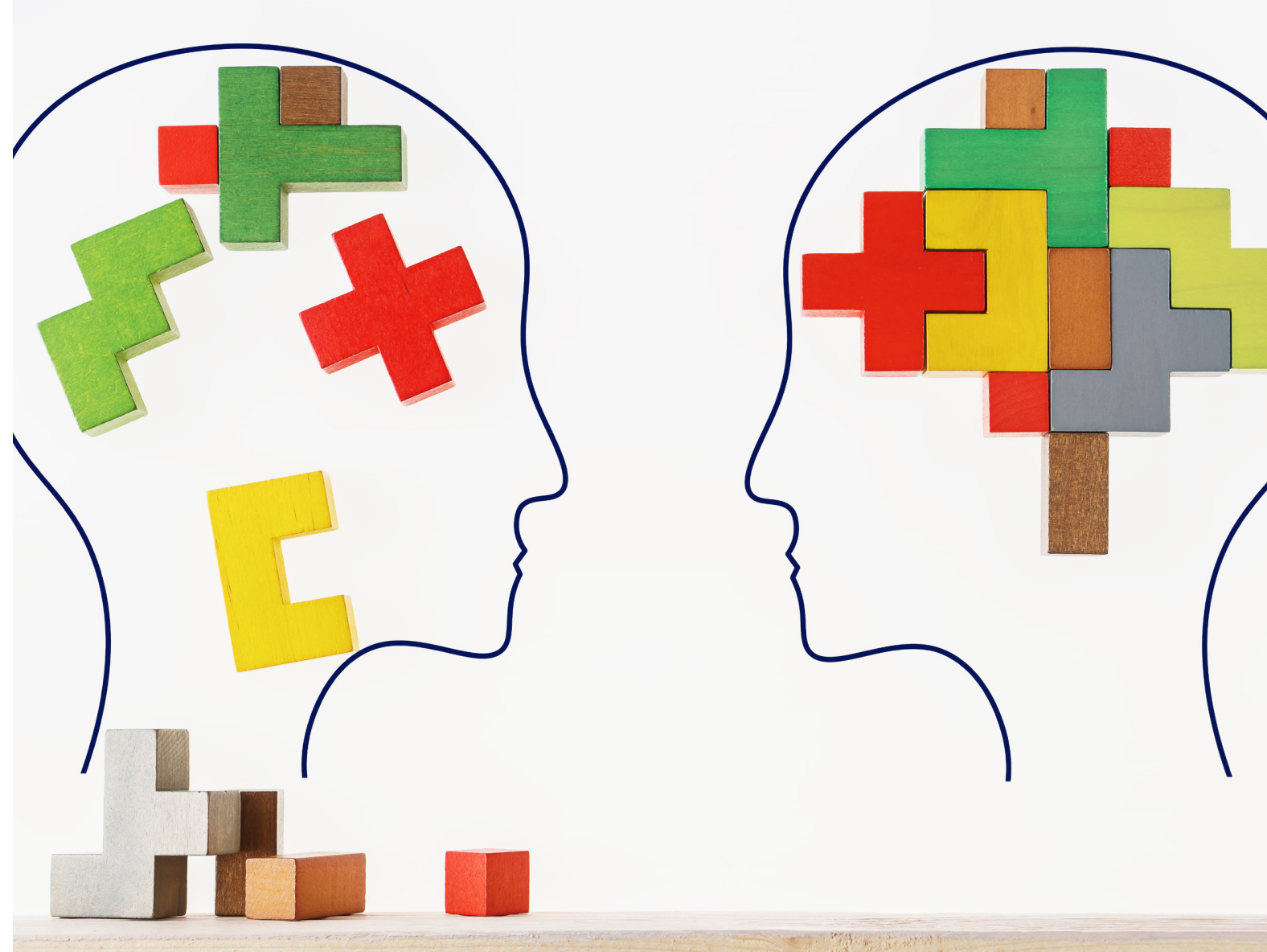


# BETWEEN THEORY AND CLINIC: THE CONTRIBUTION OF NEUROIMAGING IN THE FIELD OF CONSCIOUSNESS DISORDERS

EDITED BY: Olivia Gosseries, Steven Laureys and Caroline Schnakers  
PUBLISHED IN: Frontiers in Neurology





# frontiers

## Frontiers Copyright Statement

© Copyright 2007-2019 Frontiers Media SA. All rights reserved.

All content included on this site, such as text, graphics, logos, button icons, images, video/audio clips, downloads, data compilations and software, is the property of or is licensed to Frontiers Media SA ("Frontiers") or its licensees and/or subcontractors. The copyright in the text of individual articles is the property of their respective authors, subject to a license granted to Frontiers.

The compilation of articles constituting this e-book, wherever published, as well as the compilation of all other content on this site, is the exclusive property of Frontiers. For the conditions for downloading and copying of e-books from Frontiers' website, please see the Terms for Website Use. If purchasing Frontiers e-books from other websites or sources, the conditions of the website concerned apply.

Images and graphics not forming part of user-contributed materials may not be downloaded or copied without permission.

Individual articles may be downloaded and reproduced in accordance with the principles of the CC-BY licence subject to any copyright or other notices. They may not be re-sold as an e-book.

As author or other contributor you grant a CC-BY licence to others to reproduce your articles, including any graphics and third-party materials supplied by you, in accordance with the Conditions for Website Use and subject to any copyright notices which you include in connection with your articles and materials.

All copyright, and all rights therein, are protected by national and international copyright laws.

The above represents a summary only. For the full conditions see the Conditions for Authors and the Conditions for Website Use.

ISSN 1664-8714

ISBN 978-2-88945-842-4

DOI 10.3389/978-2-88945-842-4

## About Frontiers

Frontiers is more than just an open-access publisher of scholarly articles: it is a pioneering approach to the world of academia, radically improving the way scholarly research is managed. The grand vision of Frontiers is a world where all people have an equal opportunity to seek, share and generate knowledge. Frontiers provides immediate and permanent online open access to all its publications, but this alone is not enough to realize our grand goals.

## Frontiers Journal Series

The Frontiers Journal Series is a multi-tier and interdisciplinary set of open-access, online journals, promising a paradigm shift from the current review, selection and dissemination processes in academic publishing. All Frontiers journals are driven by researchers for researchers; therefore, they constitute a service to the scholarly community. At the same time, the Frontiers Journal Series operates on a revolutionary invention, the tiered publishing system, initially addressing specific communities of scholars, and gradually climbing up to broader public understanding, thus serving the interests of the lay society, too.

## Dedication to Quality

Each Frontiers article is a landmark of the highest quality, thanks to genuinely collaborative interactions between authors and review editors, who include some of the world's best academicians. Research must be certified by peers before entering a stream of knowledge that may eventually reach the public - and shape society; therefore, Frontiers only applies the most rigorous and unbiased reviews.

Frontiers revolutionizes research publishing by freely delivering the most outstanding research, evaluated with no bias from both the academic and social point of view. By applying the most advanced information technologies, Frontiers is catapulting scholarly publishing into a new generation.

## What are Frontiers Research Topics?

Frontiers Research Topics are very popular trademarks of the Frontiers Journals Series: they are collections of at least ten articles, all centered on a particular subject. With their unique mix of varied contributions from Original Research to Review Articles, Frontiers Research Topics unify the most influential researchers, the latest key findings and historical advances in a hot research area! Find out more on how to host your own Frontiers Research Topic or contribute to one as an author by contacting the Frontiers Editorial Office: [researchtopics@frontiersin.org](mailto:researchtopics@frontiersin.org)

# BETWEEN THEORY AND CLINIC: THE CONTRIBUTION OF NEUROIMAGING IN THE FIELD OF CONSCIOUSNESS DISORDERS

Topic Editors:

**Olivia Gosseries**, University and University Hospital of Liege, Belgium

**Steven Laureys**, University and University Hospital of Liege, Belgium

**Caroline Schnakers**, Casa Colina Hospital and Centers for Healthcare, United States

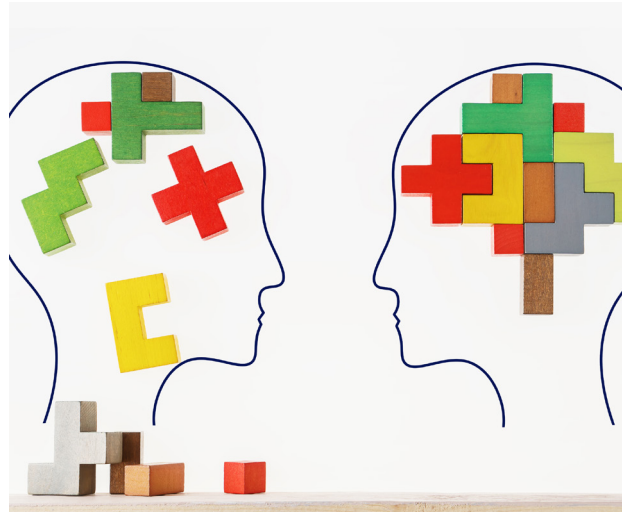


Image: Radachynskyi Serhii/Shutterstock.com

*"Let us make our future now, and let us make our dreams tomorrow's reality".*

Malala Yousafzai

This book is dedicated to all our patients and their families.

**Citation:** Gosseries, O., Laureys, S., Schnakers, C., eds. (2019). Between Theory and Clinic: The Contribution of Neuroimaging in the Field of Consciousness Disorders. Lausanne: Frontiers Media. doi: 10.3389/978-2-88945-842-4

# Table of Contents

- 05 Editorial: Between Theory and Clinic: The Contribution of Neuroimaging in the Field of Consciousness Disorders**  
Olivia Gosseries, Caroline Schnakers and Steven Laureys
- 08 Conscious While Being Considered in an Unresponsive Wakefulness Syndrome for 20 Years**  
Audrey Vanhaudenhuyse, Vanessa Charland-Verville, Aurore Thibaut, Camille Chatelle, Jean-Flory L. Tshibanda, Audrey Maudoux, Marie-Elisabeth Faymonville, Steven Laureys and Olivia Gosseries
- 17 Cortical Brain Changes in Patients With Locked-In Syndrome Experiencing Hallucinations and Delusions**  
Marco Sarà, Riccardo Cornia, Massimiliano Conson, Antonio Carolei, Simona Sacco and Francesca Pistoia
- 23 Brain, Behavior, and Cognitive Interplay in Disorders of Consciousness: A Multiple Case Study**  
Charlène Aubinet, Lesley Murphy, Mohamed A. Bahri, Stephen K. Larroque, Helena Cassol, Jitka Annen, Manon Carrière, Sarah Wannez, Aurore Thibaut, Steven Laureys and Olivia Gosseries
- 33 Functional MRI Motor Imagery Tasks to Detect Command Following in Traumatic Disorders of Consciousness**  
Yelena G. Bodien, Joseph T. Giacino and Brian L. Edlow
- 43 Do Patients Thought to Lack Consciousness Retain the Capacity for Internal as Well as External Awareness?**  
Amelie Haugg, Rhodri, Laura E. Gonzalez-Lara, Bettina Sorger, Adrian M. Owen and Lorina Naci
- 56 Network Analysis in Disorders of Consciousness: Four Problems and One Proposed Solution (Exponential Random Graph Models)**  
John Dell'Italia, Micah A. Johnson, Paul M. Vespa and Martin M. Monti
- 77 A Heartbeat Away From Consciousness: Heart Rate Variability Entropy Can Discriminate Disorders of Consciousness and is Correlated With Resting-State fMRI Brain Connectivity of the Central Autonomic Network**  
Francesco Riganello, Stephen Karl Larroque, Mohamed Ali Bahri, Lizette Heine, Charlotte Martial, Manon Carrière, Vanessa Charland-Verville, Charlène Aubinet, Audrey Vanhaudenhuyse, Camille Chatelle, Steven Laureys and Carol Di Perri
- 95 Novel Approaches to the Diagnosis of Chronic Disorders of Consciousness: Detecting Peripersonal Space by Using Ultrasonics**  
Antonino Naro, Antonino Chillura, Simona Portaro, Alessia Bramanti, Rosaria De Luca, Placido Bramanti and Rocco Salvatore Calabrò
- 106 Shining a Light on Awareness: A Review of Functional Near-Infrared Spectroscopy for Prolonged Disorders of Consciousness**  
Mohammed Rupawala, Hamid Dehghani, Samuel J. E. Lucas, Peter Tino and Damian Cruse



- 123 Multimodal Neuroimaging Approach to Variability of Functional Connectivity in Disorders of Consciousness: A PET/MRI Pilot Study**  
Carlo Cavaliere, Sivayini Kandeepan, Marco Aiello, Demetrius Ribeiro de Paula, Rocco Marchitelli, Salvatore Fiorenza, Mario Orsini, Luigi Trojano, Orsola Masotta, Keith St. Lawrence, Vincenzo Loreto, Blaine Alexander Chronik, Emanuele Nicolai, Andrea Soddu and Anna Estraneo
- 135 Longitudinal Bedside Assessments of Brain Networks in Disorders of Consciousness: Case Reports From the Field**  
Corinne A. Bareham, Judith Allanson, Neil Roberts, Peter J. A. Hutchinson, John D. Pickard, David K. Menon and Srivas Chennu
- 146 A Review of Resting-State Electroencephalography Analysis in Disorders of Consciousness**  
Yang Bai, Xiaoyu Xia and Xiaoli Li
- 155 A Systematic Review and Meta-Analysis of the Relationship Between Brain Data and the Outcome in Disorders of Consciousness**  
Boris Kotchoubey and Yuri G. Pavlov
- 170 Daytime Central Thalamic Deep Brain Stimulation Modulates Sleep Dynamics in the Severely Injured Brain: Mechanistic Insights and a Novel Framework for Alpha-Delta Sleep Generation**  
Jackie L. Gottshall, Zoe M. Adams, Peter B. Forgacs and Nicholas D. Schiff
- 184 Do Sensory Stimulation Programs Have an Impact on Consciousness Recovery?**  
Lijuan Cheng, Daniela Cortese, Martin M. Monti, Fuyan Wang, Francesco Riganello, Francesco Arcuri, Haibo Di and Caroline Schnakers



# Editorial: Between Theory and Clinic: The Contribution of Neuroimaging in the Field of Consciousness Disorders

Olivia Gosseries<sup>1,2\*</sup>, Caroline Schnakers<sup>3</sup> and Steven Laureys<sup>1,2</sup>

<sup>1</sup> Coma Science Group, University Hospital of Liege, Liege, Belgium, <sup>2</sup> GIGA-Consciousness, University of Liege, Liege, Belgium, <sup>3</sup> Research Institute, Casa Colina Hospital and Centers for Healthcare, Pomona, CA, United States

**Keywords:** disorders of consciousness, unresponsive wakefulness syndrome/vegetative state, minimally conscious state, neuroimaging, electrophysiology

## Editorial on the Research Topic

### Between Theory and Clinic: The Contribution of Neuroimaging in the Field of Consciousness Disorders

Patients surviving severe brain injury either recover quickly from coma or go through prolonged disorders of consciousness (DOC) such as unresponsive wakefulness syndrome (UWS) or minimally conscious state (MCS). While patients in MCS show signs of consciousness, patients in UWS only show reflexive behaviors. These patients are unable to communicate and present vigilance fluctuation, language impairments, and severe sensory-motor deficits. Once patients recover functional communication or use of objects, they are emerged from MCS (EMCS).

Even though behavioral assessment remains the gold standard for diagnosis, a number of studies highlight the difficulty in making the distinction between conscious and unconscious patients based on clinical examinations. Misdiagnosis can have serious consequences on patient's management, medically and ethically (i.e., regarding end-of-life decision).

The emergence of neuroimaging and neurophysiological techniques opened new opportunities to complement bedside assessment by improving diagnosis and prognosis of patients with DOC. This Research Topic, which includes 15 articles with 100 contributors, aims to give an overview on how neuroimaging research can improve diagnosis, prognosis and management of patients with DOC, and how recent applications of neuroimaging can help understand consciousness through severe brain injuries.

Vanhaudenhuyse et al. report the case of a misdiagnosis in a patient who was considered in an unresponsive wakefulness syndrome for 20 years. Repeated behavioral examinations (using the Coma Recovery Scale-Revised, CRS-R) combined with neuroimaging techniques (using positron emission tomography—PET, and magnetic resonance imaging—MRI) showed that the patient was in fact conscious and was re-diagnosed as an incomplete locked-in syndrome. Sarà et al. reported that some locked-in patients present hallucinations, and in a subgroup of 5 patients with such symptoms, they showed a reduced cortical volume in the right parahippocampal cortex, the fusiform and lingual regions, suggesting that advanced neuroimaging might help to detect small cortical changes.

In parallel, Aubinet et al. show how neuroimaging can help develop more sensitive behavioral tools to assess cognition in DOC patients. They describe the behavioral and cognitive profiles of 5 patients in MCS/EMCS alongside their neuroimaging results using structural MRI and PET. They introduce a new language-based neuropsychological tool, the *Cognitive Assessment by Visual Election* (CAVE), and showed that the cognitive profiles of the patients were consistent with the underlying brain impairments. More specifically, the presence of residual visual, motor,

## OPEN ACCESS

### Edited by:

Jan Kassubek,  
University of Ulm, Germany

### Reviewed by:

Yann Quidé,  
University of New South Wales,  
Australia

### \*Correspondence:

Olivia Gosseries  
ogosseries@uliege.be

### Specialty section:

This article was submitted to  
Applied Neuroimaging,  
a section of the journal  
Frontiers in Neurology

**Received:** 19 January 2019

**Accepted:** 07 February 2019

**Published:** 27 February 2019

### Citation:

Gosseries O, Schnakers C and  
Laureys S (2019) Editorial: Between  
Theory and Clinic: The Contribution of  
Neuroimaging in the Field of  
Consciousness Disorders.  
Front. Neurol. 10:165.  
doi: 10.3389/fneur.2019.00165

and language comprehension functions was, respectively, associated with a relative preservation of occipital, motor, and temporo-angular cortex metabolism.

Using functional MRI (fMRI) command following tasks, Bodien et al. compared the rate of covert consciousness detection by hand squeezing and tennis playing motor imagery paradigms in 10 patients with traumatic DOC and 10 healthy subjects. They found that the tennis paradigm performed better in healthy subjects, but in patients, the hand squeezing paradigm detected command following with greater accuracy. The hand squeezing paradigm may therefore be a better classifier of command following in DOC patients.

Several articles also aimed at exploring new ways to detect consciousness in DOC patients. To investigate the potential for internal and external awareness in DOC patients, Haugg et al. assessed the juxtaposed relationship between the default mode network (DMN) and the fronto-parietal (dorsal attention and executive control) networks' functional time-courses. Patients who demonstrated fMRI command following showed greater differentiation between the DMN and dorsal attention network in response to movie viewing, compared to the resting condition. This effect was similar to healthy subjects and was driven by the movie's narrative. Conversely, this pattern was not present in DOC patients who showed no fMRI-based evidence of covert awareness. Naturalistic paradigms could therefore be used to dissociate between groups of DOC patients with and without covert awareness.

Dell'Italia et al. present a different framework to estimate fMRI network properties based on Exponential Random Graph Models (ERGM), which overcomes current methodological limitations. Longitudinal data in one patient who sustained a severe traumatic brain injury show that throughout recovery from coma, brain graphs vary in their natural level of connectivity. Separable temporal ERGM can characterize network dynamics over time and show the specific pattern of formation and dissolution of connectivity after coma.

To differentiate DOC patients, Riganello et al. measured the complexity index of the heart rate variability using non-linear multi-scale entropies in 16 MCS and 14 UWS patients. Higher complexity index values were observed in MCS compared to UWS patients with high discriminative power using machine learning. The complexity index also correlated with brain connectivity in the central autonomic networks assessed with resting state fMRI. These findings suggest that this "heart" index can provide an indirect way to monitor brain connectivity in DOC patients.

Naro et al. used functional transcranial doppler to differentiate between patients in MCS and UWS by assessing cerebral blood flow velocity (CBFV) during passive movement tasks. They observed group difference changes in CBFV with the pulsatility index in 21 patients with DOC and 25 healthy controls. This rapid and easy tool may allow to identify residual top-down modulation processes from higher-order cortical areas to sensory-motor integration networks related to the peripersonal space. Another potential technique that is at its infancy in the field of DOC is the functional near-infrared spectroscopy, a non-invasive optical and portable device. Rupawala et al. review its

potential application to improve the accuracy of diagnoses and to provide new ways of communication.

A few authors tackled to better understand brain processing in DOC patients and therefore, in turn, improve diagnostic and prognostic techniques in such population. Using an hybrid PET/MR imaging, Cavaliere et al. investigated test-retest brain connectivity variability in three DOC patients. Using graph-theory and independent component analyses, they found differences between test-retest acquisitions affecting each network and each patient in a different way. Higher functional/metabolic correlation was measured in the MCS and EMCS patients compared to the UWS patient. Performing multiple acquisitions within the same session allow to assess temporal patterns of resting-state networks and improve characterization of DOC patients.

Longitudinal assessments using high-density electroencephalography (EEG) and CRS-R have also been performed on a longer time scale (with 3-monthly intervals) by Bareham et al., who showed that measures of EEG networks correlated with behavioral variations. EEG connectivity captured both stability and recovery of behavioral trajectories within and between patients. This highlights the feasibility of bedside EEG assessments in rehabilitation setting, which can complement clinical evaluation.

Bai et al. reviewed resting state EEG studies in DOC for diagnosis, prognosis, and brain interventions. Spectrum power, coherence, and entropy were the most frequently used features while power spectrum and functional connectivity had the best performance differentiating UWS from MCS and healthy subjects. Permutation entropy in the theta frequency also had high classification accuracy for differential diagnosis. Regarding prognosis, in their systematic review and meta-analysis of brain data and outcome in DOC, Kotchoubey and Pavlov report that oscillatory EEG responses, sleep spindles, and the somatosensory cortical response N20 were the best outcome predictors for DOC, whereas the poorest prognostic effects were fMRI responses to stimulation and P300. They however conclude that no practical recommendations on prognosis indicators can be given at this stage and they suggest several considerations to improve future (prognosis) studies: each group of patients should include at least 20 patients, perform blind assessments, use a flow chart to illustrate the procedure of patient selection, include the full list of measured variables, report the time since injury and the time of outcome, and describe all positive and negative results.

The last two articles refer to therapeutic options. Gottshall et al. evaluated a patient in chronic MCS who received central thalamic deep brain stimulation (CT-DBS). After 1 year of treatment discontinuation, reduced responsiveness was observed along with the abolishment of sleep spindles, marked downregulation of slow wave sleep delta power, and the return of alpha-delta sleep. The authors discuss the mechanism of sleep modulation by daytime CT-DBS in severe brain injuries and suggest a novel mechanistic framework for alpha-delta sleep generation across pathophysiology.

Cheng et al. evaluated the effect of a sensory stimulation program (3 days per week for 4 weeks) using a ABAB design (for 16 weeks) in 29 patients. Higher CRS-R total scores

were obtained during the treatment in the MCS group with increased arousal and oromotor function but not in the UWS group. Three patients also underwent fMRI and a modulation of brain activity related to treatment was found in specific brain regions.

In conclusion, this Research Topic offers some novelties in the field of severe brain injuries and DOC, including new techniques, methodology, diagnosis/prognosis improvements, and therapeutic options. We look forward to translate the neuroscientific evidence generated from these studies to the clinical context.

## AUTHOR CONTRIBUTIONS

OG wrote the editorial. CS and SL revised it.

## ACKNOWLEDGMENTS

The University and University Hospital of Liège, the Belgian National Funds for Scientific Research (FRS-FNRS), the European Union's Horizon 2020 Framework Programme for

Research and Innovation under the Specific Grant Agreement No. 720270 (Human Brain Project SGA1) and No. 785907 (Human Brain Project SGA2), Luminous project (EU-H2020-fetopen-ga686764), DOCMA project (EU-H2020-MSCA-RISE-778234), the BIAL Foundation, the French Speaking Community Concerted Research Action (ARC 12-17/01), the James McDonnell Foundation, Mind Science Foundation, IAP research network P7/06 of the Belgian Government (Belgian Science Policy), the European Commission, the Public Utility Foundation Université Européenne du Travail, and Fondazione Europea di Ricerca Biomedica.

**Conflict of Interest Statement:** The authors declare that the research was conducted in the absence of any commercial or financial relationships that could be construed as a potential conflict of interest.

*Copyright © 2019 Gosseries, Schnakers and Laureys. This is an open-access article distributed under the terms of the Creative Commons Attribution License (CC BY). The use, distribution or reproduction in other forums is permitted, provided the original author(s) and the copyright owner(s) are credited and that the original publication in this journal is cited, in accordance with accepted academic practice. No use, distribution or reproduction is permitted which does not comply with these terms.*



# Conscious While Being Considered in an Unresponsive Wakefulness Syndrome for 20 Years

Audrey Vanhaudenhuyse<sup>1,2\*</sup>, Vanessa Charland-Verville<sup>3</sup>, Aurore Thibaut<sup>3,4</sup>, Camille Chatelle<sup>3,5</sup>, Jean-Flory L. Tshibanda<sup>3,6</sup>, Audrey Maudoux<sup>2,7</sup>, Marie-Elisabeth Faymonville<sup>1,2</sup>, Steven Laureys<sup>3</sup> and Olivia Gosseries<sup>3</sup>

<sup>1</sup> Department of Algology and Palliative Care, University Hospital of Liege, Liege, Belgium, <sup>2</sup> GIGA-Consciousness, Sensation & Perception Research Group, University of Liege, Liege, Belgium, <sup>3</sup> GIGA-Consciousness, Coma Science Group & Neurology Department, University Hospital of Liege, Liege, Belgium, <sup>4</sup> Neuromodulation Center, Spaulding Rehabilitation Hospital, Harvard Medical School, Boston, MA, United States, <sup>5</sup> Laboratory for Neuroimaging of Coma and Consciousness-Department of Neurology, Massachusetts General Hospital, Harvard Medical School, Boston, MA, United States, <sup>6</sup> Department of Radiology, University Hospital of Liege and University of Liege, Liege, Belgium, <sup>7</sup> Otorhinolaryngology Head and Neck Surgery Department, University Hospital of Liege, Liege, Belgium

## OPEN ACCESS

### Edited by:

Elham Rostami,  
Academic Hospital, Sweden

### Reviewed by:

Anna Estraneo,  
IRCCS Istituti Clinici Scientifici Maugeri  
(ICS Maugeri), Italy  
Rita Formisano,  
Fondazione Santa Lucia (IRCCS), Italy

### \*Correspondence:

Audrey Vanhaudenhuyse  
avanhaudenhuyse@chuliege.be

### Specialty section:

This article was submitted to  
Neurotrauma,  
a section of the journal  
Frontiers in Neurology

Received: 23 February 2018

Accepted: 26 July 2018

Published: 28 August 2018

### Citation:

Vanhaudenhuyse A,  
Charland-Verville V, Thibaut A,  
Chatelle C, Tshibanda J-FL,  
Maudoux A, Faymonville M-E,  
Laureys S and Gosseries O (2018)  
Conscious While Being Considered in  
an Unresponsive Wakefulness  
Syndrome for 20 Years.  
Front. Neurol. 9:671.  
doi: 10.3389/fneur.2018.00671

Despite recent advances in our understanding of consciousness disorders, accurate diagnosis of severely brain-damaged patients is still a major clinical challenge. We here present the case of a patient who was considered in an unresponsive wakefulness syndrome/vegetative state for 20 years. Repeated standardized behavioral examinations combined to neuroimaging assessments allowed us to show that this patient was in fact fully conscious and was able to functionally communicate. We thus revised the diagnosis into an incomplete locked-in syndrome, notably because the main brain lesion was located in the brainstem. Clinical examinations of severe brain injured patients suffering from serious motor impairment should systematically include repeated standardized behavioral assessments and, when possible, neuroimaging evaluations encompassing magnetic resonance imaging and <sup>18</sup>F-fluorodeoxyglucose positron emission tomography.

**Keywords:** disorders of consciousness, misdiagnosis, locked-in syndrome, unresponsive wakefulness syndrome, MRI, PET, EEG, vegetative state

## INTRODUCTION

We here present the case of a 41-year-old man who was considered in an unresponsive wakefulness syndrome (UWS; previously referred to as “vegetative state”) for 20 years. In this section, we first review his medical history then we report the clinical and neuroimaging evaluations that were performed in our center 20 years after his brain injury.

## Patient's History

In 1992, the patient sustained a severe traumatic brain injury as a result of a car accident. He had no previous significant medical history. On admission to a general hospital, the Glasgow Coma Scale (1) total score was 4/15 and both pupils were in myosis. Babinski reflex was present bilaterally. The patient was intubated and mechanically ventilated. Brain CT scan revealed left parietal, basal ganglia, and retro-pontic hemorrhages. The EEG displayed a non-reactive global slowing of basic rhythms without paroxysmic activity. The patient was tracheotomized, received nasogastric feeding



and left the intensive care unit 24 days later with the diagnosis of “coma vigil.” Six weeks after the insult, the treating nurse of the neuropsychiatry department reported that the patient had moved his right hand to command, but this observation did not change the clinical diagnosis and it was never reported on later occasions. Two epileptic seizures were observed 6 months post-injury. The tracheal tube was removed 8 months after the brain trauma. Neurological examination performed 9 months post-onset reported spontaneous eye opening without reproducible response to command, and concluded to a state of “irreversible coma vigil” (i.e., permanent vegetative state). One year and 5 months post-injury, he was transferred to a chronic nursing care home with the diagnosis of “comatose state.” The patient did not receive physiotherapy, speech therapy or occupational therapy. No stimulation or rehabilitation treatment was reported by the medical team in the nursing home.

Twenty years after his brain injury, the patient was transferred to our neurology department for a diagnostic evaluation as requested by the general practitioner of his nursing care home. The request was initiated by the family of the patient who was staying in the same room who had the impression that he was conscious. The diagnosis on referral was “coma vigil.” Pharmacological treatment included diphantoine ( $4 \times 100$  mg/d—antiepileptic), mirtazapine ( $1 \times 30$  mg—antidepressant) and lormetazepam ( $1 \times 2$  mg/d—sedative benzodiazepine). Medication was not modified during the week of assessment. Hetero-anamnesis was limited given that no family could be reached.

## Clinical Assessments

The patient’s consciousness level was assessed with the Coma Recovery Scale-Revised [CRS-R, (2)]. This scale is currently considered the most validated and sensitive method for identifying behavioral signs of awareness and thus better diagnose between UWS, minimally conscious state and emergence of the minimally conscious state (2–5). It consists of six subscales: auditory, visual, motor, oromotor and verbal functions, communication, and the level of arousal. The 23 items are ordered by degree of complexity, ranging from reflexive to cognitively mediated behaviors. We recently reported that a minimum of five CRS-R assessments conducted within a short time interval (e.g., 2 weeks) was necessary to reduce misdiagnosis (6). Here, the patient underwent seven CRS-R assessments in a period of 1 week; these were performed by a team of experimented examiners at different moments of the day, and in similar environmental conditions. To assess the patient’s spatio-temporal orientation, we asked on one occasion some questions of the Mini Mental State Examination [MMSE, (7)].

Pain perception was also assessed once with the Nociception Coma Scale-Revised [NCS-R, (8)], which consists of three subscales evaluating motor, verbal, and facial expression responses; each subscore ranges from 0 to 3 (maximum total score of 9). Additional physiotherapy and otorhinolaryngology examinations were performed during the week of hospitalization.

Spontaneously, the patient showed eyes opening, chewing, left wrist and leg movements as well as visual fixation and visual pursuit; these two latter are considered as signs of consciousness

(9, 10). The CRS-R examinations straightforwardly showed that the patient was not in a UWS (Table 2). The CRS-R total score varied between 12 and 17. During every single assessment, the patient was able to repeatedly follow simple commands (e.g., close your eyes, open your mouth, lift your thumb). On two consecutive assessments, he could also functionally communicate (i.e., being able to systematically and accurately answer simple questions using a “YES/NO” codes), which means that he emerged from the minimally conscious state. The first time, the patient correctly answered the CRS-R visual questions using YES and NO cards. The second time, he responded accurately to self-related questions using a buzzer (i.e., buzz once to say yes). On three other assessments, the patient presented an intentional non-functional communication [i.e., clearly discernible communicative responses occurred on at least two out of the six questions, irrespectively of accuracy; (2)]. During all these assessments, we tried different codes of communication with the patient, such as point out YES/NO cards or rise your thumb to say YES/do not move your thumb to say NO, to finally observe that the best way to communicate was with visual fixation of YES/NO cards on the vertical axis.

Furthermore, the patient showed visual pursuits (on vertical and horizontal planes on all assessments), automatic motor responses (e.g., touch his mouth), anticipation and grimaces after nociceptive stimulations, and objects localization.

When assessing his spatio-temporal orientation using YES/NO cards, the patient was able to correctly indicate his first and last name, the names of his roommate and the mother’s roommate. He was, however, not able to give his age, to locate the hospital, neither the exact date (day, month, year) nor the season.

NCS-R assessment highlighted withdrawal flexion, groaning and grimacing in response to nociceptive stimulation (total score of 5), as well as abnormal stereotyped posture and oral movements during nursing cares (total score of 2). Physiotherapy assessment showed spasticity in flexion in the right superior limb and abnormal extension with internal rotation in the left superior limb. The feet were fixed in equine varus positions and the knees flexions were limited. The head suffered from a vicious position in deviation to the left. Otorhinolaryngology examination evidenced significant spasticity of the entire cephalic segment, major spasticity of the whole neck muscles with the impossibility to reduce left deviation. A left saliva drooling was observed but the velar reflex and nausea reflex were absent. A naso-pharyngo-laryngeal fibroscopy showed that the nasal cavities, the pharynx and the larynx were structurally normal. The laryngeal sensitivity was reduced and no cough reflex could be evoked. Food testing was attempted but was impossible to perform due to a deficient oral phase.

## Neuroimaging Assessments

For structural MRI, a high-resolution T2-weighted image was acquired (25 slices; repetition time = 3,000 ms, echo time = 88 ms, voxel size =  $0.9 \times 0.9 \times 3$  mm<sup>3</sup>, field of view =  $220 \times 220$  mm<sup>2</sup>) on a 3 Tesla scanner (Siemens Trio, Siemens Medical Solutions, Erlangen, Germany). Diffusion tensor images (DTI)



**TABLE 1 |** Behavioral responses of the patient assessed with the Coma Recovery Scale-Revised.

Day of assessment	1	2	3	4	5	6	7
Other evaluations performed the same day		EEG	PET NCS	MMSE	MRI		
<b>AUDITORY FUNCTION</b>							
4—Consistent Movement to Command* (4/4 responses of 2 different commands)				x		x	x
3—Reproducible Movement to Command* (3/4 responses of 1 command)	x	x	x		x		
2—Localization to Sound	x	x	x	x	x	x	x
1—Auditory Startle	x			x			
0—None							
<b>VISUAL FUNCTION</b>							
5—Object Recognition*		x	x	x	x	x	x
4—Object Localization: Reaching*			x	x			
3—Visual Pursuit*	x	x	x	x	x	x	x
2—Fixation*	x	x	x	x	x	x	x
1—Visual Startle	x	x	x	x	x	x	x
0—None							
<b>MOTOR FUNCTION</b>							
6—Functional Object Use <sup>#</sup>							
5—Automatic Motor Response*					x		
4—Object Manipulation*							
3—Localization to Noxious Stimulation*							
2—Flexion Withdrawal	x			x	x	x	x
1—Abnormal Posturing		x	x	x			
0—None/Flaccid							
<b>OROMOTOR/VERBAL FUNCTION</b>							
3—Intelligible Verbalization*							
2—Vocalization/Oral Movement	x	x	x	x		x	x
1—Oral Reflexive Movement	x	x	x	x		x	x
0—None					x		
<b>COMMUNICATION</b>							
2—Functional: Accurate <sup>#</sup>				x	x		
1—Non-Functional: Intentional*		x				x	x
0—None	x		x				
<b>AROUSAL</b>							
3—Attention							
2—Eye Opening w/o Stimulation	x	x	x		x	x	x
1—Eye Opening with Stimulation				x			
0—Unarousable							
Total score	12*	14*	13*	16 <sup>#</sup>	17 <sup>#</sup>	16*	16*

\*Denotes MCS. #Denotes emergence of MCS.

were acquired using an EPI sequence (TR = 5,700 ms, TE = 87 ms, 45 slices; slice thickness = 3 mm, gap = 0.3 mm, matrix size = 128\*128) and sensitized in 64 non-collinear directions using a  $b$ -value = 1,000 s/mm<sup>2</sup> and two  $b$  = 0 images. Data were acquired and analyzed similarly to our previous studies (23, 24). Images were processed using the FMRIB Software Library (FSL; version 4.1.2; <http://www.fmrib.ox.ac.uk/fsl>). Fractional anisotropy and mean diffusivity maps were obtained using FSL diffusion toolbox (25).

Structural MRI showed post-traumatic diffuse axonopathy lesions in the right middle cerebellum peduncle, right cerebral peduncle, left lenticular nucleus, corpus callosum, right superior frontal gyrus, and mesencephalic tegmentum (**Figure 1A**). There was no parenchymatic atrophy.

DTI showed a relative preservation of the white matter structure (**Figure 1B**). The global fractional anisotropy was estimated at 0.32 (normal range in healthy control subjects between 0.35 and 0.59).

For resting cerebral  $^{18}\text{F}$ -fluorodeoxyglucose positron emission tomography (FDG-PET), data were also acquired and analyzed as in our previous studies (19, 26). Before and after injection of 300 MBq of FDG, the patient was kept awake in the dark for 30 min and was then scanned on a Gemini TF PET-CT scanner (Philips Medical Systems). Data was preprocessed using spatial normalization, smoothing (Gaussian kernel of 14 mm full width at a half maximum) and proportional scaling, implemented in Statistical Parametric Mapping toolbox, SPM 12 ([www.fil.ion.ucl.ac.uk/spm](http://www.fil.ion.ucl.ac.uk/spm)). The design matrix modeled the patient and 34 age-matched healthy controls' PET-scans. We used a significance threshold of  $p < 0.05$  uncorrected in all contrast for single subject analyses.

Results showed a preservation of 99.6% of the patient's global brain metabolism as compared to healthy subjects (**Figure 1C**). Preserved brain regions encompassed the whole fronto-temporo-parietal cortex bilaterally. Hypometabolism was observed in the

mesiofrontal region, the thalamus bilaterally, the brainstem and the cerebellum (**Figure 1D**).

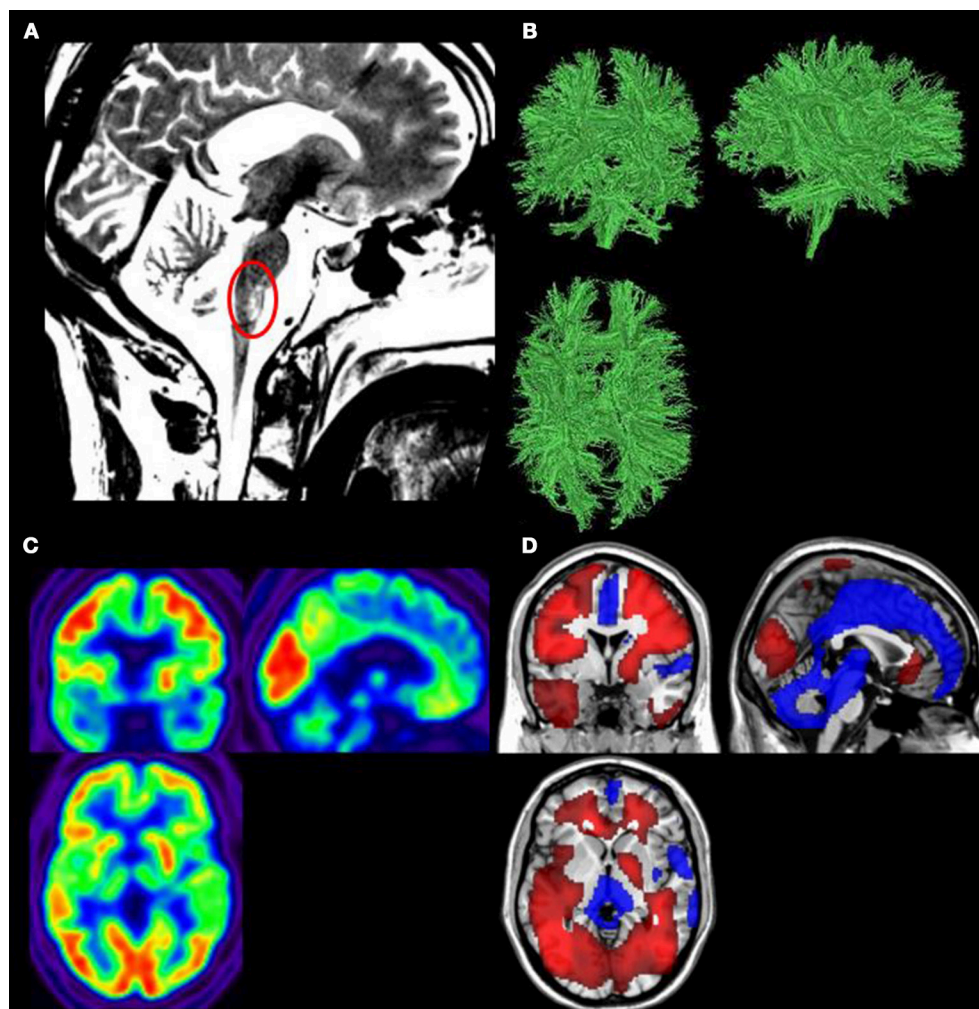
Both MRI and PET data show a brainstem lesion, which is observed in patients with locked-in syndrome [(27), **Figures 1A,D**].

A clinical EEG was also performed using 19 electrodes and interpreted by a certified neurologist. Results showed bilateral alpha activity and 8–10 Hz activities on all derivations without any paroxysmal activity.

The days of neuroimaging assessments (as well as the NCS and the MMSE) are reported in **Table 1**.

## BACKGROUND

Despite recent advances in our understanding of disorders of consciousness and the redefinition of nosological distinctions between altered states of consciousness, diagnosis of severely



**FIGURE 1 | (A)** Structural magnetic resonance imaging (MRI) showed the mesencephalic tegmentum lesion (red circle). **(B)** Diffusion tensor imaging (DTI) showed white matter structure preservation. **(C)**  $^{18}\text{F}$ -fluorodeoxyglucose positron emission tomography (FDG-PET) demonstrated a global cerebral metabolism preservation. **(D)** Areas in which FDG-PET finds significantly impaired (blue) or preserved (red) metabolism compared to controls ( $p < 0.05$ , uncorrected).

brain-damaged patients continues to represent a major clinical challenge. If neuroimaging techniques support clinical examinations and help to improve the accuracy of the diagnosis of altered state of consciousness, behavioral assessment remains the principal method used to detect awareness in these patients (28). Nowadays, standardized scales such as the CRS-R (2) are validated to assess the level of consciousness of these patients. In addition, series of studies have reported that specific clinical tools [e.g., using a mirror to assess visual pursuit (9, 10) or the own name to assess localization to sounds (29)] can increase the chance of observing behavioral responses. In spite of these developments, clinical practice shows that disentangling reflexive from voluntary behaviors can still be very difficult.

Several misdiagnosis studies have been described in patients at an early stage after severe brain damage, as well as in the long-term care (Table 2). Some studies reported cases of patients considered unconscious while they actually presented behavioral signs of consciousness when assessed more thoroughly (5, 6, 11–13, 15, 16, 19–22). Other studies recount cases of patients who were considered unconscious at the bedside but who were actually found to be conscious with neuroimaging techniques, and some of these patients could even

communicate with adapted communication code (18, 19, 30–32). Different factors can explain the high rate of diagnosis errors in patients with disorders of consciousness: the lack of knowledge about the diagnosis criteria and terminology, the absence or misuse of standardized assessment scale, the use of insensitive tools, the patients' perceptual and/or motor deficits, the presence of language impairment, the fluctuating arousal level, and the presence of pain or sedative drugs (33, 34).

Studies have highlighted the importance to properly diagnose clinical entities because patients in minimally conscious state retain some preserved capacities for cognitive processing, which is not the case in patients with UWS who only show reflex behaviors (35–37). In addition, outcome and responses to treatment of minimally conscious patients seem more favorable than those in a UWS (38–40). Clinical decisions about pain management and end-of-life are also influenced by the diagnosis (41–43). A similar yet very different group of patients are those with a locked-in syndrome [LIS; (27)]. Patients with LIS are completely conscious but they have no muscle control due to a disruption of the brainstem's cortico-spinal pathways. However, most of these patients recover minimal motor function with time, and some may even recover almost fully, as it is sometimes

**TABLE 2 |** Studies reporting misdiagnosis of UWS.

References	Method	Number of patients	Number of patients misdiagnosed	% of misdiagnosis	Etiology	Initial diagnosis	Correct diagnosis	Duration of the misdiagnosis
Tresch et al. (11)	Clinical consensus vs. Author's examination	62	11	18%	NA	UWS	MCS	Chronic (> 1 year)
Childs et al. (12)	Clinical consensus vs. Author's examination	49	18	37%	14 TBI 4 NTBI	UWS	MCS	1–3 days
Andrews et al. (13)	Clinical consensus vs. RLA (14)	40	17	42%	10 TBI 7 NTBI	UWS	15 MCS 2 EMCS	Range 2–175 days
Tavalaro and Tayson (15)	Clinical consensus vs. Family and nurses impression	1	1	NA	Stroke	UWS	LIS	6 years
Gill-Thwaites and Munday (16)	Clinical consensus vs. SMART (17)	60	27	45%	21 TBI 39 NTBI	UWS	"Higher level of functioning than VS"	Within 4 months
Schnakers et al. (5)	Clinical consensus vs. CRS-R	44	18	41%	39 TBI 64 NTBI	UWS	MCS	NA
Lukowicz et al. (18)	Clinical consensus vs. Family impression	1	1	NA	Brain tumor	"Unconscious terminal stage"	LIS	16 years
Stender et al. (19)	Clinical consensus vs. CRS-R	51	18	35%	TBI and NTBI	UWS	MCS	Mean duration of UWS: 2 years and 3 months
Sattin et al. (20)	Experience rater CRS-R vs. CRS-R with person responsible of patients	92	15	16%	25 TBI 67 NTBI	UWS	MCS	Mean duration of UWS: 2 years and 6 months
van Erp et al. (21)	Clinical consensus vs. CRS-R	41	17	41%	TBI and NTBI	UWS	MCS	Mean duration of UWS: 5 years
Cortese et al. (22)	Morning CRS-R vs. Afternoon CRS-R	7	2	30%	2 TBI 5 NTBI	UWS	MCS	1.8–6.2 years
Wannez et al. (6)	1 CRS-R vs. 5 CRS-R	62	22	35%	TBI and NTBI	UWS	MCS	Mean time since injury 4 years

UWS, unresponsive wakefulness syndrome (vegetative state—VS); MCS, minimally conscious state; EMCS, emergence of minimally conscious state; LIS, locked-in syndrome; TBI, traumatic brain injury; NTBI, non-traumatic brain injury; NA, non applicable.

the case with *incomplete LIS* (44, 45). On the other hand, some patients with LIS have other brain lesions outside the brainstem which might induce cognitive impairments (46, 47).

## DISCUSSION

Our standardized-repeated behavioral assessments detected signs of consciousness and functional communication at the patient's bedside, which indicates that the patient emerged from the minimally conscious state. The neuroimaging results confirmed that the patient was conscious and that he actually was in a LIS due to a lesion in the brainstem. Because the patient could move more than a classical LIS, the diagnosis of incomplete LIS was finally made.

This patient had a brain injury 20 years before his admission to our center and he was misdiagnosed as being unconscious all these years when he was in fact fully conscious. The lack of knowledge about differential diagnosis of disorders of consciousness during this time period can explain that the patient received the diagnosis of "coma vigil" or "vegetative state." The LIS was defined in 1966 (48), while criteria of the minimally conscious state and emergence of this state were defined much later, in 2002 (49). Moreover, 20 years ago, behavioral assessment of consciousness were limited to very few scales such as the Glasgow Coma Scale, which is not sensitive enough to detect small signs of consciousness (4). Our clinical practice shows that once stamped with the diagnosis of UWS, it is often difficult to change the label, and the first signs of recovery of consciousness can be missed. The negative associations intrinsic to the term "vegetative state" can result to diagnostic errors and can also lead to potential effect on the treatment and care (37).

This case report also shows how difficult it can be to properly assess signs of consciousness and evaluate cognitive impairment in severely brain-injured patients suffering from profound physical disabilities. In order to detect consciousness in these patients, we are limited to make inferences about the presence or absence of motor responses. Behavioral examination is very challenging because observed movements may be small, inconsistent and easily exhausted, potentially leading to diagnostic errors.

On one hand, the American Congress of Rehabilitation Medicine (50) defines the following neurobehavioral criteria of the LIS: eyes opening, evidence of basic cognitive abilities, quadriplegia or paraplegia, as well as eyes movements way of communication, usually escorted by lesions of the ventral pons. In addition, intact intellectual abilities characterize the classical LIS (46). On the other hand, emergence from the minimally conscious state is defined by the demonstration of either functional communication or functional use of objects, on two consecutive assessments. Our patient showed spontaneous eyes opening and severe motor impairment that could be related to quadriplegia. Communication, which was detected and could be possible via eye movements, was not easily reproducible: out of seven assessments, the patient was able to functionally communicate only on two consecutive assessments while a non-functional intentional communication was detected on three

evaluations. Even if the patient presented an eye-movement-based communication, the diagnosis of incomplete LIS is challenging at the behavioral level because his communication responses fluctuated a lot. In addition, we should consider that the patient's deficit in spatio-temporal orientation (such as his inability to report the exact date or to locate the hospital) could be related to his 20-years-long impossibility to read a calendar or to be informed about the world outside his room rather than to a cognitive impairment. Inconsistency of behavioral responses and difficulties to correctly answer to orientation questions could also be the result of a lack of stimulation for the past 20 years.

At the neuroimaging level, structural MRI, DTI, and FDG-PET results highlighted a preservation of global cerebral metabolism and cerebral white matter combined with a lesion in the brainstem. The brain lesions observed with the neuroimaging tools, specifically in the brainstem, are typically observed in patients with LIS (51), with additional brain lesions (46).

In 33% of cases, a previous study showed that it was the relatives of the patient with LIS who were the first to detect consciousness and ability to communicate (52). In addition, guidelines emphasize the importance that the diagnosis should be made by involving information from family members or other persons who see the patient regularly (53). Other studies have also insisted on the critical role of the family or of a close relative in the assessment of patients (54).

The story of the patient we reported here is marked by an important social isolation. Indeed, since his accident, his family and friends were disengaged from the care and his general condition. The only people in daily contact with him were members of the medical staff. Since 1994, the patient was in a long care nursing home. Even if nurses knew him very well after all these years, they always referred to him as a "vegetative state." The intrinsic negative connotation of the term "vegetative state" can lead to situations where the patients' relatives interpret this diagnosis as he is no longer a human being (but more a "vegetable"), and that there is no hope of recovery (55). The "unresponsive wakefulness syndrome" terminology was thus adopted to be more descriptive of the actual state of these patients and preventing the use of a pejorative term (35). In addition, even if the medical team usually strive to maintain these people's rights as human beings and treat them with respect, it is difficult to be optimistic and adopt a positive attitude during years when patients are very low responsive.

Recent advances in technologies have demonstrated the possibility of establishing binary communication with severe brain injury patients using solely mental processes. These brain computer interfaces (BCI) technologies have employed neural responses detectable with EEG, to provide patients with motor impairments the ability to control a computer. These interfaces usually drive software for simple communication, or control devices that influence some aspect of the patient's external environment. In addition, they provide the patient with valuable real-time feedback on their performance, enabling them to learn how to use the interface better over time [for a review, see (56, 57)]. Recently, a novel BCI based on steady-state visually evoked potential or functional near-infrared spectroscopy were developed, tested and validated with patients in LIS (58, 59).



These BCI technologies could benefit to patients who are severely motor impaired and potentially allow clinicians to detect signs of consciousness and elaborate communication with these very challenging patients.

One can point as limitation that neuropsychological testing is lacking in the evaluation of this patient. Neuropsychological testing and specifically the ones adapted for non-communicative patients (46, 60) would have been useful to better determine the patient's cognitive abilities. Another limitation is the lack of assessment during these 20 years. Indeed, the patient may have recovered slowly over these years with no expert to assess his progress. One can also argue that the patient was at some point in a functional locked-in syndrome [i.e., patients with a dissociation between extreme motor dysfunction and preserved higher cortical functions identified only by functional imaging techniques; (36)] but misdiagnosed as being in UWS because neuroimaging techniques were not available at that time to detect consciousness (61).

## CONCLUDING REMARKS

In conclusion, this report emphasizes both the complex nature of patients with severe brain injury and the necessity to use validated sensitive techniques to make an accurate diagnosis. Accurate diagnosis in the early stages will determine cares and patients management after their brain injury. If misdiagnosis of UWS is frequent for patients who actually are in a minimally conscious state, this misdiagnosis is, even if less frequent, still observed in patients who are in fact totally conscious like LIS patients. Since behavioral assessments remain the gold standard to detect consciousness, clinicians should be cautious in the scales they use to assess patients, as well as to additional cognitive impairments as a consequence of specific brain lesions. To date, the most sensitive and validated scale is the CRS-R (2). The number of CRS-R assessments has an impact on the clinical diagnosis of patients since a lack of repeated examinations in patients with DOC can lead to an underestimation of patients' level of consciousness (6). It was recently demonstrated that a minimum of five CRS-R assessments is required for a reliable clinical diagnosis in DOC (6).

This case report also emphasizes the need for neuroimaging in the assessment of consciousness to confirm or refute the clinical

diagnosis. In addition, we should notice that the diagnosis of UWS of this patient was maintained because he was abandoned early in a chronic setting, where there was no adequate expertise in the assessment of persons with disorders of consciousness and in a condition of social isolation. A close collaboration and involvement of family should be systematic in cares and assessments of patients with disorders of consciousness.

## ETHICS STATEMENT

The study was approved by the Ethics Committee of the Faculty of Medicine of the University of Liège, Belgium.

## AUTHOR CONTRIBUTIONS

AV and OG were responsible for acquisition, analysis and interpretation of data and drafting the article. VC-V was responsible for interpretation of data and drafting the article. AT, CC, J-FT, and AM were responsible for acquisition and interpretation of data and revising the article. M-EF and SL were responsible for interpretation of data and revising the article.

## ACKNOWLEDGMENTS

The study was supported by the University and University Hospital of Liège, the French Speaking Community Concerted Research Action (ARC-06/11-340), the Belgian National Funds for Scientific Research (FRS-FNRS), Human Brain Project (EU-H2020-fetflagship-hbp-sga1-ga720270), the Luminous project (EU-H2020-fetopen-ga686764), the Wallonie-Bruxelles International, the James McDonnell Foundation, Mind Science Foundation, IAP research network P7/06 of the Belgian Government (Belgian Science Policy), the European Commission, the Public Utility Foundation Université Européenne du Travail, Fondazione Europea di Ricerca Biomedica, the Bial Foundation, Plan National Cancer of Belgium (Grant number 139). VC-V, AT, AM, and OG are post-doctoral fellows, and SL is research director at FRS-FNRS. The authors thank the whole staff from the Neurology, Radiodiagnostic and Nuclear Medicine departments, the certified neurologist EEG, the University Hospital of Liège and the patient.

## REFERENCES

- Jennett B, Bond M. Assessment of outcome after severe brain damage. *Lancet Lond Engl.* (1975) 1:480–4. doi: 10.1016/S0140-6736(75)92830-5
- Giacino JT, Kalmar K, Whyte J. The JFK Coma Recovery Scale-Revised: measurement characteristics and diagnostic utility. *Arch Phys Med Rehabil.* (2004) 85:2020–9. doi: 10.1016/j.apmr.2004.02.033
- American Congress of Rehabilitation Medicine, Brain Injury-Interdisciplinary Special Interest Group, Disorders of Consciousness Task Force, Seel RT, Sherer M, Whyte J, et al. Assessment scales for disorders of consciousness: evidence-based recommendations for clinical practice and research. *Arch Phys Med Rehabil.* (2010) 91:1795–813. doi: 10.1016/j.apmr.2010.07.218
- Schnakers C, Majerus S, Giacino J, Vanhaudenhuyse A, Bruno M-A, Boly M, et al. A French validation study of the Coma Recovery Scale-Revised (CRS-R). *Brain Inj.* (2008) 22:786–92. doi: 10.1080/02699050802403557
- Schnakers C, Vanhaudenhuyse A, Giacino J, Ventura M, Boly M, Majerus S, et al. Diagnostic accuracy of the vegetative and minimally conscious state: clinical consensus versus standardized neurobehavioral assessment. *BMC Neurol.* (2009) 9:35. doi: 10.1186/1471-2377-9-35
- Wannez S, Heine L, Thonnard M, Gosseries O, Laureys S, Coma Science Group collaborators. The repetition of behavioral assessments in diagnosis of disorders of consciousness. *Ann Neurol.* (2017) 81:883–9. doi: 10.1002/ana.24962
- Folstein MF, Folstein SE, McHugh PR. "Mini-mental state". A practical method for grading the cognitive state of patients for the clinician. *J Psychiatr Res.* (1975) 12:189–98.

8. Chatelle C, De Val M-D, Catano A, Chaskis C, Seeldrayers P, Laureys S, et al. Is the nociception coma scale-revised a useful clinical tool for managing pain in patients with disorders of consciousness? *Clin J Pain* (2016) 32:321–6. doi: 10.1097/AJP.0000000000000259
9. Thonnard M, Wannez S, Keen S, Brédart S, Bruno M-A, Gosseries O, et al. Detection of visual pursuit in patients in minimally conscious state: a matter of stimuli and visual plane? *Brain Inj.* (2014) 28:1164–70. doi: 10.3109/02699052.2014.920521
10. Vanhaudenhuyse A, Schnakers C, Brédart S, Laureys S. Assessment of visual pursuit in post-comatose states: use a mirror. *J Neurol Neurosurg Psychiatry* (2008) 79:223. doi: 10.1136/jnnp.2007.121624
11. Tresch DD, Sims FH, Duthie EH, Goldstein MD, Lane PS. Clinical characteristics of patients in the persistent vegetative state. *Arch Intern Med.* (1991) 151:930–2. doi: 10.1001/archinte.1991.00400050078015
12. Childs NL, Mercer WN, Childs HW. Accuracy of diagnosis of persistent vegetative state. *Neurology* (1993) 43:1465–7. doi: 10.1212/WNL.43.8.1465
13. Andrews K, Murphy L, Munday R, Littlewood C. Misdiagnosis of the vegetative state: retrospective study in a rehabilitation unit. *BMJ* (1996) 313:13–6. doi: 10.1136/bmj.313.7048.13
14. Hagen C, Durham P. Levels of cognitive functioning. In: Professional Staff Association of Rancho Los Amigos Hospital, Editor. *Rehabilitation of the Head Injured Adult: Comprehensive Physical Management*. Downey, CA: Rancho Los Amigos Hospital (1987).
15. Tavalaro J, Tayson R. *Look Up for Yes*. New York, NY: Kodansha America, Inc. (1997).
16. Gill-Thwaites H, Munday R. The Sensory Modality Assessment and Rehabilitation Technique (SMART): a valid and reliable assessment for vegetative state and minimally conscious state patients. *Brain Inj.* (2004) 18:1255–69. doi: 10.1080/02699050410001719952
17. Gill-Thwaites H. The Sensory Modality Assessment Rehabilitation Technique—a tool for assessment and treatment of patients with severe brain injury in a vegetative state. *Brain Inj.* (1997) 11:723–34. doi: 10.1080/026990597123098
18. Lukowicz M, Matuszak K, Talar A. A misdiagnosed patient: 16 years of locked-in syndrome, the influence of rehabilitation. *Med Sci Monit Int Med J Exp Clin Res.* (2010) 16:CS18–23.
19. Stender J, Gosseries O, Bruno M-A, Charland-Verville V, Vanhaudenhuyse A, Demertzi A, et al. Diagnostic precision of PET imaging and functional MRI in disorders of consciousness: a clinical validation study. *Lancet Lond Engl.* (2014) 384:514–22. doi: 10.1016/S0140-6736(14)60042-8
20. Sattin D, Giovannetti AM, Ciaraffa F, Covelli V, Bersano A, Nigri A, et al. Assessment of patients with disorder of consciousness: do different Coma Recovery Scale scoring correlate with different settings? *J Neurol.* (2014) 261:2378–86. doi: 10.1007/s00415-014-7478-5
21. van Erp WS, Lavrijsen JCM, Vos PE, Bor H, Laureys S, Koopmans RTCM. The vegetative state: prevalence, misdiagnosis, and treatment limitations. *J Am Med Dir Assoc.* (2015) 16:85.e9–85.e14. doi: 10.1016/j.jamda.2014.10.014
22. Cortese M, Riganello F, Arcuri F, Pugliese M, Lucca L, Dolce G, et al. Coma recovery scale-r: variability in the disorder of consciousness. *BMC Neurol.* (2015) 15:5. doi: 10.1186/s12883-015-0455-5
23. Bruno MA, Fernández-Espejo D, Lehembre R, Tshibanda L, Vanhaudenhuyse A, Gosseries O, et al. Multimodal neuroimaging in patients with disorders of consciousness showing “functional hemispherectomy.” *Prog Brain Res.* (2011) 193:323–33. doi: 10.1016/B978-0-444-53839-0.00021-1
24. Tshibanda L, Vanhaudenhuyse A, Galanaud D, Boly M, Laureys S, Puybasset L. Magnetic resonance spectroscopy and diffusion tensor imaging in coma survivors: promises and pitfalls. *Prog Brain Res.* (2009) 177:215–29. doi: 10.1016/S0079-6123(09)17715-4
25. Behrens TEJ, Woolrich MW, Jenkinson M, Johansen-Berg H, Nunes RG, Clare S, et al. Characterization and propagation of uncertainty in diffusion-weighted MR imaging. *Magn Reson Med.* (2003) 50:1077–88. doi: 10.1002/mrm.10609
26. Bodart O, Gosseries O, Wannez S, Thibaut A, Annen J, Boly M, et al. Measures of metabolism and complexity in the brain of patients with disorders of consciousness. *NeuroImage Clin.* (2017) 14:354–62. doi: 10.1016/j.nicl.2017.02.002
27. Bruno MA, Nizzi MC, Laureys S, Gosseries O. The locked-in syndrome. In: Tononi G, Laureys S, Gosseries O, editors. *The Neurology of Consciousness, 2nd Edn.* New York, NY: Academic Press Elsevier (2015). p. 187–202.
28. Majerus S, Gill-Thwaites H, Andrews K, Laureys S. Behavioral evaluation of consciousness in severe brain damage. *Prog Brain Res.* (2005) 150:397–413. doi: 10.1016/S0079-6123(05)50028-1
29. Cheng L, Gosseries O, Ying L, Hu X, Yu D, Gao H, et al. Assessment of localisation to auditory stimulation in post-comatose states: use the patient's own name. *BMC Neurol.* (2013) 13:27. doi: 10.1186/1471-2377-13-27
30. Cruse D, Chennu S, Chatelle C, Bekinshtein TA, Fernández-Espejo D, Pickard JD, et al. Bedside detection of awareness in the vegetative state: a cohort study. *Lancet Lond Engl.* (2011) 378:2088–94. doi: 10.1016/S0140-6736(11)61224-5
31. Monti MM, Vanhaudenhuyse A, Coleman MR, Boly M, Pickard JD, Tshibanda L, et al. Willful modulation of brain activity in disorders of consciousness. *N Engl J Med.* (2010) 362:579–89. doi: 10.1056/NEJMoa0905370
32. Owen AM, Coleman MR, Boly M, Davis MH, Laureys S, Pickard JD. Detecting awareness in the vegetative state. *Science* (2006) 313:1402. doi: 10.1126/science.1130197
33. Gosseries O, Di H, Laureys S, Boly M. Measuring consciousness in severely damaged brains. *Annu Rev Neurosci.* (2014) 37:457–78. doi: 10.1146/annurev-neuro-062012-170339
34. Schnakers C, Bessou H, Rubi-Fessen I, Hartmann A, Fink GR, Meister I, et al. Impact of aphasia on consciousness assessment: a cross-sectional study. *Neurorehabil Neural Repair* (2015) 29:41–7. doi: 10.1177/1545968314528067
35. Laureys S, Cesia GG, Cohadon F, Lavrijsen J, León-Carrión J, Sannita WG, et al. Unresponsive wakefulness syndrome: a new name for the vegetative state or apallic syndrome. *BMC Med.* (2010) 8:68. doi: 10.1186/1741-7015-8-68
36. Bruno M-A, Vanhaudenhuyse A, Thibaut A, Moonen G, Laureys S. From unresponsive wakefulness to minimally conscious PLUS and functional locked-in syndromes: recent advances in our understanding of disorders of consciousness. *J Neurol.* (2011) 258:1373–84. doi: 10.1007/s00415-011-6114-x
37. Gosseries O, Bruno M-A, Chatelle C, Vanhaudenhuyse A, Schnakers C, Soddu A, et al. Disorders of consciousness: what's in a name? *Neurorehabilitation* (2011) 28:3–14. doi: 10.3233/NRE-2011-0625
38. Lopez-Rolon A, Vogler J, Howell K, Shock J, Czermak S, Heck S, et al. Severe disorders of consciousness after acquired brain injury: a single-centre long-term follow-up study. *NeuroRehabilitation* (2017) 40:509–17. doi: 10.3233/NRE-171438
39. Luauté J, Maucourt-Boulch D, Tell L, Quelard F, Sarraf T, Iwaz J, et al. Long-term outcomes of chronic minimally conscious and vegetative states. *Neurology* (2010) 75:246–52. doi: 10.1212/WNL.0b013e3181e8e8df
40. Thibaut A, Bruno M-A, Ledoux D, Demertzi A, Laureys S. tDCS in patients with disorders of consciousness: sham-controlled randomized double-blind study. *Neurology* (2014) 82:1112–8. doi: 10.1212/WNL.0000000000000260
41. Chatelle C, Thibaut A, Whyte J, De Val MD, Laureys S, Schnakers C. Pain issues in disorders of consciousness. *Brain Inj.* (2014) 28:1202–8. doi: 10.3109/02699052.2014.920518
42. Demertzi A, Schnakers C, Ledoux D, Chatelle C, Bruno M-A, Vanhaudenhuyse A, et al. Different beliefs about pain perception in the vegetative and minimally conscious states: a European survey of medical and paramedical professionals. *Prog Brain Res.* (2009) 177:329–38. doi: 10.1016/S0079-6123(09)17722-1
43. Demertzi A, Jox RJ, Racine E, Laureys S. A European survey on attitudes towards pain and end-of-life issues in locked-in syndrome. *Brain Inj.* (2014) 28:1209–15. doi: 10.3109/02699052.2014.920526
44. Patterson JR, Grabis M. Locked-in syndrome: a review of 139 cases. *Stroke* (1986) 17:758–64. doi: 10.1161/01.STR.17.4.758
45. Bohn Derrien L. *Je Parle: L'extraordinaire Retour à la vie D'une Locked-in Syndrome*. Paris: Editions Jean-Claude Lattès (1999).
46. Schnakers C, Majerus S, Goldman S, Boly M, Van Eeckhout P, Gay S, et al. Cognitive function in the locked-in syndrome. *J Neurol.* (2008) 255:323–30. doi: 10.1007/s00415-008-0544-0
47. Wilson BA, Hinchcliffe A, Okines T, Florschütz G, Fish J. A case study of locked-in syndrome: psychological and personal perspectives. *Brain Inj.* (2011) 25:526–38. doi: 10.3109/02699052.2011.568034
48. Plum F, Posner J. *The Diagnosis of Stupor and Coma*. Philadelphia, PA: F.A. Davis (1966).
49. Giacino JT, Ashwal S, Childs N, Cranford R, Jennett B, Katz DI, et al. The minimally conscious state: definition and diagnostic criteria. *Neurology* (2002) 58:349–53. doi: 10.1212/WNL.58.3.349



50. American Congress of Rehabilitation Medicine. Recommendations for use of uniform nomenclature pertinent to patients with severe alterations in consciousness. *Arch Phys Med Rehabil.* (1995) 76:205–9. doi: 10.1016/S0003-9993(95)80031-X
51. Laureys S, Pellas F, Van Eeckhout P, Ghorbel S, Schnakers C, Perrin F, et al. The locked-in syndrome : what is it like to be conscious but paralyzed and voiceless? *Prog Brain Res.* (2005) 150:495–511. doi: 10.1016/S0079-6123(05)50034-7
52. Bruno MA, Pellas F, Bernheim JL, Ledoux D, Goldman S, Demertzi A, et al. [Life with Locked-In syndrome]. *Rev Med Liege* (2008) 63:445–51.
53. Royal College of London. The vegetative state: guidance on diagnosis and management. *Clin Med Lond Engl.* (2003) 3:249–54.
54. Formisano R, D'Ippolito M, Riseti M, Riccio A, Caravasso CF, Catani S, et al. Vegetative state, minimally conscious state, akinetic mutism and Parkinsonism as a continuum of recovery from disorders of consciousness: an exploratory and preliminary study. *Funct Neurol.* (2011) 26:15–24.
55. Machado C, Estévez M, Carrick FR, Rodríguez R, Pérez-Nellar J, Chinchilla M, et al. Vegetative state is a pejorative term. *NeuroRehabilitation* (2012) 31:345–7. doi: 10.3233/NRE-2012-00802
56. Chatelle C, Chennu S, Noirhomme Q, Cruse D, Owen AM, Laureys S. Brain-computer interfacing in disorders of consciousness. *Brain Inj.* (2012) 26:1510–22. doi: 10.3109/02699052.2012.698362
57. Chaudhary U, Birbaumer N, Ramos-Murguialday A. Brain-computer interfaces in the completely locked-in state and chronic stroke. *Prog Brain Res.* (2016) 228:131–61. doi: 10.1016/bs.pbr.2016.04.019
58. Chaudhary U, Xia B, Silvoni S, Cohen LG, Birbaumer N. Brain-computer interface-based communication in the completely locked-in state. *PLoS Biol.* (2017) 15:e1002593. doi: 10.1371/journal.pbio.1002593
59. Lesenfants D, Habbal D, Lugo Z, Lebeau M, Horki P, Amico E, et al. An independent SSVEP-based brain-computer interface in locked-in syndrome. *J Neural Eng.* (2014) 11:035002. doi: 10.1088/1741-2560/11/3/035002
60. Trojano L, Moretta P, Estraneo A, Santoro L. Neuropsychologic assessment and cognitive rehabilitation in a patient with locked-in syndrome and left neglect. *Arch Phys Med Rehabil.* (2010) 91:498–502. doi: 10.1016/j.apmr.2009.10.033
61. Formisano R, D'Ippolito M, Catani S. Functional locked-in syndrome as recovery phase of vegetative state. *Brain Inj.* (2013) 27:1332. doi: 10.3109/02699052.2013.809555

**Conflict of Interest Statement:** The authors declare that the research was conducted in the absence of any commercial or financial relationships that could be construed as a potential conflict of interest.

Copyright © 2018 Vanhaudenhuyse, Charland-Verville, Thibaut, Chatelle, Tshibanda, Maudoux, Faymonville, Laureys and Gosseries. This is an open-access article distributed under the terms of the Creative Commons Attribution License (CC BY). The use, distribution or reproduction in other forums is permitted, provided the original author(s) and the copyright owner(s) are credited and that the original publication in this journal is cited, in accordance with accepted academic practice. No use, distribution or reproduction is permitted which does not comply with these terms.



# Cortical Brain Changes in Patients With Locked-In Syndrome Experiencing Hallucinations and Delusions

Marco Sarà<sup>1\*</sup>, Riccardo Cornia<sup>2</sup>, Massimiliano Conson<sup>3</sup>, Antonio Carolei<sup>2</sup>, Simona Sacco<sup>2</sup> and Francesca Pistoia<sup>2</sup>

<sup>1</sup> Post-Coma Intensive Rehabilitation Care Unit, San Raffaele Hospital, Cassino, Italy, <sup>2</sup> Department of Biotechnological and Applied Clinical Sciences, Neurological Institute, University of L'Aquila, L'Aquila, Italy, <sup>3</sup> Neuropsychology Laboratory, Department of Psychology, University of Campania Luigi Vanvitelli, Caserta, Italy

## OPEN ACCESS

### Edited by:

Caroline Schnakers,  
Casa Colina Centers for  
Rehabilitation, United States

### Reviewed by:

Dario Amaldi,  
Università di Genova, Italy  
Anna Estraneo,  
IRCCS Istituti Clinici Scientifici  
Maugeri (ICS Maugeri), Italy

### \*Correspondence:

Marco Sarà  
marco.sara@sanraffaele.it

### Specialty section:

This article was submitted  
to Neurotrauma,  
a section of the journal  
Frontiers in Neurology

**Received:** 29 December 2017

**Accepted:** 01 May 2018

**Published:** 17 May 2018

### Citation:

Sàrà M, Cornia R, Conson M,  
Carolei A, Sacco S and Pistoia F  
(2018) Cortical Brain Changes  
in Patients With Locked-In  
Syndrome Experiencing  
Hallucinations and Delusions.  
Front. Neurol. 9:354.  
doi: 10.3389/fneur.2018.00354

Previous evidence suggests that hallucinations and delusions may be detected in patients with the most severe forms of motor disability including locked-in syndrome (LIS). However, such phenomena are rarely described in LIS and their presence may be underestimated as a result of the severe communication impairment experienced by the patients. In this study, we retrospectively reviewed the clinical history and the neuroimaging data of a cohort of patients with LIS in order to recognize the presence of hallucinations and delusions and to correlate it with the pontine damage and the presence of any cortical volumetric changes. Ten patients with LIS were included (5 men and 5 women, mean age  $50.1 \pm 14.6$ ). According to the presence of indicators of symptoms, these patients were categorized as hallucinators ( $n = 5$ ) or non-hallucinators ( $n = 5$ ). MRI images of patients were analyzed using Freesurfer 6.0 software to evaluate volume differences between the two groups. Hallucinators showed a selective cortical volume loss involving the fusiform ( $p = 0.001$ ) and the parahippocampal ( $p = 0.0008$ ) gyrus and the orbital part of the inferior frontal gyrus ( $p = 0.001$ ) in the right hemisphere together with the lingual ( $p = 0.01$ ) and the fusiform gyrus ( $p = 0.01$ ) in the left hemisphere. Moreover, a volumetric decrease of bilateral anterior portions of the precuneus was recognized in the hallucinators (right  $p = 0.01$ ; left  $p = 0.001$ ) as compared to non-hallucinators. We suggested that the presence of hallucinations and delusions in some LIS patients could be accounted for by the combination of a damage of the corticopontocerebellar pathways with cortical changes following the primary brainstem injury. The above areas are embedded within cortico-cortical and cortico-subcortical loops involved in self-monitoring and have been related to the presence of hallucinations in other diseases. The two main limitations of our study are the small sample of included patients and the lack of a control group of healthy individuals. Further studies would be of help to expand this field of research in order to integrate existing theories about the mechanisms underlying the generation of hallucinations and delusions in neurological patients.

**Keywords:** locked-in syndrome, hallucinations, delusions, previsual, brain injury

## INTRODUCTION

False perceptions (hallucinations) and false beliefs (delusions) are mental phenomena representing the core of the symptomatology of schizophrenia. However, such symptoms are also frequently observed in persons with brain damage (1–3), but only rarely detected in patients with severe acquired brain injury, including those with locked-in syndrome (LIS) (4, 5). LIS is the result of a complete interruption of corticospinal, corticobulbar, and corticocerebellar pathways as a consequence of specific pontine damage usually resulting from a stenosis of the basilar artery. Patients with LIS are fully conscious but show quadriplegia, bilateral facial palsy, and anarthria. Vertical gaze and blinking are the only preserved movements and patients learn to communicate with the environment through eye-coded strategies. In the light of the above-reported damage, it might be expected that patients with LIS would have only symptoms pertaining to the motor domain. In reality, they can show additional symptoms, including emotional dysfunctions and motor imagery impairments, the pathophysiology of which is still a matter of debate (6–11). Moreover, when investigated using advanced techniques for cortical volumetric analyses, some patients show specific patterns of volumetric cortical changes beyond the initial brainstem damage (12, 13). Among non-motor symptoms, hallucinations and delusions are rarely described in LIS and their presence may be underestimated as a result of the extremely limited communication channel. In addition, patients with LIS, who are completely dependent on others for all their needs, may be reticent about sharing these experiences with the health-care professionals, even if they feel distressed about them.

In this study, we retrospectively reviewed the clinical history and the neuroimaging data of a cohort of patients with LIS in order to detect whether hallucinations and delusions were correlated to specific patterns of brain atrophy.

## MATERIALS AND METHODS

### Participants

Data came from patients admitted to the Post-Coma Rehabilitative Care Unit of the San Raffaele Hospital, Cassino (Italy) in the past 10 years. Patients were only included in the study if they had a diagnosis of LIS, their clinical history had been documented in detail through medical records, and if they had been scanned using a 1.5 T MRI (Espree, Siemens AG, Erlangen) during their hospital stay. Patients with a previous history of severe neurological or psychiatric disease were excluded as well as patients treated with central nervous system active drugs. For the included patients, all clinical and neuroradiological data were retrospectively scanned. The research protocol was approved by the Internal Review Board of the University of L'Aquila (20/2017) and the study was carried out in accordance with its recommendations.

### Assessment of Clinical Data

All the clinical data of the included patients were reviewed in order to (1) identify the main biographical data and clinical characteristics of the subjects; (2) classify patients according to

the Bauer classification of LIS (14); (3) categorize them into two groups based on the presence or not of hallucinations or delusions recorded in their clinical history following the brainstem damage. The Bauer classification distinguishes between a “pure” form (where the only remaining voluntary motion is vertical eye movements and blinking), an “incomplete” form (where some voluntary motor action other than eye movements is preserved) or a “total” form (complete loss of any motor output, including eye movements) (14). During the stay in the rehabilitation ward, clinical information had been collected by asking caregivers and by communicating directly with the patients using a coded communication system based on blinking and vertical eye movements. Through these movements, patients were asked to reply to closed questions (yes/no) about the presence of positive symptoms. Hallucinations were defined as the perception of visual, auditory, tactile, or olfactory stimuli in the ascertained absence of real external stimuli. Motor hallucinations were defined as an imaginary perception of a movement (for instance of a limb) in the absence of a real body movement. Delusions were defined as false beliefs based on erroneous inference about external reality that were firmly maintained by the patient despite what almost everyone else believed and despite incontestable and obvious evidence to the contrary. The presence of hallucinations was investigated through standardized screening questions in each sensory modality (15). The occurrence of delusions was mainly inferred by the reports of caregivers and further investigated through standardized screening questions (15).

In the case of positive responses to screening questions, patients were asked to better explain their experiences by using a spelling system of communication based on the selection of letters on an alphabet board through eye blinking. This allowed us to be sure about the initial detection of hallucinations and delusions and to obtain more details about individual experiences. Patients were interviewed once a week during their stay in the rehabilitation ward and considered to have had a history of hallucinations or delusions when symptoms had occurred at least once a month. The cognitive status of the patients was also documented during their stay in rehabilitation by means of the Raven's Colored Progressive Matrices (RCPM) (16).

### Volumetric Analysis of Neuroradiological Data

As specified above, patients were only included in the study if they had undergone a 1.5 T MRI acquisition (Espree, Siemens AG, Erlangen) with a standard 8-channel birdcage head coil. Two images had been acquired for each participant and each time point. The first was a high-resolution T1-weighted image (two times), acquired using a magnetization prepared rapid acquisition gradient echo sequence (repetition time 1,590 ms; echo time 2.4 ms; flip angle 0°; matrix size 192 × 192; number of slices 160; voxel size 1 mm × 1 mm × 1 mm). The second was a T2-weighted image using a fluid attenuated inversion recovery sequence (repetition time 9,000 ms; echo time 88 ms; flip angle 0°; matrix size 384 × 512; number of slices 44).

Collected MRI images were processed and analyzed using the Freesurfer image analysis suite v 6.0 software, which is innovative

software freely available online (<http://surfer.nmr.mgh.harvard.edu/>). Its functioning is based on an inflation algorithm, which allows to inflate the brain in order to minimize the metric distortions that can occur in structural analyses due to the natural presence of depressions and grooves in the brain. Inflation is followed by registration to a spherical atlas, parcellation of the cerebral cortex, and creation of a variety of surface based data. In the present study, for each participant, mean cortical volume values of 34 brain regions, according to Desikan parcellation (17), were calculated for both the hemispheres as the average of two values, the minimal distance from gray/white matter boundary and pial surface and *vice versa*. Each participant's brain was morphed and registered to an average spherical surface that finely aligns sulci and gyri across them. Cortical volume values were then mapped onto this average inflated surface, thus avoiding interference of cortical folding on the visualization. Statistical maps were generated using FreeSurfer's Query, Design, Estimate, Contrast (QDEC) interface. For each hemisphere, a general linear model of the effect of age on cortical volumes was evaluated at each vertex for male and female groups. Spatial smoothing with an isotropic kernel (FWHM = 10 mm) was applied. Data were deemed statistically significant if  $p < 0.05$ . False discovery rate (FDR) was corrected and tables of cluster size and location were generated.

## Additional Statistical Analysis

To confirm the results of QDEC, the mean volume of selected regions of interest was extracted for each participant and data were analyzed using the IBM SPSS Statistics 20 Software. An independent *t*-test and an analysis of covariance were used to compare the cortical volume of main areas between the two clinical groups. Correction for multiple comparisons was carried out using the Benjamin–Hochberg FDR correction in the selected areas. ANOVA was applied to evaluate the effects of the main biographical and clinical factors. For comparison between groups, the level of significance was fixed at  $p < 0.05$ .

## RESULTS

Ten patients with a diagnosis of LIS were included in the study (5 men and 5 women, mean age  $50.1 \pm 14.6$ ). The ventral pontine damage was a consequence of a vascular injury in nine cases and of a traumatic injury in one case. All included patients had a pure form according to the traditional classification of LIS (14). Patients did not have any previous recorded history of psychiatric symptoms and cognitive dysfunction or any additional cortical or subcortical lesions beyond the pontine damage. At the time of the interviews, all RCPM scores were within normal range after adjustment for age and education according to Italian normative studies [cutoff = 18; (16)]. A recorded history of hallucinations or delusions following the pontine damage was found for 5 of the 10 patients in the study (4 males and 1 female). Of these, a combination of visual and motor phenomena was reported in four patients, while in the fifth a history of auditory hallucinations combined with a delusional thought disorder was inferred. There were no reports of olfactory or tactile hallucinations. The median time to onset of positive symptoms was 1 month

from the initial injury, with a median duration of symptoms of 4 months. As regards the content of hallucinations, most of the patients reported visual hallucinations consisting of objects or individuals, who were moving in the room wards. As regards motor hallucinations, patients were asked to describe whether they have had any unusual feelings on their own body, and most of them reported imaginary perceptions of limbs movement, which were out of their control. Finally, the delusional thought disorder, which was recognized in one patient only, was classified as a jealous delusional disorder.

Anagraphic and clinical data of the two groups are reported in **Table 1**: the two groups were not matched by sex (non-hallucinators = 4 females; hallucinators = 1 females), but they did not differ with respect to age (non-hallucinators: mean = 43.2, SD = 17.1; hallucinators: mean = 57, SD = 8.2;  $t = -1.626$ ,  $p > 0.05$ ), education (non-hallucinators: mean = 12.6, SD = 4.5; hallucinators: mean = 12.4, SD = 3.2;  $t = 0.81$ ,  $p > 0.05$ ), time from injury (non-hallucinators: mean = 37, SD = 8.4; hallucinators: mean = 44, SD = 1.25;  $t = -0.904$ ,  $p > 0.05$ ), and general cognitive functioning (non-hallucinators: mean = 24.4, SD = 1.8; hallucinators: mean = 23.8, SD = 1.9;  $t = 0.507$ ,  $p > 0.05$ ). Moreover, the two groups were comparable with respect to their basic MRI neuroimaging findings, as none of them showed co-existing supratentorial lesions and all had the brainstem injury, which is traditionally associated with LIS. On the contrary, the advanced volumetric analysis showed the presence of cortical differences between the two groups. The FreeSurfer cluster values are shown in the **Table 2**. Specifically, patients experiencing hallucinations showed a larger atrophy with respect to patients not experiencing hallucinations/delusions in the fusiform gyrus ( $p = 0.001$ ), the parahippocampal gyrus ( $p = 0.0008$ ), and the orbital part of the inferior frontal gyrus ( $p = 0.001$ ) in the right hemisphere together with the lingual ( $p = 0.01$ ) and the fusiform gyrus ( $p = 0.01$ ) in the left hemisphere. On the other hand, patients not experiencing hallucinations/delusions showed a larger atrophy in the insula and the lateral orbitofrontal cortex bilaterally ( $p \leq 0.001$  and  $p \leq 0.0045$ ), in the left medial orbitofrontal cortex ( $p = 0.01$ ), in the right middle frontal and temporal regions ( $p \leq 0.002$ ), and in the right pars opercularis ( $p = 0.01$ ). Moreover, the precuneus showed a volumetric decrease of bilateral anterior portions in hallucinators (right  $p = 0.01$ ; left  $p = 0.001$ ) and a volumetric decrease of bilateral posterior portions in non-hallucinators (right  $p = 0.02$ ; left  $p = 0.0005$ ).

Finally, a common feature of the recognized positive phenomena was their tendency to improve when the patients were repeatedly informed about the illusory nature of their perceptions. The symptoms spontaneously improved in all the subjects with the exception of the patient experiencing a combination of hallucinations and thought delusions. In this patient, a therapy with antipsychotic drugs was required for symptoms improvement.

## DISCUSSION

Our findings demonstrated the presence of hallucinations/delusions in a subgroup of patients with LIS, who showed a larger atrophy in a set of brain areas as compared to LIS patients not experiencing hallucinations/delusions. Such cortical volumetric

**TABLE 1** | Demographic and clinical characteristics of patients.

Patients	Sex	Age at admission	Education (years)	Cause	Time from injury to admission (days)	Localization of the brainstem lesion	RCPM (raw score)	Positive symptoms
1	F	31	8	TBI	50	Pons-midbrain	25	Absent
2	F	37	17	Stroke	30	Pons	26	Absent
3	F	26	13	Stroke	40	Pons	26	Absent
4	F	56	8	Stroke	30	Pons	22	Absent
5	M	66	17	Stroke	35	Pons	23	Absent
6	M	43	17	Stroke	60	Pons-midbrain	27	Auditory hallucinations and thought delusions
7	M	62	8	Stroke	40	Pons	24	Visual/motor hallucinations
8	F	59	13	Stroke	60	Pons-medulla oblongata	22	Visual/motor hallucinations
9	M	57	13	Stroke	30	Pons	23	Visual/motor hallucinations
10	M	64	12	Stroke	30	Pons	23	Visual/motor hallucinations

All scores were within normal range on RCPM after adjustment for age and education according to Italian normative studies [cutoff = 18; (16)].

TBI: traumatic brain injury; RCPM, Raven's colored progressive matrices.

**TABLE 2** | Cluster values in FS Query, Design, Estimate, Contrast analysis, FWHM = 10, threshold of 1.31.

Cluster	Brain region	Hemisphere	Talaraich coordinates			Size	p-Value	
			X	Y	Z			
1	Insula	Left	-36.9	1.8	-5.3	864.6	0.0001	No hall < hall
2	Precuneus	Left	-6.1	-70.7	44.4	140.39	0.0005	No hall < hall
3	Paracentral	Left	-11.6	-39.3	58	102.07	0.0006	No hall < hall
4	Precentral	Left	-50.2	2	29.8	106.08	0.0009	No hall < hall
5	Precuneus	Left	-13.7	-46	49	178.86	0.0011	Hall < no hall
6	Medial orbitofrontal	Left	-6.2	20.8	20.5	151.12	0.0038	No hall < hall
7	Lateral orbitofrontal	Left	-23.5	12.5	-19.2	167.84	0.0045	No hall < hall
8	Superior parietal	Left	-15	-72.1	46.8	138.65	0.0086	No hall < hall
9	Medial orbitofrontal	Left	-7.3	41.5	-17.7	134.73	0.01	No hall < hall
10	Lateral occipital	Left	-42.6	-73.7	-9	104.94	0.0104	No hall < hall
11	Lingual	Left	-15	-66	-3.7	171.59	0.0157	Hall < no hall
12	Fusiform	Left	-32.6	-34.8	-23.1	104.11	0.017	Hall < no hall
13	Parahippocampal	Right	36.5	-38.2	-11.9	330.83	0.0008	Hall < no hall
14	Insula	Right	29.7	14.5	-12.3	103.91	0.001	No hall < hall
15	Lateral orbitofrontal	Right	18.2	13.6	-21.8	132.32	0.0011	No hall < hall
16	Pars orbitalis	Right	41.1	49.6	-7	530.71	0.0011	Hall < no hall
17	Middle-temporal	Right	54.7	-9.9	-26.3	109.93	0.0012	No hall < hall
18	Fusiform	Right	32.7	64.5	-15	653.95	0.0018	Hall < no hall
19	Caudal middle frontal	Right	38.2	7.8	44	154.3	0.0021	No hall < hall
20	Precuneus	Right	15.4	-47.2	33.3	107.71	0.0166	Hall < no hall
21	Pars opercularis	Right	34.8	15	12.7	175.54	0.0184	No hall < hall
22	Precuneus	Right	18.4	-69.9	34.9	174.11	0.0204	No hall < hall

changes do not amount to a macroscopic cortical atrophy, which is generally not a feature of LIS, but refer to subtle cortical differences, which are recognizable only by means of advanced brain volumetric analysis techniques.

The strength of our study lies with the investigation of a cognitive phenomenon, which seems to be largely underestimated in patients with LIS. In our opinion, there are several reasons for the lack of consistent descriptions of positive symptoms in LIS. First, there is the traditional view that patients with an isolated pontine lesion show motor symptoms exclusively, and cannot suffer from cognitive dysfunctions unless wide additional cortical damage occurs. Second, there are the well-known difficulties experienced by caregivers and health-care professionals in establishing a communication channel with the patients. When communication is attempted, it is commonly used to investigate the most basic needs of the patients, while exploring more complex matters such

as subjective mental experiences remains challenging. Finally, patients may have some reticence about sharing these symptoms as a consequence of the severe disability, which makes them completely dependent on others.

The main limitation of our study lies with the small number of patients included. As LIS is a very rare condition, 10 patients are considered a good size of sample to describe symptoms, which have not yet been systematically investigated. However, the above sample is far too small to shed lights on the existence of a causal relationship between subtle cortical changes and the presence of hallucinations/delusions in patients with LIS, thus prompting caution in drawing conclusions about the possible mechanism underlying this phenomenon.

Nevertheless, cortical changes in patients with LIS, experiencing hallucinations and delusions, involved areas, which have been previously linked to the presence of these symptoms



[e.g., Ref. (1)]. Specifically, our results showed a reduced cortical volume in the fusiform and lingual regions, and in the right parahippocampal cortex, of LIS patients with positive signs. This fits with many literature findings stressing the role of both ventrolateral (fusiform) and ventromedial (lingual and parahippocampal) regions of the occipito-temporal cortex in both visual hallucinations and delusions. More in detail, the fusiform area, which is a key region of the occipito-temporal ventral visual stream, plays a pivotal role in visuoperceptual processing. Much evidence demonstrated the activation of the fusiform and lingual gyri during the recognition of objects and faces and highlighted the role of brain lesions involving this area (in particular in the right hemisphere) in neuropsychological disturbances of visual processing, such as visual agnosia and prosopagnosia [e.g., Ref. (18)]. Classical evidence on the visual processing of faces and objects has also demonstrated the involvement of the parahippocampal cortex (19, 20). Moreover, ventral visual stream areas, together with the parahippocampal region, are implicated in psychotic symptoms, both hallucinations and delusions, in patients with Alzheimer's disease (21).

When compared with LIS non-experiencing productive phenomena, hallucinators also showed a cortical atrophy in the orbital part of the inferior frontal gyrus. Neurocognitive models of visual hallucinations have highlighted the role of a pathological interaction between defective visual brain areas and altered cortical control from prefrontal areas (22, 23). For instance, recent findings converged in demonstrating that a pattern of gray matter atrophy involving both posterior and frontal areas is implied in delusional development in patients with Alzheimer's disease and frontotemporal dementia (24–26). On this basis, we could suggest that, in LIS patients experiencing hallucinations/delusions, a bottom-up impairment due to alterations in posterior areas would not be effectively modulated by top-down processes in prefrontal cortex. The consequence of this would be an impaired self-monitoring, leading individuals to experience their own internal mental contents as vivid external percepts (22, 27, 28).

Patients with LIS also experienced frequent positive motor phenomena mainly represented by the perception of a limb movement in the absence of a real movement. This is consistent with literature findings showing motor awareness abnormalities as a result of various forms of brain damage (29). Here, we might speculate that the interruption of the corticocerebellar pathways, combined with cortical alterations in prefrontal cortex could have impaired the capacity to provide the system with up-to-date information about actual motor abilities (30). The co-existence of

these two factors may have led to perceptions of movement where no actual movement has occurred.

Finally, alternative explanations may be proposed for the patients showing a lesion also involving the midbrain: this kind of damage has been previously reported to be associated with the development of peduncular hallucinosis and psychosis, whose pathogenesis is still debated (31, 32). All these observations suggest that the presence of hallucinations and delusions in some LIS patients can be accounted for by the combination of a damage of the corticopontocerebellar pathways with cortical changes following the primary brainstem injury. This would confirm the notion that hallucinations belong to those symptoms which arise from the pathological involvement of different structures functionally connected each other rather than being the result of the dysfunction of a single region (33).

Moreover, it is important to stress here that non-hallucinators, as compared to hallucinators, also showed signs of atrophy in a large set of anterior and posterior cortical areas. At present, we are not able to provide any tentative explanation accounting for this finding: future studies, also involving a healthy control group, are needed to precisely define the nature of cortical changes in LIS patients with and without positive symptoms.

Finally, a specific feature of the recognized hallucinations in patients with LIS is their tendency to improve when patients are repeatedly informed by health care professionals or caregivers about the illusory nature of their experiences. Compared with patients who have psychotic illnesses, patients with LIS show a greater insight about their experiences, making hallucinations and delusions more likely to diminish in response to specific management of these symptoms, as the presence of insight improves treatment compliance (34).

Further studies would be of help to expand this field of research in order to integrate existing theories about the mechanisms underlying the generation of hallucinations and delusions in neurological patients.

## ETHICS STATEMENT

The research protocol was approved by the Internal Review Board of the University of L'Aquila (number of approval: 20/2017) and the study was carried out in accordance with its recommendations.

## AUTHOR CONTRIBUTIONS

All authors contributed to the conception of the work, to data acquisition, analysis, and interpretation and to the drafting of the paper.

## REFERENCES

- Coltheart M, Langdon R, McKay R. Delusional belief. *Annu Rev Psychol* (2011) 62:271–98. doi:10.1146/annurev.psych.121208.131622
- Fletcher PC, Frith CD. Perceiving is believing: a Bayesian approach to explaining the positive symptoms of schizophrenia. *Nat Rev Neurosci* (2009) 10:48–58. doi:10.1038/nrn2536
- Frith C. The neural basis of hallucinations and delusions. *C R Biol* (2005) 328:169–75. doi:10.1016/j.crv.2004.10.012
- Hamilton J. Auditory hallucinations in nonverbal quadriplegics. *Psychiatry* (1985) 48:382–92. doi:10.1080/00332747.1985.11024299
- Gopal M, Parasram M, Patel H, Ilorah C, Nersesyan H. Acute psychosis as main manifestation of central pontine myelinolysis. *Case Rep Neurol Med* (2017) 2017:1471096. doi:10.1155/2017/1471096
- Pistoia F, Conson M, Trojano L, Grossi D, Ponari M, Colonnese C, et al. Impaired conscious recognition of negative facial expressions in patients with locked-in syndrome. *J Neurosci* (2010) 30:7838–44. doi:10.1523/JNEUROSCI.6300-09.2010



7. Conson M, Sacco S, Sarà M, Pistoia F, Grossi D, Trojano L. Selective motor imagery defect in patients with locked-in syndrome. *Neuropsychologia* (2008) 46:2622–8. doi:10.1016/j.neuropsychologia.2008.04.015
8. Sacco S, Sarà M, Pistoia F, Conson M, Albertini G, Carolei A. Management of pathologic laughter and crying in patients with locked-in syndrome: a report of 4 cases. *Arch Phys Med Rehabil* (2008) 89:775–8. doi:10.1016/j.apmr.2007.09.032
9. Conson M, Sarà M, Pistoia F, Trojano L. Action observation improves motor imagery: specific interactions between simulative processes. *Exp Brain Res* (2009) 199:71–81. doi:10.1007/s00221-009-1974-3
10. Conson M, Pistoia F, Sarà M, Grossi D, Trojano L. Recognition and mental manipulation of body parts dissociate in locked-in syndrome. *Brain Cogn* (2010) 73:189–93. doi:10.1016/j.bandc.2010.05.001
11. Babiloni C, Pistoia F, Sarà M, Vecchio F, Buffo P, Conson M, et al. Resting state eyes-closed cortical rhythms in patients with locked-in syndrome: an EEG study. *Clin Neurophysiol* (2010) 121:1816–24. doi:10.1016/j.clinph.2010.04.027
12. Pistoia F, Cornia R, Conson M, Gosseries O, Carolei A, Sacco S, et al. Disembodied mind: cortical changes following brainstem injury in patients with locked-in syndrome. *Open Neuroimag J* (2016) 10:32–40. doi:10.2174/1874440001610010032
13. Pistoia F, Carolei A, Sacco S, Sarà M. Commentary: Embodied medicine: Mens Sana in Corpore Virtuale Sano. *Front Hum Neurosci* (2017) 21(11):381. doi:10.3389/fnhum.2017.00381
14. Bauer G, Gerstenbrand F, Rimpl E. Varieties of the locked-in syndrome. *J Neurol* (1979) 221:77–91. doi:10.1007/BF00313105
15. Willer J. *The Beginning Psychotherapist's Companion*. USA: Oxford University Press (2013).
16. Basso A, Capitani E, Laiacina M. Raven's coloured progressive matrices: normative values on 305 adult normal controls. *Funct Neurol* (1987) 2:189–94.
17. Desikan RS, Ségonne F, Fischl B, Quinn BT, Dickerson BC, Blacker D, et al. An automated labeling system for subdividing the human cerebral cortex on MRI scans into gyral based regions of interest. *Neuroimage* (2006) 31:968–80. doi:10.1016/j.neuroimage.2006.01.021
18. Gainotti G, Marra C. Differential contribution of right and left temporo-occipital and anterior temporal lesions to face recognition disorders. *Front Hum Neurosci* (2011) 5:55. doi:10.3389/fnhum.2011.00055
19. Feinberg TE, Schindler RJ, Ochoa E, Kwan PC, Farah MJ. Associative visual agnosia and alexia without prosopagnosia. *Cortex* (1994) 30:395–411. doi:10.1016/S0010-9452(13)80337-1
20. Sergent J, Ohta S, MacDonald B. Functional neuroanatomy of face and object processing. A positron emission tomography study. *Brain* (1992) 115(Pt 1): 15–36. doi:10.1093/brain/115.1.15
21. McLachlan E, Bousfield J, Howard R, Reeves S. Reduced parahippocampal volume and psychosis symptoms in Alzheimer's disease. *Int J Geriatr Psychiatry* (2018) 33:389–95. doi:10.1002/gps.4757
22. Allen P, Laroi F, McGuire PK, Aleman A. The hallucinating brain: a review of structural and functional neuroimaging studies of hallucinations. *Neurosci Biobehav Rev* (2008) 32:175–91. doi:10.1016/j.neubiorev.2007.07.012
23. Ffytche DH, Howard RJ. The perceptual consequences of visual loss: 'positive' pathologies of vision. *Brain* (1999) 122:1247–60. doi:10.1093/brain/122.7.1247
24. Fischer CE, Ting WK, Millikin CP, Ismail Z, Schweizer TA; Alzheimer Disease Neuroimaging Initiative. Gray matter atrophy in patients with mild cognitive impairment/Alzheimer's disease over the course of developing delusions. *Int J Geriatr Psychiatry* (2016) 31:76–82. doi:10.1002/gps.4291
25. Nomura K, Kazui H, Wada T, Sugiyama H, Yamamoto D, Yoshiyama K, et al. Classification of delusions in Alzheimer's disease and their neural correlates. *Psychogeriatrics* (2012) 12:200–10. doi:10.1111/j.1479-8301.2012.00427.x
26. Shinagawa S, Naasan G, Karydas AM, Coppola G, Pribadi M, Seeley WW, et al. Clinicopathological study of patients with C9ORF72-associated frontotemporal dementia presenting with delusions. *J Geriatr Psychiatry Neurol* (2015) 28:99–107. doi:10.1177/0891988714554710
27. Blakemore SJ, Smith J, Steel R, Johnstone CE, Frith CD. The perception of self-produced sensory stimuli in patients with auditory hallucinations and passivity experiences: evidence for a breakdown in self-monitoring. *Psychol Med* (2000) 30:1131–9. doi:10.1017/S0033291799002676
28. Zmigrod L, Garrison JR, Carr J, Simons JS. The neural mechanisms of hallucinations: a quantitative meta-analysis of neuroimaging studies. *Neurosci Biobehav Rev* (2016) 69:113–23. doi:10.1016/j.neubiorev.2016.05.037
29. Frith CD, Blakemore SJ, Wolpert DM. Abnormalities in the awareness and control of action. *Philos Trans R Soc Lond B Biol Sci* (2000) 355:1771–88. doi:10.1098/rstb.2000.0734
30. Moro V, Pernigo S, Tsakiris M, Avesani R, Edelstyn NM, Jenkinson PM, et al. Motor versus body awareness: voxel-based lesion analysis in anosognosia for hemiplegia and somatoparaphrenia following right hemisphere stroke. *Cortex* (2016) 83:62–77. doi:10.1016/j.cortex.2016.07.001
31. Andrews JP, Taylor J, Saunders D, Qayyum Z. Peduncular psychosis. *BMJ Case Rep* (2016). doi:10.1136/bcr-2016-216165
32. Dogan VB, Dirican A, Koksak A, Baybas S. A case of peduncular hallucinosis presenting as a primary psychiatric disorder. *Ann Indian Acad Neurol* (2013) 16:684–6. doi:10.4103/0972-2327.120469
33. Boes AD, Prasad S, Liu H, Liu Q, Pascual-Leone A, Caviness VS Jr, et al. Network localization of neurological symptoms from focal brain lesions. *Brain* (2015) 138:3061–75. doi:10.1093/brain/awv228
34. Lera G, Herrero N, González J, Aguilar E, Sanjuán J, Leal C. Insight among psychotic patients with auditory hallucinations. *J Clin Psychol* (2011) 67:701–8. doi:10.1002/jclp.20799

**Conflict of Interest Statement:** The authors declare that the research was conducted in the absence of any commercial or financial relationships that could be construed as a potential conflict of interest.

Copyright © 2018 Sarà, Cornia, Conson, Carolei, Sacco and Pistoia. This is an open-access article distributed under the terms of the Creative Commons Attribution License (CC BY). The use, distribution or reproduction in other forums is permitted, provided the original author(s) and the copyright owner are credited and that the original publication in this journal is cited, in accordance with accepted academic practice. No use, distribution or reproduction is permitted which does not comply with these terms.



# Brain, Behavior, and Cognitive Interplay in Disorders of Consciousness: A Multiple Case Study

Charlène Aubinet<sup>1\*</sup>, Lesley Murphy<sup>2</sup>, Mohamed A. Bahri<sup>3</sup>, Stephen K. Larroque<sup>1</sup>, Helena Cassol<sup>1</sup>, Jitka Annen<sup>1</sup>, Manon Carrière<sup>1</sup>, Sarah Wannez<sup>1</sup>, Aurore Thibaut<sup>1</sup>, Steven Laureys<sup>1</sup> and Olivia Gosseries<sup>1</sup>

<sup>1</sup> Coma Science Group, GIGA Consciousness and Neurology Department, University and University Hospital of Liège, Liège, Belgium, <sup>2</sup> Department for Neuro and Clinical Health Psychology, St George's University Hospital, London, United Kingdom, <sup>3</sup> GIGA-Cyclotron Research Center in Vivo Imaging, University of Liège, Liège, Belgium

## OPEN ACCESS

### Edited by:

Freimut Dankwart Juengling,  
St. Claraspital Basel, Switzerland

### Reviewed by:

Konstantinos Kalafatakis,  
University of Bristol, United Kingdom  
Roland Wiest,  
Universität Bern, Switzerland

### \*Correspondence:

Charlène Aubinet  
caubinet@uliege.be

### Specialty section:

This article was submitted to  
Applied Neuroimaging,  
a section of the journal  
Frontiers in Neurology

**Received:** 08 February 2018

**Accepted:** 25 July 2018

**Published:** 14 August 2018

### Citation:

Aubinet C, Murphy L, Bahri MA, Larroque SK, Cassol H, Annen J, Carrière M, Wannez S, Thibaut A, Laureys S and Gosseries O (2018) Brain, Behavior, and Cognitive Interplay in Disorders of Consciousness: A Multiple Case Study. *Front. Neurol.* 9:665. doi: 10.3389/fneur.2018.00665

Patients with prolonged disorders of consciousness (DoC) after severe brain injury may present residual behavioral and cognitive functions. Yet the bedside assessment of these functions is compromised by patients' multiple impairments. Standardized behavioral scales such as the *Coma Recovery Scale-Revised* (CRS-R) have been developed to diagnose DoC, but there is also a need for neuropsychological measurement in these patients. The *Cognitive Assessment by Visual Election* (CAVE) was therefore recently created. In this study, we describe five patients in minimally conscious state (MCS) or emerging from the MCS (EMCS). Their cognitive profiles, derived from the CRS-R and CAVE, are presented alongside their neuroimaging results using structural magnetic resonance imaging (MRI) and fluorodeoxyglucose positron emission tomography (FDG-PET). Scores on the CAVE decreased along with the CRS-R total score, establishing a consistent behavioral/cognitive profile for each patient. Out of these five cases, the one with highest CRS-R and CAVE performance had the least extended cerebral hypometabolism. All patients showed structural and functional brain impairments that were consistent with their behavioral/cognitive profile as based on previous literature. For instance, the presence of visual and motor residual functions was respectively associated with a relative preservation of occipital and motor cortex/cerebellum metabolism. Moreover, residual language comprehension skills were found in the presence of preserved temporal and angular cortex metabolism. Some patients also presented structural impairment of hippocampus, suggesting the presence of memory impairments. Our results suggest that brain-behavior relationships might be observed even in severely brain-injured patients and they highlight the importance of developing new tools to assess residual cognition and language in MCS and EMCS patients. Indeed, a better characterization of their cognitive profile will be helpful in preparation of rehabilitation programs and daily routines.

**Keywords:** (emergence from) minimally conscious state, behavior, cognitive functions, neuropsychological assessment, positron emission tomography, structural magnetic resonance imaging, neural correlates

## INTRODUCTION

After an acquired severe brain injury, patients generally go through a succession of altered states of consciousness: coma, unresponsive wakefulness syndrome (i.e., vegetative state—eye opening without signs of awareness) (1), minimally conscious state (MCS), and then emergence from the minimally conscious state (EMCS), when they are able to functionally communicate or use objects (2). Patients in a MCS have further been subcategorized in MCS *minus*, whose most frequent signs of consciousness are visual fixation and pursuit, automatic oriented motor reactions and localization to noxious stimulation (3), and in MCS *plus* patients who can also follow simple commands, intelligibly verbalize or intentionally communicate (4).

Previous literature has shown the importance of accurate diagnosis in DoC patients regarding daily management (i.e., pain treatment or stimulation protocols), end-of-life decisions and prognosis (5–7). Nevertheless, accurate diagnosis is challenging (8–13), with assessment being compromised by patients' multiple impairments, in particular motor skills and fluctuating arousal level (10, 11), as well as aphasia (14, 15) and impaired visual abilities (8). Several behavioral scales have been developed to assess patients' level of consciousness. Among them, the *Coma Recovery Scale-Revised* (CRS-R) (16) is currently considered the most sensitive validated diagnostic tool (17). There is still, however, a lack of standardized neuropsychological tests dedicated to the assessment of a wider range of cognitive functions in DoC patients. Indeed, although the CRS-R allows to precisely diagnose their levels of consciousness, patients' cognitive and language deficits cannot be specifically appreciated. Consequently, a new measure was recently developed on the grounds of clinical work: the *Cognitive Assessment by Visual Election* (CAVE) [(18); Murphy, unpublished thesis]. This assessment is based on the ability to understand language at a basic level and to visually fixate objects.

Due to the difficulty to behaviorally objectify signs of consciousness and cognition in this group of severely brain-injured patients, diverse neuroimaging techniques have been developed (19). A negative correlation was found between structural damage and the level of consciousness using voxel-based morphometry (VBM). The duration of a DoC has also been associated with larger brain lesions (20). Regarding functional brain imaging, active paradigms require preserved language functions and the ability to follow verbal commands, thus passive and resting state paradigms are more commonly used, either with positron emission tomography (PET) or magnetic resonance imaging (MRI) (21). Using fluorodeoxyglucose (FDG) PET, previous studies showed an association between consciousness recovery and the restoration of cerebral activity within a large frontoparietal network, comprised of two (internal and external) networks (22). The internal default mode network (DMN) encompasses the precuneus/posterior cingulate cortex, mesiofrontal/anterior cingulate cortex as well as the temporo-parietal junction, and is mainly dedicated to internal perception and self-awareness (23–25). The external lateral frontoparietal network is involved in executive control, external perception and environment awareness (22, 26). Finally, recent studies

have shown that diverse neuroimaging and neurophysiology techniques tend to lead to compatible and consensual brain data in unresponsive and MCS patients (27–29), suggesting that it would be of benefit to combine these techniques to diagnose the DoC.

The presence of residual language and cognitive functions in DoC patients has been suggested by previous neuroimaging and electrophysiology studies (30–36). For example, residual cortical activity related to language processing was shown in two MCS patients, by comparing functional connectivity after listening to intelligible and unintelligible speech (37). To remedy the lack of cognitive behavioral measurement, Sergent and colleagues (38) used electroencephalography (EEG) and showed the advantages of a multidimensional cognitive evaluation based on low-level functions (i.e., own name recognition, temporal attention, spatial attention, detection of spatial incongruence and motor planning) and higher-level functions (i.e., modulations of previous effects by the global context) in detecting residual cognitive abilities in DoC patients.

In the present paper, we aim to study the behavioral and cognitive profile of five different patients in MCS and EMCS. Performance on the CRS-R and the CAVE were compared with their neuroimaging results using FDG-PET and structural MRI. By presenting these multiple cases, the importance of the development of new assessment tools such as the CAVE to refine the cognitive profile of MCS and EMCS patients, is emphasized. Specifically, it is hypothesized that there is an association between patients' structural and functional brain damage and their behavioral/cognitive profile, consistent with previous studies establishing neural correlates of behavior, language and cognition.

## MATERIALS AND METHODS

This prospective study includes five patients who were consecutively recruited at the University Hospital of Liège. All patients completed a battery of behavioral tests and neuroimaging assessments during a one-week hospitalization, based on clinical demand. Patients with absence of visual pursuit or visual evoked potentials (as observed by an experimented ophthalmologist) were excluded, as some functional vision is required to perform the CAVE. The control group consisted of 58 healthy subjects as controls for FDG-PET (34/58) and MRI data (36/58). The study was approved by the Ethics Committee of the Faculty of Medicine of the University of Liege and written informed consents, including for publication of data, were obtained from the patients' legal representatives and from the healthy control subjects.

### Bedside Behavioral Assessments Coma Recovery Scale-Revised (CRS-R)

The CRS-R was used for clinical diagnosis. This scale includes 23 items divided in 6 sub-scales: auditory, visual, motor, oro-motor/verbal, communication, and arousal, each assessing different items of increasing complexity (16). Some of the items are diagnostic criteria for MCS (e.g., visual pursuit, automatic oriented motor reactions, or response to command) and EMCS

(i.e., functional communication and/or use of objects), and the total score ranges from 0 to 23. Following the most recent guidelines to reduce misdiagnosis (39), at least five clinical assessments within a short time interval (i.e., 1 week) were conducted. The highest CRS-R score and diagnostic category of the week was retained for final diagnosis.

### Cognitive Assessment by Visual Election (CAVE)

The CAVE includes 6 sub-tests to evaluate the recognition of real objects, numbers, written words, letters, pictures, and colors (18). Each of these sub-tests contains 10 items (**Supplementary Material I**), with a cut-off score of 8/10 based on binomial distribution. A target object is presented simultaneously with a distractor (e.g., a pen on the left and a fork on the right visual field) and the patient is asked to look at the target (e.g., “look at the pen”). As this test requires at least the preservation of visual fixation, this tool is dedicated to MCS *minus*, MCS *plus*, and EMCS patients. It usually takes between 10 and 30 min to administer, depending on the ability to objectify patient’s eye fixations and patient’s fatigue. The scoring sheet is presented in **Supplementary Material I**. An extended version of the CAVE proposes additional subtests, including a visual memory recognition exercise that was attempted with our patients (except case 4). First, patients were presented five pictures (one at a time) and asked to memorize them. Afterward, each target was presented with a distractor and they were asked to look at the previously shown picture.

### Electrophysiological Measurement

A clinical EEG was performed using 19 electrodes and interpreted by a certified neurologist to assess the severity of the encephalopathy.

### MRI

MRI data was acquired using a 3 Tesla scanner (Siemens Trio, Siemens Medical Solutions, Erlangen, Germany). Structural MRI data were obtained with T1-weighted 3D gradient echo images using 120 slices (repetition time = 2300 ms, echo time = 2.47 ms, voxel size =  $1 \times 1 \times 1.2 \text{ mm}^3$ , flip angle =  $9^\circ$ , field of view =  $256 \times 256 \text{ mm}^2$ ).

### Voxel-Based Morphometry (VBM)

A T1 voxel-based morphometry analysis of brain structure using the VBM8 toolbox (Structural Brain Mapping Group, Christian Gaser, Department of Psychiatry, University of Jena, Germany) was carried out. T1 MRI images were segmented into gray and white matter and cerebrospinal fluid using the unified segmentation module (40). These segmented gray and white matter images were used to obtain a more accurate registration model using DARTEL (41, 42). The images of each participant were then normalized into the DARTEL template in MNI space. The gray matter images were modulated to ensure the preservation of their volumes after the normalization step. The modulated normalized gray matter images were smoothed with a Gaussian isotropic kernel of 12 mm of full width at half maximum (FWHM). The differences in gray matter volume were investigated by comparing each patient with a group of 36 healthy

control subjects (mean age =  $46 \pm 16$  years old, 13 women) using a parametric two-sample *t*-test. Both the total intracranial volume and age, centered to mean and standardized to 1, were then used as covariates. Results were considered significant at family-wise error (FWE) corrected  $p < 0.05$  at cluster level and cluster defining threshold  $p < 0.001$ .

### FDG-PET

A resting 18F-FDG PET/CT scan was performed after intravenous injection of  $\sim 150 \text{ MBq}$  of FDG using a Gemini TF PET-CT scanner (Philips Medical Systems) as described elsewhere (43). The scan started 30 min after an intravenous injection of the tracer and the scan duration was 12 min. FDG-PET images for each patient were manually reoriented using SPM12. The images were then spatially normalized, smoothed (with a 14 mm FWHM Gaussian filter) and analyzed. Patient data were compared to 34 healthy control subjects (age range 19–70 years, 15 women). SPM analysis identified brain regions with decreased and relatively preserved metabolism in each patient compared to healthy control subjects (global normalization was performed by proportional scaling). The resulting set of voxel values for each contrast, constituting a statistical parametric map of the *t*-statistics ( $\text{SPM}\{t\}$ ), was transformed to the unit normal distribution ( $\text{SPM}\{Z\}$ ) and thresholded at voxel-wise  $p < 0.05$  FWE-corrected and at  $p < 0.001$  uncorrected.

## RESULTS

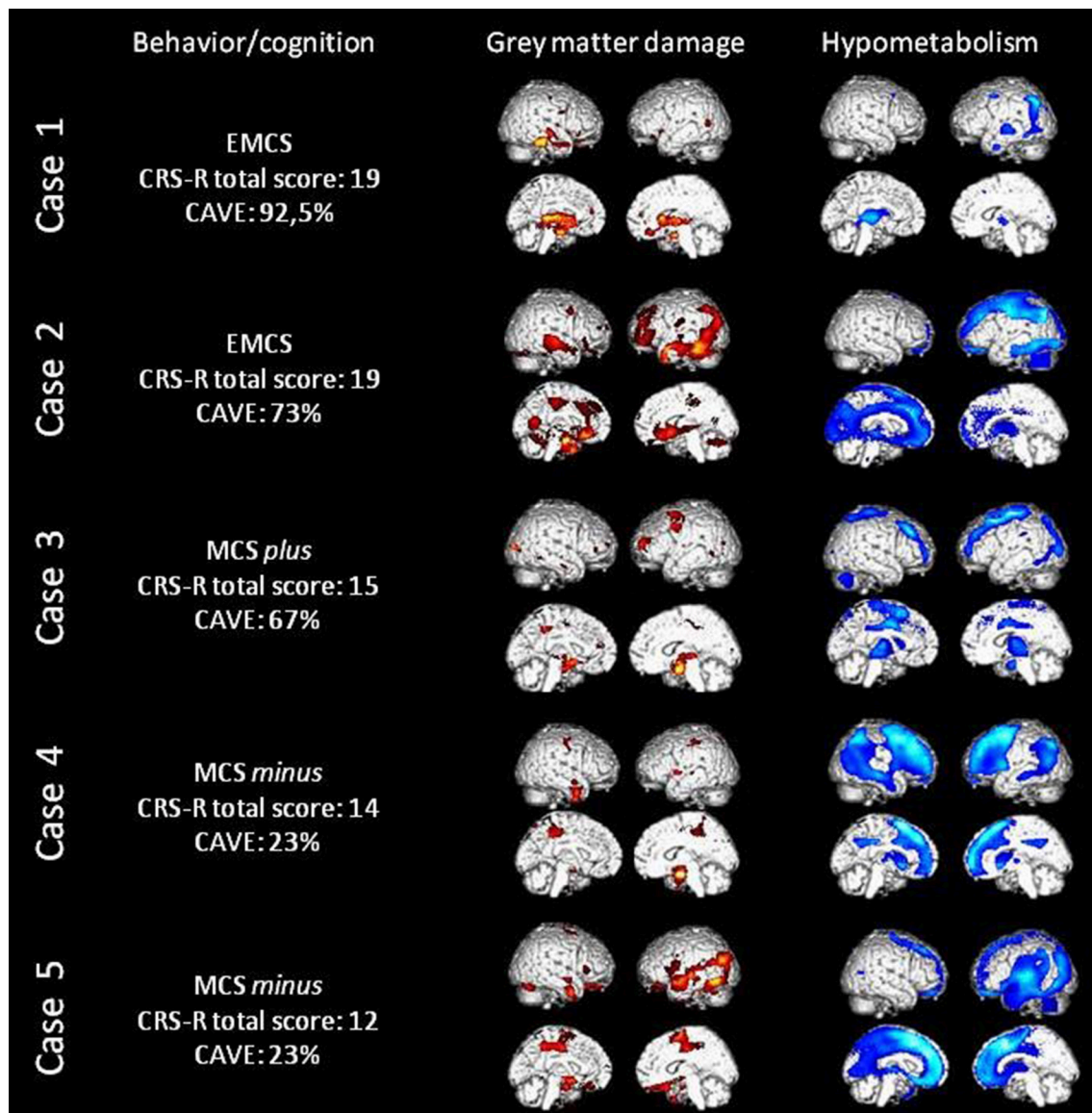
The main results of the five patients (all right-handed; age range: 20–66 years old; one woman) are presented in **Figure 1**. The CRS-R and CAVE scores are presented in **Table 1**. All VBM and PET statistical results are presented in **Table 2** (most significant data) and S1 (**Supplementary Material II**). The significant regions’ names were derived from the AAL2 atlas, using *bspmview* tool (<http://www.bobspunt.com/bspmview/>, doi: 10.5281/zenodo.168074).

### Case 1

This patient was admitted to our hospital 16 months after a traumatic brain injury. He was diagnosed as EMCS (with a total CRS-R score of 19/23) because of his ability to functionally communicate using “yes” and “no” cards. Due to fatigue and time limitation, only four CAVE sub-tests were administered. According to the cut-off score, he was able to recognize objects, numbers, written words and letters, as well as to memorize five pictures (**Table 1**). Overall, case 1 correctly responded to 92.5% of the administered items of the CAVE.

The clinical EEG showed abnormalities regarding the posterior and temporal derivations of the left hemisphere. As seen in **Table 2** and **Figure 1**, the VBM shows gray matter damage in the left hippocampus. PET hypometabolism was observed in the left thalamus and angular gyrus ( $p < 0.05$  FWE corrected), as well as the left putamen and part of the left inferior and middle temporal gyrus, the left precentral cortex and the right superior frontal cortex ( $p < 0.001$  uncorrected). The most preserved metabolism was shown in the right angular gyrus ( $p < 0.05$  FWE corrected) and in





**FIGURE 1 |** Behavioral and cognitive data, loss of gray matter volume (in red) as assessed with MRI voxel-based morphometry and cerebral hypometabolism (in blue) as assessed with FDG-PET in all five patients. Here the threshold is uncorrected 0.001 for display values (please refer to **Table 2** for corrected results).

the right insula, middle frontal cortex, post-central cortex, rolandic operculum and superior temporal cortex ( $p < 0.001$  uncorrected).

## Case 2

Case 2 had a stroke and epilepsy due to post-surgery complications 30 months before his admission to our hospital. He was diagnosed as EMCS (with a total CRS-R score of 19/23), as he was able to functionally use objects but not to functionally communicate. Using the CAFE, the patient showed a good performance in recognizing numbers and pictures (**Table 1**). He was just below the cut-off score with real objects and colors but he had more difficulties with discriminating letters and written

words and in memorizing the pictures. Unilateral spatial neglect was suspected since his performance was better when the target item was presented on his left side. Case 2 performed well for 73% of administered items.

The clinical EEG suggests significant left hemispheric damage with a nascent encephalopathy. Neuroimaging results also show left hemisphere structural and functional damage. Significant hypotrophy in the left fusiform, left medial orbitofrontal and right superior temporal cortices was noted, as well as in the left calcarine sulcus and right cerebellum. Hypometabolism was also observed in the left inferior parietal cortex ( $p < 0.05$  FWE corrected) and in the left supplementary motor area, superior frontal cortex, cingulate cortex, precuneus, fusiform cortex,

**TABLE 1 |** Behavioral scores at the CRS-R and the CAVE.

		Case 1	Case 2	Case 3	Case 4	Case 5
CRS-R	Final diagnosis	EMCS	EMCS	MCS+	MCS-	MCS-
	Auditory score	4*	4*	3*	2	1
	Visual score	5*	4*	3*	3*	3*
	Motor score	5*	6 <sup>#</sup>	5*	5*	5*
	Oromotor/verbal score	1	2	2	2	1
	Communication score	2 <sup>#</sup>	1*	0	0	0
	Arousal score	2	2	2	2	2
Total score		19	19	15	14	12
CAVE	Real objects	9/10	7/10	10/10	4/10	4/10
	Numbers	9/10	9/10	8/10	NA	3/10
	Words	9/10	6/10	1/10	2/10	1/10
	Letters	10/10	5/10	7/10	NA	1/10
	Pictures	NA	10/10	9/10	NA	3/10
	Colors	NA	7/10	5/10	NA	2/10
	Percentage of success	92.5%	73%	67%	23%	23%
	Memory	5/5	3/5	1/5	NA	1/5
	Left/right differences	No	Yes	No	No	Yes

<sup>#</sup> indicates emergence of minimally conscious state (EMCS), \* indicates MCS.

The CAVE scores in *italics* are below the cut-off score and thus considered as failed. NA, not administered.

superior parietal cortex, hippocampus and amygdala, as well as bilateral rectus gyri and thalami ( $p < 0.001$  uncorrected). The regions showing the most preserved metabolism were the right amygdala ( $p < 0.05$  FWE corrected) and the bilateral cerebellum and right middle frontal cortex, temporal, parietal and occipital lobules ( $p < 0.001$  uncorrected).

### Case 3

This patient came to our hospital 13 months after a traumatic brain injury. The diagnosis was MCS *plus* (with a total CRS-R score of 15/23) since he was able to follow simple verbal commands (e.g., “Look up,” “Turn your head” and “Close your eyes”). His cognition was more impaired than case 1 and qualitatively very different from case 2 (Table 1). He could perform some sub-tests, namely recognizing real objects, numbers and pictures. The other attempted sub-tests (including memory) led to performance lower than the cut-off score. This patient successfully responded to 67% of presented items.

The clinical EEG was biased by abundant movement artifacts. Structural damage was shown using VBM in the bilateral hippocampi and in the right precentral cortex. The PET analysis showed significant hypometabolism in bilateral precentral cortex, right middle frontal cortex, and left middle occipital cortex ( $p < 0.05$  FWE corrected), as well as in the left inferior occipital cortex, middle frontal gyrus and supplementary motor area and bilateral middle cingulate cortex and thalami ( $p < 0.001$  uncorrected). The most preserved metabolism was observed in the left supramarginal gyrus ( $p < 0.05$  FWE corrected) and

the right inferior frontal, inferior parietal, angular, and superior temporal cortex, as well as left inferior frontal, middle and superior temporal cortex ( $p < 0.001$  uncorrected).

### Case 4

Case 4 sustained a hypoxic-ischemic brain injury following an insulin overdose; she was 3 years post-hypoglycemia. This patient showed the requested visual functions, as well as automatic oriented motor reactions, therefore she was considered as being in a MCS *minus* with a CRS-R total score of 14/23. Nevertheless, she was an atypical MCS *minus* patient due to her ability to walk when guided by someone else. Using the CAVE, she failed to recognize real objects, numbers, words and colors. The remaining subtests (i.e., letters and pictures recognition) were not administered due to patient fatigue. Case 4 performed well for 23% of the administered items.

Despite the presence of muscular artifacts, the clinical EEG showed significant encephalopathy with no sign of lateralization. The neuroimaging data showed hypotrophy of the right amygdala. Moreover, hypometabolism was mainly found in the right middle frontal and cingulate cortex and in the left caudate and middle temporal cortex ( $p < 0.05$  FWE corrected), as well as in bilateral angular gyrus, caudate, putamen, thalami, and frontal cortex, in the right middle temporal and inferior parietal cortex, in the left insula and middle temporal cortex ( $p < 0.001$  uncorrected). On the contrary, the most preserved metabolism was shown in the right cerebellum ( $p < 0.05$  FWE corrected), in the bilateral insula and putamen, and in the left cerebellum, precuneus, paracentral and postcentral cortex ( $p < 0.001$  uncorrected).

### Case 5

This last patient had a stroke 13 months before his stay in our hospital. He was diagnosed as MCS *minus* with a CRS-R total score of 12/23. He did not show any residual language ability but he was able to visually fixate and track objects, as well as to automatically open his mouth when a spoon was moved toward it (i.e., automatic motor response). Similarly to case 4, this patient failed to recognize (and memorize) the visual targets, despite his high arousal enabling us to attempt all CAVE subtests. As for case 4, case 5 visually fixed the target item for 23% of the trials but left/right differences were observed.

The clinical EEG showed a symmetrical slow dysrhythmia with no paroxysm. Gray matter hypotrophy was shown in the left inferior temporal cortex and right supplementary motor area. PET results show the presence of significant hypometabolism in the left middle temporal cortex ( $p < 0.05$  FWE corrected), the bilateral superior frontal and cingulate cortex, the left thalamus, precuneus, and parietal cortex ( $p < 0.001$  uncorrected). Preserved metabolism in the right amygdala was observed ( $p < 0.05$  FWE corrected), as well as in the vermis, the bilateral cerebellum, the left hippocampus and the right parieto-occipito-temporal regions including the right precuneus and angular gyrus ( $p < 0.001$  uncorrected).



**TABLE 2 |** Regions showing significant gray matter hypotrophy, impaired and preserved metabolism.

	Brain regions	<i>p</i> (FWE-corr)	<i>T</i>	<i>x</i>	<i>y</i>	<i>z</i>
<b>GRAY MATTER</b>						
Case 1 < CTR	L hippocampus	0	6,4	−30	−15	−17
Case 2 < CTR	L fusiform cortex	0	11,5	−29	−15	−24
	L medial orbitofrontal cortex	0	8,1	−8	27	−12
	R superior temporal cortex	0,002	6,1	68	−9	−9
	L calcarine	0,035	4,9	−11	−60	11
	R cerebellum	0,038	4,3	23	−77	−30
Case 3 < CTR	R hippocampus	0,004	5,9	20	−6	−20
	L precentral cortex	0,025	4,7	−27	−4	53
	L hippocampus	0,036	4,7	−15	−6	−12
Case 4 < CTR	R amygdala	0	6,5	30	−4	−20
Case 5 < CTR	L inferior temporal cortex	0	8,0	−53	−69	−9
	R supplementary motor area	0,001	5,2	11	−1	65
<b>HYPOMETABOLISM</b>						
Case 1 < CTR	L angular gyrus	0,016	5,3	−46	−70	38
	L thalamus	0,015	5,2	−8	−18	6
Case 2 < CTR	L inferior parietal	0	15,6	−54	−26	36
Case 3 < CTR	L precentral cortex	0	12,2	−28	−18	68
	R middle frontal cortex	0,003	9,2	34	34	38
	R precentral cortex	0,012	6,0	26	−28	70
	L middle occipital cortex	0,006	5,6	−32	−90	8
	Brain stem	0,002	5,5	2	−24	−4
Case 4 < CTR	R middle frontal cortex	0	8,5	44	10	50
	L caudate	0,013	7,1	−16	12	8
	L middle temporal cortex	0	6,5	−50	−68	18
	R middle cingulate cortex	0,02	4,7	4	−50	34
Case 5 < CTR	L middle temporal cortex	0	15,4	−54	−58	20
<b>PRESERVED METABOLISM</b>						
Case 1 > CTR	R frontal lobe (white matter)	0	7,2	26	24	24
	R angular gyrus	0,041	4,5	48	−48	32
Case 2 > CTR	R amygdala	0	13,1	34	2	−24
Case 3 > CTR	R frontal lobe (white matter)	0	9,1	46	−2	18
	L supramarginal gyrus	0	9,1	−50	−28	30
Case 4 > CTR	L insula	0	10,0	−30	−8	18
	R insula	0,006	9,8	32	−4	18
	R cerebellum	0	7,0	20	−56	−20
Case 5 > CTR	R amygdala	0	17,3	34	0	−28

*L, left; R, right, CTR, healthy control subjects.*

## DISCUSSION

In this study, patients in MCS or EMCS have been assessed with a broad spectrum of (para)clinical tools. Using the CAVE, it has been possible to evaluate the cognitive profile of severely brain-injured patients, and the importance of the use of such new bedside neuropsychological assessments is highlighted. It was hypothesized that CAVE profiles would correspond to patients' cerebral structure and brain activity. Comparing all patients, the highest scorer on bedside behavioral and language-based cognitive assessments (i.e., case 1) showed less extended levels of cerebral hypometabolism. It was also

found that the percentage of success on the CAVE decreased along with the CRS-R total score (see **Table 1**), establishing a consistent behavioral/cognitive profile for each patient. The cognitive profile obtained from the CRS-R and the CAVE was mostly found to correspond to structural and functional results. As shown in **Figure 1**, both neuroimaging techniques also seem in agreement: gray matter damages are generally paralleled with hypometabolism of the same structures, and this hypometabolism is even more widespread. Below, we discuss cognitive functions in different domains and compare the behavioral results with neuroimaging findings.

## Visual Functions

All patients were able to visually fixate and pursuit objects and all showed a relative structural and metabolic preservation of occipital lobule. Regarding case 1, the ability to visually fixate objects and the use of a visually-based communication code were consistent with the absence of significant hypometabolism and gray matter hypotrophy in the occipital cortex. The difficulty to perform well with letters, words, and colors in case 3 may be consistent with the apparent hypometabolism within the left occipital cortex (44–47). In addition, number recognition appeared intact in this patient. This ability has been shown to rely on the right lateral occipital area (48), and our patient showed no significant hypometabolism in this area. Hence, our findings suggest a dissociation between letters and numbers recognition which was associated with specific occipital lesions. Both MCS *minus* patients were unable to successfully recognize the CAVE target items. Despite their ability to visually fixate one object when it was presented alone, none of these two patients showed responses to command, which suggest that they did not understand the task instructions (see next section).

Unilateral spatial neglect and/or hemianopia were suspected in case 2 and case 5 since there was a significant difference in the performance between left and right CAVE target items. Indeed, a deviation of their eyes toward their left side was noted in both patients. Karnath and coworkers have highlighted the role of a perisylvian network in spatial neglect (49), including the temporo-parietal junction, the temporal lobules and underlying insula, as well as the ventro-lateral prefrontal cortex. Accordingly, these two patients showed hypometabolism and hypotrophy of gray matter in some of these cerebral regions.

## Language and Executive Functions

Case 1 was the only patient who could functionally communicate using a “yes”/“no” code. This ability requires language and executive functions such as mental flexibility. Hence recovery of communication does not seem surprising due to the preserved metabolism and absence of gray matter damage in frontal lobules (50, 51). Besides communication, this patient was also able to follow simple commands and to understand the “look at” commands during the administration of the CAVE. Nevertheless, the EEG and PET analysis reported abnormalities regarding the posterior and temporal derivations of the left hemisphere, shown to be dedicated to semantics (52). Specifically, we found peaks of hypometabolism within the left angular gyrus, which was related to sentence comprehension (52–54). Still, this patient’s residual language skills may emerge from neural plasticity using the cerebral areas that are either around the lesion, or in the contralateral cerebral regions (55–59). Indeed, right angular gyrus and superior temporal cortex showed preserved metabolism.

In contrast, case 2 was unable to functionally communicate and read written letters and words during the CAVE assessment. This was consistent with the massive left cerebral lesion that was detected with VBM, PET and clinical EEG (52, 60). More precisely, this patient showed hypometabolism and gray matter reduction in the left fusiform cortex, known to be the “visual word form area” (54, 60, 61). Therefore, these data matched

well with his inability to recognize letters and words. Taken together, the CAVE results suggested that the more linguistic were the items, the more difficult it was for this patient to answer. Thus, it is likely that this patient had severe aphasic difficulties. Nevertheless, he was systematically able to follow (and thus understand) commands. This may correspond with the absence of hypometabolism in areas such as the left superior temporal cortex (52). In addition, similarly to case 1 it could be argued that he recovered such abilities by means of neural plasticity.

Case 3 was able to understand and follow commands and he could recognize objects, pictures and numbers. All these skills require residual language comprehension and relative preservation of semantic processing, which is related to left temporal areas (52). Accordingly, we observed the absence of gray matter hypotrophy and the presence of preserved metabolism regarding the left temporal lobule. Again, this patient showed an inability to recognize letters and written words. If this patient, contrary to case 2, did not show impairment of the left fusiform gyrus (i.e., the visual word form area), he still showed hypometabolism in regions that are very close (i.e., the left inferior and middle occipital cortex). These findings were also consistent with the patient’s inability to discriminate different colors (44, 62).

The inability of case 4 and case 5 to show language-based signs of consciousness (i.e., command-following, intelligible verbalization and communication) and to recognize CAVE items corresponded to their hypometabolism, notably regarding the left angular gyrus (52). These results implied a lack of verbal comprehension due to accumulated language and cognitive impairments. Indeed, more impaired language functions in MCS *minus* than in MCS *plus* patients was suggested by previous studies (63, 64).

## Motor Functions

Repeated assessments on the CRS-R did not demonstrate functional use of objects in case 1 but it was noted that this patient tended to grab his bed sheets and try to reach objects. Accordingly, we did not observe hypometabolism within the motor cerebral areas (**Figure 1**). Furthermore, case 2’s ability to functionally use some objects (i.e., a comb) could emerge from preserved right motor areas. Our third and fifth cases obtained the same motor subscale score at the CRS-R as case 1 since they showed automatic oriented movements with their mouth. The inability to move their limbs could thus be related to case 3’s hypometabolism of the precentral cortex and supplementary motor area and to case 5’s damage of the right supplementary motor area. Interestingly, case 4 was an atypical MCS *minus* patient because she was able to walk despite her inability to respond to commands. This capacity was probably possible because of preserved metabolism of the left paracentral and postcentral sensorimotor cortex (65–67). In addition, this patient also showed a preserved cerebellum and previous studies have highlighted its role in gait and movement coordination (68).

## Memory and Consciousness

Case 1 performed perfectly to the memory subtest. Nevertheless, it is a recognition task and other higher order memory processes

might still be impaired. Indeed, case 1 (as well as case 3) showed impaired gray matter structure in the hippocampus, which has shown to be related to episodic memory in numerous previous studies [e.g., (69, 70)]. Since memory difficulties were presented on this subtest by the other cases, one could thus hypothesize the presence of memory impairment in all five patients.

All patients were no less than minimally conscious, and at least part of the external frontoparietal network was preserved in all of them (22). Interestingly, in our atypical case 4 the metabolism of this external network seemed less preserved than the other cases. The internal DMN was probably slightly more affected than external network in our patients. For instance, the left precuneus was shown to be hypometabolic in case 2 and case 5, whereas the left temporo-parietal junctions (also involved in the DMN) seem hypometabolic in four patients. Lastly, the thalamus, known to play an important role in consciousness (71), was hypometabolic in all five patients. Since thalamo-cortical alterations were found in other brain-injured patients with chronic fatigue problems (72), case 1's fatigue might also be at least partially explained by the left thalamus functional impairment.

## Limitations

This multiple case report only provides preliminary findings; more patients are needed in order to overcome statistical limitations and confirm the relationships between cognition and brain structure and function at the group level. The heterogeneity of DoC patients makes this research very challenging. Moreover, the performance at the CAVE is multi-determined, requiring visual functions, language comprehension and other subtest-specific abilities such as reading. As such, the CAVE might allow us to detect the presence of aphasia in our patients, but it does not discriminate or specify which language functions are altered (e.g., phonology vs. semantics). New material could be included to evaluate MCS and EMCS patients' cognitive functions in a more specific way. Finally, the CAVE seems to be useful only for patients who are at least MCS *plus*.

## Conclusion

In this study, the performance of all patients using the CRS-R and the CAVE was consistent, and it mostly corresponded to their brain structure and metabolism in line with previous research on patients with focal cerebral lesions. For instance, the ability to recognize visually presented objects, or items based on their name was linked to a relative preservation of visual and language metabolism. In addition, residual language comprehension skills were found in the presence of

preserved temporal and angular cortex metabolism. These results suggest that brain-behavior relationships might be observed even in severely brain-injured patients. This research further highlights the importance of the development of behavioral assessment tools, such as the CAVE, both to inform clinical practice and for scientific interest. Clinically, besides the CRS-R this new test allows to refine the patient's cognitive profile. This knowledge will be helpful in preparation of rehabilitation programs and daily routines. Such information may be important also for the investigation of the neural correlates of behavior and cognition in patients with severe brain injury.

## AUTHOR CONTRIBUTIONS

CA, LM, and OG conceived and planned the presented research. LM previously created the CAVE. CA, OG, MB, SKL, AT, and SW contributed to data analyses and interpretation. CA, HC, JA, and MC acquired the data. CA drafted the manuscript under OG's supervision and all authors provided critical feedback and helped shape the manuscript.

## ACKNOWLEDGMENTS

The study was supported by the University and University Hospital of Liège, the French Speaking Community Concerted Research Action (ARC 12-17/01), the Belgian National Funds for Scientific Research (FRS-FNRS), Human Brain Project (EU-H2020-fetflagship-hbp-sga1-ga720270), Luminous project (EU-H2020-fetopen-ga686764), the James McDonnell Foundation, Mind Science Foundation, IAP research network P7/06 of the Belgian Government (Belgian Science Policy), the European Commission, the Public Utility Foundation 'Université Européenne du Travail,' 'Fondazione Europea di Ricerca Biomedica,' the Bial Foundation, Belgian National *Plan Cancer* (139). CA and SKL are research fellows, OG and AT are post-doctoral fellows, and SL is research director at FRS-FNRS. We thank Pr P. Maquet, Pr B. Sadzot, Dr E. Rikir and J. M. Klein from the Neurology department, University Hospital of Liège, as well as the whole Neurology staff, patients, and their families.

## SUPPLEMENTARY MATERIAL

The Supplementary Material for this article can be found online at: <https://www.frontiersin.org/articles/10.3389/fneur.2018.00665/full#supplementary-material>

## REFERENCES

- Laureys S, Celesia GG, Cohadon F, Lavrijsen J, León-Carrión J, Sannita WG, et al. Unresponsive wakefulness syndrome: a new name for the vegetative state or apallic syndrome. *BMC Med.* (2010) 8:68. doi: 10.1186/1741-7015-8-68
- Giacino JT, Ashwal S, Childs N, Cranford R, Jennett B, Katz DI. The minimally conscious state. *Neurology* (2002) 58:349–53. doi: 10.1212/WNL.58.3.349
- Wannez S, Gosseries O, Azzolini D, Martial C, Cassol H, Aubinet C, et al. Prevalence of coma-recovery scale-revised signs of consciousness in patients in minimally conscious state. *Neuropsychol Rehabil.* (2017). doi: 10.1080/09602011.2017.1310656. [Epub ahead of print].
- Bruno MA, Vanhaudenhuyse A, Thibaut A, Moonen G, Laureys S. From unresponsive wakefulness to minimally conscious PLUS and functional locked-in syndromes: recent advances in our understanding of disorders of consciousness. *J Neurol.* (2011) 258:1373–84. doi: 10.1007/s00415-011-6114-x

5. Chatelle C, Val M, De Catano A, Chaskis C, Seeldrayers P, Laureys S, et al. Is the nociception coma scale-revised a useful clinical tool for managing pain in patients with disorders of consciousness? *Clin J Pain* (2016) 32:321–6. doi: 10.1097/AJP.0000000000000259
6. Demertzi A, Ledoux D, Bruno M-A, Vanhaudenhuyse A, Gosseries O, Soddu A, et al. Attitudes towards end-of-life issues in disorders of consciousness: a European survey. *J Neurol*. (2011) 258:1058–65. doi: 10.1007/s00415-010-5882-z
7. Thibaut A, Wannez S, Donneau A-F, Chatelle C, Gosseries O, Bruno M-A, et al. Controlled clinical trial of repeated prefrontal tDCS in patients with chronic minimally conscious state. *Brain Inj.* (2017) 31:466–74. doi: 10.1080/02699052.2016.1274776
8. Andrews K, Murphy L, Munday R, Littlewood C. Misdiagnosis of the vegetative state: retrospective study in a rehabilitation unit. *BMJ* (1996) 313:13–6. doi: 10.1136/bmj.313.7048.13
9. Childs NL, Mercer WN, Childs HW. Accuracy of diagnosis of persistent vegetative state. *Neurology* (1993) 43:1465–7.
10. Gill-Thwaites H. Lotteries, loopholes and luck: misdiagnosis in the vegetative state patient. *Brain Inj.* (2006) 20:1321–8.
11. Schnakers C, Vanhaudenhuyse A, Giacino J, Ventura M, Boly M, Majerus S, et al. Diagnostic accuracy of the vegetative and minimally conscious state: clinical consensus versus standardized neurobehavioral assessment. *BMC Neurol*. (2009) 9:35. doi: 10.1186/1471-2377-9-35
12. Stender J, Gosseries O, Bruno MA, Charland-Verville V, Vanhaudenhuyse A, Demertzi A, et al. Diagnostic precision of PET imaging and functional MRI in disorders of consciousness: a clinical validation study. *Lancet* (2014) 384:514–22. doi: 10.1016/S0140-6736(14)60042-8
13. van Erp WS, Lavrijsen JCM, Vos PE, Bor H, Laureys S, Koopmans RTCM. The vegetative state: prevalence, misdiagnosis, and treatment limitations. *J Am Med Dir Assoc*. (2015) 16:85.e9–85.e14. doi: 10.1016/j.jamda.2014.10.014
14. Majerus S, Bruno MA, Schnakers C, Giacino JT, Laureys S. The problem of aphasia in the assessment of consciousness in brain-damaged patients. *Prog Brain Res*. (2009) 177:49–61. doi: 10.1016/S0079-6123(09)17705-1
15. Schnakers C, Bessou H, Rubi-Fessen I, Hartmann A, Fink GR, Meister I, et al. Impact of aphasia on consciousness assessment: a cross-sectional study. *Neurorehabil Neural Repair* (2014) 29:41–7. doi: 10.1177/1545968314528067
16. Giacino JT, Kalmar K, Whyte J. The JFK coma recovery scale-revised: measurement characteristics and diagnostic utility. *Arch Phys Med Rehabil*. (2004) 85:2020–9. doi: 10.1016/j.apmr.2004.02.033
17. Seel RT, Sherer M, Whyte J, Katz DI, Giacino JT, Rosenbaum AM, et al. Assessment scales for disorders of consciousness: evidence-based recommendations for clinical practice and research. *Arch Phys Med Rehabil*. (2010) 91:1795–813. doi: 10.1016/j.apmr.2010.07.218
18. Murphy L. The Cognitive Assessment by Visual Election (CAVE): a pilot study to develop a cognitive assessment tool for people emerging from disorders of consciousness. *Neuropsychol. Rehabil.* (2018). doi: 10.1080/09602011.2018.1454327. [Epub ahead of print].
19. Gosseries O, Pistoia F, Charland-Verville V, Carolei A, Sacco S, Laureys S. The role of neuroimaging techniques in establishing diagnosis, prognosis and therapy in disorders of consciousness. *Open Neuroimaging J.* (2016) 10:52–68. doi: 10.2174/1874440001610010052
20. Guldenmund P, Soddu A, Baquero K, Vanhaudenhuyse A, Bruno M-A, Gosseries O, et al. Structural brain injury in patients with disorders of consciousness: a voxel-based morphometry study. *Brain Inj.* (2016) 30:343–52. doi: 10.3109/02699052.2015.1118765
21. Heine L, Soddu A, Gómez F, Vanhaudenhuyse A, Tshibanda L, Thonnard M, et al. Resting state networks and consciousness: Alterations of multiple resting state network connectivity in physiological, pharmacological, and pathological consciousness states. *Front Psychol.* (2012) 3:1–12. doi: 10.3389/fpsyg.2012.00295T
22. Laureys S, Lemaire C, Maquet P, Phillips C, Franck G. Cerebral metabolism during vegetative state and after recovery to consciousness. *October* (1999) 67:121–33. doi: 10.1136/jnnp.67.1.121
23. Di Perri C, Bahri MA, Amico E, Thibaut A, Heine L, Antonopoulos G, et al. Neural correlates of consciousness in patients who have emerged from a minimally conscious state: A cross-sectional multimodal imaging study. *Lancet Neurol.* (2016) 15:830–42. doi: 10.1016/S1474-4422(16)00111-3
24. Vanhaudenhuyse A, Demertzi A, Schabus M, Noirhomme Q, Bredart S, Boly M, et al. Two distinct neuronal networks mediate the awareness of environment and of self. *J Cogn Neurosci.* (2011) 23:570–8. doi: 10.1162/jocn.2010.21488
25. Demertzi A, Antonopoulos G, Heine L, Voss HU, Crone JS, De Los Angeles C, et al. Intrinsic functional connectivity differentiates minimally conscious from unresponsive patients. *Brain* (2015) 138:2619–31. doi: 10.1093/brain/awv169
26. Thibaut A, Bruno MA, Chatelle C, Gosseries O, Vanhaudenhuyse A, Demertzi A, et al. Metabolic activity in external and internal awareness networks in severely brain-damaged patients. *J Rehabil Med.* (2012) 44:487–94. doi: 10.2340/16501977-0940
27. Bodart O, Amico E, Gómez F, Casali AG, Wannez S, Heine L, et al. Global structural integrity and effective connectivity in patients with disorders of consciousness. *Brain Stimul.* (2017) 11:358–65. doi: 10.1016/j.brs.2017.11.006
28. Bodart O, Gosseries O, Wannez S, Thibaut A, Annen J, Boly M, et al. Measures of metabolism and complexity in the brain of patients with disorders of consciousness. *NeuroImage Clin.* (2017) 14:354–62. doi: 10.1016/j.nicl.2017.02.002
29. Chennu S, Annen J, Wannez S, Thibaut A, Chatelle C, Cassol H, et al. Brain networks predict metabolism, diagnosis and prognosis at the bedside in disorders of consciousness. *Brain* (2017) 140:2120–32. doi: 10.1093/brain/awx163
30. Beukema S, Gonzalez-Lara LE, Finoia P, Kamau E, Allanson J, Chennu S, et al. A hierarchy of event-related potential markers of auditory processing in disorders of consciousness. *NeuroImage Clin.* (2016) 12:359–71. doi: 10.1016/j.nicl.2016.08.003
31. De Salvo S, Caminiti F, Bonanno L, De Cola MC, Corallo F, Caizzone A, et al. Neurophysiological assessment for evaluating residual cognition in vegetative and minimally conscious state patients: a pilot study. *Funct Neurol.* (2015) 30:237–44. doi: 10.11138/FNeur/2015.30.4.237
32. Di HB, Yu SM, Weng XC, Laureys S, Yu D, Li JQ, et al. Cerebral response to patient's own name in the vegetative and minimally conscious states. *Neurology* (2007) 68:895–9. doi: 10.1212/01.wnl.0000258544.79024.d0
33. Kotchoubey B, Lang S, Mezger G, Schmalohr D, Schneck M, Semmler A, et al. Information processing in severe disorders of consciousness: vegetative state and minimally conscious state. *Clin Neurophysiol.* (2005) 116:2441–53. doi: 10.1016/j.clinph.2005.03.028
34. Laureys S, Perrin F, Faymonville M-E, Schnakers C, Boly M, Bartsch V, et al. Cerebral processing in the minimally conscious state. *Neurology* (2004) 63:916–8. doi: 10.1212/01.WNL.0000137421.30792.9B
35. Nigri A, Catricalà E, Ferraro S, Bruzzzone MG, D'Incerti L, Sattin D, et al. The neural correlates of lexical processing in disorders of consciousness. *Brain Imaging Behav.* (2016) 11:1526–37. doi: 10.1007/s11682-016-9613-7
36. Rodriguez Moreno D, Schiff ND, Giacino J, Kalmar K, Hirsch J. A network approach to assessing cognition in disorders of consciousness. *Neurology* (2010) 75:1871–8. doi: 10.1212/WNL.0b013e3181feb259
37. Schiff ND, Rodriguez-Moreno D, Kamal A, Kim KHS, Giacino JT, Plum F, et al. fMRI reveals large-scale network activation in minimally conscious patients. *Neurology* (2005) 64:514–23. doi: 10.1212/01.WNL.0000150883.10285.44
38. Sergent C, Faugeras F, Rohaut B, Perrin F, Valente M, Tallon-Baudry C, et al. Multidimensional cognitive evaluation of patients with disorders of consciousness using EEG: a proof of concept study. *NeuroImage Clin.* (2017) 13:455–69. doi: 10.1016/j.nicl.2016.12.004
39. Wannez S, Heine L, Thonnard M, Gosseries O, Laureys S. The repetition of behavioral assessments in diagnosis of disorders of consciousness. *Ann Neurol.* (2017) 81:883–9. doi: 10.1002/ana.24962
40. Ashburner J, Friston KJ. Unified segmentation. *Neuroimage* (2005) 26:839–51. doi: 10.1016/j.neuroimage.2005.02.018
41. Ashburner J. A fast diffeomorphic image registration algorithm. *Neuroimage* (2007) 38:95–113. doi: 10.1016/j.neuroimage.2007.07.007
42. Takahashi R, Ishii K, Miyamoto N, Yoshikawa T, Shimada K, Ohkawa S, et al. Measurement of gray and white matter atrophy in dementia with lewy bodies using diffeomorphic anatomic registration through exponentiated lie algebra: a comparison with conventional voxel-based morphometry. *Am J Neuroradiol.* (2010) 31:1873–8. doi: 10.3174/ajnr.A2200
43. Bruno MA, Fernández-Espejo D, Lehenbre R, Tshibanda L, Vanhaudenhuyse A, Gosseries O, et al. Multimodal neuroimaging in patients with disorders of



- consciousness showing “functional hemispherectomy.” *Prog Brain Res.* (2011) 193:323–33. doi: 10.1016/B978-0-444-53839-0.00021-1
44. Bartels A, Zeki S. The architecture of the colour centre in the human visual brain: new results and a review. *Eur J Neurosci.* (2000) 12:172–93.
  45. Garrett AS, Flowers DL, Absher JR, Fahey FH, Gage HD, Keyes JW, et al. Cortical activity related to accuracy of letter recognition. *Neuroimage* (2000) 11:111–23. doi: 10.1006/nimg.1999.0528
  46. James KH, James TW, Jobard G, Wong ACN, Gauthier I. Letter processing in the visual system: different activation patterns for single letters and strings. *Cogn Affect Behav Neurosci.* (2005) 5:452–66.
  47. Koyama MS, Kelly C, Shehzad Z, Penesetti D, Castellanos FX, Milham MP. Reading networks at rest. *Cereb Cortex* (2010) 20:2549–59. doi: 10.1093/cercor/bhq005
  48. Park J, Hebrank A, Polk TA, Park DC. Neural dissociation of number from letter recognition and its relationship to parietal numerical processing. *J Cogn Neurosci.* (2012) 24:39–50. doi: 10.1162/jocn\_a\_00085
  49. Karnath H-O, Rorden C. The anatomy of spatial neglect. *Neuropsychologia* (2012) 50:1010–7. doi: 10.1016/j.neuropsychologia.2011.06.027
  50. Badre D, Nee DE. Frontal cortex and the hierarchical control of behavior. *Trends Cogn Sci.* (2017) 22:170–88. doi: 10.1016/j.tics.2017.11.005
  51. Munro BA, Weyandt LL, Hall LE, Oster DR, Gudmundsdottir BG, Kuhar BG. Physiological substrates of executive functioning: a systematic review of the literature. *Atten Deficit Hyperact Disord.* (2017) 10:1–20. doi: 10.1007/s12402-017-0226-9
  52. Binder JR, Desai RH, Graves WW, Conant LL. Where is the semantic system? a critical review and meta-analysis of 120 functional neuroimaging studies. *Cereb. Cortex* (2009) 19:2767–96. doi: 10.1093/cercor/bhp055
  53. Dronkers NF, Wilkins DP, Van Valin Jr RD, Redfern BB, Jaeger JJ. Lesion analysis of the brain areas involved in language comprehension. *Cognition* (2004) 92:145–77. doi: 10.1016/j.cognition.2003.11.002
  54. Friederici AD, Rüschemeyer SA, Hahne A, Fiebach CJ. The role of left inferior frontal and superior temporal cortex in sentence comprehension: localizing syntactic and semantic processes. *Cereb. Cortex* (2003) 13:170–7.
  55. Artzi M, Shiran SI, Weinstein M, Myers V, Tarrasch R. Cortical reorganization following injury early in life. (2016) 2016:8615872. doi: 10.1155/2016/8615872
  56. Heiss WD, Kessler J, Thiel A, Ghaemi M, Karbe H. Differential capacity of left and right hemispheric areas for compensation of poststroke aphasia. *Ann Neurol.* (1999) 45:430–8.
  57. Heiss WD, Thiel A. A proposed regional hierarchy in recovery of post-stroke aphasia. *Brain Lang.* (2006) 98:118–23. doi: 10.1016/j.bandl.2006.02.002
  58. Teki S, Barnes GR, Penny WD, Iverson P, Woodhead ZVJ, Griffiths TD, et al. The right hemisphere supports but does not replace left hemisphere auditory function in patients with persisting aphasia. *Brain* (2013) 136:1901–12. doi: 10.1093/brain/awt087
  59. Vitali P, Abutalebi J, Tettamanti M, Danna M, Ansaldo A-I, Perani D, et al. Training-induced brain remapping in chronic aphasia: a pilot study. *Neurorehabil Neural Repair* (2007) 21:152–60. doi: 10.1177/1545968306294735
  60. Dronkers NF, Ivanova MV, Baldo JV. What do language disorders reveal about brain–language relationships? from classic models to network approaches. *J Int Neuropsychol Soc.* (2017) 23:741–54. doi: 10.1017/S1355617717001126
  61. Carreiras M, Armstrong BC, Perea M, Frost R. The what, when, where, and how of visual word recognition. *Trends Cogn Sci.* (2014) 18:90–8.
  62. Lafer-Sousa R, Conway BR, Kanwisher NG. Color-biased regions of the ventral visual pathway lie between face- and place-selective regions in humans, as in macaques. *J Neurosci.* (2016) 36:1682–97. doi: 10.1523/JNEUROSCI.3164-15.2016
  63. Aubinet C, Heine L, Martial C, Larroque S, Majerus S, Laureys S, et al. Clinical sub-categorization of minimally conscious state according to resting functional connectivity. *Hum. Brain Mapp.* (2018). doi: 10.1002/hbm.24303
  64. Bruno MA, Majerus S, Boly M, Vanhaudenhuyse A, Schnakers C, Gosseries O, et al. Functional neuroanatomy underlying the clinical subcategorization of minimally conscious state patients. *J Neurol.* (2012) 259:1087–98. doi: 10.1007/s00415-011-6303-7
  65. Pizzamiglio S, Naeem U, Abdalla H, Turner DL. Neural correlates of single- and dual-task walking in the real world. *Front Hum Neurosci.* (2017) 11:460. doi: 10.3389/fnhum.2017.00460
  66. Seeber M, Scherer R, Wagner J, Solis-Escalante T, Müller-Putz GR. Commentary: EEG beta suppression and low gamma modulation are different elements of human upright walking. *Front Hum Neurosci.* (2015) 9:542. doi: 10.3389/fnhum.2015.00542
  67. Wagner J, Solis-Escalante T, Scherer R, Neuper C, Müller-Putz G. It's how you get there: walking down a virtual alley activates premotor and parietal areas. *Front Hum Neurosci.* (2014) 8:93. doi: 10.3389/fnhum.2014.00093
  68. Buckley E, Mazzà C, McNeill A. A Systematic review of the gait characteristics associated with cerebellar ataxia. *Gait Posture* (2017) 60:154–63. doi: 10.1016/j.gaitpost.2017.11.024
  69. Poldrack RA, Packard MG. Competition among multiple memory systems: converging evidence from animal and human brain studies. *Neuropsychologia* (2003) 41:245–51.
  70. Ranganath C. A unified framework for the functional organization of the medial temporal lobes and the phenomenology of episodic memory. *Hippocampus* (2010) 20:1263–90. doi: 10.1002/hipo.20852
  71. Crone JS, Soddu A, Höller Y, Vanhaudenhuyse A, Schurz M, Bergmann J, et al. Altered network properties of the fronto-parietal network and the thalamus in impaired consciousness. *NeuroImage Clin.* (2014) 4:240–8. doi: 10.1016/j.nicl.2013.12.005
  72. Berginström N, Nordström P, Ekman U, Eriksson J, Andersson M, Nyberg L, et al. Using functional magnetic resonance imaging to detect chronic fatigue in patients with previous traumatic brain injury: changes linked to altered striato-thalamic-cortical functioning. *J. Head Trauma Rehabil.* (2017) 33:266–74. doi: 10.1097/HTR.0000000000000340

**Conflict of Interest Statement:** The authors declare that the research was conducted in the absence of any commercial or financial relationships that could be construed as a potential conflict of interest.

Copyright © 2018 Aubinet, Murphy, Bahri, Larroque, Cassol, Annen, Carrière, Wannez, Thibaut, Laureys and Gosseries. This is an open-access article distributed under the terms of the Creative Commons Attribution License (CC BY). The use, distribution or reproduction in other forums is permitted, provided the original author(s) and the copyright owner(s) are credited and that the original publication in this journal is cited, in accordance with accepted academic practice. No use, distribution or reproduction is permitted which does not comply with these terms.





# Functional MRI Motor Imagery Tasks to Detect Command Following in Traumatic Disorders of Consciousness

Yelena G. Bodien<sup>1,2\*</sup>, Joseph T. Giacino<sup>2,3</sup> and Brian L. Edlow<sup>1,4</sup>

<sup>1</sup> Center for Neurotechnology and Neurorecovery, and Laboratory for Neuroimaging of Coma and Consciousness, Department of Neurology, Massachusetts General Hospital, Harvard Medical School, Boston, MA, United States,

<sup>2</sup> Department of Physical Medicine and Rehabilitation, Spaulding Rehabilitation Hospital, Harvard Medical School, Boston, MA, United States, <sup>3</sup> Department of Psychiatry, Massachusetts General Hospital and Harvard Medical School, Boston, MA, United States, <sup>4</sup> Athinoula A. Martinos Center for Biomedical Imaging, Massachusetts General Hospital and Harvard Medical School, Charlestown, MA, United States

## OPEN ACCESS

### Edited by:

Olivia Gosseries,  
University of Liège, Belgium

### Reviewed by:

Lorina Naci,  
Western University, Canada  
Thomas Jörg Müller,  
Private Clinic Meiringen,  
Switzerland

### \*Correspondence:

Yelena G. Bodien  
ybodien@mgh.harvard.edu

### Specialty section:

This article was submitted to  
Applied Neuroimaging,  
a section of the journal  
Frontiers in Neurology

**Received:** 18 August 2017

**Accepted:** 01 December 2017

**Published:** 18 December 2017

### Citation:

Bodien YG, Giacino JT and  
Edlow BL (2017) Functional MRI  
Motor Imagery Tasks to Detect  
Command Following in Traumatic  
Disorders of Consciousness.  
Front. Neurol. 8:688.  
doi: 10.3389/fneur.2017.00688

Severe traumatic brain injury impairs arousal and awareness, the two components of consciousness. Accurate diagnosis of a patient's level of consciousness is critical for determining treatment goals, access to rehabilitative services, and prognosis. The bedside behavioral examination, the current clinical standard for diagnosis of disorders of consciousness, is prone to misdiagnosis, a finding that has led to the development of advanced neuroimaging techniques aimed at detection of conscious awareness. Although a variety of paradigms have been used in functional magnetic resonance imaging (fMRI) to reveal covert consciousness, the relative accuracy of these paradigms in the patient population is unknown. Here, we compare the rate of covert consciousness detection by hand squeezing and tennis playing motor imagery paradigms in 10 patients with traumatic disorders of consciousness [six male, six acute, mean  $\pm$  SD age =  $27.9 \pm 9.1$  years, one coma, four unresponsive wakefulness syndrome, two minimally conscious without language function, and three minimally conscious with language function, per bedside examination with the Coma Recovery Scale-Revised (CRS-R)]. We also tested the same paradigms in 10 healthy subjects (nine male, mean  $\pm$  SD age =  $28.5 \pm 9.4$  years). In healthy subjects, the hand squeezing paradigm detected covert command following in 7/10 and the tennis playing paradigm in 9/10 subjects. In patients who followed commands on the CRS-R, the hand squeezing paradigm detected covert command following in 2/3 and the tennis playing paradigm in 0/3 subjects. In patients who did not follow commands on the CRS-R, the hand squeezing paradigm detected command following in 1/7 and the tennis playing paradigm in 2/7 subjects. The sensitivity, specificity, and accuracy (ACC) of detecting covert command following in patients who demonstrated this behavior on the CRS-R was 66.7, 85.7, and 80% for the hand squeezing paradigm and 0, 71.4, and 50% for the tennis playing paradigm, respectively. Overall, the tennis paradigm performed better than the hand squeezing paradigm in healthy subjects, but in patients, the hand squeezing paradigm detected command following with greater ACC. These findings indicate that current fMRI motor imagery paradigms frequently

fail to detect command following and highlight the need for paradigm optimization to improve the accuracy of covert consciousness detection.

**Keywords:** traumatic brain injury, consciousness, awareness, functional magnetic resonance imaging, motor imagery

## INTRODUCTION

Patients with severe traumatic brain injury (TBI) experience a period of impaired consciousness characterized by disturbances in arousal and awareness. This disorder of consciousness (DoC) may resolve acutely [i.e., in the intensive care unit (ICU)] or may be prolonged, extending weeks, months, or even years post-injury (1). The spectrum of behavioral states that comprise DoC includes coma, unresponsive wakefulness syndrome (UWS, also known as vegetative state) (2, 3), minimally conscious state (MCS) (4), and post-traumatic confusional state (5, 6). Accurate assessment of a patient's level of consciousness (LoC) is critically important to prognosis, as patients who have recovered consciousness (i.e., MCS) and especially language function have a higher likelihood of regaining cognitive function than those who have not (i.e., coma and UWS) (7–10). Thus, assessment of LoC drives early decisions about aggressive treatment and access to rehabilitative care. An inaccurate diagnosis may also prevent autonomous decision-making in patients who retain the capacity to do so.

Despite the critical importance of accurately defining a patient's LoC, the current standard for assessment in this patient population is bedside clinical examination, a method that is prone to inaccuracies due to patient impairments (e.g., speech and motor deficits that prevent verbalization or movement to command) and examiner bias. The approximate rate of misdiagnosing a conscious patient as unconscious is 40% (11–14). Standardized behavioral tools, such as the Coma Recovery Scale-Revised (CRS-R) (15), have helped improve the accuracy and precision of the bedside assessment, but the behavioral diagnosis is potentially susceptible to misinterpretation of subtle and inconsistent behaviors. Recently published guidance on the optimal frequency of CRS-R assessment may further improve the accuracy of behavioral assessment (16), but even frequent assessments with the CRS-R may fail to detect consciousness in persons whose capacity for volitional brain function is masked by limitations in self-expression. Objective markers of consciousness are therefore needed to ensure accurate diagnosis and to guide care management.

To circumvent some of the limitations of the bedside behavioral examination, recent studies have attempted to elicit evidence of consciousness by asking a patient to perform a mental imagery task in a magnetic resonance imaging (MRI) scanner

(17–24). These functional MRI (fMRI) motor imagery tasks are not confounded by speech or motor impairment and therefore may provide additional information about a patient's LoC that cannot be obtained by a behavioral assessment. Moreover, the magnitude, signal characteristics, and neuroanatomic location of brain activations detected by fMRI can be analyzed using predetermined objective algorithms that are independent of observer bias or variations in the administration and scoring of standardized behavioral measures. Several fMRI studies have identified persons with acute (24) and chronic (21, 25) DoC who demonstrate cognitive-motor dissociation (CMD) (26), which is defined by fMRI evidence of command following in the absence of behavioral evidence of command following.

Currently, there is a lack of consensus regarding which fMRI paradigms are best suited to elicit covert command following and hence a diagnosis of CMD. Although early studies used covert object naming (21), and some have employed covert counting of target words (27), most recent fMRI investigations have focused on spatial navigation and motor imagery tasks (e.g., imagine playing tennis, swimming, or squeezing the right or left hand) (17). For a review of tasks used to elicit command following in patients with DoC see Rossetti and Laureys (28) and Laureys and Schiff (29). In 2007, Boly and colleagues (30) compared the robustness of brain activation to four task-based fMRI imagery paradigms in healthy subjects: spatial navigation (imagine walking around the rooms of a house), auditory imagery (imagine a familiar song), motor imagery (imagine hitting a tennis ball), and visual imagery (imagine familiar faces). They found that the spatial navigation and tennis imagery tasks provided the most robust results in healthy subjects. Consequently, tennis motor imagery has been utilized frequently over the past decade to identify CMD in patients with DoC.

Although the fMRI tennis imagery task seems to be a viable complement to the bedside examination of patients with DoC, several studies have found high false-negative rates (FNRs) using this task (i.e., patient and healthy subjects who have behavioral evidence of command following do not demonstrate the expected activations on tennis imagery fMRI tasks) (17, 31). A hand squeezing motor imagery task has been used successfully in EEG studies (32, 33) and may be a more robust paradigm for use in the ICU, as it parallels the clinical bedside examination and may be less cognitively burdensome than imagining playing tennis. It remains unknown whether tennis playing imagery or hand squeezing imagery is a more effective paradigm for detecting conscious awareness.

Our aim in the present study was to compare fMRI activation in response to a tennis playing and hand squeezing paradigm in patients with traumatic DoC. The hand squeezing paradigm was

**Abbreviations:** DoC, disorders of consciousness; fMRI, functional magnetic resonance imaging; ICU, intensive care unit; LoC, level of consciousness; MCS±, minimally conscious state plus/minus; PTCS, post-traumatic confusional state; TBI, traumatic brain injury; UWS, unresponsive wakefulness syndrome.

chosen because it is a simple motor response that closely resembles the bedside behavioral examination, which often includes a “squeeze my hand” instruction to elicit command following. In addition, hand squeezing is more universal than playing tennis, which may be imagined differently and with varying intensity depending on an individual’s exposure to the sport. The hand squeezing task has been used successfully in other studies in acute and chronic DoC (24, 32, 33). We hypothesized that hand squeezing motor imagery will be detected with greater frequency than tennis playing motor imagery in patients diagnosed with acute and chronic traumatic DoC and in healthy controls.

## MATERIALS AND METHODS

### Experimental Design

This study was carried out in accordance with a protocol approved by the Partners Institutional Review Board. Patient surrogate decision-makers gave written informed consent in accordance with the Declaration of Helsinki. The patient cohort was prospectively recruited from an ICU, an outpatient follow-up neurology clinic, and an affiliated long-term acute hospital. Inclusion criteria were as follows: (1) age 18–65 years; and (2) head trauma with Glasgow Coma Scale score of 3–8 with no eye opening for at least 24 h after injury. Exclusion criteria were as follows: (1) life expectancy less than 6 months, as determined by a treating clinician; (2) prior severe brain injury or neurodegenerative disease; (3) penetrating TBI with intracranial metal or other body metal precluding MRI; and (4) no fluency in English prior to the injury (because the paradigms were administered in English).

Surrogate decision-makers were approached for consent  $\geq 24$  h after injury. For the ICU cohort, fMRI was performed as soon as the patient was clinically stable for transport to the MRI scanner, as determined by the treating ICU physicians and nurses. Patients with chronic DoC were scanned when they returned to the hospital for an outpatient clinic appointment or an inpatient hospitalization (e.g., for cranioplasty). Administration of sedative, anxiolytic, and/or analgesic medications was permitted for patient safety or comfort, at the discretion of the treating clinicians.

Age-matched healthy subjects were enrolled as a comparison group. Healthy subjects had no history of neurological, psychiatric, cardiovascular, pulmonary, renal, or endocrinological disease. They provided written informed consent and underwent the same fMRI protocols as the patients. All patient and healthy subject MRI scans were performed on the same scanner.

### Neurobehavioral Assessment

Demographic and clinical data were collected at the time of enrollment in accordance with the National Institutes of Health Common Data Element Guidelines for TBI.<sup>1</sup> LoC was characterized *via* behavioral evaluation with the CRS-R or based on criteria derived from the Confusion Assessment Protocol immediately prior to the fMRI (6, 34). Based on the CRS-R, each patient’s LoC was defined as coma (no arousal or

awareness), UWS (return of arousal but no awareness of self or the environment) (2, 3), or MCS (return of arousal and reliable but inconsistent evidence of awareness) (4). MCS was further subdivided into MCS– and MCS+ with the distinguishing feature being the presence of language function (i.e., at least one of the following: command following, object-recognition, or intelligible verbalization) in patients diagnosed as MCS+ (35, 36). Emergence from MCS was marked by recovery of either functional use of two common objects or basic accurate communication. The neurobehavioral assessment was conducted immediately prior to the fMRI scan. All behavioral evaluations were conducted by Brian L. Edlow.

### MRI Data Acquisition

Magnetic resonance imaging data were acquired with a 32-channel head coil on a 3 T Siemens Skyra MRI scanner (Siemens Medical Solutions, Erlangen, Germany) located in the Neurosciences ICU. Auditory stimuli were presented *via* MRI-compatible earphones (Newmatic Medical, Caledonia, MI, USA) connected to the scanner’s sound system. The blood-oxygen level dependent (BOLD) fMRI sequence utilized the following parameters: echo time (TE) = 30 ms, repetition time (TR) = 4,000 ms, in-plane resolution = 2.0 mm  $\times$  2.0 mm, slice thickness = 2 mm, interslice gap = 2.5 mm, matrix = 94  $\times$  94, field of view (FOV) = 192 mm  $\times$  192 mm, 49 slices, 2 $\times$  GRAPPA acceleration. Image acquisition parameters differed for one subject (P10) due to a change in the fMRI protocol motivated by decreasing scan time. For this subject, the fMRI sequence TE was reduced to 25 ms and TR to 3,000 ms. High-spatial resolution 3D T1-weighted multi-echo magnetization prepared gradient echo (MEMPRAGE) anatomical images were acquired for registration purposes (37): FOV = 256 mm  $\times$  256 mm, acquisition matrix = 256  $\times$  256, 176 sagittal slices (thickness 1 mm), 3 $\times$  GRAPPA acceleration, TE = 1.69, 3.55, 5.41, and 7.27 ms, TR = 2,530 ms, inversion time = 1,200–1,300 ms, 1.0 mm<sup>3</sup> isotropic resolution, and flip angle = 7°.

### fMRI Paradigms

Two fMRI motor imagery paradigms—hand squeezing and tennis playing—were performed as part of a larger fMRI and EEG study. fMRI data from the hand squeeze task have been previously reported for P1-5 and C1-10 (24). Each motor imagery fMRI paradigm utilized a block design and was comprised of two runs, with each run containing three 24-s rest blocks and two 24-s stimulation blocks. In total, 144 s of rest data and 96 s of stimulation data were analyzed for each paradigm. Prior to the first rest block, 36 s of data (9 s for P10) were acquired to obtain a stable baseline BOLD signal. These data were excluded from analysis.

The hand squeeze motor imagery task always preceded the tennis motor imagery task because the former paradigm was part of the primary aim of a larger study (24) and the latter paradigm was added as part of a secondary study aim after initiation of data collection. Similar to other studies in DoC (32, 33), subjects were instructed to imagine squeezing their right hand or to rest. During the task, instructions to “keep squeezing” or to “keep resting” were repeated at 6-s intervals. The tennis playing task

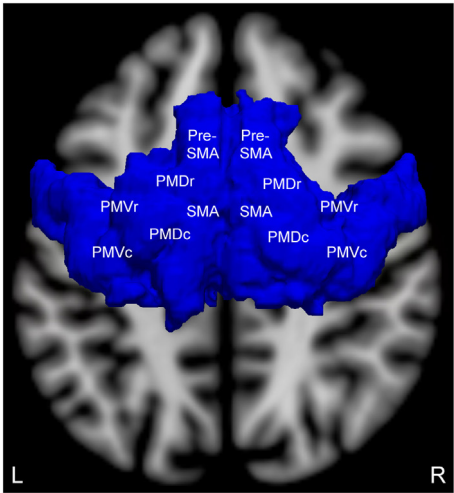
<sup>1</sup> <https://www.commondataelements.ninds.nih.gov>.

was identical to the hand squeezing task except that subjects were instructed to imagine playing tennis or to rest. During the task, instructions of “keep playing” or “keep resting” were repeated at 6-s intervals. Instructions administered before and during the fMRI are detailed in Table S1 in Supplementary Material.

fmRI Data Analysis

In a first-level analysis of the individual runs, fMRI data processing was performed using the FMRI Expert Analysis Tool (FEAT) version 6.00 in FSL 5.0.7 (FMRIB’s Software Library<sup>2</sup>). Motor imagery stimuli were contrasted against rest. Z statistic images

<sup>2</sup>www.fmrib.ox.ac.uk/fsl.



**FIGURE 1 |** Brodmann area 6 region of interest (superior view) for measuring motor imagery functional magnetic resonance imaging (fMRI) activation. This region of interest contains the supplementary motor area (SMA), pre-SMA, and the four components of the bilateral premotor cortices: premotor dorsal rostral (PMDr), premotor dorsal caudal (PMDc), premotor ventral rostral (PMVr), and premotor ventral caudal (PMVc). Adapted and reproduced with permission from Edlow et al. (24).

were thresholded ( $Z > 3.1$ ) and a corrected cluster significance threshold of  $P = 0.05$  was used. Higher-level analysis was carried out using a fixed effects model (FLAME in FSL) (38, 39). The statistical threshold for cluster significance ( $Z > 3.1$ ) and the size of the Gaussian kernel (FWHM 10 mm) were both selected to decrease false positive cluster activations (40). Additional details on analysis have been published elsewhere (24).

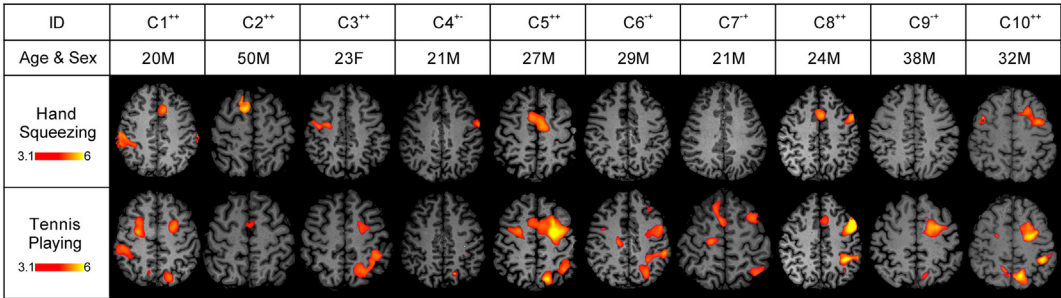
We used FEATQuery in FSL to quantify the percentage of voxels activated within a prespecified region of interest (ROI). For healthy subjects, we defined a positive response by the criterion that  $>0\%$  of ROI voxels met the aforementioned statistical threshold. For patients, we defined a positive response by two criteria, consistent with a recently proposed definition (24): (1)  $>0\%$  of ROI voxels met the statistical threshold; and (2) the percentage of activated ROI voxels was above the 2.5th percentile of a normal range (2.5th–97.5th percentile) derived from the healthy subjects’ data for each paradigm. This quantitative approach was completely automated and did not require subjective interpretation by clinical or research staff, thereby reducing potential bias that may have been introduced by knowledge of the patient’s behavioral diagnosis.

fmRI Regions of Interest

We selected an *a priori* ROI based upon fMRI studies of motor imagery in patients with chronic traumatic DoC and healthy subjects, as well as a recently published study of patients with acute traumatic DoC that used this same ROI (24). The bilateral supplementary motor areas (SMA) from the Harvard-Oxford Cortical Structural Atlas and premotor cortices (PMC) from the Juelich Histological Atlas (41) were combined as a single ROI (Figure 1). This ROI was transformed from standard atlas space into patient native fMRI space for analysis, consistent with prior fMRI studies of patients with DoC (17, 20, 24, 42, 43).

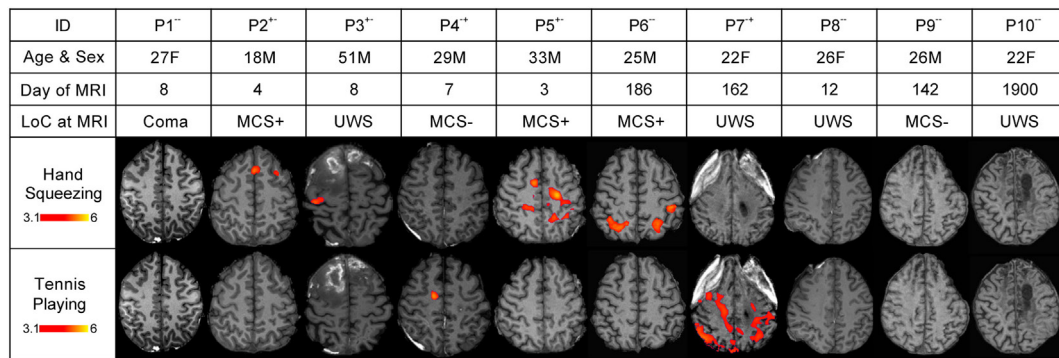
Statistical Analysis

Using the CRS-R as the reference standard and the motor imagery fMRI responses as the test criteria, we assessed the reliability of each paradigm in detecting behavioral evidence of command following by calculating the true-positive rate (TPR;

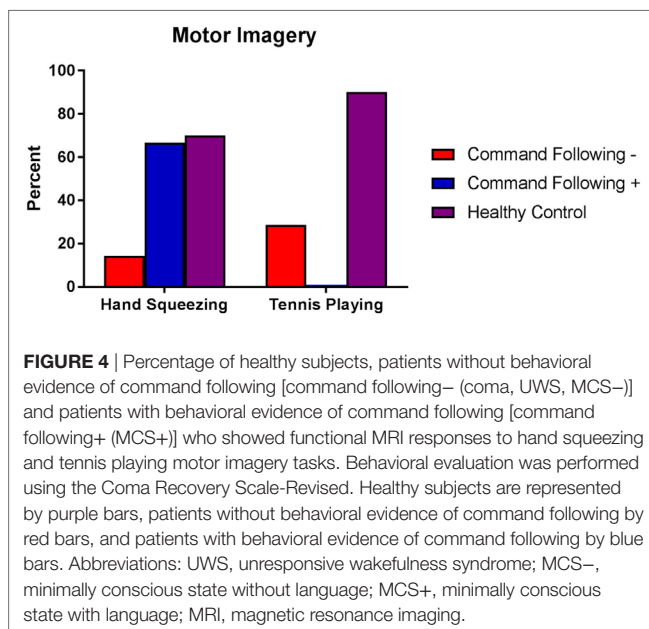


**FIGURE 2 |** Stimulus-based functional magnetic resonance imaging (fMRI) responses to hand squeezing and tennis playing motor imagery paradigms in healthy subjects. fMRI data are shown as Z-statistic images to demonstrate stimulus-specific responses. Z-Statistic images are thresholded at cluster-corrected Z scores of 3.1 (inset color bars) and superimposed upon T1-weighted axial images. In the row-labeled “ID,” a “+” indicates that an fMRI response was detected and a “–” indicates that an fMRI response was not detected during the hand squeezing and tennis playing motor imagery paradigms, respectively. Abbreviations: F, female; M, male. All images are in radiologic convention.





**FIGURE 3** | Stimulus-based functional magnetic resonance imaging (fMRI) responses to hand squeezing and tennis playing motor imagery paradigms in patients. fMRI data are shown as Z-statistic images to demonstrate stimulus-specific responses. Z-Statistic images are thresholded at cluster-corrected Z scores of 3.1 (inset color bars) and superimposed upon T1-weighted axial images. Level of consciousness (LoC) is assessed via behavioral evaluation with the Coma Recovery Scale-Revised as coma, unresponsive wakefulness syndrome (UWS), minimally conscious state without language (MCS-), or minimally conscious state with language (MCS+). In the row-labeled “ID,” a “+” indicates that an fMRI response was detected and a “-” indicates that an fMRI response was not detected during the hand squeezing and tennis playing motor imagery paradigms, respectively. Abbreviations: F, female; M, male. All images are in radiologic convention.



**FIGURE 4** | Percentage of healthy subjects, patients without behavioral evidence of command following [command following- (coma, UWS, MCS-)] and patients with behavioral evidence of command following [command following+ (MCS+)] who showed functional MRI responses to hand squeezing and tennis playing motor imagery tasks. Behavioral evaluation was performed using the Coma Recovery Scale-Revised. Healthy subjects are represented by purple bars, patients without behavioral evidence of command following by red bars, and patients with behavioral evidence of command following by blue bars. Abbreviations: UWS, unresponsive wakefulness syndrome; MCS-, minimally conscious state without language; MCS+, minimally conscious state with language; MRI, magnetic resonance imaging.

i.e. sensitivity), true-negative rate (TNR; i.e. specificity), FNR and the false-positive rate (FPR) with 95% exact confidence interval (CI) in the patient cohort. Notably, the FPR may include both false positives (i.e., patients wrongly identified on fMRI as being able to follow commands) and cases of dissociation between behavioral and fMRI responses (i.e., CMD caused by speech or motor impairments or other confounding factors). The accuracy (ACC) of each fMRI paradigm for detecting command following was calculated as  $(TP + TN)/(TP + FP + TN + FN)$ . We also calculated the TP proportions in the healthy subject cohort but not the other metrics because all healthy subjects exhibited behavioral evidence of command following.

We tested for an association between sedation (dichotomized as presence or absence) and fMRI responses, as well as between sedation and LoC at the time of fMRI (dichotomized as presence

or absence of command following), using a  $2 \times 2$  Fisher's Exact Test. Statistical analyses were performed in STATA v14s (44).

## RESULTS

### Demographics and Clinical Characteristics

Hand squeeze and tennis playing fMRI data were acquired in a convenience sample of 12 patients. One of these subjects was excluded due to severe artifact resulting from a ventriculoperitoneal shunt that prevented spatial normalization of the data. A second subject was excluded due to errors in the data acquisition of DICOM images. The final patient cohort included 10 subjects (six male, mean  $\pm$  age =  $27.9 \pm 9.1$ , six acute, one coma, four UWS, two MCS-, and three MCS+). Demographic and clinical data are presented in **Table 1**. Ten age-matched healthy subjects were recruited (nine male, mean  $\pm$  SD age =  $28.5 \pm 9.4$ , see Table S2 in Supplementary Material). There was no statistical difference in the proportion of males to females (chi-squared,  $P > 0.10$ ) or in the age of the subjects ( $t$ -test,  $P > 0.88$ ) between the patient and healthy subject groups.

### Hand Squeezing

Seven of the 10 healthy subjects demonstrated covert command following *via* the hand squeeze paradigm [70%, 95% exact CI: (34.8–93.3%), see **Table 2**, **Figures 2** and **4**. Three of the 10 patients demonstrated command following on the hand squeeze paradigm [30% (6.7–65.3), see **Table 3**, **Figures 3** and **4**. Of the three patients with behavioral evidence of command following on bedside examination, two demonstrated command following on the hand squeezing fMRI task (TP = 2/3, FN = 1/3). Of the seven patients without behavioral evidence of command following, one demonstrated command following on the hand squeeze paradigm (TN = 6/7, FP = 1/7). Consequently, the sensitivity and specificity of the hand squeeze paradigm for detecting behavioral evidence of command following were 66.7% (12.5–98.2) and 85.7% (42.1–99.6), respectively, and ACC = 80%.



**TABLE 1** | Patient demographics and clinical characteristics.

ID	Age (years)	Sex	TBI mechanism	iGCS	Day of fMRI	CRS-R at fMRI	CRS-R subscale scores at fMRI	LoC at fMRI
P1	27	F	Fall	3	8	1	A0V0M1O0C0Ar0	Coma
P2	18	M	Fall	3–7	4	12	A3V2M5O1C0Ar1	MCS+
P3	51	M	Ped vs. car	3	8	3	A0V0M1O1C0Ar1	UWS
P4	29	M	Ped vs. car	4–7	7	3	A0V0M3O0C0Ar0	MCS–
P5	33	M	Fall	3–4	3	12	A4V2M5O0C0Ar1	MCS+
P6	25	M	MVA	3–6 T	183	15	A4V3M3O2C1Ar2	MCS +
P7	22	F	Ped vs. car	3–3 T	162	5	A1V1M1O1C0Ar1	UWS
P8	26	F	Ped vs. truck	3–3 T	12	2	A0V0M1O0C0Ar1	UWS
P9	26	M	MVA	3	142	8	A1V1M3O2C0Ar1	MCS–
P10	22	F	MVA	3	1,900	5	A1V0M2O1C0Ar1	UWS

The initial GCS (iGCS) is a range defined by the best (i.e., highest) and worst (i.e., lowest) post-resuscitation GCS scores assessed by a qualified clinician who performed a reliable examination (not confounded by sedation and/or paralytics) prior to ICU admission. LoC is assessed immediately prior to fMRI via behavioral evaluation with the CRS-R as coma, UWS, MCS–, or MCS+. The subscales for the CRS-R are auditory function (A), visual function (V), motor function (M), oromotor function (O), communication (C), and arousal (Ar). CRS-R, Coma Recovery Scale-Revised; F, female; fMRI, functional MRI; GCS, Glasgow Coma Scale; LoC, level of consciousness; M, male; MCS–, minimally conscious state without language; MCS+, minimally conscious state with language; MVA, motor vehicle accident; Ped, pedestrian; T, intubated; TBI, traumatic brain injury; UWS, unresponsive wakefulness syndrome.

**TABLE 2** | Healthy control subject fMRI responses to hand squeeze and tennis motor imagery.

ID	Hand squeezing	Tennis playing
C1		+
C2	+	+
C3	+	+
C4	+	–
C5	+	+
C6	–	+
C7	–	+
C8	+	+
C9	–	+
C10	+	+
Total percent (95% exact CI)	70% (34.8–93.3)	90% (55.5–99.7)

CI, confidence interval; fMRI, functional magnetic resonance imaging.

**TABLE 3** | Patient fMRI responses to hand squeeze and tennis motor imagery.

ID	LoC at fMRI	Hand squeezing	Tennis playing
P1 <sup>a</sup>	Coma	–	–
P2 <sup>a</sup>	MCS+	+	–
P3 <sup>a</sup>	UWS	+	–
P4 <sup>a</sup>	MCS–	–	+
P5 <sup>a</sup>	MCS+	+	–
P6	MCS+	–	–
P7	UWS	–	+
P8	UWS	–	–
P9	MCS–	–	–
P10	UWS	–	–
Total percent (95% exact CI)		30% (6.7–65.3)	20% (2.5–55.6)
Sensitivity (95% exact CI)		66.7% (12.5–98.2)	0% (0–70.8)
Specificity (95% exact CI)		85.7% (42.1–99.6)	71.4% (29.0–96.3)
Accuracy		80%	50%

Sensitivity, specificity, and accuracy of motor imagery paradigm detection of command following in patients who demonstrated behavioral evidence of command following.

fMRI, functional magnetic resonance imaging; LoC, level of consciousness; MCS–, minimally conscious state without language; MCS+, minimally conscious state with language; UWS, unresponsive wakefulness syndrome; CI, confidence interval.

<sup>a</sup>The patient was receiving sedatives at the time of data acquisition (see Table S3 in Supplementary Material for details). Image acquisition parameters for P10 differed from those of the other subjects (see Materials and Methods for details).

## Tennis Playing

Nine of the 10 healthy subjects demonstrated command following *via* the tennis playing paradigm [90% (55.5–99.7)]. Two of the 10 patients demonstrated command following on the tennis playing paradigm [20% (2.5–55.6)]. Of the three patients with behavioral evidence of command following on bedside examination, none demonstrated command following on the tennis playing imagery paradigm (TP = 0/3, FN = 3/3). Of the seven patients without behavioral evidence of command following, two demonstrated command following on the tennis playing motor imagery paradigm (TN = 5/7, FP = 2/7). The sensitivity and specificity for the tennis playing paradigm for detecting behavioral evidence of command following were 0% (0–70.8) and 71.4% (29.0–96.3), respectively, and ACC = 50%.

The agreement between presence or absence of command following *via* hand squeezing and tennis playing imagery was 60% in healthy subjects and 50% in patients. Data on the percentage of voxels activated for each subject in each paradigm are presented in Tables S2 and S4 in Supplementary Material for healthy subjects and patients, respectively. For both the hand squeeze and tennis imagery paradigms, at least one healthy subject demonstrated 0% activated voxels. Therefore, all patients with >0% activated voxels in each paradigm met the predetermined criteria for having a positive response to the fMRI tasks (i.e., the ROI had >0% activated voxels and the percentage of activated voxels in the ROI exceeded the 2.5th percentile of the normal range in healthy subjects).

## Effect of Sedation on Behavioral Diagnosis and fMRI Responses

Administration of sedation ( $n = 5$ ) was not associated with LoC or fMRI responses at the time of fMRI (Fisher's Exact Test,  $df = 1$ ;  $P = 0.17$ – $0.99$  for all analyses). The types and doses of sedative, anxiolytic, and analgesic medications administered at the time of fMRI are reported in Table S3 in Supplementary Material.

## DISCUSSION

Precise assessment of LoC in patients with severe TBI is critical for guiding clinical management, providing accurate prognoses, and

gaining access to rehabilitative services. Assessment of command following is a central component of the bedside examination and diagnostic impression. However, behavioral bedside assessment is susceptible to patient-, environment-, and examiner-related biases that contribute to the high misdiagnosis rate in this patient population. Multiple fMRI paradigms that probe covert consciousness have been investigated as potential objective markers of command following, but few studies have compared the utility of these paradigms concurrently in the same patient sample (31). Head-to-head comparison of fMRI command following tasks is needed to guide paradigm selection in future studies and eventually clinical practice. In addition, defining intrasubject variability would provide an objective basis for the cautious interpretation of absent fMRI responses to motor imagery paradigms. In this study, we assessed the sensitivity, specificity, and ACC of hand squeezing and tennis playing motor imagery paradigms in a sample of patients with severe TBI whose behavioral diagnosis at the time of the fMRI was coma, UWS, or MCS.

Although the tennis paradigm had higher ACC for detecting covert command following in healthy subjects, the hand squeezing paradigm accurately identified two of three patients who demonstrated behavioral evidence of command following (MCS+) as well as one patient (UWS) who did not. Conversely, responses to the tennis paradigm were absent in all three patients who demonstrated behavioral evidence of command following and present in two (MCS-, UWS) who did not. The sensitivity and specificity, and ACC of these findings suggest that the hand squeezing paradigm is a better classifier of command following in patients who are known to follow commands at the bedside than is the tennis playing paradigm.

One objective of developing fMRI paradigms for detection of conscious awareness in DoC is the prospect of identifying patients who retain the cognitive capacity for command following but do not demonstrate it at the bedside due to confounding factors such as impairments in speech or motor function. This cohort, described as having CMD (24, 26), is at risk for early withdrawal of life-sustaining therapies and denial of access to rehabilitative care. Our tennis playing paradigm identified two such patients, neither of whom showed fMRI responses to the hand squeezing paradigm, while the hand squeezing paradigm identified one such patient. For the purpose of this study, which focused on identifying the fMRI paradigm that best detects command following and therefore tried to maximize the TPR, these patients were included in the “false positive” group when calculating specificity and ACC. However, rather than the fMRI findings being “false positives,” it is possible that these three patients retained the cognitive capacity for command following but only demonstrated it on one of the two fMRI paradigms and not on bedside evaluation. Thus, the rate of detecting CMD was higher for the tennis playing paradigm than hand squeezing, even though the hand squeezing paradigm identified patients with behavioral evidence of command following with a higher ACC than did tennis. Future studies should address this apparent discrepancy between overall ACC and CMD detection rate by increasing the sample size, increasing the number of experimental runs, and interleaving the presentation of the fMRI paradigms. When possible, administering more than one

type of command following paradigm should be considered to maximize the probability of detecting conscious awareness.

The tennis playing paradigm performed better than the hand squeezing task in the healthy control group while the opposite was true for patients. Comparison of fMRI activation profiles between healthy subjects and brain-injured patients must be performed with caution, given the multitude of factors that may influence an individual's fMRI response. For example, in healthy subjects, playing tennis, whether on the court or in one's imagination, may be a more cognitively challenging and salient task compared to a mundane hand-squeezing task. Conversely, hand squeezing may become more salient in a brain-injured patient who is asked to perform this task frequently during neurological examinations in the ICU. Furthermore, it is likely that imagining playing tennis requires multimodal processing and therefore would be expected to evoke a more distributed network than the unimodal task of imagining squeezing one's hand. If so, patients, as compared to healthy subjects, may have access to less of the distributed network required to mediate tennis imagery due to focal lesions and loss of connectivity. For those patients who are able to cognitively perform the task, the frequent repetition of the command in the clinical environment may be associated with a mental training effect and/or an increased effort applied to the task and hence a more robust fMRI response (45). It is also possible that the patients who followed commands at the bedside were actually squeezing their hand in the scanner, rather than imagining the movement, leading to more robust SMA/PMC activation. In this study, we did not systematically record hand movements during the scanning session. Future studies that compare fMRI paradigms in this patient population should consider incorporating visual or electromyographic monitoring into their paradigm.

Several limitations should be considered when interpreting the results of this study. First, although this is one of the only studies that compares the ACC of fMRI motor imagery paradigms in a patient cohort, the sample size is small and includes patients in both acute and chronic phases of recovery. Consequently, generalizing our findings to other patient groups should be done with caution and future investigations should consider larger sample sizes of more homogenous patient groups enrolled across multiple sites. Second, the CIs around the fMRI command following proportions are very wide, suggesting that our sample has high variability and that the findings may lack precision when compared to the overall population of patients with traumatic DoC. Third, at the time of the fMRI scan, several subjects were receiving pharmacological sedation. Sedatives were administered at the discretion of the treating clinicians for patient safety or comfort and therefore could not be lifted for this study. Indeed, even patients who are comatose may require sedation to treat bronchospasm caused by an endotracheal tube. Sedation is therefore a medical necessity for some critically ill patients, and it is therefore unlikely that any fMRI study of critically ill patients that aims to be generalizable will be able to exclude patients receiving sedation.

Although the effects of sedating agents on cortical responses (46) and connectivity (47) are beginning to be elucidated, the impact of these pharmacological interventions may vary with multiple patient-specific factors, including tolerance, body mass,

and metabolism. Furthermore, standardized sedation rating scales that have been validated in non-brain injured critically ill patients (e.g., the Richmond Agitation Sedation Scale) (48) are not applicable in severely brain-injured patients, for whom the behavioral effects of sedation cannot be quantitatively distinguished from the behavioral effects of the brain injury itself. As a result, we could not quantitatively measure the effect of sedation for each patient prior to scanning. Therefore, despite the lack of a statistical association between sedation and fMRI responsiveness, it is still possible that sedation affected the fMRI responses, though the results of the hand and tennis motor imagery paradigms would have been affected equally as all data were collected during the same scanning session.

Finally, we could not avoid some methodological challenges such as the hand squeezing motor imagery task always preceding the tennis playing motor imagery task. Though our findings do not suggest that this fixed order contributed to systematically poor arousal and therefore decreased fMRI responses to the tennis playing paradigm, future studies should consider randomizing the presentation of the tasks. In addition, imaging parameters for one patient, who did not show responses to either paradigm, did not conform to those of the other subjects, potentially adding variability to the data. The examiner completing the behavioral assessments for this study was not blinded to the previously determined clinical diagnosis of the patient (i.e., the diagnosis of LoC rendered by the treating physicians and nurses) and the investigator conducting the imaging analysis was not blinded to the behavioral assessment. Therefore, it is possible that the clinical diagnosis biased the behavioral assessment reported here and that, despite the automated nature of the imaging analysis, the behavioral assessment influenced the fMRI results. To avoid this potential limitation in the future, the behavioral assessment completed for study purposes should be conducted by an examiner who is not involved in the clinical care of the patient or in screening patients for inclusion in the study and the investigator conducting the imaging analysis should be blinded to the behavioral diagnosis. Finally, despite recent evidence supporting the need for serial behavioral assessment of LoC to improve diagnostic accuracy (16), we were only able to administer one CRS-R prior to the fMRI study due to the medical instability of the acutely ill patients and the limited time available to examine chronic patients returning for clinical follow-up. Future studies should aim to administer multiple behavioral assessments to establish the diagnostic baseline.

It is important to note that there was poor agreement between fMRI responses occurring during the hand squeezing and tennis playing fMRI squeezing tasks in both healthy subjects and patients. Specifically, all the healthy subjects who failed to demonstrate an fMRI response to hand squeezing or tennis imagery did show an fMRI response to the other paradigm. All of the patients who demonstrated an fMRI response to hand squeezing or tennis playing failed to show an fMRI response to the other paradigm. Fluctuation in arousal, task characteristics, prior exposure to the sport, and intersubject variability may have contributed to the inconsistencies in these findings. Future studies could consider individualizing the task such that it matches each participant's

experiences or interviewing participants and surrogates to ascertain prior exposure.

In choosing the appropriate task for detecting consciousness in patients diagnosed with DoC, investigators should carefully consider the research aims because a series of decisions (e.g., paradigm, analytic pipeline, and interpretation algorithm) related to the specific question of interest may alter the study design and findings. Furthermore, factors unrelated to cognitive ability, such as subject familiarity with the imagined task (e.g., a patient who has played tennis may be more responsive than a patient who has only watched the game on television) and analytic strategies (e.g., objective application of *a priori* ROIs versus subjective reading of fMRI activation maps) may introduce uncertainty into the data. Thus, different fMRI paradigms may lead to variable results in the same patient. We found that in patients with severe TBI diagnosed with DoC, the hand squeezing motor imagery paradigm detected covert command following with greater ACC than the tennis playing paradigm. However, the tennis playing paradigm was more sensitive in healthy subjects and identified more patients with CMD. These findings should be considered hypothesis-generating and will require replication in a larger sample of patients across multiple clinical and research sites. Clinical implementation of fMRI motor imagery paradigms for detection of consciousness will require further development, validation, and optimization of standardized approaches to fMRI data acquisition, analysis and interpretation.

## ETHICS STATEMENT

This study was carried out in accordance with a protocol approved by the Partners Institutional Review Board. Patient surrogate decision-makers gave written informed consent in accordance with the Declaration of Helsinki.

## AUTHOR CONTRIBUTIONS

The authors contributed to the following aspects of the study: YB, JG, and BE: substantial contributions to the conception or design of the work; or the acquisition, analysis, or interpretation of data for the work; drafting the work or revising it critically for important intellectual content; final approval of the version to be published; and agreement to be accountable for all aspects of the work in ensuring that questions related to the accuracy or integrity of any part of the work are appropriately investigated and resolved.

## ACKNOWLEDGMENTS

The authors thank the nursing staffs of the Massachusetts General Hospital Neurosciences ICU, Multidisciplinary ICU, and the Surgical ICU. We also thank Kellie Cahill and the MRI technologists for their assistance with data acquisition. We would like to acknowledge Dylan Tisdall and Andre van der Kouwe (Athinoula A Martinos Center for Biomedical Imaging) and Himanshu Bhat (Siemens Medical Center) for the provision of WIP711D (vNav Motion-Corrected Multiecho MPAGE) used to acquire MEMPRAGE data. We are grateful to the patients and

families in this study for their participation and support. This work was supported by grants from the National Institutes of Health (K23NS094538), the Center for Integration of Medicine & Innovative Technology (Boston, MA, USA), the American Academy of Neurology/American Brain Foundation, the James S. McDonnell Foundation, the Massachusetts General Hospital Department of Neurology and Division of Neurocritical Care and Emergency Neurology, and the National Institute on

Disability, Independent Living, and Rehabilitation Research (NIDILRR).

## SUPPLEMENTARY MATERIAL

The Supplementary Material for this article can be found online at <http://www.frontiersin.org/articles/10.3389/fneur.2017.00688/full#supplementary-material>.

## REFERENCES

- Jennett B, Plum F. Persistent vegetative state after brain damage. A syndrome in search of a name. *Lancet* (1972) 1(7753):734–7. doi:10.1016/S0140-6736(72)90242-5
- Giacino JT, Kalmar K. Diagnostic and prognostic guidelines for the vegetative and minimally conscious states. *Neuropsychol Rehabil* (2005) 15(3–4):166–74. doi:10.1080/09602010443000498
- Laureys S, Celesia GG, Cohadon F, Lavrijns J, Leon-Carrion J, Sannita WG, et al. Unresponsive wakefulness syndrome: a new name for the vegetative state or apallic syndrome. *BMC Med* (2010) 8(1):68. doi:10.1186/1741-7015-8-68
- Giacino JT, Ashwal S, Childs N, Cranford R, Jennett B, Katz DI, et al. The minimally conscious state: definition and diagnostic criteria. *Neurology* (2002) 58(3):349–53. doi:10.1212/WNL.58.3.349
- Nakase-Thompson R, Sherer M, Yablon SA, Nick TG, Trzepacz PT. Acute confusion following traumatic brain injury. *Brain Inj* (2004) 18(2):131–42. doi:10.1080/0269905031000149542
- Sherer M, Nakase-Thompson R, Yablon SA, Gontkovsky ST. Multidimensional assessment of acute confusion after traumatic brain injury. *Arch Phys Med Rehabil* (2005) 86(5):896–904. doi:10.1016/j.apmr.2004.09.029
- Hirschberg R, Giacino JT. The vegetative and minimally conscious states: diagnosis, prognosis and treatment. *Neurol Clin* (2011) 29(4):773–86. doi:10.1016/j.ncl.2011.07.009
- Nakase-Richardson R, Whyte J, Giacino JT, Pavawalla S, Barnett SD, Yablon SA, et al. Longitudinal outcome of patients with disordered consciousness in the NIDRR TBI model systems programs. *J Neurotrauma* (2012) 29(1):59–65. doi:10.1089/neu.2011.1829
- Whyte J, Nakase-Richardson R, Hammond FM, McNamee S, Giacino JT, Kalmar K, et al. Functional outcomes in traumatic disorders of consciousness: 5-Year outcomes from the national institute on disability and rehabilitation research traumatic brain injury model systems. *Arch Phys Med Rehabil* (2013) 94(10):1855–60. doi:10.1016/j.apmr.2012.10.041
- Giacino JT, Kalmar K. The vegetative and minimally conscious states: a comparison of clinical features and functional outcome. *J Head Trauma Rehabil* (1997) 12(4):36–51. doi:10.1097/00001199-199708000-00005
- Wannez S, Hoyoux T, Langohr T, Bodart O, Martial C, Wertz J, et al. Objective assessment of visual pursuit in patients with disorders of consciousness: an exploratory study. *J Neurol* (2017) 264(5):928–37. doi:10.1007/s00415-017-8469-0
- Schnakers C, Vanhaudenhuyse A, Giacino J, Ventura M, Boly M, Majerus S, et al. Diagnostic accuracy of the vegetative and minimally conscious state: clinical consensus versus standardized neurobehavioral assessment. *BMC Neurol* (2009) 9:35. doi:10.1186/1471-2377-9-35
- Andrews K, Murphy L, Munday R, Littlewood C. Misdiagnosis of the vegetative state: retrospective study in a rehabilitation unit. *BMJ* (1996) 313(7048):13–6. doi:10.1136/bmj.313.7048.13
- Childs NL, Mercer WN, Childs HW. Accuracy of diagnosis of persistent vegetative state. *Neurology* (1993) 43(8):1465–7. doi:10.1212/WNL.43.8.1465
- Kalmar K, Giacino JT. The JFK coma recovery scale – revised. *Neuropsychol Rehabil* (2005) 15(3–4):454–60. doi:10.1080/09602010443000425
- Wannez S, Heine L, Thonnard M, Gosseries O, Laureys S, Coma Science Group Collaborators. The repetition of behavioral assessments in diagnosis of disorders of consciousness: repeated CRS-R assessments for diagnosis in DOC. *Ann Neurol* (2017) 81(6):883–9. doi:10.1002/ana.24962
- Monti MM, Vanhaudenhuyse A, Coleman MR, Boly M, Pickard JD, Tshibanda L, et al. Willful modulation of brain activity in disorders of consciousness. *N Engl J Med* (2010) 362(7):579–89. doi:10.1056/NEJMoa0905370
- Coleman MR, Bekinschtein T, Monti MM, Owen AM, Pickard JD. A multimodal approach to the assessment of patients with disorders of consciousness. *Prog Brain Res* (2009) 177:231–48. doi:10.1016/S0079-6123(09)17716-6
- Owen AM, Coleman MR, Boly M, Davis MH, Laureys S, Pickard JD. Detecting awareness in the vegetative state. *Science* (2006) 313(5792):1402. doi:10.1126/science.1130197
- Coleman MR, Davis MH, Rodd JM, Robson T, Ali A, Owen AM, et al. Towards the routine use of brain imaging to aid the clinical diagnosis of disorders of consciousness. *Brain* (2009) 132(9):2541–52. doi:10.1093/brain/awp183
- Rodriguez Moreno D, Schiff ND, Giacino J, Kalmar K, Hirsch J. A network approach to assessing cognition in disorders of consciousness. *Neurology* (2010) 75(21):1871–8. doi:10.1212/WNL.0b013e3181feb259
- Di H, Boly M, Weng X, Ledoux D, Laureys S. Neuroimaging activation studies in the vegetative state: predictors of recovery? *Clin Med (Lond)* (2008) 8(5):502–7. doi:10.7861/clinmedicine.8-5-502
- Giacino JT, Hirsch J, Schiff N, Laureys S. Functional neuroimaging applications for assessment and rehabilitation planning in patients with disorders of consciousness. *Arch Phys Med Rehabil* (2006) 87(12 Suppl 2):S67–76. doi:10.1016/j.apmr.2006.07.272
- Edlow BL, Chatelle C, Spencer CA, Chu CJ, Bodien YG, O'Connor KL, et al. Early detection of consciousness in patients with acute severe traumatic brain injury. *Brain* (2017) 140(9):2399–414. doi:10.1093/brain/awx176
- Schiff ND, Rodriguez-Moreno D, Kamal A, Kim KHS, Giacino JT, Plum F, et al. fMRI reveals large-scale network activation in minimally conscious patients. *Neurology* (2005) 64(3):514–23. doi:10.1212/01.WNL.0000150883.10285.44
- Schiff ND. Cognitive motor dissociation following severe brain injuries. *JAMA Neurol* (2015) 72(12):1413. doi:10.1001/jamaneurol.2015.2899
- Naci L, Owen AM. Making every word count for nonresponsive patients. *JAMA Neurol* (2013) 70(10):1235–41. doi:10.1001/jamaneurol.2013.3686
- Rossetti AO, Laureys S. *Clinical Neurophysiology in Disorders of Consciousness Brain Function Monitoring in the ICU and Beyond [Internet]*. Vienna: Springer (2015). Available from: <http://ezproxy.unav.es:2048/login?url=http://link.springer.com/book/>
- Laureys S, Schiff ND. Coma and consciousness: paradigms (re)framed by neuroimaging. *Neuroimage* (2012) 61(2):478–91. doi:10.1016/j.neuroimage.2011.12.041
- Boly M, Coleman MR, Davis MH, Hampshire A, Bor D, Moonen G, et al. When thoughts become action: an fMRI paradigm to study volitional brain activity in non-communicative brain injured patients. *Neuroimage* (2007) 36(3):979–92. doi:10.1016/j.neuroimage.2007.02.047
- Gibson RM, Fernandez-Espejo D, Gonzalez-Lara LE, Kwan BY, Lee DH, Owen AM, et al. Multiple tasks and neuroimaging modalities increase the likelihood of detecting covert awareness in patients with disorders of consciousness. *Front Hum Neurosci* (2014) 8:950. doi:10.3389/fnhum.2014.00950
- Cruse D, Chennu S, Chatelle C, Bekinschtein TA, Fernández-Espejo D, Pickard JD, et al. Bedside detection of awareness in the vegetative state: a cohort study. *Lancet* (2011) 378(9809):2088–94. doi:10.1016/S0140-6736(11)61224-5
- Cruse D, Chennu S, Chatelle C, Fernandez-Espejo D, Bekinschtein TA, Pickard JD, et al. Relationship between etiology and covert cognition in the minimally conscious state. *Neurology* (2012) 78(11):816–22. doi:10.1212/WNL.0b013e318249f764



34. Giacino JT, Kalmar K, Whyte J. The JFK coma recovery scale-revised: measurement characteristics and diagnostic utility. *Arch Phys Med Rehabil* (2004) 85(12):2020–9. doi:10.1016/j.apmr.2004.02.033
35. Bruno M-A, Majerus S, Boly M, Vanhaudenhuyse A, Schnakers C, Gosseries O, et al. Functional neuroanatomy underlying the clinical subcategorization of minimally conscious state patients. *J Neurol* (2012) 259(6):1087–98. doi:10.1007/s00415-011-6303-7
36. Bruno M-A, Vanhaudenhuyse A, Thibaut A, Moonen G, Laureys S. From unresponsive wakefulness to minimally conscious PLUS and functional locked-in syndromes: recent advances in our understanding of disorders of consciousness. *J Neurol* (2011) 258(7):1373–84. doi:10.1007/s00415-011-6114-x
37. van der Kouwe AJW, Benner T, Salat DH, Fischl B. Brain morphometry with multiecho MPRAGE. *Neuroimage* (2008) 40(2):559–69. doi:10.1016/j.neuroimage.2007.12.025
38. Beckmann CF, Jenkinson M, Smith SM. General multilevel linear modeling for group analysis in fMRI. *Neuroimage* (2003) 20(2):1052–63. doi:10.1016/S1053-8119(03)00435-X
39. Woolrich MW, Behrens TEJ, Beckmann CF, Jenkinson M, Smith SM. Multilevel linear modelling for fMRI group analysis using Bayesian inference. *Neuroimage* (2004) 21(4):1732–47. doi:10.1016/j.neuroimage.2003.12.023
40. Eklund A, Nichols TE, Knutsson H. Cluster failure: why fMRI inferences for spatial extent have inflated false-positive rates. *Proc Natl Acad Sci U S A* (2016) 113(28):7900–5. doi:10.1073/pnas.1602413113
41. Eickhoff SB, Stephan KE, Mohlberg H, Grefkes C, Fink GR, Amunts K, et al. A new SPM toolbox for combining probabilistic cytoarchitectonic maps and functional imaging data. *Neuroimage* (2005) 25(4):1325–35. doi:10.1016/j.neuroimage.2004.12.034
42. Fernández-Espejo D, Junqué C, Vendrell P, Bernabeu M, Roig T, Bargalló N, et al. Cerebral response to speech in vegetative and minimally conscious states after traumatic brain injury. *Brain Inj* (2008) 22(11):882–90. doi:10.1080/02699050802403573
43. Bardin JC, Fins JJ, Katz DI, Hersh J, Heier LA, Tabelow K, et al. Dissociations between behavioural and functional magnetic resonance imaging-based evaluations of cognitive function after brain injury. *Brain* (2011) 134(3):769–82. doi:10.1093/brain/awr005
44. StataCorp. *Stata Statistical Software: Release*. College Station, TX: StatCorp LP (2015).
45. Kami A, Meyer G, Jezzard P, Adams MM, Turner R, Ungerleider LG. Functional MRI evidence for adult motor cortex plasticity during motor skill learning. *Nature* (1995) 377(6545):155–8. doi:10.1038/377155a0
46. Davis MH, Coleman MR, Absalom AR, Rodd JM, Johnsrude IS, Matta BF, et al. Dissociating speech perception and comprehension at reduced levels of awareness. *Proc Natl Acad Sci U S A* (2007) 104(41):16032–7. doi:10.1073/pnas.0701309104
47. Kirsch M, Guldenmund P, Ali Bahri M, Demertzi A, Baquero K, Heine L, et al. Sedation of patients with disorders of consciousness during neuroimaging: effects on resting state functional brain connectivity. *Anesth Analg* (2017) 124(2):588–98. doi:10.1213/ANE.0000000000001721
48. Sessler CN, Gosnell MS, Grap MJ, Brophy GM, O'Neal PV, Keane KA, et al. The Richmond Agitation-Sedation Scale: validity and reliability in adult intensive care unit patients. *Am J Respir Crit Care Med* (2002) 166(10):1338–44. doi:10.1164/rccm.2107138

**Conflict of Interest Statement:** The authors declare that the research was conducted in the absence of any commercial or financial relationships that could be construed as a potential conflict of interest.

Copyright © 2017 Bodien, Giacino and Edlow. This is an open-access article distributed under the terms of the Creative Commons Attribution License (CC BY). The use, distribution or reproduction in other forums is permitted, provided the original author(s) or licensor are credited and that the original publication in this journal is cited, in accordance with accepted academic practice. No use, distribution or reproduction is permitted which does not comply with these terms.





# Do Patients Thought to Lack Consciousness Retain the Capacity for Internal as Well as External Awareness?

Amelie Haugg<sup>1,2</sup>, Rhodri Cusack<sup>3</sup>, Laura E. Gonzalez-Lara<sup>4</sup>, Bettina Sorger<sup>5</sup>, Adrian M. Owen<sup>4</sup> and Lorina Naci<sup>3\*</sup>

<sup>1</sup> Department of Psychiatry, Psychotherapy and Psychosomatics, Psychiatric Hospital, University of Zurich, Zurich, Switzerland, <sup>2</sup> Neuroscience Center Zurich, Swiss Federal Institute of Technology, University of Zurich, Zurich, Switzerland, <sup>3</sup> School of Psychology, Trinity College Institute of Neuroscience, Trinity College Dublin, Dublin, Ireland, <sup>4</sup> The Brain and Mind Institute, University of Western Ontario, London, ON, Canada, <sup>5</sup> Faculty of Psychology and Neuroscience, Maastricht University, Maastricht, Netherlands

## OPEN ACCESS

### Edited by:

Olivia Gosseries,  
University of Liège, Belgium

### Reviewed by:

Martin Monti,  
UCLA Department of Psychology,  
United States  
Yuzheng Hu,  
National Institute on Drug Abuse  
(NIDA), United States

### \*Correspondence:

Lorina Naci  
naci@tcd.ie

### Specialty section:

This article was submitted to  
Applied Neuroimaging,  
a section of the journal  
Frontiers in Neurology

**Received:** 26 January 2018

**Accepted:** 06 June 2018

**Published:** 27 June 2018

### Citation:

Haugg A, Cusack R,  
Gonzalez-Lara LE, Sorger B,  
Owen AM and Naci L (2018) Do  
Patients Thought to Lack  
Consciousness Retain the Capacity  
for Internal as Well as External  
Awareness? *Front. Neurol.* 9:492.  
doi: 10.3389/fneur.2018.00492

It is well established that some patients, who are deemed to have disorders of consciousness, remain entirely behaviorally non-responsive and are diagnosed as being in a vegetative state, yet can nevertheless demonstrate covert awareness of their external environment by modulating their brain activity, a phenomenon known as cognitive-motor dissociation. However, the extent to which these patients retain internal awareness remains unknown. To investigate the potential for internal and external awareness in patients with chronic disorders of consciousness (DoC), we asked whether the pattern of juxtaposition between the functional time-courses of the default mode (DMN) and fronto-parietal networks, shown in healthy individuals to mediate the naturally occurring dominance switching between internal and external aspects of consciousness, was present in these patients. We used a highly engaging movie by Alfred Hitchcock to drive the recruitment of the fronto-parietal networks, including the dorsal attention (DAN) and executive control (ECN) networks, and their maximal juxtaposition to the DMN in response to the complex stimulus, relative to rest and a scrambled, meaningless movie baseline condition. We tested a control group of healthy participants ( $N = 13/12$ ) and two groups of patients with disorders of consciousness, one comprised of patients who demonstrated independent, neuroimaging-based evidence of covert external awareness ( $N = 8$ ), and the other of those who did not ( $N = 8$ ). Similarly to the healthy controls, only the group of patients with overt and, critically, covert external awareness showed significantly heightened differentiation between the DMN and the DAN in response to movie viewing relative to their resting state time-courses, which was driven by the movie's narrative. This result suggested the presence of functional integrity in the DMN and fronto-parietal networks and their relationship to one another in patients with covert external awareness. Similar to the effect in healthy controls, these networks became more strongly juxtaposed to one another in response to movie viewing relative to the baseline

conditions, suggesting the *potential* for internal and external awareness during complex stimulus processing. Furthermore, our results suggest that naturalistic paradigms can dissociate between groups of DoC patients with and without covert awareness based on the functional integrity of brain networks.

**Keywords:** functional Magnetic Resonance Imaging (fMRI), functional connectivity, disorders of consciousness, naturalistic stimulation, movie watching, conscious information processing

## INTRODUCTION

In the last decade, a population of patients has been identified who are demonstrably conscious, but entirely unable to speak or move willfully in any way, and remain behaviorally non-responsive for several years (1–8). Following severe brain-injury, patients may manifest a spectrum of behavioral non-responsivity, from a complete absence to minimal and inconsistent willful behavioral responses (9–11). Patients who do not show any willful behavioral responses on repeated behavioral examinations, are thought to lack awareness of oneself and one's environment and are clinically diagnosed to be in a vegetative state (VS) (12), also known as the “unresponsive wakefulness syndrome” (UWS) (13). The clinical, behavioral assessment of non-responsive patients is particularly difficult because of its reliance on the subjective interpretation of inconsistent behaviors, which are often limited by motor constraints, and can result in high misdiagnosis rates (up to 43%) (14). Recent studies have shown that, despite the complete absence of external signs of awareness, a significant minority (~14–19%) of patients thought to be in a VS are able to demonstrate conscious awareness by modulating their brain activity (2, 15) in different types of neuroimaging paradigms [e.g., (1, 3–5, 7, 8)], a phenomenon captured by the recently-coined term “cognitive motor dissociation” (CMD) (16). Despite these advances, the mental life of behaviorally non-responsive patients—particularly their capacity to have similar experiences as healthy individuals in response to everyday life events that involve both their *awareness of oneself* and *awareness of one's environment*—had until recently remained largely unknown and inaccessible to empirical investigation.

To address this challenge, Naci et al. (7, 17, 18) developed a movie-viewing paradigm for the investigation of conscious experiences of behaviorally non-responsive patients who may retain covert awareness. Movie viewing is highly suited to testing populations that exhibit large fluctuations in arousal, impaired motor control and compromised attention span, because, by creating an immersive experience, it naturally engages attention and various cognitive processes that lead to reduced movement in the scanner (19) and recruitment of strong brain activity that is synchronized across different individuals (7, 18, 20–23). Naci and colleagues focused on the assessment of executive function—a high-level cognitive function that requires conscious awareness—while participants watched a brief (8 min) and highly engaging movie by Alfred Hitchcock. The investigators found that the movie's executive demands, assessed quantitatively and qualitatively in independent control groups, predicted similar activity across individual participants in the frontal and parietal

cortex, regions that support executive processing (25–29). Thus, the time-course of the fronto-parietal activation provided a template for decoding whether behaviorally non-responsive patients have similar cognitive experiences to healthy individuals in response to the executive demands of the movie. Using this approach, Naci and colleagues demonstrated that a patient who had been behaviorally non-responsive and thought to lack consciousness for 16 years was consciously aware and could continuously engage in complex thoughts about real-world events unfolding over time (7). Thus, they provided strong evidence that some patients who are entirely behaviorally non-responsive can retain conscious awareness of their external environment (17, 24).

However, *awareness of oneself*, an aspect of consciousness routinely tested for at the patient's bedside, is more elusive and harder to measure, even in patients who demonstrate awareness of their external environment, such as those thought to be in a minimally conscious state (30). Traditionally, awareness of oneself, or internal awareness, has been assessed through self-report and, as a result, it is challenging to measure in its complete absence. Therefore, the extent to which some DoC patients, especially those who remain entirely behaviorally non-responsive and are diagnosed to be in a VS, are capable of internal awareness remains unclear. In the healthy brain, the focus of conscious awareness is thought to switch naturally over time between its internal and external aspects (31–33), a relationship mediated by the fluctuating juxtaposition or anti-correlation of functional time-courses of the default mode network (DMN) and fronto-parietal networks, as observed in the resting state (34–36). Although recent studies suggest a role for the DMN in facilitating goal-oriented behavior (37–39), this network has been shown to support a variety of internally-driven processes, including autobiographical memory, imagination, thinking about the self (40–46), and internal awareness (31, 33). Furthermore, the DMN decreases in activity when attention is directed externally (34, 47, 48), but increases in response to introspectively-oriented cognitive processes (44, 46). By contrast, the networks extending in the frontal and parietal cortices, including the dorsal attention (DAN) and executive control (ECN) networks are thought to mediate externally-driven cognitive processes, including attention, inhibition and executive control, that support external awareness (49, 50). The fronto-parietal networks increase in activity when attention is directed to external stimuli in cognitive tasks (35, 36, 51, 52).

Thus, although the relationship between the DMN and DAN/ECN to one another may depend upon the paradigm employed and the goals of the subject (53, 54), the juxtaposition

of their functional time-courses is critical for the naturally ongoing switches between internal and external awareness (31–33). As the DMN and fronto-parietal networks are juxtaposed to one another at rest (34–36), and dissociate further when attention is directed externally, we reasoned that their functional responses would be maximally juxtaposed to one another during a highly engaging stimulus.

In this study, we did not investigate internal awareness directly, but rather investigated the *potential* for internal as well as external awareness in DoC patients including patients in the vegetative and minimally conscious states. To this end, we asked whether the pattern of juxtaposition between the DMN and DAN/ECN functional time-courses observed in healthy controls (31, 55) was present in patients, who had previously demonstrated evidence of external awareness. To this end, we used the aforementioned highly engaging short movie by Alfred Hitchcock to drive the recruitment of the fronto-parietal networks and its maximal disengagement from the DMN relative to the resting state baseline, in a control group of healthy participants and severely brain-injured patients with disorders of consciousness. To circumvent the limitations of behavioral testing based on the clinical evaluation and ensure that patients categorized as unconscious indeed showed no wilful brain responses, each patient underwent a functional Magnetic Resonance Imaging (fMRI)-based assessment with a previously established command-following protocol for detecting covert awareness (5, 56). Initially, we investigated the functional connectivity of the DMN and DAN/ECN in the healthy controls during movie viewing relative to the baseline conditions. Subsequently, we tested whether DoC patients, who demonstrated independent covert external awareness, differently from patients who did not, showed a juxtaposition between the DMN and fronto-parietal functional time-courses that was strengthened by the complex stimulus.

## METHODS

### Participants

Ethical approval was obtained from the Health Sciences Research Ethics Board and the Psychology Research Ethics Board of Western University, in London Canada. All healthy participants were right-handed, native English speakers and had no history of neurological disorders. They gave informed written consent and were remunerated for their time. Thirteen and twelve healthy volunteers participated in experiment 1 and 2, respectively. The data of healthy volunteers was previously reported in studies by Naci et al. (7, 18). A convenience sample of 18 DoC patients participated in experiment 3. The patients' respective substitute decision makers provided informed written consent. Three patients were excluded from final analyses. Of these, one was excluded because of large structural brain damage and extremely enlarged ventricles that would have rendered any further analysis impossible. A second patient was excluded due to excessive movement in the scanner, which caused the termination of the scanning session. The third patient was excluded due to a "locked-in syndrome" diagnosis. Patient 1 appeared twice in the data set, with the corresponding two different scanning visits 2 years apart. In visit 1, the patient

showed the ability to perform the command following task in the scanner, whereas in visit 2 there was no evidence of command following. These differences may have been due to fluctuations in arousal or a genuine change in the patient's status of consciousness. Based on the results of the fMRI analysis, the patient's data from the 2 visits were treated as independent samples for the purpose of subsequence group analysis. Activity-based analyses on data from a subset of the patient cohort were previously reported in Naci et al. (7, 18) and Naci and Owen (5). Prior to commencing the scanning sessions, all patients were tested behaviorally at their bedside (outside of the scanner) with the Coma Recovery Scale-Revised (CRS-R) (57), which assessed each patient's behavioral responsivity along 6 sub-scales: auditory, visual, motor, oromotor/verbal, communication, and arousal (Table 1). All patients were clinically diagnosed as either VS or minimally conscious state [MCS; (30)] at the time of the image acquisition based on the CRS-R. Table 2 provides an overview of the demographic and clinical information, as well as the results of the fMRI command-following protocol for each patient.

### Stimuli and Design

In experiment 1, a group of healthy participants ( $N = 13$ ) were scanned in two different conditions, resting state (8 min) and movie-viewing (8 min) in the same session. Participants were instructed to simply relax in the resting state, and to pay attention to the movie during the stimulation condition. The movie consisted of an edited version of Alfred Hitchcock's black-and-white movie "Bang! You're Dead." It depicted a 5-year-old boy, who finds his uncle's revolver, partially loads it with bullets, and plays with it at home and in public, unaware of its power and danger. Sound in the scanner was delivered over scanner-compatible noise canceling headphones.

In experiment 2, healthy participants ( $N = 12$ ) watched a visually and auditory scrambled version of the Hitchcock movie sequence inside the scanner. To create the scrambled condition, very brief (one second) audio-visual segments of the movie were pseudo-randomized, retaining the sensory properties (visual and auditory) while removing the narrative. Written feedback at the end of the scanning session confirmed that participants were not able to uncover a storyline in the scrambled movie, or relate it to stored knowledge of previous movies they had seen.

In experiment 3, DoC patients ( $N = 15$ ) were scanned in the resting state and during viewing of the intact movie in the same session. The condition order was counterbalanced and the same procedure and scanning parameters were used for the patients as for healthy controls. To control for patient's wakefulness, eye opening was monitored inside the scanner with an infrared camera. Due to the highly limited time in the scanner, severely brain-injured patients did not undergo the scrambled movie baseline condition.

### Patient Behavioral Assessment and Command-Following fMRI Paradigm

Awareness fluctuates greatly in the chronic DoC patient group, and therefore the behavioral diagnosis based on the gold-standard measure of CRS-R is likely to fluctuate

**TABLE 1 |** Coma Recovery Scale—Revised subscale scores assessed prior to the fMRI session.

Patient ID	Diagnosis	Auditory	Visual	Motor	Oromotor/verbal	Communication	Arousal
1 Visit 1	VS	1 - Auditory startle	0 - None.	2 - Flexion withdrawal	1 - Oral reflexive	0 - None	2 - Eye opening without stimulation
Visit 2	VS	1 - Auditory startle	1 - Visual startle	2 - Flexion withdrawal	1 - Oral reflexive	0 - None	2 - Eye opening without stimulation
2	MCS	1 - Auditory startle	3 - Visual pursuit	2 - Flexion withdrawal	1 - Oral reflexive	0 - None	2 - Eye opening without stimulation
3	VS	1 - Auditory startle	1 - Visual startle	1 - Abnormal posturing	1 - Oral reflexive	0 - None	2 - Eye opening without stimulation
4	MCS	3 - Reproducible movement to command	3 - Visual pursuit	2 - Flexion withdrawal	2 - Vocalization/oral movement	0 - None	3 - Attention
5	MCS	1 - Auditory startle	3 - Visual pursuit	2 - Flexion withdrawal	1 - Oral reflexive	0 - None	1 - Eye opening with stimulation
6	VS	1 - Auditory startle	1 - Visual startle	2 - Flexion withdrawal	1 - Oral reflexive	0 - None	1 - Eye opening with stimulation
7	VS	0 - None	0 - None	2 - Flexion withdrawal	1 - Oral reflexive	0 - None	2 - Eye opening without stimulation
8	VS	2 - Localization to sound	1 - Visual startle	1 - Abnormal posturing	0 - None	0 - None	2 - Eye opening without stimulation
9	VS	0 - None	1 - Visual startle	0 - None	0 - None	0 - None	2 - Eye opening without stimulation
10	MCS	2 - Localization to sound	3 - Visual pursuit	1 - Abnormal posturing	1 - Oral reflexive	0 - None	2 - Eye opening without stimulation
11	MCS	4 - Consistent movement to command	4 - Object localization: reaching	4 - Automatic motor response	1 - Oral reflexive	1 - Non-functional: intentional	1 - Eye opening with stimulation
12	VS	1 - Auditory startle	0 - None	1 - Abnormal posturing	1 - Oral reflexive	0 - None	1 - Eye opening with stimulation
13	VS	1 - Auditory startle	0 - None	2 - Flexion withdrawal	1 - Oral reflexive	0 - None	1 - Eye opening with stimulation
14	VS	1 - Auditory startle	1 - Visual startle	0 - None	1 - Oral reflexive	0 - None	2 - Eye opening without stimulation
15	MCS	1 - Auditory startle	3 - Visual pursuit	1 - Abnormal posturing	1 - Oral reflexive	0 - None	1 - Eye opening with stimulation

VS, vegetative state; MCS, minimally conscious state.

(58). Furthermore, in some cases, as for CMD patients (59), awareness is difficult to spot behaviorally. Therefore, it was a priority of this manuscript to base evaluation of awareness on an assessment that would not falsely put covertly responding “VS patients” in a group of non-responders. Accordingly, to ensure an objective standard of awareness that was independent of the behavioral diagnosis, and also relevant but independent to the movie paradigm, awareness was assessed with a previously validated fMRI task (5) in the same scanning session as the movie paradigm.

To account for the variability of the behavioral diagnosis, we conducted on average 7 CRS-R assessments for each patient during the week of their research visit at our facility. Given this well-documented fluctuation, to follow as closely as possible the level of awareness that might be picked up by the fMRI task, here we reported the CRS-R score of the scanning day.

Each patient underwent a command following scan in the same scanning session. Stimuli. The stimuli were eleven single words (“one,” “two,” “three,” “four,” “five,” “six,” “seven,” “eight,”

“nine,” “yes,” “no”). Design. The fMRI selective auditory attention paradigm has been previously described in healthy individuals (56) and patients with DoC (5), and is designed to identify the ability to follow commands to selectively attending to stimuli, by recruiting top-down attention. On each trial, participants were instructed to either count a target word (“yes” or “no”) presented among pseudorandom distractors (spoken digits one to nine), or to relax. Each trial had an on/off design: sound (~22.5 s) followed by silence (10 s). The scan lasted 5 min, including instructions.

As seen in **Table 2**, the results of the command following task were broadly consistent with the MCS patients’ clinical diagnosis that indicated overt awareness—all but one MCS patient, who fell asleep in the scanner, were able to perform the selective attention task in the scanner [see (60, 61) for diverging results on MCS patients who could not perform a command-following task in the MRI scanner]. By contrast, 3 out of 10 VS patients showed positive command following results. This is consistent with previous findings showing that a proportion of patients

**TABLE 2 |** The patients' demographic and clinical information, fMRI command-following protocol results and functional connectivity results.

Patient ID	Age range	Diagnosis	Interval since ictus, months	Score on CRS-R	Etiology	Command following (attention)	Movie DMN-DAN Connectivity	Resting DMN-DAN Connectivity
1	Visit 1: 22–25	VS	67	6	TBI	+	0.21	0.32
	Visit 2: 26–30	VS	89	7		–	0.38	0.32
2	31–35	MCS	445	9	HBI	+	0.44	0.48
3	18–21	VS	68	6	HBI	–	0.43	0.31
4	26–30	MCS	36	13	HBI	+	0.35	0.37
5	46–50	MCS	234	8	HBI	+	0.19	0.24
6	56–60	VS	38	6	HBI	–	0.37	0.13
7	31–35	VS	25	5	HBI	–	0.47	0.35
8	18–21	VS	3	6	HBI	+	0.29	0.46
9	41–45	VS	248	3	TBI	+	0.33	0.45
10	22–25	MCS	69	9	TBI	+	0.62	0.64
11	46–50	MCS	148	15	TBI	–	0.60	0.54
12	51–55	VS	11	4	HBI	–	0.63	0.64
13	51–55	VS	79	5	HBI	–	0.60	0.52
14	18–21	VS	49	5	HBI	–	0.66	0.25
15	36–40	MCS	38	7	TBI	+	0.13	0.38

VS, vegetative state; MCS, minimally conscious state; TBI, traumatic brain injury; HBI, hypoxic-ischemic brain injury; CRS-R, Coma Recovery Scale—Revised (57). In the "Command Following (Attention)" column, "+" denotes that the patient demonstrated a positive result, or showed evidence of command-following in the scanner; "–" denotes that the patient showed no evidence of command-following during this task. The Movie connectivity and Resting connectivity columns describe functional connectivity (as described by z-values) between the DMN and DAN.

clinically diagnosed as VS are nevertheless able to modulate brain activity to command (2, 3, 15). The results of this command-following task were used to split the patient cohort into two groups: DoC+ patients were able to perform the command-following task in the scanner, DoC– patients were not able to do so. Further analyses were then performed independently for these two groups.

## Functional Data Acquisition

All participants were scanned in a 3 Tesla Siemens Tim Trio MRI scanner at the Robarts Research Institute in London, Canada. A 32-channel head coil was used for functional and anatomical scans. We acquired functional images during movie viewing (246 scans) and resting-state (256 scans) by a T2\*-weighted echo-planar sequence [33 slices, voxel size =  $3 \times 3 \times 3$  mm<sup>3</sup>, interslice gap = 25%, repetition time = 2,000 ms, echo time (TE) = 30 ms, matrix size =  $64 \times 64$ , flip angle (FA) = 75 degrees]. Furthermore, a T1-weighted 3D magnetization prepared rapid acquisition gradient echo (MPRAGE) sequence was used for anatomical scans [voxel size =  $1 \times 1 \times 1$  mm<sup>3</sup>, TE = 4.25 ms, matrix size =  $240 \times 256 \times 192$ , FA = 9 degrees]. The total anatomical scanning time was 5min 38sec. All scanning parameters were the same for healthy participants and patients.

## Preprocessing

For preprocessing and data analysis we used SPM8 (Wellcome Institute of Cognitive Neurology, <http://www.fil.ion.ucl.ac.uk/spm/software/spm8/>) and the AA pipeline software [(62), [www.automaticanalysis.org](http://www.automaticanalysis.org)]. All preprocessing and data analysis steps

were the same for healthy participants and patients. We discarded the first five volumes of each run to avoid T1-saturation effects. The preprocessing procedure included slice-time correction, motion correction, normalization into Montreal Neurological Institute (MNI) space and spatial smoothing with a Gaussian kernel of 10mm full width at half maximum. Furthermore, we applied a temporal high-pass filter with a cut-off of 1/128 Hz to each voxel and regressed out the six motion parameters (x, y, z, roll, pitch, yaw). To investigate any confounding effects of movement differences between groups and conditions, we additionally calculated the mean frame-wise displacement (63) for each participant and compared them using a mixed ANOVA, as well as paired *t*-tests. Healthy participants did not differ significantly in movement, as assessed by frame-wise displacement values, between the movie viewing and resting state condition [ $t_{(12)} = -1.91$ ,  $p = 0.08$ ]. Similarly, the patients' movement did not differ significantly. A two-factor mixed ANOVA on motion, with factors group (DoC+, DoC–) and condition (movie, rest) showed no significant main effects [group:  $F_{(1)} = 0.28$ ,  $p = 0.60$ ; condition:  $F_{(1)} = 1.01$ ,  $p = 0.33$ ] and no significant interaction [ $F_{(1,1)} = 0.53$ ,  $p = 0.48$ ]. To avoid the formation of artificial anti-correlations, a confounding effect previously reported by Murphy et al. (64) and Anderson et al. (65), we performed no global signal regression.

## Functional Network Definition

We analyzed functional connectivity within and between the three key networks that are involved in higher order processes: the DMN, DAN and ECN. The functional networks were



defined based on functionally specific regions of interest (ROIs) (19 in total, 10mm spheres), from well-established landmark coordinates published in Raichle (66). MNI coordinates for ROIs of each network can be found in **Table 3**. For the analysis of functional connectivity based on a set of network nodes pre-defined in the healthy literature (MNI standard neurological space), each patient's brain was normalized to the healthy template. Some of the ROIs may not be optimally located in a subset of the patients due to the varying location and extent of damage (see **Figure 1** for an overview of structural information on the patients' brains). The mechanism of functional re-organization that follows brain injury and leads to loss of consciousness in some cases, whereas in others to preservation of consciousness, remains poorly understood and is the focus of active research (59, 67) outside of the scope of this manuscript. Therefore, although it is impossible to ascertain the structure-to-preserved function mapping for each individual patient, we expected that any damage within the regions of interest in each patient's brain would add noise to the brain activity measurement and reduce the power to detect an effect. Therefore, if results in brain-injured patients confirmed a-priori hypotheses based on the healthy control group, they would likely present a conservative estimate of the underlying effect.

Functional Connectivity Analysis

The preprocessed mean BOLD time series of each ROI was extracted and correlated (Pearson correlation) with the time courses of all the other ROIs. We note that Pearson

correlation is a basic FC measure that, while it does not directly imply causal relations between neural regions, is advantageous for its minimal assumptions regarding the true nature of brain interactions and breath of its use in the neuroscientific literature, and thus fitting to the aims of this investigation. Based on these Pearson's correlations, we created a 19 × 19 correlation matrix (**Figure 2**). We performed this procedure separately for the movie and resting state for each participant. The average over all ROIs within a network was computed and a two-way repeated measures ANOVA and Bonferroni-corrected pairwise comparisons were performed to evaluate effects of interest. To account for the non-normalized distribution of correlation values (68), all statistical analyses were performed on z-transformed correlation values, using Fisher's r-to-z transformation. For visualization purposes, we re-transformed these z-values in correlation values.

RESULTS

Healthy Participants

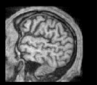
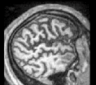
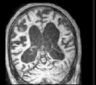
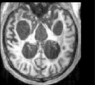
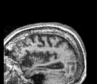

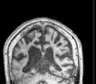

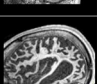

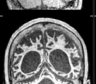

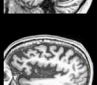

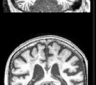

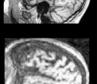
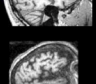
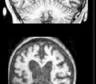
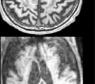
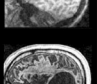
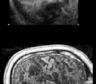
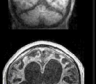
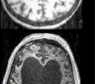
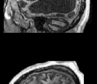
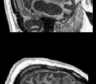
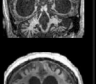
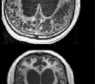
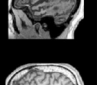
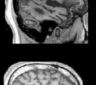
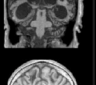
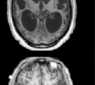
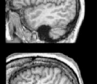
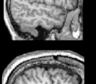
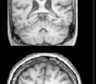
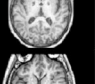
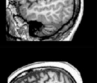
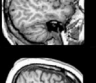
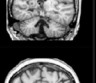
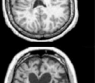
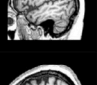
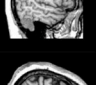
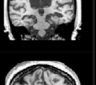
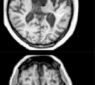
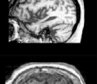
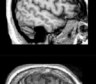
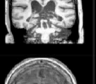
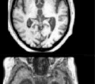
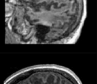
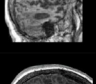
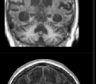
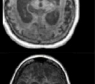
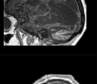
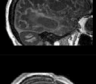
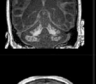
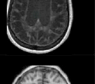
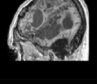
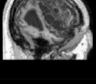

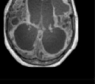
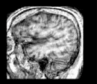

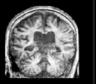
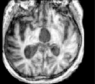
The correlation matrices for the movie viewing and resting state conditions, including all ROIs for the three networks, are shown in **Figure 2**. A two-way repeated measures ANOVA with factors condition (movie, rest) and connectivity (*within*-networks, *between*-networks) revealed a significant interaction effect [ $F_{(1,1)} = 18.52, p < 0.001$ ]. During movie viewing the connectivity between the DMN and DAN [ $t_{(12)} = 4.58, p < 0.001$ ] and DMN and ECN [ $t_{(12)} = 4.03, p < 0.005$ ] were significantly down-regulated during the movie relative to the resting state (**Figure 3A**). As the measure of connectivity (Pearson correlation) reflected the degree of similarity between the networks' functional time-courses, this result demonstrated that the functional response of each of the DAN/ECN became more dissimilar to that of the DMN during the movie relative to the resting state baseline. By comparison, functional connectivity between DAN and ECN [ $t_{(12)} = 0.23, p = 0.82$ ], as well as functional connectivity within the functional networks [DMN:  $t_{(12)} = 2.15, p = 0.052$ ; DAN:  $t_{(12)} = 1.35, p = 0.20$ ; ECN:  $t_{(12)} = 0.75, p = 0.47$ ] did not differ between the movie and resting state condition.

To further investigate whether this dissociation was indeed related to the processing of the movie's higher-order properties, including its narrative, or merely driven by the presence of sensory stimulation in the movie relative to the resting state condition, we investigated the connectivity between these networks during the intact movie relative to its scrambled version, which retained the sensory features but was devoid of the narrative (**Figure 3B**). Relative to the scrambled movie, in the intact movie we found significant down-regulation of the DMN-DAN connectivity [ $t_{(11)} = -2.289, p < 0.05$ ], but not the DMN-ECN connectivity (**Figure 3B**). This suggested that the modulation of the DMN-DAN, but not DMN-ECN, connectivity during movie viewing reflected the processing of the movie's higher-order features, including its narrative. This result was consistent with a recent study showing heightened functional differentiation with increasing stimuli meaningfulness (69).

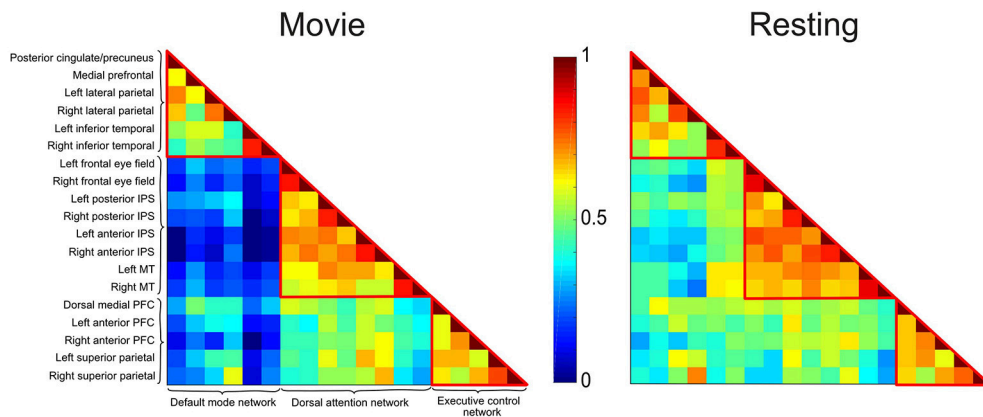
TABLE 3 | Overview of the regions of interests for the DMN, DAN, and ECN.

Network	ROI	MNI coordinates		
Default mode network	Posterior cingulate/precuneus	0	-52	27
	Medial prefrontal	-1	54	27
	Left lateral parietal	-46	-66	30
	Right lateral parietal	49	-63	33
	Left inferior temporal	-61	-24	-9
	Right inferior temporal	58	-24	-9
Dorsal attention network	Left frontal eye field	-29	-9	54
	Right frontal eye field	29	-9	54
	Left posterior IPS	-26	-66	48
	Right posterior IPS	26	-66	48
	Left anterior IPS	-44	-39	45
	Right anterior IPS	41	-39	45
	Left MT	-50	-66	-6
	Right MT	53	-63	-6
Executive control network	Dorsal medial PFC	0	24	46
	Left anterior PFC	-44	45	0
	Right anterior PFC	44	45	0
	Left superior parietal	-50	-51	45
	Right superior parietal	50	-51	45

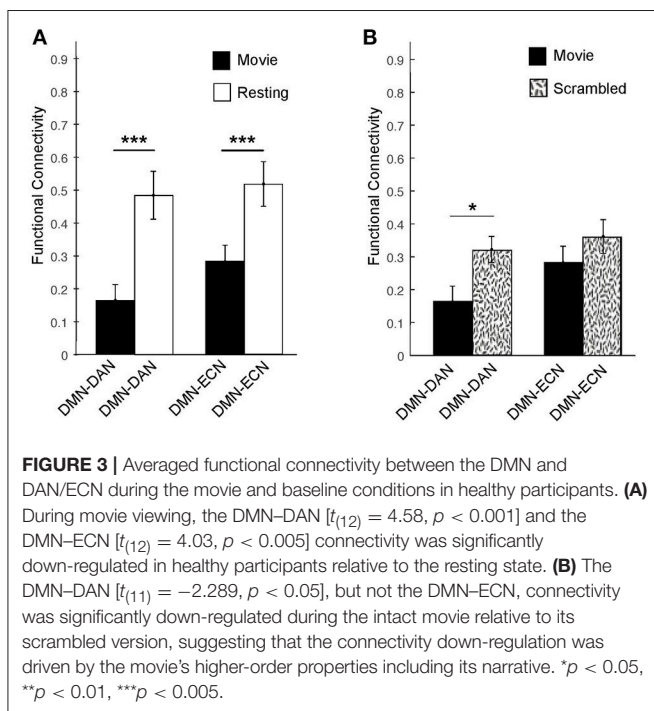
IPS, Intraparietal sulcus; MT, Middle temporal area; PFC, Prefrontal cortex.

Patient ID	Clinical Diagnosis	Imaging Command Following	Sagittal Left	Sagittal Right	Coronal	Horizontal	Radiologist notes on clinical CT/MRI
1	VS	+ (visit 1)					No acute intracranial abnormality.
	VS	- (visit 2)					
2	MCS	+					No CT/clinical MRI imaging notes.
3	VS	-					Diffuse marked cerebral atrophy and cerebellar atrophy (to a lesser extent). Areas of signal change in the caudate nuclei, putamen, pulvinar of the thalamus and insular-periinsular areas (bilaterally).
4	MCS	+					No CT/clinical MRI imaging notes.
5	MCS	+					Initial/Acute CT: generalized brain edema, partial obliteration of left quadrigeminal cistern, decreased GM/WM differentiation. Did not show hematomas or contusions.
6	VS	-					Progressive encephalomalacic changes affecting the supratentorial and infratentorial brain parenchyma. Diffuse atrophy and loss of the brain substance with associated marked ex vacuo dilation of the ventricular system which has progressed.
7	VS	-					Diffuse cerebral edema, with evolving infarcts of the basal ganglia.
8	VS	+					Extensive white matter ischemia in the frontal, parietal and occipital regions. Ischemia of the global pallidi.
9	VS	+					Severe cerebral and brainstem atrophy with periventricular leukomalacia consistent with severe brain injury. CT showed post traumatic widespread white matter disease.
10	MCS	+					Bilateral basal ganglia subarachnoid hemorrhage, intraventricular hemorrhage. Right caudate infarct, right frontal hemorrhage, small right parietal subdural
11	MCS	-					No CT/clinical MRI imaging notes.
12	VS	-					No imaging notes.
13	VS	-					Cerebral edema.
14	VS	-					Diffuse cerebral mass effect with transtentorial herniation. Suspect beginning diffuse infarction. Loss of grey matter to white matter density difference now involves a majority of cerebral hemispheres. Bifrontal craniectomies with herniation of frontal lobes.
15	MCS	+					Small left sided subdural over the left parietal lobe which measures about 6-mm at its maximum thickness. Moderately severe contralateral shift to the midline, some herniation. Subarachnoid space and the convexity sulci are totally effaced.

**FIGURE 1 |** Structural brain information for the patient cohort. Columns 4–7 give an overview of structural MRI images that were taken for each patient. On the right, clinical notes by radiologists on previous computerized tomography (CT) and/or MRI scans are listed. The sign “+” or “–” in the “Imaging Command Following” column describes whether the patient was able to successfully complete a command-following task in the MRI scanner (+), or not (–).



**FIGURE 2 |** Correlation matrices depicting the DMN, DAN, and ECN during movie viewing and resting state conditions in healthy participants. Each cell represents the color-coded connectivity between an ROI to itself (middle diagonal) or another region. The labels for the ROIs in each network are displayed on the left-hand side. Warm/cool colors depict high/low correlations as per the heat bar in the middle of the graph. During movie viewing, healthy participants showed decreased functional connectivity between the DMN and the DAN/ECN as compared to the resting state. Functional connectivity within each network, and between the DAN and ECN did not differ significantly between the two conditions.



**FIGURE 3 |** Averaged functional connectivity between the DMN and DAN/ECN during the movie and baseline conditions in healthy participants. **(A)** During movie viewing, the DMN–DAN [ $t_{(12)} = 4.58, p < 0.001$ ] and the DMN–ECN [ $t_{(12)} = 4.03, p < 0.005$ ] connectivity was significantly down-regulated in healthy participants relative to the resting state. **(B)** The DMN–DAN [ $t_{(11)} = -2.289, p < 0.05$ ], but not the DMN–ECN, connectivity was significantly down-regulated during the intact movie relative to its scrambled version, suggesting that the connectivity down-regulation was driven by the movie's higher-order properties including its narrative. \* $p < 0.05$ , \*\* $p < 0.01$ , \*\*\* $p < 0.005$ .

## DoC Patients

The results in the healthy controls suggested that the heightened differentiation between the DMN and DAN aspect of the fronto-parietal network was driven by the movie's high-order properties including its narrative. Subsequently, we investigated whether behaviorally non-responsive patients who retained covert external awareness (labeled here DoC+), and those who showed no such evidence (labeled here DoC–) [see command following (attention) in **Table 2**], showed heightened

differentiation of the functional response of the DMN and DAN networks in response to movie viewing relative to their resting state baseline connectivity.

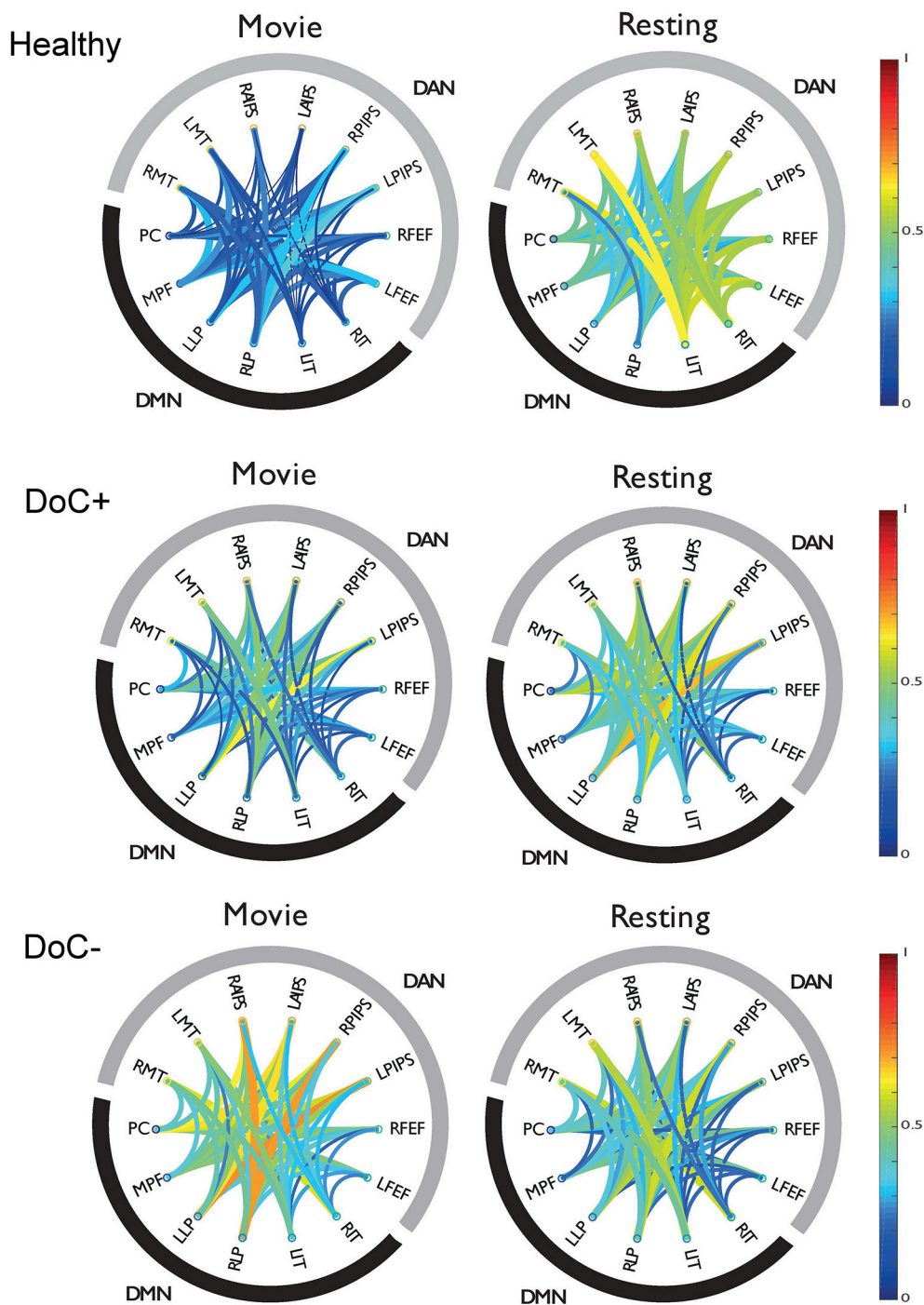
DoC+ patients showed a significant down-regulation of DMN–DAN connectivity, suggesting heightened differentiation of the networks' functional response during the movie viewing relative to the resting state (**Figure 4**) [ $t_{(7)} = -3.31, p < 0.05$ ]. By contrast, DoC– patients showed no down-regulation of the DMN–DAN connectivity, but rather a significant up-regulation of this connectivity [ $t_{(7)} = 2.99, p < 0.05$ ] during the movie relative to the resting state.

The modulatory effect of movie viewing on the DMN–DAN connectivity was highly significant different between the two patient groups [ $t_{(15)} = 4.23, p = 0.001$ ; **Figure 5A**]. Moreover, the down-regulation of DMN–DAN connectivity in the DoC+ group, and the opposite effect in the DoC– group was visible in individual patient (**Figure 5B**), although, we caution that the current analysis is not optimized to investigate statistical significance at the single-subject level. By contrast, the DMN–DAN connectivity during resting state did not differentiate the two patient types (**Figures 5C,D**).

## DISCUSSION

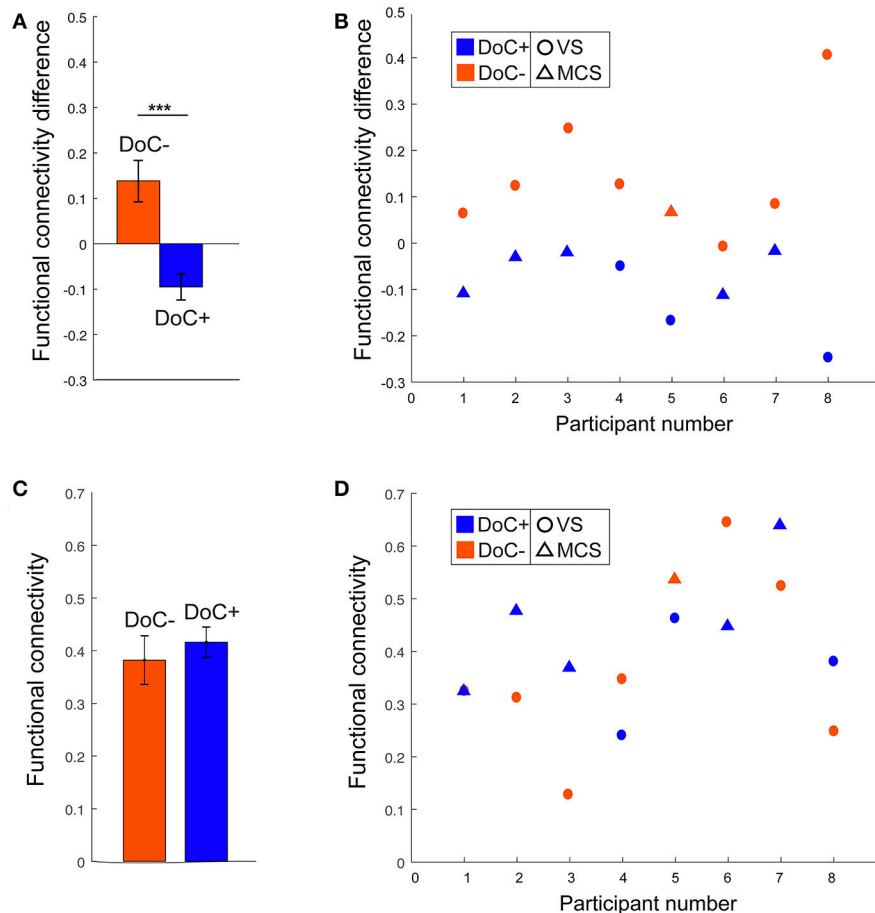
In this study, we asked whether patients with disorders of consciousness retain the potential for internal as well as external conscious awareness. To address this question, we investigated the juxtaposed relationship between the DMN and fronto-parietal (DAN, ECN) networks' functional time-courses, which are thought to support the naturally occurring fluctuations and dominance switching between internal and external awareness (31–33) in healthy individuals. We used a highly engaging external stimulus—a short movie by Alfred Hitchcock to drive maximal juxtaposition of the DMN and fronto-parietal networks relative to the resting state and scrambled, meaningless movie





**FIGURE 4 |** DMN-DAN connectivity in healthy participants and DoC patients. The schema-balls provide an overview of individual ROI connectivity and depict all possible between-ROI connections for the DMN and DAN. Warm/cool colors depict high/low correlations as per the heat bar to the right of the graph. Healthy participants showed a down-regulation of DMN–DAN connectivity during movie viewing relative to the resting state. Similarly, the DoC+ patients showed a down-regulation of DMN–DAN connectivity during movie viewing [ $t_{(7)} = -3.31, p < 0.05$ ]. By contrast, DoC-patients did not show this effect. RMT, right middle temporal visual area; LMT, left middle temporal visual area; RAIPS, right anterior intraparietal sulcus; LAIPS, left anterior intraparietal sulcus; RPIPS, right posterior intraparietal sulcus; LPIPS, left posterior intraparietal sulcus; RFEF, right frontal eye field; LFEF, left frontal eye field; RIT, right inferior temporal; LIT, left inferior temporal; RLP, right lateral parietal; LLP, left lateral parietal; MPF, medial prefrontal; PC, posterior cingulate/precuneus.





**FIGURE 5 |** DMN–DAN connectivity difference between movie viewing and the resting state and during resting state only in DoC patients. **(A)** The DoC+ and DoC– groups differed significantly on their DMN–DAN connectivity modulation during movie viewing relative to resting state [ $t_{(15)} = 4.23$ ,  $p < 0.005$ ]. **(B)** Visual inspection suggested that individual DoC+ patients displayed a down-regulation of DMN–DAN connectivity during movie viewing, illustrated by a negative value for the difference between movie and resting DMN–DAN connectivity. **(C,D)** During the resting state, there was no significant difference in DMN–DAN connectivity between the DoC+ and DoC– groups **(C)**, and no such difference could be observed at the individual patient level **(D)**. \*\*\* $p < 0.005$ .

baseline conditions. Initially we investigated the connectivity between the DMN and fronto-parietal networks in response to movie viewing and baseline conditions in healthy controls, and subsequently, in two groups of severely brain-injured patients with DoC, one comprised of patients who demonstrated independent neuroimaging-based evidence of covert external awareness, and the other of those who did not.

Healthy controls showed significantly heightened differentiation between the DMN and the DAN in response to movie viewing relative to their resting state and scrambled movie time-courses. This result suggested that the heightened differentiation during movie viewing was driven by the movie's higher-order features, including its narrative. This finding was consistent with previous studies showing a heightened dissociation between the default mode and fronto-parietal networks on paradigms requiring externally-directed attention [(48, 52, 55), but see (70) for diverging results]. The connectivity between the DMN and ECN was not modulated by the movie's

higher-order features, which may be explained by differential engagement by the movie paradigm of the DAN and ECN. Movie viewing required the ability to orient and sustain attention to the incoming auditory input, and discriminate the saliency and contextual relevance of the sensory inputs with respect to the evolving narrative—a function subserved primarily by the DAN (50), and it did not require behavioral response planning or monitoring—a function subserved primarily by the ECN (49).

Similar to healthy controls, severely brain-injured patients who had demonstrated independent evidence of covert external awareness showed significantly enhanced differentiation between the DMN and DAN functional time-course in response to movie viewing relative to the resting state baseline. This result suggested the presence of functional integrity in the default mode and fronto-parietal networks and their relationship to one another. It is worth noting that we did not investigate internal awareness directly, but rather the potential for internal awareness in addition to external awareness as indicated by the pattern of

juxtaposed time-courses of these networks. Similar to the effect in healthy participants, these networks became more strongly juxtaposed to one another in response to movie viewing, relative to their resting baseline, suggesting the *potential* for internal as well as external awareness during complex stimulus processing.

By contrast, this effect was not present in chronic DoC patients who showed no fMRI-based evidence of covert awareness. Conversely, these patients showed a diminished differentiation between the DMN and DAN time-courses during the movie viewing relative to the resting state baseline. This was consistent with previous studies showing a loss of functional differentiation between brain networks in loss of consciousness (71–73). The loss of functional differentiation in response to movie viewing relative to the resting state suggests that, in severely brain-injured patients who likely lack conscious awareness, the stimulus-evoked feed-forward processing cascade is echoed undifferentiated throughout the brain leading to similar functional responses across different networks. In this study, we had no differential hypotheses for the MCS+ vs. MCS– patients and, on this basis, we did not differentiate between MCS patients. Further, the small number of MCS patients ( $N = 6$ ) did not facilitate further separation into groups. However, it would be interesting to investigate in future studies differences between MCS+ and MCS– patients in this regard, and we would hypothesize that MCS+ patients would be more likely than MCS– to show the heightened differentiation between the DMN and DAN networks during the movie paradigm relative to the resting state, which the current data suggest is indicative of the potential for internal awareness during viewing of a naturalistic narrative.

Visual inspection suggested that this effect was present at the single-subject level and differentiated patients who had covert awareness from those who did not, not only at the group but also at the individual level and thus, may be sufficiently robust to facilitate detection of covert awareness in individual patients in the absence of other neuroimaging assessments. This hypothesis requires formal testing with a large number of patients in future studies. Notably, this effect was not present when looking at DMN–DAN connectivity in the resting state alone, suggesting that richly evocative stimulation is appropriate for differentiating between behaviorally non-responsive patients who retain covert awareness and those who don't, based on the integrity of consciousness supporting networks. Previous studies have suggested several benefits of the movie-viewing paradigm over the resting state for investigating the functional integrity of brain networks in healthy individuals. Foremost, movie-viewing creates an immersive experience that naturally

engages attention, rendering participants less likely to fall asleep and less liable to arousal fluctuations present in the resting state condition (74), it reduces movement (19, 75), and leads to strong brain activity (21, 22). Importantly, a complex and plot-driven naturalistic stimulus engages functionally distinct brain systems in a stereotypical way across different individuals (7, 17, 18, 20, 21, 23) that enables comparisons between different participants with minimized inter-subject variance with respect to specific perceptual and cognitive processes. Furthermore, the test-retest reliability of functional connectivity analyses during movie-viewing has been shown superior relative to the resting state, on average by 50% (76).

Our results suggest that these benefits extend to patient populations. To date, a large number of clinical studies investigating functional connectivity have focused on the resting state condition, due to its ease of acquisition in patient populations [e.g., (77–83)] and have provided significant insights on functional disruption in various populations relative to neurologically typical individuals. However, this approach cannot account for an important characteristic of healthy neural processing, that is, the brain's ability to re-organize its connectivity in response to external stimulation. Here, we show that naturalistic paradigms, which present complex real-world information evolving over time, can dissociate between groups of severely brain-injured chronic DoC patients with and without covert awareness, an approach that may also yield important insights when extended to other patient populations (84). Particularly, the ease of patient engagement with reduced movement and reduced arousal fluctuations is beneficial for testing a range of patient populations that, similarly to brain-injured patients, exhibit large fluctuations in arousal, impaired motor control, and compromised attention span, and thus, are difficult to test with conventional paradigms that target cognition.

## AUTHOR CONTRIBUTIONS

AH and LN: conceptualization; LN, AH, and RC: methodology; LG-L: patient recruitment; LN: data acquisition; AH and LN: formal analyses; AH and LN: manuscript preparation; BS and AO: feedback; LN: supervision.

## FUNDING

This research was supported by a Canada Excellence Research Chair to AO and a L'Oréal-Unesco for Women in Science Excellence Research Grant to LN.

## REFERENCES

- Owen AM, Coleman MR, Boly M, Davis MH, Laureys S, Pickard JD. Detecting awareness in the vegetative state. *Science* (2006) 313:1402. doi: 10.1126/science.1130197
- Monti MM, Vanhaudenhuyse A, Coleman MR, Boly M, Pickard JD, Tshibanda L, et al. Willful modulation of brain activity in disorders of consciousness. *N Engl J Med*. (2010) 362:579–89. doi: 10.1056/NEJMoa0905370
- Cruse D, Chennu S, Chatelle C, Bekinschtein TA, Fernández-Espejo D, Pickard JD, et al. Bedside detection of awareness in the vegetative state: a cohort study. *Lancet* (2012) 378:2088–94. doi: 10.1016/S0140-6736(11)61224-5
- Bardin JC, Fins JJ, Katz DI, Hersh J, Heier LA, Tabelow K, et al. Dissociations between behavioural and functional magnetic resonance imaging-based evaluations of cognitive function after brain injury. *Brain* (2011) 134:769–82. doi: 10.1093/brain/awr005

5. Naci L, Owen AM. Making every word count for nonresponsive patients. *JAMA Neurol.* (2013) 70:1235–41. doi: 10.1001/jamaneurol.2013.3686
6. Fernández-Espejo D, Owen AM. Detecting awareness after severe brain injury. *Nat Rev Neurosci.* (2013) 14:801–9. doi: 10.1038/nrn3608
7. Naci L, Cusack R, Anello M, Owen AM. A common neural code for similar conscious experiences in different individuals. *Proc Natl Acad Sci USA* (2014) 111:14277–82. doi: 10.1073/pnas.1407007111
8. Bodien YG, Giacino JT, Edlow BL. Functional MRI motor imagery tasks to detect command following in traumatic disorders of consciousness. *Front Neurol.* (2017) 8:688. doi: 10.3389/fneur.2017.00688
9. Plum F, Posner JB. *The Diagnosis of Stupor and Coma, Vol. 19.* Oxford: Oxford University Press (1982).
10. Laureys S, Owen AM, Schiff ND. Brain function in coma, vegetative state, and related disorders. *The Lancet Neurology.* (2004) 3, 537–546. doi: 10.1016/S1474-4422(04)00852-X
11. Owen AM. Disorders of consciousness. *Ann N Y Acad Sci.* (2008) 1124:225–38. doi: 10.1196/annals.1440.013
12. The Multi-Society Task Force on PVS. Medical aspects of the persistent vegetative state. *N Engl J Med.* (1994) 330:1499–508. doi: 10.1056/NEJM199405263302107
13. Laureys S, Celesia GG, Cohadon F, Lavrijssen J, León-Carrión J, Sannita WG, et al. Unresponsive wakefulness syndrome: a new name for the vegetative state or apallic syndrome. *BMC Med.* (2010) 8:68. doi: 10.1186/1741-7015-8-68
14. Schnakers C, Vanhaudenhuyse A, Giacino J, Ventura M, Boly M, Majerus S, et al. Diagnostic accuracy of the vegetative and minimally conscious state: clinical consensus versus standardized neurobehavioral assessment. *BMC Neurol.* (2009) 9:35. doi: 10.1186/1471-2377-9-35
15. Kondziella D, Friberg CK, Frokjaer VG, Fabricius M, Møller K. Preserved consciousness in vegetative and minimal conscious states: systematic review and meta-analysis. *J Neurol Neurosurg Psychiatry* (2015) 87:485–92. doi: 10.1136/jnnp-2015-310958
16. Schiff ND. Cognitive motor dissociation following severe brain injuries. *JAMA Neurol.* (2015) 72:1413–5. doi: 10.1001/jamaneurol.2015.2899
17. Sinai L, Owen AM, Naci L. Mapping preserved real-world cognition in severely brain-injured patients. *Front Biosci (Landmark Ed).* (2017) 22:815–23. doi: 10.2741/4518
18. Naci L, Sinai L, Owen AM. Detecting and interpreting conscious experiences in behaviorally non-responsive patients. *NeuroImage* (2017) 145(Pt B):304–13. doi: 10.1016/j.neuroimage.2015.11.059
19. Centeno M, Tierney TM, Perani S, Shamshiri EA, StPier K, Wilkinson C, et al. Optimising EEG-fMRI for localisation of focal epilepsy in children. *PLoS ONE* (2016) 11:e0149048. doi: 10.1371/journal.pone.0149048
20. Hasson U, Nir Y, Levy I, Fuhrmann G, Malach R. Intersubject synchronization of cortical activity during natural vision. *Science* (2004) 303:1634–40. doi: 10.1126/science.1089506
21. Bartels A, Zeki S. Brain dynamics during natural viewing conditions—a new guide for mapping connectivity *in vivo*. *Neuroimage* (2005) 24:339–49. doi: 10.1016/j.neuroimage.2004.08.044
22. Bartels A, Zeki S, Logothetis NK. Natural vision reveals regional specialization to local motion and to contrast-invariant, global flow in the human brain. *Cereb Cortex* (2007) 18:705–17. doi: 10.1093/cercor/bhm107
23. Hasson U, Malach R, Heeger DJ. Reliability of cortical activity during natural stimulation. *Trends Cogn Sci.* (2010) 14:40–8. doi: 10.1016/j.tics.2009.10.011
24. Naci L, Graham M, Owen AM, Weijer C. Covert narrative capacity: mental life in patients thought to lack consciousness. *Ann Clin Transl Neurol.* (2017) 4:61–70. doi: 10.1002/actn.376
25. Sauseng P, Klimesch W, Schabus M, Doppelmayr M. Fronto-parietal EEG coherence in theta and upper alpha reflect central executive functions of working memory. *Int J Psychophysiol.* (2005) 57:97–103. doi: 10.1016/j.ijpsycho.2005.03.018
26. Hampshire A, Owen AM. Fractionating attentional control using event-related fMRI. *Cereb Cortex* (2006) 16:1679–89. doi: 10.1093/cercor/bhj116
27. Duncan J. The multiple-demand (MD) system of the primate brain: mental programs for intelligent behaviour. *Trends Cogn Sci.* (2010) 14:172–9. doi: 10.1016/j.tics.2010.01.004
28. Ptak R, Schnider A. The attention network of the human brain: relating structural damage associated with spatial neglect to functional imaging correlates of spatial attention. *Neuropsychologia* (2011) 49:3063–70. doi: 10.1016/j.neuropsychologia.2011.07.008
29. Barbey AK, Colom R, Solomon J, Krueger F, Forbes C, Grafman J. An integrative architecture for general intelligence and executive function revealed by lesion mapping. *Brain* (2012) 135:1154–64. doi: 10.1093/brain/aws021
30. Giacino JT, Ashwal S, Childs N, Cranford R, Jennett B, Katz DI, et al. The minimally conscious state definition and diagnostic criteria. *Neurology* (2002) 58:349–53. doi: 10.1212/WNL.58.3.349
31. Vanhaudenhuyse A, Demertzi A, Schabus M, Noirhomme Q, Bredart S, Boly M, et al. Two distinct neuronal networks mediate the awareness of environment and of self. *J Cogn Neurosci.* (2011) 23:570–8. doi: 10.1162/jocn.2010.21488
32. Heine L, Soddu A, Gómez F, Vanhaudenhuyse A, Tshibanda L, Thonnard M, et al. Resting state networks and consciousness: alterations of multiple resting state network connectivity in physiological, pharmacological, and pathological consciousness states. *Front Psychol.* (2012) 3:195. doi: 10.3389/fpsyg.2012.00295
33. Demertzi A, Soddu A, Laureys S. Consciousness supporting networks. *Curr Opin Neurobiol.* (2013) 23:239–44. doi: 10.1016/j.conb.2012.12.003
34. Greicius MD, Krasnow B, Reiss AL, Menon V. Functional connectivity in the resting brain: a network analysis of the default mode hypothesis. *Proc Natl Acad Sci USA.* (2003) 100:253–8. doi: 10.1073/pnas.0135058100
35. Fox MD, Snyder AZ, Vincent JL, Corbetta M, Van Essen DC, Raichle ME. The human brain is intrinsically organized into dynamic, anticorrelated functional networks. *Proc Natl Acad Sci USA.* (2005) 102:9673–8. doi: 10.1073/pnas.0504136102
36. Sridharan D, Levitin DJ, Menon V. A critical role for the right fronto-insular cortex in switching between central-executive and default-mode networks. *Proc Natl Acad Sci USA.* (2008) 105:12569–74. doi: 10.1073/pnas.0800005105
37. Spreng RN, DuPre E, Selarka D, Garcia J, Gojkovic S, Mildner J, et al. Goal-congruent default network activity facilitates cognitive control. *J Neurosci.* (2014) 34:14108–14. doi: 10.1523/JNEUROSCI.2815-14.2014
38. Vatansever D, Menon DK, Manktelow AE, Sahakian BJ, Stamatakis EA. Default mode dynamics for global functional integration. *J Neurosci.* (2015) 35:15254–62. doi: 10.1523/JNEUROSCI.2135-15.2015
39. Vatansever D, Menon DK, Stamatakis EA. Default mode contributions to automated information processing. *Proc Natl Acad Sci USA.* (2017) 114:12821–6. doi: 10.1073/pnas.1710521114
40. Gusnard DA, Akbudak E, Shulman GL, Raichle ME. Medial prefrontal cortex and self-referential mental activity: relation to a default mode of brain function. *Proc Natl Acad Sci USA.* (2001) 98:4259–64. doi: 10.1073/pnas.071043098
41. Wicker B, Ruby P, Royet JP, Fonlupt P. A relation between rest and the self in the brain? *Brain Res Rev.* (2003) 43:224–30. doi: 10.1016/j.brainresrev.2003.08.003
42. D'argembeau A, Collette F, Van der Linden M, Laureys S, Del Fiore G, Degueldre C, et al. Self-referential reflective activity and its relationship with rest: a PET study. *Neuroimage* (2005) 25:616–24. doi: 10.1016/j.neuroimage.2004.11.048
43. Beer JS. The default self: feeling good or being right? *Trends Cogn Sci.* (2007) 11:187–9. doi: 10.1016/j.tics.2007.02.004
44. Buckner RL, Andrews-Hanna JR, Schacter DL. The brain's default network. *Ann N Y Acad Sci.* (2008) 1124:1–38. doi: 10.1196/annals.1440.011
45. Schneider F, Bempohl F, Heinzel A, Rotte M, Walter M, Tempelmann C, et al. The resting brain and our self: self-relatedness modulates resting state neural activity in cortical midline structures. *Neuroscience* (2008) 157:120–31. doi: 10.1016/j.neuroscience.2008.08.014
46. Andrews-Hanna JR, Reidler JS, Sepulcre J, Poulin R, Buckner RL. Functional-anatomic fractionation of the brain's default network. *Neuron* (2010) 65:550–62. doi: 10.1016/j.neuron.2010.02.005
47. Raichle ME, MacLeod AM, Snyder AZ, Powers WJ, Gusnard DA, Shulman GL. A default mode of brain function. *Proc Natl Acad Sci USA.* (2001) 98:676–82. doi: 10.1073/pnas.98.2.676
48. Shulman GL, Fiez JA, Corbetta M, Buckner RL, Miezin FM, Raichle ME, et al. Common blood flow changes across visual tasks: II. Decreases in cerebral cortex. *J Cogn Neurosci.* (1997) 9:648–63. doi: 10.1162/jocn.1997.9.5.648

49. Kroger JK, Sabb FW, Fales CL, Bookheimer SY, Cohen MS, Holyoak KJ. Recruitment of anterior dorsolateral prefrontal cortex in human reasoning: a parametric study of relational complexity. *Cereb Cortex* (2002) 12:477–85. doi: 10.1093/cercor/12.5.477
50. Corbetta M, Shulman GL. Control of goal-directed and stimulus-driven attention in the brain. *Nat Rev Neurosci.* (2002) 3:201–15. doi: 10.1038/nnr755
51. Seeley WW, Menon V, Schatzberg AF, Keller J, Glover GH, Kenna H, et al. Dissociable intrinsic connectivity networks for salience processing and executive control. *J Neurosci.* (2007) 27:2349–56. doi: 10.1523/JNEUROSCI.5587-06.2007
52. Dosenbach NU, Fair DA, Miezin FM, Cohen AL, Wenger KK, Dosenbach RA, et al. Distinct brain networks for adaptive and stable task control in humans. *Proc Natl Acad Sci USA.* (2007) 104:11073–8. doi: 10.1073/pnas.0704320104
53. Spreng RN, Stevens WD, Chamberlain JP, Gilmore AW, Schacter DL. Default network activity, coupled with the frontoparietal control network, supports goal-directed cognition. *Neuroimage* (2010) 53:303–17. doi: 10.1016/j.neuroimage.2010.06.016
54. Smallwood J, Brown K, Baird B, Schooler JW. Cooperation between the default mode network and the frontal-parietal network in the production of an internal train of thought. *Brain Res.* (2012) 1428:60–70. doi: 10.1016/j.brainres.2011.03.072
55. Kelly AC, Uddin LQ, Biswal BB, Castellanos FX, Milham MP. Competition between functional brain networks mediates behavioral variability. *Neuroimage* (2008) 39:527–537. doi: 10.1016/j.neuroimage.2007.08.008
56. Naci L, Cusack R, Jia VZ, Owen AM. The brain's silent messenger: using selective attention to decode human thought for brain-based communication. *J Neurosci.* (2013) 33:9385–93. doi: 10.1523/JNEUROSCI.5577-12.2013
57. Giacino JT, Kalmar K, Whyte J. The JFK coma recovery scale-revised: measurement characteristics and diagnostic utility. *Arch Phys Med Rehabil.* (2004) 85:2020–29. doi: 10.1016/j.apmr.2004.02.033
58. Wannez S, Heine L, Thonnard M, Gosseries O, Laureys S, Coma Science Group Collaborators. The repetition of behavioral assessments in diagnosis of disorders of consciousness. *Ann Neurol.* (2017) 81:883–9. doi: 10.1002/ana.24962
59. Schiff ND. Altered consciousness. In: Winn R, editor. *Youmans and Winn's Neurological Surgery, 7th Edn.* New York, NY: Elsevier Saunders (2016). p. 203–8.
60. Monti MM, Coleman MR, Owen AM. Executive functions in the absence of behavior: functional imaging of the minimally conscious state. *Prog Brain Res.* (2009) 117:249–60. doi: 10.1016/S0079-6123(09)17717-8
61. Monti MM, Rosenberg M, Finoia P, Kamau E, Pickard JD, Owen AM. Thalamo-frontal connectivity mediates top-down cognitive functions in disorders of consciousness. *Neurology* (2015) 85:1–7. doi: 10.1212/WNL.0000000000001123
62. Cusack R, Vicente-Grabovetsky A, Mitchell DJ, Wild CJ, Auer T, Linke AC, et al. Automatic analysis (aa): efficient neuroimaging workflows and parallel processing using Matlab and XML. *Front Neuroinform.* (2015) 8:90. doi: 10.3389/fninf.2014.00090
63. Power JD, Barnes KA, Snyder AZ, Schlaggar BL, Petersen SE. Spurious but systematic correlations in functional connectivity MRI networks arise from subject motion. *Neuroimage* (2012) 59:2142–54. doi: 10.1016/j.neuroimage.2011.10.018
64. Murphy K, Birn RM, Handwerker DA, Jones TB, Bandettini PA. The impact of global signal regression on resting state correlations: are anti-correlated networks introduced? *Neuroimage* (2009) 44:893–905. doi: 10.1016/j.neuroimage.2008.09.036
65. Anderson JS, Druzzal TJ, Lopez-Larson M, Jeong EK, Desai K, Yurgelun-Todd D. Network anticorrelations, global regression, and phase-shifted soft tissue correction. *Hum Brain Mapp.* (2011) 32:919–34. doi: 10.1002/hbm.21079
66. Raichle ME. The restless brain. *Brain Connect.* (2011) 1:3–12. doi: 10.1089/brain.2011.0019
67. Fernández-Espejo D, Rossit S, Owen AM. A thalamocortical mechanism for the absence of overt motor behavior in covertly aware patients. *JAMA Neurol.* (2015) 72:1442–50. doi: 10.1001/jamaneurol.2015.2614
68. Fisher RA. Frequency distribution of the values of the correlation coefficient in samples from an indefinitely large population. *Biometrika* (1915) 10:507–21. doi: 10.2307/2331838
69. Boly M, Sasai S, Gosseries O, Oizumi M, Casali A, Massimini M, et al. Stimulus set meaningfulness and neurophysiological differentiation: a functional magnetic resonance imaging study. *PLoS ONE* (2015) 10:e0125337. doi: 10.1371/journal.pone.0125337
70. Elton A, Gao W. Task-positive functional connectivity of the default mode network transcends task domain. *J Cogn Neurosci.* (2015) 27:2369–81. doi: 10.1162/jocn\_a\_00859
71. Stamatakis EA, Adapa RM, Absalom AR, Menon DK. Changes in resting neural connectivity during propofol sedation. *PLoS ONE* (2010) 5:e14224. doi: 10.1371/journal.pone.0014224
72. Massimini M, Ferrarelli F, Sarasso S, Tononi G. Cortical mechanisms of loss of consciousness: insight from TMS/EEG studies. *Arch Ital Biol.* (2012) 150:44–55. doi: 10.4449/aib.v150i2.1361
73. Casali AG, Gosseries O, Rosanova M, Boly M, Sarasso S, Casali KR, et al. A theoretically based index of consciousness independent of sensory processing and behavior. *Sci Transl Med.* (2013) 5:198ra105. doi: 10.1126/scitranslmed.3006294
74. Tagliazucchi E, Laufs H. Decoding wakefulness levels from typical fMRI resting-state data reveals reliable drifts between wakefulness and sleep. *Neuron* (2014) 82:695–708. doi: 10.1016/j.neuron.2014.03.020
75. Vanderwal T, Kelly C, Eilbott J, Mayes LC, Castellanos FX. (2015). Inscapes: a movie paradigm to improve compliance in functional magnetic resonance imaging. *NeuroImage* 122:222–32. doi: 10.1016/j.neuroimage.2015.07.069
76. Wang J, Ren Y, Hu X, Nguyen VT, Guo L, Han J, et al. Test-retest reliability of functional connectivity networks during naturalistic fMRI paradigms. *Hum Brain Mapp.* (2017) 38:2226–41. doi: 10.1002/hbm.23517
77. Sorg C, Riedl V, Mühlau M, Calhoun VD, Eichele T, Läer L, et al. Selective changes of resting-state networks in individuals at risk for Alzheimer's disease. *Proc Natl Acad Sci USA.* (2007) 104:18760–5. doi: 10.1073/pnas.0708803104
78. Greicius M. Resting-state functional connectivity in neuropsychiatric disorders. *Curr Opin Neurol.* (2008) 21:424–30. doi: 10.1097/WCO.0b013e328306f2c5
79. Boly M, Tshibanda L, Vanhaudenhuyse A, Noirhomme Q, Schnakers C, Ledoux D, et al. Functional connectivity in the default network during resting state is preserved in a vegetative but not in a braindead patient. *Hum Brain Mapp.* (2009) 30:2393–400. doi: 10.1002/hbm.20672
80. Rosazza C, Minati L. Resting-state brain networks: literature review and clinical applications. *Neurol Sci.* (2011) 32:773–85. doi: 10.1007/s10072-011-0636-y
81. Soddu A, Vanhaudenhuyse A, Demertzi A, Bruno MA, Tshibanda L, Di H, et al. Resting state activity in patients with disorders of consciousness. *Funct Neurol.* (2011) 26:37.
82. Lee MH, Smyser CD, Shimony JS. Resting-state fMRI: a review of methods and clinical applications. *Amer J Neuroradiol.* (2013) 34:1866–72. doi: 10.3174/ajnr.A3263
83. Hannawi Y, Lindquist MA, Caffo BS, Sair HI, Stevens RD. Resting brain activity in disorders of consciousness A systematic review and meta-analysis. *Neurology* (2015) 84:1272–80. doi: 10.1212/WNL.0000000000001404
84. Hasson U, Avidan G, Gelbard H, Vallines I, Harel M, Minshew N, et al. Shared and idiosyncratic cortical activation patterns in autism revealed under continuous real-life viewing conditions. *Autism Res.* (2009) 2:220–31. doi: 10.1002/aur.89

**Conflict of Interest Statement:** The authors declare that the research was conducted in the absence of any commercial or financial relationships that could be construed as a potential conflict of interest.

The reviewer MM declared a past co-authorship with one of the authors AO to the handling Editor.

Copyright © 2018 Haugg, Cusack, Gonzalez-Lara, Sorger, Owen and Naci. This is an open-access article distributed under the terms of the Creative Commons Attribution License (CC BY). The use, distribution or reproduction in other forums is permitted, provided the original author(s) and the copyright owner are credited and that the original publication in this journal is cited, in accordance with accepted academic practice. No use, distribution or reproduction is permitted which does not comply with these terms.





# Network Analysis in Disorders of Consciousness: Four Problems and One Proposed Solution (Exponential Random Graph Models)

John Dell'Italia<sup>1\*</sup>, Micah A. Johnson<sup>1</sup>, Paul M. Vespa<sup>2</sup> and Martin M. Monti<sup>1,2</sup>

<sup>1</sup> Department of Psychology, University of California, Los Angeles, Los Angeles, CA, United States, <sup>2</sup> Brain Injury Research Center, Department of Neurosurgery, David Geffen School of Medicine at UCLA, Los Angeles, CA, United States

## OPEN ACCESS

### Edited by:

Olivia Gosseries,  
University of Liège, Belgium

### Reviewed by:

Enrico Amico,  
Purdue University, United States  
Tino Prell,  
Friedrich-Schiller-Universität-Jena,  
Germany

### \*Correspondence:

John Dell'Italia  
johndellitalia@ucla.edu

### Specialty section:

This article was submitted to  
Applied Neuroimaging,  
a section of the journal  
Frontiers in Neurology

**Received:** 12 February 2018

**Accepted:** 24 May 2018

**Published:** 12 June 2018

### Citation:

Dell'Italia J, Johnson MA, Vespa PM  
and Monti MM (2018) Network  
Analysis in Disorders of  
Consciousness: Four Problems and  
One Proposed Solution (Exponential  
Random Graph Models).  
Front. Neurol. 9:439.  
doi: 10.3389/fneur.2018.00439

In recent years, the study of the neural basis of consciousness, particularly in the context of patients recovering from severe brain injury, has greatly benefited from the application of sophisticated network analysis techniques to functional brain data. Yet, current graph theoretic approaches, as employed in the neuroimaging literature, suffer from four important shortcomings. First, they require arbitrary fixing of the number of connections (i.e., density) across networks which are likely to have different “natural” (i.e., stable) density (e.g., patients vs. controls, vegetative state vs. minimally conscious state patients). Second, when describing networks, they do not control for the fact that many characteristics are interrelated, particularly some of the most popular metrics employed (e.g., nodal degree, clustering coefficient)—which can lead to spurious results. Third, in the clinical domain of disorders of consciousness, there currently are no methods for incorporating structural connectivity in the characterization of functional networks which clouds the interpretation of functional differences across groups with different underlying pathology as well as in longitudinal approaches where structural reorganization processes might be operating. Finally, current methods do not allow assessing the dynamics of network change over time. We present a different framework for network analysis, based on Exponential Random Graph Models, which overcomes the above limitations and is thus particularly well suited for clinical populations with disorders of consciousness. We demonstrate this approach in the context of the longitudinal study of recovery from coma. First, our data show that throughout recovery from coma, brain graphs vary in their natural level of connectivity (from 10.4 to 14.5%), which conflicts with the standard approach of imposing arbitrary and equal density thresholds across networks (e.g., time-points, subjects, groups). Second, we show that failure to consider the interrelation between network measures does lead to spurious characterization of both inter- and intra-regional brain connectivity. Finally, we show that Separable Temporal ERGM can be employed to describe network dynamics over time revealing the specific pattern of formation and dissolution of connectivity that accompany recovery from coma.

**Keywords:** network analysis, exponential random graph model, functional magnetic resonance imaging, coma, disorders of consciousness

## 1. INTRODUCTION

In the past 15 years, *in vivo* studies of the healthy and diseased brain have increasingly focused on approaches aimed at assessing the spontaneous functional architecture of the brain, conceived as a network of interacting regions (1). Network analyses have been successfully employed in many fields, including sociology (2), computer sciences (3), public health (4), epidemiology (5), and transportation (6), among others, to capture salient aspects of each phenomenon. Indeed, while different fields often employ different approaches to assessing network properties, they all share the common goal of characterizing important aspects of complex network function into a limited number of metrics, which can, jointly, capture both what is unique and what is shared across systems. Network approaches have also been extensively employed toward understanding specific aspects of cognition [e.g., (7)], development (8) and aging (9), and, perhaps most frequently, the pathological brain [e.g., Alzheimer's disease (10), Parkinson disease; (11), severe brain injury; (12)]. This approach has also found fruitful application in the study of human consciousness [e.g., (13–15)]. Indeed, many of the proposals of how human consciousness arises from neural function often make reference to aspects of brain activity as a network of interacting areas, such as the reverberation and spread of neural activity across fronto-parietal association regions (16, 17), the presence of synchronized long-range activity in specific frequency bands [e.g., (18, 19)] and specific neural circuits [e.g., cortico-thalamic loops; (20)], the dynamic competition between assemblies of cells (21), or to the degree to which a network possesses certain topological characteristics [e.g., integration and differentiation; (22)].

In the context of disorders of consciousness [DOC; (23)], network approaches to the study of functional connectivity have given rise to a fertile body of literature (see 24, for a recent review). Yet, there are a number of important methodological challenges which might play into the interpretation of such studies [cf., (25, 26)] and which might explain some of the contrasting results reported [e.g., the exact role of thalamo-cortical vs. cortico-cortical connectivity in recovery of consciousness; see (27–34)]. [See also (35) for further discussion].

In what follows, we propose that it is best to have both seed based and graph theoretic questions in a single model. In the neuroimaging literature, there are a number of limitations of current approaches which have hindered the ability to use a single model for combining seed based and graph theoretic approaches, but there are models that have been developed by other fields (36–40).

### 1.1. Four Problems in Current Network Analysis Approaches

Current graph theory methods as employed in neuroimaging (41, 42) suffer from a number of important shortcomings which are particularly relevant in the domain of DOC. (We note that the following discussion is in the context of network analysis as currently implemented for neuroimaging data, and is not meant to imply that other fields have not found solutions to them. In fact, as we will argue below, we are advocating for importing into

the field of neuroimaging methods that have successfully been applied in other domains).

#### 1.1.1. Problem #1: Arbitrary Enforcing of Network Density

Conventional graph theoretic approaches in neuroimaging require sparse networks. That is to say, they require networks (i.e., connectivity matrices) to have some connections (i.e., edges) with non-zero values (typically integer, in binary networks, or fractional, in weighted networks) and some with zero values—as opposed, for example, to fully connected networks in which all edges have non-zero values (i.e., each node is connected to all other nodes with non-zero edges). Yet, since brain networks are typically derived from pairwise correlations across time-series of regions of interest, the starting point for network analysis is typically a fully connected network [in fact, a complex network, which is both fully connected and has positive and negative edges; (43)]. It is thus common procedure to make the connectivity matrices sparse by fixing their density (i.e., the proportion of non-zero edges to the total number of possible edges), which is done by retaining the strongest  $d$  connections and setting all remaining ones to zero. The resulting network is thus sparse, with density  $\frac{d}{N(N-1)/2}$ , where  $N$  is the number of nodes in the network. On the one hand, this procedure ensures that any uncovered difference across networks (e.g., patients vs. volunteers; time-point A vs. time-point B) reflects some systematic aspect of their topological characteristics and not, more trivially, the fact that they have different densities. On the other hand, however, because of the lack of a principled approach to perform this procedure, it is currently typical to iteratively re-calculate network characteristics at several density levels, from a lower bound meant to ensure that networks are estimable [such that the average nodal degree is no smaller than  $2 \times \log(N)$ ; (44)] to an upper bound such that the mean small-world characteristic of networks is no smaller than 1 or 1.5 [e.g., (13)]. While conventional, the idea of enforcing graphs to have the same density across groups, time-points, or conditions is in itself problematic, because it is not hard to imagine that some graphs might be naturally denser than others [see (45)]. This is particularly relevant in the context of the typical comparisons of interest in DOC such as patients vs. healthy volunteers, patients in a Vegetative State vs. patients in a Minimally Conscious State (vs. patients in a Locked-in Syndrome), or within-patient changes over time (e.g., acute-to-chronic designs). Of course, similar problems are encountered in many other contexts (e.g., adolescents vs. older adults) and might even apply to normal, within-group, variability in the healthy brain. Mandating equal density across graphs might obscure important differences across conditions of interest, bias results, and lead to spurious findings.

One solution to the problem of network iterative thresholding is to analyze complex networks [i.e., fully connected and signed matrices; (43, 46, 47)]. Yet, despite this problem having been well documented, as shown in a recent review focused on the use of graph-theoretic approaches in the clinical context, less than 7% of 106 published papers (up to April 2016) employed complex matrices (48). All remaining studies only considered non-negative and/or sparse matrices. In addition, it is important to note two potentially unwanted limitations of using complex

matrices. First, the use of complex matrices assumes that the probability of connectivity between two regions is spatially stationary, but it is in fact well known to be inversely related to distance at both the neuronal and region levels [see, (49–51)]. Second, the use of complex matrices affects the formulation of some metrics [e.g., modularity; (43, 46)] because positive and negative edges are treated as separate sparse networks, an issue that is further complicated by the frequent use of mean-centering preprocessing strategies which are known to shift the distribution of positive and negative edges (52, 53). Furthermore, the formulation and interpretation of other metrics [e.g., path based metrics such as characteristic path length/local efficiency, betweenness centrality, etc.; (46, 54)], are also affected since the weights represent both the strength and probability of the connections (i.e., density). Thus, analyzing fully connected signed graphs does avoid the thresholding issue but at the cost of clouding the interpretation of metrics such as density and path-based graph statistics.

### 1.1.2. Problem #2: Network Measures Are Not Independent of Each-Other

A standard network analysis, as currently implemented in the field, typically assesses a number of different topological measures in parallel, such as characteristic path length, average clustering, efficiency, and small-world characteristic, among others [c.f., (43)]. Many of these characteristics, however, are not independent of each other. In fact, they are often interrelated and can greatly influence each other (55–57). Consider two metrics often employed in graph theoretic analysis of brain data: clustering coefficient and density. Clustering coefficient can be described as the level of segregated neural processing within a network (42). Density, as explained above, is a measure of the number of existing edges within a network (i.e., connection with non-zero value), divided by the total number of possible edges. These two network characteristics are strongly interrelated: It has been shown that there is a clear relationship between a network's density and its clustering coefficient (57). Similarly, dependencies between many other network measures frequently employed in the neuroimaging literature (e.g., degree, clustering coefficient, characteristic path length, and small world index) have also been reported (55, 56), highlighting the need to control for these relationships in order to minimize the potential for spurious findings [see (42, 55)]. Conventionally, this problem is addressed by arbitrarily fixing network density (see Problem #1). This approach, however, suffers from two important shortcomings. First, as explained above, different networks might well have different levels of natural—or stable—density. Second, it is a rather weak control. For example, it only addresses the dependencies of network measures on density, but ignores the many other known correlations among features of networks that are often assessed [cf., (55)], which, to date, have gone unaccounted for in virtually all of the extant literature in the field.

### 1.1.3. Problem #3: Failure to Account for Structural Information in Shaping Functional Networks

In the clinical context of DOC, despite the fact that patients are well known to have heterogeneous underlying pathology, which introduces many concerns for proper diagnosis (58,

59), functional [e.g., (13, 15, 28, 34, 60–63)] and structural connectivity (64–69) are typically investigated separately. This narrow approach is very problematic because it has been shown, in the rodent model (70) and in healthy humans (71, 72), that structural data can predict the functional connectivity as estimated by correlations in the fMRI signal, as well as EEG phase coupling in healthy volunteers (73). Failing to include both structural and functional data will have a similar effect on the analysis of functional networks as omitting any other graph metric (i.e., problem #2): it will result in improper estimation of the terms in the model and potentially spurious results. This issue is particularly important in the clinical context of DOC given their highly heterogeneous pathology and the fact that this can change over time, which affects longitudinal comparison of brain networks over time.

Diffusion weighted imaging (DWI) and blood oxygenation level dependent (BOLD) can be used in conjunction to estimate connectivity matrices using joint independent component analysis [jICA; (74)], Connectivity Independent Component Analysis [connICA; (75)] or partial least squares [PLS; (76)]. In general, all three methods produce multiple group connectivity matrices based on the covariance of BOLD and DWI data across all participants. Both jICA and connICA produce multiple components that are maximally spatially independent [for a complete explanation of jICA see (77–79) and for a complete explanation of connICA see (33)]. PLS produce a linear combination of latent variables that maximally covary with each other based on weighted structural and functional connections [for a complete explanation of PLS see (80–83)]. These methods incorporate both structural and functional connectivity in the estimation of the connectivity matrices, but they require researchers to choose the number of components (in jICA and connICA) or number of latent variables (in PLS). Changing these parameters influences the results of the connectivity estimation and the standards for these parameters are still being investigated for both jICA and connICA (78, 84–86). We thus propose an alternative to these methods that avoids the necessity to estimate the functional and structural connectivity jointly. In the approach we describe below, the structural and functional connectivity matrices are estimated separately, and the former is used as a variable in estimating graph statistics for the latter (see section 2.6 for a complete description).

### 1.1.4. Problem #4: Network Dynamics—Estimating Network Change Over Time

Finally, contrary to the assumption underlying conventional network analysis in neuroimaging, connectivity between areas is unlikely to be stationary processes. Rather, brain activity might best be viewed as a malleable and variable process over time (87). Yet, even in the few cases where this limitation has been addressed [e.g., (88)], these types of approaches do not quantify dynamic change of connectivity across time (or states). Rather, they just dissect a time-series into multiple static networks and compare them over their respective topological properties. In other words, even these approaches are static in nature and fail to capture the dynamics of network connectivity over time. In the context of DOC, for example, this means that longitudinal analysis of brain data can be employed to reveal differences in

topological properties of networks at two different time-points, but do not allow saying anything of the process of interest, which is the dynamics of how one network transitioned into another (e.g., how a network transformed as consciousness was regained over time).

## 1.2. Exponential Random Graph Models

In response to these four shortcomings of current network analysis, we present and demonstrate a novel [in the context of DOC, for other contexts within neuroimaging, cf.: (89–91)] approach to graph analysis, referred to as Exponential Random Graph Models [ERGM; (36)]. The core idea underlying ERGM is that instead of considering graphs as fixed entities which can be described in terms of topological properties (e.g., clustering, path length, small world property), it attempts to generate hypotheses about the (unobserved) stochastic processes that gave rise to an observed network (92). Contrary to the prevalent approach in neuroimaging, then, the presence/absence of an edge within a network is not considered to be a fixed property of a graph, but rather a random variable generated by a stochastic process. In other words, rather than assuming the observed network as “given” and fix, and describing its topological characteristics (e.g., characteristic path length, clustering coefficient), it tries to characterize the processes that have generated the observed network. One particularly appealing aspect of this approach is that, so long as the total number of nodes (i.e., ROIs) constituting a network remains unchanged, it allows for comparing across networks with different density levels, thereby solving problem #1. The ERGM framework uses the following exponential model:

$$P_{\theta}(Y = y) = \frac{\exp(\theta^T g(y))}{c(\theta)} \quad (1)$$

where  $\theta$  is a parameter vector that is modeled by  $g(y)$  (i.e., any statistic of the graph). The parameter  $c(\theta)$  is a normalizing constant representing the parameter estimate for all possible graphs (38). This normalizing constant is not able to be analytically solved due to the combinatorics of the graph structure. We can nonetheless approximate the unknown population mean using  $c(\theta_s)$  (i.e., the sample mean):

$$\begin{aligned} \frac{c(\theta)}{c(\theta_s)} &= E_{\theta_s} \exp(\theta - \theta_s)^T g(y_i) \\ \frac{c(\theta)}{c(\theta_s)} &\approx \frac{1}{M} \sum_{i=1}^M \exp(\theta - \theta_s)^T g(y_i) \end{aligned} \quad (2)$$

for derivations [see (38)]. These equations allows for an approximation of the population mean using sample mean. A bootstrapping method using Markov Chain Monte Carlo (MCMC) methods is used to sample and estimate the population mean. These methods assume Markovian principles of independent draws and the ability to reach equilibrium. Equilibrium is the state in which any edge that is toggled on or off results in an equally probable graph. The general method is to take the ratio of the probabilities of  $Y_{ij} = 1$  (i.e., adding a single

edge) and  $Y_{ij} = 0$  (i.e., no edge) conditioned on  $Y_{ij}^C = y_{ij}^C$  (i.e., all other pair of nodes in the graph).

$$\begin{aligned} \frac{P(Y_{ij} = 1 | Y_{ij}^C = y_{ij}^C)}{P(Y_{ij} = 0 | Y_{ij}^C = y_{ij}^C)} &= \exp \theta^* (s(Y_{ij} = 1) - s(Y_{ij} = 0)) \\ \log \frac{P(Y_{ij} = 1 | Y_{ij}^C = y_{ij}^C)}{P(Y_{ij} = 0 | Y_{ij}^C = y_{ij}^C)} &= \theta^* \Delta(s(Y_{ij})) \\ \text{LPL}(\theta) &= \sum \log [P(Y_{ij} = y_{ij}) | (Y_{ij}^C = y_{ij}^C)] \end{aligned} \quad (3)$$

where the  $\text{LPL}(\theta)$  is the log-pseudolikelihood for  $\theta$ , which is maximized by taking the maximum pseudolikelihood for  $\theta$  (38). This estimation process is performed for the model with all the parameters (i.e.,  $\theta$ ). The estimates give the mean and standard error. These estimates were tested for significance in each functional data set. Due to the MCMC, a t-statistic can be estimated and is reported in the model output along with a p-value.

For interpretation purposes, Equation 1 can be represented as follows [the full derivations can be found in (38)]:

$$\text{logit}(P_{\theta}(Y_{ij} = 1 | nactors, Y_{ij}^C)) = \sum_{k=1}^K \theta_k \delta_{Z_k(y)} \quad (4)$$

where  $k$  is the number of network statistics in the model and  $\theta_k$  is the parameter estimate for each statistic. The  $\delta_{Z_k(y)}$  is the change in network statistic if a edge were added between any node  $i$  and  $j$ . Thus, the interpretation of the network statistics involve the change in probability of an adding a edge with certain network statistic. The significance of a parameter estimate is one compared to the expected parameter estimate in a null model with the probability of all edges equal to 0.5 [i.e., (93)].

In what follows, we first demonstrate the insidiousness of problem #2 in the context of well characterized, freely-available, data on the business ties of Florentine families in the fifteenth century (94), and then we apply the powerful and flexible ERGM approach to estimating network statistics for characterizing (brain) networks in the longitudinal context of a patient recovering after coma after severe traumatic brain injury (TBI). To anticipate the key points that will follow, ERGM, which has been successfully employed in other contexts (36–40), offers a number of substantial advantages which are particularly important in the clinical context of DOC. First, it does not require imposing (and assuming) the same level of density across graphs, thus allowing estimating characteristics of each graph at its “natural” density level. Second, it allows for controlling the dependencies between network characteristics. In this sense, in contrast to the conventional approach, which can be viewed as a series of univariate regressions (i.e., one per metric) assessing the topological characteristics across groups of graphs (e.g., patient groups and controls vs. patients), ERGM is making use of a multiple regression framework (39), in which all features are considered together, and thus returns the “unique” contribution of each network measure. Third, the multiple regression framework extends to graph theoretic measures characterizing



the structural connectivity of a network, thus accounting and “parceling out” the effect of cross-sectional differences [e.g., (69)] and longitudinal changes in structural connectivity [e.g., (95, 96)] across graphs. Finally, a temporal implementation of this technique, Separable Temporal ERGM (STERGM), allows assessing the dynamic changes of network properties occurring over observations (e.g., time, clinical groups).

## 2. METHODS

### 2.1. Florentine Business Ties Data

We demonstrate the importance of problem #2 using freely available data for social network analysis. The dataset, which has been extensively characterized in previous work, describes business connections between Florentine families in the fifteenth century (94). We use this data analysis to demonstrate the interrelationship between network measures and how failure to include them in a single full model (FM) can lead to spurious results. Specifically, the relationship between network measures is manipulated by constructing two identical networks with one unique difference between them—that is, whether the Barbadori family belongs to the blue group (Figure 1, left) or the green group (Figure 1, right). As we will discuss further below, this example focuses on the relationship between node mixing terms (i.e., a measure of within-group [blue vs. green] connectivity) and a higher order term called geometrically weighted edge shared partners (GWESP; a type of triangles term; see section 2.6 for full description of both terms). To demonstrate the effects of relationships between measures, we estimate three models per each network: two partial models (PMs) including an edges term and either the higher order term ( $PM_A$ ) or the mixing terms ( $PM_B$ ), and the FM containing all terms. As we will show, for each network, PMs return spurious results with respect to both significance and magnitude of the parameter estimates.

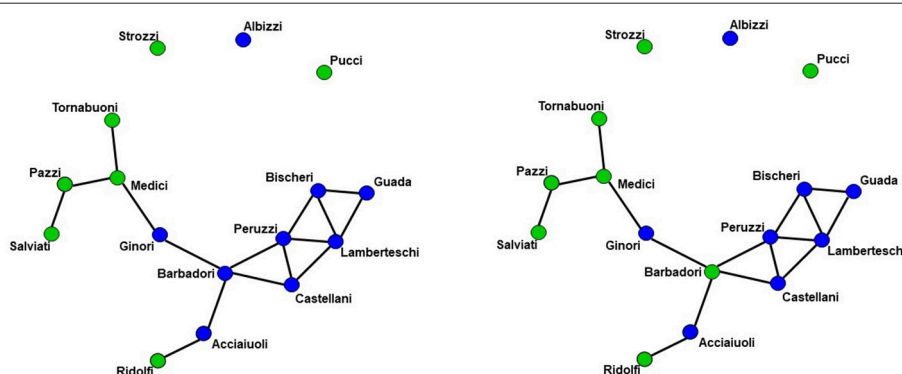
### 2.2. Patient

We demonstrate the use of ERGM models using longitudinal data from a patient recovering from a severe brain injury.

A 40 to 45 year old person suffered a severe TBI due to a fall. The patient suffered pulmonary contusion and liver laceration, and presented with a post-resuscitation Glasgow Coma Scale [GCS; (97)] of 3. Computerized tomography (CT) revealed skull fractures, traumatic subarachnoid hemorrhage, extradural hematoma, subdural hematoma, and bilateral frontal lobe contusions. At the 3 acute imaging sessions, which occurred on the 11, 18, and 25th days post-injury, the patient presented a total GCS of 6 (Eyes opening (E): 1, Verbal response (V): 1, Motor response (M): 4), 7 (E:1, V:1, M:5), and 10 (E:3, V:1, M:6), respectively. While DoC diagnoses are typically not made at such an acute stage, the behavioral profile of the patient was consistent with a vegetative state [VS; i.e., wakefulness in the absence of any behavioral sign of awareness of the self or the environment; (23)] at the first time-point, with a minimally conscious state *minus* [MCS-; i.e., wakefulness with intermittent but reproducible signs of low-level non-reflexive behaviors, such as orientation to noxious stimuli; (98)] at the second time-point, and a minimally conscious state *plus* [MCS+; i.e., wakefulness with intermittent but reproducible signs of high-level non-reflexive behaviors, such as response to command, intelligible verbalization, or gestural or verbal yes/no responses; (98)] at the third. At 6-months follow-up the patient was assessed with a Glasgow Outcome Scale—Extended [GOS-E; (99)] in-person interview and scored as being in a lower moderate disability (i.e., GOS-E = 5).

### 2.3. Experimental Design

The patient underwent 4 imaging sessions over the span of 6 months. The first 3 sessions occurred within a month post injury (see above), and the follow-up session took place 181 days post-injury. At each session the patient underwent (among other clinical and research sequences) anatomical (T1-weighted) and functional (T2\*-weighted) data protocols. T1-weighted images were acquired with a 3D MPRAGE sequence (repetition time [TR] = 1,900 ms, echo time [TE] = 3.43,  $1 \times 1 \times 1$  mm). BOLD functional data were acquired with a gradient-echo echo planar image (TR = 2,000 ms; TE = 25 ms,  $3.5 \times 3.5 \times 4$  mm). Diffusion Weighted data were acquired with an echo planar sequence (TR



**FIGURE 1 |** Florentine business ties networks. Florentine business ties data with additional grouping. **Left:** Network A. **Right:** Network B. We note that two networks are identical except for the Barbadori family being allocated to the blue group in the left graph and to the green group in the right graph.

= 9,000 ms, TE = 90 ms, 64 directions,  $3 \times 3 \times 3$ ) using a b-value of 1,000 and acquiring an additional B0 image. Acute data were acquired on the in-patient 3 Tesla Siemens TimTrio system at the Ronald Reagan University Medical Center, while chronic data were acquired on the out-patient 3 Tesla Siemens Prisma system also at the Ronald Reagan Medical Center at the University of California Los Angeles. The study was approved by the UCLA institutional review board (IRB). Informed consent was obtained from the legal surrogate, as per state regulations.

## 2.4. Data Preprocessing

### 2.4.1. BOLD Data Preprocessing

The functional data underwent a number of conventional preprocessing steps including brain extraction, slice timing correction, motion correction, band-pass filtering ( $0.08 \leq \text{Hz} \leq 0.1$ ), and removal of linear and quadratic trends. A nuisance regression was employed to parcel out signals of non-interest including motion parameters, white matter, cerebral spinal fluid, and full-brain mean signal [which has been shown to alleviate the consequences of in-scanner motion; (100)]. Affine registration of the functional data to the standard template (MNI) was performed using Advanced Normalization Tools [ANTs; (101, 102)].

### 2.4.2. DWI Data Preprocessing

The diffusion data were preprocessed using the following pipeline: DWI preprocessing, registrations, probabilistic tractography with tractography thresholding. All of these processes were run using a bash script in parallel using the GNU Parallel package (103).

#### 2.4.2.1. DWI preprocessing

All preprocessing procedures were visually checked for optimal quality. The T1-weighted data were brain extracted [optiBET; (104)] and bias field corrected [BrainSuite BFC; (105)]. The diffusion-weighted data were prepared for tractography with the following steps: (1) visual quality checking of raw images; (2) artifact checking/removal and motion correction with vector rotation [DTIprep; (106)]; (3) eddy current distortion correction followed by tensor fitting (i.e., linear fitting using weighted least squares) and estimation of diffusivity metrics [BrainSuite's BDP; (107, 108)]; (4) brain extraction of the b0 image [BET; (109)]; and (5) GPU-enhanced Bayesian estimation of the diffusion profile with up to two principal directions per voxel (i.e., allowing for crossing/kissing streamlines) using FSL's bedpostx (110, 111).

#### 2.4.2.2. Registrations

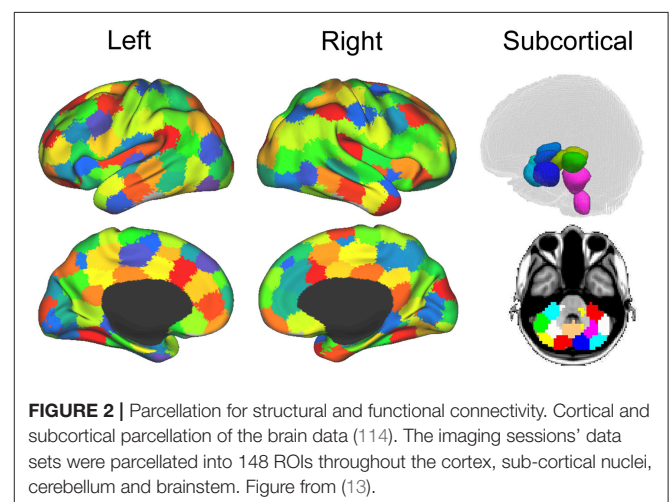
All registrations were visually checked for optimal quality. The following steps were conducted: (1) linear registration of the native diffusion data (b0 image) to the native T1-weighted data [ANTs IntermodalityIntrasubject; (102)]; (2) nonlinear registration (ANTs) of the native T1-weighted data to the Montreal Neurological Institute (MNI) standard space (MNI Avg 152 T1  $2 \times 2 \times 2$  mm standard brain); (3) forward or inverse transform concatenations [ANTs; (102)] to move between native diffusion, native T1, and the MNI template.

### 2.4.2.3. Probabilistic tractography

GPU-enhanced probabilistic tractography between all regions of the whole-brain atlas (i.e., iteratively seeding from each region to all other regions as targets) was conducted with the “matrix1” option in FSL's probtrackx2 (110, 112). A minimum distance of 4.8 mm (i.e., 2 voxel widths) was set to prevent artificial streamlines passing through contiguous regions. The output matrix of streamline counts between all regions was thresholded to remove spurious streamlines with an optimization procedure that minimizes asymmetries between the seed/target assignments for each ROI-ROI pair [MANIA; (113)].

## 2.5. Brain Network Construction

For each dataset (both the functional and diffusion data), a graph was constructed to provide a mathematical description of the brain as a functional network. Brain graphs were constructed in two steps. First, these data sets were parceled into 148 ROIs spanning the cortex, sub-cortical nuclei, cerebellum and brainstem (see **Figure 2**). This parcellation scheme, which was defined independently of our data, is made freely available by Craddock and colleagues (114). Additionally, we used the Oxford thalamic connectivity atlas (115) to further refine the parcellation of the thalamus from 6 to 14 for a total of 148 ROI (i.e., 134 Craddock ROIs and 14 Thalamic ROIs). While other parcellation schemes are available (e.g., Harvard-Oxford atlas, AAL atlas), the present one has two main advantages [cf., (13)]. First, being functionally defined, it clusters spatially proximal voxels by the homogeneity of their functional connections as opposed to clustering voxels by anatomical position which, as exemplified by the case of the precentral gyrus ROIs in both the AAL and the Harvard-Oxford atlases, might cluster together functionally distinct sub-regions. Second, at our chosen level of resolution, the Craddock ROIs have almost 50% more granularity as either structural atlas (i.e., 148 ROIs vs., 90 and 112 for the AAL and Harvard-Oxford atlases, respectively). Following parcellation, the average time-course of all voxel within each ROI were extracted and correlated across each pair of regions.



**FIGURE 2** | Parcellation for structural and functional connectivity. Cortical and subcortical parcellation of the brain data (114). The imaging sessions' data sets were parcellated into 148 ROIs throughout the cortex, sub-cortical nuclei, cerebellum and brainstem. Figure from (13).

Functional connectivity was assessed with a partial correlation method using the Markov Network Toolbox [MoNeT; (116)] in MATLAB. This approach, referred to as R3 (as in resampling, random penalization, and random effects), combines a penalized maximum likelihood estimation—or graphical lasso—procedure with a resampling-based (bootstrapped) model selection procedure, on whitened BOLD timeseries, to infer fully-data driven stable functional connectivity estimates at the single-subject (or group) level. Under this approach, each fMRI time series is repeatedly bootstrapped in order to estimate the within-subject variability and matrices of penalty parameters which reduce selection bias and variability. This method thus reduces the spurious connections from indirect sources arising from the high dimensionality of fMRI data often seen when using the conventional Pearson's  $r$  method. Using partial correlations with regularization parameters, the indirect sources are eliminated and the sparsity of each matrix is determined by the within subject variability. Thus, each functional data set returns a connectivity matrix that represents connectivity from direct sources, rather than indirect ones, and that is sparse, as determined on a single-subject basis through bootstrapping and regularization. This latter point side-steps entirely the need for arbitrary and iterative thresholding approaches (42). It is important to point out, however, another important difference between the partial correlations approach described above and the standard correlation approach to estimating brain networks as performed by most previous work [e.g., (13, 117, 118)]. On the one hand, the conventional correlational approach has the advantage of allowing straightforward interpretation of the elements of adjacency matrices as strength of the functional connectivity between nodes. On the other hand, the matrices generated are fully connected and thus requiring application of a non-linear transformation (e.g., thresholding) in order to render them sparse – a condition necessary for application of many common graph theory metrics (42). In contrast, the partial correlation method employed here returns a sparse matrix. However, it does so at the cost of losing interpretability of graph weights which can now be seen as the functional connectivity between two nodes  $i$  and  $j$  after controlling for the correlations with other nodes in the neighborhood (i.e., connected with) – say –  $i$ . For this reason, matrices obtained with this novel methodology are typically binarized, thus resulting in a sparse matrix of ones and zeros indexing the presence/absence of functional connectivity between each pair of nodes (i.e., ROIs).

## 2.6. Graph Statistics

All ERGM models we used to analyze the patient data included the same graph statistics. The model used for all the data sets was specified as follows:

$$P_{\theta}(Y = y) = \frac{\exp(\theta_1 \text{edges} + \theta_2 \text{nodecov}(\text{degree}) + \theta_3 \text{nodecov}(\text{efficiency}) + \theta_4 \text{nodecov}(\text{cluster}) + \theta_5 \text{nodemix}(\text{latent}) + \theta_6 \text{nodemix}(\text{resting}) + \theta_7 \text{gwesp}(\alpha = \lambda))}{c(\theta)} \quad (5)$$

Edges refers to the total number of edges for each functional connectivity graph. This term allows control for the density of

each graph. In this sense it is thus similar to the intercept in a linear regression and is thus typically not interpreted or further analyzed.

There are four nodal covariate terms for the diffusion data—three nodal covariates (i.e., degree, efficiency and cluster) and the nodemix (latent) term –and a nodal covariate for the functional connectivity (i.e., nodemix for resting). Degree is the number of edges for each structural node. Efficiency is the local efficiency of each node. Cluster is the clustering coefficient of each node. The nodecov term estimates the probability of functional connectivity edge as a function of each distribution of the structural terms (i.e., degree, local efficiency and clustering coefficient). A positive coefficient indicates an increase in the probability of a functional connectivity edge as structural term increases in magnitude. On the other hand, a negative coefficient indicates an increase in probability of a functional connectivity edge as the structural term decreases.

As shown in Equation (5), there are two nodemix terms: latent and resting. The nodemix (latent) is the within and between module connectivity of the structural connectivity. Thus, this mixing term represents the probability of a functional connectivity edge given the modular membership based on the structural connectivity. The number of modules and modular membership of each node is determined by a position latent cluster ERGM (119, 120). These models have shown to be able to use a latent space model with an a priori determined number of dimensions using the parameter  $d$  (3 dimensions). The nodes are arranged in a euclidean system with proximity equating to probability of an edge. The clusters are determined by the parameter  $G$  (3, 4, 7, and 6 for Acute first, second, third sessions and Chronic session, respectively). This parameter sets the number of Gaussian spherical clusters that are introduced in the latent space. The estimation of position latent cluster ERGM is a two step Bayesian estimation, but the exact specification is beyond the scope of this paper [see (119)].

The nodemix (resting) is our mixing term for determining the inter- and intra-regional connectivity of the resting state networks and sub-cortical regions of the functional data. Multiple parameter estimates were produced for this term. Additionally, these mixing terms used the exogenous node labels for each node's membership in the seven resting state networks (121) and sub-cortical regions. Each node of the brain network was labeled either: frontoparietal, visual, somato-motor, limbic, dorsal attention, ventral attention, default, subcortex and thalamus. Each combination of the inter- and intra-regional connectivity produced a mixing term and parameter estimate. For example, one inter-regional mixing term would be frontoparietal and thalamic connectivity. This parameter estimate would give the probability of an edge existing between the frontoparietal network and thalamus. An example of intra-

regional mixing term would be frontoparietal to frontoparietal. This term would express the probability of an edge within the

frontoparietal network. These mixing terms were used to assess the connectivity between the within the resting state networks, between the resting state networks, within the sub-cortical regions, between the sub-cortical regions, and between resting state networks and sub-cortical regions. This term incorporates questions that would be addressed using seed based connectivity analyses.

The geometrically weighted edged shared partners (GWESP) can be expressed by this equation (37):

$$\theta_t = \log \lambda_t$$

$$v(y; \theta_t) = e^{\theta_t} \sum_{i=1}^{n-2} [1 - (1 - e^{-\theta_t})^i] EP_i(y) \quad (6)$$

In this equation,  $v$  is the GWESP term and  $\theta_t$  is the log of the decay parameter that was fixed in all the data sets. The  $EP_i(y)$  is the edge shared partners term for the entire graph. It accounts for the number of each type of edge shared partner. An edged shared partner is triangle that shares a common base. Edge shared partners is a metric used to quantify the amount of clustering in the form of transitivity in a network. High positive parameter estimates indicate that transitivity is present above and beyond all the other statistics in the model. Transitivity is a higher order relationship present in most graphs which are the local and/or global communication and the amount of local cohesion. Differences in transitivity between patients could be a key change that occurs from injury. This would be a disruption of the clustering found within the patient's brain. This type of disruption would hamper local and/or global communication and additionally it would indicate a lack of local cohesion within a network.

The analysis was performed using the ERGM package (40) in R. There are two ERGMs used on the patient data. A FM and used all the terms from Equation (5). The FM was fit multiple times to get assess the proper  $\lambda$  (the decay parameter) for the GWESP term. The range of  $\lambda$  began at 0.05 and increase by increments of 0.05 up to 2.0. Each iteration was checked by inspecting the diagnostics of the MCMC. The models that have the best fit for the parameter estimate GWESP were chosen (i.e.,  $\lambda = 0.45$ ). A second model, the PM was fit. The structural terms (i.e., the three nodecov and the nodemix for latent) were omitted from this model to demonstrate the effects on the rest of the parameter estimates.

The FM's graph statistics were chosen based on two reasons: the type of functional data being analyzed (i.e., resting state data) and the first three problems outlined above (see sections 1.1.1–1.1.3). The nodemix (resting) terms were chosen because this patient's functional connectivity matrices were estimated from the BOLD correlations during the resting state scans. Thus, the intra- and inter- regional connectivity would be best characterized by putative resting state networks. The number of resting networks were chosen based on a data driven approach [i.e., (121)] that estimates a number of networks based on stability of clusters [for details on the clustering algorithm see (122)] estimated from 1,000 subjects' functional data. A seven network parcellation was chosen because it minimized the instability

(121) and matches what has been previously discussed in the literature [e.g., (123–126)]. Additionally, the thalamus group was added because of its possible involvement in DOC [e.g., (28, 29, 32, 127)] or anesthesia induced loss of consciousness [e.g., (117, 118, 128, 129)]. Finally, the subcortical and cerebellum groups were added to ensure every node fit a grouping label.

The edges term allows for networks with varying density to be modeled and compared (cf., Problem #1, section 1.1.1). The higher order term (i.e., GWESP) describes the local and/or global communication which could be an important aspect in the recovery from brain injury [e.g., (14, 32, 130)], and because it alleviates the problem of interrelation among graph theoretic measures (cf., Problem #2, section 1.1.2) by accounting for the higher order term's variance and thus avoiding it being improperly allocated to lower order terms (i.e., edges, node mixing, and structural terms). As shown below, failing to include the higher order term can affect the estimation of parameters in either magnitude or sign. Structural connectivity is important because, as stated in third problem (cf., section 1.1.3), it can be severely affected by TBI, systematically changing over time and/or patient cohorts, and because it is interrelated with functional connectivity. Thus, we chose four terms for the structural connectivity that would capture the number of connections of each node (i.e., degree), a measure of integration [i.e., local efficiency (42)], and higher order relationships (i.e., clustering and modularity). The two higher order terms were chosen because they capture two different higher order dynamics: local grouping of nodes [i.e., clustering coefficient (42)] and community structure [i.e., modularity; (42)].

The models were assessed by using goodness of fit (GOF) plots (38). After the model was estimated, a thousand simulations were run from the model statistics. These simulations were compared to the original graph's probabilities for each graph statistic (e.g., the probability of nodes with a specific degree, probability edge shared partners and the probability minimum geodesic distances). This is to ensure that the model represents a graph similar to the original data that it was modeled from. The metrics chosen for this example is degree distribution, edge wise shared partner, minimum geodesic distance (another form of local path length) and the nodal covariates from Equation 5. These are the most commonly used graph metrics because they capture important characteristics of graphs that capture the central tendencies and clustering of graphs. The MCMC diagnostics were assessed for each parameter estimate. The GOF plots were used to assess the fit of the FM and all four GOF plots was assessed for goodness of fit.

## 2.7. Separable Temporal Exponential Random Graph Model

STERGM (131) is an extension of the original ERGM. It is used to assess the dynamics of networks as they change over time. The same underlying methods for estimating ERGM is used in STERGM. A model with network statistics is used to estimate the parameter estimates for a network that changes over time. To achieve this, two separate networks are investigated. A formation



network is generated conditional on forming edges,

$$P(Y^+ = y^+ | Y^t; \theta^+) = \frac{\exp(\theta^+ g(y^+, X))}{c(\theta^+, X, Y^+(Y^t))}, y^+ \in Y^+(y^t) \quad (7)$$

where a formation network  $Y^+$  is characterized by formation parameters  $\theta^+$  (131). The formation network statistics are  $g(y^+, X)$  and the normalizing constant is  $c(\theta^+, X, Y^+(Y^t))$ . The second network formed is a dissolution network that is conditional on the edges that dissolve. This network is represented by the same variables labeled with minus instead of a plus,

$$P(Y^- = y^- | Y^t; \theta^-) = \frac{\exp(\theta^- g(y^-, X))}{c(\theta^-, X, Y^-(Y^t))}, y^- \in Y^-(y^t) \quad (8)$$

where a dissolution network  $Y^-$  is characterized by dissolution parameters  $\theta^-$  (131). The dissolution network statistics are  $g(y^-, X)$  and the normalizing constant is  $c(\theta^-, X, Y^-(Y^t))$ . These networks can form a new network at time  $t + 1$  by applying formation and dissolution networks on  $y^t$ . This can be expressed as:

$$Y^{t+1} = Y^t \cup (Y^+ - Y^t) - (Y^t Y^-) \quad (9)$$

The formation and dissolution networks are independent of each other across the  $t + 1$  time points (131). STERGM has the unique ability to model networks as they transform over time enabling research questions about the dynamics of a network. The same model in Equation 5 was used in both the formation and dissolution models. The quantifications of these networks are similar to ERGM, but these two models slightly change the interpretation of the parameter estimates. In the formation model, a positive parameter estimate indicates a tendency for edges for a network statistic form at time point  $t + 1$ , and a negative parameter estimate indicates a lack of formation of edges for a particular network statistic at time point  $t + 1$ . The dissolution model has two separate interpretations based on the sign of the parameter estimate. A negative parameter estimates are interpreted as edges are more likely to dissolve and positive parameters indicate edges are more likely to be preserved. Despite these differences in interpretation, all the same procedures were used in STERGM as were used in ERGM (PM, FM, quality control using MCMC diagnostics, and assessing fit using GOF) for both the formation and dissolution models.

## 3. RESULTS

### 3.1. Florentine Business Ties

Network A has both the mixing term and triangles term as significant model statistics when modeling them separately (i.e.,  $PM_A$  and  $PM_B$  see **Table 1**). When they are combined together into the FM, the mixing term remains significant but the triangle term is no longer significant. Thus, the FM for the Florentine business ties properly attributes the variance of each graph theory statistic and the selective mixing term remains significant. The network B has just the triangles term significant in the  $PM_A$  and FM. The mixing term is neither significant in the  $PM_B$  nor the FM.

### 3.2. Patient Recovery

Consistent with the argument we made in the introduction, as shown in **Figure 3** (bottom row), the brain network construction using MoNeT resulted in four graphs with different estimated densities. Specifically, the three acute sessions returned graph densities of 10.4, 13.5, 12.9%, for the first, second, and third time-points, respectively, while the chronic session presented a graph density of 14.5%. Overall, then, the density differential between acute session 1 and chronic session was 4.1%, and the general acute-to-chronic pattern appeared to be a trend toward greater density. The structural connectivity (**Figure 3**, top row), on the other hand, had less variability in the densities of the graphs over time (i.e., 6.6, 6, 5.3, and 5.3%; a total difference of 1.3% between acute session 1 and chronic session).

#### 3.2.1. Integrating Functional and Structural Connectivity

When we compared the properties of the network as estimated relying exclusively on functional connectivity (i.e., PM) as compared to when both functional and structural connectivity were jointly considered (i.e., FM), the PM included two significant positive inter-regional connectivity parameters (i.e., between thalamus and subcortex and between limbic network and subcortex; see top of **Figure 4**) which were no longer significant once structural connectivity was included (i.e., in the PM), suggesting their spurious status. More broadly, the positive parameter estimates became less positive and the negative parameter estimates became more negative. The only structural terms that were significant were the nodal covariate mixing term for connectivity between latent clusters 2 and 3 and within latent clusters 3 (see **Table 2**).

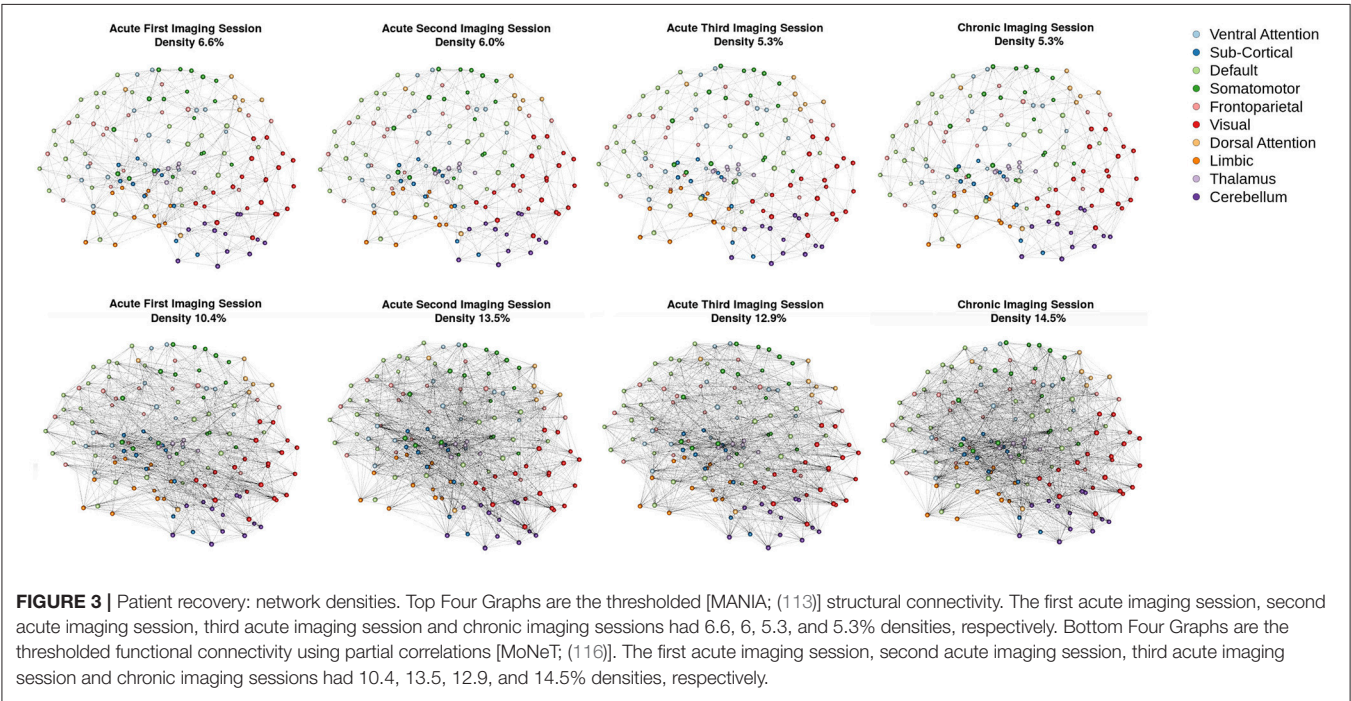
At the second acute time-point, the PM and the FM again differed, with the latter showing an additional significant positive parameter estimate for connections between dorsal attention network and subcortex (see bottom **Figure 4**), three inter-regional connectivity parameter estimates that became non-significant (i.e., connections between cerebellum and subcortex, default network and frontoparietal network and visual network and dorsal attention; see bottom **Figure 4**) and two intra-regional connectivity parameter estimates that became non-significant (i.e., connections within the subcortex and ventral attention network; see bottom **Figure 4**). Overall, the parameter estimates both increased and decreased in magnitude with or without changing significance. Similar to the first acute session, the structural terms were only significant for the nodal covariate mixing term (i.e., between latent clusters 1 and 3, and within latent clusters 1, 2, 3, and 4; see **Table 2**).

In the third acute session, six inter-regional positive parameter estimates (i.e., connections between cerebellum and dorsal attention network, frontoparietal network and dorsal attention network, frontal parietal network and ventral attention network, dorsal attention network and somatomotor network, limbic network and visual network and limbic network and subcortex; see right **Figure 5**) and three intra-regional positive parameter estimates (i.e., connections within the dorsal attention network, somatomotor network and ventral attention network; see **Figure 5**) became non-significant once structural connectivity

TABLE 1 | Florentine business ties models.

	ERGM Parameter Estimates					
	Network A			Network B		
	PM <sub>A</sub>	PM <sub>B</sub>	FM	PM <sub>A</sub>	PM <sub>B</sub>	FM
Edges	−2.44*** (0.40)	−3.42*** (0.72)	−3.54*** (0.70)	−2.46*** (0.39)	−2.27*** (0.43)	−2.75*** (0.49)
Nodal Covariate Mixing: Within Group 0		1.63 (0.95)	1.60 (0.88)		0.15 (0.75)	0.31 (0.65)
Nodal Covariate Mixing: Within Group 1		2.60** (0.80)	2.16** (0.82)		1.17 (0.61)	0.91 (0.48)
GWESP (Fixed 0.8)	0.53* (0.23)		0.32 (0.28)	0.54* (0.23)		0.50* (0.23)

Three models are run on each network in **Figure 4**: PM<sub>A</sub>, PM<sub>B</sub>, FM. The PM<sub>A</sub> has just the edges and triangles term. The PM<sub>B</sub> has just the edges and mixing term. The FM has all three terms. Each term has a parameter estimate, a standard error in parenthesis and a p-value indicated by asterisks. The LATEX code to create this table was produced by the R package called texreg (132). \**p* < 0.05; \*\**p* < 0.01; \*\*\**p* < 0.001.

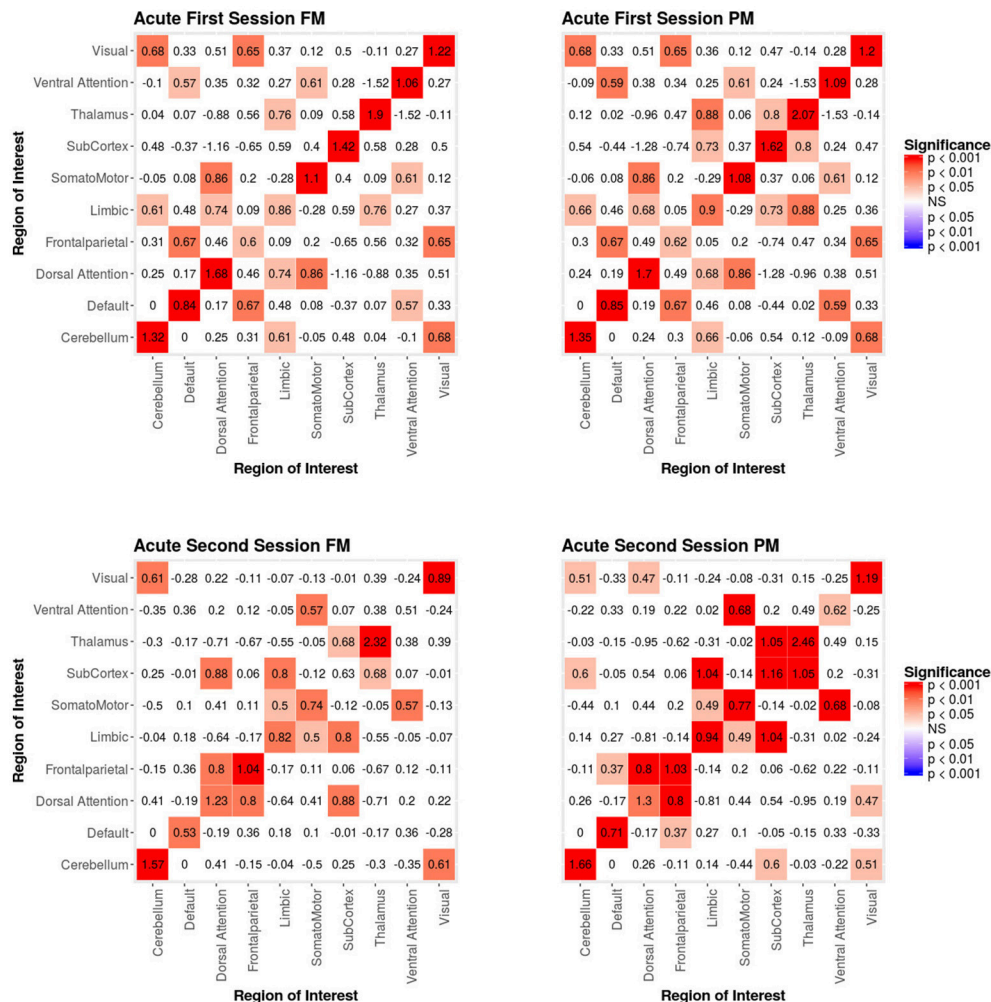


was included in the model. Similar to the first acute session, the parameter estimates generally decreased in magnitude. Finally, consistent with the first two acute sessions, the only significant structural feature was the nodal covariate mixing term (i.e., between latent clusters 2 and 3, latent clusters 1 and 4, latent clusters 1 and 6, latent clusters 3 and 6 and latent clusters 5 and 7, and within latent clusters 1, 2, 3, 4, 5, 6, and 7; see **Table 3**).

In the chronic session, two inter-regional positive parameter estimates became non-significant after inclusion of the structural connectivity terms (i.e., between default network and frontoparietal network and default network and visual network; see right **Figure 5**). Conversely, unlike in the acute sessions, we also observed the reverse effect, with the the visual

network and ventral attention network parameter estimate became significant in the FM. Additionally, the structural terms were only significant for the nodal covariate mixing term (i.e., between latent clusters 1 and 3, latent clusters 2 and 3, latent clusters 1 and 4, latent clusters 3 and 5, latent clusters 4 and 5, latent clusters 1 and 6 and latent clusters 2 and 6 and within latent clusters 4; see **Table 3**).

Finally, across all imaging sessions the GWESP parameter estimate was reduced in magnitude (see **Tables 2, 3**) by the addition of the structural terms, with the largest difference seen in third acute session (see **Table 3**). Additionally, the GOF (see **Figure 6**) are fit for every statistic in all of the FM. All the GOF terms fit well except for a portion of the edge shared partners, but



**FIGURE 4 |** Patient recovery ERGM. Comparison of results for the FM and PM for acute sessions 1 and 2. The left figures display the FM mixing term results for the Acute first and second sessions. The mixing term term accounts for the inter- and intra-regional connectivity. The legend displays tints of red for significant positive parameter estimates. The right figures display the PM mixing term results for the Acute first and second sessions. The coloring scheme is the same as the FM. These figures are symmetric within each model because the graphs are undirected.

in the model statistics (the far right in **Figure 6**) are well fit to the original data.

As we will discuss below, the differences we are reporting between the results obtained with the conventional model (i.e., PM), estimated form functional connectivity alone, and those obtained with the (i.e., FM), estimated from both the functional and structural connectivity, demonstrates the risk of drawing spurious conclusions when relying on the PM.

### 3.3. STERGM

The STERGM allowed us to look at the temporal dynamics of recovery post severe brain injury with two parallel models: a formation model and a dissolution model. The formation model produces parameter estimates describing how likely it is that new connections (i.e., edges) form throughout the recovery from coma, while the dissolution model produces parameter estimates

describing how likely it is that existing connections dissolve (or persist) throughout recovery.

In our index patient, the formation model showed a significant negative edges parameter estimate and a significant positive GWESP parameter estimate, the latter implying a tendency to form edges over time that close triangles (see **Table 4**). Additionally, none of the structural nodal covariates were found to be significant (see **Table 4**). There were, however, four significantly positive parameter estimates for intra-regional connectivity (i.e., default network, frontoparietal network, thalamus, and visual network; see left **Figure 7**), three significantly negative parameter estimates for inter-regional connectivity (i.e., between default network and visual network, somatomotor network and frontoparietal network, and ventral attention network and visual network; see left **Figure 7**), and two significantly positive parameter estimates for inter-regional connectivity (i.e., between default network and thalamus,



**TABLE 2 |** Patient recovery ERGM.

	ERGM Parameter Estimates			
	First Acute		Second Acute	
	PM	FM	PM	FM
Edges	−6.29*** (0.28)	−6.34*** (0.56)	−7.64*** (0.36)	−7.71*** (0.59)
Nodal Covariate: Degree (Structural)		0.00 (0.00)		0.00 (0.01)
Nodal Covariate: Local Efficiency (Structural)		0.10 (0.44)		0.35 (0.35)
Nodal Covariate: Cluster Coefficient (Structural)		−0.08 (0.34)		−0.33 (0.29)
Nodal Covariate Mixing: Latent Cluster 1 to 1 (Structural)		0.03 (0.08)		1.01*** (0.15)
Nodal Covariate Mixing: Latent Cluster 2 to 2 (Structural)		0.07 (0.17)		0.82*** (0.11)
Nodal Covariate Mixing: Latent Cluster 1 to 3 (Structural)		−0.11 (0.08)		0.33** (0.12)
Nodal Covariate Mixing: Latent Cluster 2 to 3 (Structural)		−0.28* (0.12)		0.16 (0.11)
Nodal Covariate Mixing: Latent Cluster 3 to 3 (Structural)		0.24* (0.10)		0.91*** (0.12)
Nodal Covariate Mixing: Latent Cluster 1 to 4 (Structural)				0.23 (0.13)
Nodal Covariate Mixing: Latent Cluster 2 to 4 (Structural)				0.22 (0.12)
Nodal Covariate Mixing: Latent Cluster 3 to 4 (Structural)				−0.09 (0.12)
Nodal Covariate Mixing: Latent Cluster 4 to 4 (Structural)				0.86*** (0.13)
GWESP (Fixed 0.45)	2.09*** (0.13)	2.07*** (0.13)	3.11*** (0.21)	2.94*** (0.20)

Parameter estimates for the FM and PM of the Acute first and second sessions. The mixing term for resting state are excluded because they are in **Figure 4**. All of the structural parameter estimates are listed in the FM columns. The edges and GWESP parameter estimates are for the functional connectivity in the PMs and FMs. The LATEX code to create this table was produced by the R package called texreg (132). \* $p < 0.05$ ; \*\* $p < 0.01$ ; \*\*\* $p < 0.001$ .

and somatomotor network and ventral attention network; see left **Figure 7**). The dissolution model has a significantly negative edges parameter estimate and significantly positive GWESP parameter estimate (see **Table 4**). Also, none of the structural terms were significant for the dissolution model. Additionally, all ten parameter estimates for intra-regional connectivity (i.e., cerebellum, default network, dorsal attention network, frontoparietal network, limbic network, somatomotor network, subcortex, thalamus, ventral attention network, and visual network) significantly positive (see right **Figure 7**) and 11 significantly positive parameter estimates for inter-regional connectivity (i.e., between cerebellum and visual network, default network and frontoparietal network, dorsal attention network and frontoparietal network, dorsal attention network and somatomotor network, dorsal attention network and ventral attention network, dorsal attention network and visual network,

frontoparietal network and thalamus, somatomotor network and ventral attention network, subcortex and thalamus, and thalamus and visual network; see right **Figure 7**). Finally, the GOF (see **Figure 8**) were fit well for every statistic in both the formation and dissolution model. Overall, the model was thus well fit for both the formation and dissolution models. All the GOF terms fit well except for a portion of the edge shared partners, but in the model statistics are well fit to the original data.

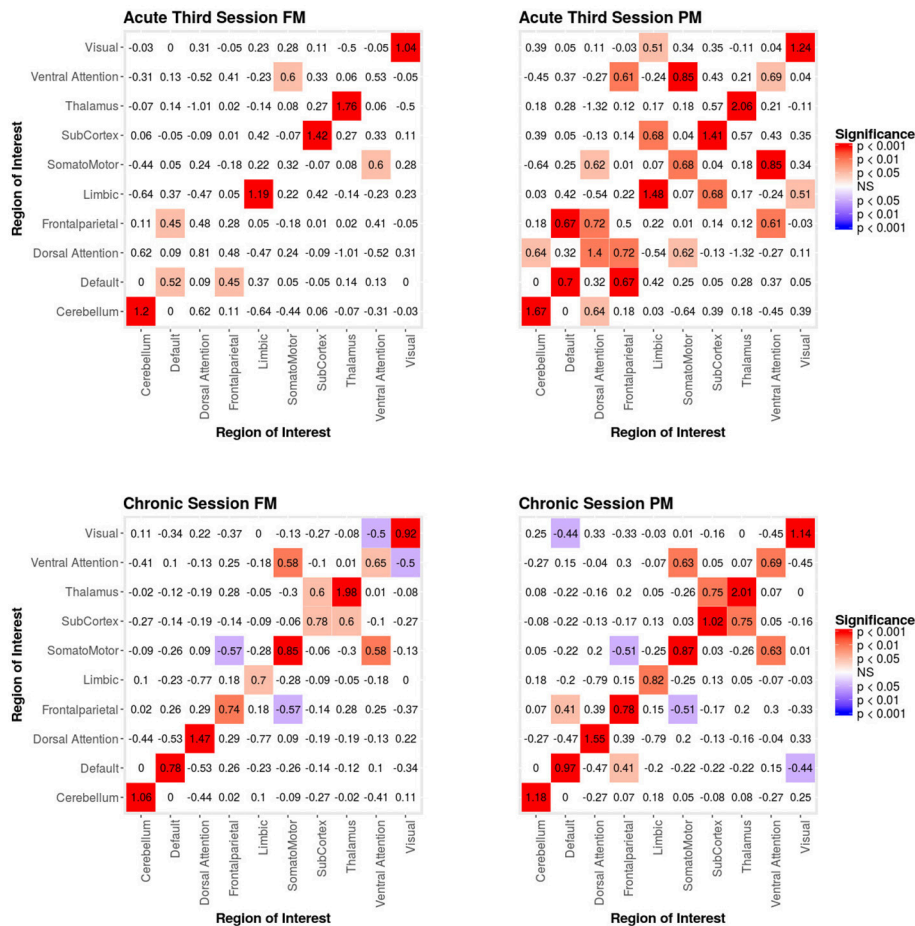
## 4. DISCUSSION

In this work, we have addressed four issues which, while general to the implementation of network theory in the field of functional neuroimaging, are particularly relevant to studies in the clinical context of DOC. In what follows we discuss how the approach we have demonstrated above in a patient recovering from coma resolves specifically each of the four problems outlined in the introduction. The first three problems discussed were solved using a single model which controls for (i) the density of the functional connectivity, (ii) the effects of variance/change in structural connectivity on the functional metrics, while (iii) modeling the intra- and inter-connectivity of the resting state networks and the effects of higher order terms (i.e., GWESP). The final problem was resolved using STERGM to model the network dynamics in recovering from coma.

### 4.1. Solution to Problem #1: Use Natural Density, Not Arbitrarily Fixed Density (i.e., Use a Multiple Regression Framework—Part I)

As our longitudinal data shows, consistent with results from other domains of neuroscience [see (45, 133)], brain graphs are susceptible to having different “natural” levels of density at which they are the most stable and which might thus be ideal to estimate network properties. In our data, over the progression of 6 months post injury, as the patient recovered consciousness and cognitive function, the natural brain graph density went from 10.4 to 14.5%. These density differences were revealed thanks to the use of MoNeT (116), a tool which combines a penalized maximum likelihood estimation with a resampling-based (bootstrapped) model selection procedure in order to find the most stable level of sparse brain graph given a set of time-dependent measurements (e.g., fMRI data). On the one hand, as we will explain below, these differences might well reflect important aspects of network dynamics in the recovery of consciousness post severe brain injury. On the other hand, regardless of the ultimate interpretation of the finding in of itself, had we employed the standard approach and enforced equal density across brain graphs in order to allow comparability (42, 55), these differences would have been obscured and would have introduced a bias in the direct comparison of topological properties across graphs. Ultimately, an accurate estimation of the connectivity is necessary to correctly model the connectivity. ERGM and STERGM allow for controlling the density without having to fix the density for all graphs. This allows for data driven approaches to allow the density to vary based on the stability





**FIGURE 5 |** Patient recovery ERGM. Comparison of results for the FM and PM for acute session 3 and chronic session. The left figures display the FM mixing term results for the Acute third session and Chronic session. The mixing term term accounts for the inter- and intra-regional connectivity. The legend displays tints of red for significant positive parameter estimates and the significant negative parameter estimates are colored in tints of blue. The right figures display the PM mixing term results for the Acute third session and Chronic session. The coloring scheme is the same as the FM. These figures are symmetric within each model because the graphs are undirected.

of the connectivity estimates. This natural variance could reveal differences in graph statistics that would otherwise be masked by fixing density. Overall, this result further demonstrates that, when arbitrarily enforcing equal density across graphs, we are in fact biasing our results toward the graphs with natural density closest to the threshold employed. While we show this in the context of time, it immediately translates to cross-sectional analyses that are also typical of the field of DOC (e.g., healthy controls vs. patients), with the prediction that the more different the natural density across groups, the greater the bias in the results.

## 4.2. Solution to Problem #2: Control for Interrelations Across Network Metrics (i.e., Use a Multiple Regression Framework—Part II)

As discussed above, ERGM can cope with comparing graphs with different natural densities because it factors in density as

a variable in the model (in other words, it controls explicitly for different densities). Similarly, ERGM can also control for interrelations across the many metrics that are typically estimated by explicitly including them all in a single model. As mentioned in the introduction, this approach is akin to performing a multiple regression model in which each network feature is evaluated for its unique contribution to the graph, as opposed to the current graph theoretic approach dominating in neuroimaging, which is akin to running several single-variable regressions, one per topological feature investigated. The Florentine business networks were used to demonstrate the effect of leaving out significant contributing factors to the model, something that renders our ERGM vulnerable to correlations between graph properties similar to the current conventional approached (42). As shown in **Table 1**, using PMs can lead to incorrectly estimating the magnitude or the significance of network measures. For example, in network A (**Figure 1**, left), the failure to include the mixing terms leads to a significant

**TABLE 3 |** Patient Recovery ERGM.

	ERGM Parameter Estimates			
	Third Acute		Chronic	
	PM	FM	PM	FM
Edges	−7.97*** (0.36)	−7.27*** (0.63)	−8.05*** (0.42)	−8.07*** (0.57)
Nodal Covariate: Degree (Structural)		−0.01 (0.01)		0.01 (0.01)
Nodal Covariate: Local Efficiency (Structural)		0.02 (0.12)		−0.11 (0.16)
Nodal Covariate: Cluster Coefficient (Structural)		−0.22 (0.15)		0.33 (0.17)
Nodal Covariate Mixing: Latent Cluster 1 to 1 (Structural)		2.33*** (0.42)		0.34 (0.24)
Nodal Covariate Mixing: Latent Cluster 2 to 2 (Structural)		1.17*** (0.23)		−0.06 (0.24)
Nodal Covariate Mixing: Latent Cluster 1 to 3 (Structural)		−0.48 (0.44)		−0.34* (0.17)
Nodal Covariate Mixing: Latent Cluster 2 to 3 (Structural)		0.47* (0.23)		−0.51** (0.17)
Nodal Covariate Mixing: Latent Cluster 3 to 3 (Structural)		1.24*** (0.24)		0.29 (0.15)
Nodal Covariate Mixing: Latent Cluster 1 to 4 (Structural)		1.25*** (0.26)		−0.52** (0.20)
Nodal Covariate Mixing: Latent Cluster 2 to 4 (Structural)		0.35 (0.24)		−0.55** (0.19)
Nodal Covariate Mixing: Latent Cluster 3 to 4 (Structural)		0.35 (0.23)		−0.55*** (0.16)
Nodal Covariate Mixing: Latent Cluster 4 to 4 (Structural)		1.11*** (0.23)		0.56** (0.18)
Nodal Covariate Mixing: Latent Cluster 1 to 5 (Structural)		−0.35 (0.51)		−0.20 (0.20)
Nodal Covariate Mixing: Latent Cluster 2 to 5 (Structural)		−0.01 (0.26)		−0.26 (0.20)
Nodal Covariate Mixing: Latent Cluster 3 to 5 (Structural)		0.27 (0.26)		−0.52** (0.17)
Nodal Covariate Mixing: Latent Cluster 4 to 5 (Structural)		0.16 (0.26)		−0.39* (0.19)
Nodal Covariate Mixing: Latent Cluster 5 to 5 (Structural)		2.09*** (0.31)		0.42 (0.23)
Nodal Covariate Mixing: Latent Cluster 1 to 6 (Structural)		1.20*** (0.30)		−0.42* (0.20)
Nodal Covariate Mixing: Latent Cluster 2 to 6 (Structural)		0.60* (0.24)		−0.37* (0.18)
Nodal Covariate Mixing: Latent Cluster 3 to 6 (Structural)		−0.95* (0.40)		−0.23 (0.16)
Nodal Covariate Mixing: Latent Cluster 4 to 6 (Structural)		0.39 (0.24)		−0.22 (0.17)
Nodal Covariate Mixing: Latent Cluster 5 to 6 (Structural)		0.37 (0.29)		−0.03 (0.18)
Nodal Covariate Mixing: Latent Cluster 6 to 6 (Structural)		1.74***		0.30

(Continued)

**TABLE 3 |** Continued

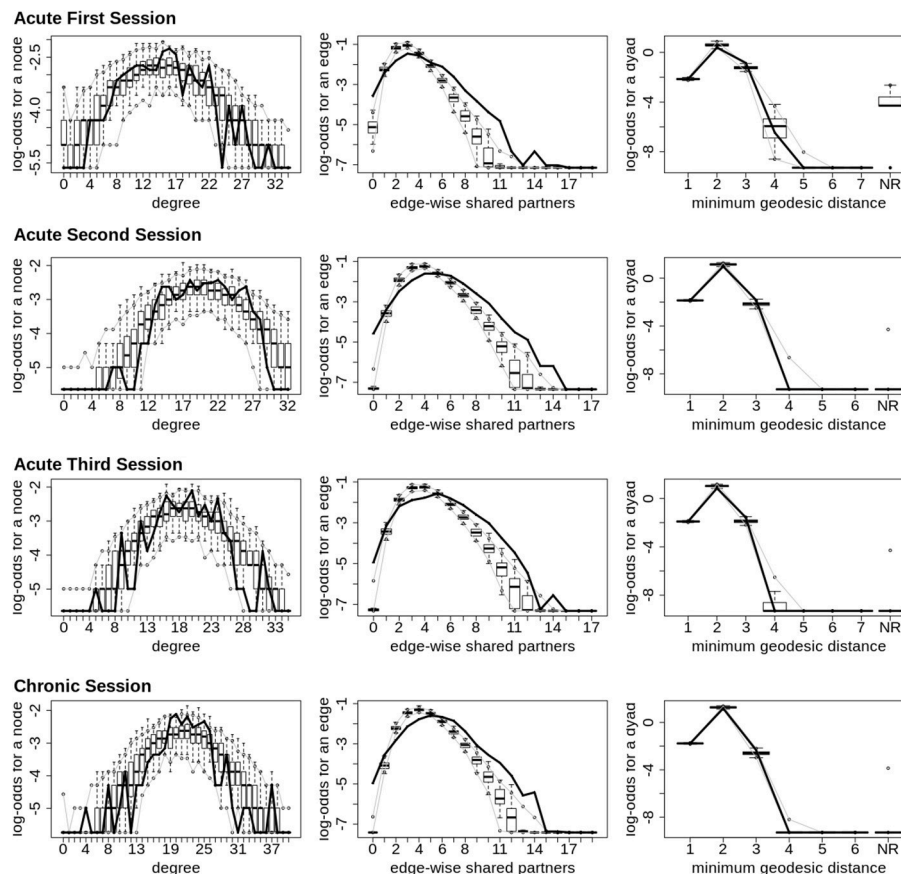
	ERGM Parameter Estimates			
	Third Acute		Chronic	
	PM	FM	PM	FM
		(0.29)		(0.19)
Nodal Covariate Mixing: Latent Cluster 1 to 7 (Structural)		−0.54 (0.51)		
Nodal Covariate Mixing: Latent Cluster 2 to 7 (Structural)		0.42 (0.24)		
Nodal Covariate Mixing: Latent Cluster 3 to 7 (Structural)		0.28 (0.25)		
Nodal Covariate Mixing: Latent Cluster 4 to 7 (Structural)		−0.15 (0.27)		
Nodal Covariate Mixing: Latent Cluster 5 to 7 (Structural)		0.59* (0.26)		
Nodal Covariate Mixing: Latent Cluster 6 to 7 (Structural)		0.30 (0.27)		
Nodal Covariate Mixing: Latent Cluster 7 to 7 (Structural)		1.48*** (0.26)		
GWESP (Fixed 0.45)	3.23*** (0.20)	2.87*** (0.20)	3.48*** (0.24)	3.28*** (0.24)

Parameter estimates for the FM and PM of the Acute third session and Chronic session. The mixing term for resting state are excluded because they are in **Figure 5**. All of the structural parameter estimates are listed in the FM columns. The edges and GWESP parameter estimates are for the functional connectivity in the PMs and FMs. The LATEX code to create this table was produced by the R package called texreg (132). \* $p < 0.05$ ; \*\* $p < 0.01$ ; \*\*\* $p < 0.001$ .

GWESP term, however, it appears to be overestimated as compared to the FM (where it is not significant). In other words, on the basis of the PM results, one would be justified in concluding that triadic closure (i.e., the tendency for edges to appear where they complete triangles) is a key stochastic process underlying the network. Yet, the FM shows that this result is spurious and is in fact due to the mixing term—that is, to the dynamics of within-group connectivity, and not triadic closure. As shown in **Table 1**, changing group membership of one node alone, preserving all other aspects of the network, affected both qualitatively and quantitatively the network measures (compare the FM columns for  $PM_A$  and  $PM_B$  in **Table 1**). Similarly to Network A, Network B's PMs returned different parameter estimates than the FM. As we will discuss below, a similar effect is at play in the neuroimaging data where, failure to include structural information, could have lead to incorrectly attributing to functional connectivity between the fronto-parietal and the default mode networks a network characteristic that is in fact due to structural connectivity (i.e., problem #3, cf., **Figure 4, 5**).

### 4.3. Solution to Problem #3: Adjust for the Effects of Structural Connectivity on Functional Connectivity (i.e., Use a Multiple Regression Framework—Part III)

As shown in the results, ERGM is capable of addressing the currently unresolved issue of integrating functional and



**FIGURE 6 |** Patient recovery ERGM. Goodness of fit plots for the four FM (i.e., Acute Session 1, Acute Session 2, Acute Session 3 and Chronic Session). The black line marks the respective networks; the box-and-whiskers indicate the model data obtained from the 1000 simulations of each model (see section 2.6).

structural connectivity in a unique framework (37, 38, 40). Analogously to the two previous points, the solution employed by ERGM is to include structural connectivity terms in the model, thus explicitly adjusting for the relationship between the structural and functional connectivity. In our data, inclusion of structural terms in the model affected all other parameter estimates, empirically demonstrating that, in the context of recovery of consciousness after severe brain injury, failing to include structural connectivity is tantamount to mis-specifying the model [similarly to not including network density (i.e., problem #1)] or not modeling all estimated metrics in a single model [(i.e., problem #2)]. While we recognize that this is likely to be an issue in any field where structural connectivity might differ across groups and/or individuals, there is also little doubt that this is particularly problematic in the context of DOC where the underlying structural architecture is likely to be substantially different from healthy volunteers [e.g., (64, 134)], across different clinical groups [e.g., (69)], and over time [e.g., (96, 135) as well as in the data presented here].

Specifically, our results show that when structural data are included (i.e., in the FMs), the probability of inter- and intra-regional connectivity changes—as compared to the

PMs—including: parameter estimates with a higher magnitude in the PM (e.g., connections between default network and ventral attention network, limbic network to thalamus, and within limbic network in the Acute First session), parameters with a lower magnitude in PM (e.g., connections between visual network and cerebellum, visual network and subcortex or visual network and thalamus in the Acute Second session), and parameters which went from non-significant in the PM to significant in the FM (e.g., connections between dorsal attention network and subcortex in the Acute Second session or connections between visual network and ventral attention in the Chronic session) and viceversa (e.g., connections between default network and frontoparietal network in the Chronic session or connections between thalamus and subcortex in the Acute First session). These results have immediate theoretical implications for the field of DOC in as much as the partial ERGM model in our patient shows increased likelihood of connectivity between the default mode and the fronto-parietal networks throughout recovery from coma (see Figure 4, 5). This could be (mistakenly) construed as bearing on the issue of the relationship between the “external awareness” and “internal awareness” networks in DOC (136, 137). For example, the relationship between these

**TABLE 4 |** Patient Recovery STERGM.

	STERGM Parameter Estimates	
	Formation	Dissolution
Edges	−10.03*** (1.04)	−3.56* (1.79)
Nodal Covariate: Degree (Structural)	0.01 (0.01)	0.03 (0.02)
Nodal Covariate: Local Efficiency (Structural)	−0.14 (0.64)	−1.27 (1.64)
Nodal Covariate: Cluster Coefficient (Structural)	0.34 (0.49)	1.33 (1.25)
Nodal Covariate Mixing: Latent Cluster 1 to 1 (Structural)	−0.04 (0.09)	−0.01 (0.21)
Nodal Covariate Mixing: Latent Cluster 2 to 2 (Structural)	0.04 (0.17)	0.30 (0.41)
Nodal Covariate Mixing: Latent Cluster 1 to 3 (Structural)	−0.12 (0.09)	−0.11 (0.24)
Nodal Covariate Mixing: Latent Cluster 2 to 3 (Structural)	−0.04 (0.11)	0.19 (0.32)
Nodal Covariate Mixing: Latent Cluster 3 to 3 (Structural)	−0.00 (0.14)	−0.13 (0.32)
GWESP (Fixed 0.75)	3.26*** (0.33)	
GWESP (Fixed 0.25)		0.27*** (0.08)

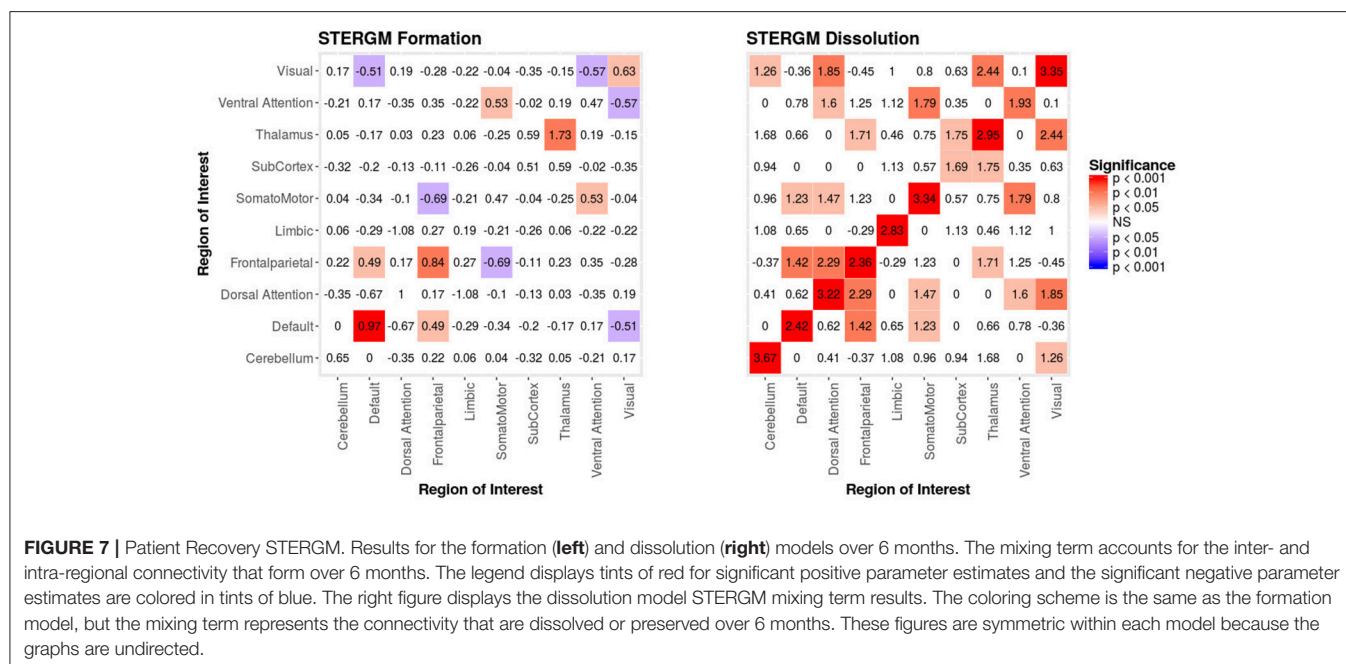
Parameter estimates for the formation and dissolution models. The mixing term for resting state are excluded because they are in **Figure 7**. All of the structural parameter estimates are listed in the FM columns. The edges and GWESP parameter estimates are for the functional connectivity in the formation and dissolution models. The LATEX code to create this table was produced by the R package called *texreg* (132). \* $p < 0.05$ ; \*\* $p < 0.01$ ; \*\*\* $p < 0.001$ .

two networks was no longer observed once structural data was included in the FM exposing the initial finding as spurious and likely reflecting improper attribution of variance due to leaving out the structural terms from the model.

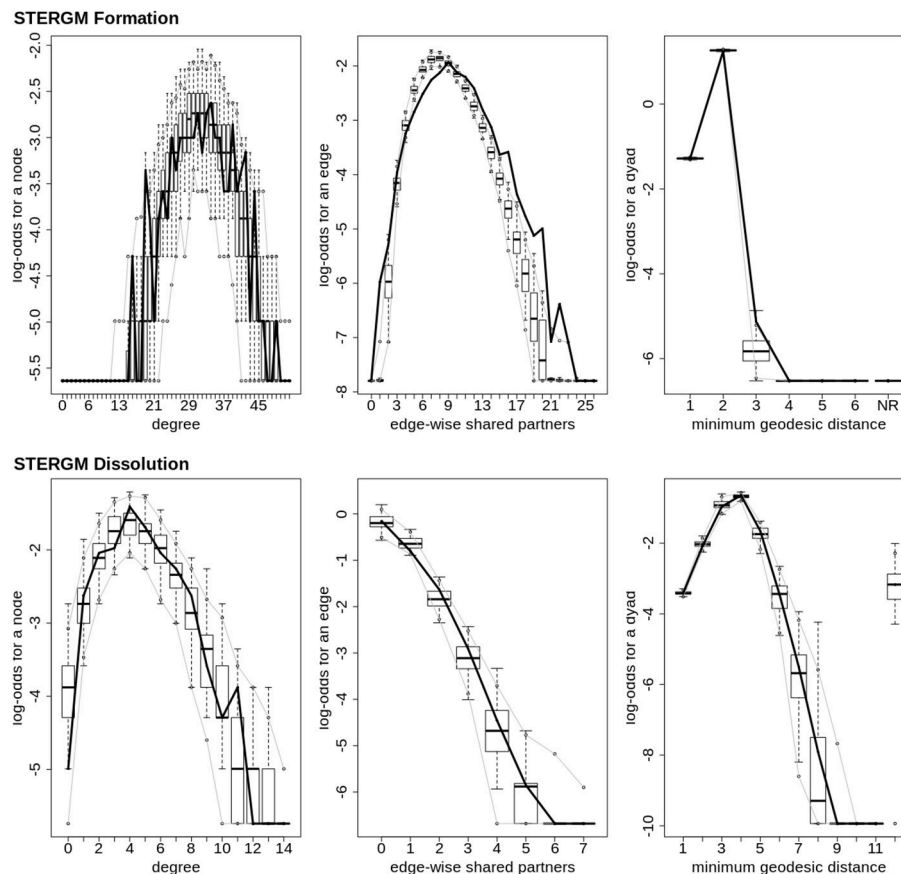
Finally, we note that ERGM has an important advantage over other techniques in the context of integrating functional and structural connectivity. Indeed, previous approaches only made use of the structural connectivity in order to predict the functional network (71, 72) or in order to jointly estimate the functional and structural connectivity (74–76). ERGM, however, allows estimating the influence of structural connectivity on the properties of the functional networks, something which, even at the level of one patient alone, has a large enough effect to change the significance and/or magnitude of the network's parameter estimates.

#### 4.4. Solution to Problem #4: Assess Dynamics of Change Across Time-Points, Not Static Differences Across Time-Points

Finally, an additional advantage of this new approach is the ability to directly analyze network dynamics over time—an issue that is very important in the context of loss and recovery of consciousness after severe brain injury (28, 34). In our example data, the two STERGM models uncovered a strong positive parameter estimates for intra-regional connectivity in all networks, for the dissolution model, indicating that in the process of recovery there are strong tendencies to preserve existing edges across time. Additionally, there are four positive parameter estimates for the formation of new edges, implying that as our patient recovered he was more likely to establish new connectivity within and between networks. Taken together, the tendency of our patient to maintain existing connections







**FIGURE 8 |** Patient recovery STERGM. Goodness of fit plots for the formation (top) and dissolution (bottom) models. The black line marks the formation and dissolution networks observed over time in the patient's graphs between the first Acute session and the Chronic session; the box-and-whiskers indicate the model data obtained from the 1000 simulations of each model (see section 2.6).

and develop novel ones might well explain why we observed a tendency over time for the “natural” density of networks to increase throughout recovery. It should also be pointed out that while we did not find any negative parameter estimate in the dissolution model, a significant negative estimate could be interpreted as evidence for neural reorganization, another important advantage of ERGM in the context of DOC [e.g., (95)].

#### 4.5. Limitations

It is important to consider two important limitations of the work above. First, we have presented the use of ERGM in the context of a single patient. On the one hand, ERGM was specifically developed to allow meaningful analysis of single graphs. Indeed, unlike neurosciences and other experimental biological and behavioral sciences, some fields do not typically have multiple graphs to compare (e.g., multiple subjects, multiple time-points), but rather have a single graph from which meaningful inferences are drawn [e.g., sociology (2), transportation (6), and public health (4)]. On the other hand, although—formally—inferences could be legitimately drawn from a single case, in the context of DoC and clinical work, brain-derived network analyses reflect

much of the heterogeneity of the underlying conditions, thus making inferences drawn from individual cases questionable in their generality and applicability to other patients. Furthermore, at this initial stage, there are no baseline or control measurements against which to compare one patient's parameters derived from the (ST)ERGM. Second, because of the pragmatics and reality of clinical work, acute scans, which happened in an in-patient setting, were performed on a 3 Tesla Siemens TimTrio system while follow-up MR data were acquired in an out-patient setting, on a 3 Tesla Siemens Prisma system. The impact of such a variable on the model parameters remains to be assessed in larger samples, including in healthy volunteers. We thus leave it to future cohort studies to interpret in detail the significance of the specific ERGM and STERGM parameters with respect to the issue of loss and recovery of consciousness after severe brain injury.

#### 5. CONCLUSIONS AND FUTURE WORK

Network analyses are an attempt to synthesize complex processes into a small number of metrics. In this paper we have introduced a novel [in the context of DOC, for other contexts within

neuroimaging, cf.: (89–91)] approach to estimating network properties, ERGMs, which overcome four important challenges faced by current graph theoretic approaches to brain data and which are particularly consequential in the context of DOC. The main advantage of ERGM over current approaches is the fact that it adopts a multiple regression framework *in lieu* of multiple parallel simple regressions (i.e., one per each metric). Under this multiple regression framework, brain networks can be compared across densities—since the density of each will be controlled for within the model. This side-steps the issue of having to impose the same arbitrary sparsity across networks which are likely to have very different stable levels of density, as is the case, for example, between severely brain injured patients and controls or in longitudinal recovery. Similarly, by including in a unified model structural and functional data, it is possible to acknowledge and control for the fact that patients surviving severe brain injury are likely to have very heterogeneous brain pathology and thus profound differences in structural substrate—a fact that is currently ignored in the extant literature. Even in one patient alone, direct comparison of the conventional PM with the FM demonstrated how failing to

consider structural information can lead to spurious results and erroneous conclusions. Furthermore, ERGM can be extended to assess dynamics of change thus allowing to discover the network evolution that govern loss and recovery of consciousness over time, as opposed to comparing static graphs at different time-points.

Finally, we end this paper by pointing out that the reader can implement (ST)ERGM as performed here using the freely distributed `ergm` package (40) in R and the Markov Network Toolbox [MoNeT; (116)] in MATLAB.

## AUTHOR CONTRIBUTIONS

JD, MM, and PV designed the experiment. JD and MJ analyzed the data. JD and MM interpreted the results. JD drafted the manuscript, all authors provided feedback.

## FUNDING

This work was supported by the Tiny Blue Dot foundation (to MM) and the Brain Injury Research Center at UCLA.

## REFERENCES

- Raichle ME, MacLeod AM, Snyder AZ, Powers WJ, Gusnard DA, Shulman GL. A default mode of brain function. *Proc Natl Acad Sci USA*. (2001) **98**:676–82. doi: 10.1073/pnas.98.2.676
- Freeman LC. Centrality in social networks conceptual clarification. *Soc Netw*. (1978) **1**:215–39. doi: 10.1016/0378-8733(78)90021-7
- McQuillan JM. Graph theory applied to optimal connectivity in computer networks. *SIGCOMM Comput Commun Rev*. (1977) **7**:13–41. doi: 10.1145/1024857.1024860
- Luke DA, Harris JK. Network analysis in public health: history, methods, and applications. *Annu Rev Public Health* (2007) **28**:69–93. doi: 10.1146/annurev.publhealth.28.021406.144132
- Lucek PR, Ott J. Neural network analysis of complex traits. *Genet Epidemiol*. (1997) **14**:1101–6. doi: 10.1002/(SICI)1098-2272(1997)14:6<1101::AID-GEPI90>3.0.CO;2-K
- Guimera R, Mossa S, Turtschi A, Amaral LN. The worldwide air transportation network: anomalous centrality, community structure, and cities' global roles. *Proc Natl Acad Sci USA*. (2005) **102**:7794–9. doi: 10.1073/pnas.0407994102
- Cao H, Plichta MM, Schäfer A, Haddad L, Grimm O, Schneider M, et al. Test–retest reliability of fMRI-based graph theoretical properties during working memory, emotion processing, and resting state. *Neuroimage* (2014) **84**:888–900. doi: 10.1016/j.neuroimage.2013.09.013
- Fransson P, Åden U, Blennow M, Lagercrantz H. The functional architecture of the infant brain as revealed by resting-state fMRI. *Cereb Cortex* (2010) **21**:145–54. doi: 10.1093/cercor/bhq071
- Micheliyannis S, Vourkas M, Tsirka V, Karakontstantaki E, Kanatsouli K, Stam CJ. The influence of ageing on complex brain networks: a graph theoretical analysis. *Hum Brain Mapp*. (2009) **30**:200–8. doi: 10.1002/hbm.20492
- Sanz-Arigita EJ, Schoonheim MM, Damoiseaux JS, Rombouts SARB, Maris E, Barkhof F, et al. Loss of 'small-world' networks in Alzheimer's disease: graph analysis of fMRI resting-state functional connectivity. *PLoS ONE* (2010) **5**:e13788. doi: 10.1371/journal.pone.0013788
- Wu T, Wang L, Chen Y, Zhao C, Li K, Chan P. Changes of functional connectivity of the motor network in the resting state in Parkinson's disease. *Neurosci. Lett*. (2009) **460**:6–10. doi: 10.1016/j.neulet.2009.05.046
- Pandit AS, Expert P, Lambiotte R, Bonnelle V, Leech R, Turkheimer FE, et al. Traumatic brain injury impairs small-world topology. *Neurology* (2013) **80**:1826–33. doi: 10.1212/WNL.0b013e3182929f38
- Monti MM, Lutkenhoff ES, Rubinov M, Boveroux P, Vanhaudenhuyse A, Gosseries O, et al. Dynamic change of global and local information processing in propofol-induced loss and recovery of consciousness. *PLoS Comput Biol*. (2013) **9**:e1003271. doi: 10.1371/journal.pcbi.1003271
- Chennu S, Fioino P, Kamau E, Allanson J, Williams GB, Monti MM, et al. Spectral signatures of reorganised brain networks in disorders of consciousness. *PLoS Comput Biol*. (2014) **10**:e1003887. doi: 10.1371/journal.pcbi.1003887
- Crone JS, Lutkenhoff ES, Bio BJ, Laureys S, Monti MM. Testing proposed neuronal models of effective connectivity within the Cortico-basal Ganglia-thalamo-cortical loop during loss of consciousness. *Cereb Cortex* (2017) **27**:2727–38. doi: 10.1093/cercor/bhw112
- Baars BJ. The conscious access hypothesis: origins and recent evidence. *Trends Cogn. Sci.* (2002) **6**:47–52. doi: 10.1016/S1364-6613(00)01819-2
- Baars BJ, Ramsoy TZ, Laureys S. Brain, conscious experience and the observing self. *Trends Neurosci.* (2003) **26**:671–5. doi: 10.1016/j.tins.2003.09.015
- Engel AK, Singer W. Temporal binding and the neural correlates of sensory awareness. *Trends Cogn. Sci.* (2001) **5**:16–25. doi: 10.1016/S1364-6613(00)01568-0
- Tallon-Baudry C. The roles of gamma-band oscillatory synchrony in human visual cognition. *Front Biosci.* (2009) **14**:321–32. doi: 10.2741/3246
- Dehaene S, Changeux JP. Ongoing spontaneous activity controls access to consciousness: a neuronal model for inattention blindness. *PLoS Biol.* (2005) **3**:e141. doi: 10.1371/journal.pbio.0030141
- Crick F, Koch C. A framework for consciousness. *Nat Neurosci.* (2003) **6**:119–26. doi: 10.1038/nn0203-119
- Tononi G. Consciousness as integrated information: a provisional manifesto. *Biol Bull.* (2008) **215**:216–42. doi: 10.2307/25470707
- Monti MM, Laureys S, Owen AM. The vegetative state. *BMJ* (2010) **341**:c3765. doi: 10.1136/bmj.c3765
- Hannawi Y, Lindquist MA, Caffo BS, Sair HI, Stevens RD. Resting brain activity in disorders of consciousness: A systematic review and meta-analysis. *Neurology* (2015) **84**:1272–80. doi: 10.1212/WNL.0000000000001404

25. Soddu A, Vanhaudenhuyse A, Demertzi A, Bruno MA, Tshibanda L, Di H, et al. Resting state activity in patients with disorders of consciousness. *Funct Neurol.* (2011) **26**:37.
26. Boly M, Massimini M, Garrido MI, Gosseries O, Noirhomme Q, Laureys S, et al. Brain connectivity in disorders of consciousness. *Brain Connect.* (2012) **2**:1–10. doi: 10.1089/brain.2011.0049
27. Laureys S, Faymonville ME, Degueldre C, Fiore GD, Damas P, Lambermont B, et al. Auditory processing in the vegetative state. *Brain* (2000) **123**(Pt 8):1589–601. doi: 10.1093/brain/123.8.1589
28. Laureys S, Faymonville ME, Luxen A, Lamy M, Franck G, Maquet P. Restoration of thalamocortical connectivity after recovery from persistent vegetative state. *Lancet* (2000) **355**:1790–1. doi: 10.1016/S0140-6736(00)02271-6
29. Vanhaudenhuyse A, Noirhomme Q, Tshibanda LJF, Bruno MA, Boveroux P, Schnakers C, et al. Default network connectivity reflects the level of consciousness in non-communicative brain-damaged patients. *Brain* (2010) **133**:161–71. doi: 10.1093/brain/awp313
30. Boly M, Tshibanda L, Vanhaudenhuyse A, Noirhomme Q, Schnakers C, Ledoux D, et al. Functional connectivity in the default network during resting state is preserved in a vegetative but not in a brain dead patient. *Hum Brain Mapp.* (2009) **30**:2393–400. doi: 10.1002/hbm.20672
31. Boly M, Garrido MI, Gosseries O, Bruno MA, Boveroux P, Schnakers C, et al. Preserved feedforward but impaired top-down processes in the vegetative state. *Science* (2011) **332**:858–62. doi: 10.1126/science.1202043
32. Crone JS, Soddu A, Höller Y, Vanhaudenhuyse A, Schurz M, Bergmann J, et al. Altered network properties of the fronto-parietal network and the thalamus in impaired consciousness. *Neuroimage* (2014) **4**:240–8. doi: 10.1016/j.neuroimage.2013.12.005
33. Amico E, Marinazzo D, Di Perri C, Heine L, Annen J, Martial C, et al. Mapping the functional connectome traits of levels of consciousness. *Neuroimage* (2017) **148**:201–11. doi: 10.1016/j.neuroimage.2017.01.020
34. Crone JS, Bio BJ, Vespa PM, Lutkenhoff ES, Monti MM. Restoration of thalamo-cortical connectivity after brain injury: recovery of consciousness, complex behavior, or passage of time? *J Neurosci Res.* (2017) **96**:671–687. doi: 10.1002/jnr.24115
35. Monti MM. Cognition in the vegetative state. *Annu Rev Clin Psychol.* (2012) **8**:431–54. doi: 10.1146/annurev-clinpsy-032511-143050
36. Holland PW, Leinhardt S. An exponential family of probability distributions for directed graphs. *J Am Statist Assoc.* (1981) **76**:33–50. doi: 10.1080/01621459.1981.10477598
37. Hunter DR. Curved exponential family models for social networks. *Soc Netw.* (2007) **29**:216–30. doi: 10.1016/j.socnet.2006.08.005
38. Hunter DR, Handcock MS, Butts CT, Goodreau SM, Morris M. *ergm*: a package to fit, simulate and diagnose exponential-family models for networks. *J Stat Softw.* (2008) **24**:nihpa54860.
39. Goodreau SM, Kitts JA, Morris M. Birds of a feather, or friend of a friend? Using exponential random graph models to investigate adolescent social networks. *Demography* (2009) **46**:103–25. doi: 10.1353/dem.0.0045
40. Handcock MS, Hunter DR, Butts CT, Goodreau SM, Krivitsky PN, Morris M. *ergm: Fit, Simulate and Diagnose Exponential-Family Models for Networks*. R package version 3.8.0. (2017). Available online at: <https://CRAN.R-project.org/package=ergm>
41. Bullmore E, Sporns O. The economy of brain network organization. *Nat Rev Neurosci.* (2012) **13**:336–49. doi: 10.1038/nrn3214
42. Rubinov M, Sporns O. Complex network measures of brain connectivity: uses and interpretations. *Neuroimage* (2010) **52**:1059–69. doi: 10.1016/j.neuroimage.2009.10.003
43. Rubinov M, Sporns O. Weight-conserving characterization of complex functional brain networks. *Neuroimage* (2011) **56**:2068–79. doi: 10.1016/j.neuroimage.2011.03.069
44. Watts DJ, Strogatz SH. Collective dynamics of “small-world” networks. *Nature* (1998) **393**:440. doi: 10.1038/30918
45. Nielsen JA, Zielinski BA, Fletcher PT, Alexander AL, Lange N, Bigler ED, et al. Multisite functional connectivity MRI classification of autism: ABIDE results. *Front Hum Neurosci.* (2013) **7**:599. doi: 10.3389/fnhum.2013.00599
46. Fornito A, Zalesky A, Breakspear M. Graph analysis of the human connectome: promise, progress, and pitfalls. *Neuroimage* (2013) **80**:426–44. doi: 10.1016/j.neuroimage.2013.04.087
47. Fornito A, Zalesky A, Bullmore E. *Fundamentals of Brain Network Analysis*. Amsterdam: Elsevier (2016).
48. Hallquist MN, Hillary FG. Graph theory approaches to functional network organization in brain disorders: a critique for a brave new small-world. *bioRxiv* (2018) 243741. doi: 10.1101/NETN\_a\_00054
49. Hellwig B. A quantitative analysis of the local connectivity between pyramidal neurons in layers 2/3 of the rat visual cortex. *Biol Cybernet.* (2000) **82**:111–21. doi: 10.1007/PL00007964
50. Averbeck BB, Seo M. The statistical neuroanatomy of frontal networks in the macaque. *PLoS Comput Biol.* (2008) **4**:e1000050. doi: 10.1371/journal.pcbi.1000050
51. Braitenberg V, Schüz A. “Global activity, cell assemblies and Synfire Chains,” In: *Cortex: Statistics and Geometry of Neuronal Connectivity*. Berlin: Springer (1998). p. 193–204.
52. Murphy K, Birn RM, Handwerker DA, Jones TB, Bandettini PA. The impact of global signal regression on resting state correlations: are anti-correlated networks introduced? *Neuroimage* (2009) **44**:893–905. doi: 10.1016/j.neuroimage.2008.09.036
53. Saad Z, Gotts SJ, Murphy K, Chen G, Jo HJ, Martin A, et al. Trouble at rest: how correlation patterns and group differences become distorted after global signal regression. *Brain Connect.* (2012) **2**:25–32. doi: 10.1089/brain.2012.0080
54. Wang Y, Ghumare E, Vandenberghe R, Dupont P. Comparison of different generalizations of clustering coefficient and local efficiency for weighted undirected graphs. *Neural Comput.* (2017) **29**:313–31. doi: 10.1162/NECO\_a\_00914
55. van Wijk BCM, Stam CJ, Daffertshofer A. Comparing brain networks of different size and connectivity density using graph theory. *PLoS ONE* (2010) **5**:e13701. doi: 10.1371/journal.pone.0013701
56. Braun U, Plichta MM, Esslinger C, Sauer C, Haddad L, Grimm O, et al. Test-retest reliability of resting-state connectivity network characteristics using fMRI and graph theoretical measures. *Neuroimage* (2012) **59**:1404–12. doi: 10.1016/j.neuroimage.2011.08.044
57. Zalesky A, Fornito A, Bullmore E. On the use of correlation as a measure of network connectivity. *Neuroimage* (2012) **60**:2096–106. doi: 10.1016/j.neuroimage.2012.02.001
58. Bruno MA, Fernández-Espejo D, Lehenbre R, Tshibanda L, Vanhaudenhuyse A, Gosseries O, et al. Multimodal neuroimaging in patients with disorders of consciousness showing “functional hemispherectomy.” *Prog Brain Res.* (2011) **193**:323–33. doi: 10.1016/B978-0-444-53839-0.00021-1
59. Coleman M, Bekinschtein T, Monti M, Owen A, Pickard J. A multimodal approach to the assessment of patients with disorders of consciousness. *Prog Brain Res.* (2009) **177**:231–48. doi: 10.1016/S0079-6123(09)17716-6
60. Boly M, Moran R, Murphy M, Boveroux P, Bruno MA, Noirhomme Q, et al. Connectivity changes underlying spectral EEG changes during propofol-induced loss of consciousness. *J Neurosci.* (2012) **32**:7082–90. doi: 10.1523/JNEUROSCI.3769-11.2012
61. Ku SW, Lee U, Noh GJ, Jun IG, Mashour GA. Preferential inhibition of frontal-to-parietal feedback connectivity is a neurophysiologic correlate of general anesthesia in surgical patients. *PLoS ONE* (2011) **6**:e25155. doi: 10.1371/journal.pone.0025155
62. Lee U, Kim S, Noh GJ, Choi BM, Hwang E, Mashour GA. The directionality and functional organization of frontoparietal connectivity during consciousness and anesthesia in humans. *Conscious Cogn.* (2009) **18**:1069–78. doi: 10.1016/j.concog.2009.04.004
63. Rosanova M, Gosseries O, Casarotto S, Boly M, Casali AG, Bruno MA, et al. Recovery of cortical effective connectivity and recovery of consciousness in vegetative patients. *Brain* (2012) **135**:1308–20. doi: 10.1093/brain/awr340
64. Fernández-Espejo D, Bekinschtein T, Monti MM, Pickard JD, Junque C, Coleman MR, et al. Diffusion weighted imaging distinguishes the vegetative state from the minimally conscious state. *Neuroimage* (2011) **54**:103–12. doi: 10.1016/j.neuroimage.2010.08.035
65. Fernández-Espejo D, Soddu A, Cruse D, Palacios EM, Junque C, Vanhaudenhuyse A, et al. A role for the default mode network in the bases of disorders of consciousness. *Ann Neurol.* (2012) **72**:335–43. doi: 10.1002/ana.23635

66. Newcombe VFJ, Williams GB, Scoffings D, Cross J, Carpenter TA, Pickard JD, et al. Aetiological differences in neuroanatomy of the vegetative state: insights from diffusion tensor imaging and functional implications. *J Neurol Neurosurg Psychiatry* (2010) **81**:552–61. doi: 10.1136/jnnp.2009.196246
67. Wilson C. Aetiological differences in neuroanatomy of the vegetative state: insights from diffusion tensor imaging and functional implications. *J Neurol Neurosurg Psychiatry* (2010) **81**:475–6. doi: 10.1136/jnnp.2010.205815
68. Tollard E, Galanaud D, Perlberg V, Sanchez-Pena P, Le Fur Y, Abdenour L, et al. Experience of diffusion tensor imaging and 1H spectroscopy for outcome prediction in severe traumatic brain injury: preliminary results. *Crit Care Med*. (2009) **37**:1448–55. doi: 10.1097/CCM.0b013e31819cf050
69. Zheng ZS, Reggente N, Lutkenhoff E, Owen AM, Monti MM. Disentangling disorders of consciousness: insights from diffusion tensor imaging and machine learning. *Hum Brain Mapp.* (2017) **38**:431–43. doi: 10.1002/hbm.23370
70. Díaz-Parra A, Osborn Z, Canals S, Moratal D, Sporns O. Structural and functional, empirical and modeled connectivity in the cerebral cortex of the rat. *Neuroimage* (2017) **159**:170–84. doi: 10.1016/j.neuroimage.2017.07.046
71. Bettinardi RG, Deco G, Karlaftis VM, Van Hartevelt TJ, Fernandes HM, Kourtzi Z, et al. How structure sculpts function: unveiling the contribution of anatomical connectivity to the brain's spontaneous correlation structure. *Chaos Interdiscipl J Nonlin Sci.* (2017) **27**:047409. doi: 10.1063/1.4980099
72. Messé A, Rudrauf D, Giron A, Marrelec G. Predicting functional connectivity from structural connectivity via computational models using MRI: an extensive comparison study. *Neuroimage* (2015) **111**:65–75. doi: 10.1016/j.neuroimage.2015.02.001
73. Finger H, Bönstrup M, Cheng B, Messé A, Hilgetag C, Thomalla G, et al. Modeling of large-scale functional brain networks based on structural connectivity from DTI: comparison with EEG derived phase coupling networks and evaluation of alternative methods along the modeling path. *PLoS Comput Biol.* (2016) **12**:e1005025. doi: 10.1371/journal.pcbi.1005025
74. Kessler D, Angstadt M, Welsh RC, Sripatha C. Modality-spanning deficits in attention-deficit/hyperactivity disorder in functional networks, gray matter, and white matter. *J Neurosci.* (2014) **34**:16555–66. doi: 10.1523/JNEUROSCI.3156-14.2014
75. Amico E, Goñi J. Mapping hybrid functional-structural connectivity traits in the human connectome. arXiv: 171002199. (2017).
76. Mišić B, Betzel RF, De Reus MA, Van Den Heuvel MP, Berman MG, McIntosh AR, et al. Network-level structure-function relationships in human neocortex. *Cereb Cortex* (2016) **26**:3285–96. doi: 10.1093/cercor/bhw089
77. Calhoun VD, Adali T, Giuliani NR, Pekar JJ, Kiehl KA, Pearlson GD. Method for multimodal analysis of independent source differences in schizophrenia: combining gray matter structural and auditory oddball functional data. *Hum Brain Mapp.* (2006) **27**:47–62. doi: 10.1002/hbm.20166
78. Calhoun VD, Liu J, Adal T. A review of group ICA for fMRI data and ICA for joint inference of imaging, genetic, and ERP data). *Neuroimage* (2009) **45**:S163–72. doi: 10.1016/j.neuroimage.2008.10.057
79. Sui J, Pearlson G, Caprihan A, Adali T, Kiehl KA, Liu J, et al. Discriminating schizophrenia and bipolar disorder by fusing fMRI and DTI in a multimodal CCA+ joint ICA model. *Neuroimage* (2011) **57**:97–106. doi: 10.1016/j.neuroimage.2011.05.055
80. McIntosh AR, Lobaugh NJ. Partial least squares analysis of neuroimaging data: applications and advances. *Neuroimage* (2004) **23**:S250–63. doi: 10.1016/j.neuroimage.2004.07.020
81. Abdi H. Partial least squares regression and projection on latent structure regression (PLS Regression). *Wiley Interdiscipl Rev Comput Stat* (2010) **2**:97–106. doi: 10.1002/wics.51
82. Krishnan A, Williams LJ, McIntosh AR, Abdi H. Partial Least Squares (PLS) methods for neuroimaging: a tutorial and review. *Neuroimage* (2011) **56**:455–75. doi: 10.1016/j.neuroimage.2010.07.034
83. McIntosh AR, Mišić B. Multivariate statistical analyses for neuroimaging data. *Annu Rev Psychol.* (2013) **64**:499–525. doi: 10.1146/annurev-psych-113011-143804
84. Hyvärinen A, Oja E. Independent component analysis: algorithms and applications. *Neural Netw.* (2000) **13**:411–30. doi: 10.1016/S0893-6080(00)00026-5
85. Abou-Elseoud A, Starck T, Remes J, Nikkinen J, Tervonen O, Kiviniemi V. The effect of model order selection in group PICA. *Hum Brain Mapp.* (2010) **31**:1207–16. doi: 10.1002/hbm.20929
86. Ray KL, McKay DR, Fox PM, Riedel MC, Uecker AM, Beckmann CF, et al. ICA model order selection of task co-activation networks. *Front Neurosci.* (2013) **7**:237. doi: 10.3389/fnins.2013.00237
87. Ioannides AA. Dynamic functional connectivity. *Curr Opin Neurobiol.* (2007) **17**:161–70. doi: 10.1016/j.conb.2007.03.008
88. Barttfeld P, Uhrig L, Sitt JD, Sigman M, Jarraya B, Dehaene S. Signature of consciousness in the dynamics of resting-state brain activity. *Proc Natl Acad Sci USA.* (2015) **112**:887–92. doi: 10.1073/pnas.1418031112
89. Simpson SL, Hayasaka S, Laurienti PJ. Exponential random graph modeling for complex brain networks. *PLoS ONE* (2011) **6**:e20039. doi: 10.1371/journal.pone.0020039
90. Simpson SL, Moussa MN, Laurienti PJ. An exponential random graph modeling approach to creating group-based representative whole-brain connectivity networks. *Neuroimage* (2012) **60**:1117–26. doi: 10.1016/j.neuroimage.2012.01.071
91. Simpson SL, Lyday RG, Hayasaka S, Marsh AP, Laurienti PJ. A permutation testing framework to compare groups of brain networks. *Front Comput Neurosci.* (2013) **7**:171. doi: 10.3389/fncom.2013.00171
92. Robins G, Pattison P, Kalish Y, Lusher D. An introduction to exponential random graph ( $p^*$ ) models for social networks. *Soc Netw.* (2007) **29**:173–91. doi: 10.1016/j.socnet.2006.08.002
93. Erdős P, Rényi A. On random graphs I. *Publ Math.* (1959) **6**:290–7.
94. Kent DV. *The Rise of the Medici: Faction in Florence, 1426-1434*. Oxford: Oxford University Press (1978).
95. Voss HU, Uluç AM, Dyke JP, Watts R, Kobylarz EJ, McCandliss BD, et al. Possible axonal regrowth in late recovery from the minimally conscious state. *J Clin Invest.* (2006) **116**:2005–11. doi: 10.1172/JCI27021
96. Thengone DJ, Voss HU, Fridman EA, Schiff ND. Local changes in network structure contribute to late communication recovery after severe brain injury. *Sci Transl Med.* (2016) **8**:368re5. doi: 10.1126/scitranslmed.aaf6113
97. Teasdale G, Jennett B. Assessment of coma and impaired consciousness: a practical scale. *Lancet* (1974) **304**:81–4. doi: 10.1016/S0140-6736(74)91639-0
98. Bruno MA, Vanhaudenhuyse A, Thibaut A, Moonen G, Laureys S. From unresponsive wakefulness to minimally conscious PLUS and functional locked-in syndromes: recent advances in our understanding of disorders of consciousness. *J Neurol.* (2011) **258**:1373–84. doi: 10.1007/s00415-011-6114-x
99. Wilson JL, Pettigrew LE, Teasdale GM. Structured interviews for the Glasgow Outcome Scale and the extended Glasgow Outcome Scale: guidelines for their use. *J Neurotr.* (1998) **15**:573–85. doi: 10.1089/neu.1998.15.573
100. Power JD, Barnes KA, Snyder AZ, Schlaggar BL, Petersen SE. Spurious but systematic correlations in functional connectivity MRI networks arise from subject motion. *Neuroimage* (2012) **59**:2142–54. doi: 10.1016/j.neuroimage.2011.10.018
101. Avants BB, Epstein CL, Grossman M, Gee JC. Symmetric diffeomorphic image registration with cross-correlation: evaluating automated labeling of elderly and neurodegenerative brain. *Med Image Anal.* (2008) **12**:26–41. doi: 10.1016/j.media.2007.06.004
102. Avants BB, Tustison NJ, Song G, Cook PA, Klein A, Gee JC. A reproducible evaluation of ANTs similarity metric performance in brain image registration. *Neuroimage* (2011) **54**:2033–44. doi: 10.1016/j.neuroimage.2010.09.025
103. Tange O. Gnu parallel—the command-line power tool. *USENIX Magaz.* (2011) **36**:42–7.
104. Lutkenhoff ES, Rosenberg M, Chiang J, Zhang K, Pickard JD, Owen AM, et al. Optimized brain extraction for pathological brains (optiBET). *PLoS ONE* (2014) **9**:e115551. doi: 10.1371/journal.pone.0115551
105. Shattuck DW, Sandor-Leahy SR, Schaper KA, Rottenberg DA, Leahy RM. Magnetic resonance image tissue classification using a partial volume model. *Neuroimage* (2001) **13**:856–76. doi: 10.1006/nimg.2000.0730
106. Oguz I, Farzinfar M, Matsui J, Budin F, Liu Z, Gerig G, et al. DTIPrep: quality control of diffusion-weighted images. *Front Neuroinform.* (2014) **8**:4. doi: 10.3389/fninf.2014.00004
107. Bhushan C, Haldar JP, Joshi AA, Leahy RM. Correcting susceptibility-induced distortion in diffusion-weighted MRI using constrained nonrigid



- registration. In: *Signal and Information Processing Association Annual Summit and Conference (APSIPA), Asia-Pacific Signal and Information Processing Association Annual Summit and Conference*. Hollywood, CA (2012).
108. Haldar JP, Leahy RM. Linear transforms for Fourier data on the sphere: application to high angular resolution diffusion MRI of the brain. *Neuroimage* (2013) **71**:233–47. doi: 10.1016/j.neuroimage.2013.01.022
  109. Smith SM. Fast robust automated brain extraction. *Hum Brain Mapp.* (2002) **17**:143–55. doi: 10.1002/hbm.10062
  110. Behrens TE, Woolrich MW, Jenkinson M, Johansen-Berg H, Nunes RG, Clare S, et al. Characterization and propagation of uncertainty in diffusion-weighted MR imaging. *Magnet Res Med.* (2003) **50**:1077–88. doi: 10.1002/mrm.10609
  111. Hernández M, Guerrero GD, Cecilia JM, García JM, Inuggi A, Jbabdi S, et al. Accelerating fibre orientation estimation from diffusion weighted magnetic resonance imaging using GPUs. *PLoS ONE* (2013) **8**:e61892. doi: 10.1371/journal.pone.0061892
  112. Behrens TE, Berg HJ, Jbabdi S, Rushworth MF, Woolrich MW. Probabilistic diffusion tractography with multiple fibre orientations: What can we gain? *Neuroimage* (2007) **34**:144–55. doi: 10.1016/j.neuroimage.2006.09.018
  113. Shadi K, Bakhshi S, Gutman DA, Mayberg HS, Dovrolis C. A symmetry-based method to infer structural brain networks from probabilistic tractography data. *Front Neuroinform.* (2016) **10**:46. doi: 10.3389/fninf.2016.00046
  114. Craddock RC, James GA, Holtzheimer PE, Hu XP, Mayberg HS. A whole brain fMRI atlas generated via spatially constrained spectral clustering. *Hum Brain Mapp.* (2012) **33**:1914–28. doi: 10.1002/hbm.21333
  115. Behrens T, Johansen-Berg H, Woolrich M, Smith S, Wheeler-Kingshott C, Boulby P, et al. Non-invasive mapping of connections between human thalamus and cortex using diffusion imaging. *Nat Neurosci.* (2003) **6**:750. doi: 10.1038/nn1075
  116. Narayan M, Allen GI, Tomson S. Two sample inference for populations of graphical models with applications to functional connectivity. arXiv: 150203853. (2015).
  117. Boveroux P, Vanhaudenhuyse A, Bruno MA, Noirhomme Q, Lauwick S, Luxen A, et al. Breakdown of within-and between-network resting state functional magnetic resonance imaging connectivity during propofol-induced loss of consciousness. *Anesthesiol J Am Soc Anesthesiol.* (2010) **113**:1038–53. doi: 10.1097/ALN.0b013e3181f697f5
  118. Schrouff J, Perlberg V, Boly M, Marrelec G, Boveroux P, Vanhaudenhuyse A, et al. Brain functional integration decreases during propofol-induced loss of consciousness. *Neuroimage* (2011) **57**:198–205. doi: 10.1016/j.neuroimage.2011.04.020
  119. Handcock MS, Raftery AE, Tantrum JM. Model-based clustering for social networks. *J R Statist Soc Ser A* (2007) **170**:301–54.
  120. Krivitsky PN, Handcock MS. Fitting position latent cluster models for social networks with latentnet. *J Stat Softw.* (2008) **24**. doi: 10.18637/jss.v024.i05
  121. Yeo BTT, Krienen FM, Sepulcre J, Sabuncu MR, Lashkari D, Hollinshead M, et al. The organization of the human cerebral cortex estimated by intrinsic functional connectivity. *J Neurophysiol.* (2011) **106**:1125–65. doi: 10.1152/jn.00338.2011
  122. Lashkari D, Vul E, Kanwisher N, Golland P. Discovering structure in the space of fMRI selectivity profiles. *Neuroimage* (2010) **50**:1085–98. doi: 10.1016/j.neuroimage.2009.12.106
  123. Buckner RL. Human functional connectivity: new tools, unresolved questions. *Proc Natl Acad Sci USA.* (2010) **107**:10769–70. doi: 10.1073/pnas.1005987107
  124. Cohen AL, Fair DA, Dosenbach NU, Miezin FM, Dierker D, Van Essen DC, et al. Defining functional areas in individual human brains using resting functional connectivity MRI. *Neuroimage* (2008) **41**:45–57. doi: 10.1016/j.neuroimage.2008.01.066
  125. Fox MD, Corbetta M, Snyder AZ, Vincent JL, Raichle ME. Spontaneous neuronal activity distinguishes human dorsal and ventral attention systems. *Proc Natl Acad Sci USA.* (2006) **103**:10046–51. doi: 10.1073/pnas.0604187103
  126. Vincent JL, Kahn I, Snyder AZ, Raichle ME, Buckner RL. Evidence for a frontoparietal control system revealed by intrinsic functional connectivity. *J Neurophysiol.* (2008) **100**:3328–42. doi: 10.1152/jn.90355.2008
  127. Zhou J, Liu X, Song W, Yang Y, Zhao Z, Ling F, et al. Specific and nonspecific thalamocortical functional connectivity in normal and vegetative states. *Conscious Cogn.* (2011) **20**:257–68. doi: 10.1016/j.concog.2010.08.003
  128. Martuzzi R, Ramani R, Qiu M, Rajeevan N, Constable RT. Functional connectivity and alterations in baseline brain state in humans. *Neuroimage* (2010) **49**:823–34. doi: 10.1016/j.neuroimage.2009.07.028
  129. Stamatakis EA, Adapa RM, Absalom AR, Menon DK. Changes in resting neural connectivity during propofol sedation. *PLoS ONE* (2010) **5**:e14224. doi: 10.1371/journal.pone.0014224
  130. Schröter MS, Spormaker VI, Schorer A, Wohlschläger A, Czisch M, Kochs EF, et al. Spatiotemporal reconfiguration of large-scale brain functional networks during propofol-induced loss of consciousness. *J Neurosci.* (2012) **32**:12832–40. doi: 10.1523/JNEUROSCI.6046-11.2012
  131. Krivitsky PN, Handcock MS. A separable model for dynamic networks. *J R Statist Soc.* (2014) **76**:29–46. doi: 10.1111/rssb.12014
  132. Leifeld P. texreg: Conversion of Statistical Model Output in R to LATEX and HTML Tables. *J Stat Softw.* (2013) **55**:62. doi: 10.18637/jss.v055.i08
  133. The ADHD-200 Consortium. The ADHD-200 consortium: a model to advance the translational potential of neuroimaging in clinical neuroscience. *Front Syst Neurosci.* (2012) **6**:62. doi: 10.3389/fnsys.2012.00062
  134. Lutkenhoff ES, Chiang J, Tshibanda L, Kamau E, Kirsch M, Pickard JD, et al. Thalamic and extrathalamic mechanisms of consciousness after severe brain injury. *Ann Neurol.* (2015) **78**:68–76. doi: 10.1002/ana.24423
  135. Lutkenhoff ES, McArthur DL, Hua X, Thompson PM, Vespa PM, Monti MM. Thalamic atrophy in antero-medial and dorsal nuclei correlates with six-month outcome after severe brain injury. *Neuroimage Clin.* (2013) **3**:396–404. doi: 10.1016/j.nicl.2013.09.010
  136. Boly M, Phillips C, Balteau E, Schnakers C, Degueldre C, Moonen G, et al. Consciousness and cerebral baseline activity fluctuations. *Human Brain Mapp.* (2008) **29**:868–74. doi: 10.1002/hbm.20602
  137. Boly M, Phillips C, Tshibanda L, Vanhaudenhuyse A, Schabus M, Dang-Vu G T T Moonon, et al. Intrinsic brain activity in altered states of consciousness. *Ann N Y Acad Sci.* (2008) **1129**:119–29. doi: 10.1196/annals.1417.015

**Conflict of Interest Statement:** The authors declare that the research was conducted in the absence of any commercial or financial relationships that could be construed as a potential conflict of interest.

Copyright © 2018 Dell'Italia, Johnson, Vespa and Monti. This is an open-access article distributed under the terms of the Creative Commons Attribution License (CC BY). The use, distribution or reproduction in other forums is permitted, provided the original author(s) and the copyright owner are credited and that the original publication in this journal is cited, in accordance with accepted academic practice. No use, distribution or reproduction is permitted which does not comply with these terms.



# A Heartbeat Away From Consciousness: Heart Rate Variability Entropy Can Discriminate Disorders of Consciousness and Is Correlated With Resting-State fMRI Brain Connectivity of the Central Autonomic Network

## OPEN ACCESS

### Edited by:

Freimut Dankwart Juengling,  
St. Claraspital Basel, Switzerland

### Reviewed by:

Jordi A. Matias-Guiu,  
Hospital Clínico San Carlos, Spain  
Vishwadeep Ahluwalia,  
Georgia Institute of Technology,  
United States

### \*Correspondence:

Francesco Riganello  
f.riganello@istitutosananna.it  
Stephen Karl Larroque  
lrq3000@gmail.com

†These authors have contributed  
equally to this work as first authors

### Specialty section:

This article was submitted to  
Applied Neuroimaging,  
a section of the journal  
Frontiers in Neurology

Received: 24 May 2018

Accepted: 24 August 2018

Published: 12 September 2018

### Citation:

Riganello F, Larroque SK, Bahri MA,  
Heine L, Martial C, Carrière M,  
Charland-Verville V, Aubinet C,  
Vanhaudenhuyse A, Chatelle C,  
Laureys S and Di Perri C (2018) A  
Heartbeat Away From Consciousness:  
Heart Rate Variability Entropy Can  
Discriminate Disorders of  
Consciousness and Is Correlated With  
Resting-State fMRI Brain Connectivity  
of the Central Autonomic Network.  
Front. Neurol. 9:769.  
doi: 10.3389/fneur.2018.00769

Francesco Riganello<sup>1,2\*†</sup>, Stephen Karl Larroque<sup>1\*†</sup>, Mohamed Ali Bahri<sup>3</sup>, Lizette Heine<sup>4</sup>,  
Charlotte Martial<sup>1</sup>, Manon Carrière<sup>1</sup>, Vanessa Charland-Verville<sup>1</sup>, Charlene Aubinet<sup>1</sup>,  
Audrey Vanhaudenhuyse<sup>5</sup>, Camille Chatelle<sup>1</sup>, Steven Laureys<sup>1</sup> and Carol Di Perri<sup>1,6</sup>

<sup>1</sup> Coma Science Group, GIGA-Consciousness, University & Hospital of Liege, Liege, Belgium, <sup>2</sup> Research in Advanced NeuroRehabilitation, Istituto S. Anna, Crotone, Italy, <sup>3</sup> GIGA-Cyclotron Research Center in vivo Imaging, University of Liege, Liege, Belgium, <sup>4</sup> Centre de Recherche en Neurosciences, Inserm U1028 - CNRS UMR5292, University of Lyon 1, Bron, France, <sup>5</sup> Sensation & Perception Research Group, GIGA-Consciousness, University & Hospital of Liege, Liege, Belgium, <sup>6</sup> Centre for Clinical Brain Sciences, University of Edinburgh, Edinburgh, United Kingdom

**Background:** Disorders of consciousness are challenging to diagnose, with inconsistent behavioral responses, motor and cognitive disabilities, leading to approximately 40% misdiagnoses. Heart rate variability (HRV) reflects the complexity of the heart-brain two-way dynamic interactions. HRV entropy analysis quantifies the unpredictability and complexity of the heart rate beats intervals. We here investigate the complexity index (CI), a score of HRV complexity by aggregating the non-linear multi-scale entropies over a range of time scales, and its discriminative power in chronic patients with unresponsive wakefulness syndrome (UWS) and minimally conscious state (MCS), and its relation to brain functional connectivity.

**Methods:** We investigated the CI in short (CI<sub>s</sub>) and long (CI<sub>l</sub>) time scales in 14 UWS and 16 MCS sedated. CI for MCS and UWS groups were compared using a Mann-Whitney exact test. Spearman's correlation tests were conducted between the Coma Recovery Scale-revised (CRS-R) and both CI. Discriminative power of both CI was assessed with One-R machine learning model. Correlation between CI and brain connectivity (detected with functional magnetic resonance imagery using seed-based and hypothesis-free intrinsic connectivity) was investigated using a linear regression in a subgroup of 10 UWS and 11 MCS patients with sufficient image quality.

**Results:** Higher CI<sub>s</sub> and CI<sub>l</sub> values were observed in MCS compared to UWS. Positive correlations were found between CRS-R and both CI. The One-R classifier selected CI<sub>l</sub> as the best discriminator between UWS and MCS with 90% accuracy, 7% false positive and 13% false negative rates after a 10-fold cross-validation test. Positive correlations

were observed between both CI and the recovery of functional connectivity of brain areas belonging to the central autonomic networks (CAN).

**Conclusion:** CI of MCS compared to UWS patients has high discriminative power and low false negative rate at one third of the estimated human assessors' misdiagnosis, providing an easy, inexpensive and non-invasive diagnostic tool. CI reflects functional connectivity changes in the CAN, suggesting that CI can provide an indirect way to screen and monitor connectivity changes in this neural system. Future studies should assess the extent of CI's predictive power in a larger cohort of patients and prognostic power in acute patients.

**Keywords:** heart rate variability entropy (HRV), disorders of consciousness (DOC), unresponsive wakefulness syndrome/vegetative state (UWS/VS), minimally conscious state, functional connectivity, resting-state fMRI, machine learning

## INTRODUCTION

Disorders of consciousness are a spectrum of pathologies affecting one's ability to interact with the external world. They are increasingly becoming a worldwide health concern, whether of traumatic (1, 2) or non-traumatic (3–6) cause, with its share of ethically challenging questions including life and death decisions (7–9). Indeed, differential diagnosis of the clinical entities of disorders of consciousness raises crucial ethical and medical issues, including pain treatment and end-of-life decisions (8, 10, 11).

Despite the definition of such a unified name, these disorders are in fact covering a broad population of very heterogeneous pathologies with diverse etiologies, injuries and outcomes. This heterogeneity can make them hardly distinguishable in the clinical practice (9), leading to a reported misdiagnosis rate between 33 and 41% for the clinical consensus (12, 13). Although the clinical characterization of disorders of consciousness can now be more reliably assessed using specifically designed scales such as the Coma Recovery Scale-Revised (CRS-R) (14), practicing them requires a specific training of the physicians and, although lower, might still induce diagnosis errors inherent to any behavior-based clinical assessment due to the patient's possible inability to respond (13). Indeed, these assessments rely on observing the patient's motor actions, and their absence

does not necessarily relate to the absence of consciousness, as there are several other factors that might hamper the patient's responsiveness to the assessment (motor disabilities, language understanding difficulties, fluctuating consciousness because of natural awareness fluctuations or the influence of drugs side effects, patient's willingness to collaborate among other factors) (13). Neuroimaging has been proposed as a complementary tool to help in assessment and decision making for these critical conditions (13, 15, 16). However, these techniques are usually highly costly, complex, and time consuming. Alternative methods, such as probing physiological signals of peripheral organs like the heart, have been proposed to overcome these issues (17–19).

Heart rate is defined as the numbers of heartbeats per minute; the Heart Rate Variability (HRV) is the fluctuation in the time intervals between adjacent heartbeats. These fluctuations represent the output of a complex brain-heart two-way interaction system (20–22). Indeed, HRV analysis provides a window into the brain's function. HRV has been observed to rapidly and flexibly modulate response to environmental changes and can be disrupted by neurological and non-neurological diseases usually involving the autonomic nervous system (23–29). The HRV recording technique is non-invasive, inexpensive to acquire and has an excellent signal-to-noise ratio compared to signals investigated in neuroimaging or clinical neurophysiology (30).

HRV is analyzed in time and frequency domains and by non-linear methods (31). In the time domain, this is quantified by the amount of heartbeats variability observed during monitoring periods in the range of 1 min to more than 24 h. In the frequency domain, HRV is calculated as the absolute or relative amount of signal energy within the component bands. Fast Fourier Transformation (FFT), Auto-regression or Wavelet modeling are used to separate the HRV into its main components: Ultra Low Frequency (ULF), Very Low Frequency (VLF), Low Frequency (LF), and High Frequency (HF) (31).

As the sequence of heart beats is not regular and exhibit complex fluctuation patterns over a wide range of time scales, HRV is better described by the mathematical chaos (32, 33), therefore non-linear analyses are appropriate to model this type

**Abbreviations:** ACC, anterior cingulate cortex; AC-PC, anterior commissure - posterior commissure; ANOX, anoxic; ANS, autonomic nervous system; ARCA, cardiac arrest; BOLD, blood-oxygen-level dependent; CAN, central autonomic network; CI, complexity index; CI<sub>L</sub>, complexity index in the long term (average of multiscale entropies from 6 to 10); CI<sub>S</sub>, complexity index in the short term (average of multiscale entropies from 1 to 5); CNS, central nervous system; CRS-R, Coma Recovery Scale - Revised; CSF, cerebro-spinal fluid; ECG, electrocardiogram; EPI, echo-planar imaging; FFT, Fast Fourier Transform; fMRI, functional magnetic resonance imaging; GM, grey matter; HEM, hemorrhagic; HRV, heart rate variability; ICC, intrinsic connectivity contrast; LOC, Lateral Occipital Cortex; MCS, minimally conscious state; MFG, middle Frontal Gyrus; MNI, Montreal Neurological Institute; MPFC, Medial Prefrontal Cortex; MRI, magnetic resonance imaging; MSE, multiscale entropy; MTG, middle Temporal Gyrus; PCC, posterior cingulate cortex; PPG, photoplethysmographic; SE, sample entropy; SPL, Superior Parietal Lobule; STG, Superior Temporal Gyrus; TBI, traumatic brain injury; UWS, unresponsive wakefulness syndrome, previously persistent vegetative syndrome (PVS); WM, white matter.

of time series. These analyses quantify the unpredictability and complexity of the interbeat intervals (IBI) series. Poincaré plot (34), detrended fluctuation analysis (35), approximate entropy (36), sample entropy (SE) (37), and multiscale entropy (MSE) (38) are among the most commonly applied methods of non-linear analysis used in the HRV analysis.

MSE was developed to investigate the information content in non-linear signals at different temporal scales (coarse-graining), using generally the SE in order to quantify the degree of unpredictability of time series. In other words, applying MSE on top of the HRV allows to measure the diversity of the heart beat intervals: higher entropy indicates a more unpredictable and diverse heart beats sequence, and conversely lower entropy indicates a more regular and predictable heart beats. Considering the complex brain-heart interactions system mentioned above, it is conceivable that the HRV entropy might be a way to measure the health status of this system, with a low value being indicative of low reactivity to the external/internal stimulus. Indeed, MSE on HRV was shown to be a marker of health status of biological systems (39–41). The Complexity Index (CI) is calculated from the MSE measures and is defined as the sum of the entropies computed for different scales (i.e., at different levels of resolution of the signal). The CI thus provides a scalar score, which is the aggregation of MSE over multiple time scales, and it allows to get insights into the integrated complexity of the measured system (41).

Heart rate, as well as respiration rate, glands, smooth muscles functions and biological sensors are under the control of the Autonomic Nervous System (ANS), which is in charge of maintaining the homeostasis without any conscious control (42). The sympathetic (“fight or flight system”) and parasympathetic (“rest and digest” system) branches of the ANS have an antagonistic role and are connected to the brain by the spinal nerves (43). By doing so, they modulate the ANS functional status through inputs from thermoregulation, baroreceptors, chemoreceptors, renin-angiotensin-aldosterone balance and atrial and ventricular receptors (18, 44–46).

The Central Autonomic Network (CAN) has been proposed as an integrative model where neural structures and heart function are involved and functionally linked in the affective, cognitive and autonomic regulation (47, 48). The CAN is defined as covering the structures of the brainstem (periaqueductal gray matter, nucleus ambiguus, and ventromedial medulla), limbic structure (amygdala and hypothalamus), prefrontal cortex (anterior cingulate, insula, orbitofrontal, and ventromedial cortex) and cerebellum (22, 49, 50). Some brain regions of the CAN (dorsolateral prefrontal cortex, mediodorsal thalamus, hippocampus, caudate, septal nucleus and middle Temporal Gyrus) seem to be unique to humans (51–53). The interplay between Central Nervous System (CNS) and ANS is functionally modeled as a setup involving the above-cited structures connecting to the brainstem solitary tract (NTS) via feed-forward and feedback loops. These coupled structures and their oscillatory signals, integrated in the NTS by the efferent parts of the vagus nerve, are coupled with organs outside the brain in a bidirectional way. Through this two-way interaction, peripheral oscillations, such as those in the heart, lung, immunological

system and kidney, can lead to changes in the CAN, as well as be influenced by the CAN (54–57). HRV measurements are thought to reflect heart rate interaction and ANS dynamics and, to some extent and indirectly, higher brain functions (58–61), and thus might be relevant for diagnostic purposes (62, 63).

In the present study, we aimed to characterize and investigate the discriminative power of the CI in sedated patients suffering from disorders of consciousness, more specifically diagnosed as either unresponsive wakefulness syndrome (UWS, i.e., vegetative state—eye opening without signs of awareness) or minimally conscious (MCS—displaying non-reflexive behaviors) according to the CRS-R clinical assessment. In the light of the above mentioned studies, we hypothesized an impaired two-way brain heart connection (due to the loss of the biological complexity linked to physiologic mechanism) (14, 58), and consequently lower values of CI in UWS patients on average compared to MCS. We further expected CI values to be correlated with each patient's behavioral assessment as measured with the Coma Recovery Scale Revised (CRS-R) (14). In addition, we expected the CI measures to possess some discriminative power on the diagnosis when used in a machine learning model such as One-R classifier, an algorithm deriving a single association rule between the most discriminating feature and the diagnosis classification (64).

With the aim of investigating brain regions' involvement in the HRV entropy, we further investigated the relationship between the CI measures and the brain connectivity patterns, and whether there are different patterns for UWS and MCS that are correlated with changes in the CI values. In this optic, we correlated, using a linear parametric regression, the per-subject CI values with brain regions connectivity patterns as detected by whole-brain resting-state functional magnetic resonance imagery (fMRI). fMRI is a non-invasive technique used to investigate the spontaneous temporal coherence in blood-oxygen-level dependent (BOLD) signal fluctuations related to the amount of synchronized neural activity (i.e., functional connectivity) existing between distinct brain locations (65). Combined with a regression of the physiological noise by principal components analysis via aCompCor, this approach, novel in its application to HRV studies, allows to investigate whole brain connectivity patterns without any task and with minimal assumptions compared to other approaches such as cardiac gating (52, 66). Given the findings of previous studies suggesting that CI is involved with autonomic nervous system structures (67–69), we hypothesized that the CI values would be correlated with brain regions belonging to the CAN, with higher CI values being predictive of greater positive correlations in this network.

## METHODS

### Participants

This study included patients diagnosed as either UWS or MCS according to the Coma Recovery Scale - Revised (CRS-R) (14, 70) and diagnosed as either UWS or MCS who underwent an MRI examination under Propofol sedation together with electrocardiography (ECG) recordings. Exclusion criteria were (i) artifacts in ECG recording (ii) ECG acquisition and



neuroimaging examination in patients less than 2 weeks from brain insult, (iii) large focal brain damage, i.e.,  $>2/3$  of one hemisphere, as stated by a certified neuroradiologist, (iv) motion parameters  $>3$  mm in translation and 3 degrees in rotation. Additional exclusion criteria were applied for patients included in the MRI analysis: (v) suboptimal segmentation and normalization due to movement or metallic artifacts as stated by a certified neuroradiologist, (vi) non gaussian-like fMRI signal shape after denoising.

From an initial dataset of 67 sedated patients with ECG and imaging acquisition, 37 patients were discarded because of too many artifacts in the ECG recording. The 30 remaining patients formed the subgroup S1 with 14 patients (7 males, mean age  $51 \pm 14$ ; 7 females, age  $46 \pm 18$ ; 7 ARCA [cardiac arrest], 2 ANOX [anoxic], 1 TBI [traumatic brain injury], 2 HEM [hemorrhagic], 1 ANOX+TBI [anoxic and traumatic], 1 other [metabolic, epilepsy, etc.]) being diagnosed as UWS and 16 patients (10 males mean age  $44 \pm 17$ ; 7 females, mean age  $41 \pm 17$ ; all patients mean age  $42 \pm 17$ ; 2 ARCA, 2 ANOX, 10 TBI, 1 HEM, 1 ANOX+TBI) as MCS (**Table 1**). For the correlation analysis between the CI values and brain regions connectivity differences as detected by resting-state fMRI, nine additional patients were discarded because of movement or metallic artifact in the fMRI data, or because of suboptimal segmentation or signal shape during the preprocessing as stated above (additional details are in the Supplementary Materials, **Appendix B**). The subgroup S2 for fMRI analysis therefore included 21 patients with 10 UWS patients (5 males, mean age  $54 \pm 11$ ; 5 females, mean age  $50 \pm 18$ ; 5 ARCA, 2 ANOX, 2 HEM, 1 ANOX+TBI) and 11 MCS patients (5 males, mean age  $37 \pm 17$ ; 6 females, mean age  $40 \pm 16$ ; all patients mean age  $38 \pm 16$ ; 1 ARCA, 2 ANOX, 7 TBI, 1 HEM) (**Table 1**). The evolution time since the brain injury up to the ECG/MRI assessment is described in **Table 1**. The patients were matched between MCS and UWS for diagnosis, age, gender, etiology and onset, for both subgroups.

The study was approved by the Ethics Committee of the Faculty of Medicine of the University of Liège and written informed consents, including for publication of data, were obtained from the patients' legal representatives and from the healthy control subjects in accordance with the Declaration of Helsinki.

## Sedation Protocol

Patients were sedated to reduce the severity of movement artifact during the fMRI data acquisition. The sedation was obtained by Propofol infusion keeping the concentration to a minimum [average:  $1.7 \mu\text{g/mL}$ , range:  $[1, 2.5] \mu\text{g/mL}$ ] (71). The sedation was administered through intravenous infusion by a target-controlled infusion system [Diprifusor, pharmacokinetic model of Marsh et al. (72), Alaris TM, Alaris Medical Belgium B.V., Strombeek-Bever, Belgium] in order to obtain constant plasma concentration. Propofol was chosen for immobilization purpose for its short induction and recovery times, and because generally it does not need additional sedatives (73). Moreover is one of the most available anesthetic agent with common clinical application and well-established safety as well as being well-studied (74). There

is also preliminary evidence that Propofol has also might not significantly reduce the residual resting-state functional connectivity observed in UWS and MCS patients (71). During data acquisition, the patients wore headphone and earplug. The stability of their vital parameters was controlled by continuous monitoring of blood pressure, ECG, respiration and pulse-oximetry.

## ECG Procedure

### ECG Data Acquisition

Electrocardiographic activity was recorded during the 10 min of fMRI data acquisition using the scanner's built-in equipment. The cardiac cycle was monitored by a photoplethysmographic sensor (PPG) placed on the right index finger and ECG's three leads positioned on the chest of the patients (leads I, II, and III are used and acquired in parallel via the ECG channels to display a prominent peak of the QRS ECG complex).

### ECG Data Preprocessing

The ECG signal and PPG was cleaned of noise using a FFT filter without detrending (SigView software; <http://www.sigview.com/>). The series of consecutive intervals between heartbeats (tachogram) were extracted from ECG and PPG. After a visual analysis for ectopic beat or missing data, the MSE was calculated and analyzed to measure the complexity of the nonlinearity and non-stationary properties of the signal using the HRV Advanced Analysis software version 2.2 (75). Studies demonstrated that PPG and ECG measures have superimposable results in the temporal and frequency domains and in nonlinear dynamic analyses (76). The results between ECG and PPG signals were manually compared as an additional sanity check about the correct acquisition of the signal (**Figure 1**).

### ECG Data Analysis

The MSE approach (38, 41) was applied to quantify the degree of irregularity over a range of time scales ( $\tau$ ). The method involves the construction of coarse-grained IBI time series and the quantification of the degree of irregularity of each of these. We then extracted 10 min from the tachogram. The time series from  $\tau = 1$ –10 were constructed by averaging the IBI/tachogram's data points within non-overlapping windows of increasing length,  $\tau$  (**Figure 2**).

Finally, the SE was applied for each coarse-grained constructed (37, 77) (Equation 1). The purpose of SE is to look for patterns in a time series and quantify its degree of predictability or regularity (77). The parameters involved in the calculation of the SE are the dimensional phase space  $m$  and the tolerance for accepting matches of two patterns  $r$  and were set to  $m = 2$  and  $r = 0.15$  (41, 78).

$$S_E(m, r, N) = -\ln \frac{\phi^{m+1}(r)}{\phi^m(r)}$$

Equation (1): SE: Sample Entropy;  $m$ : distance between time series points to be compared;  $r$ : radius of similarity;  $N$ : length of

**TABLE 1** | Demographic information of patients.

ID	CRS-R diagnosis	CRS-R total score	CRS-R subscore	Etiology	Age	Days since onset
1	<b>UWS</b>	<b>3</b>	<b>S101100</b>	<b>OTHER</b>	<b>15–24</b>	<b>18</b>
2	<b>UWS</b>	<b>3</b>	<b>S001101</b>	<b>ANOX</b>	<b>55–64</b>	<b>21</b>
3	<b>UWS</b>	<b>3</b>	<b>S001101</b>	<b>ARCA</b>	<b>65–74</b>	<b>31</b>
4	UWS	4	S002101	ARCA	55–64	24
5	<b>UWS</b>	<b>4</b>	<b>S001201</b>	<b>ANOX+TBI</b>	<b>45–54</b>	<b>46</b>
6	MCS	5	S102101	TBI	15–24	38
7	<b>MCS</b>	<b>5</b>	<b>S030101</b>	<b>HEM</b>	<b>45–54</b>	<b>30</b>
8	UWS	5	S201101	ARCA	35–44	733
9	<b>UWS</b>	<b>5</b>	<b>S102101</b>	<b>ARCA</b>	<b>65–74</b>	<b>18</b>
10	<b>UWS</b>	<b>5</b>	<b>S002102</b>	<b>ARCA</b>	<b>65–74</b>	<b>43</b>
11	<b>MCS</b>	<b>6</b>	<b>S012102</b>	<b>TBI</b>	<b>15–24</b>	<b>31</b>
12	<b>UWS</b>	<b>6</b>	<b>S111102</b>	<b>ARCA</b>	<b>45–54</b>	<b>37</b>
13	UWS	6	S102102	HEM	55–64	248
14	<b>UWS</b>	<b>6</b>	<b>S101202</b>	<b>ARCA</b>	<b>45–54</b>	<b>101</b>
15	UWS	6	S111201	TBI	25–34	1017
16	<b>MCS</b>	<b>7</b>	<b>S302101</b>	<b>ARCA</b>	<b>45–54</b>	<b>209</b>
17	<b>MCS</b>	<b>7</b>	<b>S230101</b>	<b>TBI</b>	<b>25–34</b>	<b>534</b>
18	<b>UWS</b>	<b>7</b>	<b>S102202</b>	<b>HEM</b>	<b>45–54</b>	<b>353</b>
19	<b>UWS</b>	<b>8</b>	<b>S112202</b>	<b>ANOX</b>	<b>15–24</b>	<b>462</b>
20	<b>MCS</b>	<b>9</b>	<b>S311211</b>	<b>TBI</b>	<b>15–24</b>	<b>432</b>
21	<b>MCS</b>	<b>10</b>	<b>S232201</b>	<b>TBI</b>	<b>35–44</b>	<b>1294</b>
22	<b>MCS</b>	<b>10</b>	<b>S331102</b>	<b>ANOX</b>	<b>25–34</b>	<b>2407</b>
23	MCS	10	S115201	TBI	45–54	220
24	<b>MCS</b>	<b>11</b>	<b>S305201</b>	<b>TBI</b>	<b>25–34</b>	<b>561</b>
25	<b>MCS</b>	<b>11</b>	<b>S305102</b>	<b>ANOX</b>	<b>15–24</b>	<b>624</b>
26	MCS	12	S305202	TBI	15–24	660
27	<b>MCS</b>	<b>13</b>	<b>S335101</b>	<b>TBI</b>	<b>35–44</b>	<b>319</b>
28	MCS	15	S345102	ANOX+TBI	45–54	2086
29	MCS	16	S345202	ARCA	45–54	290
30	<b>MCS</b>	<b>16</b>	<b>S335212</b>	<b>TBI</b>	<b>55–64</b>	<b>4322</b>

In bold: patients included in fMRI analysis (S2 group). Days since onset: evolution time since the brain injury up to the ECG/fMRI acquisition. CRS-R subscore represent the subitems scores of the best CRS-R during the period of assessment (in order: “S” prefix for subscore then auditory, visual, motor, oromotor/verbal, communication and arousal scores). The rejection details for the patients discarded from the fMRI analysis are available in the Supplementary materials (Appendix B). ARCA, cardiac arrest; TBI, traumatic brain injury; HEM, hemorrhagic; ANOX, anoxic.

the time series;  $\phi$ : probability that points  $m$  distance apart would be within the distance  $r$ .

The CI of the MSE is calculated as the area under the SE time scale curve (Equation 2).

$$C_I = \sum_{i=1}^N S_E(i)$$

Equation 2: CI summations of quantitative values of the Sample Entropy of  $N$  coarse-grained time scale.

The CI provides insights into the integrated complexity of a system, over a range of time scales of interest. The summations of quantitative SE values over time scales 1–5 and over time scales 6–10 represent the complexity index calculated in short ( $CI_s$ ) and long time scales ( $CI_l$ ), respectively (41), corresponding to high frequency (0.15–0.4 Hz) and low frequency band (0.04–0.15 Hz) respectively.

## MRI Procedure

### MRI Data Acquisition

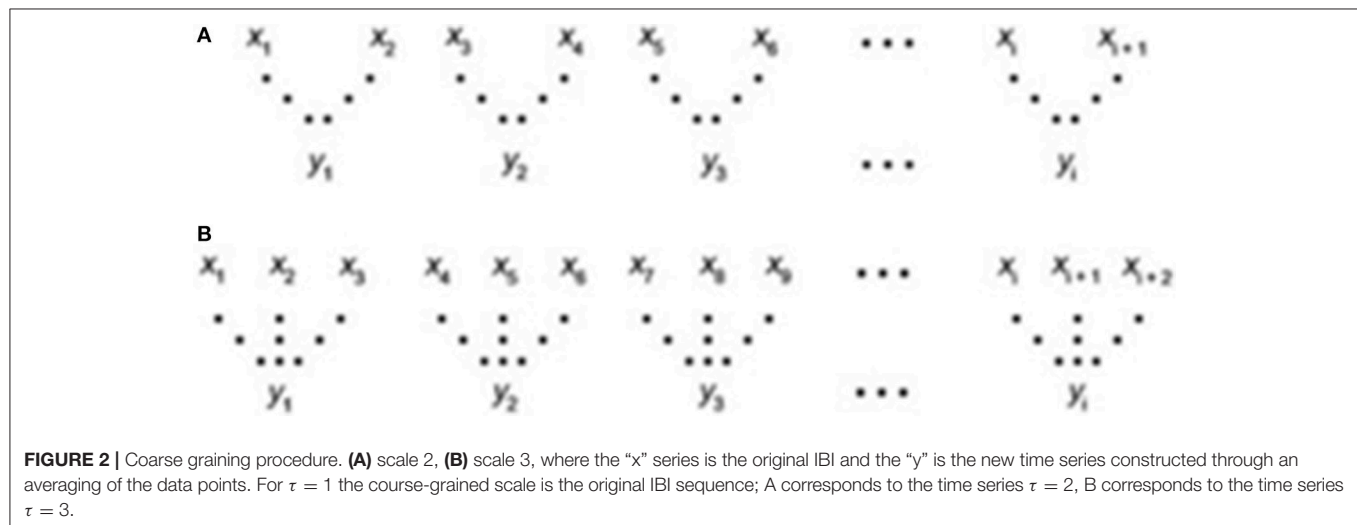
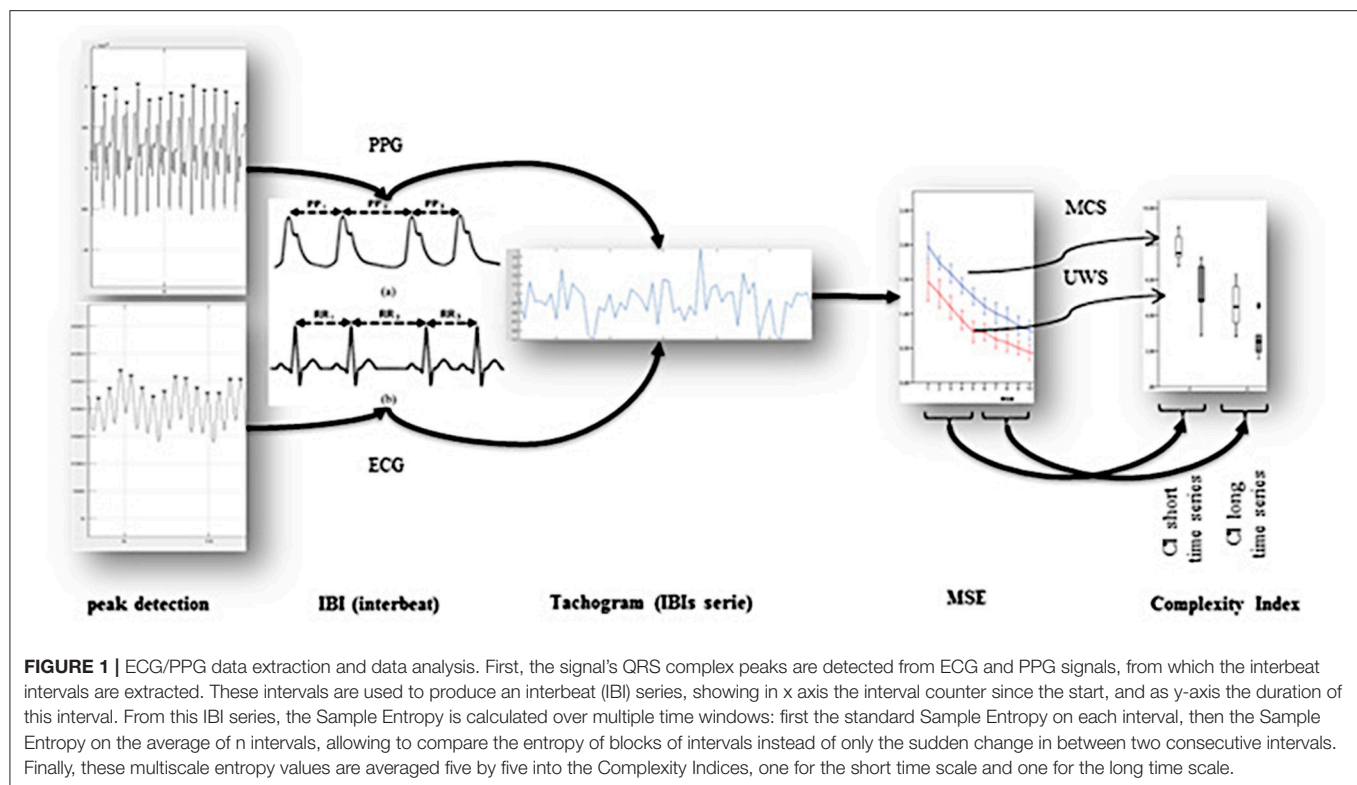
All structural and functional images of the MCS and UWS patients were acquired on a 3 Tesla Siemens Magnetom TrioTim magnetic resonance image machine at the University Hospital of Liège.

### Structural Imaging

A high-resolution T1-weighted image was acquired for each patient (T1-weighted 3D gradient echo images using 120 slices, repetition time = 2,300 ms, echo time = 2.47 ms, voxel size =  $1 \times 1 \times 1 \text{ mm}^3$ , flip angle = 9 degrees, field of view =  $256 \times 256 \text{ mm}^2$ ) in order to allow for precise segmentation and coregistration as well as denoising.

### Resting-state fMRI

Multislices T2\*-weighted fMRI images were obtained during 10 min for each patient by using Echo Planar Imaging (EPI)



sequence with axial slice orientation (300 volumes, 32 slices, voxel size =  $3.0 \times 3.0 \times 3.75 \text{ mm}^3$ , repetition time = 2,000 ms, echo time = 30 ms, flip angle =  $78^\circ$ , field of view = 192 mm, matrix size =  $64 \times 64 \times 32$ , delay = 0, slice order = sequential descending). As a standard protocol, all subjects were instructed to keep their eyes closed and not to think of anything in particular. Head motion was restricted by placement of a comfortable padding around each participant's head, and earplugs and headphones were placed on the patient's ears. The first three initial volumes were automatically discarded by the MRI scanner (dummy scans)

to allow for longitudinal magnetization to reach steady-state (79).

## MRI Data Pre-processing

### Structural imaging

Structural ( $T1^*$ -weighted) MRI images were manually reoriented to the anterior commissure/posterior commissure (AC-PC) scheme and then normalized and segmented into gray matter, white matter, cerebrospinal fluid, skull, and soft tissue outside the brain, using the “old segmentation” module and standard tissue probability map of Statistical

Parametric Mapping 12 (SPM12) ([www.fil.ion.ucl.ac.uk/spm](http://www.fil.ion.ucl.ac.uk/spm)).

### Resting-state fMRI

Functional volumes were first manually reoriented and coregistered to the structural images, and then preprocessed by using SPM12 (SPM, RRID:SCR\_007037). First, the EPI volumes were corrected for the temporal difference in acquisition among different slices using the slice timing correction module with the reference slice set to the first temporal slice, and then the images were realigned for head motion correction using a two-steps procedure: (1) realignment to the first volume and creation of the mean image, (2) then all images were realigned to the mean EPI image. The mean EPI image across all realigned volumes was then auto-coregistered to the structural image. Then the structural image was segmented into three tissues: gray matter (GM), white matter (WM), and cerebro-spinal fluid (CSF) in the subject's space, producing as a by-product of the segmentation the parameters of the transform from the subject's space to Montreal Neurological Institute (MNI) space. This transform was then used to normalize the structural image, the co-registered EPI images and the segmented tissues. Finally, all the coregistered and normalized EPI images were smoothed with an isotropic Gaussian kernel (8 mm full-width-at-half-maximum). A manual inspection of the whole BOLD timeseries motion was conducted from the SPM motion file to exclude any subject where the translational head displacement was greater than 1 mm, or if the rotational displacement was greater than 0.1 radians. With the aim of reducing loss of signal or whole subjects exclusion due to motion artifacts (80), we used the “scrubbing” technique from the ART toolbox (Artifact Detection Tools, RRID:SCR\_005994)<sup>1</sup> for artifactual volume detection and rejection using a composite motion measure (largest voxel movement) with a “liberal” threshold (global threshold 9.0, motion threshold 2.0, use scan-to-scan motion and global signal). With this approach, a volume was defined as an outlier (artifact) if the largest voxel movement detected was above the specified thresholds. We subsequently included outliers in the global mean signal intensity and motion as nuisance regressors (i.e., one regressor per outlier in the first-level general linear model). Thus, the temporal structure of the data was not disrupted. Several parameters were included in a linear regression using CONN v17F (Connectivity Toolbox, RRID:SCR\_009550) and SPM12 to remove possible spurious variances from the data. These were (i) six head motion parameters obtained in the realigning step, (ii) scrubbing the outlier scans detected by ART's composite motion measure, (iii) non-neuronal sources of noise estimated using the anatomical component-based noise correction method [aCompCor; (81, 82)], which consists in regressing out the representative signals of no interest from subject-specific white matter and cerebro-spinal fluid, which were the top five principal components (PCA) from the white matter and the top five from cerebrospinal fluid per-subject mask (81). Then the residual time

series were linearly detrended (no despiking) and temporally band-pass filtered (0.008–0.09 Hz) using CONN's denoising procedure.

## Statistical Analyses

### ECG Statistical Analyses

In both the entire patient group S1 and the subgroup undergoing fMRI analysis S2, the CI<sub>s</sub> and CI<sub>i</sub> measures average per MCS and UWS groups were compared using a Mann-Whitney exact test. Correlation between the CRS-R total score—the sum of all CRS-R items of the best assessment over a week—with the CI<sub>s</sub> on one hand, and between the CRS-R total score and CI<sub>i</sub> on the other hand was analyzed using the Spearman's correlation test. Significance of tests was set to  $p < 0.05$ .

### Machine Learning Model

WEKA (Waikato Environment for Knowledge Analysis, RRID:SCR\_001214), an open source toolbox for machine learning analysis (64)<sup>2</sup> was used to assess the discriminative power of the CI measures by a machine-learning model called the One-R classifier (83), with the objective of predicting the CRS-R diagnosis of UWS or MCS given a patient's CI measures. The retained CRS-R diagnosis was the final best diagnosis over a week of CRS-R assessments. One-R (83) is a fast and very simple algorithm deriving a one level decision tree. It operates by generating a separate rule for each individual attribute of the dataset (CI<sub>s</sub> and CI<sub>i</sub>) based on error rate. To generate the rule, each attribute is discretized into bins calculating the percentage that each class (MCS and UWS) appears within each bin. Finally, the rule for the final decision tree is chosen by selecting the attribute with minimum error to perform the diagnostic classification. This algorithm was chosen as it reported the best results in our case while being the most simple and thus robust model after running multiple simulations with various machine learning algorithms known to derive efficient models for diagnosis (84), the results of these simulations are available in the supplementary materials (**Appendix A**). The dataset used to generate the model consisted of the CI<sub>s</sub> and CI<sub>i</sub> values of the S1 group, and the objective was to predict the patient's diagnosis (UWS or MCS). To assess the performance of this model in generalization, a 10-fold cross-validation test (85) was conducted, thus the S1 group was split into 10 parts of equal number of patients, and the model was learnt on 9 parts and tested on the 10th part. This process was performed 10 times in total to use each part as the test set at some point, and metrics were calculated as the average over all 10 tests. Several metrics were calculated on both the 10-fold cross-validation test results, the S1 subgroup results and the S2 subgroup results such as the sensitivity (rate of MCS correctly classified), specificity (rate of UWS correctly classified), false positive and negative rates of MCS and UWS classification, accuracy (MCS and UWS predicted conditions), F1-score (86) [a measure of the test's accuracy that takes in consideration the harmonic mean

<sup>1</sup>NITRC: Artifact Detection Tools (ART): Tool/Resource Info. Available at: [https://www.nitrc.org/projects/artifact\\_detect/](https://www.nitrc.org/projects/artifact_detect/) (Accessed March 1, 2018).

<sup>2</sup>Weka 3 - Data Mining With Open Source Machine Learning Software in Java. Available online at: <https://www.cs.waikato.ac.nz/ml/weka/> (Accessed April 27, 2018).



of sensitivity and its precision also called the Dice similarity coefficient, ranging values between 0 [worst precision and sensitivity] and 1 [perfect precision and sensitivity] and the Matthews Correlation Coefficient (87) [a correlation coefficient between the observed and predicted binary classifications, ranging values between 1 [perfect prediction], 0 [random prediction], and  $-1$  [total disagreement between prediction and observation]].

### Resting-state fMRI Analyses

Functional magnetic resonance imaging is a non-invasive technique used to investigate the spontaneous temporal coherence in blood-oxygen-level dependent (BOLD) signal fluctuations related to the amount of synchronized neural activity (i.e., functional connectivity) existing between distinct brain locations (65).

With the aim of investigating the possible brain connectivity changes associated with a change of the CI values, we conducted a whole-brain resting-state fMRI functional connectivity analysis using a seed-to-voxel correlation analysis to observe changes in correlation of the BOLD signal in the whole brain with respect to the specified seed regions. Using CONN, we extracted from fMRI BOLD time series from a region of interest (the seed) and measured the temporal correlation between this signal and the time series of all other brain voxels. We have also conducted a voxel-to-voxel analysis by correlating the activity of all fMRI BOLD voxels to all other voxels via the Intrinsic Connectivity Contrast [ICC; in Conn toolbox; (88, 89)] as a quantification measure of global brain connectivity. In short, ICC quantifies the degree, including positive and negative correlations, of each voxel with all other brain voxels, which is then standardized against the average voxel degree as the mean and variance 1 to derive a Z-score. In other words, a positive ICC means that a brain region is significantly more connected to the rest of the brain compared to the average voxel connectivity.

The seeds were defined as spheres of 5 mm radius around the peak coordinates of main structures of the ANS/CAN (90): the Superior Temporal Gyrus (STG)  $[-44, -6, 11]$  &  $[44, -6, 11]$ , the Dorso-Lateral Prefrontal Cortex (DLPFC)  $[-43, 22, 34]$  &  $[22, 34, 42]$ , the Fronto-Insular cortex (FI)  $[-40, 18, -12]$  &  $[42, 10, -12]$ , the Paracingulate cortex (PC)  $[0, 44, 28]$ , the anterior cingulate cortex/mesoprefrontal cortex (ACC/MPFC)  $[-1, 54, 27]$ , the posterior cingulate cortex/precuneus (PCC/precuneus)  $[0, -52, 27]$ , cerebellum  $[-4, -56, -40]$ , thalamus  $[-4, -12, 0]$ ,  $[4, -12, 0]$ . Their coordinates have been taken from previous studies in order to avoid circularity (16). We used the averaged time series to estimate whole brain positive correlation  $r$  maps, and the  $t$ -test contrasts. In the design matrix, we applied a contrast to regress out the average connectivity of MCS and UWS patients and to highlight any connectivity difference that is correlated only with the complexity index. We did two different correlation tests for  $CI_s$  and  $CI_l$ .

Finally, we examined global brain connectivity patterns (without a priori seed) between each voxel and the rest of the brain using the ICC measure. We used the same design matrix to highlight only the connectivity differences correlated only with  $CI_s$  and then  $CI_l$ .

Age standardized to unitary standard deviation and centered to the mean was used a regressor of nuisance in the design matrices for both the seed-based and the hypothesis-free analyses.

Statistical results were generated with CONN and considered significant with multiple comparison correction at the topological level with non-parametric permutation test cluster-mass  $p$ -FWE  $< 0.1$  and with primary voxel-wise threshold  $p$ -uncorrected  $< 0.001$  with 1000 iterations. CONN 17f was patched with a permutation test patch to allow for generalized permutation of residuals ([https://www.nitrc.org/forum/message.php?msg\\_id=23131](https://www.nitrc.org/forum/message.php?msg_id=23131)). The significant regions names were derived from the Harvard-Oxford atlas (Harvard - Oxford Cortical Structural Atlas, RRID:SCR\_001476), using bspmview tool<sup>3</sup> Visualizations were generated using CONN, MRICron (RRID:SCR\_002403), NiLearn (RRID:SCR\_001362) (91), Python (Python Programming Language, RRID:SCR\_008394) and an in-house python script (<https://github.com/lrq3000/neuro-python-plotting>).

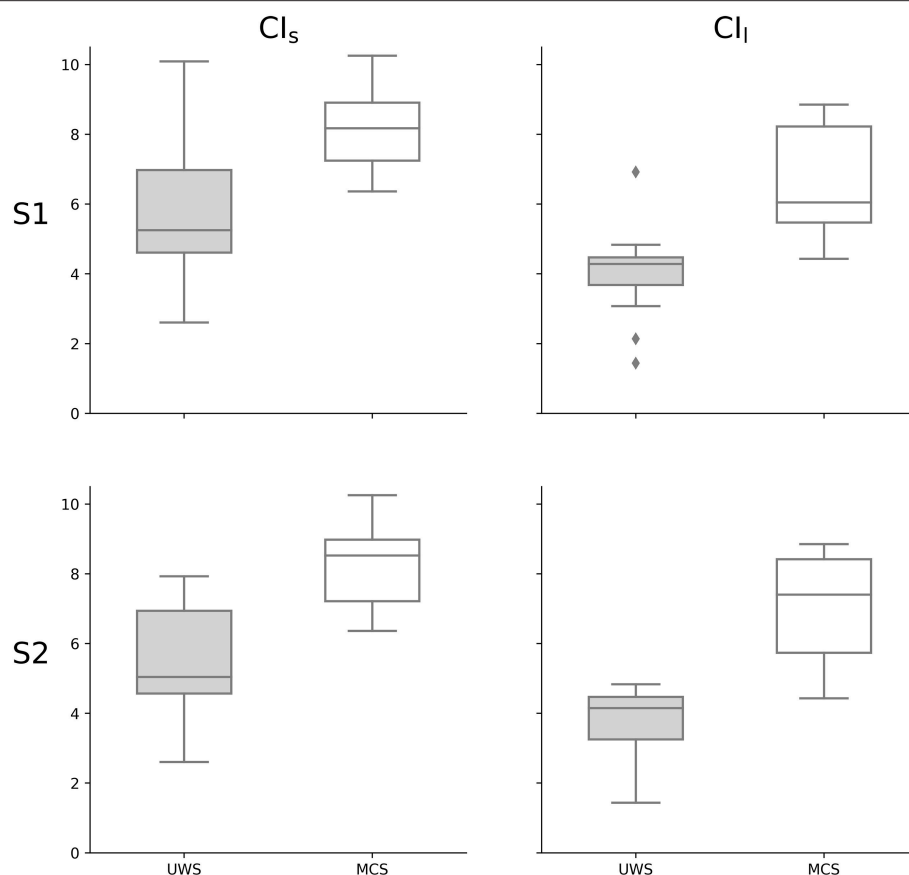
## RESULTS

In the S1 group, when comparing the CI values of MCS and UWS patients, higher values of  $CI_s$  ( $z = -3.346$ ,  $p < 0.001$ ) and of  $CI_l$  ( $z = -4.095$ ,  $p < 0.0001$ ) were observed for the MCS group compared to the UWS group (**Figures 2, 3**). A stronger correlation was found between the CRS-R total score and  $CI_l$  (Spearman's  $\rho = 0.671$ ,  $p < 0.0001$ ) compared to the moderate correlation between CRS-R total score and  $CI_s$  (Spearman's  $\rho = 0.579$ ,  $p < 0.001$ ) (**Figure 5**). The results of the S1 group are superimposable to the subgroup S2 who underwent fMRI analysis. In the S2 subgroup, higher values of  $CI_s$  ( $z = -3.063$ ,  $p = 0.002$ ) and of  $CI_l$  ( $z = -3.556$ ,  $p < 0.001$ ) were observed in the MCS group compared to the UWS group (**Figure 3**). A stronger correlation was found between the CRS-R total score and  $CI_l$  (Spearman's  $\rho = 0.676$ ,  $p < 0.001$ ) compared to the moderate correlation between CRS-R total score and  $CI_s$  (Spearman's  $\rho = 0.619$ ,  $p = 0.003$ ) (**Figure 5**).

Using the machine learning One-R classifier, the  $CI_l$  was selected as the most discriminating feature for the diagnostic classification of MCS and UWS patients. The model's accuracy in the classification of MCS and UWS patients was 93%, with a correct classification of MCS and UWS of 94 and 93% respectively (**Table 2**). The false positive (UWS as MCS) and false negative (MCS as UWS) rates were 7 and 6% respectively. F1-score and Matthews Correlation Coefficient were 94 and 0.87 respectively, evidencing a high performance of the model in the diagnostic classification. Superimposable results were obtained in the 10-fold cross-validation test (**Table 2**), with an accuracy of 90% and a correct MCS and UWS classification of 88 and 93% respectively. The false positive and false negative rates were 7 and 13% respectively.

These results showed that most MCS patients displayed more complex HRV patterns compared to UWS patients. In addition,

<sup>3</sup>BSPMVIEW|bspmview. Available online at: <http://www.bobsput.com/bspmview/DOI.10.5281/zenodo.168074> (Accessed March 1, 2018).



**FIGURE 3 |** Complexity Index statistical analysis comparing UWS and MCS patients summarized as a box plot. Higher values of  $CI_s$  ( $z = -3.346$ ,  $p < 0.001$ ) and of  $CI_l$  ( $z = -4.095$ ,  $p < 0.0001$ ) were observed for MCS group compared to UWS using Mann-Whitney's test. The 1st row compares the entire group of patients S1 ( $n = 30$ ), while the 2nd row compares the subgroup of patients S2 ( $n = 21$ ) who underwent fMRI analysis. The 1st column represents the complexity index (CI) in short time scale, while the 2nd column is for the long time scale. White boxes represent MCS patients; gray boxes the UWS patients. The boxes range from Q1 to Q3, while the whiskers are defined at the 1.5 interquartile range, and the black lines are the medians, points are outliers.

the CI measures showed strong discriminative power when used to predict the diagnosis of a patient. Under the frame of the brain-heart two-way interaction and with the aim to observe how this complexity is linked to the brain activity, we investigated the resting state fMRI of a subset of 24 patients who had sufficient image quality to ensure successful analysis. We chose to focus on only positive correlations, using one-sided statistical test and multiple comparison correction at the cluster level with non-parametric permutation test (**Figure 6**). Both CI were positively correlated with an increase of the brain's functional connectivity in CAN regions. Increased values of  $CI_s$  were associated with increased connectivity between the Fronto-Insular cortex with the Superior Frontal Gyrus and between the Paracingulate cortex with two clusters covering the inferior and middle Temporal Gyrus, the Frontal Operculum and the Insular cortex.  $CI_l$  values positively correlated with an increase of connectivity between the Paracingulate cortex with the right Frontal Pole, between the Superior Temporal Gyrus (STG) with the Superior Parietal Lobule (SPL) and finally between the Dorso-Lateral Prefrontal Cortex (DLPFC) located in the Middle Frontal Gyrus (MFG) with the left and right Frontal Pole. The Anterior Cingulate Cortex, the

Medial Prefrontal Cortex, the Thalamus and the Cerebellum did not show significant results. Statistical tables are available in the Supplementary materials (**Appendix B**).

The ICC showed a positive correlation between the  $CI_s$  and the intrinsic connectivity (i.e., an overall connectivity with the rest of the brain) in a cluster covering the Middle Temporal Gyrus (MTG) and the STG and between the  $CI_l$  and the intrinsic connectivity of the MFG. Of interesting note, both the seed-based and the hypothesis-free analyses found an increase of connectivity in the STG and MFG correlated with an increase of CI. By comparing only the functional connectivity of MCS to UWS patients, without CI measures, no significant results were found except for the ICC analysis (see the Supplementary materials, **Appendix B**).

## DISCUSSION

We investigated the HRV and more specifically the CI of the MSE in MCS and UWS sedated patients, tested its discriminative power for diagnosis and investigated the possible

**TABLE 2 |** One-R classifier results and confusion matrix.

Confusion Matrix		Classifier: One-R		
MCS (true)	MCS as UWS (false negative)	Rule: $CI_l < 4.876 \rightarrow \text{UWS}$ $CI_l \geq 4.876 \rightarrow \text{MCS}$	Test dataset results	fMRI test (S2 subgroup)
15	1			
1	13			
UWS as MCS (false positive)	UWS (true)			
		Full training test (S1 group)	10-fold cross-validation	
True positive (MCS) rate (%)		94	88	92
True negative (UWS) rate (%)		93	93	100
False negative rate (%)		6	13	8
False positive rate (%)		7	7	0
Precision MCS classification (%)		94	94	100
Precision UWS classification (%)		93	87	91
accuracy (%)		93	90	95
F1-score (%)		94	90	96
Matthews Correlation Coefficient[−1:1]		0.87	0.80	0.91

The confusion matrix is based on the S1 group. The One-R classifier is a simple machine learning decision tree model that derives a single rule from the single most contributing parameter to predict the patient's diagnosis. This model deduced that the long term complexity index ( $CI_l$ ) is the best predictor of patient's diagnosis, with a threshold of  $\sim 4.9$ , below which the patient should be diagnosed as unresponsive (UWS) and above as minimally conscious (MCS). The 10-fold cross-validation test shows that this model is quite robust and reliable, with 90% accuracy, 7% false positive rate, 13% false negative rate and a F1-score, combining both accuracy and recall, of 90%. For comparison, a baseline Zero-R rule always predicting MCS as the diagnosis would have an accuracy of 53% on the S1 group dataset. Additional machine learning models and results can be found in the Supplementary materials (Appendix A).

neural correlates sources of CI modulation via a resting-state fMRI analysis. The present study is the first to show that baseline HRV entropy, more specifically the  $CI_l$ , can be a reliable predictor of the clinical level of consciousness, and furthermore the first to estimate the direct relationship between  $CI_l$  and CRS-R and between  $CI_l$  and the brain functional connectivity using simultaneously acquired resting-state fMRI.

Group-wise, we found higher values of  $CI_l$  in MCS patients compared to UWS patients (Figure 3). This difference was observed for both the  $CI_s$  (linked to the parasympathetic modulation) with moderate significance and the  $CI_l$  (linked to the sympathetic modulation) with strong significance. Moreover, the values of  $CI_l$  were correlated to the CRS-R total score (Figure 5), with MCS patients generally displaying a higher-end  $CI_l$  value compared to UWS patients, with only UWS patients having  $CI_l$  values in the lower-end (Figures 4, 5).

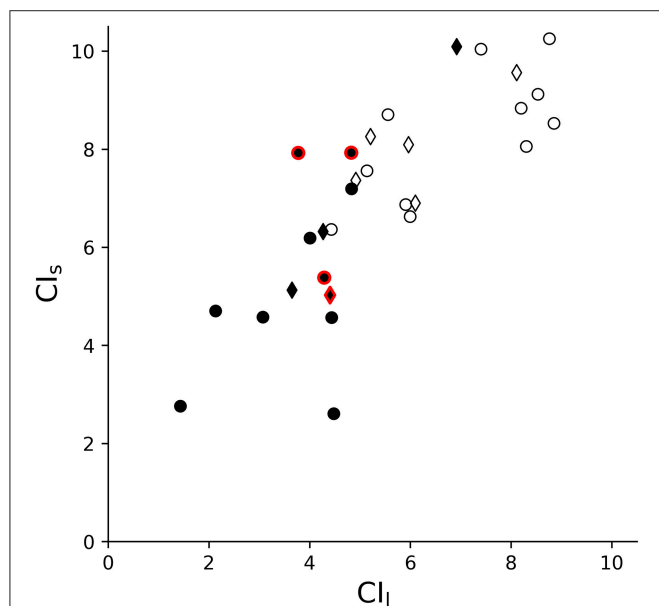
To assess the discriminative power of  $CI_l$  for disorders of consciousness, we built a machine learning model based on the One-R rule association algorithm, using both  $CI_l$  as input features, with the objective to predict whether a patient is MCS (positive condition) or UWS (negative condition). The One-R algorithm derives a single rule from the single most contributing parameter to predict the patient's diagnosis. This classifier deduced that  $CI_l$  was the best predictor of patient's diagnosis, with a threshold of  $\sim 4.9$ , below which the patient should be diagnosed as UWS and above as MCS. According to the best standards in machine learning for neuroimaging, we conducted a 10-fold cross-validation test to evaluate the generalizable performance of this model (85) (Table 2), which showed that this model is quite robust and reliable, with 90%

accuracy, 7% false positive rate, 13% false negative rate and a F1-score, combining both accuracy and recall, of 90%. For comparison, a baseline Zero-R rule always predicting MCS as the diagnosis would have an accuracy of 53% on the S1 group dataset. Thus, the model reported a high accuracy performance, while having low false positive and negative rates compared to the CRS-R gold standard. Since the One-R model is a very simple classifier with a linear decision frontier based on only one feature, this suggests that  $CI_l$  is a highly discriminative measure for UWS and MCS. Considering the much higher misdiagnosis rate of about 40% by human assessors not using the CRS-R, even after nation-wide efforts to reduce it (12, 13), and considering the very simple machine learning model used here, these results strongly suggest that heart rate  $CI_l$  might have an application as a complementary assessment tool and might help physician in their decision process by providing a supplementary hypothesis-free evaluation of the patient's state of consciousness.

Finally, the fMRI analysis reported a positive correlation between the  $CI_l$  and the connectivity in several brain areas belonging to the CAN/ANS (Figure 6), using both seed-based, thus guided, approach and voxel-based, thus hypothesis-free, approach. Indeed, the voxel-based ICC results showed that, even without any a priori about the spatial location of connectivity changes associated with higher  $CI_l$  values, we could observe that higher  $CI_l$  values were associated with brain regions belonging to the CAN/ANS.

Many studies have reported the potential usefulness of HRV analysis (in both time and frequency domains, as well as non-linear analysis) in consciousness studies (18, 19, 92). They observed better autonomic response to specific stimuli

(i.e., music, visual, acoustic), higher sympathetic activation, modulation in peak of the low frequency band or ratio between low and high frequency power in MCS than in UWS (93–101).



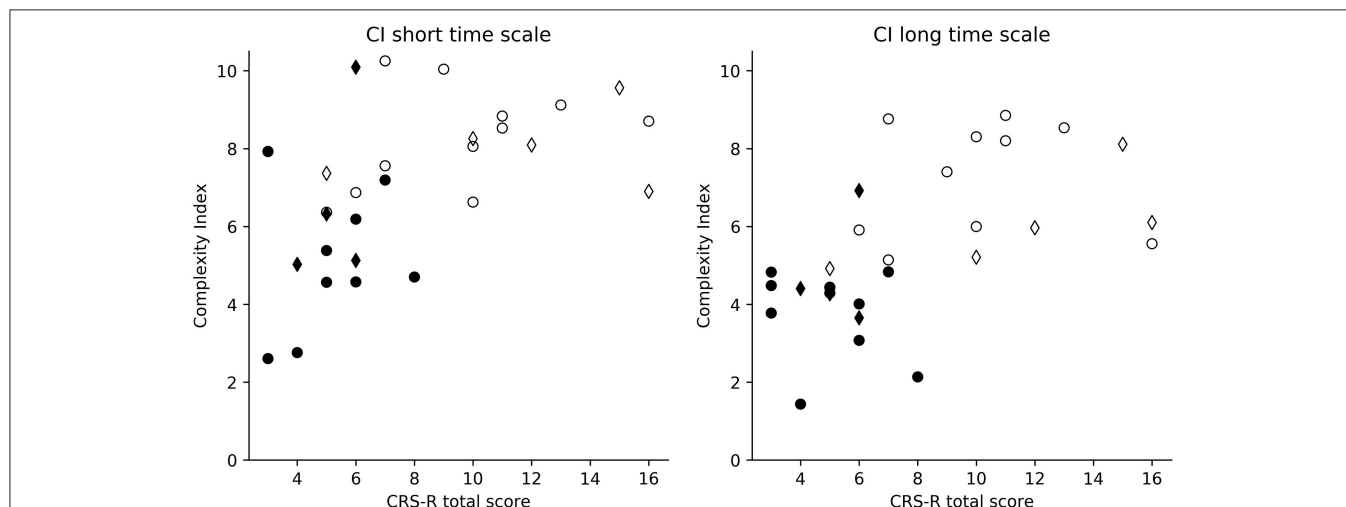
**FIGURE 4 |** Dispersion graph of  $CI_l$  and  $CI_s$ . This shows that the repartition of patients relatively to the  $CI$  is defined by the diagnosis, with UWS patients usually on the lower-end and MCS patients on the higher-end, showing some degree of linear separability. White circles and diamonds represent MCS patients; black circles and diamonds the UWS patients. Diamonds represent the patients discharged for the fMRI analysis (i.e., only included in S1,  $n = 30$ ) while the circles are the patients included in the fMRI analysis (S2 group,  $n = 21$ ). Outlined in red are patients in subacute state (i.e., with MRI acquisition between 2 and 4 weeks from brain insult).

A greater HRV responsiveness in time and frequency domains to emotional stimuli than to non-emotional stimuli has been observed in MCS patients compared to UWS (97) and similarly for nociceptive stimuli (92) and auditory oddball tasks (102).

In the frequency domain, modulation of sympathetic response (observed by the normalized unit of low frequency) has been associated to musical stimuli (selected to elicit specific emotional response) in UWS patients (95), MCS patients and healthy subjects (93), allowing the experimenters to classify the subjects' emotional responses as positive or negative. For acute traumatic patients, pre-hospital low entropy has been associated with mortality, independently of GCS score or Injury Severity Score (103). MSE measured within the first 24 h can identify trauma patients at increased risk of subsequent hospital death (69) and predict robustly within 3 h of admission the death of the patients occurring days later (104). SE has proved useful for rapid identification of trauma patients with potentially lethal injuries (105). In pediatric patients, the reduction of heart rate dynamics was shown to correlate negatively with disease severity and outcome (106).

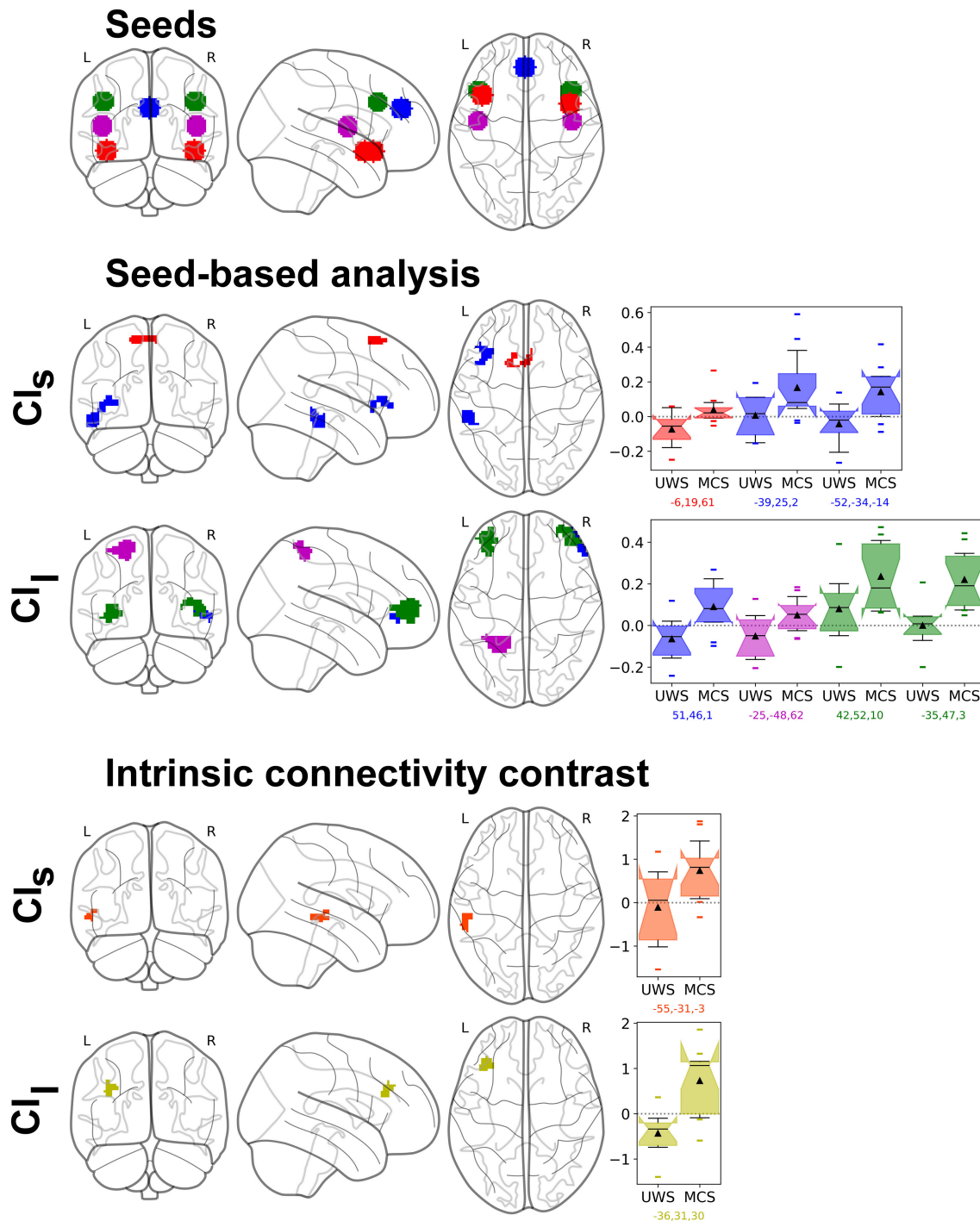
However, few studies have reported results in the non-linear domain (i.e., approximate entropy, sample entropy, multiscale entropy, etc.) in chronic patients with disorders of consciousness. In these few studies, lower values of approximate and sample entropy have been reported in UWS than MCS patients compared to healthy subjects following musical stimuli with increasing structural complexity (107, 108). Studies with anesthetized healthy subjects have reported decreased entropy during anesthesia (109, 110). Decreased sample entropy and approximate entropy values have also been reported in UWS and MCS compared to healthy subjects (103, 105).

We here investigated the HRV of mostly chronic patients with disorders of consciousness by using the MSE, which is a non-linear analysis that can capture



**FIGURE 5 |** Dispersion graphs of the correlation between CRS-R total score and  $CI$ . This shows the per-subject  $CI$  value relatively to the patient's CRS-R total score. Both  $CI_l$  (Spearman's  $\rho = 0.671$ ,  $p < 0.0001$ ) and  $CI_s$  (Spearman's  $\rho = 0.579$ ,  $p < 0.001$ ) were correlated with the CRS-R total score. S1 (diamond and circle markers,  $n = 30$ ) and S2 (circle markers,  $n = 21$ ) groups were compared for  $CI_s$  (left) and  $CI_l$  (right). White circles represent MCS patients; black circles the UWS patients. Diamonds represent the patients discharged for the fMRI analysis while the circle markers represent the patients included in the fMRI analysis (S2 group).





**FIGURE 6 |** Resting-state fMRI analysis results of the parametric regression between CI and UWS/MCS patients' connectivity changes in the S2 group ( $n = 21$ ). Top row shows the seeds: Fronto-Insular (FI, red), Paracingulate cortex (PC, blue), Superior Temporal Gyrus (STG, magenta), Dorso-lateral prefrontal cortex (DLPFC, green). Middle rows show the seed-based analysis results, with same colors as the seeds, and effect size as box plots (range Q1-Q3, whiskers interquartile 1.5, black line as median, black triangle as mean, points as outliers), first with the CI in short time scale ( $CI_S$ ) and then long time scale ( $CI_L$ ). We can see a positive correlation of the  $CI_S$  with the connectivity between FI with Superior Frontal Gyrus (red) and between PC with two clusters covering the Temporal Gyrus (inferior and middle), the Frontal Operculum and the Insular Cortex (blue). The  $CI_L$  is positively correlated with the connectivity between PC and the right Frontal Pole (blue), between STG with the Superior Parietal Lobule (magenta) and between DLPFC and the left and right Frontal Poles (green). Bottom rows show the hypothesis-free intrinsic connectivity correlation (ICC) results, with a positive correlation between values of  $CI_S$  and an increase of intrinsic connectivity of the posterior Middle Temporal Gyrus (pMTG) and posterior STG (orange); and a correlation between  $CI_L$  and an increase of intrinsic connectivity in the Middle Frontal Gyrus (MFG) (yellow). Statistical significance was considered at permutation of residuals test cluster-mass  $p\text{-FWE} < 0.1$  and primary threshold  $p\text{-uncorrected} < 0.001$ .

a wider dynamic range of interaction between heart and brain than simple entropy or variability in the linear (time) or spectral (frequency) domains, and therefore potentially bear more diagnostic and prognostic information.

Indeed, cardiovascular signals are largely analyzed using traditional time and frequency domain measures, however these measures are not capable of measuring dynamic changes in the autonomic control of the heart rate, thus failing to account for important properties related to multiscale organization and brain-heart non-equilibrium dynamics (111–113).

The brain-heart dynamic processes, that characterize the cardiac signal output, can be described as non-linear, non-stationary, asymmetric and with multiscale variability (i.e. small perturbation can cause large effects, the system's output has dynamical properties that can change over time, the system dissipates energy as it operates far-from-equilibrium, and exhibits spatio-temporal patterns over a range of scales) (114).

In contrast, these dynamic processes in healthy conditions exhibit complex fluctuations that are reduced or absent in pathological conditions, where we can observe less complex outputs (115) expressed by an increased randomness (e.g., in a subject with atrial fibrillation) or augmented periodicity (e.g., in UWS patients).

Our results in the non-linear domain showing higher CI in MCS than UWS are in line with the above-cited literature and further characterize the complexity of brain-heart interactions. Our findings are also highly significant compared to previous studies using other types of analysis (100, 107, 108, 116). This confirms that the extra information extracted using non-linear analyses can lead to better differential diagnosis with high discriminative power, even higher than that of the clinical consensus without CRS-R (13), which can potentially be applied to clinical practice in a near future.

Several fMRI studies on healthy subjects have shown the complexity of interaction of the heart with the Central Autonomic Network (22, 52, 53, 117, 118). Valenza and colleagues have shown that the insular cortex, frontal gyrus, lateral occipital cortex, paracingulate and cingulate gyrus and precuneus cortices, as well as subcortical structures including the thalamus are involved in the modulation of the CAN/ANS network-mediated cardiovascular control (119). The causal, directed interactions between brain regions at rest (brain-brain networks) and between resting-state brain activity and the ANS outflow (brain-heart links) have been studied by Duggento et al. (120) showing that the amygdala, hypothalamus, brainstem and, among others, medial, middle and superior frontal gyri, superior temporal pole, paracentral lobule and cerebellar regions are involved in modulating the CAN. Previous studies reported that  $CI_s$  is probably linked to the vagal control of HRV, while  $CI_l$  seems to be more related (although not exclusively) to the sympathetic control of HRV (41, 78, 121, 122).

While most of these studies used active tasks paradigms or cardiac gating to investigate HRV (52, 66), the fMRI results

of our study extend the previous findings by offering a new approach with two innovations: (1) by studying the resting-state connectivity changes, after the regression of physiological noise by principal components analysis via aCompCor, rather than by using an active paradigm or cardiac gating, which allows to estimate how the CI relates to the baseline cognitive abilities of the patient; (2) by investigating the direct correlation between the heart rate's complexity modulation (as measured by the CI) with the brain areas connectivity in regions involving the autonomic system, in order to identify some of the cerebral sources of HRV modulation. We found that both  $CI_s$  and  $CI_l$  are linked to the brain's functional connectivity of the CAN/ANS, with higher CI values being correlated with a recovery of CAN/ANS faculties. Indeed, by looking at the effect sizes, we can observe that the correlation is positive in MCS and usually close to null for UWS, suggesting a recovery of real positive connectivity in MCS as compared to UWS. Of note, we observed that the DLPFC, which seem to be a component of the CAN unique to humans (52, 53, 123), had a greater connectivity with the Frontal Poles correlatively with the  $CI_l$ .

This highlights that (impaired) complex brain-heart interactions characterize chronic patients with disorders or consciousness, and that the CI can reflect these connectivity changes at resting state, in the form of a scalar value summarizing the connectivity changes of multiple regions of the CAN/ANS. This further suggests that the CI could potentially be used as a fast, inexpensive and entirely non-invasive method of screening and monitoring connectivity changes in the CAN/ANS networks. Combined with the observation of a high discriminative power using a model as simple as the one rule association of the One-R machine learning model, CI could represent a very interesting alternative for medical centers that cannot afford expensive MRI machines as well as for highly busy medical centers as a preliminary screening method. Furthermore, this method can work even for patients with extensive brain damages that might prevent neuroimaging methods from functioning.

Although less practical and affordable than ECG, future studies should investigate whether screening directly the functional connectivity change patterns in the CAN might also yield predictive value for the diagnosis, although we expect with less sensitivity than the CI. Indeed, our fMRI results suggest that the CI measures reflect an aggregation of various functional connectivity changes in the CAN, which allows for increased sensitivity compared to any single seed analysis.

Interestingly, one of the three UWS patients with a high CI evolved into a MCS state one year later after the assessment considered here. The CI measures might prove clinically relevant not only for diagnosis but also as outcome predictors. Future studies to assess the prediction power the CI measures are warranted.

This study is however not free of limitations. As patients suffering from disorders of consciousness notably move a lot (e.g., spasms, spasticity) and since fMRI data are very sensitive to movement, Propofol was here used in low doses

in order to avoid movement artifacts during the fMRI scan acquisition, as required by clinical practice. HRV entropy is known to be profoundly affected by general anesthesia and it can play more roles in the monitoring of anesthetic depth (124). SE decreases after induction of anesthesia (110) and decrease of HRV entropy following Sevoflurane and Propofol anesthesia (109) has been observed. However, there is preliminary evidence that sedation might not exert a significant influence on the resting-state functional connectivity of UWS and MCS patients, since the impairment following the brain injury somehow overshadows the sedation effect (71, 125).

The ECG used in this study was acquired simultaneously to MRI, as was the standard procedure at the time at the Hospital of Liège. It would however be interesting for future studies to additionally acquire ECG outside of MRI acquisitions, which would be useful to derive additional metrics and assess the possible influence of MRI auditory noise on resting-state ECG. Indeed, a previous work observed that MCS patients show a phase shift of their cardiac cycle to global regularities in auditory signal (102), thus it is conceivable that the auditory noise induced by a MRI machine might impact the ECG.

Recently, there were a few findings about the circadian rhythm and body temperature fluctuations in disorders of consciousness, finding that several parameters such as the HRV, the body temperature and the circadian rhythm are correlated with the prognosis (126, 127). Furthermore, the preliminary results from an ongoing work investigating the day-to-night variations of the HRV in disorders of consciousness seem to indicate that the circadian cycle impacts directly the HRV, with more difference between groups being highlighted during the day. If this is confirmed on a bigger sample, this would indicate that ECG acquisition should be preferentially done during the day, as was done in our study (128).

Although the difficulty to recruit and analyze such a challenging population of patients should be noted, the relatively limited number of patients, heterogeneity of their etiology and time of disease onset can represent a limit for this study. For instance, outcome studies have highlighted that there is a correlation between the etiology and the final diagnosis (129). Due to the heterogeneity of our cohort of patients, a characterization of etiology is not possible. Future studies with a larger cohort of patients are needed to evaluate the relationship between the heart rate CI measures and the etiologies. The  $CI_I$  threshold found by the OneR classifier seems to be quite stable according to the 10-fold cross-validation test, but this threshold should be confirmed in practice on a larger population and on multiple centers in order to account for inter-scanners variability. Furthermore, we used the CRS-R diagnosis as the gold standard for most analyses and notably machine learning, which, like other behavior-based clinical assessment methods, might produce false negative errors as explained in the introduction, as previous studies observed UWS patients retaining covert consciousness (13, 130, 131). Finally, for the fMRI analysis, the CI, being based on the HRV, correlation with brain

regions connectivity results might be partly influenced by blood irrigation variation.

## CONCLUSION

Our findings show that the MSE analysis of HRV and in particular the CI could be a useful tool to measure the degree of complexity in the brain-heart interaction and the response of the CAN/ANS systems to external stimulations. With the CI being correlated and even predictive of the clinical level of consciousness as assessed by the CRS-R, this could represent a fast, effective, inexpensive, and particularly easy to use tool to evaluate the level of consciousness in patients with disorders of consciousness. In particular, our findings show that CI has potential to be a useful supporting metric in the differential diagnosis between UWS and MCS, as well as a way to monitor patients' consciousness and brain connectivity evolution, in particular with patients that cannot be assessed with neuroimaging because of artifacts or extensive brain damage.

## AUTHOR CONTRIBUTIONS

FR and SKL contributed equally to this work. FR and SKL conceived, planned, and conducted the research and analyses. FR, SKL, and CD interpreted the results. FR designed the methods and scripts for data preprocessing and analysis on ECG and SKL and MB designed the methods and scripts for data preprocessing and analysis on fMRI. FR and SKL realized the visualizations. LH, CM, MC, VC-V, CA, AV, and CC carried the data acquisitions. CD provided guidance and supervision on the whole study. CD, SL, and CC provided supervision and resources. FR, SKL, and CD drafted the manuscript and all authors provided critical feedback and helped shape the final manuscript.

## FUNDING

This research was supported by the University and Hospital of Liège, the Belgian National Funds for Scientific Research (F.R.S.-F.N.R.S.), the French Speaking Community Concerted Research Action (ARC 12-17/01), Center-TBI (FP7-HEALTH-602150), Human Brain Project (EU-H2020-fetflagship-hbp-sga1-ga720270), Luminous project (EU-H2020-fetopen-ga686764), the James McDonnell Foundation, the Mind Science Foundation, IAP research network P7/06 of the Belgian Government (Belgian Science Policy), the Public Utility Foundation Université Européenne du Travail, Fondazione Europea di Ricerca Biomedica, the Bial Foundation, Belgian National Plan Cancer, the European Space Agency, Belspo and the European Commission. SKL is a FRS-FNRS research fellows, CD is post-doctoral FRS-FNRS fellow, and SL is research director at FRS-FNRS. We are highly grateful to the members of the Liège Coma Science Group for their assistance in clinical evaluations. We thank Pr P. Maquet, Pr B. Sadzot, Dr E. Rikir, Dr J.-F.L. Tshibanda, J. Klein and the whole teams from the Neurology, Radiodiagnostic and Nuclear Medicine departments, University Hospital of Liège, the Cyclotron of the University of Liège, as

well as the patients and their families, A.NIETO-CASTANON of the Department of Speech, Language, and Hearing sciences, Boston University (USA) and S.WHITFIELD-GABRIELI of the Gabrieli Lab, Massachusetts Institute of Technology (USA) for their kind technical advices.

## REFERENCES

- Meaney DF, Morrison B, Dale Bass C. The mechanics of traumatic brain injury: a review of what we know and what we need to know for reducing its societal burden. *J Biomech Eng.* (2014) 136:021008. doi: 10.1115/1.4026364
- Roebuck-Spencer T, Cernich A. Epidemiology and Societal Impact of Traumatic Brain Injury. In: *Handbook on the Neuropsychology of Traumatic Brain Injury Clinical Handbooks in Neuropsychology*. New York, NY: Springer (2014). p. 3–23.
- Erkkinen MG, Kim MO, Geschwind MD. Clinical neurology and epidemiology of the major neurodegenerative diseases. *Cold Spring Harb Perspect Biol.* (2018) 10:a033118. doi: 10.1101/cshperspect.a033118
- Gitler AD, Dhillon P, Shorter J. Neurodegenerative disease: models, mechanisms, and a new hope. *Dis Model Mech.* (2017) 10:499–502. doi: 10.1242/dmm.030205
- Pisa FE, Biasutti E, Drigo D, Barbone F. The prevalence of vegetative and minimally conscious states: a systematic review and methodological appraisal. *J Head Trauma Rehabil.* (2014) 29:E23–30. doi: 10.1097/HTR.0b013e3182a4469f
- van Erp WS, Lavrijsen JCM, Vos PE, Bor H, Laureys S, Koopmans RTCM. The Vegetative State: Prevalence, Misdiagnosis, and Treatment Limitations. *J Am Med Dir Assoc.* (2015) 16:85.e9–85.e14. doi: 10.1016/j.jamda.2014.10.014
- Demertzi A, Ledoux D, Bruno M-A, Vanhaudenhuyse A, Gosseries O, Soddu A, et al. Attitudes towards end-of-life issues in disorders of consciousness: a European survey. *J Neurol.* (2011) 258:1058–65. doi: 10.1007/s00415-010-5882-z
- Riganello F, Macri S, Allea E, Petrini C, Soddu A, Leòn-Carrión J, et al. Pain perception in unresponsive wakefulness syndrome may challenge the interruption of artificial nutrition and hydration: neuroethics in action. *Neurocrit Care* (2016) 7:202. doi: 10.3389/fneur.2016.00202
- Fins JJ. Clinical pragmatism and the care of brain damaged patients: toward a palliative neuroethics for disorders of consciousness. In: Laureys S, editor. *Progress in Brain Research The Boundaries of Consciousness: Neurobiology and Neuropathology*. Amsterdam: Elsevier (2011). 565–82.
- Bosco A, Lancioni GE, Belardinelli MO, Singh NN, O'Reilly MF, Sigafos J. Vegetative state: efforts to curb misdiagnosis. *Cogn Process* (2010) 11:87–90. doi: 10.1007/s10339-009-0355-y
- Andrews K. Medical decision making in the vegetative state: withdrawal of nutrition and hydration. *NeuroRehabilitation* (2004) 19:299–304.
- Schnakers C, Vanhaudenhuyse A, Giacino J, Ventura M, Boly M, Majerus S, et al. Diagnostic accuracy of the vegetative and minimally conscious state: clinical consensus versus standardized neurobehavioral assessment. *BMC Neurol.* (2009) 9:35. doi: 10.1186/1471-2377-9-35
- Stender J, Gosseries O, Bruno M-A, Charland-Verville V, Vanhaudenhuyse A, Demertzi A, et al. Diagnostic precision of PET imaging and functional MRI in disorders of consciousness: a clinical validation study. *Lancet Lond Engl.* (2014) 384:514–22. doi: 10.1016/S0140-6736(14)60042-8
- Giacino JT, Kalmar K, Whyte J. The JFK coma recovery scale-revised: measurement characteristics and diagnostic utility. *Arch Phys Med Rehabil.* (2004) 85:2020–29. doi: 10.1016/j.apmr.2004.02.033
- Di Perri C, Heine L, Amico E, Soddu A, Laureys S, Demertzi A. Technology-based assessment in patients with disorders of consciousness. *Ann Ist Super Sanita* (2014) 50:209–20. doi: 10.4415/ANN\_14\_03\_03
- Demertzi A, Antonopoulos G, Heine L, Voss HU, Crone JS, de Los Angeles C, et al. Intrinsic functional connectivity differentiates minimally conscious from unresponsive patients. *Brain* (2015) 138:2619–31. doi: 10.1093/brain/awv169
- Riganello F, Sannita WG. Residual brain processing in the vegetative state. *J Psychophysiol.* (2009) 23:18–26. doi: 10.1027/0269-8803.23.1.18
- Riganello F, Garbarino S, Sannita WG. Heart rate variability, homeostasis, and brain function: a tutorial and review of application. *J Psychophysiol.* (2012) 26:178–203. doi: 10.1027/0269-8803/a000080
- Ryan ML, Thorson CM, Otero CA, Vu T, Proctor KG. Clinical applications of heart rate variability in the triage and assessment of traumatically injured patients. *Anesthesiol Res Pract.* (2011) 2011:416590. doi: 10.1155/2011/416590
- Palma J-A, Benarroch EE. Neural control of the heart: recent concepts and clinical correlations. *Neurology* (2014) 83:261–71. doi: 10.1212/WNL.0000000000000605
- Porges SW. The polyvagal theory: New insights into adaptive reactions of the autonomic nervous system. *Cleve Clin J Med.* (2009) 76:S86–S90. doi: 10.3949/ccjm.76.s2.17
- Thayer JF, Lane RD. A model of neurovisceral integration in emotion regulation and dysregulation. *J Affect Disord.* (2000) 61:201–16.
- Javorka M, Trunkvalterova Z, Tonhajzerova I, Javorkova J, Javorka K, Baumert M. Short-term heart rate complexity is reduced in patients with type 1 diabetes mellitus. *Clin Neurophysiol.* (2008) 119:1071–81. doi: 10.1016/j.clinph.2007.12.017
- Arbit B, Azarbal B, Hayes SW, Gransar H, Germano G, Friedman JD, et al. Prognostic contribution of exercise capacity, heart rate recovery, chronotropic incompetence, and myocardial perfusion single-photon emission computerized tomography in the prediction of cardiac death and all-cause mortality. *Am J Cardiol.* (2015) 116:1678–84. doi: 10.1016/j.amjcard.2015.08.037
- Kleiger RE, Miller JP, Bigger Jr. JT, Moss AJ. Decreased heart rate variability and its association with increased mortality after acute myocardial infarction. *Am J Cardiol.* (1987) 59:256–62. doi: 10.1016/0002-9149(87)90795-8
- Schnell I, Potchter O, Epstein Y, Yaakov Y, Hermesh H, Brenner S, et al. The effects of exposure to environmental factors on Heart Rate Variability: an ecological perspective. *Environ Pollut.* (2013) 183:7–13. doi: 10.1016/j.envpol.2013.02.005
- Whitsel EA, Quibrera PM, Christ SL, Liao D, Prineas RJ, Anderson GL, et al. Heart rate variability, ambient particulate matter air pollution, and glucose homeostasis: the environmental epidemiology of arrhythmogenesis in the women's health initiative. *Am J Epidemiol.* (2009) 169:693–703. doi: 10.1093/aje/kwn400
- Carney RM, Blumenthal JA, Freedland KE, et al. Low heart rate variability and the effect of depression on post-myocardial infarction mortality. *Arch Intern Med.* (2005) 165:1486–91. doi: 10.1001/archinte.165.13.1486
- Harrison NA, Cooper E, Voon V, Miles K, Critchley HD. Central autonomic network mediates cardiovascular responses to acute inflammation: relevance to increased cardiovascular risk in depression? *Brain Behav Immun.* (2013) 31:189–96. doi: 10.1016/j.bbi.2013.02.001
- Nait-Ali A. *Advanced Biosignal Processing*. Berlin; Heidelberg: Springer Science & Business Media (2009).
- Task Force of the European Society of Cardiology and the North American Society of Pacing and Electrophysiology. Heart rate variability: standards of measurement, physiological interpretation and clinical use. *Circulation* (1996) 93:1043–65.
- Goldberger AL. Is the normal heartbeat chaotic or homeostatic? *News Physiol.* (1991) 6:87–91. doi: 10.1152/physiologyonline.1991.6.2.87
- Wu GQ, Arzeno NM, Shen LL, Tang DK, Zheng DA, Zhao NQ, et al. Chaotic signatures of heart rate variability and its power spectrum in health, aging and heart failure. *PLoS ONE* (2009) 4:e4323. doi: 10.1371/journal.pone.0004323
- D'Addio G, Pinna GD, Maestri R, Corbi G, Ferrara N, Rengo F. Quantitative poincare plots analysis contains relevant information related to heart rate variability dynamics of normal and pathological subjects. In *Computers in*

## SUPPLEMENTARY MATERIAL

The Supplementary Material for this article can be found online at: <https://www.frontiersin.org/articles/10.3389/fneur.2018.00769/full#supplementary-material>



- Cardiology*, 2004 (IEEE), 457–60. Available online at: <http://ieeexplore.ieee.org/abstract/document/1442973/> (Accessed April 19, 2017).
35. Echeverria JC, Woolfson MS, Crowe JA, Hayes-Gill BR, Croaker GD, Vyas H. Interpretation of heart rate variability via detrended fluctuation analysis and  $\alpha\beta$  filter. *Chaos* (2003) 13:467–75. doi: 10.1063/1.1562051
  36. Fusheng Y, Bo H, Qingyu T. Approximate Entropy and Its Application to Biosignal Analysis. In: Akay M, editor. *Nonlinear Biomedical Signal Processing*. John Wiley & Sons, Inc (2000). p. 72–91. Available online at: <http://onlinelibrary.wiley.com/doi/10.1002/9780470545379.ch3/summary> [Accessed May 19, 2014]
  37. Aboy M, Cuesta-Frau D, Austin D, Mico-Tormos P. Characterization of sample entropy in the context of biomedical signal analysis. In: *Engineering in medicine and Biology Society, 2007. EMBS 2007. 29th Annual International Conference of the IEEE*. IEEE (2007). p. 5942–5. Available online at: <http://ieeexplore.ieee.org/abstract/document/4353701/> (Accessed October 14, 2017).
  38. Costa M, Goldberger AL, Peng CK, others. *Multiscale Entropy Analysis (MSE)*. (2000). Available online at: <http://physionet.cps.unizar.es/physiotools/mse/tutorial/tutorial.pdf> (Accessed September 26, 2015).
  39. Voss A, Heitmann A, Schroeder R, Peters A, Perz S. Short-term heart rate variability–age dependence in healthy subjects. *Physiol Meas*. (2012) 33:1289–311. doi: 10.1088/0967-3334/33/8/1289
  40. Voss A, Schulz S, Schroeder R, Baumert M, Caminal P. Methods derived from nonlinear dynamics for analysing heart rate variability. *Philos Trans R Soc Math Phys Eng Sci*. (2009) 367:277–96. doi: 10.1098/rsta.2008.0232
  41. Costa M, Goldberger AL, Peng C-K. Multiscale entropy analysis of biological signals. *Phys Rev E* (2005) 71:021906. doi: 10.1103/PhysRevE.71.021906
  42. Thayer JF, Lane RD. Claude Bernard and the heart–brain connection: Further elaboration of a model of neurovisceral integration. *Neurosci Biobehav Rev*. (2009) 33:81–8. doi: 10.1016/j.neubiorev.2008.08.004
  43. Gabella G. Autonomic Nervous System. In: *eLS* (John Wiley & Sons, Ltd). doi: 10.1038/npg.els.0000081/full
  44. Badra LJ, Cooke WH, Hoag JB, Crossman AA, Kuusela TA, Tahvanainen KU, Eckberg DL. Respiratory modulation of human autonomic rhythms. *Am J Physiol Heart Circ Physiol*. (2001) 280:H2674–88. doi: 10.1152/ajpheart.2001.280.6.H2674
  45. Bentley MT, Paolone VJ. Heart rate variability and thermoregulation during resting cold-water immersion and upper body exercise. *Med Sci Sports Exerc*. (2003) 35:S254.
  46. Bonsignore MR. Baroreflex control of heart rate during sleep in severe obstructive sleep apnoea: effects of acute CPAP. *Eur Respir J*. (2006) 27:128–35. doi: 10.1183/09031936.06.00042904
  47. Benarroch EE. The central autonomic network: functional organization, dysfunction, and perspective. *Mayo Clin Proc*. (1993) 68:988–1001.
  48. Benarroch E, Singer W, Mauermann M. *Autonomic Neurology*. Oxford, UK: Oxford University Press (2014).
  49. Cechetto DF, Shoemaker JK. Functional neuroanatomy of autonomic regulation. *NeuroImage* (2009) 47:795–803. doi: 10.1016/j.neuroimage.2009.05.024
  50. Gianaros PJ, Sheu LK. A review of neuroimaging studies of stressor-evoked blood pressure reactivity: Emerging evidence for a brain-body pathway to coronary heart disease risk. *NeuroImage* (2009) 47:922–36. doi: 10.1016/j.neuroimage.2009.04.073
  51. Benarroch EE. Enteric nervous system functional organization and neurologic implications. *Neurology* (2007) 69:1953–7. doi: 10.1212/01.wnl.0000281999.56102.b5
  52. Napadow V, Dhond R, Conti G, Makris N, Brown EN, Barbieri R. Brain correlates of autonomic modulation: combining heart rate variability with fMRI. *NeuroImage* (2008) 42:169–77. doi: 10.1016/j.neuroimage.2008.04.238
  53. Thayer JF. What the heart says to the brain (and vice versa) and why we should listen. *Psychol Teme* (2007) 16:241–50.
  54. Aysin B, Aysin E. Effect of respiration in heart rate variability (HRV) analysis. *Conf IEEE Eng Med Biol Soc*. (2006) 1:1776–9. doi: 10.1109/IEMBS.2006.260773
  55. Ce G. Effects of relaxation and music therapy on patients in a coronary care unit with presumptive acute myocardial infarction. *Heart Lung J Crit Care* (1989) 18:609–16.
  56. Drawz PE, Babineau DC, Brecklin C, He J, Kallem RR, Soliman EZ, et al. Heart rate variability is a predictor of mortality in chronic kidney disease: a report from the CRIC study. *Am J Nephrol*. (2013) 38:517–28. doi: 10.1159/000357200
  57. Ernst G. Heart-Rate variability—more than heart beats? *Front Public Health* (2017) 5:240. doi: 10.3389/fpubh.2017.00240
  58. Appelhans BM, Lueken LJ. Heart rate variability as an index of regulated emotional responding. *Rev Gen Psychol*. (2006) 10:229–40. doi: 10.1037/1089-2680.10.3.229
  59. Frazier TW, Strauss ME, Steinhauer SR. Respiratory sinus arrhythmia as an index of emotional response in young adults. *Psychophysiology* (2004) 41:75–83. doi: 10.1046/j.1469-8986.2003.00131.x
  60. Mashin VA, Mashina MN. Analysis of the heart rate variability in negative functional states in the course of psychological relaxation sessions. *Hum Physiol*. (2000) 26:420–5. doi: 10.1007/BF02760270
  61. Nickel P, Nachreiner F. Psychometric properties of the 0.1 HZ component of HRV as an indicator of mental strain. *Proc Hum Factors Ergon Soc Annu Meet* (2000) 44:2747–50. doi: 10.1177/154193120004401284
  62. Samuels MA. The brain–heart connection. *Circulation* (2007) 116:77–84. doi: 10.1161/CIRCULATIONAHA.106.678995
  63. Valentini M, Parati G. Variables influencing heart rate. *Prog Cardiovasc Dis*. (2009) 52:11–19. doi: 10.1016/j.pcad.2009.05.004
  64. Witten IH, Frank E, Hall MA, Pal CJ. *Data Mining: Practical Machine Learning tools and Techniques*. Morgan Kaufmann (2016).
  65. Biswal B, Yetkin FZ, Haughton VM, Hyde JS. Functional connectivity in the motor cortex of resting human brain using echo-planar MRI. *Magn Reson Med*. (1995) 34:537–41.
  66. Brooks JCW, Faull OK, Pattinson KTS, Jenkinson M. Physiological noise in brainstem fMRI. *Front Hum Neurosci*. (2013) 7:623. doi: 10.3389/fnhum.2013.00623
  67. Lin P-F, Lo M-T, Tsao J, Chang Y-C, Lin C, Ho Y-L. Correlations between the signal complexity of cerebral and cardiac electrical activity: a multiscale entropy analysis. *PLoS ONE* (2014) 9:e87798. doi: 10.1371/journal.pone.0087798
  68. Riganello F. Responsiveness and the Autonomic Control–CNS Two-Way Interaction in Disorders of Consciousness. In: Monti MM, Sannita WG, editors. *Brain Function and Responsiveness in Disorders of Consciousness*. Cham: Springer International Publishing (2016). p. 145–55. Available at: [http://link.springer.com/10.1007/978-3-319-21425-2\\_11](http://link.springer.com/10.1007/978-3-319-21425-2_11) [Accessed December 4, 2015]
  69. Norris PR, Stein PK, Morris JA. Reduced heart rate multiscale entropy predicts death in critical illness: a study of physiologic complexity in 285 trauma patients. *J Crit Care* (2008) 23:399–405. doi: 10.1016/j.jcrc.2007.08.001
  70. Schnakers C. Clinical assessment of patients with disorders of consciousness. *Arch Ital Biol*. (2012) 150:36–43. doi: 10.4449/aib.v150i2.1371
  71. Kirsch M, Guldenmund P, Ali Bahri M, Demertzi A, Baquero K, Heine L, et al. Sedation of patients with disorders of consciousness during neuroimaging: effects on resting state functional brain connectivity. *Anesth Analg*. (2017) 124:588–98. doi: 10.1213/ANE.0000000000001721
  72. Marsh B, White M, Morton N, Kenny GNC. Pharmacokinetic model driven infusion of propofol in children. *Br J Anaesth*. (1991) 67:41–8.
  73. Young C, Knudsen N, Hilton A, Reves JG. Sedation in the intensive care unit. *Crit Care Med*. (2000) 28:854–66. doi: 10.1093/bjaceaccp/mkn005
  74. Machata A-M, Willschke H, Kabon B, Kettner SC, Marhofer P. Propofol-based sedation regimen for infants and children undergoing ambulatory magnetic resonance imaging. *Br J Anaesth*. (2008) 101:239–43. doi: 10.1093/bja/aen153
  75. Tarvainen MP, Niskanen J-P, Lipponen JA, Ranta-Aho PO, Karjalainen PA. Kubios HRV–heart rate variability analysis software. *Comput Methods Programs Biomed*. (2014) 113:210–20. doi: 10.1016/j.cmpb.2013.07.024
  76. Lu G, Yang F, Taylor JA, Stein JF. A comparison of photoplethysmography and ECG recording to analyse heart rate variability in healthy subjects. *J Med Eng Technol*. (2009) 33:634–41. doi: 10.3109/03091900903150998

77. Richman JS, Lake DE, Moorman JR. Sample entropy. *Methods Enzymol.* (2004) 384:172–84. doi: 10.1016/S0076-6879(04)84011-4
78. Silva LEV, Cabella BCT, Neves UP da C, Murta Junior LO. Multiscale entropy-based methods for heart rate variability complexity analysis. *Phys Stat Mech Its Appl.* (2015) 422:143–52. doi: 10.1016/j.physa.2014.12.011
79. Di Perri C, Bahri MA, Amico E, Thibaut A, Heine L, Antonopoulos G, et al. Neural correlates of consciousness in patients who have emerged from a minimally conscious state: a cross-sectional multimodal imaging study. *Lancet Neurol.* (2016) 15:830–42. doi: 10.1016/S1474-4422(16)00111-3
80. Power JD, Mitra A, Laumann TO, Snyder AZ, Schlaggar BL, Petersen SE. Methods to detect, characterize, and remove motion artifact in resting state fMRI. *NeuroImage* (2014) 84:320–41. doi: 10.1016/j.neuroimage.2013.08.048
81. Behzadi Y, Restom K, Liu J, Liu TT. A Component Based Noise Correction Method (CompCor) for BOLD and Perfusion Based fMRI. *NeuroImage* (2007) 37:90–101. doi: 10.1016/j.neuroimage.2007.04.042
82. Chai XJ, Castañón AN, Öngür D, Whitfield-Gabrieli S. Anticorrelations in resting state networks without global signal regression. *NeuroImage* (2012) 59:1420–8. doi: 10.1016/j.neuroimage.2011.08.048
83. Holte RC. Very simple classification rules perform well on most commonly used datasets. *Mach Learn.* (1993) 11:63–90.
84. Wahbeh AH, Al-Radaideh QA, Al-Kabi MN, Al-Shawakfa EM. A comparison study between data mining tools over some classification methods. *Int J Adv Comput Sci Appl.* (2011) 8:18–26. doi: 10.14569/SpecialIssue.2011.010304
85. Varoquaux G, Raamana PR, Engemann D, Hoyos-Idrobo A, Schwartz Y, Thirion B. Assessing and tuning brain decoders: cross-validation, caveats, and guidelines. *NeuroImage* (2017) 145:166–79. doi: 10.1016/j.neuroimage.2016.10.038
86. Sokolova M, Japkowicz N, Szpakowicz S. Beyond accuracy, F-score and ROC: a family of discriminant measures for performance evaluation. In: Sattar A, Kang B, editors. *AI 2006: Advances in Artificial Intelligence*, Berlin; Heidelberg: Springer Berlin Heidelberg, (2006). 1015–21.
87. Powers D. Evaluation: from precision, recall and F-factor to ROC, informedness, markedness & correlation. *J Mach Learn Technol.* (2011) 2:37–63. doi: 10.9735/2229-3981
88. Martuzzi R, Ramani R, Qiu M, Shen X, Papademetris X, Constable RT. A whole-brain voxel based measure of intrinsic connectivity contrast reveals local changes in tissue connectivity with anesthetic without a priori assumptions on thresholds or regions of interest. *Neuroimage* (2011) 58:1044–50. doi: 10.1016/j.neuroimage.2011.06.075
89. Scheinost D, Benjamin J, Lacadie CM, Vohr B, Schneider KC, Ment LR, et al. The intrinsic connectivity distribution: a novel contrast measure reflecting voxel level functional connectivity. *Neuroimage* (2012) 62:1510–9. doi: 10.1016/j.neuroimage.2012.05.073
90. Talairach JT, Tournoux PP. *Co-planar Stereotaxic Atlas of the Human Brain*. New York, NY: Stuttg Ger Theime (1988).
91. Abraham A, Pedregosa F, Eickenberg M, Gervais P, Mueller A, Kossaifi J, et al. Machine learning for neuroimaging with scikit-learn. *Front Neuroinform.* (2014) 8:14. doi: 10.3389/fninf.2014.00014
92. Tobaldini E, Toschi-Dias E, Trimarchi PD, Brena N, Comanducci A, Casarotto S, et al. Cardiac autonomic responses to nociceptive stimuli in patients with chronic disorders of consciousness. *Clin Neurophysiol.* (2018) 129:1083–9. doi: 10.1016/j.clinph.2018.01.068
93. Riganello F, Quintieri M, Candelieri A, Conforti D, Dolce G. Heart rate response to music: an artificial intelligence study on healthy and traumatic brain-injured subjects. *J Psychophysiol.* (2008) 22:166–74. doi: 10.1027/0269-8803.22.4.166
94. Lee Y-C, Lei C-Y, Shih Y-S, Zhang W-C, Wang H-M, Tseng C-L, et al. HRV response of vegetative state patient with music therapy. In: *2011 Annual International Conference of the IEEE Engineering in Medicine and Biology Society*. Boston, MA (2011). doi: 10.1109/IEMBS.2011.6090488
95. Riganello F, Candelieri A, Quintieri M, Conforti D, Dolce G. Heart rate variability: an index of brain processing in vegetative state? An artificial intelligence, data mining study. *Clin Neurophysiol.* (2010) 121:2024–34. doi: 10.1016/j.clinph.2010.05.010
96. Machado C, Korein J, Aubert E, Bosch J, Alvarez MA, Rodríguez R, et al. Recognizing a mother's voice in the persistent vegetative state. *Clin EEG Neurosci.* (2007) 38:124–6. doi: 10.1177/155005940703800306
97. Gutiérrez J, Machado C, Estévez M, Olivares A, Hernández H, Perez J, et al. Heart rate variability changes induced by auditory stimulation in persistent vegetative state. *Int J Disabil Hum Dev.* (2010) 9:357–62. doi: 10.1515/IJDHD.2010.041
98. Yen BS, Wang H-M, Hou MC, Huang S-C, Chou L-C, Hsu S-Y, et al. The relationship between music processing and electrocardiogram (ECG) in vegetative state (VS). In: *Proceedings of 2010 IEEE International Symposium on Circuits and Systems (ISCAS)*. Paris (2010). p. 2239–42.
99. Wijnen VJM, Heutink M, Boxtel GJM van, Eilander HJ, Gelder B de. Autonomic reactivity to sensory stimulation is related to consciousness level after severe traumatic brain injury. *Clin Neurophysiol.* (2006) 117:1794–807. doi: 10.1016/j.clinph.2006.03.006
100. Papaioannou V, Giannakou M, Maglaveras N, Sofianos E, Giala M. Investigation of heart rate and blood pressure variability, baroreflex sensitivity, and approximate entropy in acute brain injury patients. *J Crit Care* (2008) 23:380–6. doi: 10.1016/j.jcrc.2007.04.006
101. Riganello F, Cortese MD, Dolce G, Sannita WG. Visual pursuit response in the severe disorder of consciousness: modulation by the central autonomic system and a predictive model. *BMC Neurol.* (2013) 13:164. doi: 10.1186/1471-2377-13-164
102. Raimondo F, Rohaut B, Demertzi A, Valente M, Engemann D, Salti M, et al. Brain-heart interactions reveal consciousness in non-communicating patients. *Ann Neurol.* (2017) 82:578–91. doi: 10.1002/ana.25045
103. Batchinsky AI, Cancio LC, Salinas J, Kuusela T, Cooke WH, Wang JJ, et al. Prehospital loss of R-to-R interval complexity is associated with mortality in trauma patients. *J Trauma* (2007) 63:512–8. doi: 10.1097/TA.0b013e318142d2f0
104. Norris PR, Anderson SM, Jenkins JM, Williams AE, Morris JA Jr. Heart rate multiscale entropy at three hours predicts hospital mortality in 3,154 trauma patients. *Shock Augusta Ga* (2008) 30:17–22. doi: 10.1097/SHK.0b013e318164e4d0
105. Batchinsky AI, Salinas J, Kuusela T, Necsoiu C, Jones J, Cancio LC. Rapid prediction of trauma patient survival by analysis of heart rate complexity: impact of reducing data set size. *Shock* (2009) 32:565–71. doi: 10.1097/SHK.0b013e3181a993dc
106. Goldstein B, Fiser DH, Kelly MM, Mickelsen D, Ruttimann U, Pollack MM. Decomplexification in critical illness and injury: Relationship between heart rate variability, severity of illness, and outcome. *Crit Care Med.* (1998) 26:352.
107. Sarà M, Sebastiano F, Sacco S, Pistoia F, Onorati P, Albertini G, et al. Heart rate non linear dynamics in patients with persistent vegetative state: a preliminary report. *Brain Inj.* (2008) 22:33–7. doi: 10.1080/02699050701810670
108. Riganello F, Cortese MD, Arcuri F, Quintieri M, Dolce G. How can music influence the autonomic nervous system response in patients with severe disorder of consciousness? *Front Neurosci.* (2015) 9:461. doi: 10.3389/fnins.2015.00461
109. Huang H-H, Lee Y-H, Chan H-L, Wang Y-P, Huang C-H, Fan S-Z. Using a short-term parameter of heart rate variability to distinguish awake from isoflurane anesthetic states. *Med Biol Eng Comput.* (2008) 46:977–84. doi: 10.1007/s11517-008-0342-y
110. Naraghi L, Peev MP, Esteve R, Chang Y, Berger DL, Thayer SP, et al. The influence of anesthesia on heart rate complexity during elective and urgent surgery in 128 patients. *J Crit Care* (2015) 30:145–9. doi: 10.1016/j.jcrc.2014.08.008
111. Notarius C. Limitations of the use of spectral analysis of heart rate variability for the estimation of cardiac sympathetic activity in heart failure. *Europace* (2001) 3:29–38. doi: 10.1053/eupc.2000.0136
112. Shaffer F, McCraty R, Zerr CL. A healthy heart is not a metronome: an integrative review of the heart's anatomy and heart rate variability. *Psychol Clin Settings* (2014) 5:1040. doi: 10.3389/fpsyg.2014.01040
113. Costa MD, Davis RB, Goldberger AL. Heart rate fragmentation: a new approach to the analysis of cardiac interbeat interval dynamics. *Front Physiol.* (2017) 8:255. doi: 10.3389/fphys.2017.00255
114. Costa MD, Peng C-K, Goldberger AL. Multiscale analysis of heart rate dynamics: entropy and time irreversibility measures. *Cardiovasc Eng.* (2008) 8:88–93. doi: 10.1007/s10558-007-9049-1

115. Goldberger AL, Amaral LAN, Hausdorff JM, Ivanov PC, Peng C-K, Stanley HE. Fractal dynamics in physiology: alterations with disease and aging. *Proc Natl Acad Sci USA*. (2002) 99:2466–72. doi: 10.1073/pnas.012579499
116. Kim SW, Jeon HR, Kim JY, Kim Y. Heart rate variability among children with acquired brain injury. *Ann Rehabil Med*. (2017) 41:951–60. doi: 10.5535/arm.2017.41.6.951
117. Critchley HD. Neural mechanisms of autonomic, affective, and cognitive integration. *J Comp Neurol*. (2005) 493:154–66. doi: 10.1002/cne.20749
118. Thayer JF, Åhs F, Fredrikson M, Sollers JJ, Wager TD. A meta-analysis of heart rate variability and neuroimaging studies: implications for heart rate variability as a marker of stress and health. *Neurosci Biobehav Rev*. (2012) 36:747–56. doi: 10.1016/j.neubiorev.2011.11.009
119. Valenza G, Duggento A, Passamonti L, Diciotti S, Tessa C, Toschi N, et al. Resting-state brain correlates of cardiovascular complexity. In: *Engineering in Medicine and Biology Society (EMBC), 2017 39th Annual International Conference of the IEEE*. Jeju Island: IEEE. p. 3317–20.
120. Duggento A, Bianciardi M, Passamonti L, Wald LL, Guerrisi M, Barbieri R, et al. Globally conditioned Granger causality in brain–brain and brain–heart interactions: a combined heart rate variability/ultra-high-field (7 T) functional magnetic resonance imaging study. *Philos Trans R Soc Math Phys Eng Sci*. (2016) 374:20150185. doi: 10.1098/rsta.2015.0185
121. Fazan FS, Brognara F, Fazan Junior R, Murta Junior LO, Virgilio Silva LE. Changes in the complexity of heart rate variability with exercise training measured by multiscale entropy-based measurements. *Entropy* (2018) 20:47. doi: 10.3390/e20010047
122. Silva LEV, Silva CAA, Salgado HC, Fazan R. The role of sympathetic and vagal cardiac control on complexity of heart rate dynamics. *Am J Physiol Heart Circ Physiol*. (2017) 312:H469–77. doi: 10.1152/ajpheart.00507.2016
123. Benarroch EE. The autonomic nervous system: basic anatomy and physiology. *Contin Lifelong Learn Neurol*. (2007) 13:13–32. doi: 10.1212/01.CON.0000299964.20642.9a
124. Mäenpää M, Laitio T, Kuusela T, Penttilä J, Kaisti K, Aalto S, et al. Delta entropy of heart rate variability along with deepening anesthesia. *Anesth Analg*. (2011) 112:587–92. doi: 10.1213/ANE.0b013e318208074d
125. Guldenmund P, Demertzi A, Boveroux P, Boly M, Vanhaudenhuyse A, Bruno M-A, et al. Thalamus, brainstem and salience network connectivity changes during propofol-induced sedation and unconsciousness. *Brain Connect*. (2013) 3:273–85. doi: 10.1089/brain.2012.0117
126. Blume C, Lechinger J, Santhi N, del Giudice R, Gnjezda M-T, Pichler G, et al. Significance of circadian rhythms in severely brain-injured patients: a clue to consciousness? *Neurology* (2017) 88:1933–41. doi: 10.1212/WNL.0000000000003942
127. Schabus M, Wisłowska M, Angerer M, Blume C. Sleep and circadian rhythms in severely brain-injured patients – a comment. *Clin Neurophysiol*. (2018) 129:1780–4. doi: 10.1016/j.clinph.2018.03.048
128. Angerer M. *Neural and Cardiological Signatures of Conscious Processing and Circadian Rhythms in Brain-Injured Patients*. Master thesis, University of Salzburg, Austria (2017).
129. Bruno M-A, Ledoux D, Vanhaudenhuyse A, Gosseries O, Thibaut A, Laureys S. Prognosis of patients with altered state of consciousness. In: *Coma and Disorders of Consciousness*. London: Springer (2012). p. 11–23.
130. Monti MM, Vanhaudenhuyse A, Coleman MR, Boly M, Pickard JD, Tshibanda L, et al. Willful modulation of brain activity in disorders of consciousness. *N Engl J Med*. (2010) 362:579–89. doi: 10.1056/NEJMoa0905370
131. Gibson RM, Fernández-Espejo D, Gonzalez-Lara LE, Kwan BY, Lee DH, Owen AM, et al. Multiple tasks and neuroimaging modalities increase the likelihood of detecting covert awareness in patients with disorders of consciousness. *Front Hum Neurosci*. (2014) 8:950. doi: 10.3389/fnhum.2014.00950

**Conflict of Interest Statement:** The authors declare that the research was conducted in the absence of any commercial or financial relationships that could be construed as a potential conflict of interest.

Copyright © 2018 Riganello, Larroque, Bahri, Heine, Martial, Carrière, Charland-Verville, Aubinet, Vanhaudenhuyse, Chatelle, Laureys and Di Perri. This is an open-access article distributed under the terms of the Creative Commons Attribution License (CC BY). The use, distribution or reproduction in other forums is permitted, provided the original author(s) and the copyright owner(s) are credited and that the original publication in this journal is cited, in accordance with accepted academic practice. No use, distribution or reproduction is permitted which does not comply with these terms.



# Novel Approaches to the Diagnosis of Chronic Disorders of Consciousness: Detecting Peripersonal Space by Using Ultrasonics

Antonino Naro, Antonino Chillura, Simona Portaro, Alessia Bramanti, Rosaria De Luca, Placido Bramanti and Rocco Salvatore Calabrò\*

IRCCS centro Neurolesi Bonino-Pulejo, Messina, Italy

## OPEN ACCESS

### Edited by:

Olivia Gosseries,  
University of Liège, Belgium

### Reviewed by:

Francesca Pistoia,  
University of L'Aquila, Italy  
Caroline Schnakers,  
University of California, Los Angeles,  
United States  
Aurore Thibaut,  
University of Liège, Belgium

### \*Correspondence:

Rocco Salvatore Calabrò  
salbro77@tiscali.it

### Specialty section:

This article was submitted to  
Applied Neuroimaging,  
a section of the journal  
Frontiers in Neurology

**Received:** 25 August 2017

**Accepted:** 18 January 2018

**Published:** 05 February 2018

### Citation:

Naro A, Chillura A, Portaro S,  
Bramanti A, De Luca R, Bramanti P  
and Calabrò RS (2018) Novel  
Approaches to the Diagnosis of  
Chronic Disorders of Consciousness:  
Detecting Peripersonal Space  
by Using Ultrasonics.  
Front. Neurol. 9:47.  
doi: 10.3389/fneur.2018.00047

The assessment of behavioral responsiveness in patients suffering from chronic disorders of consciousness (DoC), including Unresponsive Wakefulness Syndrome (UWS) and Minimally Conscious State (MCS), is challenging. Even if a patient is unresponsive, he/she may be covertly aware in reason of a cognitive-motor dissociation, i.e., a preservation of cognitive functions despite a solely reflexive behavioral responsiveness. The approach of an external stimulus to the peripersonal space (PPS) modifies some biological measures (e.g., hand-blink reflex amplitude) to the purpose of defensive responses from threats. Such modulation depends on a top-down control of subcortical neural circuits, which can be explored through changes in cerebral blood flow velocity (CBFV), using functional transcranial Doppler (fTCD) and, thus, gaining useful, indirect information on brain connectivity. These data may be used for the DoC differential diagnosis. We evaluated the changes in CBFV by measuring the pulsatility index (PI) in 21 patients with DoC (10 patients with MCS and 11 with UWS) and 25 healthy controls (HC) during a passive movement and motor imagery (MI) task in which the hand of the subject approached and, then, moved away from the subject's face. In the passive movement task, the PI increased progressively in the HCs when the hand was moved toward the face and, then, it decreased when the hand was removed from the face. The PI increased when the hand was moved toward the face in patients with DoC, but then, it remained high when the hand was removed from the face and up to 30 s after the end of the movement in the patients with MCS (both MCS+ and MCS-) and 1 min in those with UWS, thus differentiating between patients with MCS and UWS. In the MI task, all the HCs, three out of four patients with MCS+, and one out of six patients with MCS- showed an increase-decrease PI change, whereas the remaining patients with MCS and all the patients with UWS showed no PI changes. Even though there is the possibility that our findings will not be replicated in all patients with DoC, we propose fTCD as a rapid and very easy tool to differentiate between patients with MCS and UWS, by identifying residual top-down modulation processes from higher-order cortical areas to sensory-motor integration networks related to the PPS, when using passive movement tasks.

**Keywords:** peripersonal space, chronic disorders of consciousness, transcranial ultrasound, motor imagery, cerebral blood flow



## INTRODUCTION

Patients with chronic disorders of consciousness (DoC), including unresponsive wakefulness syndrome (UWS) and minimally conscious state (MCS), show a deterioration of the awareness of self and the environment despite a preserved wakefulness (1, 2). The differential diagnosis between these two entities is essentially based on clinical scales [including the JFK Coma Recovery Scale-Revised (CRS-R)] (3) that focus on the level of behavioral responsiveness to different types of stimuli (4). While patients with UWS disclose no voluntary behavioral responses, individuals with MCS show variable signs of consciousness and are subcategorized into MCS+ and MCS− based on the level of complexity of observed behavioral responses. Specifically, the former shows command following, intelligible verbalization or gestural or “intentional communication,” while the latter only shows minimal levels of behavioral interaction (i.e., non-reflex movements) (5).

Nonetheless, making the distinction between MCS and UWS patients is challenging, as reflected by the high misdiagnosis rate (6). Indeed, the clinical presentations of these two entities can be relatively similar in many cases, although having different levels of awareness, and discriminating between reflexive and willful behavior can be difficult (7). In fact, the clinical assessment can be biased by several sources of false negative results, including abnormalities in brain arousal and attention, sensory and motor output impairment, language comprehension, restraining and immobilizing techniques, and pain (8–10). These aspects can determine clinical conditions that have been labeled as MCS\*, cognitive-motor dissociation, Functional Locked-In Syndrome, Vegetative State with hidden consciousness or with preserved islands of consciousness (5, 11–16), in which a behaviorally unresponsive patient is covertly aware, i.e., aware but unable to manifest it (owing to, e.g., a severe motor impairment, with particular regard to the motor cortico-thalamocortical circuits) (17).

Therefore, advanced paraclinical approaches complementing the clinical assessment, including functional neuroimaging and neurophysiology, aimed at demonstrating covert willful behavior (e.g., by looking at task-dependent and task-independent brain activation as compared to that observed in conscious healthy controls) could help in DoC differential diagnosis. About that, the evaluation of the peripersonal space (PPS) may be useful. PPS defines the region of space immediately surrounding the body in which objects can be grasped and manipulated. It has been observed that a stimulus approaching the PPS provokes a more vigorous defensive reaction than a homologous stimulus outside the PPS (18–23). This modulation depends on a cortico-thalamo-brainstem top-down control of the bottom-up information (arousing, in turn, the top-down control) (20, 21). Thus, any difference in behavioral response should be the result of some stimulus becoming salient through a voluntary top-down process (24). At the same time, the assessment of behavior-related brain responses may disclose useful information, albeit indirect, on the degree of deterioration of the cortical-thalamocortical connectivity in patients with DoC and, thus, on the level of awareness.

An easy and quick way to study PPS and the related top-down control may consist of the assessment of its neurovascular function by using functional transcranial doppler (fTCD) sonography. fTCD represents an extension of the standard TCD, allowing to assess the modulation of cerebral hemodynamics during brain activation paradigms, e.g., the execution of motor tasks, motor imagery (MI), and sensory stimulation (25–27). In fact, mental and motor activities augment regional metabolism and modify auto-regulatory mechanisms that, in turn, influence cerebrovascular resistance, thus resulting in an increase in cerebral blood flow velocity (CBFV) (28–32). By measuring CBFV, it is possible to estimate functional connectivity subserving the execution of a motor task, given that cerebral blood flow indirectly assesses the functional connectivity among the hubs constituting brain networks while transferring information across brain regions (33). In fact, cerebral blood flow is proportionate to the functional connectivity strength in a connection–distance dependent fashion and to the level of behavioral performance (33). fTCD has a low spatial resolution and is an easy tool in comparison to more sophisticated devices [including functional magnetic resonance imaging (fMRI) and electroencephalography (EEG)], it is non-invasive, readily available, easily repeatable, and has an excellent temporal resolution (5 ms) to document hemodynamic changes (34).

To the best of our knowledge, no study has yet investigated hemodynamic changes related to PPS perturbation by using fTCD. This study aims to measure the modulation of CBFV related to stimuli approaching the PPS-face; these hemodynamic changes should reflect the level of integrity of the top-down cortical-thalamo-brainstem pathways and, indirectly, the level of awareness.

## MATERIALS AND METHODS

### Participants

Twenty-two patients with DoC attending our neurorehabilitation units (12 males and 10 females, mean age  $52 \pm 17$  years, range 19–73; MCS:  $53 \pm 16$  years; UWS:  $54 \pm 18$  years; 11 patients were in a UWS—disease duration  $9 \pm 6$  months and 10 in an MCS—disease duration  $8 \pm 4$  months) were consecutively included in the study. The DoC diagnosis was based on the neurobehavioral assessments (performed twice a day for 1 month before the assessment for study eligibility, using the CRS-R) (35) and the available functional studies (neuroimaging and EEG). Only five patients previously underwent advanced analyses, which furnished results in keeping with the clinical diagnosis. Moreover, patients with MCS were categorized into MCS+ and MCS− based on the level of complexity of observed behavioral responses (response to the command, intelligible verbalization, and intentional communication) (5).

Persons with hemodynamic stenosis of neck vessels (as measured by cervical and TCD ultrasound to exclude hemodynamically significant stenosis in the target territory), cardiovascular/hemodynamic instability, severe spasticity that limits upper limb movements, hypo/hypercapnia, and vasodilatory or vasoconstrictor drug treatment, were excluded from the

study. fTCD measurements were compared with 25 healthy control subjects (HC) (11 males and 14 females, mean age  $55 \pm 15$  years, range 25–75), who did not show hemodynamic stenosis of neck vessels and did not take vasodilatory or vasoconstrictor drugs. The clinical and demographic characteristics are shown in **Table 1**. The level of behavioral responsiveness was assessed using the CRS-R (which was performed twice a day for 1 month before study inclusion by two trained and experienced neurologists). The best CRS-R score observed was used for the analyses. The research followed the principles of the Declaration of Helsinki and was approved by the Ethics Committee of the Institute. HC and the legal surrogates of patients with DoC gave their written informed consent to participate in the study.

## Experimental Procedure

The participant was lying supine on a bed, in a quiet and mild-lighted room, with the eyes open (CRS-R arousal protocol guaranteed this in patients with DoC). The right upper limb was lying along the trunk with the palm facing up, the right arm in a position that allowed the forearm to move toward the

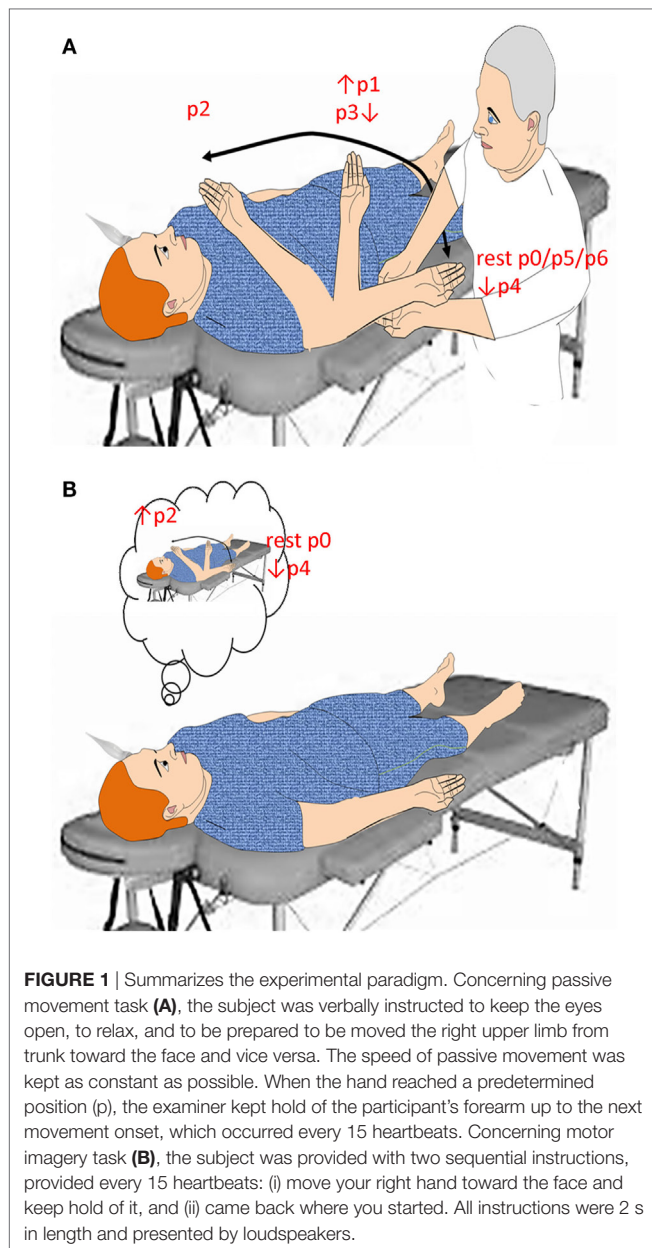
eyes (without touching the face) (**Figure 1**). Blood pressure (from left upper limb) and heart rate (HR) were continuously monitored. The subjects were provided with two motor tasks in random order. In the “passive movement” task, an experimenter mobilized the right upper limb across five different positions, so as to move the hand toward and backward the face, i.e., forearm extended on the arm ( $p0 = 180^\circ$ ), forearm flexed on the arm at  $90^\circ$  ( $p1$ ), forearm flexed on the arm at  $10^\circ$  ( $p2$ ), and then going back to  $90^\circ$  ( $p3$ ), and  $180^\circ$  ( $p4$ ) (**Figure 1A**). The speed of passive movements was kept as constant as possible. Each movement occurred every 15 heartbeats. During each stationary period, the examiner kept hold of the participant's forearm. This experiment was performed to verify the role of the two afferent pathways (optic and proprioceptive) in the modulation of cerebral hemodynamic responses.

In the “motor imagery” task, all participants were instructed to mentally perform an upper limb flexion movement toward the face (i.e., from  $p0$  to  $p2$ ) and an extension movement backward the face (i.e., from  $p2$  to  $p4$ ) (**Figure 1B**). Each movement occurred every 15 heartbeats. This experiment was conducted to evaluate whether and how MI affects cerebral hemodynamics.

**TABLE 1** | Clinical–demographic characteristics.

	Age (years)	Gender	BI	DD (months)	CRS-R	RF	Treatment
MCS+ ( $n = 4$ )	63	M	V	6	18	1.7	B, A
	25	M	V	12	17	5.7	B
	65	F	T	16	16	2	AED
	63	M	T	7	16	1.7	B, LD
MCS– ( $n = 6$ )	53	F	V	6	14	4.7	B, LD
	56	F	T	6	12	None	B, LD, A
	64	M	T	8	14	1.6	LD
	54	M	T	5	11	3.8	AED, A
	62	F	V	7	9	None	LD, A
	20	M	V	7	9	2	B
Mean $\pm$ SD	53 $\pm$	6M	5T	8 $\pm$	14 $\pm$		
	16	4F	5V	4	3		
UWS ( $n = 11$ )	67	M	T	8	6	1	B, LD, AED, A
	60	M	T	6	6	2	LD, A
	19	M	V	5	6	4	B, AED
	65	M	T	7	6	2.6	LD, AED
	53	F	T	18	5	3.7	LD, AED, A
	73	M	V	24	5	4.7	B, LD, AED, A
	20	M	V	4	5	2.4	AED
	65	F	T	7	4	4.7	LD, AED, A
	55	F	T	6	4	5.7	AED
	57	M	T	6	4	None	B, LD
	59	F	V	6	3	2.6	B, A
Mean $\pm$ SD	54 $\pm$	7M	7T	9 $\pm$	5 $\pm$		
	18	4F	4V	6	1		
Mean $\pm$ SD	54 $\pm$	7M	7T	9 $\pm$	5 $\pm$		
	18	4F	4V	6	1		

BI, etiology of brain injury; CRS-R, Coma Recovery Scale-Revised; DD, disease duration; F, female; M, male; MCS, Minimally Conscious State; T, traumatic; UWS, Unresponsive Wakefulness Syndrome; V, vascular; RF, risk factors (1. physical inactivity, 2. tobacco, 3. blood lipids, 4. hypertension, 5. obesity, 6. family history, 7. diabetes, 8. coagulopathies); LD, L-DOPA; AED, antiepileptic drugs; A, analgesics; B, baclofen; (+), patients with MCS+.



As a control experiment, we performed a condition in which the experimenter's hand entered the PPS-face, without actual movement of the subject of his or her own body in 10 out of 25 HCs. fTCD was recorded during this task with the same modalities of the "passive movement" task.

By using fTCD, we measured the pulsatility index (PI) from the middle (MCA), anterior (ACA), and posterior (PCA) cerebral artery at rest ( $p0_{rest}$ ) and during the entire motor task. The resting condition ( $p0_{rest}$ ) allowed the establishment of the regulatory parameters for subsequent sessions. We also measured PI from MCA 30 (p5) and 60 s (p6) after the end of the passive movement (p5 and p6 being identical to p0). The main experiments were repeated twice, to control for any variation within the subjects, averaging the results obtained from the two trials. The fTCD

recording was performed twice for each intracranial vessel. The head was held in place by a headrest to minimize head movements. All HCs were asked to avoid caffeine, alcohol, and nicotine for 24 h before the measurement, due to these substances well-known effects on vascular reactivity (36).

## Functional Transcranial Doppler

Functional transcranial Doppler was performed by using a conventional color-coded ultrasound system equipped with a 2–5 MHz phased array transducer (iU22 Philips, Healthcare Solutions, Bothell, WA, USA). The examination was performed through the left temporal acoustic bone window and with the transducer placed anteriorly to the tragus and upwards of the zygomatic arch. The fTCD probe was fixed on the head of the participant by using a hard hat to guarantee the same displacement over the measures and conditions. The peak systolic velocity (PSV), end-diastolic velocity, mean velocity ( $V_m$ ), and PI were measured for each intracranial vessel and were averaged. Age- and gender-corrected PI was calculated, according to the formula  $(PSV - EVD)/V_m$ .

## Statistical Analysis

Pulsatility index and HR modulation were analyzed by using an ANOVA with the factors: *hand-position* (six levels for passive movement:  $p0 \rightarrow p1$ ,  $p1 \rightarrow p2$ ,  $p2 \rightarrow p3$ ,  $p3 \rightarrow p4$ ,  $p4 \rightarrow p5$ , and  $p5 \rightarrow p6$ ; two levels for MI:  $p0 \rightarrow p2$  and  $p2 \rightarrow p4$ ), *task* (two levels: passive movement and MI), and *group* (three levels: HC, MCS, and UWS). We did not aim at assessing the differences between the fTCD of the three main brain vessels as no between-vessel differences have been reported (25, 26). A  $p$ -value  $< 0.05$  was considered significant. Conditional on a significant  $F$ -value for the *hand-position* factor, *post hoc t*-tests were performed for each group and motor task (with Bonferroni correction,  $\alpha = 0.0125$ ). The Greenhouse–Geisser method was applied to compensate for the possible effects of non-sphericity in the compared measurements. All data are presented as mean  $\pm$  SD or as percent changes, where appropriate.

Given that the patients with vascular brain damage frequently have long-lasting vascular risk factors (such as arterial hypertension), which may affect cerebral hemodynamics and modify the mechanisms of cerebral vascular autoregulation (including the limits within the standard window of autoregulation), brain injury etiology and cardiovascular risk factors were included as covariates in the multivariate analysis.  $\beta$  values [standardized regression coefficients (SRCs)], which is a measure of how strongly each predictor variable influences the criterion (dependent) variable, are provided. The higher the  $\beta$  value, the greater the impact of the predictor variable on the criterion variable. If the  $\beta$  coefficient is equal or nearly to 0, then there is no relationship between the variables.

Clinical-electrophysiological correlations (among CRS-R, PI, and HR) were assessed by using the Spearman correlation test.

In the context of single-subject sensitivity analysis, we employed a linear regression model; SRCs were considered as direct measures of sensitivity. The sensitivity and specificity of the electrophysiological measures employed to distinguish accurately between MCS and UWS were calculated by measuring the

area under the curve (AUC) of receiver operating characteristic (ROC). Finally, intraindividual variability between the trials was also calculated in terms of SD of the individual's scores over the trials, thus reflecting the degree of within-person fluctuation over time. Higher scores reflected greater variability.

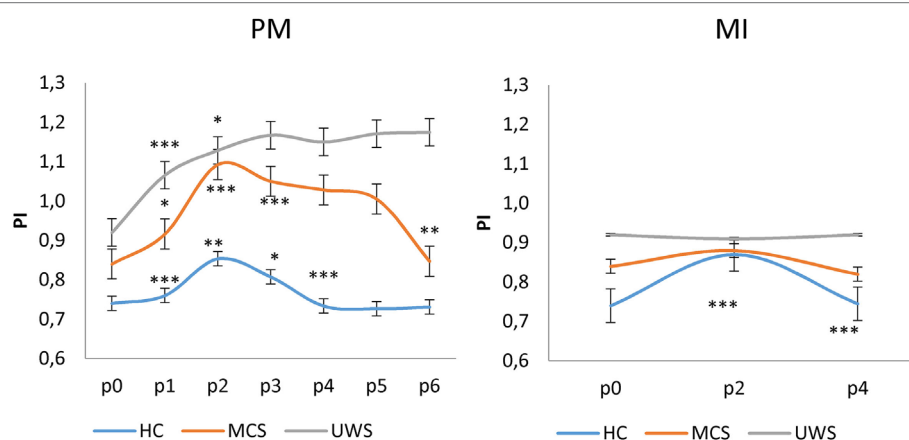
## RESULTS

All the participants completed the experimental study without any side effect. Clinical, neurobehavioral, and functional study data were all concordant in the same patient for the diagnosis of either MCS or UWS. At baseline ( $p_{0\text{rest}}$ ), all the patients showed higher PI and HR values than HC individuals did ( $p < 0.001$ ). Moreover, PI and HR values at rest were higher in patients with UWS than with MCS ( $p = 0.01$ ), with no differences between MCS+ and MCS- ( $p > 0.1$ ) (Figures 2 and 3; Table S1 in Supplementary Material). Nonetheless, some patients with MCS and UWS diverged from this trend, showing lower/higher PI and HR values (Table S1 in Supplementary Material). An example of CBF from the left anterior, middle, and posterior cerebral arteries at rest in one HC, one patient with MCS, and one patient with UWS is provided in Figure 4.

Motor imagery and passive movement tasks yielded significantly different effects on PI [ $\text{task} \times \text{group} \times \text{hand-position}$   $F_{(12,516)} = 17$ ,  $p < 0.001$ ]. In detail, passive movement task determined significantly different changes of PI across the hand positions between the groups [ $\text{group} \times \text{hand-position}$   $F_{(10,430)} = 26$ ,  $p < 0.001$ ;  $\text{group}$   $F_{(2,86)} = 24$ ,  $p < 0.001$ ;  $\text{hand-position}$   $F_{(5,215)} = 21$ ,  $p < 0.001$ ]. In fact, all the HCs showed significant changes of PI values across the hand positions [ $\text{hand-position}$  effect  $F_{(5,120)} = 138$ ,  $p < 0.001$ ], according to the following schema:  $p_0 < p_1 < p_2 > p_3 > p_4 \approx p_5 \approx p_6$ , with  $p_3 \approx p_1$  and  $p_0 \approx p_4 \approx p_5 \approx p_6$  (Figures 2 and 5; Table S1 in Supplementary Material; Table 2). All the patients with MCS

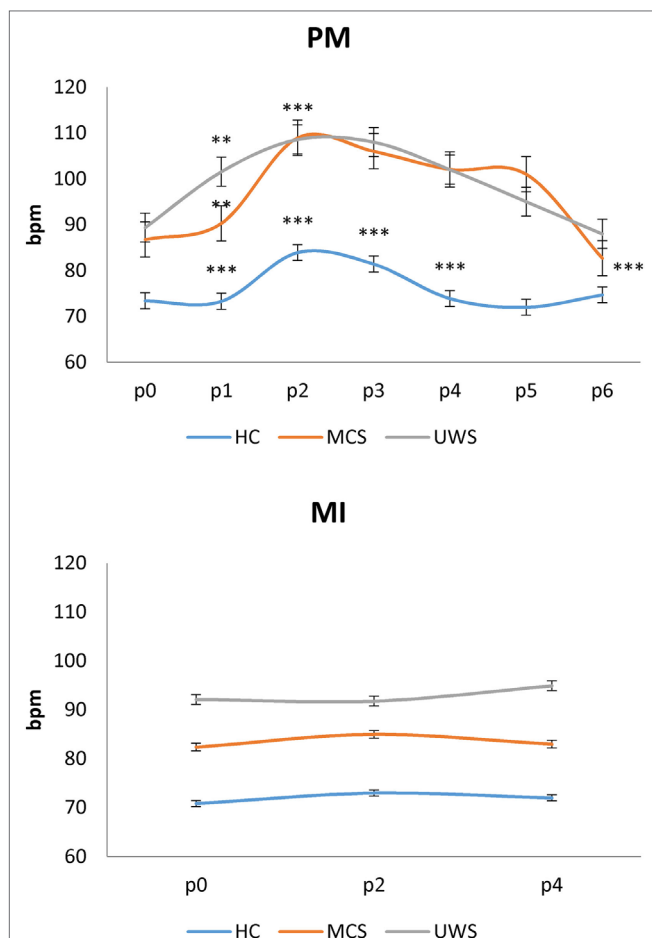
showed significant changes of PI values across hand positions [ $\text{hand-position}$  effect  $F_{(5,45)} = 6.9$ ,  $p < 0.001$ ], with a pattern that differed from that observed in the HC:  $p_0 < p_1 < p_2 > p_3 \approx p_4 \approx p_5 > p_6$  (where  $p_6 \approx p_0$ ). There were no significant differences between patients with MCS+ and MCS- ( $\text{group}$  effect  $p = 0.2$ ). Instead, all the patients with UWS showed a global increase of PI during the passive motor (PM) task, without the significant PI modulation according to the following pattern:  $p_0 < p_1 < p_2 \approx p_3 \approx p_4 \approx p_5 \approx p_6$  ( $\text{hand-position}$  effect  $p = 0.7$ ). Therefore, the PI increased when the hand was moved toward the face in patients with DoC, as observed in the HCs. However, PI remained high when the hand was removed from the face, differently from what observed in the HCs. Further, the high levels of PI lasted up to 30 s after the end of the movement in patients with MCS (both MCS+ and MCS-) and 1 min in those with UWS. An example of CBF changes from the left middle cerebral artery across the positions (p) explored during the PM task in one HC, one patient with MCS, and one patient with UWS is provided in Figure 5. Intraindividual variability between the two trials was very low in all the participants ( $p < 0.005$ ).

Motor imagery task significantly influenced the PI across hand positions between the groups [ $\text{group} \times \text{hand-position}$   $F_{(10,430)} = 10$ ,  $p < 0.001$ ;  $\text{group}$   $F_{(2,86)} = 11$ ,  $p < 0.001$ ;  $\text{hand-position}$   $F_{(1,43)} = 19$ ,  $p < 0.001$ ]. Indeed, all the HCs showed significant changes of PI values across the hand positions (p) according to the following schema:  $p_0 < p_2 > p_4$ , with  $p_0 \approx p_4$  [ $\text{hand-position}$  effect  $F_{(1,43)} = 48$ ,  $p < 0.001$ ] (Figures 2 and 6; Table S1 in Supplementary Material; Table 2). Such a pattern was barely appreciable in the MCS group ( $\text{hand-position}$  effect  $p = 0.06$ ), in which three patients out of four with MCS+ and one patient out of six with MCS- showed such pattern. Thus, we found no significant intra-MCS difference ( $p = 0.1$ ), although the PI modulation in the three patients with MCS+ was greater than that observed in the patient with MCS-. On the other hand, PI modulation was absent in all



**FIGURE 2** | Shows mean ( $\pm$ SD; vertical error bar) pulsatility index (PI) values during passive movement (PM) and motor imagery (MI) tasks for each group [healthy controls (HC), minimally conscious state (MCS), and unresponsive wakefulness syndrome (UWS)] across the hand positions (p) explored. There was a significant difference at  $p_0$  (baseline) between the PI values of HCs and patients with disorders of consciousness ( $p < 0.001$ ), and between patients with MCS and UWS ( $p = 0.01$ ). PM induced a significantly different PI modulation at each p among the groups ( $p < 0.001$ ). On the contrary, MI induced a significant increase of PI at  $p_2$  and decrease at  $p_4$  only in the HCs. \*Refer to the significance of intragroup PI change at each p as compared to the previous one (Bonferroni corrected  $p$ -value, \*\*\* $p < 0.001$ , \*\* $p = 0.001$ , \* $p < 0.0125$ ).





**FIGURE 3** | Shows mean ( $\pm$ SD; vertical error bar) heart rate values [in beats per minute (bpm)] during passive movement (PM) and motor imagery (MI) tasks for each group [healthy controls (HC), minimally conscious state (MCS), and unresponsive wakefulness syndrome (UWS)] across the hand positions (p) explored. There was a significant difference at p0 (baseline) between the bpm values of HCs and patients with disorders of consciousness ( $p < 0.001$ ), and between patients with MCS and UWS ( $p = 0.01$ ). PM induced a significantly different bpm modulation at each p among the groups ( $p < 0.001$ ). On the contrary, MI did not induce any significant bpm change. \*Refer to the significance of intragroup pulsatility index change at each p as compared to the previous one (Bonferroni corrected  $p$ -value, \*\*\* $p < 0.001$ , \*\* $p = 0.001$ , \* $p < 0.0125$ ).

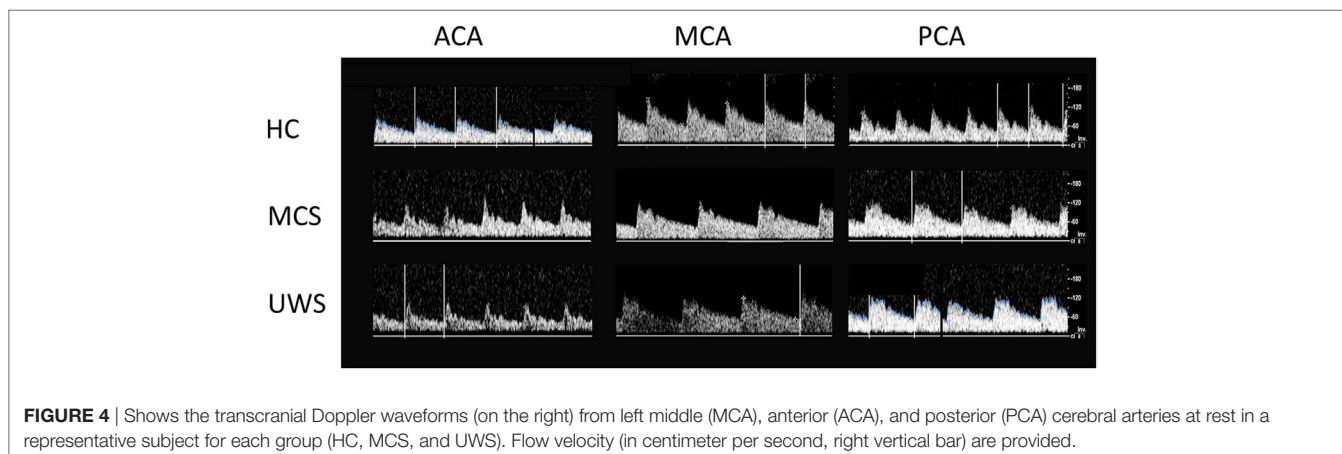
the patients with UWS (*hand-position* effect  $p = 0.7$ ). An example of CBF changes from the left middle cerebral artery across the positions (p) explored during the MI task in one HC, one patient with MCS, and one patient with UWS is provided in **Figure 6**. Intraindividual variability between the two trials was very low in all the participants ( $p < 0.005$ ).

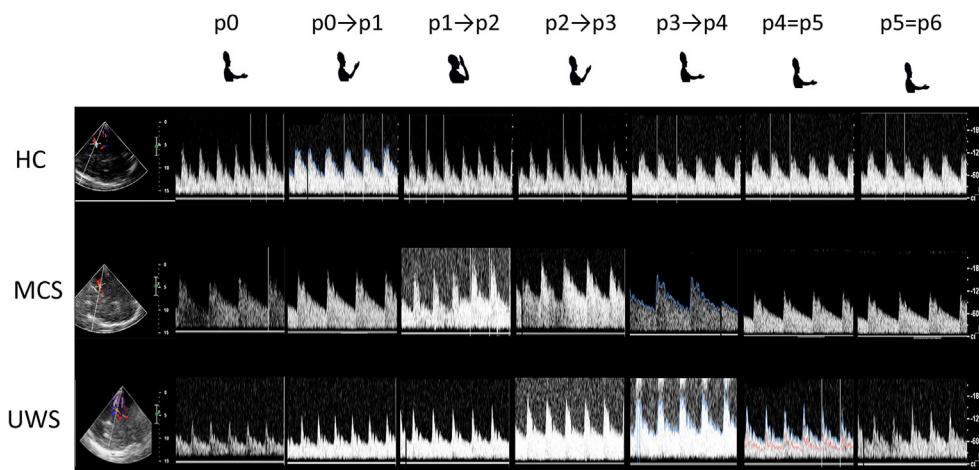
Heart rate during passive movement showed a pattern of increase from p0 to p2 and a decrease from p2 to p6 in each group [*hand-position*  $F_{(5,215)} = 9$ ,  $p < 0.001$ ; *group*  $\times$  *hand-position*  $p = 0.1$ ; *group*  $p = 0.9$ ] as suggested by the significant *hand-position* effect in HC [ $F_{(5,120)} = 54$ ,  $p < 0.001$ ], patients with MCS [ $F_{(5,45)} = 4.9$ ,  $p = 0.001$ ] and with UWS [ $F_{(5,50)} = 6.6$ ,  $p < 0.001$ ] (**Figure 3**; **Table 3**). On the contrary, HR did not significantly change during MI in any group (all interactions and effects  $p > 0.1$ ) (**Figure 3**).

In the control experiment (10 subjects), in which the experimenter's hand entered the PPS-face while the subject remained still, we did not document any significant PI changes across the entire range of movement.

We found a significant correlation between the best CRS-R score and the PI modulation during passive movement ( $r = 0.623$ ,  $p = 0.002$ ). There were no significant effects of clinical-demographic characteristics (age,  $\beta = 0.01$ ,  $p = 0.5$ ; gender,  $\beta = 0.01$ ,  $p = 0.4$ ; disease duration,  $\beta = 0.26$ ,  $p = 0.5$ ; and treatment,  $\beta = 0.13$ ,  $p = 0.6$ ) on PI changes across motor tasks, as well as an effect of blood pressure and HR on PI (all  $p > 0.1$ ). Also, brain etiology ( $\beta = 0.01$ ,  $p = 0.4$ ) and risk factors ( $\beta = 0.01$ ,  $p = 0.7$ ) did not influence the dependent variable PI.

Concerning the sensitivity analysis, we employed a linear regression model; SRCs were considered as direct measures of sensitivity. We found that the PI changes from p0 to p2 and from p2 to p4 (which were the most significant intervals), were the most predictive values for DoC diagnosis during the passive movement task (SRC = 0.05,  $p = 0.01$ ). Finally, the ROC analysis with PI value and CRS-R score as factors showed that the diagnostic accuracy of the overall PI magnitude modulation during passive movement was good (AUC = 0.6), with a sensitivity and specificity concerning DoC category of 100%. In contrast, MI task-induced PI magnitude modulation was poorly associated with CRS-R score (AUC = 0.3) (**Figure 7**), with a sensitivity of 40% and a specificity of 100% concerning DoC category.





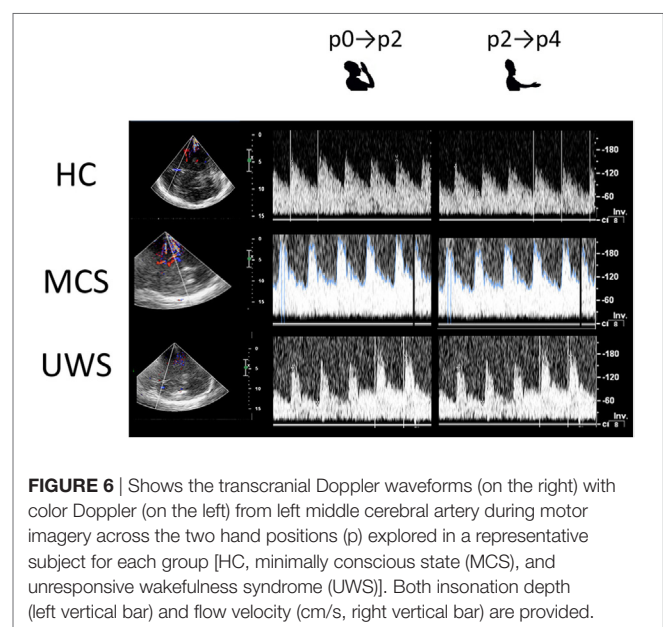
**FIGURE 5 |** Shows the transcranial Doppler waveforms (on the right) with color Doppler (on the left) from left middle cerebral artery during passive mobilization across the six hand positions (p) explored in a representative subject for each group [healthy controls, minimally conscious state (MCS), and unresponsive wakefulness syndrome (UWS)]. Both insonation depth (left vertical bar) and flow velocity (centimeter per second, right vertical bar) are provided.

**TABLE 2 |** Post hoc *t*-test concerning pulsatility index modulation at each hand position (p) as compared to the previous one (significant when *p*-value <0.0125), during the passive motor (PM) and motor imagery (MI) task in patients with minimally conscious state (MCS) and unresponsive wakefulness syndrome (UWS), and in healthy controls (HC). MI data of patients with UWS were not significant.

Group	PM	t-Value	p-Value
	Hand position		
HC	p0–p1	–8	<0.001
	p1–p2	–3.9	0.001
	p2–p3	2.8	0.01
	p3–p4	6.6	<0.001
	p4–p5	>0.1	>0.1
	p5–p6	>0.1	>0.1
MCS	p0–p1	–2.9	0.01
	p1–p2	–6.5	<0.001
	p2–p3	6.5	<0.001
	p3–p4	>0.1	>0.1
	p4–p5	>0.1	>0.1
	p5–p6	5.1	0.001
UWS	p0–p1	–7.2	<0.001
	p1–p2	–3.3	0.01
	p2–p3	>0.1	>0.1
	p3–p4	>0.1	>0.1
	p4–p5	>0.1	>0.1
	p5–p6	>0.1	>0.1
Group	MI	t-Value	p-Value
	Hand position		
HC	p0–p2	–8.2	<0.001
	p2–p4	6.5	<0.001
MCS	p0–p2	–2.1	0.07
	p2–p4	2.3	0.04

## DISCUSSION

To the best of our knowledge, this is the first attempt to characterize PPS in patients with DoC. Our data suggest that fTCD evaluation



**FIGURE 6 |** Shows the transcranial Doppler waveforms (on the right) with color Doppler (on the left) from left middle cerebral artery during motor imagery across the two hand positions (p) explored in a representative subject for each group [HC, minimally conscious state (MCS), and unresponsive wakefulness syndrome (UWS)]. Both insonation depth (left vertical bar) and flow velocity (cm/s, right vertical bar) are provided.

of PPS functions may be useful to corroborate the differential diagnosis of patients with DoC. In fact, all the patients with DoC showed an increased baseline vascular reactivity (i.e., higher PI and HR values) as compared to HC individuals, in keeping with the uncoupling of CBF and cerebral metabolic rate arising from reduced cerebral glucose consumption and oxygen uptake after extensive brain injury (37–39). Even though the patients with UWS showed higher PI and HR values at baseline than those with MCS, some patients diverged from their group trend, in that they had lower/higher PI and HR values. Moreover, CRS-R scores did not correlate with baseline PI and HR values. On the other hand, the assessment of CBFV during the PM task targeting the PPS allowed differentiating between patients with MCS and UWS. Even though the PI increased when the hand was moved toward

the face in patients with DoC, it remained high when the hand was removed from the face and up to 30 s after the end of the movement in the patients with MCS (both MCS+ and MCS−) and 1 min in those with UWS, thus differentiating between patients with MCS and UWS. This pattern of CBFV changes is in keeping with the protective role played by PPS toward the potential threats approaching body parts. This role is reflected by a more vigorous defensive reactions elicited when stimuli are located inside rather than outside the PPS (18, 19, 21, 22). The lack of an early normalization of CBFV in patients with DoC may be related to a dysfunction in the regulation of temporized brain activity or in the replenishing of the metabolite levels after increased brain activity (40, 41). The strong impairment of brain metabolism and

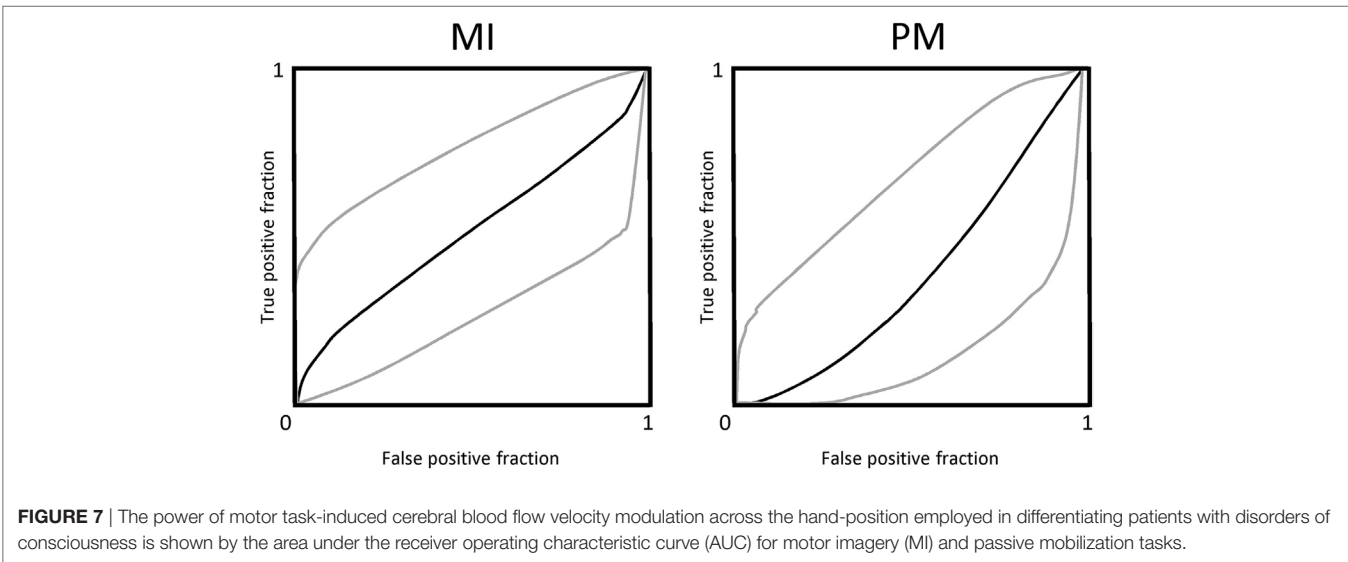
the tonic cortical and subcortical dis-excitability may account for the delay in CBFV normalization observed in patients with DoC (42–44). Additionally, a dysfunctional neurovascular coupling, i.e., the close spatial and temporal relationships between the neural activity and CBF, also accounts for the lack of CBFV normalization following a task (39, 45).

Noteworthy, our findings may agree with the reported correlation between the behavioral responsiveness of patients with DoC and the degree of cortico-subcortical connectivity breakdown and subcortical hyper-connectivity (46). In fact, the magnitude and extent of PI modulation during PM task (but not the baseline values) were correlated with the CRS-R scoring, i.e., the lower and more reflex the behavioral responsiveness, the higher and longer the PI increase. Therefore, CBFV regulation may reflect the partial preservation of top-down modulation processes from higher-order cortical areas to sensory-motor integration networks related to the PPS (16, 20, 21, 24, 47, 48), in patients with MCS but not in those with UWS.

Interestingly, four patients with MCS (three with MCS+ and one with MCS−) showed a barely appreciable PI modulation during the MI task. Studies testing MI in patients with MCS disclosed a high rate of false negative, i.e., a patient can have some motor function but does not demonstrate brain activity when asked to imagine a task (49–51). According to these issues, PI modulation during MI does not seem a very reliable method for differentiating the MCS status, but it may only furnish information about the differential diagnosis between MCS and UWS. The lack of sensitivity of PI modulation during MI task may depend on the nature of the brain processes related to stimuli approaching PPS, i.e., protective response, which is not the case of MI. Moreover, it is likely that that passive movement induces a neurovascular activation that is not detectable during MI, which instead represents an internally triggered event (52). Finally, the simplicity of the movement required, in comparison to the more complex MI tasks formerly employed (i.e., playing tennis or in-house navigation), could have yielded non-specific cerebral blood flow responses that are independent of the motor task.

**TABLE 3 |** Post hoc *t*-test concerning heart rate (HR) modulation at each hand position (p) as compared to the previous one (significant when *p*-value < 0.0125), during the passive motor task in patients with minimally conscious state (MCS) and unresponsive wakefulness syndrome (UWS), and in healthy controls (HC). HR data of motor imagery were not significant.

Group	Hand position	<i>t</i> -Value	<i>p</i> -Value
HC	p0–p1	−7.4	<0.001
	p1–p2	−5.5	<0.001
	p2–p3	8.2	<0.001
	p3–p4	14	<0.001
	p4–p5		>0.1
	p5–p6		>0.1
MCS	p0–p1	−3.3	0.008
	p1–p2	−2.9	0.02
	p2–p3	2.4	0.04
	p3–p4		>0.1
	p4–p5		>0.1
	p5–p6	4.2	0.001
UWS	p0–p1	−3.5	0.006
	p1–p2	−5.1	<0.001
	p2–p3		>0.1
	p3–p4		>0.1
	p4–p5		>0.1
	p5–p6		>0.1



Heart rate showed a common pattern of modulation during passive movement task without any correlation to PI and CRS-R, whereas it did not change during MI. Thus, hemodynamic factors like HR seem to not bias PI while performing such motor tasks.

## Limitations

The small sample enrolled represents a main limitation of our study. Moreover, none of the patients with MCS had borderline CRS-R scores between MCS and UWS (i.e., in the range of 6–8), and only 2 patients with MCS had a score of 9. This issue might have magnified the observed fTCD differences between patients with MCS and UWS. Also, we did not find fTCD differences between MCS+ and MCS–, which may depend on the CRS-R scores the patients with MCS– reported (up to 14, which makes them in the higher boundaries of MCS–). If we had available patients with MCS– with CRS-R score in the range of 6–8, we could have differentiated patients with MCS+ and MCS–. Therefore, future studies with a larger number of patients, a more varied CRS-R score range, and long-term outcomes, should be undertaken to confirm the possible use of fTCD as a complementary diagnostic tool. Also, fMRI or PET-scans should be used to confirm our findings, as fTCD could represent an approach that indicates the subject candidates to undergo advanced and sophisticated neuroimaging paradigms.

Functional transcranial doppler measures CBFV rather than absolute cerebral blood flow. An estimation of the latter can be made if the diameter of the insonated vessel remains constant (25, 26), but there is not sufficient data to demonstrate this issue in our work. fTCD has an interesting temporal resolution, but the spatial resolution is unfortunately low so that we cannot be precise on spatialized cerebral hemodynamics.

We did not measure right arm electromyography to exclude possible voluntary muscular activity during the passive movement, even though previous studies have ruled out significant biasing effects on CBFV of muscle activation during a passive movement task (25, 26).

A possible contribution from peripheral covariates (including beat-to-beat arterial blood pressure, HR, PaCO<sub>2</sub>, breath-by-breath end-tidal CO<sub>2</sub>, and the neural activation stimulus represented by the go-signal) could lead to the inaccurate assessment of CBFV, particularly during MI (25, 26). About that, blood pressure and HR were monitored and did not significantly correlate with PI values. However, a larger assessment of such peripheral covariates will be necessary. In fact, it would be important to specifically identify the presence of a dysautonomic syndrome and of other alteration of the mechanisms of cerebral vascular autoregulation. However, the blood pressure and HR (which were monitored during the experimental session) changed according to a common waxing–waning pattern. Moreover, brain etiology and the presence of risk factors (both added to the multivariate analysis) did not significantly influence the PI changes. Nonetheless, larger samples should be investigated to define these issues better.

Finally, one could be concerned that PI modification may be simply related to hand movement protocol rather than to PPS violation response. However, the condition, in which the experimenter's hand entered the PPS while the upper limb of the participant was not moved, showed no significant PI changes.

Therefore, it is reasonable that PI changes are related to PPS violation rather than to the hand movement.

## Conclusions

Functional transcranial Doppler could be a promising, quick, and easy tool for the bedside differential diagnosis between patients with MCS and UWS. Indeed, fTCD helps to identify CBF changes that are related to top-down modulation processes from higher-order cortical areas to sensory-motor integration networks related to the PPS, when using passive movement tasks. Despite the small sample size and the simplicity of the methodology as compared to those more advanced (53, 54) our approach may also allow the clinician to identify the candidates for carrying out advanced and sophisticated neuroimaging tools when they are not readily available.

## ETHICS STATEMENT

All procedures performed in studies involving human participants were in accordance with the ethical standards of the institutional and/or national research committee and with the 1964 Helsinki declaration and its later amendments or comparable ethical standards. Our Local Ethic Committee approved the study.

## INFORMED CONSENT

Healthy subject and the legal surrogates of patients with Disorder of Consciousness gave their written informed consent to study participation.

## AUTHOR CONTRIBUTIONS

AN, RC, and PB: substantial contributions to the conception and design of the work, and interpretation of data; revising the work critically for important intellectual content; final approval of the version to be published; agreement to be accountable for all aspects of the work in ensuring that questions related to the accuracy or integrity of any part of the work are appropriately investigated and resolved. AC, SP, AB, and RL: acquisition and analysis of data; drafting the work; final approval of the version to be published; and agreement to be accountable for all aspects of the work in ensuring that questions related to the accuracy or integrity of any part of the work are appropriately investigated and resolved.

## SUPPLEMENTARY MATERIAL

The Supplementary Material for this article can be found online at <http://www.frontiersin.org/articles/10.3389/fneur.2018.00047/full#supplementary-material>.

**TABLE S1** | Shows individual pulsatility index (PI) values during passive mobilization and motor imagery (MI) for each group [healthy controls (HC), minimally conscious state (MCS)±, and unresponsive wakefulness syndrome (UWS), with their coma recovery scale-revised score in parentheses] across the six positions explored and the two imagined movements (p). The patients with MCS whose pulsatility index values differed from those of the other individuals belonging to the same subgroup (MCS+ or MCS–) are highlighted in red.



## REFERENCES

- Multi-Society Task Force on PVS. Medical aspects of the persistent vegetative state. *N Engl J Med* (1994) 330:1499–508. doi:10.1056/NEJM199405263302107
- Giacino JT, Ashwal S, Cranford R, Jennett B, Katz DI, et al. The minimally conscious state: definition and diagnostic criteria. *Neurology* (2002) 58:349–53. doi:10.1212/WNL.58.3.349
- Giacino JT, Kalmar K, Whyte J. The JFK Coma Recovery Scale-Revised: measurement characteristics and diagnostic utility. *Arch Phys Med Rehabil* (2004) 85:2020–9. doi:10.1016/j.apmr.2004.02.033
- Laureys S, Owen AM, Schiff ND. Brain function in coma, vegetative state, and related disorders. *Lancet Neurol* (2004) 3:537–46. doi:10.1016/S1474-4422(04)00852-X
- Bruno MA, Vanhaudenhuyse A, Thibaut A, Moonen G, Laureys S. From unresponsive wakefulness to minimally conscious PLUS and functional locked-in syndromes: recent advances in our understanding of disorders of consciousness. *J Neurol* (2011) 258(7):1373–84. doi:10.1007/s00415-011-6114-x
- van Erp WS, Lavrijsen JC, Vos PE, Bor H, Laureys S, Koopmans RT. The vegetative state: prevalence, misdiagnosis, and treatment limitations. *J Am Med Dir Assoc* (2015) 16:e9–85. doi:10.1016/j.jamda.2014.10.014
- Guldenmund P, Stender J, Heine L, Laureys S. Mindsight: diagnostics in disorders of consciousness. *Crit Care Res Prac* (2012) 2012:624724. doi:10.1155/2012/624724
- Majerus S, Bruno MA, Schnakers C, Giacino JT, Laureys S. The problem of aphasia in the assessment of consciousness in brain-damaged patients. *Prog Brain Res* (2009) 177:49–61. doi:10.1016/S0079-6123(09)17705-1
- Bruno MA, Vanhaudenhuyse A, Schnakers C, Boly M, Gosseries O, Demertzi A, et al. Visual fixation in the vegetative state: an observational case series PET study. *BMC Neurol* (2010) 10:35. doi:10.1186/1471-2377-10-35
- Schnakers C, Chatelle C, Majerus S, Gosseries O, De Val M, Laureys S. Assessment and detection of pain in noncommunicative severely brain-injured patients. *Expert Rev Neurother* (2010) 10:1725–31. doi:10.1586/ern.10.148
- Shea N, Bayne T. The vegetative state and the science of consciousness. *Br J Philos Sci* (2010) 61:459–84. doi:10.1093/bjps/axp046
- Formisano R, D'Ippolito M, Riseti M, Riccio A, Caravasso CF, Catani S, et al. Vegetative state, minimally conscious state, akinetic mutism and Parkinsonism as a continuum of recovery from disorders of consciousness, an exploratory and preliminary study. *Funct Neurol* (2011) 26:15–24.
- Formisano R, Pistoia F, Sarà M. Disorders of consciousness, A taxonomy to be changed? *Brain Injury* (2011) 25:638. doi:10.3109/02699052.2011.572948
- Formisano R, D'Ippolito M, Catani S. Functional locked-in syndrome as recovery phase of vegetative state. *Brain Injury* (2013) 27:1332. doi:10.3109/02699052.2013.809555
- Gosseries O, Zasler ND, Laureys S. Recent advances in disorders of consciousness: focus on the diagnosis. *Brain Inj* (2014) 28:1141–50. doi:10.3109/02699052.2014.920522
- Schiff ND. Cognitive motor dissociation following severe brain injuries. *JAMA Neurol* (2015) 72:1413–5. doi:10.1001/jamaneurol.2015.2899
- Fernández-Espejo D, Rossit S, Owen AM. A thalamocortical mechanism for the absence of overt motor behavior in covertly aware patients. *JAMA Neurol* (2015) 72(12):1442–50. doi:10.1001/jamaneurol.2015.2614
- Cooke DF, Graziano MS. Defensive movements evoked by air puff in monkeys. *J Neurophysiol* (2003) 90:3317–29. doi:10.1152/jn.00513.2003
- Graziano MS, Cooke DF. Parieto-frontal interactions, personal space, and defensive behavior. *Neuropsychologia* (2006) 44:845–59. doi:10.1016/j.neuropsychologia.2005.09.011
- Sambo CF, Forster B, Williams SC, Iannetti GD. To blink or not to blink: fine cognitive tuning of the defensive peripersonal space. *J Neurosci* (2012) 32:12921–7. doi:10.1523/JNEUROSCI.0607-12.2012
- Sambo CF, Liang M, Cruccu G, Iannetti GD. Defensive peripersonal space: the blink reflex evoked by hand stimulation is increased when the hand is near the face. *J Neurophysiol* (2012) 107:880–9. doi:10.1152/jn.00731.2011
- de Vignemont F, Iannetti GD. How many peripersonal spaces? *Neuropsychologia* (2015) 70:327–34. doi:10.1016/j.neuropsychologia.2014.11.018
- Bisio A, Garbarini F, Biggio M, Fossataro C, Ruggeri P, Bove M. Dynamic shaping of the defensive peripersonal space through predictive motor mechanisms: when the “near” becomes “far”. *J Neurosci* (2017) 37:2415–24. doi:10.1523/JNEUROSCI.0371-16.2016
- Sussman TJ, Jin J, Mohanty A. Top-down and bottom-up factors in threat-related perception and attention in anxiety. *Biol Psychol* (2016) 121(PtB):160–72. doi:10.1016/j.biopsycho.2016.08.006
- Salinet AS, Panerai RB, Robinson TG. Effects of active, passive and motor imagery paradigms on cerebral and peripheral hemodynamics in older volunteers: a functional TCD study. *Ultrasound Med Biol* (2012) 38:997–1003. doi:10.1016/j.ultrasmedbio.2012.02.016
- Salinet AS, Robinson TG, Panerai RB. Active, passive, and motor imagery paradigms: component analysis to assess neurovascular coupling. *J Appl Physiol* (2013) 114:1406–12. doi:10.1152/jappphysiol.01448.2012
- Malojčić B, Giannakopoulos P, Sorond FA, Azevedo E, Diomedes M, Oblak JP, et al. Ultrasound and dynamic functional imaging in vascular cognitive impairment and Alzheimer's disease. *BMC Med* (2017) 15:27. doi:10.1186/s12916-017-0799-3
- Lassen NA, Ingvar DH, Skinhoj E. Brain function and blood flow. *Sci Am* (1978) 239:62–71. doi:10.1038/scientificamerican1078-62
- Aaslid R. Visually evoked dynamic blood-flow response of the human cerebral circulation. *Stroke* (1987) 18:771–5. doi:10.1161/01.STR.18.4.771
- Aaslid R, Lindegaard KF, Sorteberg W, Nornes H. Cerebral autoregulation dynamics in humans. *Stroke* (1989) 20:45–52. doi:10.1161/01.STR.20.1.45
- Panerai RB, Deverson ST, Mahony P, Hayes P, Evans DH. Effect of CO<sub>2</sub> on dynamic cerebral autoregulation measurement. *Physiol Meas* (1999) 20:265–75. doi:10.1088/0967-3334/20/3/304
- Moody M, Panerai RB, Eames PJ, Potter JF. Cerebral and systemic hemodynamic changes during cognitive and motor activation paradigms. *Am J Physiol Regul Integr Comp Physiol* (2005) 288:R1581–8. doi:10.1152/ajpregu.00837.2004
- Liang X, Zou Q, He Y, Yang Y. Coupling of functional connectivity and regional cerebral blood flow reveals a physiological basis for network hubs of the human brain. *Proc Natl Acad Sci U S A* (2013) 110(5):1929–34. doi:10.1073/pnas.1214900110
- Rosengarten B, Deppe M, Kaps M, Klingelhofer J. Methodological aspects of functional transcranial Doppler sonography and recommendations for simultaneous EEG recording. *Ultrasound Med Biol* (2012) 38:989–96. doi:10.1016/j.ultrasmedbio.2012.02.027
- Wannez S, Heine L, Thonnard M, Gosseries O, Laureys S, Coma Science Group Collaborators. The repetition of behavioral assessments in diagnosis of disorders of consciousness. *Ann Neurol* (2017) 81(6):883–9. doi:10.1002/ana.24962
- Mathew RJ, Wilson WH. Substance abuse and cerebral blood flow. *Am J Psychiatry* (1991) 148(3):292–305. doi:10.1176/ajp.148.3.292
- Shan G, Yining H, Xia H, Yicheng Z, Bo W, Shunwei L. Transcranial Doppler characteristics in persistent vegetative status, locked-in syndrome and brain death. *Chin Med Sci J* (1999) 14(4):211–4.
- Daboussi A, Minville V, Leclerc-Foucras S, Geeraerts T, Esquerré JP, Payoux P, et al. Cerebral hemodynamic changes in severe head injury patients undergoing decompressive craniotomy. *J Neurosurg Anesthesiol* (2009) 21(4):339–45. doi:10.1097/ANA.0b013e3181b1dbba
- Perez-Nellar J, Machado C, Scherle CE, Chinchilla M. TCD diastolic velocity decay and pulsatility index increment in PVS cases. *Can J Neurol Sci* (2010) 37:831–6. doi:10.1017/S0317167100051520
- Donahue MJ, Stevens RD, de Boorder M, Pekar JJ, Hendrikse J, van Zijl PC, et al. Hemodynamic changes after visual stimulation and breath holding provide evidence for an uncoupling of cerebral blood flow and volume from oxygen metabolism. *J Cereb Blood Flow Metab* (2009) 29(1):176–85. doi:10.1038/jcbfm.2008.109
- Harders AG, Laborde G, Droste DW, Rastogi E. Brain activity and blood flow velocity changes: a transcranial Doppler study. *Int J Neurosci* (1989) 47(1–2):91–102.
- Heiss WD. PET in coma and in vegetative state. *Eur J Neurol* (2012) 19:207–11. doi:10.1111/j.1468-1331.2011.03489.x
- Lapitskaya N, Gosseries O, De Pasqua V, Pedersen AR, Nielsen JF, de Noordhout AM, et al. Abnormal corticospinal excitability in patients with disorders of consciousness. *Brain Stimul* (2013) 6:590–7. doi:10.1016/j.brs.2013.01.002
- Bagnato S, Boccagni C, Sant'Angelo A, Prestandrea C, Rizzo S, Galardi G. Patients in a vegetative state following traumatic brain injury display a reduced intracortical modulation. *Clin Neurophysiol* (2012) 123:1937–41. doi:10.1016/j.clinph.2012.03.014

45. Girouard H, Iadecola C. Neurovascular coupling in the normal brain and in hypertension, stroke, and Alzheimer disease. *J Appl Physiol* (2006) 100:328–35. doi:10.1152/jappphysiol.00966.2005
46. Annen J, Heine L, Ziegler E, Frasso G, Bahri M, Di Perri C, et al. Function-structure connectivity in patients with severe brain injury as measured by MRI-DWI and FDG-PET. *Hum Brain Mapp* (2016) 37:3707–20. doi:10.1002/hbm.23269
47. Schiff ND. Recovery of consciousness after brain injury: a mesocircuit hypothesis. *Trends Neurosci* (2010) 33:1–9. doi:10.1016/j.tins.2009.11.002
48. Fridman EA, Beattie BJ, Broft A, Laureys S, Schiff ND. Regional cerebral metabolic patterns demonstrate the role of anterior forebrain mesocircuit dysfunction in the severely injured brain. *Proc Natl Acad Sci U S A* (2014) 111:6473–8. doi:10.1073/pnas.1320969111
49. Monti MM, Rosenberg M, Finoia P, Kamau E, Pickard JD, Owen AM. Thalamo-frontal connectivity mediates top-down cognitive functions in disorders of consciousness. *Neurology* (2015) 84:167–73. doi:10.1212/WNL.0000000000001123
50. Cruse D, Chennu S, Chatelle C, Bekinschtein T, Fernández-Espejo D, Pickard J, et al. Bedside detection of awareness in the vegetative state: a cohort study. *Lancet* (2011) 378:2088–94. doi:10.1016/S0140-6736(11)61224-5
51. Cruse D, Chennu S, Fernández-Espejo D, Payne WL, Young GB, Owen AM. Detecting awareness in the vegetative state: electroencephalographic evidence for attempted movements to command. *PLoS One* (2012) 7:e49933. doi:10.1371/journal.pone.0049933
52. Oishi K, Kasai T, Maeshima T. Autonomic response specificity during motor imagery. *J Physiol Anthropol Appl Human Sci* (2000) 19:255–61. doi:10.2114/jpa.19.255
53. Stender J, Gosseries O, Bruno MA, Charland-Verville V, Vanhaudenhuyse A, Demertzi A, et al. Diagnostic precision of PET imaging and functional MRI in disorders of consciousness: a clinical validation study. *Lancet* (2014) 384(9942):514–22. doi:10.1016/S0140-6736(14)60042-8
54. Schiff N, Ribary U, Moreno D, Beattie B, Kronberg E, Blasberg R. Residual cerebral activity and behavioural fragments in the persistent vegetative state. *Brain* (2002) 125:1210–34. doi:10.1093/brain/awf131

**Conflict of Interest Statement:** The authors declare that the research was conducted in the absence of any commercial or financial relationships that could be construed as a potential conflict of interest.

The reviewer AT and handling editor declared their shared affiliation.

Copyright © 2018 Naro, Chillura, Portaro, Bramanti, De Luca, Bramanti and Calabrò. This is an open-access article distributed under the terms of the Creative Commons Attribution License (CC BY). The use, distribution or reproduction in other forums is permitted, provided the original author(s) and the copyright owner are credited and that the original publication in this journal is cited, in accordance with accepted academic practice. No use, distribution or reproduction is permitted which does not comply with these terms.



# Shining a Light on Awareness: A Review of Functional Near-Infrared Spectroscopy for Prolonged Disorders of Consciousness

Mohammed Rupawala<sup>1\*</sup>, Hamid Dehghani<sup>1,2</sup>, Samuel J. E. Lucas<sup>3</sup>, Peter Tino<sup>2</sup> and Damian Cruse<sup>4</sup>

<sup>1</sup> Centre for Doctoral Training in Physical Sciences for Health, University of Birmingham, Birmingham, United Kingdom,

<sup>2</sup> School of Computer Science, University of Birmingham, Birmingham, United Kingdom, <sup>3</sup> School of Sport, Exercise and Rehabilitation Sciences, University of Birmingham, Birmingham, United Kingdom, <sup>4</sup> School of Psychology, University of Birmingham, Birmingham, United Kingdom

## OPEN ACCESS

### Edited by:

Olivia Gosseries,  
University of Liège, Belgium

### Reviewed by:

Ujwal Chaudhary,  
Universität Tübingen, Germany  
Konstantinos Kalafatakis,  
University of Bristol, United Kingdom

### \*Correspondence:

Mohammed Rupawala  
mxr510@student.bham.ac.uk

### Specialty section:

This article was submitted to  
Applied Neuroimaging,  
a section of the journal  
Frontiers in Neurology

Received: 21 December 2017

Accepted: 30 April 2018

Published: 22 May 2018

### Citation:

Rupawala M, Dehghani H,  
Lucas SJE, Tino P and Cruse D  
(2018) Shining a Light on Awareness:  
A Review of Functional Near-Infrared  
Spectroscopy for Prolonged  
Disorders of Consciousness.  
Front. Neurol. 9:350.  
doi: 10.3389/fneur.2018.00350

Qualitative clinical assessments of the recovery of awareness after severe brain injury require an assessor to differentiate purposeful behavior from spontaneous behavior. As many such behaviors are minimal and inconsistent, behavioral assessments are susceptible to diagnostic errors. Advanced neuroimaging tools can bypass behavioral responsiveness and reveal evidence of covert awareness and cognition within the brains of some patients, thus providing a means for more accurate diagnoses, more accurate prognoses, and, in some instances, facilitated communication. The majority of reports to date have employed the neuroimaging methods of functional magnetic resonance imaging, positron emission tomography, and electroencephalography (EEG). However, each neuroimaging method has its own advantages and disadvantages (e.g., signal resolution, accessibility, etc.). Here, we describe a burgeoning technique of non-invasive optical neuroimaging—functional near-infrared spectroscopy (fNIRS)—and review its potential to address the clinical challenges of prolonged disorders of consciousness. We also outline the potential for simultaneous EEG to complement the fNIRS signal and suggest the future directions of research that are required in order to realize its clinical potential.

**Keywords: disorders of consciousness, functional near-infrared spectroscopy, electroencephalography, motor imagery, data fusion, brain-computer interface**

## INTRODUCTION

In the UK, every 3 minutes an individual is hospitalized due to a traumatic (e.g., fall, assault, motor vehicle accident) or non-traumatic (e.g., stroke, brain hemorrhage, anoxia) brain injury, equating to approximately 300,000 admissions per year.<sup>1</sup> While many patients experience little or no long-term effects, a significant number of patients will develop a prolonged disorder of consciousness (PDOC), such as a vegetative state or minimally conscious state. Patients in a vegetative state [also known as unresponsive wakefulness syndrome (1)] are clinically awake, with eyes open and preserved reflexes, yet appear to be unaware of their surroundings or of themselves [for a detailed

<sup>1</sup><https://www.headway.org.uk/about-brain-injury/further-information/statistics/>.

review of the PDOC states, please refer to Ref. (2)]. Patients in a minimally conscious state exhibit inconsistent but purposeful evidence of awareness, such as visual pursuit and following verbal commands (3).

Partial or full recovery following severe brain injury can in many cases involve transitioning between each of these states (4). The progression is generally smooth (4) and therefore the difficulty lies in accurately determining and diagnosing a patient in a single state using qualitative clinical assessment methods. The need to accurately detect awareness remains a thorough subject of research as misdiagnoses can lead to inappropriate healthcare decisions (5). Standardized behavioral assessments are the current “gold standard” for detecting signs of awareness (6, 7). However, as clinicians must rely on observable behaviors to determine a patient’s level of awareness, it is possible that a significant proportion of patients can be misdiagnosed if they are unable to produce purposeful behaviors due to a motor impairment. Indeed it has been estimated that 15% of patients (8) who meet the behavioral gold standard for vegetative state have a cognitive-motor dissociation (9) or covert awareness (10) that can only be detected with brain imaging.

In the first demonstration of covert command-following, Owen et al. asked a patient who fulfilled all clinical criteria for a diagnosis of vegetative state to undertake two motor imagery tasks in the functional magnetic resonance imaging (fMRI) scanner; the first involved playing a game of tennis and the second, a spatial navigation task, involved imagining visiting the rooms of her house (11). As is seen in healthy individuals when completing the same tasks, significant activity was observed in the patient’s supplementary motor area (SMA) while imagining playing tennis, and in the parahippocampal gyrus, the posterior parietal cortex, and the lateral premotor cortex (PMC) when imagining moving around her house. This brain imaging evidence of the patient following the commands indicated that she was aware, despite the fact that she was unable to demonstrate it with her behavior. Subsequently, by assigning each imagery task to a “yes” or “no” communication output, several patients have been able to answer a series of questions about themselves and their lives (12–15), hinting at the potential for brain–computer interfaces (BCIs) and assistive devices for this patient group. Here, a BCI is defined using the definition proposed by Wolpaw et al.: a device that “provides the brain with a new, non-muscular communication and control channel” [(16), p. 768]. In this context, a BCI serves to directly measure neural activity associated with the users’ intent and translate the recorded signals into corresponding control signals for BCI applications.

Despite the success of fMRI in the field of PDOC, the technology is limited because many patients’ reduced mobility requires them to be transported to advanced facilities that feature such equipment. Furthermore, fMRI systems are unsuitable for those with metallic implants, are highly sensitive to motion artifacts, and require patients to lay supine. A portable, inexpensive, and non-magnetic method for measuring the same hemodynamic response as measured by fMRI could be used to translate the successes of fMRI to the bedside.

The hemodynamic response is a collective term for the set of physiological responses that take place during the onset

of neuronal activations. For example, the blood oxygenation level-dependent (BOLD) signal detected in fMRI systems are sensitive to changes in cerebral blood flow, cerebral metabolic rate of oxygen and cerebral blood volume (17). Increases in these elements during neural activation result in slight increases in the local magnetic resonance signal and thus small changes in the BOLD signal that can be detected by fMRI.

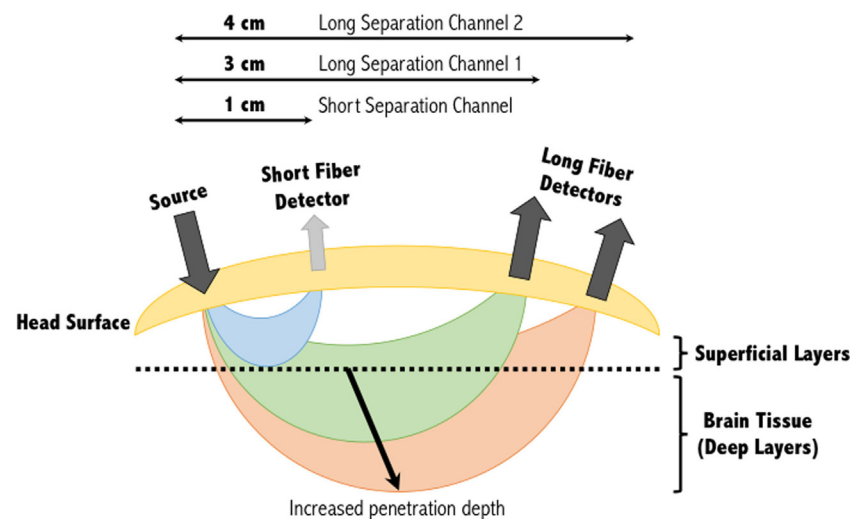
Functional near-infrared spectroscopy (fNIRS) is an alternative method to fMRI that similarly measures BOLD-like hemodynamic responses (18, 19). Furthermore, this method is portable, inexpensive, fast, non-invasive and has limited contraindications (18, 20, 21). Nevertheless, without sophisticated hardware and signal processing techniques, the technology offers significantly reduced spatial resolution, due to the diffuse nature of light propagation in tissue. fNIRS devices detect changes in the concentration of oxygenated ([HbO]) and deoxygenated ([HbR]) hemoglobin molecules in the blood. fNIRS, like fMRI, is an “indirect” neuroimaging tool in the sense that it monitors hemodynamic responses to neural activations on the basis that neural activations are tightly coupled to vascular processes; a process known as neurovascular coupling. Based on these properties, fNIRS has been shown to have a broad spectrum of uses including studies of vision (20), hearing (22), speech (23), learning (24), emotion (25), and pain (26), and as such, recently has also begun demonstrating its use within the field of PDOC (27–29). Furthermore, as a component of neurovascular coupling relies on end to end asynchronous electrical signaling to drive neural activations, there is growing interest in simultaneous electroencephalography (EEG)-fNIRS—both of which share similar advantageous properties (e.g., portability, inexpensive, and non-invasive) (27).

In this review, we provide a basic overview of fNIRS and its instrumentation [for an in-depth review, please refer to Ref. (30)], followed by discussions of its use within the field of PDOC. We explore the current paradigms used to detect awareness and demonstrate how fNIRS both independently and when simultaneously combined with EEG can accurately monitor changes in neural activity. Next, we explore recent advances to improve the spatial resolution of the signal and methods to advance analysis of the hemodynamic response. Finally, we discuss the potential of fNIRS as a BCI to aid in communication and to improve accuracy of clinical diagnoses.

## PRINCIPLES AND fNIRS INSTRUMENTATION

Spectroscopy is based on the study of light signals. In the near-infrared (NIR) range of light, with wavelengths between ~600 and 900 nm, biological tissues are effectively transparent. The low molar absorptivity of lipids and water in this region enables light to effectively penetrate and be maximally absorbed by oxygenated (HbO) and deoxygenated (HbR) hemoglobin (31, 32). These primary light-absorbing compounds in tissue in the NIR range are called chromophores (31). Optical neuroimaging using fNIRS typically requires the use of a set of light-emitting diodes (light sources) on the scalp, and an equal or larger set of detectors,



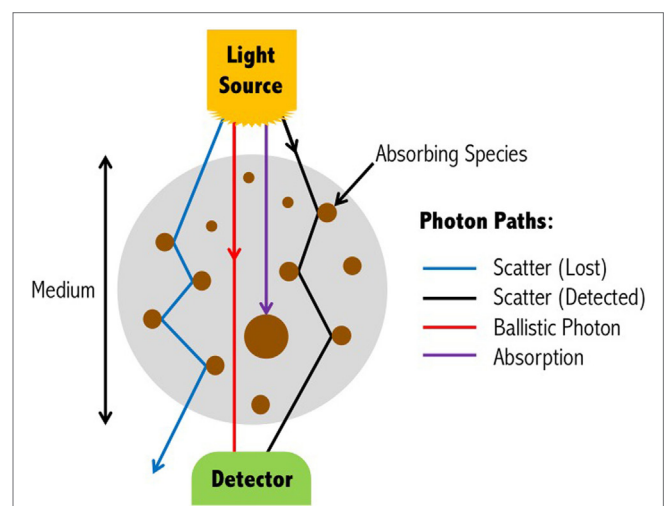


**FIGURE 1** | Banana shape profiles of the sampled functional near-infrared spectroscopy signal at multiple source-detector distances. A single source and detector constitute the simplest NIRS channel. Depending on the source-detector separation distance, and the subjects' skull and scalp thicknesses, the light may or may not sufficiently penetrate the superficial layers to sample the deeper layers. A separation of 3 cm is commonly used, however, increasing this to 4 cm can increase the penetration depth of the light sampled tissues. Short separation channels are located within 1 cm of the source and can provide physiological (noise) data within the superficial layers. This activity can then be regressed from the long separation channel, resulting in a signal corresponding to activity solely within deep brain tissues. Figure adapted from Ref. (34). No permissions were required.

depending on the number of source-detector channels required. NIR light of wavelengths specific to each biological chromophore will be absorbed primarily by that chromophore (HbO, HbR, and cytochrome *c*-oxidase). Scattered light then follows a trajectory back toward the surface of the scalp, in a characteristic “banana” shape, where it is captured and recorded by, for example, photo-detectors (**Figure 1**) (33).

*Absorption* and *scattering* are the two main attenuating interactions that take place between light and tissue (**Figure 2**). As light from a source penetrates through the layers of the head, specific wavelengths will be absorbed by the absorbing (chromophore) components within the different media. The photons that reach the detector on the scalp are primarily those that have scattered within the medium, and therefore have traveled a greater distance than the geometrical (straight-line) distance between the light source and detector. The measured intensity at multiple wavelengths is then used to separate the absorption due to different chromophores. Due to the scattering properties of light on route to the detector, the fNIRS signal has limited spatial resolution of the underlying chromophore concentrations with respect to its location in the head, but contains rich contrast (i.e., a small change in attenuation change will result in a large measured intensity change).

The depth within the skull that can be studied using fNIRS is largely dependent on the inter-optode distance or source-detector separation distance as it is also referred. As a general approximation, the penetration depth achievable is approximately a third to half the source-detector separation distance (21, 36). At greater source-detector separation distances, deeper penetration of light is achieved at the cost of poorly resolved images due to less light being captured by the detector (**Figure 1**). Diffuse optical tomography can improve this resolution by employing a large



**FIGURE 2** | Light propagation paths through a medium. Depending on the wavelength of the emitted light, photons may either be absorbed by the medium, scatter to the extent that they are no longer detectable, scatter and yet be detected, or travel through the scattering medium in a straight-line (ballistic photon). For functional near-infrared spectroscopy devices, ballistic photon paths are highly unlikely to occur due to source and detectors being positioned on the surface of the head, and the light propagating directly into the brain. Figure adapted from Ref. (35). No permissions were required.

number of over-lapping measurements, each generating their own banana-like trajectory. Combining these signals allows a deeper three-dimensional reconstruction of the hemodynamic signals from the brain (37).

Hemodynamic signal integrity can be readily compromised by the effect of superficial layers on the detected signal. These

layers of tissue are assumed to have a constant attenuation effect on the light signal; however, there is a slight effect due to extracerebral signal components (38). The attenuating layers in the head include the skin, scalp, skull, cerebrospinal fluid, gray matter and white matter, in addition to the chromophores within the blood. Of these however, the scalp and skull have been shown to be most significant (39). Traditionally, it was assumed that hemodynamic changes in the overlying tissue layers were uncorrelated with the changes in brain function. However, research has shown that the systemic physiological signals from superficial layers can exponentially decay the light from the emitter (40); that is to say that NIRS measurements are inherently most sensitive (have largest magnitude) to tissue nearest the source and detector (40). Major contributors of physiological interference include heartbeat (1–1.5 Hz) (41), respiration (0.2–0.5 Hz) (42), low-frequency oscillations including Mayer waves (~0.1 Hz) (43), and task-related changes in systemic physiology (44).

The mean scalp plus skull thickness in an adult human is typically 10–18 mm [average modeled values of ~7 mm for scalp and ~6 mm for skull as reported by Ref. (39)]. Okada and Delpy showed that increasing the skull thickness from 4 to 10 mm would result in an 80% loss in NIR signal intensity (45). In contrast, Strangman et al. argued that the scalp consistently had a greater influence on NIRS brain sensitivity than skull (39). In addition, they looked at how source-detector separations could overcome this and found that as separations increased above 20 mm (mean sensitivity of 0.06), the effect of the superficial layers became less influential, with near-maximal sensitivity to brain tissue being achieved at or above 45 mm (mean sensitivity of 0.19) (39). Other methods of effectively detecting absorption changes from deep brain tissues while keeping a normal source-detector separation distance (e.g., 45 mm) include the use of independent component analysis (ICA) (46), principle component analysis (47), and model-based analysis such as the general linear model (GLM) (48).

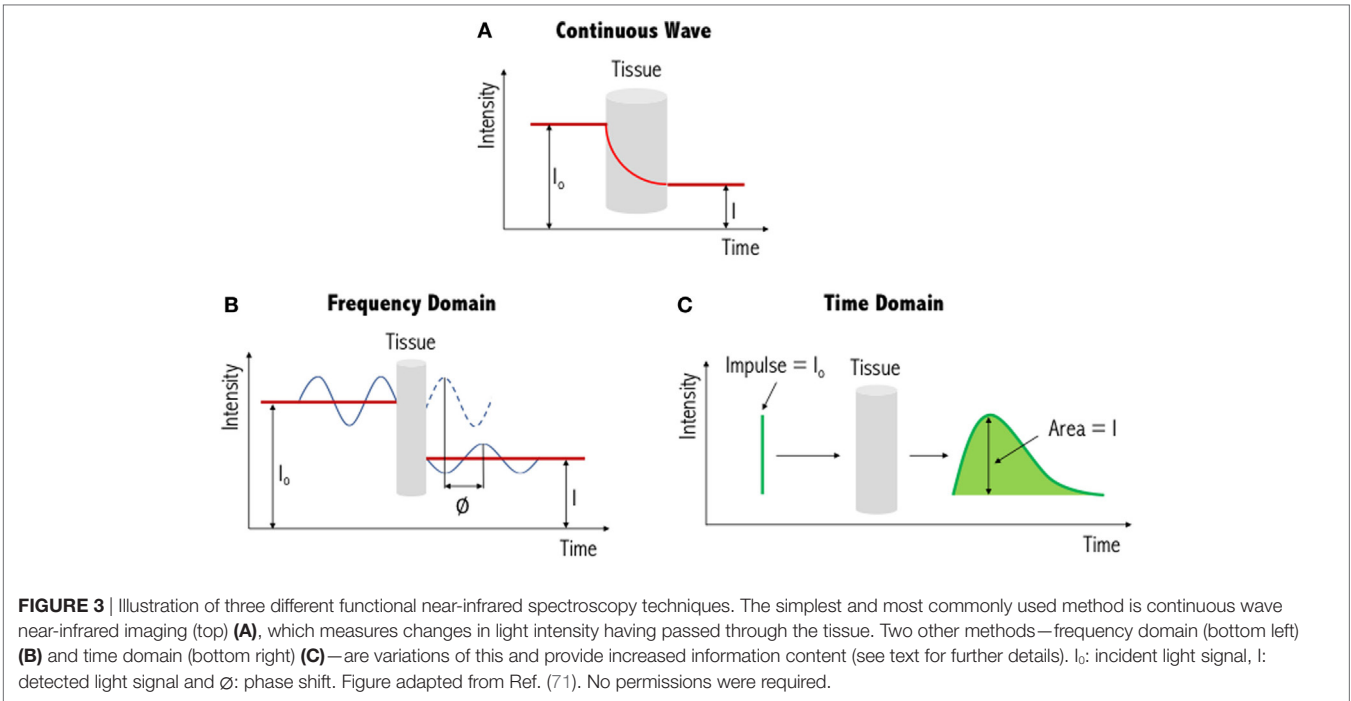
With multiple-distance optodes (i.e., a short separation channel and long separation channel), some groups have shown this method to advance a GLM approach in eliminating superficial effects (49–51). In this approach, short separation detectors that are located in the activation area but have shorter source-detector separation distances (<10 mm) are more sensitive to activity in the superficial layers, whereas the signal received at the long separation detectors are sensitive to both the brain and superficial layers (**Figure 1**). Regressing out the short separation signal from the long separation signal effectively filters out the superficial component [see (44) for more information about how the data from the short separation channel is regressed from that of the long separation channel]. Other approaches to improve deep tissue spatial resolution with multiple-distance probes include the use of multi-distance probes along with ICA (52), and diffuse optical tomography (53). Alternatively, low processing options to eliminate physiological signals include low-pass filtering (only to eliminate cardiac oscillations) (54) and wavelet filtering (55).

According to a recent investigation by Pfeifer et al., the lack of a standardized signal processing method or guideline for fNIRS data is likely to cause novice users to employ data analysis tools provided by commercial companies (i.e., a “black box”) which are unlikely to take into account the parameters of the study (56) and

may increase false positives or false negatives in the final published results (57). Indeed, Pfeifer et al. demonstrated statistical discrepancies between a “black box” signal processing stream, and that of a relatively simple self-implemented signal processing stream that involved motion artifact removal and band-pass filtering of [HbO] and [HbR] data (56). With increasingly widespread use of NIRS devices across biomedical research, the field will clearly benefit from standardization, as adopted in much of fMRI research (e.g., FMRIB Software Library and Statistical Parametric Mapping) (58–63). Furthermore, when using signal processing methods as provided by manufactures, it is paramount that the research team have an advanced understanding of every step to ensure that the data and conclusions are reliable and interpretable.

The three types of systems that are primarily used for NIR imaging are continuous wave (**Figure 3A**), frequency domain (**Figure 3B**) and time domain/resolved (**Figure 3C**). Of these, continuous wave devices are the most common instruments for measuring the fNIRS signal. These devices emit light at a constant intensity and measure changes in the intensity of the re-emerging (i.e., diffusely reflected) light, having passed through the tissues. To quantify chromophore concentrations from the recorded light intensities requires modeling of the medium through which the light has propagated. The earliest model is the Beer–Lambert law, proposed following work by the French mathematician Bouguer in the 1700s (please refer to discussions and citations in (64)). This type of spectroscopy represents a linear relationship between absorbance and concentration of an absorbing species, and as such has been widely used in colorimetric analysis, with similar principles applied to biological tissue. Biological tissue, such as the brain, is a highly scattering environment. To account for such scattering of light, Delpy et al. developed the modified Beer–Lambert law (65, 66). This has been used widely in continuous wave devices as a means to derive concentration changes of each chromophore (HbO, HbR, and total hemoglobin, HbT). In order to gain absolute concentration values, as opposed to the changes in concentration of each chromophore, other methods of chromophore estimation include spatially resolved spectroscopy (67, 68), time-resolved spectroscopy (69), and phase-resolved spectroscopy (70) systems. The output values of these systems can be seen as approximations as several assumptions are used to determine the optical properties of the tissues (i.e., light scattering and absorption coefficients).

In addition to continuous wave measurements, two other diffuse optical measurements that have been developed include frequency domain and time domain fNIRS. In the former, light sources emit light continuously, like continuous wave-fNIRS; however, the amplitude is modulated at frequencies in the MHz range. The absorption and scattering properties of tissues are then obtained by recording the amplitude decay and phase shift (delay) of the detected signal with respect to the incident beam (43). In time-resolved fNIRS, short (picosecond) incident light pulses are introduced into tissues and as they penetrate through the various layers (i.e., skin, skull, cerebrospinal fluid, and brain) the signal is broadened and attenuated. As the photons leave the tissue, the recorded temporal distribution by the time domain system, and the shape of this distribution, provides information about tissue absorption and scattering. Advantages and disadvantages of these three systems are summarized in **Table 1**. From **Table 1**, we can



**FIGURE 3 |** Illustration of three different functional near-infrared spectroscopy techniques. The simplest and most commonly used method is continuous wave near-infrared imaging (top) **(A)**, which measures changes in light intensity having passed through the tissue. Two other methods—frequency domain (bottom left) **(B)** and time domain (bottom right) **(C)**—are variations of this and provide increased information content (see text for further details).  $I_0$ : incident light signal,  $I$ : detected light signal and  $\phi$ : phase shift. Figure adapted from Ref. (71). No permissions were required.

**TABLE 1 |** Advantages and disadvantages of the three commonly used functional near-infrared spectroscopy techniques.

Measurement type	Advantages	Disadvantages	Reference
Continuous wave	<ul style="list-style-type: none"><li>■ High sampling rate</li><li>■ Can be miniaturized—ease in portability</li><li>■ Simple to use</li><li>■ Low cost</li></ul>	<ul style="list-style-type: none"><li>■ Low penetration depth—increased sensitivity to superficial layers</li><li>■ Difficult to separate absorption and scattering</li></ul>	(71, 72)
Frequency domain	<ul style="list-style-type: none"><li>■ High sampling rate</li><li>■ Relatively accurate separation of absorption and scattering</li></ul>	<ul style="list-style-type: none"><li>■ Moderate penetration depth—sensitive to superficial layers</li></ul>	(73, 74)
Time domain	<ul style="list-style-type: none"><li>■ High spatial resolution</li><li>■ High penetration depth—mean time-of-flight and variance values can separate brain tissue from superficial layers</li><li>■ Most accurate separation of absorption and scattering</li></ul>	<ul style="list-style-type: none"><li>■ Low sampling rate—greater loss of photons</li><li>■ Instrument size/weight is larger</li><li>■ Stabilization/cooling required</li><li>■ Costlier system as most advanced</li><li>■ Can be more susceptible to noise—can impact the usefulness of studying variance values</li></ul>	(75, 76)

Table adapted from Ref. (21).

see that while continuous wave fNIRS devices offer a cheap and portable method of rapidly capturing brain hemodynamic activity, their simplicity limits the spatial resolution and the penetration depth that can be achieved in comparison with frequency- and time-domain fNIRS systems.

## MOTOR IMAGERY PARADIGMS WITH fNIRS

Motor imagery is the imagined movement of the body while keeping the muscles still. Motor imagery tasks can provide proxies of command-following for those patients who may be aware but unable to produce purposeful overt behaviors. However, motor imagery-BOLD activation is not always detectable in all participants; indeed, Fernández-Espejo et al. found no appropriate activation in 20% of healthy participants in one study (77).

A variety of motor imagery paradigms have been examined for use with fNIRS (Table 2), the majority of which require activation of the hand and foot areas of the cortical homunculus. Motor imagery tasks can be divided into visual and kinesthetic tasks. In the former, the participant visualizes the movement while in the latter the participant imagines the feelings and sensations produced by the movement. Kinesthetic motor imagery is more often used as it has been shown to recruit more of the cortical motor system (78). Coyle et al. used a continuous wave-fNIRS system to demonstrate that when three healthy participants imagined squeezing a ball, their [HbO] increased reliably above that from rest in the C3 and C4 regions of the motor cortex (based on the EEG international 10-20 system), regions predominantly associated with hand movements (79). Interestingly, after averaging each participants' data over 20 trials, hemodynamics following motor imagery activation could be prominently distinguished by

**TABLE 2** | Comprehensive list of functional near-infrared spectroscopy motor imagery studies, including those that have also been applied within a brain-computer interface (BCI) setting.

	Measurement type	Channel density	Wavelengths (nm)	Reference
Motor imagery	Time domain	4	760, 830	(80, 82)
	Continuous wave	18	760, 850	(83)
	Continuous wave	24	695, 830	(84)
	Continuous wave	24	695, 830	(85)
	Continuous wave	48	695, 830	(86)
Motor imagery-BCI	Time domain	4	760, 830	(87) <sup>a</sup>
	Frequency domain	8	690, 830	(88)
	Continuous wave	2	760, 880	(79)
	Continuous wave	4	760, 870	(89, 90)
	Continuous wave	16	760, 850	(27) <sup>a</sup>
	Continuous wave	20	780, 805, 830	(91)
	Continuous wave	24	695, 830	(92)
	Continuous wave	24	695, 830	(93)
	Continuous wave	24	695, 830	(92)
	Continuous wave	24	695, 830	(94)
	Continuous wave	24	695, 830	(95, 96)
	Continuous wave	24	760, 830	(97)
	Continuous wave	24	760, 850	(98)
	Continuous wave	24	780, 805, 830	(99)
	Continuous wave	31, 14	780, 805, 830	(100)
	Continuous wave	34	760, 830	(101)
	Continuous wave	40	760, 830	(102)
	Continuous wave	45	780, 805, 830	(103)
	Continuous wave	48	780, 805, 830	(104)
	Continuous wave	50	780, 805, 830	(105)
	Continuous wave	50	780, 805, 830	(106, 107)
	Continuous wave	52	695, 830	(108)
	Continuous wave	52	780, 830	(109)
	Unknown	1	700, 880	(110)
	Unknown	24	740, 808, 850	(111)

Included are the types of measurements being recorded, channel density, and the types of wavelengths being operated.

<sup>a</sup>Indicates studies that have been conducted on patients with prolonged disorder of consciousness or locked-in-syndrome (please refer to **Table 3**).

eye from that of baseline prior to signal processing. Although this may indicate that such experimental paradigms can generate profound neuroactivational changes, it is important to note that their findings were based off a small cohort of three participants. Nevertheless, the authors were further able to show that, by solely studying HbO changes, motor imagery could be used to correctly classify a user's intent ~80% of the time. Other types of motor imagery paradigms that have established significant hemodynamic signal changes with fNIRS include tennis arm-swinging motion (80) and a finger tapping sequence (81).

Aside from these, of popular interest with fNIRS is the ability to differentiate activations from left- and right-hand movements whether that be tapping, gripping or flexing of the wrist. Sitaram et al. reported that fNIRS recordings of motor imagery for left- and right-hand tapping were similar to motor execution recordings, but smaller in magnitude (91). Nevertheless, from the data it was clear that the hemodynamic responses for left-hand and right-hand motor imagery had distinct patterns that could be used by a classifier to discriminate between the two classes. As such, the researchers of this study were able to achieve approximately 89% accuracy using their classifier, with similar results being achieved

by others (87% accuracy achieved when distinguishing between imagined right-wrist and left-wrist flexion) (91, 101).

To add to the hand tapping motor imagery paradigm, recently there has been significant interest in separating left and right foot tapping's using fNIRS. When using a four-class motor imagery paradigm (left/right foot/hand) in a BCI setting, Batula et al. achieved an average classification accuracy of approximately 46% over three participants (chance = 25%; two participants had a classification accuracy over 50%) (93). Nevertheless, the authors suggested that improved performance could be achieved by utilizing more informative features or classifiers through a more detailed inspection of the activation patterns, or a better selection of motor tasks. However, from their confusion matrix, it can be seen that right foot was most frequently misclassified. This is not surprising as distinguishing between left and right foot using fNIRS is challenging as the foot motor areas are near or within the longitudinal fissure between brain hemispheres (112). Nevertheless, improvements to classification accuracies could be achieved by using a single "feet" or leg motor imagery task (113), or by providing feedback training to strengthen the participants motor imagery abilities (114).

Many of the NIRS systems currently employed in motor imagery research are continuous wave (**Table 2**), and so require extensive montage (source and detector layout) development and data processing. However, time domain-NIRS devices have the potential to enhance depth sensitivity as they record the arrival times of individual photons to build a distribution of times of flight (115, 116). Early work by Abdalmalak et al. assessed the feasibility of time domain fNIRS to detect brain activity during motor imagery (80). Seven participants performed tennis-playing imagery of which four showed prominent activity in either the PMC alone or PMC and SMA, as detected by fMRI. During the task, increases in blood flow and volume in the PMC and/or SMA led to an increase in light absorption, and thus a decrease in the number of photons,  $N$ , reaching the detector and their mean time-of-flight,  $\langle t \rangle$ . These changes in  $N$  and  $\langle t \rangle$  precisely occurred during the onset of motor imagery and not during rest for the four participants that likewise showed fMRI activity. On a small scale, this study demonstrated good agreement between both imaging modalities, strengthening the argument for the use of fNIRS in motor imagery. However, in three of the seven healthy participants, who were demonstrably aware, no activity was detected by either imaging modality. While no method will be perfectly sensitive (77), it is clear that considerably greater levels of sensitivity are required before this method may be used clinically. Therefore, the same authors tested 15 healthy participants with the same tennis-playing imagery task and instead evaluated the mean and variance, which have greater depth sensitivity, and report sensitivity values between 86 and 93% in the SMA and PMC, the highest being for  $\langle t \rangle$  as the data are less influenced by noise (82). Furthermore, of the 15 participants that took part in the study, 93% generated responses that were detectable by fMRI and 87% by fNIRS, a considerable improvement over their earlier work (80) and a clear demonstration of the power of advances in physical and computational methods to improve detection of clinically meaningful information from fNIRS signals. These promising results also confirm that time domain



fNIRS is an alternative means of reducing scalp contamination and for enhancing the sensitivity to brain activity, and thus may be a well-suited tool for use on patients with PDOC. To the best of our knowledge, time domain fNIRS data have not yet been reported in patients with PDOC.

Research in patients with PDOC has, however, been accomplished using other fNIRS devices. Molteni et al. detected residual functional activity in two minimally conscious state patients using a commercially available NIRS device (although undefined in the manuscript) and a protocol that involved somatosensory, passive movement, and active movement stimulations (28). While somatosensory stimulation (using a vibrating pillow) elicited a weak response over the somatosensory cortex, passive movement stimulation (hand movement with the assistance of the experimenter) generated clearer hemodynamic responses (increase in HbO, decrease in HbR). Active movement tasks (self-performed hand opening and closing) generated the weakest hemodynamic response in the hand region of M1 in both patients; however, this was expected as the patients were unable to move their hands autonomously and showed no signs of engagement with the task. Furthermore, their T1-weighted MRI brain scans indicated the presence of severe atrophy that could have allowed for fluid accumulation. An excess in cerebrospinal fluid would have increased the attenuation of the NIRS signal (see earlier discussions) thereby reducing the chance of a measurable response to the task. Overall, as a primary study, the authors were able to show that residual brain activity can be detected in patients with PDOC using fNIRS and favors the use of motor imagery as a means of overcoming the need for patients to execute movements, which may not always be possible.

In a study by Kempny et al., 16 patients (11 in a minimally conscious state and 5 in a vegetative state) performed a kinesthetic motor imagery task of squeezing a ball with their right-hand whilst being evaluated with continuous wave-fNIRS (27). In addition, healthy participants were asked to physically perform and kinesthetically imagine the same task in order to obtain patterns that could be used to validate responses in patients with PDOC. A typical fNIRS response to movement and motor imagery is an increase in the [HbO] accompanied by a less pronounced decrease in the [HbR] (117, 118). However, the groups in this study exhibited two types of responses during motor imagery; the typical responses and an inverted response (decrease in [HbO] and an increase in [HbR]). Furthermore, minimally conscious patients, in comparison with those in a vegetative state, more often exhibited a hemodynamic response that was similar to that of healthy participants. Fluctuations in hemodynamic patterns have been shown to depend on the location of the probe and the difficulty of the task (106), highlighting the importance of normative data from healthy individuals against which to compare a given patient's response. Kempny et al. further identified that the greatest reduction in [HbO] was found on the right hemisphere of the head across all three groups during motor imagery (27). Regions of hemodynamic activation were in line with previous studies (118, 119), with greater activation observed on the ipsilateral side [see (95) for similar results]. While this may seem unusual as one would expect primarily activation of the contralateral areas during hand motor imagery,

Batula et al. demonstrated that this is not always the case, in particular when the left-hand is involved, which generated a more bilateral activation pattern during motor imagery (95), a pattern confirmed by fMRI (120, 121).

The above studies demonstrate the feasibility of fNIRS in the field of PDOC. However, there is much to do to ensure that the signals measured are sufficiently reliable and interpretable for use in clinical contexts. Below we suggest one potential means of achieving that goal.

## SIMULTANEOUS EEG-fNIRS

One means of improving the sensitivity of fNIRS, while maintaining portability, is to combine it with simultaneously acquired EEG. During neural activity, glucose and oxygen are rapidly consumed from the local capillary bed. This reduction in metabolites stimulates the brain to increase local cerebral blood flow and cerebral blood volume. A number of models have been proposed that both physiologically and mathematically demonstrate the association between electrical and hemodynamic responses (122, 123), strengthening the existence of neurovascular coupling. This has led some to even study the phenomenon at the bedside, highlighting the delay in the vascular response in comparison to neural activation during stimulus onset (124). As such, this reinforces the argument for the simultaneous use of fNIRS along with an electrophysiological method to better understand the underlying brain activity in patients with PDOC.

During neural activity, summation of ionic fluxes across large numbers of synchronously activated neurons (dipoles) can cause changes in electric fields that can be measured directly using EEG with high temporal resolution (millisecond timeframe). EEG passively measures scalp surface potentials and has been widely explored for identifying covertly aware patients (125) and monitoring rehabilitation success (126) within the field of PDOC [for a detailed overview of EEG, see Ref. (127)]. EEG shares many advantageous properties with fNIRS including its portability, low cost and non-invasiveness. Nevertheless, EEG is prone to blink artifacts, which can be readily eliminated with the use of computational tools such as ICA (128). Alternatively, and depending on the outcomes of the study, participants could close their eyes; however, this can corrupt task-related signatures with physiological noise (129, 130). For example, Verleger reported that refraining from blinking lowered the amplitude of the characteristic P3 peak (a positive-going component of an EEG signal) during an auditory task (130). In addition to ocular movements, the spatial resolution of EEG can be relatively poor. This is due to the spatial smearing of the EEG signal, through a process known as volume conduction (131), as each dipole exerts influence in nearly all directions and not just on the scalp immediately above the dipole. Computational tools, such as the use of spatial filters [e.g., the surface Laplacian (132)], offer a solution to improve the spatial resolution of the dataset. However, this can be further enhanced when EEG is used simultaneously with fNIRS, because the improved spatial resolution offered by fNIRS can provide some degree of information regarding the active source's location, thus complementing EEG findings.

Demonstrating the link between brain hemodynamics and electrophysiology, Zama and Shimada reported a strong correlation in healthy individuals between the magnitudes of the change in HbO in contralateral PMC and the EEG-detected readiness potential approximately 1,000 ms before movement onset (133). As both electrical and optical tools measure different aspects of brain activity and do not interfere with one another, there is also potential that simultaneously acquired EEG and NIRS data will contain complementary information about brain activity and/or neurovascular function that cannot be observed when using these systems independently.

While EEG electrode positioning is commonly based on the International 10-20 and 10-10 positioning systems, there is no accepted standard for NIRS optode placement on the scalp, although attempts have been made to match the International 10-20 system used in EEG (134). Low electrical impedance is desired for high-quality EEG because neural signals are small (microvolts) relative to background noise (135). This is achieved by using electrode pastes and gels. Improving optical coupling for fNIRS devices is achieved by increasing the efficiency of light transmission between the optode and the head. Light can be lost both at the source and the detector if air gaps are introduced (136); however, this loss can be minimized if optodes are positioned in direct contact with the scalp surface. During simultaneous use, electrode gels and pastes on the scalp for EEG recording can negatively impact the transmission of light for fNIRS. Giacometti and Diamond designed an EEG-fNIRS head probe that linked NIRS channels through EEG electrodes (137). Their head probe can stretch to fit a wide range of head sizes and account for head shape variability while maintaining contact pressure on the scalp. Furthermore, relative to other commercial products, their head probe was found to have improved accuracy (i.e., the sensor is placed on the location where it corresponds with the EEG 10-10 standardized system, 83.2%) and precision (i.e., the sensor is placed on the same location on a particular head every time, 39.5%). This design is, however, limited by the number of combined optode-electrodes that can be positioned on the scalp (**Figure 4**). Cooper et al. designed an integrated opto-electrode probe that housed both an EEG electrode and an optical fiber bundle (138). With this device, they observed a hemodynamic response during a finger-to-thumb opposition task alongside an EEG readiness potential. Open-source and commercial hardware is therefore available to promote research into simultaneous EEG-fNIRS for detection of covert consciousness and cognition.

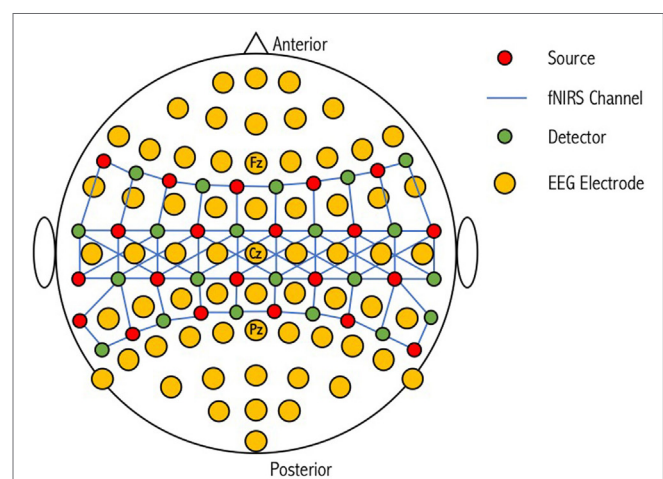
## Simultaneous EEG-fNIRS in BCI Applications

The majority of EEG-fNIRS studies have been within the field of BCIs. BCIs are used for several applications including spelling devices, environmental control, navigation in virtual reality, simple computer games, cursor control applications, and control of prostheses and robotic arms (139–142). The most commonly studied signals in BCI are those of EEG. Neuronal oscillations observed in EEG are categorized into five specific frequency bands: delta, <4 Hz; theta, 4–7 Hz; alpha, 8–12 Hz [also known as mu activity when recorded from sensorimotor areas (143)]; beta, 12–30 Hz, and gamma >30 Hz. A decrease in oscillatory

activity in a specific frequency band is known as an event-related desynchronization, whereas a corresponding increase is called an event-related synchronization. Event-related desynchronization/synchronization patterns are produced in motor imagery as a result of mu and beta frequency band activity within the EEG signal (144). There have been several applications of EEG-based BCI in the field of PDOC, rehabilitation, and for other conditions resulting from a traumatic brain injury or motor impairing disease [for a detailed list of references, please refer to Ref. (145)].

In fNIRS BCI, features for classification are mostly extracted from hemodynamic signals (HbO, HbR, and HbT), such as peak amplitude, mean value, variance, slope, skewness, kurtosis, wavelet transform, and those from genetic algorithms (146). A combination of these then makes a training set that are used to train a classifier (supervised learning) before applying a test data set for it to detect brain-signal patterns (147). For a two-class problem (i.e., left- and right-hand imagery) support vector machines (SVM) are greatly favored, as they attempt to maximize the distance between the separating hyperplane and the nearest training points—or so-called support vectors (146). Other classifiers include linear discriminant analysis (LDA), artificial neural networks, and hidden Markov models (148). The classified signals are then sent to an external device to generate the desired response. In neurofeedback tasks, the response is a display of the accuracy of the users' intent, based on their brain activity allowing self-regulation of brain functions.

There has been a growing interest for the use of fNIRS BCI as a communications device for patients in a locked-in state. Locked-in-syndrome (LIS) is a condition in which patients are aware but have limited or no means to move or communicate (149). As a result, they share similar challenges as those diagnosed with PDOC (i.e., patients in an early minimally conscious



**FIGURE 4** | Schematic representation of a combined optode-electrode head probe. The electroencephalography (EEG) international 10-20 positioning system is used to form the base for 64 EEG electrodes. NIRS sources and detectors are then placed in close proximity to these electrodes to form corresponding channels of different lengths. An increase in the number of sources and detectors used results in an increase in channel complexity and an overall improvement in the resolution of the sampled tissue. Figure adapted from Ref. (100). No permissions were required.

state are clinically aware but can lack the mobility to respond to commands). Naito et al. examined the ability of patients with LIS to communicate “yes” or “no” answers to several questions through either performing a mental calculation or by mentally singing (assigned “yes”), or by staying mentally relaxed (assigned “no”) (150). Frontal lobe activity was measured using a self-devised continuous wave-NIRS device, and the extracted amplitude and phase data were used in a discriminant analysis to classify the patients’ response. Of the 17 patients with LIS participating in the study, only 40% (i.e.,  $n = 7$ ) had significantly differentiating responses. From these seven patients, the average rate of correct detection of their intention was 80%. The limited applicability of this BCI in patients with LIS can be accounted for by the lack of specificity of optode placement, as well as the partial filtering applied to the dataset. A low pass filter with a cutoff frequency of 0.1 Hz was applied, and hence this may not have completely eliminated Mayer waves, which are known to readily corrupt the NIRS signal when sampled from the superficial layers (110).

Functional near-infrared spectroscopy is a relatively novel technique in the field of motor imagery-based BCIs, with EEG still viewed by many as the gold standard. **Table 2** displays a list of several fNIRS motor imagery studies, with the majority being extended for use in BCI research. On the whole, there is widespread use of continuous wave-fNIRS devices as these low-cost instruments are relatively easy to set up and use. The number of channels used for a study ranges between 1 and 52; however, this is dependent on the number of sources and detectors available for a particular device and the region of the head it is required to cover. Furthermore, those studies using less than 24 channels have generally been experimental for example to test novel probe or sensor designs. With respect to the type of wavelengths used, these range between 695 and 850 nm, all of which are within the acceptable limits to measure changes in the biological chromophores. More complex and costlier instruments such as time domain (see section 3) and frequency domain fNIRS have had far less use within this research community. Koo et al. demonstrated the reliability of a hybrid (fNIRS and EEG) self-paced motor imagery-based BCI using a frequency domain NIRS system (88). Here, self-paced motor imagery is where the onset of motor imagery is not known, and neither are the brain signals corresponding to the detected motor imagery (in cue-based motor imagery, the start or cue of the motor imagery is known, hence a BCI system can recognize the motor imagery from the participants brain signals). While a frequency domain system was used for the study, which aided in the hybrid BCI achieving true positive rates of 88% (i.e., the BCI well recognized the intentions of the participants), it was clear that no phase data was extracted and analyzed, and thus the instrument was analyzed as if it were a continuous wave system. The majority of work using frequency domain systems has not yet extended beyond motor execution studies (i.e., tapping tasks), with those using the device either evaluating both time-domain and frequency domain (phase) parameters (151), or fast optical signals (152, 153) [see Ref. (73, 154) for more information regarding fast optical signals and event-related optical signals].

Several research groups have opted for a hybrid BCI approach whereby NIRS features are used to support and complement

EEG-based BCI. Fazli et al. conducted motor execution and EEG-based, visual feedback controlled motor imagery tasks on 14 healthy right-handed volunteers, requiring them to perform left- and right-hand gripping (98). Twenty-four fNIRS channels (8 sources and 16 detectors) and 37 EEG electrodes were used for data acquisition. The NIRS data were then low pass filtered (0.2 Hz) and baseline corrected before using the modified Beer–Lambert law to calculate concentration changes of hemoglobin. Time-averaged concentration changes (HbO and HbR), using a sliding window, were then used as features for LDA classification. EEG band-pass filtered coefficients in the alpha and beta bands were spatially filtered using a method known as common spatial patterns (155) before the LDA classifier was computed. The LDA results from EEG, [HbO], [HbR], and combinations of all three were fed into a meta-classifier before testing. On average for motor imagery, combining EEG with either [HbO], [HbR], or both, had a classification accuracy of approximately 82%, statistically significant than the accuracies of the individual methods (EEG: ~78%, HbO: ~72%, HbR: 65%). However, it has recently been shown that both age and feedback can affect motor imagery patterns during simultaneous EEG-fNIRS data acquisition (83).

Use of a large number of fNIRS channels and/or EEG electrodes during simultaneous EEG-fNIRS acquisition can in some cases be suboptimal due to the high dimensionality of the data and the associated computational costs during classification. One approach to dimensionality reduction is the widely used EEG spatial filtering method of common spatial patterns. Importantly, applying this method to fNIRS data will align the EEG and fNIRS processing streams, allowing for more meaningful comparisons across modalities while improving classification accuracies when used simultaneously in BCI applications. The common spatial patterns method in multichannel EEG (155) efficiently reduces the number of features for classification to those that have highly discriminative properties between tasks. Conversely, in fNIRS, the majority of published studies have employed channel-wise HbO and HbR as features for classification (89, 102). This high feature dimension space requires more trials and a longer training time to train the classifier—first introduced by Bellman as the “curse of dimensionality” (156). Furthermore, a high feature dimension may increase the complexity and instability of the classifier. Zhang et al. evaluated a common spatial patterns algorithm on multichannel fNIRS data and found significant improvement in classification accuracy in both motor execution and motor imagery tasks relative to a conventional high dimension feature space (average accuracy with 180 feature dimensions—54%, average accuracy with 18 feature dimensions derived from common spatial patterns—74%) (111). A benefit of high density EEG is that the whole head coverage allows the researcher to confirm the physiological plausibility of the spatial pattern maps associated with each task—i.e., is the activity restricted to electrodes over contralateral sensorimotor cortices for hand imagery? The fNIRS probes used in the work by Zhang et al. were positioned over the motor cortex as this region is primarily activated during a hand tapping task (111). While focusing on a small area of the scalp is beneficial from the perspective of statistical multiple-comparisons and data



dimensionality, it is not possible to ensure that the recorded hemodynamic changes are physiologically plausible, or whether they reflect a general amplification in blood flow across the entire brain. Therefore, future fNIRS research could extend toward greater scalp coverage so as to minimize the research gap and align the common spatial patterns methods of fNIRS with those of EEG, while aiming to balance the benefits against the increased preparation time and reduced portability and comfort of whole-head systems.

Recently, there has been interest into the use of a “few-channel” approach for BCIs, based on previous research demonstrating focal neural activation in specific motor tasks. Ge et al. demonstrated the accuracy of a few-channel BCI using EEG-fNIRS on participants conducting a left- and right-hand gripping motor imagery task (100). To validate which few-channels to use for the BCI (i.e., feature extraction and classification steps), the initial paradigm was performed simultaneously using a 64-channel EEG electrode set and 52-channel fNIRS set. Of these 52-channels however, 31 (11 detectors and 11 sources) were placed over the sensorimotor cortices (C3-Cz-C4 in 10-20 nomenclature). From the 64 EEG and 31 fNIRS channels, electrodes at positions C3, Cz, and C4 and 14 fNIRS channels (6 sources and 6 detectors) centered around C3 and C4, were used for the few-channel EEG-fNIRS BCI, as these showed distinct neural activity during both left and right motor imagery tasks [see **Figure 3** in Ref. (100) for further information on the montage layout]. Following feature extraction, fusion of both EEG and fNIRS datasets, and classification using SVM, the researchers were able to demonstrate that few-channel EEG-fNIRS had a significantly higher classification accuracy for 11 out of 12 participants than either of the individual modalities (average classification accuracies: EEG—75%, fNIRS—57%, EEG-fNIRS—81%) (100).

In the validation step, source analysis for both the 64 EEG and 31 fNIRS channels was performed to localize the neural signals during the motor imagery task. Source analysis effectively attempts to solve the question of what brain tissues/areas are being probed by a given measurement. In EEG, source analysis involves estimating solutions to the ill-posed inverse problem. Due to the effects of volume conduction, sources (i.e., dipoles) all over the brain may contribute to a measured signal at the scalp. However, an infinite number of source configurations (i.e., radial and tangential) may generate a particular pattern of voltage at the scalp (127). Source analysis thus requires estimating the final surface voltage pattern and then working backward to determine which neural sources generated that voltage pattern. As a result of this, the inverse problem can be seen as a NP-hard (non-deterministic polynomial-time hard) problem, where no absolute answer is available. Nevertheless, several methods are available, based on certain assumptions, to obtain approximate solutions (157, 158). In fNIRS, the question for source analysis becomes more specific as we aim to understand the depth penetration of the instrument. Light propagation through scattering media, such as the head (heterogeneous structure) is inherently complex and as such mathematical models of this process (radiative transport equation and its diffusion equation) are difficult to solve analytically

(74). Estimations can however be made by solving the diffusion equation for optically homogenous tissues with infinite, semi-infinite, or slab boundary conditions (159, 160). Two types of numerical approaches can also be used to gain information about sensitivity and penetration depth in complex tissue: (1) approaches based on finite element and finite difference analysis or (2) Monte Carlo simulations of photon propagation through the tissue. The latter was used by Strangman et al. to highlight that an increase in source-detector separation increased sensitivities of higher level gray matter samples, however at the cost of exponentially decaying sensitivity in-depth penetration (161). Returning to the study of Ge et al., standardized low-resolution electrical tomographic analysis (158) was used to compute an inverse solution for the EEG motor imagery data, whereas digitized points and topographical maps of the changes in HbO, superimposed onto the surface of a standard three-dimensional head model, were used for the fNIRS data (100).

These methodological advances have ultimately aided efforts to improve BCI communication in patients with LIS at the bedside (162, 163). Most recently, Chaudhary et al. demonstrated that patients with LIS could be trained (using feedback) to directly communicate through their hemodynamic signatures “yes” and “no” answers to a number of individually tailored personal questions (163). Patients were specifically asked to think (not imagine) “yes” or “no” when answering the auditorily presented questions while data were recorded from frontocentral brain regions. In the training period, questions with known “yes” or “no” answers were presented. However, to add to the complexity, the trained classifier was then tested using open questions (e.g., quality of life questions: “You have back pain”) to which only the patient could answer. Findings demonstrated that when most patients were instructed to answer “yes” there was an increase in oxygenation that was not followed by a decrease when providing a negative response. As such, the mean relative change in [HbO] across each of the channels was used as a feature to train the SVM classifier through a fivefold cross-validation procedure. Overall, in three quarters of patients it was found that the correct response rate for feedback and open question sessions exceeded 75%. This study marks a huge leap in the capabilities of fNIRS BCI, especially when compared to the study a decade ago by Naito et al. (150). Furthermore, in many cases, it sets the stage for the use of simultaneous EEG-fNIRS BCI in patients with PDOC. Nevertheless, caution should be taken since these results were based off a small cohort of four patients. Additionally, the underlying neurocognitive mechanism is unclear, as responses were not detected via a proxy mental action (i.e., in motor imagery) but by apparent processing of the “correctness” of the statements—i.e., that they were indeed experiencing back pain, rather than that they were performing a mental behavior to signal that they were experiencing back pain. The lack of a clear neurocognitive model may impede its utility in a wider patient group.

This school of thought is opposed to the more widely used method of using proxy behaviors for communication—e.g., imagining playing tennis to answer “yes.” This approach importantly does not rely on unclear models of neurocognitive processing but makes use of a clear signal of volitional



command-following. However, command-following places higher cognitive demands on the communicator as they must map the appropriate response onto an arbitrary behavior and produce that behavior. Conversely, the approach of Chaudhary et al. (163) assumes that the communicator's passive experience of the correctness of the statement is sufficient to provide the communicative output and is therefore a potentially more functional method for patients with limited cognitive resources as a result of brain injury.

In a recent comparison to the continuous wave device used by Chaudhary et al. (163), which is prone to be increasingly sensitive to light absorption in superficial layers and thus less reliable at detecting brain activity, Abdalmalak et al. (87) tested their previously designed four-channel time-resolved fNIRS system (80, 82), which enhances depth sensitivity by discriminating between early and late arriving photons (see previous discussions between continuous wave and time domain systems). With this technique, they detected motor imagery (imagining playing tennis) from a patient who was diagnosed with an acute form of locked-in-state. Furthermore, by using motor imagery as a proxy for communication and by analyzing the mean time-of-flight signals (converted to HbO and HbR and classified using SVM), they detected yes/no responses to a series of questions addressed to the same patient. The accuracy of the answers was confirmed by the patient's residual eye-movement communication channel. While this method has the potential to be translated to patients with PDOC, postinjury functional reorganization of the brain may affect the choice of probe placement, and ischemia or hematoma can impede scattering and absorption of light. As such, structural imaging data would contribute significantly to increasing the accuracy of fNIRS BCI methods. Furthermore, it is necessary to take into account any medications or sedatives used by the patient, as some are known

to cause hemodynamic fluctuations that could be misinterpreted as being task-related (164).

## FROM COMMUNICATION TO ADVANCES IN REHABILITATION

Improving diagnostic accuracy and establishing a means of communication between clinicians and patients has been a significant goal of the field of PDOC over the last two decades. However, there has also been significant research into potential therapies and treatments via pharmacological interventions and neuromodulation techniques, such as deep brain stimulation and spinal cord stimulation (165–167). fNIRS provides a non-invasive means of quantifying the neurophysiological and neurocognitive impact of these approaches.

Unlike deep brain stimulation where an electrode is implanted directly within the brain rupturing the safety of the blood–brain barrier to external pathogens, in spinal cord stimulation the electrode is implanted in the epidural space to stimulate the ascending transmission pathways and regulate the awareness circuit (e.g., the mesocircuit) (168, 169). This method has been applied to PDOC with some promising effects. Kanno et al. reported that 54% of patients (109 out of 201) in a vegetative state began demonstrating purposeful behaviors (170), whereas Yamamoto et al. reported 70% of patients (7 out of 10) recovered from the minimally conscious state (i.e., demonstrated functional interactive communication and/or functional use of two different objects) following spinal cord stimulation use (166). Spinal cord stimulation is known to enhance cerebral blood flow and increase cerebral glucose metabolism (166, 168, 171), stimulate neurotransmitter and neuromodulator release (171, 172), and excite nerve conduction and electrical activity within regions of the brain (168, 171). This multitude

**TABLE 3 |** Summary of the current literature using functional near-infrared spectroscopy (fNIRS) in patients with prolonged disorder of consciousness (PDOC) or locked-in-syndrome (LIS).

Diagnosis	Number of patients	Overview of main results	Reference
PDOC	2—MCS	<ul style="list-style-type: none"> <li>Functional activation (i.e., [HbO] and [HbR]) during passive and somatosensory stimulation</li> <li>Weak brain activations during active hand opening and closing</li> </ul>	Molteni et al., 2013 (28)
PDOC	5—UWS/VS 11—MCS	<ul style="list-style-type: none"> <li>Hemispheric differences during motor imagery of squeezing a ball with the right hand</li> <li>Patients in a minimally conscious state shared fNIRS profiles similar to healthy participants</li> </ul>	Kempny et al., 2016 (27)
PDOC	7—UWS/VS 2—MCS	<ul style="list-style-type: none"> <li>In eight of the nine patients, spinal cord stimulation for 30 s induced sustained cerebral blood volume changes in the prefrontal cortex (an area important in the consciousness system; measured through an increase in [HbT])</li> <li>An inter-stimulus interval of 2 min significantly improved amplitudes of the HbT across blocks</li> </ul>	Zhang et al., 2018 (29)
LIS	40	<ul style="list-style-type: none"> <li>The intentions of 23 patients were successfully detected (80% correctly identified) by assigning different mental tasks to “yes” and “no” responses</li> </ul>	Naito et al., 2007 (150)
LIS	1	<ul style="list-style-type: none"> <li>The responses to open sentences were detected by instructing the patient to think “yes” and “no” to several questions</li> <li>72% of responses were correctly identified at the bedside</li> </ul>	Gallegos-Ayala et al., 2014 (162)
LIS	4	<ul style="list-style-type: none"> <li>Communication using open sentences was established by instructing the patient to think “yes” and “no” to several questions</li> <li>For three out of the four patients, classification accuracies exceeded 75%</li> </ul>	Chaudhary et al., 2017 (163)
LIS	1	<ul style="list-style-type: none"> <li>Without any prior training, tennis-playing motor imagery was used successfully by a patient as a proxy to communicate responses to three questions</li> <li>Results were confirmed by the patient's residual eye-movement communication channel</li> <li>Responses were similar to that of healthy participants performing the same task</li> </ul>	Abdalmalak et al., 2017 (87)

MCS, minimally conscious state; UWS, unresponsive wakefulness syndrome; VS, vegetative state.

of effects may ultimately come together to enhance the recovery process of such patients.

Assessing brain responses during spinal cord stimulation in patients in a minimally conscious state has previously been achieved using EEG. Previous studies have shown significantly altered relative power and synchronization in the delta (1–4 Hz) and gamma (30–45 Hz) bands in the frontal areas following spinal cord stimulation (173), with gamma activity in the frontal cortex causing transient global effects (widespread connectivity and network alterations) and long-lasting local effects (local connectivity alternations that persist beyond stimulation) (174). The drawback with EEG, however, is that brain responses during spinal cord stimulation cannot be measured in real-time due to interference from the stimulator's electrical field. fNIRS on the other hand is not limited by this issue.

Using an eight-channel fNIRS device (device type not specified in the manuscript), Zhang et al. provided insights into the mechanisms of spinal cord stimulation for PDOC, in addition to quantifying the neuromodulation effects of different stimulation parameters (29). In the prefrontal cortices of eight patients with PDOC, the researchers found a characteristic profile of an increase in [HbT] when stimulation was switched on, followed by a gradual return to baseline after stimulation was switched off. No such meaningful profile was observed in the occipital cortex. Furthermore, in the prefrontal cortex, both patients in the minimally conscious state showed significant increases in HbT across blocks, while such a profile was only present in two out of the six patients in the vegetative state. These results hint that it may be possible to partially increase cerebral blood flow in patients with PDOC via spinal cord stimulation, and that fNIRS can be used as a real-time monitor of these physiological consequences. Continued use of fNIRS alongside explorative therapies for PDOC has potential to guide clinicians in tailoring stimulation protocols to optimize desired physiological responses and ultimately increase the success of rehabilitation efforts.

## CONCLUSIONS AND FUTURE PERSPECTIVES

Functional near-infrared spectroscopy is in its infancy relative to fMRI and EEG, which have an already substantial literature in the study of PDOC. However, fNIRS is attracting interest in PDOC research as it can provide moderate spatial and temporal resolution of brain data *via* a portable and non-invasive device (please refer to **Table 3** for an overall summary of the literature using fNIRS in patients with PDOC or LIS). Therefore, it has potential to improve the accuracy of diagnoses and even provide access to communication devices for more patients than could be achieved with, for example, fMRI alone.

## REFERENCES

1. Laureys S, Celesia G, Cohadon F, Lavrijzen J, Leon-Carrion J, Sannita W, et al. Unresponsive wakefulness syndrome: a new name for the vegetative state or apallic syndrome. *BMC Med* (2010) 8:68. doi:10.1186/1741-7015-8-68

Following in the footsteps of fMRI and EEG research in PDOC, the majority of fNIRS research has focused on detecting covert command-following *via* sensorimotor activity during imagined actions. However, for clinical applications, fNIRS is so far insufficiently sensitive to detect task-relevant activation in single-subject data. Furthermore, no fNIRS study has yet differentiated between vegetative and minimally conscious states, suggesting limited diagnostic utility so far. However, as the sensorimotor cortex is easily probed by scalp-based sensors, and often a target for other hemodynamic markers of covert command-following (i.e., fMRI), the PDOC field should commit to developing sensitive fNIRS markers of motor imagery.

Due to the relative infancy of fNIRS, there remains significant work to do in terms of hardware, signal processing, and analyses, especially for those researchers and clinicians who are not experts in optical imaging. For example, the vast majority of fNIRS work in motor imagery has been conducted with less sensitive but simpler continuous wave devices. Further research into the operations of more advanced fNIRS systems (e.g., high channel density frequency domain and time domain devices) and subsequent knowledge transfer to clinical and biomedical science users will enable greater resolution of clinically meaningful brain responses. Indeed, across the broad physical and computational sciences of optical imaging, there has been significant work in improving the sensitivity of the brain tissue sampled, the depth of the measure, and the tools and models used to examine light propagation and detection. Recent successes in combining fNIRS and EEG analyses for BCIs also indicate that the technology is reaching the standards required for clinical applicability in PDOC.

It is clear that for fNIRS to realize its potential in PDOC assessment, research teams must incorporate multidisciplinary expertise in cognition, clinical practice, physical sciences, and computational sciences. With principled paradigms for diagnosing covert awareness in combination with state-of-the-art devices and algorithms for data modeling, and feature extraction/classification, fNIRS, and perhaps more so EEG-fNIRS, has great potential to improve diagnostic accuracy in PDOC and enable patients to communicate their true mental state to the outside world.

## AUTHOR CONTRIBUTIONS

MR wrote the initial draft of the paper. MR and DC revised the draft. All the authors contributed to subsequent drafts.

## FUNDING

MR gratefully acknowledges funding from EPSRC through a studentship from the Sci-Phy-4-Health Centre for Doctoral Training (EP/L016346/1).

2. Laureys S, Owen AM, Schiff ND. Brain function in coma, vegetative state, and related disorders. *Lancet Neurol* (2004) 3:537–46. doi:10.1016/S1474-4422(04)00852-X
3. Giacino JT, Ashwal S, Childs N, Cranford R, Jennett B, Katz DI, et al. The minimally conscious state: definition and diagnostic criteria. *Neurology* (2002) 58:349–53. doi:10.1212/WNL.58.3.349

4. Gosseries O, Vanhaudenhuyse A, Bruno M-A, Demertzi A, Schnakers C, Boly M, et al. Disorders of consciousness: coma, vegetative and minimally conscious states. In: Cvetkovic D, Cosic I, editors. *States of Consciousness*. Berlin, Heidelberg: Springer (2011). p. 29–55.
5. Andrews K. Medical decision making in the vegetative state: withdrawal of nutrition and hydration. *NeuroRehabilitation* (2004) 19:299–304.
6. Giacino JT, Kalmar K, Whyte J. The JFK coma recovery scale-revised: measurement characteristics and diagnostic utility. *Arch Phys Med Rehabil* (2004) 85:2020–9. doi:10.1016/j.apmr.2004.02.033
7. Morrissey A-M, Gill-Thwaites H, Wilson B, Leonard R, McLellan L, Pundole A, et al. The role of the SMART and WHIM in behavioural assessment of disorders of consciousness: clinical utility and scope for a symbiotic relationship. *Neuropsychol Rehabil* (2017):1–12. doi:10.1080/09602011.2017.1354769
8. Kondziella D, Friberg CK, Frokjaer VG, Fabricius M, Möller K. Preserved consciousness in vegetative and minimal conscious states: systematic review and meta-analysis. *J Neurol Neurosurg Psychiatry* (2016) 87:485–92. doi:10.1136/jnnp-2015-310958
9. Schiff ND. Cognitive motor dissociation following severe brain injuries. *JAMA Neurol* (2015) 72:1413–5. doi:10.1001/jamaneurol.2015.2899
10. Fernández-Espejo D, Rossit S, Owen AM. A thalamocortical mechanism for the absence of overt motor behavior in covertly aware patients. *JAMA Neurol* (2015) 72:1442–50. doi:10.1001/jamaneurol.2015.2614
11. Owen AM, Coleman MR, Boly M, Davis MH, Laureys S, Pickard JD. Detecting awareness in the vegetative state. *Science* (2006) 313:1402. doi:10.1126/science.1130197
12. Monti MM, Vanhaudenhuyse A, Coleman MR, Boly M, Pickard JD, Tshibanda L, et al. Willful modulation of brain activity in disorders of consciousness. *N Engl J Med* (2010) 362:579–89. doi:10.1056/NEJMoa0905370
13. Fernández-Espejo D, Owen AM. Detecting awareness after severe brain injury. *Nat Rev Neurosci* (2013) 14:801–9. doi:10.1038/nrn3608
14. Naci L, Owen A. Making every word count for nonresponsive patients. *JAMA Neurol* (2013) 70:1235–41. doi:10.1001/jamaneurol.2013.3686
15. Bardin JC, Fins JJ, Katz DI, Hersch J, Heier LA, Tabelow K, et al. Dissociations between behavioural and functional magnetic resonance imaging-based evaluations of cognitive function after brain injury. *Brain* (2011) 134:769–82. doi:10.1093/brain/awr005
16. Wolpaw JR, Birbaumer N, McFarland DJ, Pfurtscheller G, Vaughan TM. Brain-computer interfaces for communication and control. *Clin Neurophysiol* (2002) 113:767–91. doi:10.1016/S1388-2457(02)00057-3
17. Buxton RB, Uludağ K, Dubowitz DJ, Liu TT. Modeling the hemodynamic response to brain activation. *Neuroimage* (2004) 23:S220–33. doi:10.1016/j.neuroimage.2004.07.013
18. Villringer A, Chance B. Non-invasive optical spectroscopy and imaging of human brain function. *Trends Neurosci* (1997) 20:435–42. doi:10.1016/S0166-2236(97)01132-6
19. Huppert TJ, Hoge RD, Diamond SG, Franceschini MA, Boas DA. A temporal comparison of BOLD, ASL, and NIRS hemodynamic responses to motor stimuli in adult humans. *Neuroimage* (2006) 29:368–82. doi:10.1016/j.neuroimage.2005.08.065
20. Gratton G, Corballis PM, Cho E, Fabiani M, Hood DC. Shades of gray matter: noninvasive optical images of human brain responses during visual stimulation. *Psychophysiology* (1995) 32:505–9. doi:10.1111/j.1469-8986.1995.tb02102.x
21. Strangman G, Boas DA, Sutton JP. Non-invasive neuroimaging using near-infrared light. *Biol Psychiatry* (2002) 52:679–93. doi:10.1016/S0006-3223(02)01550-0
22. Zaramella P, Freato F, Amigoni A, Salvadori S, Marangoni P, Suppiej A, et al. Brain auditory activation measured by near-infrared spectroscopy (NIRS) in neonates. *Pediatr Res* (2001) 49:213–9. doi:10.1203/00006450-200102000-00014
23. Cannestra AF, Wartenburger I, Obrig H, Villringer A, Toga AW. Functional assessment of Broca's area using near infrared spectroscopy in humans. *Neuroreport* (2003) 14:1961–5. doi:10.1097/00001756-200310270-00016
24. Leon-Carrion J, Izzetoglu M, Izzetoglu K, Martin-Rodriguez JF, Damas-Lopez J, Barroso y Martin JM, et al. Efficient learning produces spontaneous neural repetition suppression in prefrontal cortex. *Behav Brain Res* (2010) 208:502–8. doi:10.1016/j.bbr.2009.12.026
25. Leon-Carrion J, Damas J, Izzetoglu K, Pourrezai K, Martin-Rodriguez JF, Barroso y Martin JM, et al. Differential time course and intensity of PFC activation for men and women in response to emotional stimuli: a functional near-infrared spectroscopy (fNIRS) study. *Neurosci Lett* (2006) 403:90–5. doi:10.1016/j.neulet.2006.04.050
26. Yucel MA, Aasted CM, Petkov MP, Borsook D, Boas DA, Becerra L. Specificity of hemodynamic brain responses to painful stimuli: a functional near-infrared spectroscopy study. *Sci Rep* (2015) 5:9469. doi:10.1038/srep09469
27. Kempny AM, James L, Yelden K, Dupont S, Farmer S, Playford ED, et al. Functional near infrared spectroscopy as a probe of brain function in people with prolonged disorders of consciousness. *Neuroimage Clin* (2016) 12:312–9. doi:10.1016/j.nicl.2016.07.013
28. Molteni E, Arrigoni F, Bardoni A, Galbiati S, Villa F, Colombo K, et al. Bedside assessment of residual functional activation in minimally conscious state using NIRS and general linear models. *Conf Proc IEEE Eng Med Biol Soc* (2013) 2013:3551–4. doi:10.1109/EMBC.2013.6610309
29. Zhang Y, Yang Y, Si J, Xia X, He J, Jiang T. Influence of inter-stimulus interval of spinal cord stimulation in patients with disorders of consciousness: a preliminary functional near-infrared spectroscopy study. *Neuroimage Clin* (2018) 17:1–9. doi:10.1016/j.nicl.2017.09.017
30. Ferrari M, Quaresima V. A brief review on the history of human functional near-infrared spectroscopy (fNIRS) development and fields of application. *Neuroimage* (2012) 63:921–35. doi:10.1016/j.neuroimage.2012.03.049
31. Jobsis FF. Noninvasive, infrared monitoring of cerebral and myocardial oxygen sufficiency and circulatory parameters. *Science* (1977) 198:1264–7. doi:10.1126/science.929199
32. Ferrari M, Giannini I, Sideri G, Zanette E. Continuous non invasive monitoring of human brain by near infrared spectroscopy. *Adv Exp Med Biol* (1985) 191:873–82. doi:10.1007/978-1-4684-3291-6\_88
33. Gratton G, Maier JS, Fabiani M, Mantulin WW, Gratton E. Feasibility of intracranial near-infrared optical scanning. *Psychophysiology* (1994) 31:211–5. doi:10.1111/j.1469-8986.1994.tb01043.x
34. Davies DJ, Su Z, Clancy MT, Lucas SJE, Dehghani H, Logan A, et al. Near-infrared spectroscopy in the monitoring of adult traumatic brain injury: a review. *J Neurotrauma* (2015) 32:933–41. doi:10.1089/neu.2014.3748
35. León-Carrión J, León-Domínguez U. Functional near-infrared spectroscopy (fNIRS): principles and neuroscientific applications. In: Bright P, editor. *Neuroimaging – Methods*. InTech (2012). p. 47–74. Available from: <https://www.intechopen.com/books/neuroimaging-methods>
36. Cui W, Kumar C, Chance B. Experimental study of migration depth for the photons measured at sample surface. *Proc. SPIE 1431, Time-Resolved Spectroscopy and Imaging of Tissues*. (Vol. 1431), Los Angeles, CA (1991). p. 1412–31.
37. Gervain J, Mehler J, Werker JF, Nelson CA, Csibra G, Lloyd-Fox S, et al. Near-infrared spectroscopy: a report from the McDonnell infant methodology consortium. *Dev Cogn Neurosci* (2011) 1:22–46. doi:10.1016/j.dcn.2010.07.004
38. Kohl-Bareis M, Obrig H, Steinbrink J, Malak J, Uludag K, Villringer A. Noninvasive monitoring of cerebral blood flow by a dye bolus method: separation of brain from skin and skull signals. *J Biomed Opt* (2002) 7:464–70. doi:10.1117/1.1482719
39. Strangman GE, Zhang Q, Li Z. Scalp and skull influence on near infrared photon propagation in the Colin27 brain template. *Neuroimage* (2014) 85:136–49. doi:10.1016/j.neuroimage.2013.04.090
40. Boas DA, Dale AM, Franceschini MA. Diffuse optical imaging of brain activation: approaches to optimizing image sensitivity, resolution, and accuracy. *Neuroimage* (2004) 23:S275–88. doi:10.1016/j.neuroimage.2004.07.011
41. Gratton G, Corballis PM. Removing the heart from the brain: compensation for the pulse artifact in the photon migration signal. *Psychophysiology* (1995) 32:292–9. doi:10.1111/j.1469-8986.1995.tb02958.x
42. Franceschini MA, Boas DA, Zourabian A, Diamond SG, Nadgir S, Lin DW, et al. Near-infrared spirometry: noninvasive measurements of venous saturation in piglets and human subjects. *J Appl Physiol* (2002) 92:372–84. doi:10.1152/jappl.2002.92.1.372
43. Obrig H, Neufang M, Wenzel R, Kohl M, Steinbrink J, Einhaupl K, et al. Spontaneous low frequency oscillations of cerebral hemodynamics and metabolism in human adults. *Neuroimage* (2000) 12:623–39. doi:10.1006/nimg.2000.0657
44. Kirilina E, Jelzow A, Heine A, Niessing M, Wabnitz H, Bruhl R, et al. The physiological origin of task-evoked systemic artefacts in functional



- near infrared spectroscopy. *Neuroimage* (2012) 61:70–81. doi:10.1016/j.neuroimage.2012.02.074
45. Okada E, Delpy DT. Near-infrared light propagation in an adult head model. II. Effect of superficial tissue thickness on the sensitivity of the near-infrared spectroscopy signal. *Appl Opt* (2003) 42:2915–22. doi:10.1364/AO.42.002915
  46. Katura T, Sato H, Fuchino Y, Yoshida T, Atsumori H, Kiguchi M, et al. Extracting task-related activation components from optical topography measurement using independent components analysis. *J Biomed Opt* (2008) 13:54008. doi:10.1117/1.2981829
  47. Virtanen J, Noponen T, Meriläinen P. Comparison of principal and independent component analysis in removing extracerebral interference from near-infrared spectroscopy signals. *J Biomed Opt* (2009) 14:54032. doi:10.1117/1.3253323
  48. Plichta MM, Heinzel S, Ehls A-C, Pauli P, Fallgatter AJ. Model-based analysis of rapid event-related functional near-infrared spectroscopy (fNIRS) data: a parametric validation study. *Neuroimage* (2007) 35:625–34. doi:10.1016/j.neuroimage.2006.11.028
  49. Yücel MA, Selb J, Aasted CM, Petkov MP, Becerra L, Borsook D, et al. Short separation regression improves statistical significance and better localizes the hemodynamic response obtained by near-infrared spectroscopy for tasks with differing autonomic responses. *Neurophotonics* (2015) 2:35005. doi:10.1117/1.NPh.2.3.035005
  50. Gagnon L, Perdue K, Greve DN, Goldenholz D, Kaskhedikar G, Boas DA. Improved recovery of the hemodynamic response in diffuse optical imaging using short optode separations and state-space modeling. *Neuroimage* (2011) 56:1362–71. doi:10.1016/j.neuroimage.2011.03.001
  51. Gagnon L, Cooper RJ, Yücel MA, Perdue KL, Greve DN, Boas DA. Short separation channel location impacts the performance of short channel regression in NIRS. *Neuroimage* (2012) 59:2518–28. doi:10.1016/j.neuroimage.2011.08.095
  52. Funane T, Atsumori H, Katura T, Obata AN, Sato H, Tanikawa Y, et al. Quantitative evaluation of deep and shallow tissue layers' contribution to fNIRS signal using multi-distance optodes and independent component analysis. *Neuroimage* (2014) 85:150–65. doi:10.1016/j.neuroimage.2013.02.026
  53. Dehghani H, White BR, Zeff BW, Tizzard A, Culver JP. Depth sensitivity and image reconstruction analysis of dense imaging arrays for mapping brain function with diffuse optical tomography. *Appl Opt* (2009) 48:D137–43. doi:10.1364/AO.48.00D137
  54. Franceschini MA, Fantini S, Thompson JH, Culver JP, Boas DA. Hemodynamic evoked response of the sensorimotor cortex measured noninvasively with near-infrared optical imaging. *Psychophysiology* (2003) 40:548–60. doi:10.1111/1469-8986.00057
  55. Lina J-M, Dehaes M, Matteau-Pelletier C, Lesage F. Complex wavelets applied to diffuse optical spectroscopy for brain activity detection. *Opt Express* (2008) 16:1029–50. doi:10.1364/OE.16.001029
  56. Pfeifer MD, Scholkmann F, Labruyère R. Signal processing in functional near-infrared spectroscopy (fNIRS): methodological differences lead to different statistical results. *Front Hum Neurosci* (2018) 11:641. doi:10.3389/fnhum.2017.00641
  57. Tachtsidis I, Scholkmann F. False positives and false negatives in functional near-infrared spectroscopy: issues, challenges, and the way forward. *Neurophotonics* (2016) 3:31405. doi:10.1117/1.NPh.3.3.031405
  58. Frackowiak RSJ, Friston KJ, Frith CD, Dolan RJ, Price CJ, Zeki S, et al., editors. *Human Brain Function*. 2nd ed. California, USA: Academic Press (2004).
  59. Friston KJ. Imaging cognitive anatomy. *Trends Cogn Sci* (1997) 1:21–7. doi:10.1016/S1364-6613(97)01001-2
  60. Smith SM, Jenkinson M, Woolrich MW, Beckmann CF, Behrens TEJ, Johansen-Berg H, et al. Advances in functional and structural MR image analysis and implementation as FSL. *Neuroimage* (2004) 23:S208–19. doi:10.1016/j.neuroimage.2004.07.051
  61. Jenkinson M, Beckmann CF, Behrens TEJ, Woolrich MW, Smith SM. FSL. *Neuroimage* (2012) 62:782–90. doi:10.1016/j.neuroimage.2011.09.015
  62. Strother SC. Evaluating fMRI preprocessing pipelines. *IEEE Eng Med Biol Mag* (2006) 25:27–41. doi:10.1109/EMMB.2006.1607667
  63. Caballero-Gaudes C, Reynolds RC. Methods for cleaning the BOLD fMRI signal. *Neuroimage* (2017) 154:128–49. doi:10.1016/j.neuroimage.2016.12.018
  64. Maikala RV. Modified Beer's Law—historical perspectives and relevance in near-infrared monitoring of optical properties of human tissue. *Int J Ind Ergon* (2010) 40:125–34. doi:10.1016/j.ergon.2009.02.011
  65. Delpy DT, Cope M, van der Zee P, Arridge S, Wray S, Wyatt J. Estimation of optical pathlength through tissue from direct time of flight measurement. *Phys Med Biol* (1988) 33:1433–42. doi:10.1088/0031-9155/33/12/008
  66. Patterson MS, Chance B, Wilson BC. Time resolved reflectance and transmittance for the noninvasive measurement of tissue optical properties. *Appl Opt* (1989) 28:2331–6. doi:10.1364/AO.28.002331
  67. Suzuki S, Takasaki S, Ozaki T, Kobayashi Y. Tissue oxygenation monitor using NIR spatially resolved spectroscopy. *Proc. SPIE 3597, Optical Tomography and Spectroscopy of Tissue III*. (Vol. 3597), San Jose, CA (1999). p. 3511–97.
  68. Matcher SJ, Kirkpatrick PJ, Nahid K, Cope M, Delpy DT. Absolute quantification methods in tissue near-infrared spectroscopy. *Proc. SPIE 2389, Optical Tomography, Photon Migration, and Spectroscopy of Tissue and Model Media: Theory, Human Studies, and Instrumentation*. (Vol. 2389), San Jose, CA (1995). p. 2310–89.
  69. Miwa M, Ueda Y, Chance B. Development of time-resolved spectroscopy system for quantitative noninvasive tissue measurement. *Proc. SPIE 2389, Optical Tomography, Photon Migration, and Spectroscopy of Tissue and Model Media: Theory, Human Studies, and Instrumentation*. (Vol. 2389), San Jose, CA (1995). p. 2388–9.
  70. Duncan A, Whitlock TL, Cope M, Delpy DT. Multiwavelength, wideband, intensity-modulated optical spectrometer for near-infrared spectroscopy and imaging. *Proc. SPIE 1888, Photon Migration and Imaging in Random Media and Tissues*. (Vol. 1888), Los Angeles, CA (1993). p. 248–58.
  71. Scholkmann F, Kleiser S, Metz AJ, Zimmermann R, Mata Pavia J, Wolf U, et al. A review on continuous wave functional near-infrared spectroscopy and imaging instrumentation and methodology. *Neuroimage* (2014) 85:6–27. doi:10.1016/j.neuroimage.2013.05.004
  72. Siegel AM, Marota JJA, Boas DA. Design and evaluation of a continuous-wave diffuse optical tomography system. *Opt Express* (1999) 4:287–98. doi:10.1364/OE.4.000287
  73. Gratton G, Fabiani M. Fast optical imaging of human brain function. *Front Hum Neurosci* (2010) 4:52. doi:10.3389/fnhum.2010.00052
  74. Pogue BW, Patterson MS. Frequency-domain optical absorption spectroscopy of finite tissue volumes using diffusion theory. *Phys Med Biol* (1994) 39:1157–80. doi:10.1088/0031-9155/39/7/008
  75. Chance B, Leigh JS, Miyake H, Smith DS, Nioka S, Greenfield R, et al. Comparison of time-resolved and -unresolved measurements of deoxyhemoglobin in brain. *Proc Natl Acad Sci U S A* (1988) 85:4971–5. doi:10.1073/pnas.85.14.4971
  76. Torricelli A, Contini D, Pifferi A, Caffini M, Re R, Zucchelli L, et al. Time domain functional NIRS imaging for human brain mapping. *Neuroimage* (2014) 85:28–50. doi:10.1016/j.neuroimage.2013.05.106
  77. Fernández-Espejo D, Norton L, Owen AM. The clinical utility of fMRI for identifying covert awareness in the vegetative state: a comparison of sensitivity between 3T and 1.5T. *PLoS One* (2014) 9:e95082. doi:10.1371/journal.pone.0095082
  78. Guillot A, Collet C, Nguyen VA, Malouin F, Richards C, Doyon J. Brain activity during visual versus kinesthetic imagery: an fMRI study. *Hum Brain Mapp* (2009) 30:2157–72. doi:10.1002/hbm.20658
  79. Coyle SM, Ward TE, Markham CM. Brain-computer interface using a simplified functional near-infrared spectroscopy system. *J Neural Eng* (2007) 4:219–26. doi:10.1088/1741-2560/4/3/007
  80. Abdalmalak A, Milej D, Diop M, Naci L, Owen AM, St Lawrence K. Assessing the feasibility of time-resolved fNIRS to detect brain activity during motor imagery. *Proc. SPIE 9690, Clinical and Translational Neurophotonics; Neural Imaging and Sensing; and Optogenetics and Optical Manipulation*, 969002. (Vol. 9690), San Francisco, CA (2016). 969002 p.
  81. Iso N, Moriuchi T, Sagari A, Kitajima E, Iso F, Tanaka K, et al. Monitoring local regional hemodynamic signal changes during motor execution and motor imagery using near-infrared spectroscopy. *Front Physiol* (2015) 6:416. doi:10.3389/fphys.2015.00416
  82. Abdalmalak A, Milej D, Diop M, Shokouhi M, Naci L, Owen AM, et al. Can time-resolved NIRS provide the sensitivity to detect brain activity during motor imagery consistently? *Biomed Opt Express* (2017) 8:2162–72. doi:10.1364/BOE.8.002162



83. Zich C, Debener S, Thoenes A-K, Chen L-C, Kranczioch C. Simultaneous EEG-fNIRS reveals how age and feedback affect motor imagery signatures. *Neurobiol Aging* (2016) 49:183–97. doi:10.1016/j.neurobiolaging.2016.10.011
84. Wriessnegger SC, Kurzmann J, Neuper C. Spatio-temporal differences in brain oxygenation between movement execution and imagery: a multichannel near-infrared spectroscopy study. *Int J Psychophysiol* (2008) 67:54–63. doi:10.1016/j.ijpsycho.2007.10.004
85. Amemiya K, Ishizu T, Ayabe T, Kojima S. Effects of motor imagery on inter-manual transfer: a near-infrared spectroscopy and behavioural study. *Brain Res* (2010) 1343:93–103. doi:10.1016/j.brainres.2010.04.048
86. Kober SE, Wood G. Changes in hemodynamic signals accompanying motor imagery and motor execution of swallowing: a near-infrared spectroscopy study. *Neuroimage* (2014) 93:1–10. doi:10.1016/j.neuroimage.2014.02.019
87. Abdalmalak A, Milej D, Norton L, Debicki DB, Gofton T, Diop M, et al. Single-session communication with a locked-in patient by functional near-infrared spectroscopy. *Neurophotonics* (2017) 4:40501. doi:10.1117/1.NPh.4.4.040501
88. Koo B, Lee H-G, Nam Y, Kang H, Koh CS, Shin H-C, et al. A hybrid NIRS-EEG system for self-paced brain computer interface with online motor imagery. *J Neurosci Methods* (2015) 244:26–32. doi:10.1016/j.jneumeth.2014.04.016
89. Holper L, Wolf M. Single-trial classification of motor imagery differing in task complexity: a functional near-infrared spectroscopy study. *J Neuroeng Rehabil* (2011) 8:34. doi:10.1186/1743-0003-8-34
90. Muehleemann T, Haensse D, Wolf M. Wireless miniaturized in-vivo near infrared imaging. *Opt Express* (2008) 16:10323–30. doi:10.1364/OE.16.010323
91. Sitaram R, Zhang H, Guan C, Thulasidas M, Hoshi Y, Ishikawa A, et al. Temporal classification of multichannel near-infrared spectroscopy signals of motor imagery for developing a brain-computer interface. *Neuroimage* (2007) 34:1416–27. doi:10.1016/j.neuroimage.2006.11.005
92. Yin X, Xu B, Jiang C, Fu Y, Wang Z, Li H, et al. A hybrid BCI based on EEG and fNIRS signals improves the performance of decoding motor imagery of both force and speed of hand clenching. *J Neural Eng* (2015) 12:36004. doi:10.1088/1741-2560/12/3/036004
93. Batula AM, Ayaz H, Kim YE. Evaluating a four-class motor-imagery-based optical brain-computer interface. *Conf Proc IEEE Eng Med Biol Soc* (2014) 2014:2000–3. doi:10.1109/EMBC.2014.6944007
94. Stangl M, Bauernfeind G, Kurzmann J, Scherer R, Neuper C. A hemodynamic brain-computer interface based on real-time classification of near infrared spectroscopy signals during motor imagery and mental arithmetic. *J Near Infrared Spectrosc* (2013) 21:157–71. doi:10.1255/jnirs.1048
95. Batula AM, Mark JA, Kim YE, Ayaz H. Comparison of brain activation during motor imagery and motor movement using fNIRS. *Comput Intell Neurosci* (2017) 2017:5491296. doi:10.1155/2017/5491296
96. Batula AM, Kim YE, Ayaz H. Virtual and actual humanoid robot control with four-class motor-imagery-based optical brain-computer interface. *Biomed Res Int* (2017) 2017:1463512. doi:10.1155/2017/1463512
97. Qureshi NK, Naseer N, Noori FM, Nazeer H, Khan RA, Saleem S. Enhancing classification performance of functional near-infrared spectroscopy-brain-computer interface using adaptive estimation of general linear model coefficients. *Front Neurobot* (2017) 11:33. doi:10.3389/fnbot.2017.00033
98. Fazli S, Mehnert J, Steinbrink J, Curio G, Villringer A, Müller K-R, et al. Enhanced performance by a hybrid NIRS-EEG brain computer interface. *Neuroimage* (2012) 59:519–29. doi:10.1016/j.neuroimage.2011.07.084
99. Thanh Hai N, Cuong NQ, Dang Khoa TQ, Van Toi V. Temporal hemodynamic classification of two hands tapping using functional near-infrared spectroscopy. *Front Hum Neurosci* (2013) 7:516. doi:10.3389/fnhum.2013.00516
100. Ge S, Yang Q, Wang R, Lin P, Gao J, Leng Y, et al. A brain-computer interface based on a few-channel EEG-fNIRS bimodal system. *IEEE Access* (2017) 5:208–18. doi:10.1109/ACCESS.2016.2637409
101. Naseer N, Hong K-S. Classification of functional near-infrared spectroscopy signals corresponding to the right- and left-wrist motor imagery for development of a brain-computer interface. *Neurosci Lett* (2013) 553:84–9. doi:10.1016/j.neulet.2013.08.021
102. Hong K-S, Naseer N, Kim Y-H. Classification of prefrontal and motor cortex signals for three-class fNIRS-BCI. *Neurosci Lett* (2015) 587:87–92. doi:10.1016/j.neulet.2014.12.029
103. Abibullaev B, An J, Lee SH, Moon J II. Design and evaluation of action observation and motor imagery based BCIs using near-infrared spectroscopy. *Measurement* (2017) 98:250–61. doi:10.1016/j.measurement.2016.12.001
104. Nagaoka T, Sakatani K, Awano T, Yokose N, Hoshino T, Murata Y, et al. Development of a new rehabilitation system based on a brain-computer interface using near-infrared spectroscopy. *Adv Exp Med Biol* (2010) 662:497–503. doi:10.1007/978-1-4419-1241-1\_72
105. Hwang H-J, Lim J-H, Kim D-W, Im C-H. Evaluation of various mental task combinations for near-infrared spectroscopy-based brain-computer interfaces. *J Biomed Opt* (2014) 19:77005. doi:10.1117/1.JBO.19.7.077005
106. Mihara M, Miyai I, Hattori N, Hatakenaka M, Yagura H, Kawano T, et al. Neurofeedback using real-time near-infrared spectroscopy enhances motor imagery related cortical activation. *PLoS One* (2012) 7:e32234. doi:10.1371/journal.pone.0032234
107. Mihara M, Hattori N, Hatakenaka M, Yagura H, Kawano T, Hino T, et al. Near-infrared spectroscopy-mediated neurofeedback enhances efficacy of motor imagery-based training in poststroke victims. *Stroke* (2013) 44:1091–8. doi:10.1161/STROKEAHA.111.674507
108. Kaiser V, Bauernfeind G, Kreilinger A, Kaufmann T, Kübler A, Neuper C, et al. Cortical effects of user training in a motor imagery based brain-computer interface measured by fNIRS and EEG. *Neuroimage* (2014) 85:432–44. doi:10.1016/j.neuroimage.2013.04.097
109. Kanoh S, Murayama Y-M, Miyamoto K, Yoshinobu T, Kawashima R. A NIRS-based brain-computer interface system during motor imagery: system development and online feedback training. *Conf Proc IEEE Eng Med Biol Soc* (2009) 2009:594–7. doi:10.1109/IEMBS.2009.5333710
110. Coyle S, Ward T, Markham C. Physiological noise in near-infrared spectroscopy: implications for optical brain computer interfacing. *Conf Proc IEEE Eng Med Biol Soc* (2004) 6:4540–3. doi:10.1109/IEMBS.2004.1404260
111. Zhang S, Zheng Y, Wang D, Wang L, Ma J, Zhang J, et al. Application of a common spatial pattern-based algorithm for an fNIRS-based motor imagery brain-computer interface. *Neurosci Lett* (2017) 655:35–40. doi:10.1016/j.neulet.2017.06.044
112. Cheyne D, Kristeva R, Deecke L. Homuncular organization of human motor cortex as indicated by neuromagnetic recordings. *Neurosci Lett* (1991) 122:17–20. doi:10.1016/0304-3940(91)90182-S
113. Hsu W-C, Lin L-F, Chou C-W, Hsiao Y-T, Liu Y-H. EEG classification of imaginary lower limb stepping movements based on fuzzy support vector machine with kernel-induced membership function. *Int J Fuzzy Syst* (2017) 19:566–79. doi:10.1007/s40815-016-0259-9
114. Miller KJ, Schalk G, Fetz EE, den Nijs M, Ojemann JG, Rao RPN. Cortical activity during motor execution, motor imagery, and imagery-based online feedback. *Proc Natl Acad Sci U S A* (2010) 107:4430–5. doi:10.1073/pnas.0913697107
115. Diop M, St Lawrence K. Improving the depth sensitivity of time-resolved measurements by extracting the distribution of times-of-flight. *Biomed Opt Express* (2013) 4:447–59. doi:10.1364/BOE.4.000447
116. Diop M, St Lawrence K. Deconvolution method for recovering the photon time-of-flight distribution from time-resolved measurements. *Opt Lett* (2012) 37:2358–60. doi:10.1364/OL.37.002358
117. Sato T, Ito M, Suto T, Kameyama M, Suda M, Yamagishi Y, et al. Time courses of brain activation and their implications for function: a multichannel near-infrared spectroscopy study during finger tapping. *Neurosci Res* (2007) 58:297–304. doi:10.1016/j.neures.2007.03.014
118. Leff DR, Orihuela-Espina F, Elwell CE, Athanasiou T, Delpy DT, Darzi AW, et al. Assessment of the cerebral cortex during motor task behaviours in adults: a systematic review of functional near infrared spectroscopy (fNIRS) studies. *Neuroimage* (2011) 54:2922–36. doi:10.1016/j.neuroimage.2010.10.058
119. Wilson TW, Kurz MJ, Arpin DJ. Functional specialization within the supplementary motor area: a fNIRS study of bimanual coordination. *Neuroimage* (2014) 85:445–50. doi:10.1016/j.neuroimage.2013.04.112
120. Verstynen T, Diedrichsen J, Albert N, Aparicio P, Ivry RB. Ipsilateral motor cortex activity during unimanual hand movements relates to task complexity. *J Neurophysiol* (2005) 93:1209–22. doi:10.1152/jn.00720.2004
121. Cramer SC, Finklestein SP, Schaechter JD, Bush G, Rosen BR. Activation of distinct motor cortex regions during ipsilateral and contralateral finger movements. *J Neurophysiol* (1999) 81:383–7. doi:10.1152/jn.1999.81.1.383

122. Huneau C, Benali H, Chabriat H. Investigating human neurovascular coupling using functional neuroimaging: a critical review of dynamic models. *Front Neurosci* (2015) 9:467. doi:10.3389/fnins.2015.00467
123. Croce P, Zappasodi F, Merla A, Chiarelli A. Exploiting neurovascular coupling: a Bayesian sequential Monte Carlo approach applied to simulated EEG fNIRS data. *J Neural Eng* (2017) 14:46029. doi:10.1088/1741-2552/aa7321
124. Jelzow A, Koch S, Wabnitz H, Steinbrink J, Obrig H, Macdonald R. Combined EEG and time-resolved NIRS to study neuro-vascular coupling in the adult brain. *Biomedical Optics and 3-D Imaging, OSA Technical Digest (CD) (Optical Society of America, 2010) JMA63*. Miami, FL (2010).
125. Cruse D, Chennu S, Chatelle C, Bekinschtein TA, Fernández-Espejo D, Pickard JD, et al. Bedside detection of awareness in the vegetative state: a cohort study. *Lancet* (2011) 378:2088–94. doi:10.1016/S0140-6736(11)61224-5
126. O'Kelly J, James L, Palaniappan R, Taborin J, Fachner J, Magee WL. Neurophysiological and behavioral responses to music therapy in vegetative and minimally conscious states. *Front Hum Neurosci* (2013) 7:884. doi:10.3389/fnhum.2013.00884
127. Jackson AF, Bolger DJ. The neurophysiological bases of EEG and EEG measurement: a review for the rest of us. *Psychophysiology* (2014) 51:1061–71. doi:10.1111/psyp.12283
128. Hoffmann S, Falkenstein M. The correction of eye blink artefacts in the EEG: a comparison of two prominent methods. *PLoS One* (2008) 3:e3004. doi:10.1371/journal.pone.0003004
129. Li L. The differences among eyes-closed, eyes-open and attention states: an EEG study. *2010 6th International Conference on Wireless Communications Networking and Mobile Computing (WiCOM)*. Chengdu, China (2010). p. 1–4.
130. Verleger R. The instruction to refrain from blinking affects auditory P3 and N1 amplitudes. *Electroencephalogr Clin Neurophysiol* (1991) 78:240–51. doi:10.1016/0013-4694(91)90039-7
131. van den Broek SP, Reinders F, Donderwinkel M, Peters MJ. Volume conduction effects in EEG and MEG. *Electroencephalogr Clin Neurophysiol* (1998) 106:522–34. doi:10.1016/S0013-4694(97)00147-8
132. Carvalhaes C, de Barros JA. The surface Laplacian technique in EEG: theory and methods. *Int J Psychophysiol* (2015) 97:174–88. doi:10.1016/j.ijpsycho.2015.04.023
133. Zama T, Shimada S. Simultaneous measurement of electroencephalography and near-infrared spectroscopy during voluntary motor preparation. *Sci Rep* (2015) 5:16438. doi:10.1038/srep16438
134. Okamoto M, Dan H, Sakamoto K, Takeo K, Shimizu K, Kohno S, et al. Three-dimensional probabilistic anatomical cranio-cerebral correlation via the international 10–20 system oriented for transcranial functional brain mapping. *Neuroimage* (2004) 21:99–111. doi:10.1016/j.neuroimage.2003.08.026
135. Kappenman ES, Luck SJ. The effects of electrode impedance on data quality and statistical significance in ERP recordings. *Psychophysiology* (2010) 47:888–904. doi:10.1111/j.1469-8986.2010.01009.x
136. Noponen TEJ, Kotilahti K, Nissila I, Kajava T, Merilainen PT. Effects of improper source coupling in frequency-domain near-infrared spectroscopy. *Phys Med Biol* (2010) 55:2941–60. doi:10.1088/0031-9155/55/10/010
137. Giacometti P, Diamond SG. Compliant head probe for positioning electroencephalography electrodes and near-infrared spectroscopy optodes. *J Biomed Opt* (2013) 18:27005. doi:10.1117/1.JBO.18.2.027005
138. Cooper RJ, Everdell NL, Enfield LC, Gibson AP, Worley A, Hebden JC. Design and evaluation of a probe for simultaneous EEG and near-infrared imaging of cortical activation. *Phys Med Biol* (2009) 54:2093–102. doi:10.1088/0031-9155/54/7/016
139. Blankertz B, Dornhege G, Krauledat M, Müller K-R, Curio G. The non-invasive Berlin brain-computer interface: fast acquisition of effective performance in untrained subjects. *Neuroimage* (2007) 37:539–50. doi:10.1016/j.neuroimage.2007.01.051
140. Velliste M, Perel S, Spalding MC, Whitford AS, Schwartz AB. Cortical control of a prosthetic arm for self-feeding. *Nature* (2008) 453:1098–101. doi:10.1038/nature06996
141. Sellers EW, Donchin E. A P300-based brain-computer interface: initial tests by ALS patients. *Clin Neurophysiol* (2006) 117:538–48. doi:10.1016/j.clinph.2005.06.027
142. Millan Jdel R, Renkens F, Mourino J, Gerstner W. Noninvasive brain-actuated control of a mobile robot by human EEG. *IEEE Trans Biomed Eng* (2004) 51:1026–33. doi:10.1109/TBME.2004.827086
143. Kropotov JD. Chapter 2.2 – alpha rhythms. In: Levy N, editor. *Functional Neuromarkers for Psychiatry*. San Diego: Academic Press (2016). p. 89–105.
144. Graimann B, Allison B, Pfurtscheller G. Brain-computer interfaces: a gentle introduction. In: Graimann B, Pfurtscheller G, Allison B, editors. *Brain-Computer Interfaces. The Frontiers Collection*. Berlin, Heidelberg: Springer (2009). p. 1–27.
145. Mikołajewska E, Mikołajewski D. Non-invasive EEG-based brain-computer interfaces in patients with disorders of consciousness. *Mil Med Res* (2014) 1:14. doi:10.1186/2054-9369-1-14
146. Naseer N, Hong K-S. fNIRS-based brain-computer interfaces: a review. *Front Hum Neurosci* (2015) 9:3. doi:10.3389/fnhum.2015.00003
147. Naseer N, Noori FM, Qureshi NK, Hong K-S. Determining optimal feature-combination for LDA classification of functional near-infrared spectroscopy signals in brain-computer interface application. *Front Hum Neurosci* (2016) 10:237. doi:10.3389/fnhum.2016.00237
148. Naseer N, Qureshi NK, Noori FM, Hong K-S. Analysis of different classification techniques for two-class functional near-infrared spectroscopy-based brain-computer interface. *Comput Intell Neurosci* (2016) 2016:5480760. doi:10.1155/2016/5480760
149. Laureys S, Pellas F, Van Eeckhout P, Ghorbel S, Schnakers C, Perrin F, et al. The locked-in syndrome: what is it like to be conscious but paralyzed and voiceless? *Prog Brain Res* (2005) 150:495–511. doi:10.1016/S0079-6123(05)50034-7
150. Naito M, Michioka Y, Ozawa K, Ito Y, Kiguchi M, Kanazawa T. A communication means for totally locked-in ALS patients based on changes in cerebral blood volume measured with near-infrared light. *IEICE Trans Inf Syst* (2007) E90–D:1028–37. doi:10.1093/ietisy/e90-d.7.1028
151. Gratton G, Fabiani M, Friedman D, Franceschini MA, Fantini S, Corballis P, et al. Rapid changes of optical parameters in the human brain during a tapping task. *J Cogn Neurosci* (1995) 7:446–56. doi:10.1162/jocn.1995.7.4.446
152. Wolf M, Wolf U, Choi JH, Gupta R, Safonova LP, Paunescu LA, et al. Functional frequency-domain near-infrared spectroscopy detects fast neuronal signal in the motor cortex. *Neuroimage* (2002) 17:1868–75. doi:10.1006/nimg.2002.1261
153. Morren G, Wolf M, Lemmerling P, Wolf U, Choi JH, Gratton E, et al. Detection of fast neuronal signals in the motor cortex from functional near infrared spectroscopy measurements using independent component analysis. *Med Biol Eng Comput* (2004) 42:92–9. doi:10.1007/BF02351016
154. Gratton G, Fabiani M. Chapter 15. Fast optical signals: principles, methods, and experimental results. 2nd ed. In: Frostig RD, editor. *In Vivo Optical Imaging of Brain Function*. Boca Raton, FL: CRC Press/Taylor & Francis (2009). p. 435–60.
155. Blankertz B, Tomioka R, Lemm S, Kawanabe M, Müller K-R. Optimizing spatial filters for robust EEG single-trial analysis. *IEEE Signal Process Mag* (2008) 25:41–56. doi:10.1109/MSP.2008.4408441
156. Bellman R. *Dynamic Programming*. Princeton: Princeton University Press (1957).
157. Hallex H, Vanrumste B, Grech R, Muscat J, De Clercq W, Vergult A, et al. Review on solving the forward problem in EEG source analysis. *J Neuroeng Rehabil* (2007) 4:46. doi:10.1186/1743-0003-4-46
158. Grech R, Cassar T, Muscat J, Camilleri KP, Fabri SG, Zervakis M, et al. Review on solving the inverse problem in EEG source analysis. *J Neuroeng Rehabil* (2008) 5:25. doi:10.1186/1743-0003-5-25
159. Arridge SR, Cope M, Delpy DT. The theoretical basis for the determination of optical pathlengths in tissue: temporal and frequency analysis. *Phys Med Biol* (1992) 37:1531–60. doi:10.1088/0031-9155/37/7/005
160. Schweiger M, Arridge SR, Delpy DT. Application of the finite-element method for the forward and inverse models in optical tomography. *J Math Imaging Vis* (1993) 3:263–83. doi:10.1007/BF01248356
161. Strangman GE, Li Z, Zhang Q. Depth sensitivity and source-detector separations for near infrared spectroscopy based on the Colin27 brain template. *PLoS One* (2013) 8:e66319. doi:10.1371/journal.pone.0066319
162. Gallegos-Ayala G, Furdea A, Takano K, Ruf CA, Flor H, Birbaumer N. Brain communication in a completely locked-in patient using bedside near-infrared spectroscopy. *Neurology* (2014) 82:1930–2. doi:10.1212/WNL.0000000000000449
163. Chaudhary U, Xia B, Silvoni S, Cohen LG, Birbaumer N. Brain-computer interface-based communication in the completely locked-in state. *PLoS Biol* (2017) 15:e1002593. doi:10.1371/journal.pbio.1002593

164. Yeom S-K, Won D-O, Chi SI, Seo K-S, Kim HJ, Müller K-R, et al. Spatio-temporal dynamics of multimodal EEG-fNIRS signals in the loss and recovery of consciousness under sedation using midazolam and propofol. *PLoS One* (2017) 12:e0187743. doi:10.1371/journal.pone.0187743
165. Schiff ND, Giacino JT, Kalmar K, Victor JD, Baker K, Gerber M, et al. Behavioural improvements with thalamic stimulation after severe traumatic brain injury. *Nature* (2007) 448:600–3. doi:10.1038/nature06041
166. Yamamoto T, Katayama Y, Obuchi T, Kobayashi K, Oshima H, Fukaya C. Spinal cord stimulation for treatment of patients in the minimally conscious state. *Neurol Med Chir* (2012) 52:475–81. doi:10.2176/nmc.52.475
167. Yamamoto T, Katayama Y, Obuchi T, Kobayashi K, Oshima H, Fukaya C. Deep brain stimulation and spinal cord stimulation for vegetative state and minimally conscious state. *World Neurosurg* (2013) 80:S30.e1–9. doi:10.1016/j.wneu.2012.04.010
168. DellaPapa GM, Fukaya C, La Rocca G, Zhong J, Visocchi M. Neuromodulation of vegetative state through spinal cord stimulation: where are we now and where are we going? *Stereotact Funct Neurosurg* (2013) 91:275–87. doi:10.1159/000348271
169. Schiff ND. Recovery of consciousness after brain injury: a mesocircuit hypothesis. *Trends Neurosci* (2010) 33:1–9. doi:10.1016/j.tins.2009.11.002
170. Kanno T, Morita I, Yamaguchi S, Yokoyama T, Kamei Y, Anil SM, et al. Dorsal column stimulation in persistent vegetative state. *Neuromodulation* (2009) 12:33–8. doi:10.1111/j.1525-1403.2009.00185.x
171. Visocchi M, DellaPapa GM, Esposito G, Tufo T, Zhang W, Li S, et al. Spinal cord stimulation and cerebral hemodynamics: updated mechanism and therapeutic implications. *Stereotact Funct Neurosurg* (2011) 89:263–74. doi:10.1159/000329357
172. Georgiopoulos M, Katsakiori P, Kefalopoulou Z, Ellul J, Chroni E, Constantoyannis C. Vegetative state and minimally conscious state: a review of the therapeutic interventions. *Stereotact Funct Neurosurg* (2010) 88:199–207. doi:10.1159/000314354
173. Bai Y, Xia X, Li X, Wang Y, Yang Y, Liu Y, et al. Spinal cord stimulation modulates frontal delta and gamma in patients of minimally consciousness state. *Neuroscience* (2017) 346:247–54. doi:10.1016/j.neuroscience.2017.01.036
174. Bai Y, Xia X, Liang Z, Wang Y, Yang Y, He J, et al. Frontal connectivity in EEG gamma (30–45 Hz) respond to spinal cord stimulation in minimally conscious state patients. *Front Cell Neurosci* (2017) 11:177. doi:10.3389/fncel.2017.00177

**Conflict of Interest Statement:** The authors declare that the research was conducted in the absence of any commercial or financial relationships that could be construed as a potential conflict of interest.

Copyright © 2018 Rupawala, Dehghani, Lucas, Tino and Cruse. This is an open-access article distributed under the terms of the Creative Commons Attribution License (CC BY). The use, distribution or reproduction in other forums is permitted, provided the original author(s) and the copyright owner are credited and that the original publication in this journal is cited, in accordance with accepted academic practice. No use, distribution or reproduction is permitted which does not comply with these terms.



# Multimodal Neuroimaging Approach to Variability of Functional Connectivity in Disorders of Consciousness: A PET/MRI Pilot Study

## OPEN ACCESS

### Edited by:

Caroline Schnakers,  
Casa Colina Centers for Rehabilitation,  
United States

### Reviewed by:

Athena Demertzi,  
Université de Liège, Belgium  
Ingrid Poulsen,  
Rigshospitalet, Denmark

### \*Correspondence:

Carlo Cavaliere  
ccavaliere@sdn-napoli.it

†These authors have contributed  
equally to this work

### Specialty section:

This article was submitted to  
Applied Neuroimaging,  
a section of the journal  
Frontiers in Neurology

**Received:** 01 March 2018

**Accepted:** 24 September 2018

**Published:** 18 October 2018

### Citation:

Cavaliere C, Kandeepan S, Aiello M,  
Ribeiro de Paula D, Marchitelli R,  
Fiorenza S, Orsini M, Trojano L,  
Masotta O, St. Lawrence K, Loreto V,  
Chronik BA, Nicolai E, Soddu A and  
Estraneo A (2018) Multimodal  
Neuroimaging Approach to Variability  
of Functional Connectivity in Disorders  
of Consciousness: A PET/MRI Pilot  
Study. *Front. Neurol.* 9:861.  
doi: 10.3389/fneur.2018.00861

Carlo Cavaliere<sup>1,2\*</sup>, Sivayini Kandeepan<sup>3†</sup>, Marco Aiello<sup>1</sup>, Demetrius Ribeiro de Paula<sup>3</sup>,  
Rocco Marchitelli<sup>1</sup>, Salvatore Fiorenza<sup>4</sup>, Mario Orsini<sup>1</sup>, Luigi Trojano<sup>5</sup>, Orsola Masotta<sup>4</sup>,  
Keith St. Lawrence<sup>6</sup>, Vincenzo Loreto<sup>4</sup>, Blaine Alexander Chronik<sup>3</sup>, Emanuele Nicolai<sup>1</sup>,  
Andrea Soddu<sup>3†</sup> and Anna Estraneo<sup>4†</sup>

<sup>1</sup> IRCCS SDN, Istituto di Ricerca Diagnostica e Nucleare, Naples, Italy, <sup>2</sup> Coma Science Group, GIGA-Research, University  
and University Hospital of Liege, Liege, Belgium, <sup>3</sup> Department of Physics and Astronomy, Brain and Mind Institute, Western  
University, London, ON, Canada, <sup>4</sup> Neurorehabilitation Unit and Research Laboratory for Disorder of Consciousness, Maudsley  
Hospital, London, UK, <sup>5</sup> IRCCS, Telese Terme, Italy, <sup>6</sup> Department of Psychology, University of Campania "Luigi Vanvitelli," Caserta, Italy, <sup>7</sup> Lawson  
Health Research Institute London, Medical Biophysics, University of Western Ontario, London, ON, Canada

Behavioral assessments could not suffice to provide accurate diagnostic information in individuals with disorders of consciousness (DoC). Multimodal neuroimaging markers have been developed to support clinical assessments of these patients. Here we present findings obtained by hybrid fludeoxyglucose (FDG)-PET/MR imaging in three severely brain-injured patients, one in an unresponsive wakefulness syndrome (UWS), one in a minimally conscious state (MCS), and one patient emerged from MCS (EMCS). Repeated behavioral assessment by means of Coma Recovery Scale-Revised and neurophysiological evaluation were performed in the two weeks before and after neuroimaging acquisition, to ascertain that clinical diagnosis was stable. The three patients underwent one imaging session, during which two resting-state fMRI (rs-fMRI) blocks were run with a temporal gap of about 30 min. rs-fMRI data were analyzed with a graph theory approach applied to nine independent networks. We also analyzed the benefits of concatenating the two acquisitions for each patient or to select for each network the graph strength map with a higher ratio of fitness. Finally, as for clinical assessment, we considered the best functional connectivity pattern for each network and correlated graph strength maps to FDG uptake. Functional connectivity analysis showed several differences between the two rs-fMRI acquisitions, affecting in a different way each network and with a different variability for the three patients, as assessed by ratio of fitness. Moreover, combined PET/fMRI analysis demonstrated a higher functional/metabolic correlation for patients in EMCS and MCS compared to UWS.



In conclusion, we observed for the first time, through a test-retest approach, a variability in the appearance and temporal/spatial patterns of resting-state networks in severely brain-injured patients, proposing a new method to select the most informative connectivity pattern.

**Keywords:** PET/MRI, unresponsive wakefulness syndrome, minimally conscious state, diagnosis, brain connectivity, resting-state fMRI, graph theory, glucose metabolism

## INTRODUCTION

The improvements of medical interventions in the acute and post-acute phase of severe acquired brain injury and the failure of treatments to restore brain functions keep increasing the number of patients with prolonged disorders of consciousness (DoC) (1). These severe clinical conditions entail heavy ethical and social implications, impact health care policies and determine strong psychological distress in patients' families (2–4). Distinguishing patients in unresponsive wakefulness syndrome, UWS [i.e. patients showing eyes opening but no behavioral evidence of consciousness (5)] from patients in minimally conscious state, MCS [i.e., patients showing minimal, inconsistent but clearly discernible intentional behaviors (6)] is pivotal for decision making in the entire care pathway of patients with DoC. Indeed, patients in MCS are more likely to have a better outcome (7, 8) and a higher probability of clinical response to therapeutic interventions than patients in UWS (9–11). However, in spite of the evolution of neuroscientific and medical understanding on DoC, the clinical recognition of volitional behavior still remains a very difficult task (8, 12).

Patients' clinical signs of consciousness are frequently variable across days and even within the same day (13). These inconsistencies have been often linked to temporal fluctuations of vigilance/awareness. For this reason, at least five repeated behavioral assessments by means of validated assessment tools, such as Coma Recovery Scale-Revised (CRS-R) (14), are strongly recommended for improving diagnostic accuracy (15).

However, behavioral assessment might be complicated by possible co-existing severe visuo-perceptual, motor or language disabilities that limit clinical expression of consciousness (7, 16). In this context, a multimodal diagnostic approach, combining clinical and instrumental evaluations, could help detecting signs of consciousness and making a correct diagnosis (17–19). Neuroimaging methods, particularly those not requiring patients' active response, such as resting-state functional MRI (rs fMRI) or 18F FDG-PET, can recognize residual neural activity and functional connectivity into resting state networks (RSNs), such as the default-mode network (DMN), specifically associated with awareness level in such patients, independently from their abilities to produce overt purposeful behaviors (20–22). Moreover, multimodal imaging integration allows collecting a plethora of information undetectable at patients' bedside, but

only simultaneous acquisition of neuroimaging data can assure inter-modality comparability of the findings extracted within the same temporal framework, thus reducing the influence of clinically fluctuations typical of patients with DoC. Additionally, the simultaneous acquisition of structural and functional data by hybrid imaging techniques like PET/MR can improve the patient's compliance, by shortening imaging sessions and reducing logistic issues (23).

The present clinical and neuroimaging pilot study aimed at: (1) investigating possible variability in brain functional connectivity in two distinct fMRI acquisitions within one neuroimaging exam through a test-retest approach; (2) evaluating the relationships of spontaneous functional brain activity with metabolic activity in different levels of consciousness.

For these purposes we combined simultaneous neuroimaging methods (fMRI and PET) and repeated rs-fMRI acquisition in a sample of three severely brain-injured patients with different level of consciousness in stabilized clinical diagnosis of UWS, MCS and emergence from MCS [EMCS, i.e., patient who recovered functional communication or/and functional object use; (5, 6)].

## MATERIALS AND METHODS

### Participants

We screened for the study severely brain-injured patients consecutively admitted to the neurorehabilitation Unit at Maugeri Clinical and Scientific Institutes, in Telese Terme (Italy) from February 2017 to July 2017, fulfilling the following inclusion criteria: (i) clinical diagnosis of UWS, MCS or EMCS according to standard diagnostic criteria (5, 6); (ii) time from onset longer than 1 month; (iii) traumatic, vascular or anoxic brain injury. We excluded from the study patients with: (i) severe pathologies independent from the brain injury (e.g., premorbid history of psychiatric or neurodegenerative diseases); (ii) mixed etiology (e.g., both traumatic and anoxic); (iii) not stabilized and severe general clinical conditions; (iv) contra-indication for MRI (e.g., ferromagnetic aneurysm clips, pacemaker); (v) large brain damage (>50% of total brain volume), as stated by a certified neuroradiologist, and motion parameters >3 mm in translation and 3° in rotation. Patients were also excluded if their clinical diagnosis had changed in the week before the neuroimaging acquisition.

The study was approved by the local Ethics Committee of IRCCS Pascale (Protocol number: 3/15), and performed according to the ethical standards laid down in the 1964 Helsinki

**Abbreviations:** DoC, disorder of consciousness; UWS, unresponsive wakefulness syndrome; MCS, minimally conscious state; CRS-R, Coma Recovery Scale-Revised; PET, positron emission tomography; FDG, fludeoxyglucose; fMRI, functional magnetic resonance imaging.

Declaration and its later amendments. Written informed consent was obtained from the legal guardian of patient.

## Experimental Procedures

### Clinical Assessment

One week before and one week after neuroimaging recording, all enrolled patients underwent at least five clinical evaluations, using the Italian version of the CRS-R (24), in order to confirm stabilized clinical diagnosis of UWS, MCS or EMCS and to gather the best CRS-R total score. Patients' consciousness level (measured by CRS-R total and sub-scores) was also assessed in the "neuroimaging" day by one skilled psychologist (OM) (Table S1).

### Neurophysiological Evaluation

Standard EEG and event related potentials (ERP) were recorded to complement behavioral assessment and to reduce risk of misdiagnosis. For this purpose we acquired neurophysiological exams at patients' bed in 2 days in the week before PET/MRI session and in 2 days in the week after neuroimaging exam, and the best organization of EEG background activity and reactivity was considered for classification of neurophysiological patterns, complementing patients' clinical diagnosis. In the presence of artifacts in more than 50% of EEG recording time, EEG acquisition was repeated in the day after. Two skilled clinical neurophysiologists (VL and SF, blinded to patients' etiology, clinical diagnosis and CRS-R score) reviewed neurophysiological exams.

*Standard EEG* was recorded by 19 electrodes placed on the scalp, according to international 10–20 system (O1, O2, Pz, P3, P4, T5, T6, C3, C4, Cz, T3, T4, Fz, F3, F4, F7, F8, Fp1, and Fp2). We recorded EEG for (at least) 35 min, according to standard procedure of eye-closed waking rest, with filter settings 0.53–70 Hz, and notch filter on. For the analysis of predominant activity, forced eye closing was obtained by cotton wool in awake patient (spontaneous eye opening). To analyse EEG reactivity, eye opening and (forced) eye closing were alternated three times during EEG recording. We classified EEG background activity on the basis of frequency and amplitude of predominant cortical activity present in >50% of recordings, into one of five severity categories, according to criteria recently proposed for patients with prolonged DoC [(25), Appendix 1].

*ERP* were obtained by means of a simple "oddball" paradigm using auditory stimulation and classified as "present" when P300 cortical response was recorded; in presence of N100 component the exam ERP was considered "absent," whereas lack of N100 was considered as a not reliable exam (26).

### PET/MRI Acquisition Protocol

PET/MRI data were simultaneously acquired in the resting state using a Biograph mMR tomograph (Siemens Healthcare, Erlangen, Germany) designed with a multi-ring LSO detector block embedded into a 3 T magnetic resonance scanner. Vacuumed pillows were used to minimize head movements within the scanner. The PET/MRI was acquired in the morning after customary nursing procedures. Moreover, we used some strategies to ensure patients' best vigilance state by: (i)

stopping possible sedative drugs (such as benzodiazepine) 15 h before scanning; (ii) administering CRS-R vigilance protocol (14) before PET/MRI acquisition and during neuroimaging exam at the end of first resting state MRI acquisition; (iii) monitoring eyes opening by means of a video camera located into MRI scanner. In case of appearance of clinical signs of possible drowsiness (i.e., persistence of eye closing), MRI acquisition was stopped and CRS-R vigilance protocol was administered.

Nominal axial and transverse resolution of the PET system was 4.4 and 4.1 mm FWHM, respectively, at 1 cm from the isocenter. Additional technical details on the scanner are reported elsewhere (27).

A dynamic brain PET study was performed after the intravenous bolus administration of 18F-fluorodeoxyglucose (18F-FDG) tracer. PET and rs-fMRI data acquisition started simultaneously following the i.v. injection of 5 MBq/Kg of 18F-FDG.

No food or sugar were administered to the subjects for at least 6 h prior to FDG injection. Blood glucose was measured at arrival at the PET center in all cases, and FDG was injected only if glycaemia was below 120 mg/dl.

The PET data were acquired in list mode for 60 min; matrix size was  $256 \times 256$ . PET emission data were reconstructed with ordered subset-expectation maximization (OSEM) algorithm (21 subsets, 4 iterations) and post-filtered with a three-dimensional isotropic gaussian of 4 mm at FWHM. Attenuation correction was performed using MR-based attenuation maps derived from a dual echo ( $TE = 1.23\text{--}2.46$  ms) Dixon-based sequence (repetition time 3.60 ms), allowing for reconstruction of fat-only, water-only and of fat–water images (28).

During PET acquisition, the following MRI sequences were sequentially run:

- (i) First rs-fMRI acquisition (named "T1") by a T2\*-weighted single-shot EPI sequence (voxel-size  $4 \times 4 \times 4$  mm<sup>3</sup>, TR/TE = 1000/21.4 ms, flip angle =  $82^\circ$ , 480 time points, FOV read = 256 mm, multiband factor = 2, distance factor = 0, TA = 8'06");
- (ii) Three-dimensional T1-weighted magnetization-prepared rapid acquisition gradient-echo sequence (MPRAGE, 240 sagittal planes,  $256 \times 214$  mm field of view, voxel size  $0.8 \times 0.8 \times 0.8$  mm<sup>3</sup>, TR/TE/TI 2400/2.25/1000 ms, flip angle  $8^\circ$ , TA = 6'18");
- (iii) Three-dimensional T2-weighted sequence (240 sagittal planes,  $256 \times 214$  mm field of view, voxel size  $0.8 \times 0.8 \times 0.8$  mm<sup>3</sup>, TR/TE 3370/563 ms, TA = 6'46");
- (iv) Three-dimensional fluid attenuation inversion recovery (FLAIR, 160 sagittal planes,  $192 \times 192$  mm field of view, voxel size  $1 \times 1 \times 1$  mm<sup>3</sup>, TR/TE/TI 5000/334/1800 ms, TA = 6'42");
- (v) Second rs-fMRI acquisition (named "T2") by a T2\*-weighted single-shot EPI sequence (voxel-size  $4 \times 4 \times 4$  mm<sup>3</sup>, TR/TE = 1000/21.4 ms, flip angle =  $82^\circ$ , 480 time points, FOV read = 256 mm, multiband factor = 2, distance factor = 0, TA = 8'06").

In addition, during the same scanning session, axial diffusion weighted images were also acquired for clinical purpose. The two rs-fMRI acquisitions (T1 and T2) were separated by a 30 min interval.

### fMRI and FDG-PET Processing

Resting state fMRI analysis was performed based on a methodology fully described by Ribeiro and colleagues (29). Independent component analysis (ICA) (30) followed by template matching to identify RSNs and machine learning classification to automatically recognize a neuronal source was used. We extracted the weighted graphs for each of the nine networks of interest as described in the paper (29) and calculated the graph strength (GS) for each of the 1015 nodes. Finally, for each network we calculated the correlation between the GS and the metabolic values.

Nine RSNs of interest are recognized: auditory, default mode network (DMN), extrinsic-control network left (ECNL), extrinsic-control network right (ECNR), salience, sensorimotor, visual lateral (VL), visual medial (VM) and visual occipital (VO). The RSNs are assigned as the components with maxima goodness-of-fit (similarity test) when compared to a binary predefined template while considering all the RSNs simultaneously. The templates for each RSN were selected by an expert after visual inspection from a set of spatial maps resulting from a Group ICA decomposition performed on 12 independently assessed controls and were confirmed by another

ROI is considered as a node of a graph; the edges connecting the nodes typically carry weights describing the correlation, or the degree of connectivity between each pair of nodes. After decomposing the whole brain to components using ICA, the weighted matrices ( $w_{ij}$ ) for each of the nine components are obtained by calculating the edge weights using the Equation (1):

$$w_{ij} = |z_i| + |z_j| - |z_i - z_j| \quad (1)$$

where  $w_{ij}$  represents the edge weight between nodes “ $i$ ” and “ $j$ ,” and  $z_i, z_j$  are the  $z$ -values which are obtained from the scalar map of the independent component of interest for the nodes “ $i$ ” and “ $j$ ,” respectively.

Furthermore, the two fMRI acquisitions which were obtained for all three patients within a time interval of 30 min and the FDG-PET data, were manually co-registered with their structural images. These data, along with the concatenated data (combined T1 and T2), underwent an automated pipeline in GraphICAR, which includes further minute realignment and adjustment for movement-related effects, fine co-registration, segmentation of the structural and FDG-PET image, and spatial normalization into standard stereotactic Montreal Neurological Institute (MNI) space as performed in SPM8. Considering the relevance of motion for these dataset, as already reported in Soddu et al. (32), motion parameters such as the mean displacement ( $\Delta$ ) and the displacement speed ( $\Sigma$ ) during the full acquisition were calculated using the equations explicitly given by Equations 2, and 3,

$$\Delta = \left\langle \sqrt{\text{Tra}X^2 + \text{Tra}Y^2 + \text{Tra}Z^2 + \text{Rot}X^2 + \text{Rot}Y^2 + \text{Rot}Z^2} \right\rangle \quad (2)$$

$$\Sigma = \left\langle \sqrt{\Delta_{TR}\text{Tra}X^2 + \Delta_{TR}\text{Tra}Y^2 + \Delta_{TR}\text{Tra}Z^2 + \Delta_{TR}\text{Rot}X^2 + \Delta_{TR}\text{Rot}Y^2 + \Delta_{TR}\text{Rot}Z^2} \right\rangle \quad (3)$$

expert for accuracy of structural labeling (31). Subsequently a classifier trained on an 11-dimensional space called “fingerprint,” that provides both spatial (i.e., degree of clustering, skewness, kurtosis, spatial entropy) and temporal information (i.e., one-lag autocorrelation, temporal entropy, power of five frequency bands: 0–008 Hz, 0.008–0.02 Hz, 0.02–0.05 Hz, 0.05–0.1 Hz, and 0.1–0.25 Hz) of the ICs, is used to select only the neuronal components from the extracted networks (31). Signals arising from changes in local hemodynamics which result solely from alterations in neuronal activity represented by low-frequency (0.01–0.05 Hz) are called neuronal signals. Non-neuronal signals for fMRI data represents cardiovascular signal dominated by higher frequency and head movement.

Once the neuronal components are identified, a graph theoretical approach was applied on the ICs (GraphICAR, BraiNet-Brain Imaging Solution Inc.-Sarnia, ON, Canada) to visualize and calculate the graph properties of each network (30, 32, 33). GraphICAR is a software in which single-subject ICA with 30 components was ordered using the infomax algorithm as implemented in the Group-ICA of fMRI toolbox (RRID: SCR-001953; <http://mialab.mrn.org/software/gift/>). Instead of working at the voxel level (around 100,000 voxels) for the analysis, the cortex was parcellated into 1015 regions of interests (ROIs) with anatomical meaning, using the Lausanne 2008 Atlas with functions from the Connectome Mapping Toolkit (34). Each

Where  $\Delta_{TR}$  represents the variation of a parameter over a TR.

Motion curves were regressed out from the fMRI data when performing the preprocessing using Art repair (RRID:SCR-005990; <http://cibsr.stanford.edu/tools/human-brain-project/artrepair-software.html>), but not the motion parameters. Instead these parameters were just calculated to estimate how much the patients have moved in the scanner during each acquisition.

Segmentation of the images in GraphICAR was performed at the subject level to create its own segmentation (35). Following these preprocessing steps, ICA was applied and  $w_{ij}$  matrices for each of the nine networks were obtained. Simultaneously the scalar maps of the FDG-PET for the 1015 parcellated regions of the cortex were obtained.

The  $w_{ij}$  matrices which have the dimensions of  $1015 \times 1015$  were thresholded such that the  $w_{ij}$  values that are less than the threshold were set to zero while the values greater than the threshold were kept as it is. Thresholds were selected from 0 to 1 in steps of 0.01 and the mean over the thresholded  $w_{ij}$  matrices were obtained. The graph strengths ( $S_i$ ) for each of the 1015 regions for all three subjects and for the nine networks were calculated from the thresholded  $w_{ij}$ , using the Equation (4):

$$S_i = \sum_{j=1}^N W_{ij} \quad (4)$$



where “N” is the total number of regions.

Graph strength (GS) was tested at the network level for proportionality with metabolic activity. In particular, only regions with GS values greater than the thresholded GS (values greater than half of the maximum GS value for the network of interest) were visualized and selected for subsequent calculations.

Non-neuronal networks were removed and the networks classified as neuronal were chosen for the analysis. Using the GS values, the regions belonging to each network (mask), regions outside the network and regions missing in the network for patients in EMCS, MCS and UWS were plotted in different colors for T1, T2 and concatenated data. In the case where the networks from both acquisitions were neuronal, the ratio of fit (ROF) (Equation 5), a measure assessing accuracy of network representation in the analysis, was calculated (Table 1).

$$ROF = \frac{(\text{regions inside the mask} - \text{regions outside the mask})}{(\text{total number of regions which should belong to the mask})} \quad (5)$$

Positive value of ROF indicates a high resemblance of the network (higher the value, better the resemblance), while a negative value means a distorted network. The difference between ROF ( $\Delta ROF$ ) values for T1 and T2 acquisitions of each RSN was used to assess IC variability.

Scalar maps representing the GS for each network were presented by choosing the acquisition with the highest ROF value (best finding) between the two acquisitions and was used for further analysis.

As recalled above, DMN includes several cortical regions whose metabolic activity is thought to be related to level of consciousness (20–22). We believe that presenting the GS directly on the normalized structural images, especially for the DMN has relevance, because it shows the anatomical pattern of the network and permits to visualize the level of disruption or completeness. However, we believe it would be too redundant to present the GS for all networks in the same modality. To ascertain whether the concatenated data or the data corresponding to the acquisition with the best network between T1 and T2 provided the best representation of the network, both concatenated and best acquisition data were plotted.

## Statistical Analysis

Correlation between FDG-PET and GS was performed to measure the similarity between the FDG-PET metabolic maps and the GS activity maps for the whole brain. In order to get the most representative value of the GS for each region from all the networks, the maximum value out of all the neuronal networks for that region was chosen. The z-scores of the GS and PET for each region were calculated and the scatter plots of FDG-PET versus GS were presented for the best and concatenated data for the three patients. “Corrcoeff” function as implemented in MATLAB, which returns the Pearson correlation value ( $r$ ) between the FDG-PET and GS of the 1015 parcellated ROI was calculated and presented along with the statistical  $p$  value for testing the null-hypothesis of no correlation. The  $p$ -value is computed by transforming the correlation into a t-statistical

variable having  $N-2$  degrees of freedom, with  $N$  the number of data points. Furthermore, the distribution of the GS for the best and concatenated data and FDG-PET were estimated.

## RESULTS

### Clinical Features

From a sample of nine severely brain-injured patients, we could consider for PET/fMRI analysis two representative patients with prolonged DoC and one patient emerged from MCS (Figure 1). Detailed descriptions of patients’ clinical features are provided in Appendix and the CRS-R total and subscores in Supplemental Material (Table S1). In synthesis, one anoxic patient was in UWS (F, 43 year old; time since injury: 8 months; best CRS-R total score: 6; CRS-R total score at neuroimaging study: 6), 1 traumatic patient in MCS (M, 18 year old; time since injury: 3 months; best CRS-R total score: 11; CRS-R total score at neuroimaging study: 11), and 1 anoxic patient emerged from MCS 25 days before the neuroimaging study (M, 57 year old; time since injury: 10 months; best CRS-R total score: 22; CRS-R total score at neuroimaging study: 22). The best CRS-R total scores collected in each patient in the weeks before and after the neuroimaging session and in the PET/MRI day are described in Figure 2.

### Neurophysiological Findings

The best neurophysiological findings out of 4 EEGs and 4 ERPs recorded in each patient are summarized in Figure 2. In the patient in UWS we observed a poor organization of cortical activity with predominant EEG delta activity with amplitude less than  $20 \mu V$  over most brain regions, not reactive to eye closing (i.e., Low Voltage, LV category) and lack of P300. In the patient in MCS we observed predominant reactive posterior theta EEG activity (amplitude  $>20 \mu V$ ), with frequent posterior alpha rhythm (i.e., mildly abnormal, MiA category) in 3 out of 4 EEG recordings. A P300 cortical response was recorded at least following “oddball” paradigm in 3 out of 4 exams. In the patient in EMCS, a predominant reactive posterior theta EEG activity (amplitude  $\geq 20 \mu V$ ), with frequent posterior alpha rhythms (i.e., mildly abnormal, MiA EEG category) was recorded in 2 out of 4 EEG recordings. In all EEG acquisitions, the background activity showed reactivity to eye opening and closing. The “oddball” paradigm evoked a positive cortical component (i.e., P300) in 3 out of 4 exams.

### Within-Session fMRI Variability

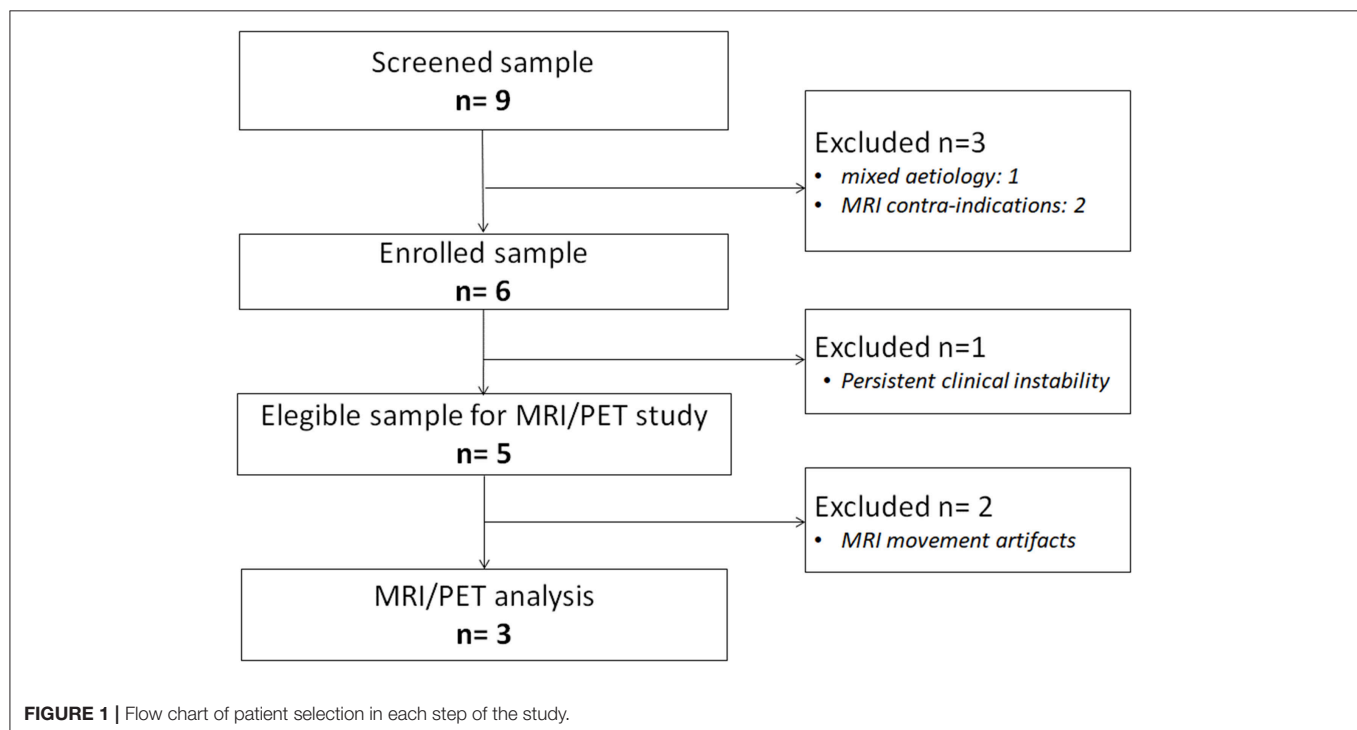
In the patient in EMCS, the DMN appeared spatially preserved during the first (T1) rs-fMRI acquisition ( $ROF = 0.19$  vs.  $ROF = 0.01$  at T2), with a main neuronal component (Figure 3, Table 1). The ECN was well preserved in both acquisitions on the left, although in the T2 rs-fMRI there was some superposition due to other regions, as shown by the negative value of ROF ( $-0.08$  vs.  $ROF = 0.12$  at T1), while it appeared inconsistent on the right, and not neuronal in T1 acquisition. Auditory and salience networks were partially preserved and evident only in the T2 scan. Moreover, the auditory appeared more lateralized to the left (Figure 3, Table 1). Sensorimotor was spatially preserved in T1, where it appeared wider for the co-activation of many nodes



**TABLE 1** | ROF values calculated from regions belonging to the GS values, separated into the regions belonging to the network itself and outside the network.

Networks	EMCS							MCS							UWS						
	T1			T2				T1			T2				T1			T2			
	In	Out	ROF	In	Out	ROF	ΔROF	In	Out	ROF	In	Out	ROF	ΔROF	In	Out	ROF	In	Out	ROF	ΔROF
Auditory				85	87	−0.01	0.01	41	26	0.06	36	9	0.10	−0.04				108	162	−0.20	0.20
DMN	81	13	0.19	78	76	0.01	0.18	82	8	0.21	107	44	0.18	0.03	53	123	−0.20				−0.20
ECNL	46	27	0.12	57	70	−0.08	0.20	20	142	−0.80	48	88	−0.26	−0.54	29	158	−0.84				−0.84
ECNR				11	0	0.08	−0.08	30	49	−0.15	46	125	−0.60	0.45							
Saliency				30	108	−0.67	0.67	58	303	−2.11	46	228	−1.57	−0.54	16	52	−0.31	37	235	−1.71	1.40
Sensorimotor	39	213	−1.71	2	27	−0.25	−1.46	42	30	0.12	41	13	0.27	−0.15	36	69	−0.32				−0.32
VL				35	179			4	79	−0.56	10	75	−0.49	−0.07				42	108	−0.50	0.50
VM	125	37	0.32	37	22	0.05	0.27	93	21	0.26	48	53	−0.02	0.28							
VO								41	54	−0.07	93	57	0.20	−0.27				6	14	−0.04	0.04

"In" and "Out" represent the total number of regions belonging to and outside of the network. Values of the non-neuronal networks are not presented.

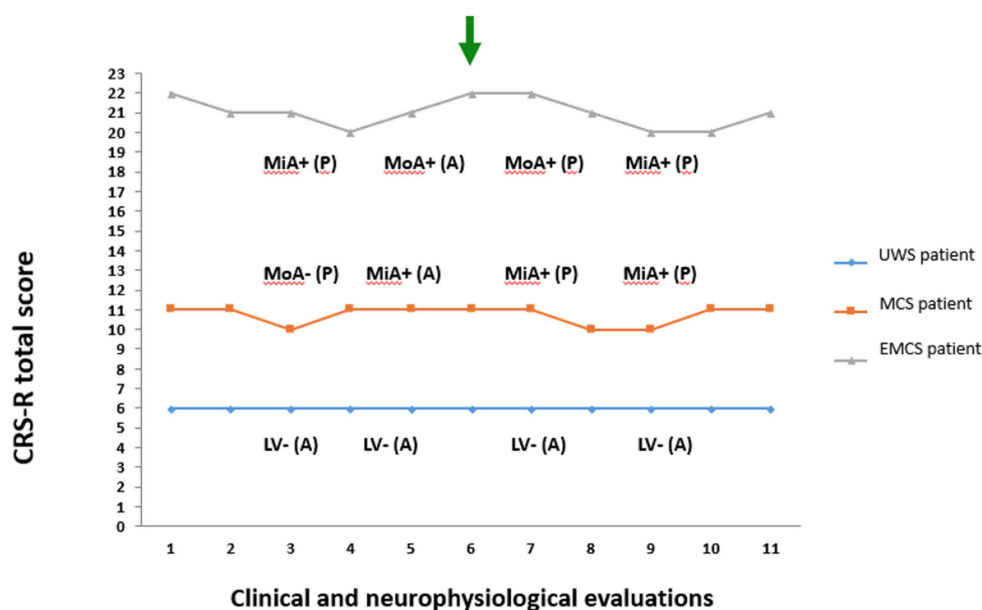


outside the network (ROF = −1.71). VL and VO were recognized as not neuronal in both scans, while VM appeared well preserved with a better spatial pattern in T1 acquisition (ROF = 0.32 vs. 0.05 at T2) (Figure 3, Table 1).

In the patient in MCS, the preservation of DMN was clear in both acquisitions (T1 and T2), with ROF values of 0.21 and 0.18, respectively. The ECN was partially recognized for both hemispheres in both acquisitions although the number of nodes outside the network was high as highlighted by the negative values of ROF (Figure 3, Table 1). Auditory and sensorimotor networks appeared well preserved in both acquisitions, with a complementary mirrored visualization for the auditory one between T1 and T2. On the other hand, the salience network

was evident in both acquisitions, but with a spread co-activation of nodes outside the network (ROF = −2.11 and −1.57 at T1 and T2, respectively) (Figure 3, Table 1). As for the three visual networks, while the VL was recognized as neuronal in both T1 and T2, but with a poor spatial representation, both VM and VO appeared temporal and spatially preserved with a better visualization of VM at T1 (ROF = 0.26 vs. −0.02 at T2), and of VO at T2 (ROF = 0.20 vs. −0.07 at T1) (Figure 3, Table 1).

In the patient in UWS, ECNR was not found in both acquisitions, while the DMN and ECNL were partially detected in T1, although with high number of regions outside the networks revealed by negative values of ROF (−0.20 and −0.84 respectively) (Figure 3, Table 1). In the same manner,



**FIGURE 2 |** Coma Recovery Scale-Revised total score and neurophysiological (EEG and evoked related potential) evaluations recorded in the 3rd and 5th day before PET/fMRI exam and in the 7th and 9th day after the PET/fMRI exam. The green arrow marks the day of neuroimaging acquisition. The blue diamond and line denote the patient in unresponsive wakefulness syndrome (UWS). The orange square and line denote the patient in minimally conscious state (MCS). The gray triangle and line denote the patient emerged from MCS (EMCS). CRS-R, Coma Recovery Scale-Revised; P, presence of P300 on evoked related potential; A, absence of P300 on evoked related potential; +, presence of EEG reactivity to eye opening and closing; -, absence of EEG reactivity to eye opening and closing; MiA, mildly abnormal EEG background activity; MoA, moderately abnormal EEG background activity; DS, Diffuse slowing EEG background activity; LV, Low voltage EEG background activity.

the salience network was detected in both acquisitions along with more regions outside the network (ROF = -0.31 and -1.71 respectively). Auditory and sensorimotor networks were identified only in one acquisition, with a higher number of regions belonging outside of the network (ROF = -0.20, -0.32) (Figure 3, Table 1). Finally, out of the three visual networks, contrary to the other two patients, VM was not identified in either acquisition. VL and few regions of VO were detected in the second acquisition (Figure 3, Table 1).

Summarizing, a wider variability was found for ICs representation in the patient in EMCS (mean  $|\Delta\text{ROF}| = 0.32$ ) and in UWS (mean  $|\Delta\text{ROF}| = 0.39$ ) than in MCS case (mean  $|\Delta\text{ROF}| = 0.26$ ).

## Mutual fMRI Findings

When considering the best finding between the two rs-fMRI acquisitions (T1 and T2) for each network, ICA components classified as neuronal networks were 61, 100, and 44% for patients in EMCS, MCS, and UWS (Figure S1), respectively. In the patient in EMCS, the DMN and VM networks were fully preserved, and most regions of ECN and sensorimotor were detected as well (Figure S1). Regions belonging to the spatial pattern and extra regions were identified in the auditory network, while mainly regions that did not belong to the salience network were detected. Out of the three visuals, only the VM was identified as neuronal with a good spatial representation of the network. In the patient in MCS (Figure S1), almost all the networks except the salience network seem to be well preserved, despite ECNR being spread

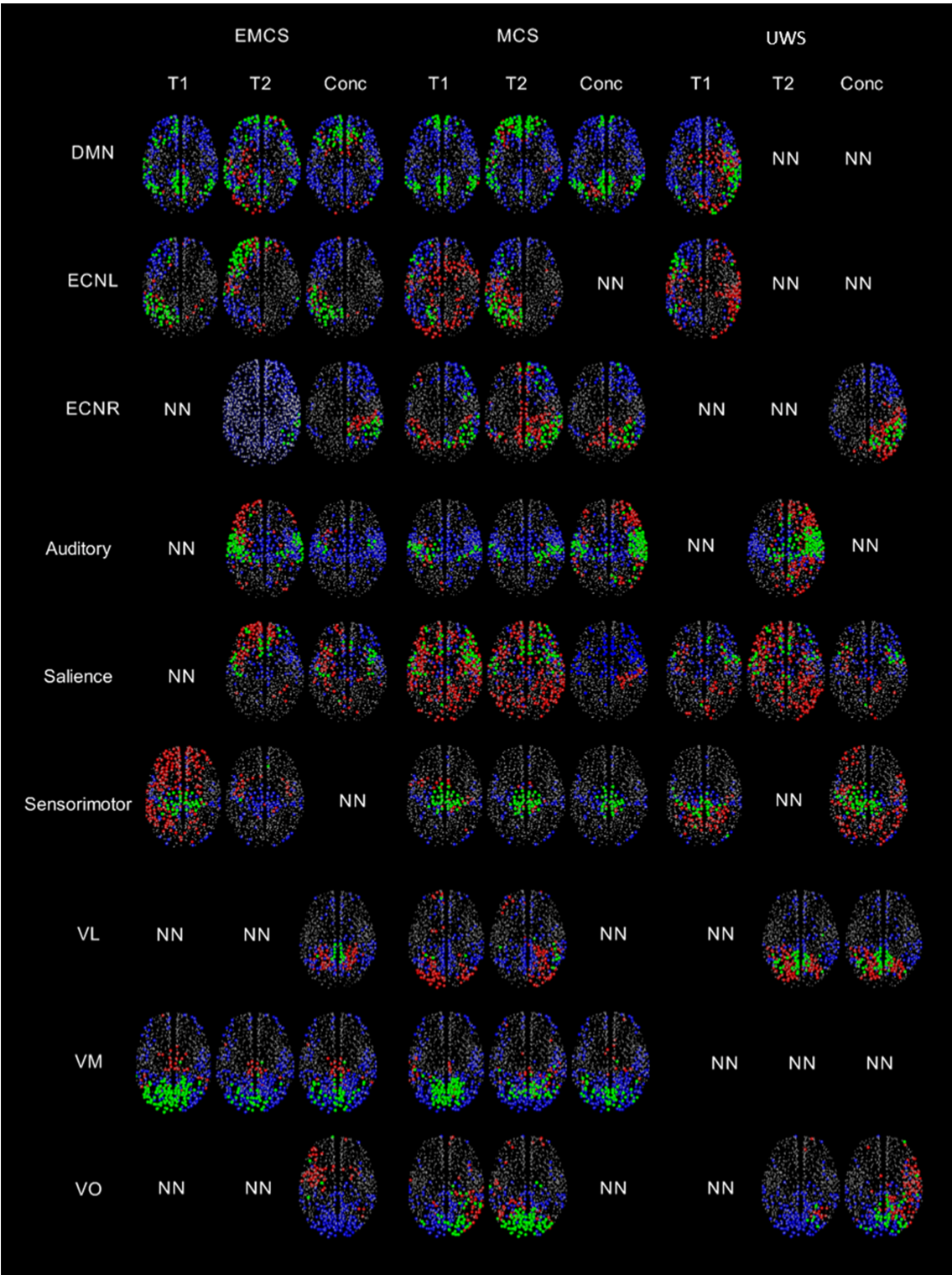
out to both hemispheres and VL being lateralized. In the patient in UWS, the spatial patterns of most of the networks (except the sensorimotor and VM) were not well defined (Figure S1).

The head displacement of the patient in EMCS in the scanner during both T1 and T2 acquisitions was 0.09, whereas for the patient in MCS they were 0.03 and 0.06, respectively. Overall the lowest displacement was observed for the patient in UWS with the values of 0.02 and 0.04 respectively (Figure S2). The speed of the patients in the scanner for the T1 and T2 acquisitions of patient in EMCS were  $2.0 \times 10^{-4}$  and  $3.7 \times 10^{-4}$ , for patient in MCS:  $2.9 \times 10^{-5}$  and  $1.9 \times 10^{-4}$ , and for patient in UWS:  $6.3 \times 10^{-4}$  and  $5.6 \times 10^{-5}$  respectively (Figure S2).

Looking at the spatial distribution of the three most representative axial slices of the GS implemented on the normalized structure of the DMN network, in the best acquisition of both EMCS and MCS, this network was preserved throughout the brain, while in the patient in UWS, the GS seems to be highlighted mostly in the areas outside the network (Figure S3). In the concatenated case, the network was present only in the patient in MCS, but in the patient in EMCS, only the frontal part was found while in the patient in UWS, the network was not even recognized. In this figure, the GS values from 0.5 to 1 were represented in the jet color notation.

## Functional-Metabolic Correlation

Considering the functional-metabolic correlation in these patients, a significant positive correlation ( $p < 0.05$ ) existed between the FDG-PET and GS for all three patients when



**FIGURE 3 |** A visual representation of the regions highlighted by the thresholded GS (values greater than half of the maximum GS value for the network), separated by the regions within and outside the network for patients in EMCS, MCS and UWS for nine RSNs. Regions belonging to the network and having GS values greater than the thresholded GS are represented by green, regions which should be in the network but do not have GS values greater than the thresholded GS are represented by blue, regions outside the network but have GS values greater than the thresholded GS are represented by red color. NN represents non-neuronal networks. Here the size of the circle doesn't represent the value of the GS, all the regions with a GS value are plotted evenly.

considering the whole brain (**Figure S4**). In the best ICs pattern, EMCS had the highest correlation ( $r = 0.19$ ,  $p < 0.01$ ), whereas in the concatenated case, the MCS had the highest correlation ( $r = 0.21$ ,  $p < 0.01$ ). This implies that, when both results are reasonably good, concatenated data seems to give a better representation. It's evident that overall the patient in UWS had the lowest correlation out of all three patients with correlation values of 0.08 ( $p = 0.02$ ) and 0.10 ( $p < 0.01$ ) for the best and concatenated data respectively. The positive skewness value of 0.31 for the FDG-PET distribution (**Figure S5**) of the patient in EMCS indicated that there were many regions metabolically more active than the mean PET value. In the UWS instance, many regions were lower or similar in activity to the mean value, as confirmed by the negative skewness value of  $-0.01$ .

## DISCUSSION

In the present pilot study, we investigated variability within a period of about 30 min in brain functional connectivity in three severely brain-injured patients (two patients still with DoC and one patient emerged from DoC). Moreover, we employed a methodological approach based on the graph theory and independent component analysis, to decompose brain connectivity maps in different networks and to correlate it to glucose metabolic activity simultaneously acquired through a PET/MRI scanner. We could demonstrate several differences between the two rs-fMRI acquisitions affecting in a different way each network and with a different variability in the three patients.

Functional connectivity assessed among the nodes belonging to different resting-state networks is sensitive to normal aging (36) and levels of consciousness (37–40), representing a potential biomarker of disease in longitudinal studies (41). Although being quite variable during pathological conditions, RSNs examined with a test-retest approach are thought to be highly reproducible within the same sample (42, 43). In a recent paper (44), co-activation patterns approach has been used in DoC patients, demonstrating heterogeneous spatial reconfiguration of DMN but also similar fluctuations of the BOLD signal in patients compared to control individuals. While these authors referred to BOLD signal oscillations during a single resting-state fMRI session, we scheduled two resting-state acquisitions with a 30-min interval, to investigate through a test-retest approach possible variability in functional connectivity within RSNs. Several differences were found between T1 and T2 session, with higher variability for the EMCS and the UWS case, compared to the patient in MCS. These findings apparently did not fit the substantial stability in the clinical diagnosis demonstrated by repeated behavioral assessments in the present brain-injured patients. However, we could speculate that this novel methodological approach is suitable to detect minimal fluctuations in brain connectivity not sufficient to determine relevant behavioral changes (i.e., by changes in clinical diagnosis), but nonetheless likely related to the variations detected by multiple CRS-R total scores and neurophysiological assessments. However, the nature and clinical significance of the fluctuations of the functional connectivity observed here remain to be

established. Furthermore, multimodal investigations, possibly combining neuroimaging and neurophysiological assessment, are necessary to ascertain if variability in brain connectivity is associated to temporal variability of EEG activity characterizing patients with high probability of vigilance fluctuations (45).

On the basis of these considerations, we suggest that this innovative approach for neuroimaging analysis could permit clinicians to better identify the best functional brain performance, needed for the diagnostic classification of patients with high likelihood of clinical misdiagnosis. These findings could be extremely interesting, mainly for patients who are clinically diagnosed as UWS, where possible minimal and inconsistent signs of consciousness may not be recognized by behavioral assessments, leading to possible misdiagnosis (12, 46–48), and for detecting subtle signs of recovery of consciousness (8, 49, 50).

The same methodology should be applied to larger patient samples, also including a high number of patients without fluctuations of CRS-R total score, to comprehend which variations of functional connectivity might be related to substantial clinical fluctuations or to a basic variability of neuronal network.

The differences in spatial patterns observed in the two acquisitions within the same patient might be due to motion and artifacts. These artifacts affect the nine networks in different manner (32). However, the present findings suggest that not necessarily one acquisition is capable of detecting spared or impaired networks reliably. This observation suggests acquiring more than one acquisition during the scanning interval and to develop a gold standard for choosing the best one.

The GS scalar maps of most networks were more similar to the standard template of the networks in the patients in EMCS and MCS than in the patient in UWS. Specifically, all the networks of the patient in MCS and the important networks (but VL and VO) of the patient in EMCS were recognized. This implies that the brain functional organization was relatively preserved for the patients in EMCS and MCS. However, the auditory and salience networks had higher GS in regions outside the network likely in relation to the brain lesion. In the patient in MCS, although the salience network behaved as neuronal, the spatial pattern was not well-defined, suggesting that this network was distorted and metabolically impaired. Although seven out of the nine networks could be recognized in the patient in UWS, they had hyper-connectivity (confirmed by the negative ROF values), resembling non-normal condition. This might be related to the severe pathological condition of the patient in UWS affecting the spatial patterns of most networks (32).

A significant positive correlation was observed between the FDG-PET and GS for all three patients, although the  $r$  values were small. Overall, a higher correlation was observed for the patient in EMCS and MCS compared to the UWS case while using the concatenated data. The negative skewness value for the FDG-PET of the patient in UWS (FDG-PET values region by region were normalized by the global signal or mean all over the 1015 regions), is explained by the fact that there are only few regions with metabolic activity above the mean value. In the patient in EMCS, the distribution of the FDG-PET is tailed



toward the left with a positive skewness value showing that there are several regions more metabolically active than the average, favoring conscious behavior.

## Limitations of the Study

The present study had several limitations. First, we acknowledge that the low number of patients was a major limitation. We selected three patients with different clinical diagnosis (i.e., UWS, MCS and EMCS), to preliminarily investigate possible variability in fMRI connectivity in patients with different level of consciousness. The small sample size did not allow any generalization, but we hope that our preliminary study could serve as a starting point for devising multicenter studies on larger samples, comparing data of patients with different levels of consciousness, different etiologies and in different disease phases. Second, we could not calculate rigorous associations between patients' behavioral profiles (measured by repeated CRS-R assessments) and their possible brain connectivity variability, since the two features could not be measured in the same time window. Also, we did not perform clinical assessments immediately before and at the end of MRI acquisition since it could not ensure a strictly closed evaluation of possible patients' fluctuation in the two fMRI acquisitions.

May be the best tool to quantitatively assess even sub-clinical variations of cortical activity that could be correlated with repeated resting state fMRI seems to be prolonged EEG monitoring (45). However, we would underline that we enrolled patients in stabilized clinical diagnosis (even though in slightly fluctuated CRS-R scores), as demonstrated by repeated clinical assessments in the weeks before and after neuroimaging day, and with time from brain injury more than 1 month in order to minimize possible biases related to spontaneous clinical changes in the two different resting MRI acquisitions. Third, a lack of specific alertness level monitoring (such as EEG recording) during scanning acquisition could be a limit for the analysis within and between subjects, since we could not exclude variations in wakefulness as confounders for intrinsic functional connectivity analysis (51). However, we used some strategies to ensure patients' best vigilance state as described above.

Finally, the lack of a control group was a limitation of the present study, although the choice of the best reference group for patients with DoC is still debated (healthy subjects vs. injured patients that recovered consciousness, like for EMCS). Nevertheless, rs-fMRI functional connectivity metrics, mainly extracted by ICA, have demonstrated a high test-retest reproducibility (42). Moreover, other studies have demonstrated the potential of rs-fMRI functional-metabolic correlation assessed by simultaneous PET/MRI in healthy subjects (52), and in other neurological conditions, like Alzheimer disease (53).

## CONCLUSIONS

Since repeated acquisitions within 30 min showed relevant variability through a test-retest fMRI approach, we suggest performing multiple acquisitions within the same session to pick the best findings and possibly to compare these findings

in longitudinal acquisitions. This procedure, together with the combined simultaneous acquisition of fMRI and PET, could provide useful information for improving characterization of patients with DoC. In a not well-defined number of patients with clinical diagnosis of unresponsive wakefulness syndrome, paraclinical testing (such as fMRI by active task or acquisition in resting state) could reveal cortically mediated cognitive functions (the so-called covert cognition). In this context our approach (i.e., double resting fMRI acquisitions combined with PET scanner) could help clinicians to increase the probability of detecting (spared) functional connectivity, which might provide diagnostic and prognostic information.

## ETHICS STATEMENT

All procedures performed in the studies involving human participants were in accordance with the ethical standards of the institutional review boards of PLA Army General Hospital and with the 1964 Helsinki Declaration and its later amendments or comparable ethical standards.

## AUTHOR CONTRIBUTIONS

CC and SK: Study concept and design, analysis and interpretation of data, manuscript preparation; MA, OM, and EN: Imaging protocol design and acquisition; RM: Interpretation of data and manuscript revision; DR: Processing the data; LT: Revision of manuscript; VL: Acquisition of data, analysis and interpretation of data; SF: Neurophysiological data acquisition, analysis, and interpretation of data; MO: Clinical assessment, analysis and interpretation of data; BC and KS: Study concept and design; AS: Study concept and design, interpretation of data and critical revision of manuscript; AE: Study concept and design, interpretation of data and critical revision of manuscript for intellectual content.

## FUNDING

This work was supported by Italian Ministry of Health, Ricerca Finalizzata, project code PE-2013-02358145.

## SUPPLEMENTARY MATERIAL

The Supplementary Material for this article can be found online at: <https://www.frontiersin.org/articles/10.3389/fneur.2018.00861/full#supplementary-material>

**Figure S1** | GS scalar maps of the nine RSNs of patients in EMCS, MCS, and UWS. From the two acquisitions, only the networks classified as neuronal are shown. When both acquisitions had neuronal components, the highest ROF value was used to choose the best spatial pattern of the network. The size of the circle represents the strength of the GS. The darker the circle, the higher the GS. Only the GS values greater than 0.5 of the maximum GS value of that network are plotted.

**Figure S2** | Motion curves illustrate translation (in mm) for x (blue), y (red), and z (orange) and rotation (in °) for pitch (blue), roll (red), and yaw (orange) parameters, and the time courses of each the nine RSNs (auditory, DMN, ECNL, ECNR, salience, sensorimotor, VL, VM, and VO) over 480 s.

**Figure S3** | Three most representative axial slices of the GS implemented on the normalized structure of the DMN network are presented for the three patients for the best functional pattern and concatenated data.

**Figure S4** | Scatter plots for the EMCS, MCS and patients in UWS showing the correlation between the FDG-PET and GS of the 1015 parcellated ROI. Solid line indicates the best linear fit to the data and on the northeast corner of each scatter plot the linear correlation value is reported along with its statistical  $p$ -value.

**Figure S5** | Distribution plots of GS for the best acquisition, concatenated data and FDG-PET for patients in EMCS, MCS and UWS.

**Table S1** | Coma Recovery Scale-Revised total and subscores in the three patients collected in the day of neuroimaging and 5 days in 1 week before and after.

**Appendix 1** | Classification criteria for visual analysis of EEG background activity.

## REFERENCES

- Bernat JL. Chronic disorders of consciousness. *Lancet* (2006) 367:1181–92. doi: 10.1016/S0140-6736(06)68508-5
- Sattin D, De Torres L, Dolce G, Arcuri F, Estraneo A, Cardinale V, et al. Analysis of Italian regulations on pathways of care for patients in a vegetative or minimally conscious state. *Funct Neurol*. (2017) 32:159. doi: 10.11138/FNeur/2017.32.3.159
- Moretta P, Estraneo A, De Lucia L, Cardinale V, Loreto V, Trojano L. A study of the psychological distress in family caregivers of patients with prolonged disorders of consciousness during in-hospital rehabilitation. *Clin Rehabil*. (2014) 28:717–25. doi: 10.1177/0269215514521826
- Moretta P, Masotta O, Crispino E, Castronovo G, Ruvolo S, Montalbano C, et al. Psychological distress is associated with altered cognitive functioning in family caregivers of patients with disorders of consciousness. *Brain Inj*. (2017) 31:1088–93. doi: 10.1080/02699052.2017.1290278
- Multi-Society Task Force on PVS. Medical aspects of the persistent vegetative state. *N Engl J Med*. (1994) 330:1499–508. doi: 10.1056/NEJM199405263302107
- Giacino JT, Ashwal S, Childs N, Cranford R, Jennett B, Katz DI, et al. The minimally conscious state definition and diagnostic criteria. *Neurology* (2002) 58:349–53. doi: 10.1212/WNL.58.3.349
- Estraneo A, Moretta P, Loreto V, Santoro L, Trojano L. Clinical and neuropsychological long-term outcomes after late recovery of responsiveness: a case series. *Arch Phys Med Rehabil*. (2014) 95:711–6. doi: 10.1016/j.apmr.2013.11.004
- Estraneo A, Trojano, L. Prognosis in Disorders of Consciousness. In: Schnakers C, Laureys S, Editors. *Coma and Disorders of Consciousness*. Cham: Springer (2018). pp. 17–36.
- Schnakers C, Monti MM. Disorders of consciousness after severe brain injury: therapeutic options. *Curr Opin Neurol*. (2017) 30:573–9. doi: 10.1097/WCO.0000000000000495
- Estraneo A, Pascarella A, Moretta P, Masotta O, Fiorenza S, Chirico G, et al. Repeated transcranial direct current stimulation in prolonged disorders of consciousness: a double-blind cross-over study. *J Neurol Sci*. (2017) 375:464–470. doi: 10.1016/j.jns.2017.02.036
- Cavaliere C, Aiello M, Di Perri C, Amico E, Martial C, Thibaut A, et al. Functional connectivity substrates for tDCS response in minimally conscious state patients. *Front Cell Neurosci*. (2016) 10:257. doi: 10.3389/fncel.2016.00257
- Schnakers C, Vanhaudenhuyse A, Giacino J, Ventura M, Boly M, Majerus S, et al. Diagnostic accuracy of the vegetative and minimally conscious state: clinical consensus versus standardized neurobehavioral assessment. *BMC Neurology* (2009) 9:35. doi: 10.1186/1471-2377-9-35
- Cortese MD, Riganello F, Arcuri F, Pugliese ME, Lucca LF, Dolce G, et al. Coma recovery scale-r: variability in the disorder of consciousness. *BMC Neurol*. (2015) 15:186. doi: 10.1186/s12883-015-0455-5
- Giacino JT, Kalmar K, Whyte J. The JFK coma recovery scale-revised: measurement characteristics and diagnostic utility. *Arch Phys Med Rehabil*. (2004) 85:2020–9. doi: 10.1016/j.apmr.2004.02.033
- Wannez S, Heine L, Thonnard M, Gosseries O, Laureys S. (2017). The repetition of behavioral assessments in diagnosis of disorders of consciousness. *Ann Neurol*. 81:883–9. doi: 10.1002/ana.24962
- Majerus S, Gill-Thwaites H, Andrews K, Laureys S. Behavioral evaluation of consciousness in severe brain damage. *Prog Brain Res*. (2005) 150:397–413. doi: 10.1016/S0079-6123(05)50028-1
- Cavaliere C, Aiello M, Di Perri C, Fernandez-Espejo D, Owen AM, Soddu A. Diffusion tensor imaging and white matter abnormalities in patients with disorders of consciousness. *Front Hum Neurosci*. (2015) 8:1028. doi: 10.3389/fnhum.2014.01028
- Schiff ND. Multimodal neuroimaging approaches to disorders of consciousness. *J Head Trauma Rehabil*. (2006) 21:388–97. doi: 10.1097/00001199-200609000-00003
- Bruno MA, Majerus S, Boly M, Vanhaudenhuyse A, Schnakers C, Gosseries O, et al. Functional neuroanatomy underlying the clinical subcategorization of minimally conscious state patients. *J Neurol*. (2012) 259:1087–98. doi: 10.1007/s00415-011-6303-7
- Coleman MR, Davis MH, Rodd JM, Robson T, Ali A, Owen AM, et al. Towards the routine use of brain imaging to aid the clinical diagnosis of disorders of consciousness. *Brain* (2009) 132:2541–52. doi: 10.1093/brain/awp183
- Soddu A, Gómez F, Heine L, Di Perri C, Bahri MA, Voss HU, et al. Correlation between resting state fMRI total neuronal activity and PET metabolism in healthy controls and patients with disorders of consciousness. *Brain Behav*. (2016) 6:e00424. doi: 10.1002/brb3.424
- Stender J, Gosseries O, Bruno MA, Charland-Verville V, Vanhaudenhuyse A, Demertzi A, et al. Diagnostic precision of PET imaging and functional MRI in disorders of consciousness: a clinical validation study. *Lancet* (2014) 384:514–22. doi: 10.1016/S0140-6736(14)60042-8
- Aiello M, Cavaliere C, Salvatore, M. Hybrid PET/MR imaging and brain connectivity. *Front Neurosci*. (2016) 10:64. doi: 10.3389/fnins.2016.00064
- Estraneo A, Moretta P, De AT, Gatta G, Giacino JT, Trojano, L. An Italian multicentre validation study of the coma recovery scale-revised. *Eur J Phys Rehabil Med*. (2015) 51:627–34.
- Estraneo A, Loreto V, Guarino I, Boemia V, Paone G, Moretta P, et al. Standard EEG in diagnostic process of prolonged disorders of consciousness. *Clin Neurophysiol*. (2016) 127:2379–85. doi: 10.1016/j.clinph.2016.03.021
- Duncan CC, Barry RJ, Connolly JF, Fischer C, Michie PT, Näätänen R, et al. Event-related potentials in clinical research: guidelines for eliciting, recording, and quantifying mismatch negativity, P300, and N400. *Clin Neurophysiol*. (2009) 120:1883–908. doi: 10.1016/j.clinph.2009.07.04
- Delso G, Fürst S, Jakoby B, Ladebeck R, Ganter C, Nekolla SG, et al. (2011). Performance measurements of the Siemens mMR integrated whole-body PET/MR scanner. *J Nucl Med*. 52:1914–22. doi: 10.2967/jnumed.111.092726
- Berker Y, Franke J, Salomon A, Palmowski M, Donker HC, Temur Y, et al. MRI-based attenuation correction for hybrid PET/MRI systems: a 4-class tissue segmentation technique using a combined ultrashort-echo-time/Dixon MRI sequence. *J Nucl Med*. (2012) 53:796–804. doi: 10.2967/jnumed.111.092577
- Ribeiro de Paula D, Ziegler E, Abeyasinghe PM, Das TK, Cavaliere C, Aiello M, et al. A method for independent component graph analysis of resting-state fMRI. *Brain Behav*. (2017) 7:e00626. doi: 10.1002/brb3.626
- Beckmann CF, DeLuca M, Devlin JT, Smith SM. Investigations into resting-state connectivity using independent component analysis. *Philos Trans R Soc Lond B Biol Sci*. (2005) 360:1001–13. doi: 10.1098/rstb.2005.1634
- Demertzi A, Gomez F, Crone JS, Vanhaudenhuyse A, Tshibanda L, Noirhomme Q, et al. Multiple fMRI system-level baseline connectivity is disrupted in patients with consciousness alterations. *Cortex* (2014) 52:35–46. doi: 10.1016/j.cortex.2013.11.005
- Soddu A, Vanhaudenhuyse A, Bahri M, Bruno MA, Boly M, Demertzi A, et al. Identifying the default mode component in spatial IC analysis of

- patients with disorders of consciousness. *Hum Brain Mapp.* (2012) 33:778–96. doi: 10.1002/hbm.21249
33. Maudoux A, Lefebvre P, Demertzi A, Cabay JE, Vanhaudenhuyse A, Laureys S, et al. Connectivity graph analysis of the auditory resting state network in tinnitus. *Brain Res.* (2012) 16:10–21. doi: 10.1016/j.brainres.2012.05.006
  34. Gerhard S, Daducci A, Lemkaddem A, Meuli R, Thiran JP, Hagmann, P. The connectome viewer toolkit: an open source framework to manage, analyze, and visualize connectomes. *Front Neuroinform.* (2011) 6:3. doi: 10.3389/fninf.2011.00003
  35. Fischl B, Salat, DH, Busa E, Makris N, Rosen B, Dale AM, et al. (2002) Whole brain segmentation: automated labeling of neuroanatomical structures in the human brain. *Neuron* 33:341–55. doi: 10.1016/S0896-6273(02)00569-X
  36. Greicius MD, Krasnow B, Reiss AL, Menon, V. Functional connectivity in the resting brain: a network analysis of the default mode hypothesis. *Proc Natl Acad Sci USA.* (2003) 100:253–8. doi: 10.1073/pnas.0135058100
  37. Bonhomme V, Vanhaudenhuyse A, Demertzi A, Bruno MA, Jaquet O, Bahri MA, et al. Resting-state network-specific breakdown of functional connectivity during ketamine alteration of consciousness in volunteers. *Anesthesiology* (2016) 125:873–88. doi: 10.1097/ALN.0000000000001275
  38. Guldenmund P, Gantner IS, Baquero K, Das T, Demertzi A, Boveroux P, et al. Propofol-induced frontal cortex disconnection: a study of resting-state networks, total brain connectivity, and mean BOLD signal oscillation frequencies. *Brain Connect.* (2016) 6:225–37. doi: 10.1089/brain.2015.0369
  39. Demertzi A, Antonopoulos G, Heine L, Voss HU, Crone JS, de Los Angeles C, et al. Intrinsic functional connectivity differentiates minimally conscious from unresponsive patients. *Brain* (2015) 138:2619–31. doi: 10.1093/brain/awv169
  40. Vanhaudenhuyse A, Noirhomme Q, Tshibanda LJE, Bruno MA, Boveroux P, Schnakers C, et al. Default network connectivity reflects the level of consciousness in non-communicative brain-damaged patients. *Brain* (2009) 133:161–71. doi: 10.1093/brain/awp313
  41. Persson J, Pudas S, Nilsson LG, Nyberg L. Longitudinal assessment of default-mode brain function in aging. *Neurobiolaging* (2014) 35:2107–17. doi: 10.1016/j.neurobiolaging.2014.03.012
  42. Jovicich J, Minati L, Marizzoni M, Marchitelli R, Sala-Llonch R, Bartres-Faz D, et al. Longitudinal reproducibility of default-mode network connectivity in healthy elderly participants: a multicentric resting-state fMRI study. *Neuroimage* (2016) 124:442–54. doi: 10.1016/j.neuroimage.2015.07.010
  43. Termenon M, Jaillard A, Delon-Martin C, Achard, S. Reliability of graph analysis of resting state fMRI using test-retest dataset from the Human Connectome Project. *Neuroimage* (2016) 142:172–87. doi: 10.1016/j.neuroimage.2016.05.062
  44. Di Perri C, Amico E, Heine L, Annen J, Martial C, Larroque SK, et al. Multifaceted brain networks reconfiguration in disorders of consciousness uncovered by co-activation patterns. *Hum Brain Mapp.* (2018) 39:89–103. doi: 10.1002/hbm.23826
  45. Piarulli A, Bergamasco M, Thibaut A, Cologan V, Gosseries O, Laureys, S. EEG ultradian rhythmicity differences in disorders of consciousness during wakefulness. *J Neurol.* (2016) 263:1746–60. doi: 10.1007/s00415-016-8196-y
  46. Owen AM, Coleman MR, Boly M, Davis MH, Laureys S, Pickard JD. Detecting awareness in the vegetative state. *Science* (2006) 313:1402–1402. doi: 10.1126/science.1130197
  47. Owen AM, Coleman MR. Functional neuroimaging of the vegetative state. *Nat Rev Neurosci.* (2008) 9:235. doi: 10.1038/nrn2330
  48. Owen AM, Coleman MR. Detecting awareness in the vegetative state. *Ann N Y Acad Sci.* (2008) 1129:130–8. doi: 10.1196/annals.1417.018
  49. Estraneo A, Moretta P, Loreto V, Lanzillo L, Santoro L, Trojano L. Late recovery of responsiveness and consciousness after traumatic, anoxic or hemorrhagic long-lasting vegetative state. *Neurology* (2010) 75:239–45. doi: 10.1212/WNL.0b013e3181e8e8cc
  50. Steppacher I, Kaps M, Kissler J. Will time heal? A long-term follow-up of severe disorders of consciousness. *Ann ClinTransl Neurol.* (2014) 1:401–8. doi: 10.1002/acn3.63
  51. Tagliazucchi E, Laufs, H. Decoding wakefulness levels from typical fMRI resting-state data reveals reliable drifts between wakefulness and sleep. *Neuron* (2014) 7: 695–708. doi: 10.1016/j.neuron.2014.03.020
  52. Aiello M, Salvatore E, Cachia A, Pappatà S, Cavaliere C, Prinster A, et al. Relationship between simultaneously acquired resting-state regional cerebral glucose metabolism and functional MRI: A PET/MR hybrid scanner study. *Neuroimage* (2015) 113:111–21. doi: 10.1016/j.neuroimage.2015.03.017
  53. Marchitelli R, Aiello M, Cachia A, Quarantelli M, Cavaliere C, Postiglione A, et al. Simultaneous resting-state FDG-PET/fMRI in Alzheimer Disease: relationship between glucose metabolism and intrinsic activity. *NeuroImage* (2018) 176:246–58. doi: 10.1016/j.neuroimage.2018.04.048

**Conflict of Interest Statement:** The authors declare that the research was conducted in the absence of any commercial or financial relationships that could be construed as a potential conflict of interest.

The reviewer AD declared a shared affiliation, with no collaboration, with one of the authors CC to the handling Editor.

Copyright © 2018 Cavaliere, Kandeepan, Aiello, Ribeiro de Paula, Marchitelli, Fiorenza, Orsini, Trojano, Masotta, St. Lawrence, Loreto, Chronik, Nicolai, Soddu and Estraneo. This is an open-access article distributed under the terms of the Creative Commons Attribution License (CC BY). The use, distribution or reproduction in other forums is permitted, provided the original author(s) and the copyright owner(s) are credited and that the original publication in this journal is cited, in accordance with accepted academic practice. No use, distribution or reproduction is permitted which does not comply with these terms.



# Longitudinal Bedside Assessments of Brain Networks in Disorders of Consciousness: Case Reports From the Field

Corinne A. Bareham<sup>1</sup>, Judith Allanson<sup>2</sup>, Neil Roberts<sup>3</sup>, Peter J. A. Hutchinson<sup>1</sup>, John D. Pickard<sup>1</sup>, David K. Menon<sup>4</sup> and Srivas Chennu<sup>1,5\*</sup>

<sup>1</sup> Department of Clinical Neurosciences, University of Cambridge, Cambridge, United Kingdom, <sup>2</sup> Cambridge University Hospitals NHS Foundation Trust, Cambridge, United Kingdom, <sup>3</sup> Sawbridgeworth Medical Services, Jacobs & Gardens Neuro Centres, Sawbridgeworth, United Kingdom, <sup>4</sup> Division of Anaesthesia, University of Cambridge, Cambridge, United Kingdom, <sup>5</sup> School of Computing, University of Kent, Canterbury, United Kingdom

## OPEN ACCESS

### Edited by:

Olivia Gosseries,  
University of Liège, Belgium

### Reviewed by:

Armand Mensen,  
Universität Bern, Switzerland  
Jacobo Diego Sitt,  
Institut National de la Santé et de la  
Recherche Médicale (INSERM),  
France

### \*Correspondence:

Srivas Chennu  
sc785@kent.ac.uk

### Specialty section:

This article was submitted to  
Applied Neuroimaging,  
a section of the journal  
Frontiers in Neurology

**Received:** 08 February 2018

**Accepted:** 27 July 2018

**Published:** 21 August 2018

### Citation:

Bareham CA, Allanson J, Roberts N,  
Hutchinson PJA, Pickard JD,  
Menon DK and Chennu S (2018)  
Longitudinal Bedside Assessments of  
Brain Networks in Disorders of  
Consciousness: Case Reports From  
the Field. *Front. Neurol.* 9:676.  
doi: 10.3389/fneur.2018.00676

Clinicians are regularly faced with the difficult challenge of diagnosing consciousness after severe brain injury. As such, as many as 40% of minimally conscious patients who demonstrate fluctuations in arousal and awareness are known to be misdiagnosed as unresponsive/vegetative based on clinical consensus. Further, a significant minority of patients show evidence of hidden awareness not evident in their behavior. Despite this, clinical assessments of behavior are commonly used as bedside indicators of consciousness. Recent advances in functional high-density electroencephalography (hdEEG) have indicated that specific patterns of resting brain connectivity measured at the bedside are strongly correlated with the re-emergence of consciousness after brain injury. We report case studies of four patients with traumatic brain injury who underwent regular assessments of hdEEG connectivity and Coma Recovery Scale-Revised (CRS-R) at the bedside, as part of an ongoing longitudinal study. The first, a patient in an unresponsive wakefulness state (UWS), progressed to a minimally-conscious state several years after injury. HdEEG measures of alpha network centrality in this patient tracked this behavioral improvement. The second patient, contrasted with patient 1, presented with a persistent UWS diagnosis that paralleled with stability on the same alpha network centrality measure. Patient 3, diagnosed as minimally conscious minus (MCS-), demonstrated a significant late increase in behavioral awareness to minimally conscious plus (MCS+). This patient's hdEEG connectivity across the previous 18 months showed a trajectory consistent with this increase alongside a decrease in delta power. Patient 4 contrasted with patient 3, with a persistent MCS- diagnosis that was similarly tracked by consistently high delta power over time. Across these contrasting cases, hdEEG connectivity captures both stability and recovery of behavioral trajectories both within and between patients. Our preliminary findings highlight the feasibility of bedside hdEEG



assessments in the rehabilitation context and suggest that they can complement clinical evaluation with portable, accurate and timely generation of brain-based patient profiles. Further, such hdEEG assessments could be used to estimate the potential utility of complementary neuroimaging assessments, and to evaluate the efficacy of interventions.

**Keywords:** consciousness, electroencephalography, brain networks, longitudinal assessment, disorders of consciousness, minimally conscious state, unresponsive wakefulness state

## INTRODUCTION

Recent years have seen substantial advances in the research and development of both behavioral tools and imaging methods to detect the level of awareness in patients with prolonged disorders of consciousness (pDOC), defined as those persisting 4 weeks or more after injury (1). Nonetheless, making an accurate clinical diagnosis remains challenging with the most recent figures indicating a misdiagnosis rate of almost 40%, when based on clinical consensus (2).

One of the factors contributing to this rate of misdiagnosis is the lack of a standardized diagnostic tool, or a gold standard for establishing the state of consciousness of a patient. The Coma Recovery Scale-Revised (CRS-R) (3) is considered the most valid scale for the systematic assessment of behavioral awareness in these patients (4) and has helped to identify those patients that have been misdiagnosed based on clinical examination (1). The CRS-R has subscales of assessment along different dimensions of behavioral responsiveness, which aim to distinguish those patients that show reflexive responses only (Unresponsive Wakefulness State/Vegetative State; UWS/VS), to those who show a degree of awareness with/without command following (Minimally Conscious State; MCS-/MCS+ respectively), to those who have emerged from minimal consciousness, as evidenced by functional object use and/or functional and accurate communication (Emerged from Minimally Conscious State; EMCS). Unfortunately, the 40% misdiagnosis rate comes from a large proportion of the MCS patients misdiagnosed as UWS in the absence of systematic behavioral assessment with methods like the CRS-R (2, 5).

Cases of some misdiagnosed patients have been found to demonstrate covert awareness using imaging techniques such as functional magnetic resonance imaging [fMRI (6, 7)] and electroencephalography [EEG (8)]. This highlights the potential utility of imaging techniques to assist with diagnosis in pDOC, especially considering that patients have typically sustained extremely severe brain injury that can lead to deficits to language, motor or general attention and arousal functioning that could lead to a failure to detect consciousness using a behavioral scale (9). Advances in neuroimaging, particularly fMRI, have found specific paradigms to measure cognition and have identified neural correlates, including prominently the Default Mode Network, which are associated with consciousness state in pDOC (10–13). Prominently, fMRI has been used to detect covert awareness and conscious experience in a significant minority of patients (6, 14).

The potential application of fMRI to develop a clinical diagnostic tool is problematic though, as it is not always

readily available, feasible, or affordable, making it unsuitable for widespread application. While MRI assessments could be employed where suitable and feasible to build a detailed picture of brain structure and function, its use for regular patient follow-up is unlikely to be viable in the typical clinical context. Once patients leave the acute clinical care setting, they are often relocated to a rehabilitation center or nursing home for long-term care and rehabilitation. Typically, they are not followed up with regular fMRI assessments. Without regular follow-up of patients who might present variable and delayed improvements in behavior, it is difficult to determine the prognostic value of fMRI-based measures.

One promising avenue of neuroimaging research is the use of high-density EEG (hdEEG). Research has indicated that functional networks in the brain at rest, captured using various measures, are associated with the state of consciousness in pDOC (15–18). In particular, topologically structured networks of spectral connectivity in the alpha band have been shown to reflect consciousness levels in both patients (16, 18) and in healthy participants as they lose and regain consciousness during sedation (19). This research has repeatedly demonstrated that resting frontoparietal network connectivity might be an important EEG-based indicator of the state of consciousness. Most recently, Chennu et al. (18) showed that such network metrics estimated from resting state hdEEG could predict CRS-R diagnosis, 12-month outcomes and the presence/absence of frontoparietal metabolism [as measured by Positron Emission Tomography (20, 21)] in a large group of pDOC patients. Moreover, MCS patients who were misdiagnosed as UWS showed no differences in any of the measured hdEEG network metrics to the patients correctly diagnosed as MCS. This suggests that assessment of hdEEG networks could have both diagnostic and prognostic clinical value. One major benefit is that hdEEG assessments can be administered at the bedside, allowing for regular and repeated assessment to track the patient's trajectory of recovery. However, despite this potential, there is a substantial translational gap to viable clinical applications. The current national clinical guidelines for pDOC in the United Kingdom (UK) state that resting EEG cannot discriminate between UWS and MCS patients (1) and is not currently used routinely in a clinical setting for diagnostic purposes. This is primarily because, as it stands, there is no EEG-based clinical tool that has been developed, standardized or trialed in a large cohort of pDOC patients.

A related hurdle to the establishment of clinical utility is the fact that the vast majority of neuroimaging research in pDOC to date has taken a cross-sectional approach to compare patient diagnostic groups, using convenience sampling

conducted at a particular point in time. This has generated valuable scientific insights about the nature of neural dysfunction in these states. However, inconsistencies between patients in regard to assessment methods can lead to poor validity or replicability, particularly if data collected is combined from multiple sites. Moreover, information from more fine-grained measures at the individual patient level can get lost using a cross-sectional approach. If the aim is to translate neuroimaging assessments from the bench to the clinic, we need to demonstrate that longitudinal monitoring in individual patients can produce consistent estimates of brain activity at the bedside. To address this translational gap, here we describe our prospective BETADOC (BEDside Test of Awareness for Disorders Of Consciousness) research study, which is amongst the first to apply a consistent method to collect hdEEG assessments and CRS-R assessments longitudinally in a group of pDOC patients, by systematically assessing them every 3 months over a period of 2 years. By conducting repeated and standardized brain network analyses of the data using a previously published pipeline (18), we track how fine-grained measures of resting state brain networks vary and progress alongside the behavioral trajectory of individual patients. This approach is enabling us to conduct longitudinal validation of hdEEG network metrics that we have previously shown to be associated with diagnosis and prognosis of consciousness in a cross-sectional study (18).

The overarching aim of the BETADOC study is to validate EEG-based metrics that accurately describe changes in the structure of hdEEG networks as individual patients recover over time. Using a longitudinal design, we can assess both the diagnostic and prognostic utility of hdEEG network metrics with multiple data points collected from each patient. In this original research report, we show preliminary results from four traumatic brain injury (TBI) patients in pDOC from the BETADOC project. The first patient progressed from UWS to MCS-, in contrast with the second patient who remained in UWS. The third patient transitioned from MCS- to MCS+, while the fourth patient remained in MCS-. We juxtapose the trajectories of individual patient's CRS-R scores with hdEEG visualizations and metrics identified *a priori*, based on prior research in an independent sample of patients (18). By demonstrating the robust relationship between these brain network metrics and CRS-R scores as patients progress through their individual trajectories, we provide a first sample of the evidence base required for viable clinical applications of resting state hdEEG assessments in pDOC.

## MATERIALS AND METHODS

### Ethics

This study was carried out in accordance with the recommendations of the UK National Health Service Research Ethics Committee for Cambridgeshire. The study protocol was approved by the committee (reference: 16/EE/0006). Patients' next-of-kin gave written informed consent prior to enrolment in the study, in accordance with the UK Mental Capacity Act 2005 and Declaration of Helsinki.

## Participants

We included two pDOC patients whose CRS-R scores reflected a transition to a progressively higher consciousness state across assessments, one from UWS to MCS- and one from MCS- to MCS+. These two patients were contrasted with two other patients whose CRS-R scores remained unchanged and reflected a stable UWS and MCS- state. All four patients had an etiology of traumatic brain injury following a road traffic accident (584–3,251 days since injury). As described further below, they were assessed using the CRS-R to ascertain behavioral diagnosis, and with high-density resting EEG to examine their brain activity. The same researcher (CAB) assessed each patient at their bedside every 3 months in the neurological center where they resided.

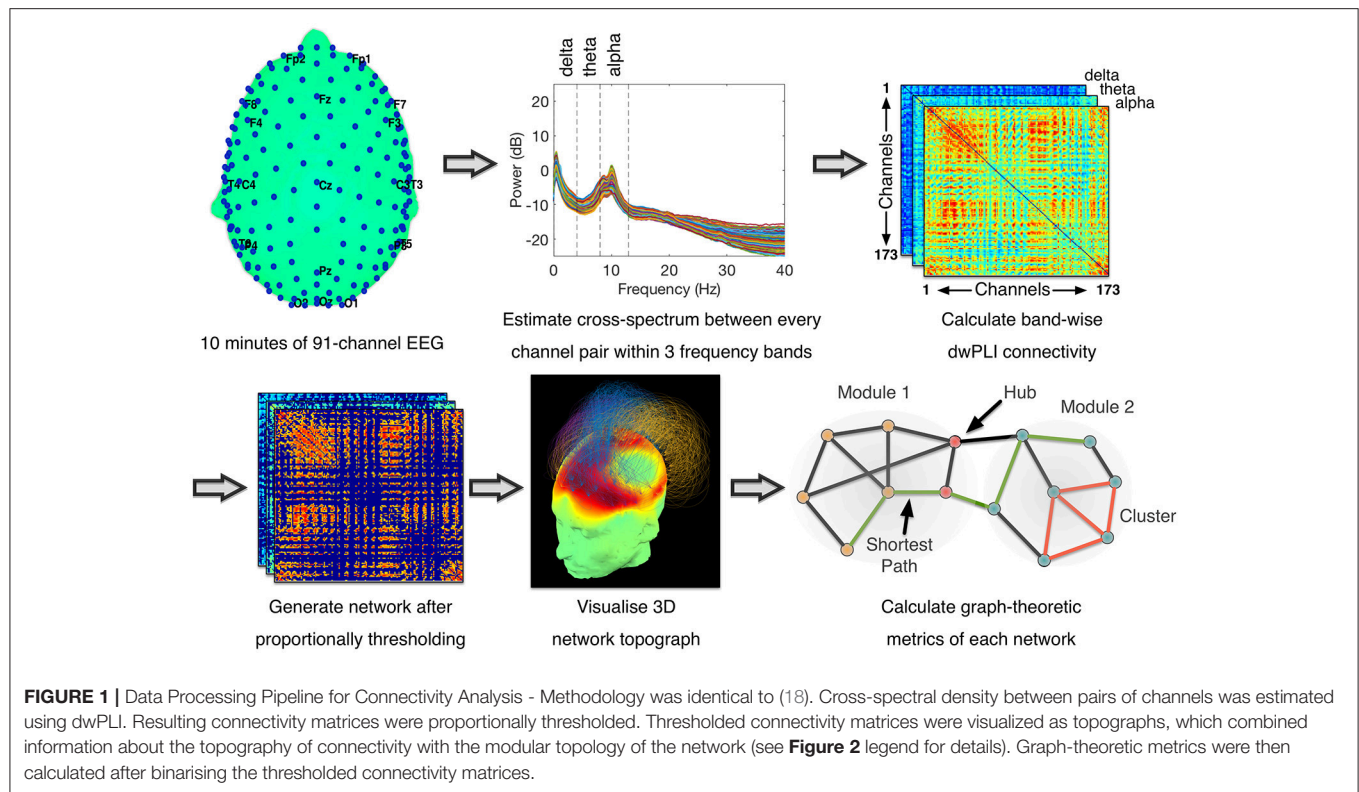
## Coma Recovery Scale-Revised

The Coma Recovery Scale - Revised (CRS-R) is a behavioral assessment of awareness for pDOC (3). The 23-item scale is split into subscales that measure the auditory, visual, motor, oromotor/verbal, communication, and arousal levels of the patient. Some items are considered to be signs of consciousness, with the most complex items indicating EMCS. Formal comparison of available behavioral scales to assess awareness in this patient group indicated the CRS-R as one of the most reliable (22). The CRS-R was administered by the same trained neuropsychologist (CAB) with each patient at each time point. Time of day, and patient postural position was also noted although it was requested that patients were sitting upright in chair if possible.

## High-Density EEG Resting State

Fifteen minutes of resting state data was collected using a 128-channel saline electrode net [Electrical Geodesics (EGI)]. Data was collected at a sampling rate of 500 Hz and was later down-sampled to 250 Hz offline. Prior to EEG collection, the CRS-R was administered to assist with ensuring patients were awake with their eyes open. Patients' behaviors and EEG data were monitored online to ensure recordings were free from seizure activity.

The pre-processing and artifact rejection method was identical to that in Chennu et al. (18), as visualized in **Figure 1**. Briefly, data from electrodes near the eyes, face and neck was removed, leaving 91 electrodes for further analysis. Data was filtered at 0.5–45 Hz and then epoched to 10-second epochs. Each epoch thus generated was baseline-corrected relative to the mean voltage over the entire epoch. Data containing excessive eye movement or muscular artifact was rejected by a quasi-automated procedure: abnormally noisy channels and epochs were identified by calculating their normalized variance and then manually rejected or retained by visual inspection. After artifact rejection, there was on average 10.74 min of data ( $SD = 2.50$ ) from each assessment for estimation of power and connectivity. This involved rejection of an average of 17% of the data in each assessment ( $SD = 19\%$ ). Independent Components Analysis (ICA) based on the Infomax ICA algorithm (23) was used to visually identify and reject noisy components (Mean = 41%,  $SD = 17\%$ ). Finally, previously rejected channels (Mean = 18%,



$SD = 10\%$ ) were interpolated using spherical spline interpolation, and data were re-referenced to the average of all channels.

Using a multitaper method with five Slepian tapers (24), spectral and cross-spectral decompositions within the canonical delta (0.5–4 Hz), theta (4–8 Hz) and alpha (8–13 Hz) frequency bands were computed at bins of 0.1 Hz. Spectral power values were normalized by dividing the power at each bin by the total power over all three bands and multiplying by 100 (17). Alongside, the cross-spectral decomposition was used to estimate the debiased weighted phase lag index (dwPLI) (25) metric of connectivity between every pair of electrodes. dwPLI minimizes the effects of volume conduction on the estimation of brain connectivity, and is further minimally biased at small sample sizes (25). Within each frequency band, dwPLI values at the peak frequency of the oscillatory signal across all channels were used to represent the connectivity between channel pairs. From each subject's dataset, the dwPLI values across all channel pairs were used to construct symmetric  $91 \times 91$  dwPLI connectivity matrices for the delta, theta and alpha bands.

The dwPLI matrices thus constructed were thresholded proportionally to preserve 90–10% of the largest dwPLI values in steps of 2.5%. Specifically, at the 90% threshold, only the 10% of the weakest network edges were discarded. At the 10% threshold, 90% of the weakest edges were discarded. This lowest threshold of 10% ensured that the average degree was not smaller than  $2 \log(N)$ , where  $N$  is the number of nodes in the network (i.e.,  $N = 91$ ). This in turn guaranteed that the resulting networks could be estimated (26). Further, graph connection densities

within this range of thresholds have been shown to be sensitive to the estimation of “true” topological structure therein (27, 28).

After applying each of these thresholds, matrices were binarised, i.e., non-zero values were set to 1. These matrices were then modeled as networks with channels as nodes and binarised dwPLI values as connections between them. These networks were analyzed using graph theory algorithms to calculate a pre-defined set of summary metrics previously evaluated in an independent dataset (18)—clustering coefficient, characteristic path length, modularity, participation coefficient and modular span—at each value of the proportional threshold. The clustering coefficient of a network captures its local efficiency (26), while the characteristic path length measures the average topological distance between pairs of nodes in a graph, providing a measure of global efficiency (26). Modularity, calculated here using the Louvain algorithm (29), is a network metric that captures the degree to which the nodes of a network can be parcellated into densely connected, topologically distinct modules (30). Given a modular decomposition, the participation coefficient of a node is an inter-modular measure of its centrality (31). A larger standard deviation in participation coefficient of network nodes indicates a diversity of connectivity, and hence the presence of hub nodes that link many modules together in an efficient network. Here, we used the standard deviation of participation coefficients to measure network centrality as the presence of diversely connected nodes with central hubs (32, 33). Finally, modular span is average weighted topographical distance (over the scalp) spanned by a module identified in a network (16). Network metrics were averaged over all connection densities



considered, to reduce them down to scalar values when plotting them alongside CRS-R scores.

For each patient, the measures were normalized for plotting to show the percentage of change relative to the first assessment in that patient. Further, to estimate the stability of each brain-based metric estimated at each assessment, we repeated the above power, connectivity and network analyses 25 times, each time randomly sampling 80% of the retained epochs. The minimum and maximum values obtained over the 25 repetitions were represented as error bars during plotting.

The above data analysis pipeline was implemented using EEGLAB (34), FieldTrip (35), the Brain Connectivity Toolbox (36), and custom MATLAB scripts. The pipeline was automated except for manual checks for and removal of artifactual channels, trials and independent components.

## RESULTS

### Patient 1: UWS to MCS–

Patient 1 (age range: 45–50) was first admitted to hospital nearly 9 years previous to the first hdEEG assessment (3,251 days since injury). Glasgow Coma Scale (GCS) at time of incident was unavailable. At the time of the first assessment, the patient had been in a prolonged UWS with no means of communication, tetraparesis and cognitive difficulties since their injury. There was a noted history of seizures and also some hospital admissions for chest infections. The patient was being treated using Sodium Valproate for management of seizures.

**Figure 2A** shows this patient's trajectory of CRS-R scores from UWS to MCS–, evidenced by visual pursuit on the visual subscale of the CRS-R. The cross-sectional study in an independent group of patients conducted by Chennu et al. (18) showed that the measure of EEG networks that distinguished UWS from MCS– patients was alpha network centrality, measured as the standard deviation of participation coefficients across the nodes in the network [see **Figure 1C** in Chennu et al. (18)]. Further, they showed that these hubs were located along a frontoparietal axis of nodes with high connectivity in both locked-in patients and healthy controls [see **Figure 1A** in Chennu et al. (18)].

Here, within a single patient over a longitudinal period, we observed a visually evident association between their CRS-R score (**Figure 2A**) and this measure, the normalized alpha band participation coefficient (**Figure 2B**), as the patient progressed from a UWS to an MCS– diagnosis. **Figure 2C** plots 3D network topographs visualizing alpha connectivity measured at each assessment. We recorded the highest CRS-R score of 8 at the 6th assessment, when frontoparietal connectivity was most evident in the patient's alpha band network (**Figure 2C**, far right).

### Patient 2: Stable UWS

Patient 2 (age range: 20–25) was admitted to hospital more than 19 months previous to the first hdEEG assessment (584 days since injury). The GCS at time of incident was unavailable. The patient was noted to have widespread intraparenchymal contusions, subarachnoid and subdural hemorrhages as well as base of skull fractures. The patient underwent decompressive craniectomy for raised intercranial pressure and since then, had

a cranioplasty. The patient had hydrocephalus and underwent ventriculoperitoneal shunt insertion. The patient's clinical course was complicated with autonomic storming which was managed with Propranolol and Clonidine. At the time of assessment, the patient showed only reflexive behaviors with tetraparesis and no effective means of communication.

**Figure 3A** shows this patient's trajectory of CRS-R scores, indicating a diagnosis of UWS throughout. Only three assessments were obtained from this patient. Over these assessments, there was no change observed in CRS-R diagnosis and behavior remained reflexive, with either presence/absence of reflexive responses noted at each assessment in the CRS-R sub-scales. Alongside, there was relatively little variation in alpha network centrality (**Figure 3B**) across assessments. We observed elevated connectivity during the last assessment (**Figure 3C**), corresponding with the highest CRS-R score recorded in this patient.

### Patient 3: MCS– to MCS+

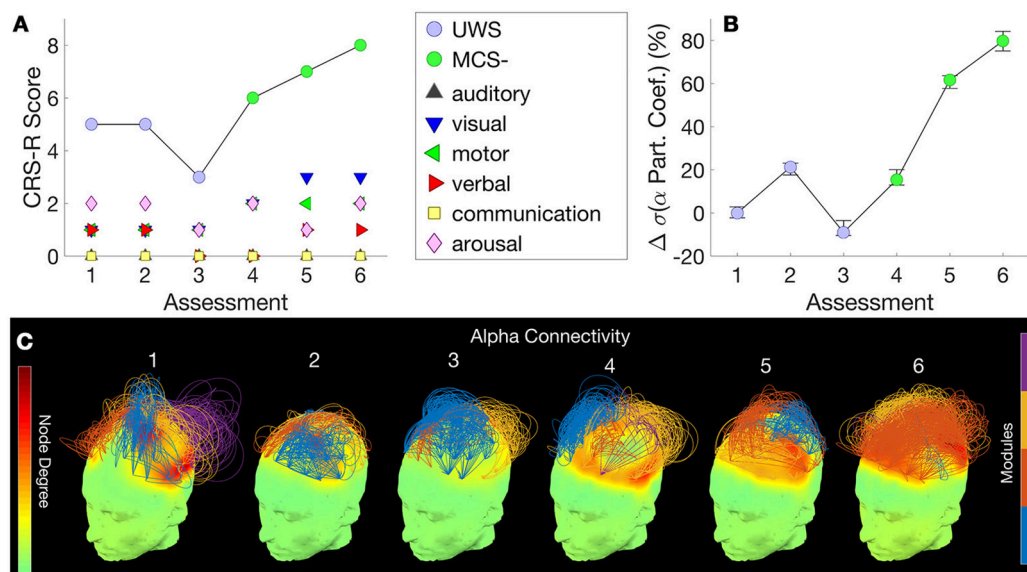
Patient 3 (age range: 20–25) was admitted to hospital almost 2 years previous to the first assessment (633 days since injury). This patient was noted to have grade 3 diffuse axonal injury, diffuse subarachnoid hemorrhage and intraventricular hemorrhage as well as bilateral frontotemporal contusions. Their clinical course was complicated by delayed onset rhabdomyolysis, multi-organ failure including acute renal failure for which they had renal replacement therapy. They also suffered a cardiac arrest resulting in hypoxic brain injury.

Approximately 9 months following injury the patient was noted to have a Glasgow Coma Scale (GCS) score of 6/15 and an EEG analysis of event-related potentials completed during their stay in a rehabilitation center showed positive in response to visual stimuli, but auditory ERPs were only positive for stimuli on the right. The patient's clinical course was complicated by seizures and recurrent aspiration pneumonia, supraventricular tachycardia and autonomic storming. They are currently treated with Phenytoin for seizure management.

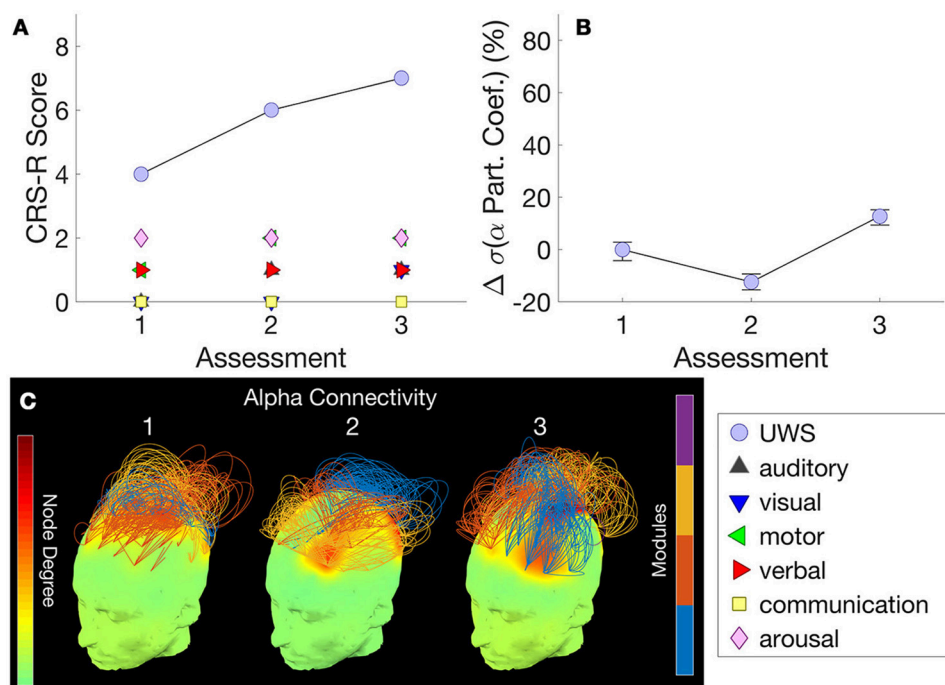
**Figure 4A** shows this patient's trajectory of CRS-R scores from an MCS– to an MCS+ state across time, evidenced by reproducible movement to command on the auditory function scale and inconsistent but intentional attempts to communicate using eye-blinks. Chennu et al. (18) showed that the best hdEEG discriminator of MCS– vs MCS+ patients was delta power [see **Figure 1C** in Chennu et al. (18)]. In this individual patient, the change in mean normalized delta power validated this finding, inversely mirroring changes in CRS-R over the transition from MCS– to MCS+ (**Figure 4B**).

Further detail is provided by the delta power topography in **Figure 4C**. At assessment 3, we recorded a low CRS-R score of 4 and a diagnosis of UWS, as the patient was less responsive (despite the application of deep pressure stimulation recommended by CRS-R guidelines). Consistent with this, delta power was relatively high at almost all channels, and dominated over 90% of total spectral power (**Figure 4B**). This proportion then dropped to just over 50% at assessments 5 and 6, when we recorded improved CRS-R scores of 8 and 15.

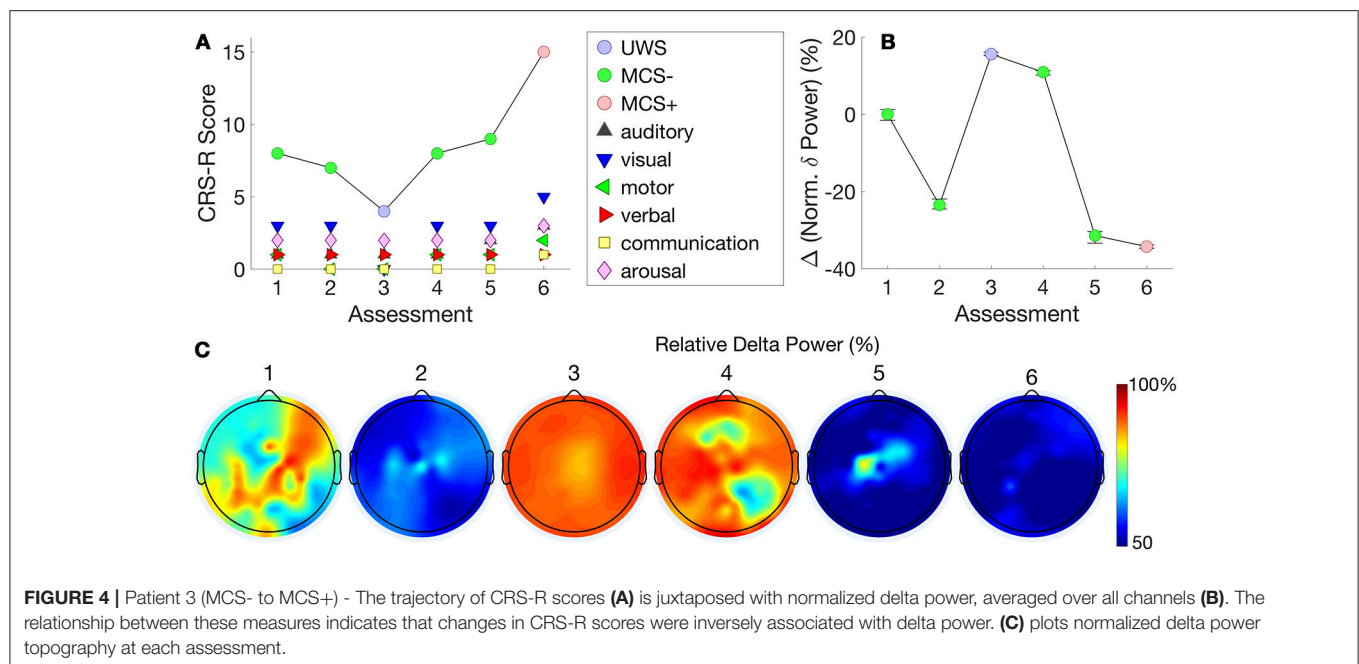




**FIGURE 2 |** Patient 1 (UWS to MCS-) - CRS-R scores, subscores and diagnosis at each assessment **(A)** are juxtaposed with the normalized standard deviation of participation coefficients estimated from the patient's hdEEG alpha band network at each assessment **(B)**. Consecutive assessments were separated by 3 months. Error bars indicate range of values obtained over 25 repetitions over random subsamples of the original data. **(C)** visualizes alpha band network topographs at each assessment. In each topograph, the color map over the scalp depicts degrees of nodes in the network (left color scale). Arcs connect pairs of nodes, and their normalized heights indicate the strength of connectivity between them. The color of an arc identifies the module to which it belongs, with groups of arcs in the same color highlighting connectivity within a module (right color scale). Topological modules within the network were identified by the Louvain algorithm (16, 18). For visual clarity, of the strongest 30% of connections, only intramodular connections are plotted.



**FIGURE 3 |** Patient 2 (Stable UWS) - **(A)** shows this patient's trajectory of CRS-R scores and stable diagnosis. Correspondingly, **(B)** demonstrates the relatively consistent standard deviations of the alpha band participation coefficients. **(C)** presents alpha band network topographs at each assessment.



**FIGURE 4 |** Patient 3 (MCS- to MCS+) - The trajectory of CRS-R scores (A) is juxtaposed with normalized delta power, averaged over all channels (B). The relationship between these measures indicates that changes in CRS-R scores were inversely associated with delta power. (C) plots normalized delta power topography at each assessment.

## Patient 4: Stable MCS-

Patient 4 (age range 30–35) was admitted to hospital nearly 4 years previous to the first assessment (1,406 days since injury). Their GCS score was 3/15 at the scene. The patient sustained a right acute subdural hemorrhage as well as multiple skull vault fractures. The patient underwent decompressive craniectomy and later developed hydrocephalus that was managed with an external ventricular drain (since removed). The patient's clinical course was complicated with autonomic storming which required treatment with Bisoprolol and Clonidine. The patient also developed sepsis that was treated with intravenous antibiotics. It was noted that further imaging showed a left middle cerebral artery territory infarct.

Figure 5A shows this patient's very stable trajectory of CRS-R scores. The patient's diagnoses on the CRS-R remained at MCS- throughout the assessments, evidenced by consistent visual pursuit. All other behaviors remained reflexive. In contrast to Patient 3, who showed a progression in normalized delta power alongside a progression in CRS-R scores, Figure 5B shows this patient's stable plateau in delta power that did not change from the first to subsequent assessments. Figure 5C shows that normalized delta power remained high across assessments consistent with a diagnosis of persistent MCS-.

For completeness, Supplementary Figure 1 depicts trajectories of alpha network centrality in Patients 3 and 4, and conversely, normalized delta power in Patients 1 and 2.

## DISCUSSION

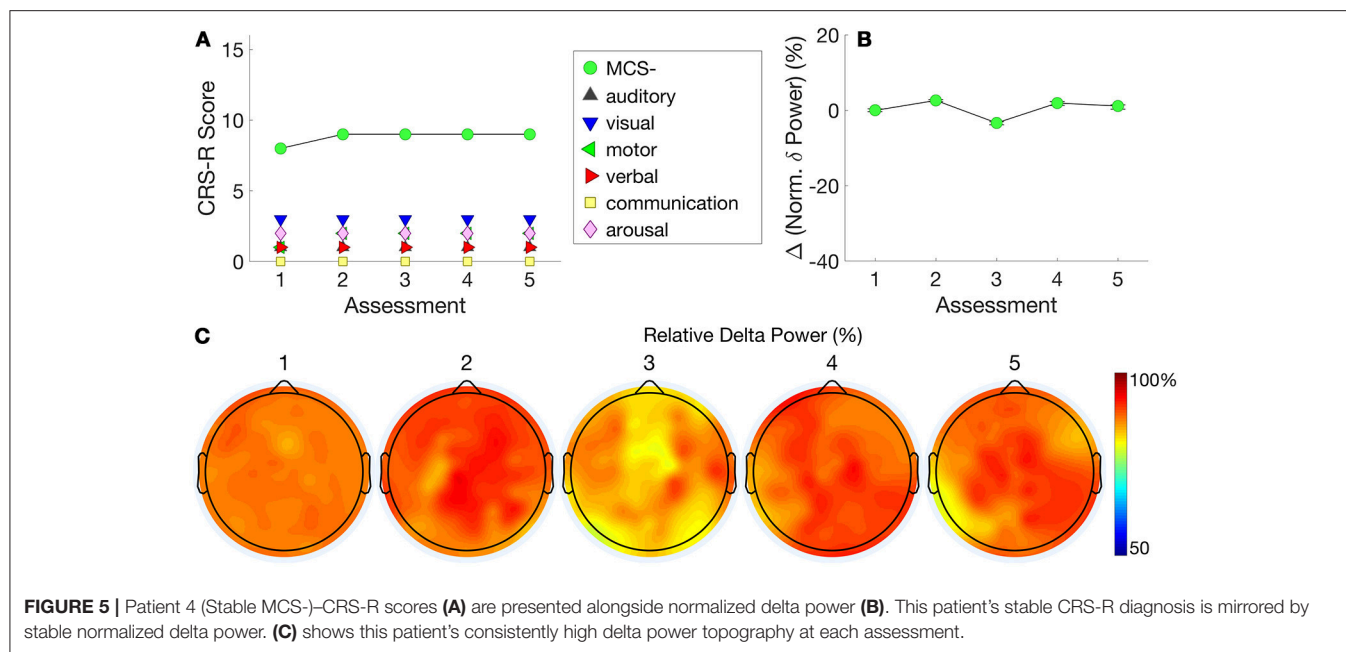
We have demonstrated a longitudinal approach to the systematic assessment of pDOC patients using a combination of behavioral and brain-based methods at their bedside in a residential neurological center. This is a novel framework that goes beyond

most existing research in pDOC, which has typically conducted cross-sectional assessments by transporting patients to specialist hospital centers with advanced neuroimaging facilities. The BETADOC study aims to translate the wealth of neuroscientific evidence generated from these previous studies to the clinical context. This study, to our knowledge, is the first to do so in the UK. Our preliminary findings show that measures of hdEEG networks were correlated with behavioral variations in individual pDOC patients assessed repeatedly at 3-monthly intervals.

## hdEEG Assessments in pDOC

We have explored the reliability and stability of hdEEG measures in the contrasting cases considered. Patients 1 and 3 show a progressive transition in CRS-R diagnoses, whilst patients 2 and 4 showed a stable level of behavioral responsiveness over time. Evidence from behaviorally stable patients 2 and 4 lends to the specificity and validity of the hdEEG measures previously identified with cross-sectional analysis (18). Here, the same measures identified as important to detect corresponding within-subject transitions in consciousness were similarly able to demonstrate stability in patients with a persistent and unchanging diagnosis.

In patient 1, whose behavioral scores progressed from UWS to MCS-, we found that the centrality of the patient's alpha band network, as measured by participation coefficients, tracked this improvement longitudinally. This finding was consistent with and extends beyond the cross-sectional analysis in Chennu et al. (18) indicating that standard deviation of alpha participation coefficients was the best discriminator of UWS vs MCS- patients at the group level. The weak alpha connectivity evident in Patient 1's hdEEG network during initial assessments was congruent with a CRS-R diagnosis of UWS. Nevertheless, the patient's hdEEG network evolved over many months of repeated assessments, and



we observed the presence of increased frontoparietal connectivity at the 6th assessment, in keeping with an increased CRS-R score and behavioral evidence of consciousness. Broadly speaking, there is considerable evidence linking the presence of robust frontoparietal alpha networks with conscious awareness, from research into other altered states, including sleep (37) and sedation (19, 38) in particular. That hdEEG metrics derived from alpha connectivity can track fine-grained longitudinal changes in behavioral state of an individual pDOC patient, even after a long intervening period since the original brain injury (7 years in case of Patient 1), is valuable new knowledge that speaks to the clinical utility of repeated hdEEG network assessments of consciousness.

## Diverse Metrics Contribute to Discriminative Utility

However, this is not to suggest that graph-theoretic metrics are uniquely useful in this context. A relatively simpler estimation of delta band power best discriminated MCS- from MCS+ patients in Chennu et al. (18). Here too, we found that in Patient 3, who progressed from MCS- to MCS+, decrease in delta power was associated with this improvement. In contrast to Patient 3, Patient 4 showed relatively little change in their MCS-state, consistent with a stable level of delta power over multiple assessments. This is in congruence with another independent report of large-scale screening of hdEEG-derived measures by Sitt et al. which showed that different measures were best able to discriminate different states of consciousness (17), and could be beneficially combined. Further, Sitt et al. too reported both positive and negative correlations between hdEEG measures and states of consciousness. More generally, increased power and connectivity in low frequency bands has been reported in pDOC (39), and attributed to partial cortical deafferentation and

the consequent intrinsic tendency of such weakly interacting neuronal oscillators to synchronize (40).

## From Theory to Practice

Taken together, our preliminary findings from the BETADOC project highlight the potential for clinical utility of hdEEG assessments to provide detailed and valuable information about brain activity in individual pDOC patients, across a range of behavioral and clinically relevant stratifications of consciousness. As highlighted earlier, one of the strengths of this project is the longitudinal approach to patient assessment.

Though we have focused on the correspondence between longitudinal changes hdEEG metrics and CRS-R scores here to demonstrate their face validity, the aim of these metrics is not solely to track the CRS-R. Indeed, there are specific data points where there are apparent mismatches between the hdEEG metric and the CRS-R. For example, Patient 3 had similar CRS-R scores at assessments 2 and 4 but different levels of normalized delta power. The magnitude of change in a hdEEG metric, which is unbounded, is not expected to exactly match the magnitude of change in CRS-R, which is by definition bounded between 0 and 23. Rather, we expect that the availability of hdEEG metrics at the bedside could complement the CRS-R by providing brain-based information that cannot be ascertained exclusively via behavioral examination. In doing so, hdEEG assessments could be valuable in reducing the rate of misdiagnosis in practice. As an example, in patients diagnosed with aphasia or with language-related deficits, the behavioral communication necessary for administering the CRS-R might not be possible. In such cases where behavioral assessment is difficult to administer reliably, the entirely passive assessment of conscious state estimated by hdEEG activity could be useful. More generally, having multiple assays of consciousness in individual patients should

eventually lead to more accurate estimation, as is known to be the case with repeated CRS-R assessments (41). Indeed, combining diagnostic information from multiple complementary modalities of assessment would promote a rational, consilience-based approach. This is because the ground truth about the patient's subjective conscious state is fundamentally uncertain (42). In the absence of a gold standard for consciousness, convergent information from multiple modalities would increase clinical confidence in the estimation of conscious state. Conversely, divergence, for example where hdEEG indicates a higher conscious state than the CRS-R, can prognosticate the eventual recovery of behavioral consciousness (18).

Another distinct context in which hdEEG assessments add value beyond complementing behavioral assessments is in the identification of patients with the potential for hidden consciousness not expressed in their behavior. This possibility, demonstrated prominently with command following using tennis imagery in seemingly UWS patients (6, 7), has led to the realization that such patients present with a dissociation between cognitive and motor function, rather than unresponsive unconsciousness (43). In these patients, a CRS-R assessment would fail to identify any signs of consciousness due to its absence in behavior. In this context, previous cross-sectional research has highlighted that assessment of hdEEG networks can identify robust alpha connectivity networks in UWS patients who demonstrate evidence of command following with tennis imagery (16). This points to the particular utility of hdEEG assessments in this significant minority of patients who would be misdiagnosed even with systematic behavioral assessment at the bedside.

Finally, the repeatability of hdEEG assessments at the bedside serves as the basis for future work toward demonstrating its utility in the clinical context. Indeed, while the diagnostic and prognostic value of EEG has been highlighted in previous cross-sectional studies of pDOC (8, 16–18, 44, 45), our early evidence speaks to its value within the context of the individual. This is important for advancing beyond the state of the art, from research to clinical practice. Should regular and repeated hdEEG assessments be incorporated into a clinical framework, they could assist with informing clinical decision making on behalf of the patient, addressing an unmet need highlighted in clinical guidelines (1). In particular, as these assessments can be reliably conducted at the bedside, they could be used to identify patients who might benefit from further examination, be it with clinical or neuroimaging methods. Further, we advance the case for exploiting the repeatability of these assessments to evaluate therapeutic and pharmacological interventions. As these often have mixed results in clinical populations (46), hdEEG could be used to better understand the underlying causes of this variable response to treatment. Ultimately, this will contribute to a more evidence-based application of precision medicine tailored to the specific needs and individual histories of pDOC patients.

## Limitations

The findings reported here are preliminary, due to the limited number of patients we were able to include from an ongoing longitudinal study, and hence caution is warranted in

their interpretation. In particular, equal numbers of repeated assessments in a large cohort of patients would be ideal for characterizing the trajectory of change in behavior and hdEEG measures. This would enable us to not only arrive at a more accurate behavioral diagnosis, but also identify patients with clear evidence of sustained recovery, in contrast to patients with ongoing fluctuations in behavior. Future research will aim to discover and describe the range of trajectories observed at the cohort level.

Another limitation worth noting is that the patients presented here all had traumatic etiology, hence generalization to other etiologies needs to be the focus of further investigation. Nevertheless, the results presented here are promising as, in this small sample, they suggest that regular and repeated assessment of patients can track variation in CRS-R and brain networks over time. In doing so, our findings point to the potential utility of hdEEG for complementing systematic behavioral assessments at the bedside.

## AUTHOR CONTRIBUTIONS

SC, CAB, JA, DKM, JDP, and PJAHH contributed to conception and design of the study; SC developed computational methods and tools. CAB collected the data and organized the database. JA conducted detailed neurological examinations of patients. NR contributed clinical information about patients. CAB and SC conducted the data analysis and wrote the manuscript. All authors contributed to manuscript revision, read and approved the submitted version.

## FUNDING

The authors received funding from the Evelyn Trust [SC, Ref: 15/07], UK Engineering and Physical Sciences Research Council [SC, Ref: EP/P033199/1], the UK National Institute for Health Research (NIHR) as part of the Acute Brain Injury and Repair Theme of the Cambridge Biomedical Research Centre [PJAHH], the NIHR Research Professorship [PJAHH], the NIHR Cambridge BRC [PJAHH and DKM], the NIHR Brain Injury Healthcare Technology Cooperative [JDP], the NIHR Senior Investigator award [DKM] and the James S. McDonnell Foundation [JDP]. This research was undertaken with the support of the Alan Turing Institute (UK Engineering and Physical Sciences Research Council Grant Number EP/N510129/1).

## ACKNOWLEDGMENTS

We would like to thank the patients, their families, carers, and treating clinicians for their participation in this study. We thank Mark Wallis and the High-Performance Computing facility at the University of Kent for providing computational support and resources (<https://www.kent.ac.uk/hpc/>).

## SUPPLEMENTARY MATERIAL

The Supplementary Material for this article can be found online at: <https://www.frontiersin.org/articles/10.3389/fneur.2018.00676/full#supplementary-material>



## REFERENCES

- Turner-Stokes L. Prolonged disorders of consciousness: new national clinical guidelines from the Royal College of Physicians, London. *Clin Med.* (2014) 14:4–5. doi: 10.7861/clinmedicine.14-1-4
- Schnakers C, Vanhaudenhuyse A, Giacino J, Ventura M, Boly M, Majerus S, et al. Diagnostic accuracy of the vegetative and minimally conscious state: clinical consensus versus standardized neurobehavioral assessment. *BMC Neurol.* (2009) 9:35. doi: 10.1186/1471-2377-9-35
- Kalmar K, Giacino JT. The JFK Coma Recovery Scale–Revised. *Neuropsychol Rehabil* (2005) 15:454–60. doi: 10.1080/09602010443000425
- Bodien YG, Carlowicz CA, Chatelle C, and Giacino JT. Sensitivity and specificity of the coma recovery scale–revised total score in detection of conscious awareness. *Arch Phys Med Rehabil.* (2016) 97:490–492.e1. doi: 10.1016/j.apmr.2015.08.422
- Childs NL, Mercer WN, and Childs HW. Accuracy of diagnosis of persistent vegetative state. *Neurology* (1993) 43:1465–7. doi: 10.1212/WNL.43.8.1465
- Owen AM, Coleman MR, Boly M, Davis MH, Laureys S, and Pickard JD. Detecting awareness in the vegetative state. *Science* (2006) 313:1402. doi: 10.1126/science.1130197
- Monti MM, Vanhaudenhuyse A, Coleman MR, Boly M, Pickard JD, Tshibanda L, et al. Willful Modulation of Brain Activity in Disorders of Consciousness. *N Eng J Med.* (2010) 362:579–89. doi: 10.1056/NEJMoa0905370
- Cruse D, Chennu S, Chatelle C, Bekinschtein TA, Fernández-Espejo D, Pickard JD, et al. Bedside detection of awareness in the vegetative state? Authors' reply. *Lancet* (2012) 379:1702. doi: 10.1016/S0140-6736(12)60715-6
- Gosseries O, Zasler ND, and Laureys S. Recent advances in disorders of consciousness: focus on the diagnosis. *Brain Injury* (2014) 28:1141–50. doi: 10.3109/02699052.2014.920522
- Vanhaudenhuyse A, Noirhomme Q, Tshibanda LJ-F, Bruno M-A, Boveroux P, Schnakers C, et al. Default network connectivity reflects the level of consciousness in non-communicative brain-damaged patients. *Brain* (2010) 133:161–71. doi: 10.1093/brain/awp313
- Fernandez-Espejo D, Soddu A, Cruse D, Palacios EM, Junque C, Vanhaudenhuyse A, et al. A role for the default mode network in the bases of disorders of consciousness. *Ann Neurol.* (2012) 72:335–43. doi: 10.1002/ana.23635
- Demertzi A, Antonopoulos G, Heine L, Voss HU, Crone JS, De Los Angeles C, et al. Intrinsic functional connectivity differentiates minimally conscious from unresponsive patients. *Brain* (2015) 138:2619–31. doi: 10.1093/brain/awv169
- Lant ND, Gonzalez-Lara LE, Owen AM, and Fernandez-Espejo D. Relationship between the anterior forebrain mesocircuit and the default mode network in the structural bases of disorders of consciousness. *Neuroimage Clin.* (2016) 10:27–35. doi: 10.1016/j.nicl.2015.11.004
- Naci L, Cusack R, Anello M, and Owen AM. A common neural code for similar conscious experiences in different individuals. *Proc Natl Acad Sci USA.* (2014) 111:14277–82. doi: 10.1073/pnas.1407007111
- King JR, Sitt JD, Faugeras F, Rohaut B, El Karoui I, Cohen L, et al. Information sharing in the brain indexes consciousness in noncommunicative patients. *Curr Biol.* (2013) 23:1914–9. doi: 10.1016/j.cub.2013.07.075
- Chennu S, Finoia P, Kamau E, Allanson J, Williams GB, Monti MM, et al. Spectral signatures of reorganised brain networks in disorders of consciousness. *PLOS Comput Biol.* (2014) 10:e1003887. doi: 10.1371/journal.pcbi.1003887
- Sitt JD, King JR, El Karoui I, Rohaut B, Faugeras F, Gramfort A, et al. Large scale screening of neural signatures of consciousness in patients in a vegetative or minimally conscious state. *Brain* (2014) 137:2258–70. doi: 10.1093/brain/awu141
- Chennu S, Anen J, Wannez S, Thibaut A, Chatelle C, Cassol H, et al. Brain networks predict metabolism, diagnosis and prognosis at the bedside in disorders of consciousness. *Brain* (2017) 140:2120–32. doi: 10.1093/brain/awx163
- Chennu S, O'Connor S, Adapa R, Menon DK, and Bekinschtein TA. Brain connectivity dissociates responsiveness from drug exposure during propofol-induced transitions of consciousness. *PLOS Comput Biol.* (2016) 12:e1004669. doi: 10.1371/journal.pcbi.1004669
- Stender J, Gosseries O, Bruno M-A, Charland-Verville V, Vanhaudenhuyse A, Demertzi A, et al. Diagnostic precision of PET imaging and functional MRI in disorders of consciousness: a clinical validation study. *Lancet* (2014) 384:514–22. doi: 10.1016/S0140-6736(14)60042-8
- Stender J, Mortensen, Kristian N, Thibaut A, Darkner S, Laureys S, Gjedde A, Kupers R. et al. The minimal energetic requirement of sustained awareness after brain injury. *Curr Biol.* (2016) 26:1494–9. doi: 10.1016/j.cub.2016.04.024
- American Congress of Rehabilitation Medicine, Brain Injury-Interdisciplinary Special Interest Group, Disorders of Consciousness Task Force, Seel RT, Sherer M, Whyte J, et al. Assessment scales for disorders of consciousness: evidence-based recommendations for clinical practice and research. *Arch Phys Med Rehabil.* (2010) 91:1795–813. doi: 10.1016/j.apmr.2010.07.218
- Loewy DH, Campbell KB, and Bastien C. The mismatch negativity to frequency deviant stimuli during natural sleep. *Electroencephalogr Clin Neurophysiol.* (1996) 98:493–501. doi: 10.1016/0013-4694(96)95553-4
- Mitra PP, and Pesaran B. Analysis of dynamic brain imaging data. *Biophys J.* (1999) 76:691–708. doi: 10.1016/S0006-3495(99)77236-X
- Vinck M, Oostenveld R, Van Wingerden M, Battaglia F, and Pennartz CM. An improved index of phase-synchronization for electrophysiological data in the presence of volume-conduction, noise and sample-size bias. *Neuroimage* (2011) 55:1548–65. doi: 10.1016/j.neuroimage.2011.01.055
- Watts DJ, and Strogatz SH. Collective dynamics of 'small-world' networks. *Nature* (1998) 393:440–2. doi: 10.1038/30918
- Lynall ME, Bassett DS, Kerwin R, Mckenna PJ, Kitzbichler M, Muller U, et al. Functional connectivity and brain networks in schizophrenia. *J Neurosci.* (2010) 30:9477–87. doi: 10.1523/JNEUROSCI.0333-10.2010
- Achard S, Delon-Martin C, Vértes PE, Renard F, Schenck M, Schneider F, et al. Hubs of brain functional networks are radically reorganized in comatose patients. *Proc Natl Acad Sci USA.* (2012) 109:20608–13. doi: 10.1073/pnas.1208933109
- Blondel VD, Guillaume J-L, Lambiotte R, and Lefebvre E. Fast unfolding of communities in large networks. *J Stat Mech.* (2008) 2008:P10008. doi: 10.1088/1742-5468/2008/10/P10008
- Fortunato S. Community detection in graphs. *Phys Rep.* (2010) 486:75–174. doi: 10.1016/j.physrep.2009.11.002
- Guimera R, and Nunes Amaral LA. Functional cartography of complex metabolic networks. *Nature* (2005) 433:895–900. doi: 10.1038/nature03288
- Van Den Heuvel MP, and Sporns O. Rich-club organization of the human connectome. *J Neurosci.* (2011) 31:15775–86. doi: 10.1523/JNEUROSCI.3539-11.2011
- Bertolero M, Yeo B, and D'Esposito M. The diverse club: the integrative core of complex networks. *ArXiv(preprint)* (2017) doi: 10.1038/s41467-017-01189-w
- Delorme A, and Makeig S. EEGLAB: an open source toolbox for analysis of single-trial EEG dynamics including independent component analysis. *J Neurosci Methods* (2004) 134:9–21. doi: 10.1016/j.jneumeth.2003.10.009
- Oostenveld R, Fries P, Maris E, and Schoffelen J-M. FieldTrip: open source software for advanced analysis of MEG, EEG, and invasive electrophysiological data. *Comput Int Neurosci.* (2011) 2011:156869. doi: 10.1155/2011/156869
- Rubinov M, and Sporns O. Complex network measures of brain connectivity: uses and interpretations. *NeuroImage* (2010) 52:1059–69. doi: 10.1016/j.neuroimage.2009.10.003
- Comsa IM, Bekinschtein TA, and Chennu S. Transient topographical dynamics of the electroencephalogram predict brain connectivity and behavioural responsiveness during drowsiness. *bioRxiv(preprint)* (2017). doi: 10.1101/231464
- Purdon PL, Pierce ET, Mukamel EA, Prerau MJ, Walsh JL, Wong KFK, et al. Electroencephalogram signatures of loss and recovery of consciousness from propofol. *Proc Natl Acad Sci USA.* (2013) 110:1142–51. doi: 10.1073/pnas.1221180110
- Schiff ND, Nauvel T, and Victor JD. Large-scale brain dynamics in disorders of consciousness. *Curr Opin Neurobiol.* (2014) 25:7–14. doi: 10.1016/j.conb.2013.10.007

40. Williams ST, Conte MM, Goldfine AM, Noirhomme Q, Gosseries O, Thonnard M, et al. Common resting brain dynamics indicate a possible mechanism underlying zolpidem response in severe brain injury. *eLife* (2013) 2:e01157. doi: 10.7554/eLife.01157
41. Wannez S, Heine L, Thonnard M, Gosseries O, and Laureys S, Coma Science Group C. The repetition of behavioral assessments in diagnosis of disorders of consciousness. *Ann Neurol*. (2017) 81:883–9. doi: 10.1002/ana.24962
42. Peterson A. Consilience, clinical validation, and global disorders of consciousness. *Neurosci Conscious*. (2016) 2016:niw011. doi: 10.1093/nc/niw011
43. Schiff ND. Cognitive motor dissociation following severe brain injuries. *JAMA Neurol*. (2015) 72:1413–5. doi: 10.1001/jamaneurol.2015.2899
44. Cruse D, Chennu S, Fernández-Espejo D, Payne WL, Young G, Adrian M, Owen et al. Detecting awareness in the vegetative state: electroencephalographic evidence for attempted movements to command. *PLoS ONE* (2012) 7:e49933. doi: 10.1371/journal.pone.0049933
45. Cruse D, Gantner I, Soddu A, and Owen AM. Lies, damned lies and diagnoses: Estimating the clinical utility of assessments of covert awareness in the vegetative state. *Brain Inj* (2014) 28:1197–201. doi: 10.3109/02699052.2014.920517
46. Thonnard M, Gosseries O, Demertzi A, Lugo Z, Vanhaudenhuyse A, Bruno MA, et al. Effect of zolpidem in chronic disorders of consciousness: a prospective open-label study. *Funct Neurol*. (2013) 28:1–6. doi: 10.11138/FNeur/2013.28.4.259

**Conflict of Interest Statement:** The authors declare that the research was conducted in the absence of any commercial or financial relationships that could be construed as a potential conflict of interest.

Copyright © 2018 Bareham, Allanson, Roberts, Hutchinson, Pickard, Menon and Chennu. This is an open-access article distributed under the terms of the Creative Commons Attribution License (CC BY). The use, distribution or reproduction in other forums is permitted, provided the original author(s) and the copyright owner(s) are credited and that the original publication in this journal is cited, in accordance with accepted academic practice. No use, distribution or reproduction is permitted which does not comply with these terms.



# A Review of Resting-State Electroencephalography Analysis in Disorders of Consciousness

Yang Bai<sup>1</sup>, Xiaoyu Xia<sup>2</sup> and Xiaoli Li<sup>3\*</sup>

<sup>1</sup>Institute of Electrical Engineering, Yanshan University, Qinhuangdao, China, <sup>2</sup>Department of Neurosurgery, PLA Army General Hospital, Beijing, China, <sup>3</sup>State Key Laboratory of Cognitive Neuroscience and Learning, IDG/McGovern Institute for Brain Research, Beijing Normal University, Beijing, China

## OPEN ACCESS

### Edited by:

Olivia Gosseries,  
University of Liège, Belgium

### Reviewed by:

Quentin Noirhomme,  
Maastricht University, Netherlands  
Damian Cruse,  
University of Western Ontario,  
Canada

### \*Correspondence:

Xiaoli Li  
xiaoli@bnu.edu.cn

### Specialty section:

This article was submitted to  
Applied Neuroimaging,  
a section of the journal  
Frontiers in Neurology

**Received:** 25 June 2017

**Accepted:** 25 August 2017

**Published:** 11 September 2017

### Citation:

Bai Y, Xia X and Li X (2017)  
A Review of Resting-State  
Electroencephalography Analysis  
in Disorders of Consciousness.  
Front. Neurol. 8:471.  
doi: 10.3389/fneur.2017.00471

Recently, neuroimaging technologies have been developed as important methods for assessing the brain condition of patients with disorders of consciousness (DOC). Among these technologies, resting-state electroencephalography (EEG) recording and analysis has been widely applied by clinicians due to its relatively low cost and convenience. EEG reflects the electrical activity of the underlying neurons, and it contains information regarding neuronal population oscillations, the information flow pathway, and neural activity networks. Some features derived from EEG signal processing methods have been proposed to describe the electrical features of the brain with DOC. The computation of these features is challenging for clinicians working to comprehend the corresponding physiological meanings and then to put them into clinical applications. This paper reviews studies that analyze spontaneous EEG of DOC, with the purpose of diagnosis, prognosis, and evaluation of brain interventions. It is expected that this review will promote our understanding of the EEG characteristics in DOC.

**Keywords:** electroencephalography, disorder of consciousness, vegetative state, minimally conscious state, unresponsive wakefulness syndrome

## INTRODUCTION

Following severe damage to the brain, caused by trauma, stroke, or anoxia, patients may fall into a coma (1, 2). When they move out of a coma, they may evolve into a vegetative state (VS) or a minimally conscious state (MCS) according to observable behavioral features (3). Among them, VS (4), or unresponsive wakefulness syndrome (5), is defined by periods of preserved behavioral arousal (6), but unresponsiveness to external stimuli and an absence of awareness (7). MCS shows signs of fluctuating yet reproducible remnants of non-reflex behaviors (8). The disorders of consciousness (DOC) including coma, VS, and MCS pose challenges to clinicians and neuroscientists for diagnosis, treatment, and daily care (3, 9, 10). A correct diagnosis of MCS and VS is of decisive importance for therapeutic strategy making, as patients with MCS generally show greater responses to some treatments (11).

In clinical practice, electroencephalography (EEG) recordings are often used as a tool to help clinicians with diagnoses and prognoses (10, 12). Analyses of resting-state EEG and event-related potential (ERP) are commonly employed (9). An ERP analysis objectively examines sensory and cognitive functions by averaging repeated stimulus-evoked EEG activity (2, 13). Several passive and active paradigms have been used in patients with DOC (13–17). However, the passive paradigms, such as mismatch negativity and somatosensory-evoked potentials, are overly dependent on the basic perceptual function and cortical sensors, which are commonly less preserved in DOC patients

following severe brain injuries (2, 18). The active paradigms, such as motor imagery, require the active participation of patients. This poses several problems when working with DOC patients, such as their impaired cognitive function, fluctuations of arousal levels, fatigue, and subclinical seizure activity. EEG recordings taken in a resting state denote spontaneous neural activity, which is relevant to the fundamental brain state (3, 19). Therefore, appropriate features derived from resting-state EEG may be helpful in monitoring the brain condition of DOC and contribute to decision-making related to these patients' care. In this paper, we present a review of studies on resting-state EEG in DOC and attempt to improve our knowledge of EEG features in the diagnosis, prognosis, and evaluation of brain interventions in cases of DOC.

## THE EEG ANALYSIS FOR DIAGNOSIS

Since MCS patients are considered to benefit relatively easily from some specific treatments, compared to VS (11, 20), the ability to differentiate an MCS from a VS would offer great value in making decisions about treatment. In clinical practice, many standardized behavioral scales are used in the assessment of consciousness of brain-injured patients, such as the Glasgow Coma Scale (GCS) (21) and the Coma Recovery Scale-Revised (CRS-R) (22). Among them, the GCS is widely used in the early hours of a patient's admission, and the CRS-R is used throughout the recovery (1). However, a high ratio of misdiagnoses can be caused by clinicians' subjective judgments, motor function injuries, and patients' fluctuating levels of awareness (10, 16, 23). Therefore, one of the primary applications of EEG studies in DOC patients is auxiliary diagnosis. **Table 1** summarizes the studies we reviewed in this paper.

Spectrum powers have demonstrated the ability to discriminate between MCS and VS. VS patients have shown increased delta power but decreased alpha power, compared to those with MCS (35, 44). In comparison with healthy subjects, VS patients have shown higher delta and theta frequency powers, and both MCS and VS patients have shown decreased alpha power (39). Moreover, the ratios between higher frequencies (alpha + beta) and lower frequencies (delta + theta) have shown a positive correlation with patients' CRS-R scores (24, 39) and a correlation with regional glucose metabolism in MCS ( $n = 4$ ) (24). Considering the spatial distribution, cortical EEG sources showed that the MCS and VS have significant variations of delta in the frontal region, theta in the frontal and parietal regions, alpha and beta in the central region, and gamma in the parietal region (43).

Spectral entropy analysis has found that the MCS has higher entropy value than the VS (18, 31), and the entropy values were correlated with CRS-R (31). The spectral entropy of the MCS changes over time, and periodicities closely resemble being awake in healthy subjects (44). Therefore, the spectral entropy value and its periodic characteristic have been suggested as potential indices for differentiating the MCS from VS. Some other spectrum-derived indices have been introduced in DOC research, such as BIS. BIS was demonstrated to discriminate between an unconscious state and a conscious one (with a value of 50) in one study (25). It could effectively distinguish the VS from the MCS (26).

Entropy theory has also been applied in the time domain of EEG. Approximate entropy (28–30), Lempel–Ziv complexity (30), permutation entropy (18), and Kolmogorov–Chaitin complexity (18) indices have been proposed to investigate the association of EEG complexity with the consciousness levels of DOC patients. Generally, the VS had lower EEG complexity than the MCS, and the control had the highest (30). Among the indices, Kolmogorov–Chaitin complexity and permutation entropy have been indicated as capable of discriminating the MCS from the VS (18, 45).

Functional connectivity is a crucial method for examining consciousness (40, 67). Among the connectivity methods, coherence was the earliest connectivity measurement used in DOC research (62). The results of one study showed that the frontal regions and their connections with the left temporal and parieto-occipital areas could differentiate the MCS and severe neurocognitive disorders, and this difference was consistent with the results of a Granger causality (27). Similarly, a study of coherence performed by Leon-Carrion et al. showed significant differences in full bandwidth (delta, theta, alpha, and beta) in MCS patients with severe neurocognitive disorders (34). However, the coherence methodology has inherent defects that prevent it from being considered as an ideal method for describing global networks (68, 69). Lehenbre et al. compared three connectivity methods (coherence, the imaginary part of coherence, and the phase lag index) and found that significantly lower connectivity of the VS than the MCS could be detected by the imaginary part of coherence and the phase lag index, but failed with coherence (35). Another study addressed 44 indices and proved that partial coherence, directed transfer function, and generalized partial directed coherence were methods with above-chance accuracy for the distinction of an MCS from a VS (with accuracy levels of 0.88, 0.80, and 0.78, respectively) (40).

Furthermore, some other connectivity approaches have been employed, such as weighted symbolic mutual information (wSMI), cross-approximate entropy (32), debiased weighted phase lag index (dwPLI) (46), symbolic transfer entropy, and multivariate Granger causality (41). Among them, wSMI has demonstrated a dissociation with consciousness levels in DOC patients (36), and it was significantly lower in VS in theta and alpha bands (18). Similarly, connectivity and network parameters measured by dwPLI in delta and alpha bands also provided valuable approaches to discriminate different consciousness levels in DOC patients (46).

New approaches using non-strict resting-state EEG might provide new perspectives for finding physiological features that may contribute to diagnoses. Standard EEG patterns in DOC patients showed a difference between the MCS and VS in sleeping states (33). The occurrence of EEG patterns, including sleep spindles, slow wave activity, and the variability of brain rhythms (theta, alpha, and beta), were demonstrated to have significant correlations with the patients' behavioral diagnoses (37). Bonfiglio et al. proposed that the detection of blink-related oscillations contributed to the differential diagnoses between the MCS and VS (38, 42). Blink-related delta oscillations linked with awareness of the surrounding environment, which was a criterion for assessing consciousness. The detection of blink-related activity differs



**TABLE 1 |** Summary of studies using resting-state EEG for diagnosis, prognosis, and evaluation of intervention and basic researches.

Objectives	Literatures	Methods	Subjects	Accuracy/sensitivity/specificity (%)	Main results
Diagnosis	Coleman et al. (24)	Spectrum power ratio	MCS 4, VS 6	–/–/–	VS showed significantly higher EEG power ratio than MCS
	Schnakers et al. (25)	BIS	VS 32, Coma 11	–/75/75	BIS could differentiate unconscious from conscious
	Schnakers et al. (26)		EMCS 13, MCS 30, VS 13, Coma 16	–/–/–	
	Pollonini et al. (27)	Coherence, Granger causality	MCS 7, SND 9	100/–/–	Number of connections within and between brain regions could differentiate MCS from SND
	Sara and Pistoia (28)	ApEn	VS 10, control 10	–/–/–	ApEn was lower in VS than in controls
	Sarà et al. (29)		VS 38, control 40	–/100/97.5	
	Wu et al. (30)	Lempel–Ziv complexity, ApEn, cross-approximate entropy	MCS 16, VS 21, control 30	–/–/–	VS had lowest non-linear indices than MCS and control had highest indices
	Gosseries et al. (31)	State entropy, response entropy	MCS 26, VS 24, Coma 6	–/89/90	EEG entropy of MCS was higher than VS
	Wu et al. (32)	Cross-approximate entropy	MCS 20, VS 30, control 30	–/–/–	Interconnection of local and distant cortical networks in MCS was superior to that of VS
	Landsness et al. (33)	Slow wave activity	MCS 6, VS 5	–/–/–	MCS showed an alternating sleep pattern; VS preserved behavioral sleep but no sleep EEG patterns;
	Leon-Carrion et al. (34)	Coherence, Granger causality	MCS 7, SND 9	–/–/–	MCS showed frontal cortex disconnection from other cortical regions
					Significant difference in full bandwidth coherence between SND and MCS
	Lehembre et al. (35)	Spectrum power, coherence, imaginary part of coherence, phase lag index	MCS 18, VS 10, Acute/subacute 15	–/–/–	VS showed increased delta, decreased alpha power, and lower connectivity than MCS
	King et al. (36)	wSMI	MCS 68, VS 75, CS 24, control 14	–/–/–	wSMI increases as a function separate VS from MCS
	Malinowska et al. (37)	Matching pursuit decomposition, Slow wave activity, K-complexes	LIS 1, MCS 20, VS 11	87/–/–	Sleep EEG patterns correlated with patients' diagnosis
	Bonfiglio et al. (38)	Blink-related delta oscillations	MCS 5, VS 4, control 12	–/–/–	Patients showed abnormal blink-related delta oscillations
	Lechinger et al. (39)	Spectrum power	MCS 9, VS 8, control 14	–/–/–	Ratios between frequencies (above 8 Hz) and (below 8 Hz) correlated with CRS-R
	Höller et al. (40)	A total of 44 indices	MCS 22, VS 27, control 23	Partial coherence: MCS vs. VS (88), control vs. MCS (96), control vs. VS (98) Transfer function: MCS vs. VS (80), control vs. MCS (87), control vs. VS (84) Partial coherence: MCS vs. VS (78), control vs. MCS (93), control vs. VS (96)	Connectivity was crucial for determining the level of consciousness
	Sitt et al. (18)	Spectrum power, spectral entropy, Kolmogorov–Chaitin complexity, phase locking index, wSMI, permutation entropy	MCS 68, VS 75, CS 24, control 14	Best cross-validated single measure: MCS vs. VS (AUC = 71 ± 4) Whole set of measures: MCS vs. VS (AUC = 78 ± 4) The most discriminative measure was wSMI, which separated VS from MCS	
	Marinazzo et al. (41)	Multivariate Granger causality, transfer entropy	MCS 10, EMCS 5, VS11, control 10	–/–/–	In VS, the central, temporal, and occipital electrodes showed asymmetry between incoming and outgoing information
	Bonfiglio et al. (42)	Blink-related synchronization/desynchronization	MCS 4, VS 5, control 12	–/–/–	Blink-related synchronization/desynchronization could differentiate MCS from VS

(Continued)

**TABLE 1 |** Continued

Objectives	Literatures	Methods	Subjects	Accuracy/sensitivity/specificity (%)	Main results
	Naro et al. (43)	Spectrum power, LORETA	MCS 7, VS 6, control 10	–/–/–	Alpha was the most significant LORETA data correlating with the consciousness level
	Piarulli et al. (44)	Spectrum power, spectral entropy	MCS 6, VS 6	–/–/–	MCS showed higher theta and alpha, lower delta, higher spectral entropy, and higher time variability than VS
	Thul et al. (45)	Permutation entropy, symbolic transfer entropy	MCS 7, VS 8, control 24	Permutation entropy: Control vs. MCS (Max AUC = 0.74), control vs. VS (Max AUC = 0.91), MCS vs. VS (Max AUC = 0.74) Symbolic transfer entropy: Control vs. MCS (Max AUC = 0.80), control vs. VS (Max AUC = 0.80), MCS vs. VS (Max AUC = 0.71)	
	Chennu et al. (46)	dwPLI, brain network	MCS 66, VS 23, control 26	VS vs. MCS: Alpha participation coefficient (AUC = 0.83, accuracy = 79%), alpha median connectivity (AUC = 0.82), alpha modular span (AUC = 0.78) MCS– vs. MCS+: delta power averaged over all channels (AUC = 0.79)	
Prognosis	Babiloni et al. (47)	Cortical sources estimated by LORETA	VS 50, control 30	Power of alpha source predicted the follow-up recovery	
	Wu et al. (30)	Lempel–Ziv complexity, ApEn, cross-approximate entropy	MCS 16, VS 21, control 30	Non-linear indices of patients who recovered increased than those in non-recovery	
	Fingelkurts et al. (48)	EEG oscillatory microstates	MCS 11, VS 14	Diversity and variability of EEG for non-survivors were significantly lower than for survivors	
	Sarà et al. (29)	ApEn	VS 38, control 40	Patients with lowest ApEn either died or remained in VS, patients with highest ApEn became MCS or partial or full recovery	
	Cologan et al. (49)	Sleep spindles	MCS 10, VS 10	Patients who clinically improved within 6 months have more sleep spindles	
	Arnaldi et al. (50)	Sleep patterns	MCS 6, VS 20	Sleep patterns were valuable predictors of a positive clinical outcome in sub-acute patients	
	Schorr et al. (51)	Spectrum power, coherence	MCS 15, VS 58, control 24	Short- and long-range coherence had a diagnostic value in the prognosis of recovery from VS	
	Wisłowska et al. (52)	Spectral power, sleep patterns, permutation entropy	MCS 17, VS 18, control 26	Sleep patterns did not systematically vary between day and night in patients Day–night changes in EEG power spectra and signal complexity were revealed in MCS, but not VS Sleep patterns were linearly related to outcome	
	Chennu et al. (46)	dwPLI, brain network	MCS 66, VS 23, control 26	Delta band connectivity and network had a clear relationship with outcomes	
Treatment evaluation	Williams et al. (53)	Spectrum power, coherence, zolpidem	Patients response in zolpidem 3	Spectral peak of 6–10 Hz with high spatial coherence was a predictor of zolpidem responsiveness	
	Manganotti et al. (54)	Spectrum power, 20 Hz rTMS	MCS 3, VS 3	rTMS over M1 induced long-lasting behavioral and neurophysiological modifications in one MCS patient	
	Carboncini et al. (55)	Spectrum power, phase synchronization, midazolam	MCS 1	Change in the power spectrum was observed after midazolam Midazolam induced significant connectivity changes	
	Cavinato et al. (56)	Coherence, simple sensory stimuli	MCS 11, VS 15	Increase in short-range parietal and long-range fronto-parietal coherences in gamma frequencies was seen in the controls and MCS VS showed no modifications in EEG patterns after stimulation	
	Pisani et al. (57)	Slow wave activity, 5 Hz rTMS	MCS 4, VS 6	Following the real rTMS, a preserved sleep–wake cycle, a standard temporal progression of sleep stages appeared in all MCS but none of VS	
	Naro et al. (58)	Spectrum power, coherence, tACS	MCS 12, VS 14, control 15	TACS entrained theta and gamma oscillations and strengthened the connectivity patterns within frontoparietal networks in all the control, partial MCS, and some VS	
	Naro et al. (59)	Spectrum power, coherence, otDCS	MCS 10, VS 10, control 10	Fronto-parietal networks modulation, theta and gamma power modulation, and coherence increase were paralleled by a transient CRS-R improvement, only in MCS individuals	
	Naro et al. (60)	Lagged-phase synchronization, network parameters, rTMS	MCS 9, VS 11, control 10	Two VS patients showed a residual rTMS-induced modulation of the functional correlations between the default mode network and the external awareness networks, as observed in MCS	

(Continued)

TABLE 1 | Continued

Objectives	Literatures	Methods	Subjects	Accuracy/sensitivity/specificity (%)	Main results
Basic research	Bai et al. (61)	Relative power, coherence, bio coherence, MCS with 5, 20, 50, 70, 100 Hz	MCS 11	Significantly altered relative power and synchronization was found in delta and gamma bands after one SCS stimulation using 5, 70, or 100 Hz	
	Davey et al. (62)	Spectrum power, coherence	VS 1	Bio coherence showed that coupling within delta was significantly decreased after stimulation using 70 Hz	
	Babiloni et al. (63)	Spectrum power, LORETA	LIS 13, control 15	Greater low-frequency power, less high-frequency power, and reduced coherence were over the more damaged right hemisphere	
	King et al. (36)	EEG oscillatory microstates	MCS 7, VS 14	Power of delta and alpha was abnormal in LIS	
	Sitt et al. (18)	Spectrum power	LIS 1, MCS 2, control 5	Decreased number of EEG microstate types was associated with altered states of consciousness	
	Varotto et al. (64)	Partial directed coherence	VS 18, control 10	Unawareness was associated with the lack of diversity in EEG alpha-rhythmic microstates	
	Chennu et al. (46)	dwPLI, graph theoretic network	MCS 19, VS 13, control 26	One MCS and one LIS showed motor imagery task performance through spectral change which was different from control	
	Forgasz et al. (65)	Sleep patterns	EMCS 13, MCS 23, VS 8	VS patients showed a significant and widespread decrease in delta band connectivity, whereas the alpha activity was hyper-connected in the central and posterior cortical regions	
	Pavlov et al. (66)	Sleep patterns	VS 15	Network of patients had reduced local and global efficiency, and fewer hubs in the alpha band	
				Patients with evidence of covert command-following had well-organized EEG background and relative preservation of cortical metabolic activity	

ApEn, approximate entropy; wSML, weighted symbolic mutual information; MCS, transcranial alternating current stimulation; tDCS, oscillatory transcranial direct current stimulation; rTMS, repetitive transcranial magnetic stimulation; SCS, spinal cord stimulation; CS, conscious patients; SND, severe neurocognitive disorders; LIS, locked-in syndrome; MCS, minimally conscious state; EMCS, emergence from MCS; VS, vegetative state; dwPLI, debiased weighted phase lag index; AUC, area under the receiver operating characteristic curve.

from the classical resting-state measurement. However, although it included an event input, the resting-state blinking used in the studies was also a type of spontaneous activity which differed from external stimulus used in ERP.

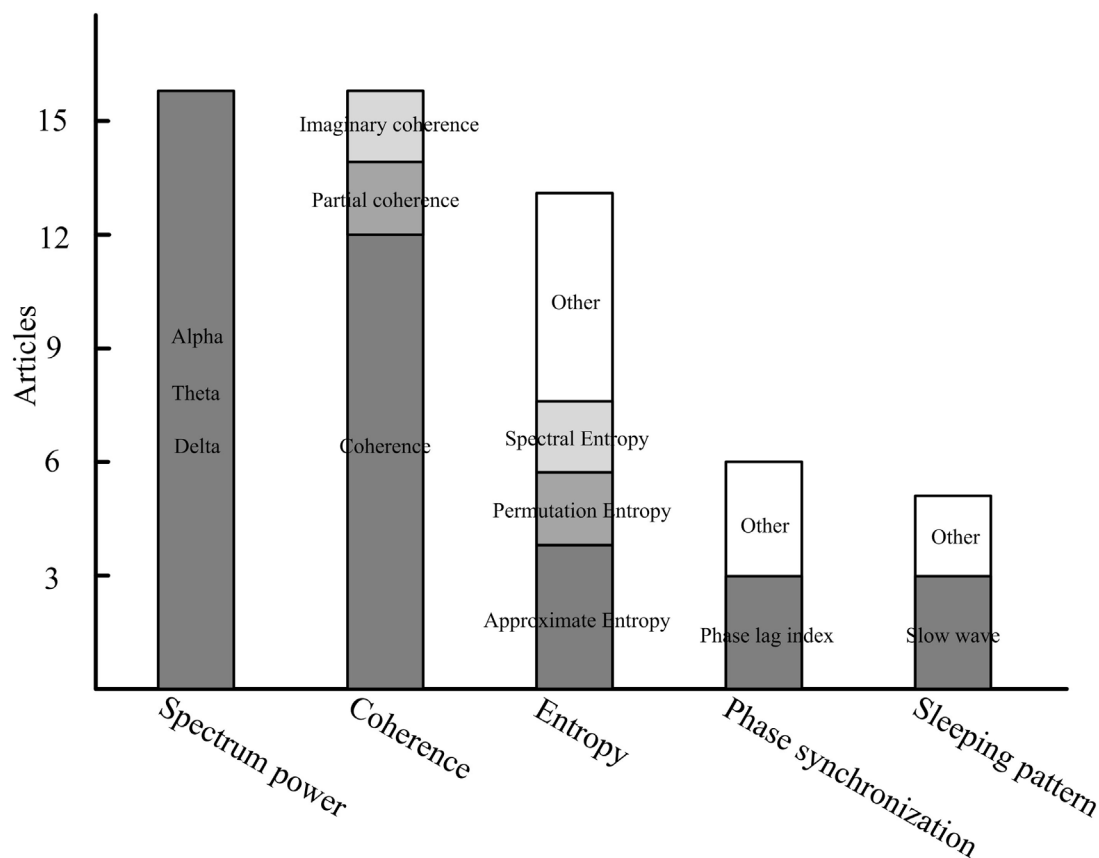
THE EEG ANALYSIS FOR PROGNOSIS

The prognosis for survival and recovery of DOC is still difficult under present clinical conditions (70, 71). Generally, the outcomes at 3 and 6 months following the first assessment were selected to observe the predictive performance of the measures. After 3 months of observation, the spectrum power of EEG recordings showed potentially positive performance in predicting the outcomes of a persistent VS (a patient stays in a VS over 1 month after brain injury) (47). Measured by the level of the cognitive functioning scale (LCF), 12 of 50 patients recovered (from LCF I–II to LCF V–VIII). All the patients stayed in a chronic DOC state at the first evaluation. Compared to healthy subjects, the power of alpha in the occipital region showed progressive decay from healthy subjects to recovered patients and then to non-recovered patients. Therefore, the alpha oscillation was implied as a predictor of the possibility of consciousness recovery (47).

Studies using 6 months of observation have shown an association of non-linear analysis indices with the follow-up recovery. Lempel–Ziv complexity, ApEn, and cross-approximate entropy have been suggested as being capable of predicting outcomes of DOC patients (10 of 37 recovered, with Glasgow Outcome Scale scores decreasing to 3). The first evaluation was conducted on patients who stayed in a chronic DOC state after the onset of brain injury for less than 6 months; the patients with increasing indices under painful stimuli had a higher probability of recovery (30). Coincidentally, another study also found that the highest ApEn might correspond to partial or full consciousness improvement at 6 months after the first assessment (29). The prognostic value of resting-state EEG in predicting survival or non-survival 6 months after brain injury was also proven by EEG oscillatory microstate analyses (48). The first EEG recording of the patients was obtained between 14 days and 3 months after acute brain events. The diversity and variability of EEG oscillations and the probability of the appearance of delta, theta (slow and fast), and alpha oscillations were shown to be potential prognostic features in predicting the outcomes of DOC at the group level. In a recent study, 39 of 61 patients had positive outcomes (assessed by Glasgow Outcome Scale-Extended) at 1 year following the first assessment (46). EEG analysis of the patients found that the connectivity and brain network parameters in delta band had a clear relationship with their outcomes. Meanwhile, EEG sleep patterns were also demonstrated valuable predictors of patients’ clinical outcomes (49, 50, 52). Especially, the density of sleep spindles provided significantly predictive and valuable information about the clinical outcomes of DOC patients.

THE EEG ANALYSIS FOR THE EVALUATION OF BRAIN INTERVENTION

Due to a variety of etiological, brain injury, and cortical conditions, DOC patients have shown various responses to treatment



**FIGURE 1** | The primary features in resting-state electroencephalography studies of disorders of consciousness.

therapies (20, 72). A precise evaluation of the cerebral responses in the treatment would be helpful for understanding the mechanism of the intervention and facilitate the creation of individual therapeutic strategies. In practice, behavioral changes induced by treatment might be long-lasting accumulated effects that could not be observed immediately. Recently, indices based on EEG analyses were applied to monitor the instantaneous cerebral responses in pharmacological and non-pharmacological brain interventions (16).

Spectrum power, connectivity of coherence, and phase synchronization have been used to assess the cerebral changes of patients in pharmacological treatment (53, 55). For MCS patients who respond to midazolam, spectrum power changes and connectivity changes were found after taking the medication (55). While under zolpidem treatment, all patients showed a distinct low-frequency oscillatory peak at approximately 6–10 Hz over the fronto-central regions (53). Resting-state EEG in non-pharmacological interventions have been investigated in DOC treatment, such as spinal cord stimulation (61), repetitive transcranial magnetic stimulation (rTMS) (54, 57, 60), sensory stimuli (56), transcranial alternating current stimulation (58), and oscillatory transcranial direct current stimulation (59). The fronto-parietal networks of the MCS in the theta and gamma bands have been demonstrated as being responsive to transcranial

current stimulation, with little reactivity found in the VS (58, 59). This modulation of a consciousness-related network may suggest more benefits to the MCS than the VS from transcranial current stimulation, and the differential cortical responses between the MCS and VS might provide a stimulus-response approach for diagnoses. Similarly, the different EEG responses between the MCS and VS have also been demonstrated in rTMS, proven by spectrum power (54), complex network parameters (60), and slow wave activity in sleeping (57). In addition, we have attempted to use resting-state EEG as an assistive method for parameter selection in spinal cord stimulations of patients with DOC (61).

## SUMMARY AND CONCLUSION

The characteristics that have been applied in DOC-related studies could be generally classified into five categories: the spectrum, entropy, connectivity, the network, and the sleeping pattern. We summarize the primary features that are frequently used in DOC studies (Figure 1). We found that spectrum power, coherence, and entropy were the most frequently used features in differentiating consciousness levels, predicting follow-up outcome or measuring patients' cortical response to brain intervention. Comparisons of various methods with multiple indices were performed in two studies (18, 40). Indices derived from spectrum, non-linear



analysis, information theory, and functional connectivity were investigated. A discrimination performance of the measures supports power spectrum and functional connectivity as having the best performance in separating the VS from the MCS and healthy subjects (18). In addition, permutation entropy in the theta frequency also has relatively higher classification accuracy in distinguishing the MCS and VS.

Spectral power measures the strength of neuronal oscillations, which depend on the spontaneously activity of underlying oscillators (neurons) (73). Spectral power at some specific frequency can reveal relationships between the activity of groups of neurons and consciousness levels (24, 39). Reviewing the studies, increases of low power (delta and theta), and decreases of high power (alpha) were common spectrum characteristics of patients with DOC. In comparing the MCS and VS, the latter has increased delta and decreased alpha power than the former. Therefore, a power ratio index may be first considered to help us qualitatively assess the consciousness state of patients. In predicting the follow-up outcomes, alpha power should always receive attention. In addition, theta and alpha bands are also critical frequency bands in assessing cortical responses to brain interventions.

Since the neuronal oscillations and synchronization are two essential features of the conscious brain (74), synchronization should be a critical feature in understanding the consciousness of patients with DOC. Synchronization analysis could reveal direct structural connections or indirect information flows, and it could concurrently provide temporal causality and spatial links (2, 75). Non-directed (coherence, the phase locking index, partial directed coherence, the imaginary part of coherence, the dwPLI, cross-approximate entropy, and wSMI) and directed (transfer entropy, symbolic transfer entropy, mutual information, and Granger causality) connectivity measurements were used to reveal the “disconnection” characteristics of patients with DOC (32, 64). Among the measurements, coherence is the most commonly used method. In addition, disconnection between the frontal and other regions, especially the fronto-parietal, was shown to be a

significant biomarker, whether assessing the consciousness level or evaluating the brain response to intervention. However, when taking the synchronization feature into actual clinical operation, the reference location, artifact robustness, volume conduction, interesting regions, and cautious physiological explanations should be taken into account.

Similar to EEG complexity in a sleep or anesthesia state (76–78), the complexity measures in DOC were based on the hypothesis that neural activities would be suppressed in a brain of a low consciousness level, and thus fewer components would be included in the EEG signals. EEG complexity, whether measured in the time domain (such as approximate entropy, Lempel–Ziv complexity, Kolmogorov–Chaitin complexity, and permutation entropy) or the frequency domain (BIS and spectral entropy), provided relatively effective and readily comprehensible indices (range of 0–1 or 0–100, with higher value corresponding to higher consciousness level) to describe brain electrical activities under different consciousness states. Therefore, complexity characteristics may have potential value in quantitatively describing the consciousness level of patients with DOC and finally are implanted into monitors for daily caring.

## AUTHOR CONTRIBUTIONS

YB and XX reviewed the articles and written the manuscript. XL guided the whole work.

## FUNDING

This research was supported by the National Natural Science Foundation of China (No. 61273063, No. 81230023) and the Beijing Municipal Science and Technology Commission (No. Z141107002514111), and the commercialization of research findings was supported by the Beijing Municipal Commission of Education.

## REFERENCES

- Gosseries O, Vanhaudenhuyse A, Bruno M-A, Demertzi A, Schnakers C, Boly MM, et al. Disorders of consciousness: coma, vegetative and minimally conscious states. In: Cvetkovic D., Cosic I., editors. *States of Consciousness*. Berlin: Springer (2011). p. 29–55.
- Gosseries O, Di H, Laureys S, Boly M. Measuring consciousness in severely damaged brains. *Annu Rev Neurosci* (2014) 37:457–78. doi:10.1146/annurev-neuro-062012-170339
- Giacino JT, Fins JJ, Laureys S, Schiff ND. Disorders of consciousness after acquired brain injury: the state of the science. *Nat Rev Neurol* (2014) 10(2): 99–114. doi:10.1038/nrneuro.2013.279
- Jennett B, Plum F. Persistent vegetative state after brain damage. A syndrome in search of a name. *Lancet* (1972) 1(7753):734–7. doi:10.1016/S0140-6736(72)90242-5
- Laureys S, Celesia GG, Cohadon F, Lavrijssen J, Leon-Carrion J, Sannita WG, et al. Unresponsive wakefulness syndrome: a new name for the vegetative state or apallic syndrome. *BMC Med* (2010) 8:68. doi:10.1186/1741-7015-8-68
- Laureys S, Owen AM, Schiff ND. Brain function in coma, vegetative state, and related disorders. *Lancet Neurol* (2004) 3(9):537–46. doi:10.1016/S1474-4422(04)00852-X
- Laureys S, Boly M. The changing spectrum of coma. *Nat Clin Pract Neurol* (2008) 4(10):544–6. doi:10.1038/ncpneu0887
- Giacino JT, Ashwal S, Childs N, Cranford R, Jennett B, Katz DI, et al. The minimally conscious state: definition and diagnostic criteria. *Neurology* (2002) 58(3):349–53. doi:10.1212/WNL.58.3.349
- Cruse D, Monti MM, Owen AM. Neuroimaging in disorders of consciousness: contributions to diagnosis and prognosis. *Future Neurol* (2011) 6(2):291–9. doi:10.2217/fnl.10.87
- Gantner IS, Bodart O, Laureys S, Demertzi A. Our rapidly changing understanding of acute and chronic disorders of consciousness: challenges for neurologists. *Future Neurol* (2013) 8(1):43–54. doi:10.2217/fnl.12.77
- Thibaut A, Bruno MA, Ledoux D, Demertzi A, Laureys S. tDCS in patients with disorders of consciousness: sham-controlled randomized double-blind study. *Neurology* (2014) 82(13):1112–8. doi:10.1212/WNL.0000000000000260
- Fernandez-Espejo D, Owen AM. Detecting awareness after severe brain injury. *Nat Rev Neurosci* (2013) 14(11):801–9. doi:10.1038/nrn3608
- Cruse D, Chennu S, Chatelle C, Bekinschtein TA, Fernandez-Espejo D, Pickard JD, et al. Bedside detection of awareness in the vegetative state: a cohort study. *Lancet* (2011) 378(9809):2088–94. doi:10.1016/S0140-6736(11)61224-5
- Cruse D, Chennu S, Fernandez-Espejo D, Payne WL, Young GB, Owen AM. Detecting awareness in the vegetative state: electroencephalographic evidence

- for attempted movements to command. *PLoS One* (2012) 7(11):e49933. doi:10.1371/journal.pone.0049933
15. Cruse D, Beukema S, Chennu S, Malins JG, Owen AM, McRae K. The reliability of the N400 in single subjects: implications for patients with disorders of consciousness. *Neuroimage Clin* (2014) 4:788–99. doi:10.1016/j.nicl.2014.05.001
  16. Gosseries O, Pistoia F, Charland-Verville V, Carolei A, Sacco S, Laureys S. The role of neuroimaging techniques in establishing diagnosis, prognosis and therapy in disorders of consciousness. *Open Neuroimag J* (2016) 10:52–68. doi:10.2174/1874440001610010052
  17. Monti MM, Sannita WG. *Brain Function and Responsiveness in Disorders of Consciousness*. Switzerland: Springer International Publishing (2016).
  18. Sitt JD, King JR, El Karoui I, Rohaut B, Faugeras F, Gramfort A, et al. Large scale screening of neural signatures of consciousness in patients in a vegetative or minimally conscious state. *Brain* (2014) 137(Pt 8):2258–70. doi:10.1093/brain/awu141
  19. Stam C, Montez T, Jones B, Rombouts S, Van Der Made Y, Pijnenburg Y, et al. Disturbed fluctuations of resting state EEG synchronization in Alzheimer's disease. *Neurophysiol Clin* (2005) 116(3):708–15. doi:10.1016/j.clinph.2004.09.022
  20. Guerra A, Costantini EM, Maatta S, Ponzo D, Ferreri F. Disorders of consciousness and electrophysiological treatment strategies: a review of the literature and new perspectives. *Curr Pharm Des* (2014) 20(26):4248–67. doi:10.2174/13816128113196660648
  21. Teasdale G, Jennett B. Assessment of coma and impaired consciousness. A practical scale. *Lancet* (1974) 2(7872):81–4. doi:10.1016/S0140-6736(74)91639-0
  22. Giacino JT, Kalmar K, Whyte J. The JFK Coma Recovery Scale-revised: measurement characteristics and diagnostic utility. *Arch Phys Med Rehabil* (2004) 85(12):2020–9. doi:10.1016/j.apmr.2004.02.033
  23. Schnakers C, Vanhaudenhuyse A, Giacino J, Ventura M, Boly M, Majerus S, et al. Diagnostic accuracy of the vegetative and minimally conscious state: clinical consensus versus standardized neurobehavioral assessment. *BMC Neurol* (2009) 9:35. doi:10.1186/1471-2377-9-35
  24. Coleman MR, Menon DK, Fryer TD, Pickard JD. Neurometabolic coupling in the vegetative and minimally conscious states: preliminary findings. *J Neurol Neurosurg Psychiatry* (2005) 76(3):432–4. doi:10.1136/jnnp.2004.045930
  25. Schnakers C, Majerus S, Laureys S. Bispectral analysis of electroencephalogram signals during recovery from coma: preliminary findings. *Neuropsychol Rehabil* (2005) 15(3–4):381–8. doi:10.1080/09602010443000524
  26. Schnakers C, Ledoux D, Majerus S, Damas P, Damas F, Lambermont B, et al. Diagnostic and prognostic use of bispectral index in coma, vegetative state and related disorders. *Brain Inj* (2008) 22(12):926–31. doi:10.1080/02699050802530565
  27. Pollonini L, Pophale S, Situ N, Wu MH, Frye RE, Leon-Carrion J, et al. Information communication networks in severe traumatic brain injury. *Brain Topogr* (2010) 23(2):221–6. doi:10.1007/s10548-010-0139-9
  28. Sara M, Pistoia F. Complexity loss in physiological time series of patients in a vegetative state. *Nonlinear Dynamics Psychol Life Sci* (2010) 14(1):1–13.
  29. Sarà M, Pistoia F, Pasqualetti P, Sebastiano F, Onorati P, Rossini PM. Functional isolation within the cerebral cortex in the vegetative state: a nonlinear method to predict clinical outcomes. *Neurorehabil Neural Repair* (2011) 25(1):35–42. doi:10.1177/1545968310378508
  30. Wu DY, Cai G, Yuan Y, Liu L, Li GQ, Song WQ, et al. Application of nonlinear dynamics analysis in assessing unconsciousness: a preliminary study. *Clin Neurophysiol* (2011) 122(3):490–8. doi:10.1016/j.clinph.2010.05.036
  31. Gosseries O, Schnakers C, Ledoux D, Vanhaudenhuyse A, Bruno MA, Demertzi A, et al. Automated EEG entropy measurements in coma, vegetative state/unresponsive wakefulness syndrome and minimally conscious state. *Funct Neurol* (2011) 26(1):25–30.
  32. Wu DY, Cai G, Zorowitz RD, Yuan Y, Wang J, Song WQ. Measuring interconnection of the residual cortical functional islands in persistent vegetative state and minimal conscious state with EEG nonlinear analysis. *Clin Neurophysiol* (2011) 122(10):1956–66. doi:10.1016/j.clinph.2011.03.018
  33. Landsness E, Bruno MA, Noirhomme Q, Riedner B, Gosseries O, Schnakers C, et al. Electrophysiological correlates of behavioural changes in vigilance in vegetative state and minimally conscious state. *Brain* (2011) 134(Pt 8):2222–32. doi:10.1093/brain/awr152
  34. Leon-Carrion J, Leon-Dominguez U, Pollonini L, Wu M-H, Frye RE, Dominguez-Morales MR, et al. Synchronization between the anterior and posterior cortex determines consciousness level in patients with traumatic brain injury (TBI). *Brain Res* (2012) 1476:22–30. doi:10.1016/j.brainres.2012.03.055
  35. Lehenbre R, Marie-Aurelie B, Vanhaudenhuyse A, Chatelle C, Collogan V, Leclercq Y, et al. Resting-state EEG study of comatose patients: a connectivity and frequency analysis to find differences between vegetative and minimally conscious states. *Funct Neurol* (2012) 27(1):41–7.
  36. King JR, Sitt JD, Faugeras F, Rohaut B, El Karoui I, Cohen L, et al. Information sharing in the brain indexes consciousness in noncommunicative patients. *Curr Biol* (2013) 23(19):1914–9. doi:10.1016/j.cub.2013.07.075
  37. Malinowska U, Chatelle C, Bruno M-A, Noirhomme Q, Laureys S, Durka PJ. Electroencephalographic profiles for differentiation of disorders of consciousness. *Biomed Eng Online* (2013) 12(1):109. doi:10.1186/1475-925X-12-109
  38. Bonfiglio L, Olcese U, Rossi B, Frisoli A, Arrighi P, Greco G, et al. Cortical source of blink-related delta oscillations and their correlation with levels of consciousness. *Hum Brain Mapp* (2013) 34(9):2178–89. doi:10.1002/hbm.22056
  39. Lechinger J, Bothe K, Pichler G, Michitsch G, Donis J, Klimesch W, et al. CRS-R score in disorders of consciousness is strongly related to spectral EEG at rest. *J Neurol* (2013) 260(9):2348–56. doi:10.1007/s00415-013-6982-3
  40. Höller Y, Thomschewski A, Bergmann J, Kronbichler M, Crone JS, Schmid EV, et al. Connectivity biomarkers can differentiate patients with different levels of consciousness. *Clin Neurophysiol* (2014) 125(8):1545–55. doi:10.1016/j.clinph.2013.12.095
  41. Marinazzo D, Gosseries O, Boly M, Ledoux D, Rosanova M, Massimini M, et al. Directed information transfer in scalp electroencephalographic recordings: insights on disorders of consciousness. *Clin EEG Neurosci* (2014) 45(1):33–9. doi:10.1177/1550059413510703
  42. Bonfiglio L, Piarulli A, Olcese U, Andre P, Arrighi P, Frisoli A, et al. Spectral parameters modulation and source localization of blink-related alpha and low-beta oscillations differentiate minimally conscious state from vegetative state/unresponsive wakefulness syndrome. *PLoS One* (2014) 9(3):e93252. doi:10.1371/journal.pone.0093252
  43. Naro A, Bramanti P, Leo A, Cacciola A, Bramanti A, Manuli A, et al. Towards a method to differentiate chronic disorder of consciousness patients' awareness: the low-resolution brain electromagnetic tomography analysis. *J Neurol Sci* (2016) 368:178–83. doi:10.1016/j.jns.2016.07.016
  44. Piarulli A, Bergamasco M, Thibaut A, Cologan V, Gosseries O, Laureys S. EEG ultradian rhythmicity differences in disorders of consciousness during wakefulness. *J Neurol* (2016) 263(9):1746–60. doi:10.1007/s00415-016-8196-y
  45. Thul A, Lechinger J, Donis J, Michitsch G, Pichler G, Kochs EF, et al. EEG entropy measures indicate decrease of cortical information processing in disorders of consciousness. *Neurophysiol Clin* (2016) 127(2):1419–27. doi:10.1016/j.clinph.2015.07.039
  46. Chennu S, Annen J, Wannez S, Thibaut A, Chatelle C, Cassol H, et al. Brain networks predict metabolism, diagnosis and prognosis at the bedside in disorders of consciousness. *Brain* (2017) 140(8):2120–32. doi:10.1093/brain/awx163
  47. Babiloni C, Sara M, Vecchio F, Pistoia F, Sebastiano F, Onorati P, et al. Cortical sources of resting-state alpha rhythms are abnormal in persistent vegetative state patients. *Clin Neurophysiol* (2009) 120(4):719–29. doi:10.1016/j.clinph.2009.02.157
  48. Fingelkurts AA, Fingelkurts AA, Bagnato S, Boccagni C, Galardi G. Life or death: prognostic value of a resting EEG with regards to survival in patients in vegetative and minimally conscious states. *PLoS One* (2011) 6(10):e25967. doi:10.1371/journal.pone.0025967
  49. Cologan V, Drouot X, Parapatics S, Delorme A, Gruber G, Moonen G, et al. Sleep in the unresponsive wakefulness syndrome and minimally conscious state. *J Neurotrauma* (2013) 30(5):339–46. doi:10.1089/neu.2012.2654
  50. Arnaldi D, Terzaghi M, Cremascoli R, De Carli F, Maggioni G, Pistarini C, et al. The prognostic value of sleep patterns in disorders of consciousness in the sub-acute phase. *Clin Neurophysiol* (2016) 127(2):1445–51. doi:10.1016/j.clinph.2015.10.042
  51. Schorr B, Schlee W, Arndt M, Bender A. Coherence in resting-state EEG as a predictor for the recovery from unresponsive wakefulness syndrome. *J Neurol* (2016) 263(5):937–53. doi:10.1007/s00415-016-8084-5
  52. Wislowska M, Giudice RD, Lechinger J, Wielek T, Heib DP, Pitiot A, et al. Night and day variations of sleep in patients with disorders of consciousness. *Sci Rep* (2017) 7(1):266. doi:10.1038/s41598-017-00323-4

53. Williams ST, Conte MM, Goldfine AM, Noirhomme Q, Gosseries O, Thonnard M, et al. Common resting brain dynamics indicate a possible mechanism underlying zolpidem response in severe brain injury. *Elife* (2013) 2:e01157. doi:10.7554/eLife.01157
54. Manganotti P, Formaggio E, Storti SF, Fiaschi A, Battistin L, Tonin P, et al. Effect of high-frequency repetitive transcranial magnetic stimulation on brain excitability in severely brain-injured patients in minimally conscious or vegetative state. *Brain Stimul* (2013) 6(6):913–21. doi:10.1016/j.brs.2013.06.006
55. Carboncini MC, Piarulli A, Virgillito A, Arrighi P, Andre P, Tomaiuolo F, et al. A case of post-traumatic minimally conscious state reversed by midazolam: clinical aspects and neurophysiological correlates. *Restor Neurol Neurosci* (2014) 32(6):767–87. doi:10.3233/RNN-140426
56. Cavinato M, Genna C, Manganotti P, Formaggio E, Storti SF, Campostrini S, et al. Coherence and consciousness: study of fronto-parietal gamma synchrony in patients with disorders of consciousness. *Brain Topogr* (2015) 28(4):570–9. doi:10.1007/s10548-014-0383-5
57. Pisani LR, Naro A, Leo A, Arico I, Pisani F, Silvestri R, et al. Repetitive transcranial magnetic stimulation induced slow wave activity modification: a possible role in disorder of consciousness differential diagnosis? *Conscious Cogn* (2015) 38:1–8. doi:10.1016/j.concog.2015.09.012
58. Naro A, Bramanti P, Leo A, Russo M, Calabrò RS. Transcranial alternating current stimulation in patients with chronic disorder of consciousness: a possible way to cut the diagnostic Gordian knot? *Brain Topogr* (2016) 29(4):623–44. doi:10.1007/s10548-016-0489-z
59. Naro A, Russo M, Leo A, Cannavò A, Manuli A, Bramanti A, et al. Cortical connectivity modulation induced by cerebellar oscillatory transcranial direct current stimulation in patients with chronic disorders of consciousness: a marker of covert cognition? *Neurophysiol Clin* (2016) 127(3):1845–54. doi:10.1016/j.clinph.2015.12.010
60. Naro A, Leo A, Manuli A, Cannavò A, Bramanti A, Bramanti P, et al. How far can we go in chronic disorders of consciousness differential diagnosis? The use of neuromodulation in detecting internal and external awareness. *Neuroscience* (2017) 349:165–73. doi:10.1016/j.neuroscience.2017.02.053
61. Bai Y, Xia X, Li X, Wang Y, Yang Y, Liu Y, et al. Spinal cord stimulation modulates frontal delta and gamma in patients of minimally consciousness state. *Neuroscience* (2017) 346:247–54. doi:10.1016/j.neuroscience.2017.01.036
62. Davey MP, Victor JD, Schiff ND. Power spectra and coherence in the EEG of a vegetative patient with severe asymmetric brain damage. *Clin Neurophysiol* (2000) 111(11):1949–54. doi:10.1016/S1388-2457(00)00435-1
63. Babiloni C, Pistoia F, Sara M, Vecchio F, Buffo P, Conson M, et al. Resting state eyes-closed cortical rhythms in patients with locked-in-syndrome: an EEG study. *Clin Neurophysiol* (2010) 121(11):1816–24. doi:10.1016/j.clinph.2010.04.027
64. Varotto G, Fazio P, Rossi Sebastiano D, Duran D, D'Incerti L, Parati E, et al. Altered resting state effective connectivity in long-standing vegetative state patients: an EEG study. *Clin Neurophysiol* (2014) 125(1):63–8. doi:10.1016/j.clinph.2013.06.016
65. Forgacs PB, Conte MM, Fridman EA, Voss HU, Victor JD, Schiff ND. Preservation of electroencephalographic organization in patients with impaired consciousness and imaging-based evidence of command-following. *Ann Neurol* (2014) 76(6):869–79. doi:10.1002/ana.24283
66. Pavlov YG, Gais S, Muller F, Schonauer M, Schapers B, Born J, et al. Night sleep in patients with vegetative state. *J Sleep Res* (2017) 7:266. doi:10.1111/jsr.12524
67. Sanders RD, Tononi G, Laureys S, Sleigh JW. Unresponsiveness ≠ unconsciousness. *J Am Soc Anesthesiol* (2012) 116(4):946–59. doi:10.1097/ALN.0b013e318249d0a7
68. Fein G, Raz J, Brown FF, Merrin EL. Common reference coherence data are confounded by power and phase effects. *Electroencephalogr Clin Neurophysiol* (1988) 69(6):581–4. doi:10.1016/0013-4694(88)90171-X
69. Srinivasan R, Nunez PL, Silberstein RB. Spatial filtering and neocortical dynamics: estimates of EEG coherence. *IEEE Trans Biomed Eng* (1998) 45(7):814–26. doi:10.1109/10.686789
70. Giacino JT, Kalmar K. Diagnostic and prognostic guidelines for the vegwive and minimally conscious states. *Neuropsychol Rehabil* (2005) 15(3–4):166–74. doi:10.1080/09602010443000498
71. Bagnato S, Boccagni C, Prestandrea C, Sant'Angelo A, Castiglione A, Galardi G. Prognostic value of standard EEG in traumatic and non-traumatic disorders of consciousness following coma. *Neurophysiol Clin* (2010) 121(3):274–80. doi:10.1016/j.clinph.2009.11.008
72. Georgiopoulos M, Katsakiori P, Kefalopoulou Z, Ellul J, Chroni E, Constantoyannis C. Vegetative state and minimally conscious state: a review of the therapeutic interventions. *Stereotact Funct Neurosurg* (2010) 88(4):199–207. doi:10.1159/000314354
73. Buzsaki G, Draguhn A. Neuronal oscillations in cortical networks. *Science* (2004) 304(5679):1926–9. doi:10.1126/science.1099745
74. Ward LM. Synchronous neural oscillations and cognitive processes. *Trends Cogn Sci* (2003) 7(12):553–9. doi:10.1016/j.tics.2003.10.012
75. Boly M, Massimini M, Garrido MI, Gosseries O, Noirhomme Q, Laureys S, et al. Brain connectivity in disorders of consciousness. *Brain Connect* (2012) 2(1):1–10. doi:10.1089/brain.2011.0049
76. Acharya R, Faust O, Kannathal N, Chua T, Laxminarayan S. Non-linear analysis of EEG signals at various sleep stages. *Comput Methods Programs Biomed* (2005) 80(1):37–45. doi:10.1016/j.cmpb.2005.06.011
77. Li X, Cui S, Voss LJ. Using permutation entropy to measure the electroencephalographic effects of sevoflurane. *Anesthesiology* (2008) 109(3):448–56. doi:10.1097/ALN.0b013e318182a91b
78. Li D, Li X, Liang Z, Voss LJ, Sleigh JW. Multiscale permutation entropy analysis of EEG recordings during sevoflurane anesthesia. *J Neural Eng* (2010) 7(4):046010. doi:10.1088/1741-2560/7/4/046010

**Conflict of Interest Statement:** The authors declare that the research was conducted in the absence of any commercial or financial relationships that could be construed as a potential conflict of interest.

The reviewer, QN, and handling editor declared their shared affiliation.

Copyright © 2017 Bai, Xia and Li. This is an open-access article distributed under the terms of the Creative Commons Attribution License (CC BY). The use, distribution or reproduction in other forums is permitted, provided the original author(s) or licensor are credited and that the original publication in this journal is cited, in accordance with accepted academic practice. No use, distribution or reproduction is permitted which does not comply with these terms.



# A Systematic Review and Meta-Analysis of the Relationship Between Brain Data and the Outcome in Disorders of Consciousness

**Boris Kotchoubey<sup>1\*</sup> and Yuri G. Pavlov<sup>1,2</sup>**

<sup>1</sup>Institute of Medical Psychology, University of Tübingen, Tübingen, Germany, <sup>2</sup>Department of Psychology, Ural Federal University, Yekaterinburg, Russia

## OPEN ACCESS

### Edited by:

Olivia Gosseries,  
University of Liège, Belgium

### Reviewed by:

Renate Rutiku,  
University of Tartu, Estonia  
Andrea Piarulli,  
Università degli Studi di Pisa, Italy;  
University of Liège, Belgium

### \*Correspondence:

Boris Kotchoubey  
boris.kotchoubey@uni-tuebingen.de

### Specialty section:

This article was submitted  
to Applied Neuroimaging,  
a section of the journal  
Frontiers in Neurology

**Received:** 29 January 2018

**Accepted:** 20 April 2018

**Published:** 08 May 2018

### Citation:

Kotchoubey B and Pavlov YG (2018)  
A Systematic Review and  
Meta-Analysis of the Relationship  
Between Brain Data and the  
Outcome in Disorders  
of Consciousness.  
Front. Neurol. 9:315.  
doi: 10.3389/fneur.2018.00315

A systematic search revealed 68 empirical studies of neurophysiological [EEG, event-related brain potential (ERP), fMRI, PET] variables as potential outcome predictors in patients with Disorders of Consciousness (diagnoses Unresponsive Wakefulness Syndrome [UWS] and Minimally Conscious State [MCS]). Data of 47 publications could be presented in a quantitative manner and systematically reviewed. Insufficient power and the lack of an appropriate description of patient selection each characterized about a half of all publications. In more than 80% studies, neurologists who evaluated the patients' outcomes were familiar with the results of neurophysiological tests conducted before, and may, therefore, have been influenced by this knowledge. In most subsamples of datasets, effect size significantly correlated with its standard error, indicating publication bias toward positive results. Neurophysiological data predicted the transition from UWS to MCS substantially better than they predicted the recovery of consciousness (i.e., the transition from UWS or MCS to exit-MCS). A meta-analysis was carried out for predictor groups including at least three independent studies with  $N > 10$  per predictor per improvement criterion (i.e., transition to MCS versus recovery). Oscillatory EEG responses were the only predictor group whose effect attained significance for both improvement criteria. Other perspective variables, whose true prognostic value should be explored in future studies, are sleep spindles in the EEG and the somatosensory cortical response N20. Contrary to what could be expected on the basis of neuroscience theory, the poorest prognostic effects were shown for fMRI responses to stimulation and for the ERP component P300. The meta-analytic results should be regarded as preliminary given the presence of numerous biases in the data.

**Keywords:** consciousness, improvement criteria, meta-analysis, minimally conscious state, neurophysiological markers, prognosis, publication bias, unresponsive wakefulness syndrome

...the quality of methodological reporting in the social and behavioral science research literature is poor. Reports are often silent or ambiguous on important methodological and procedural matters making it difficult for the analyst to determine what was done. The metaanalyst who develops elaborate and detailed methodological criteria for study selection, therefore, will most likely find that study reports do not provide sufficient information for those criteria to be confidently applied. [Lipsey and Wilson (1) (p. 22)]



A systematic analysis of several published datasets can yield substantial new knowledge as compared with the data of each single experiment (2). This insight, increasingly admitted during the last decades, underlies the use of meta-analyses and other kinds of quantitative reviews that can largely overcome the subjectivity and deliberateness of the “good old” narrative reviews. The domain of the severe Disorders of Consciousness (DoC) is, however, still dominated by the latter genre. Thus a brief overview of journal publications about brain imaging data in DoC for the last 5 years reveals that almost every fourth paper (exactly, 33 of the 137 papers) is a narrative review. Book publications further increase this number.

The notion DoC most usually includes two diagnostic entities: the vegetative state, or unresponsive wakefulness syndrome (UWS), and the minimally conscious state (MCS) (3, 4). To the best of our knowledge, the first systematic analysis of neurophysiological data in DoC was devoted to the question whether these data confirm the reality of the distinction between UWS and MCS (5). The authors came to the conclusion that there were no reliable differences in terms of neurophysiological variables (mainly EEG, PET, and fMRI) between the two diagnoses.

Hannawi et al. (6) concentrated on brain imaging studies and performed a voxel-based meta-analysis of 13 PET and fMRI studies in DoC patients, in which the corresponding data were reported. The authors identified a number of structures whose resting state activity was significantly decreased in patients as compared with healthy controls. On the other hand, they did not find convincing differences between UWS and MCS, which was in line with Liberati et al. (5). Kondziella et al. (7) came, however, to a different conclusion that brain connectivity data in rest and under passive stimulation (but not in active instruction conditions) reliably differ between UWS and MCS. Unfortunately, inclusion criteria in this study were not completely clear; thus the question still remains open whether late event-related brain potential (ERP) components (P300, N400) can be regarded as indicators of cortical connectivity, and therefore, the authors should either include all P300 and N400 studies in their analysis (if they answer this question positively), or exclude all of them (if they answer it negatively), but instead, they included only some of them. The data were not checked for publication bias, that is, the tendency for positive results or stronger effects to get published more readily than negative results or weaker effects (8). The simplest index of this bias is a negative correlation between the size of the obtained effect and its reliability (9). On the other hand, Kondziella et al. (7) indicated a bias in patient selection. The risk of this bias was estimated as “high” in 81.4% of the analyzed studies and as “uncertain” in further 11.6%.

Also, Bender et al. (10) were interested in the abilities of neurophysiological techniques to distinguish between UWS and MCS. Their meta-analysis aimed not at the presence and size of the effects, but at the parameters of sensitivity and specificity. The authors concluded “... that modern diagnostic techniques can already make a major contribution to the diagnostic assessment of MCS.” The inspection of their empirical findings yields a modest support for this conclusion, because good sensitivity and specificity values were found only for the measures of quantitative EEG; ERP and fMRI measures revealed, to the contrary,

only moderate specificity and rather low sensitivity that did not significantly differ from chance.

Kotchoubey (11) carried out a quantitative analysis of 61 reports on ERPs in DoC. ERPs are the most frequently used neurophysiological technique in DoC, which, however, does not mean that they are also most useful. In general, the results of the analysis were rather disappointing. Most studies possessed such a low statistical power that their findings can at best be regarded as “preliminary results.” In addition, there was strong evidence for a publication bias toward positive findings.

However, there were good news. The above-mentioned deficits mainly concerned the studies where ERPs were compared between UWS and MCS, which largely concurs with the conclusions of Liberati et al. (5). The negative tendencies were substantially less expressed in the literature about the relationship between ERP and the prognosis of DoC outcome. Furthermore, the power of the prognostic studies correlated positively, and the effect sizes (ESs) correlated negatively, with the rank of journals where the data were reported. This indicated that weaker but more reliable effects could be published more successfully in top-ranking journals than strong but less reliable ones.

Like all areas in which there is no golden diagnostic standard, meta-analyses of novel diagnostic tests in the domain of DoC have a strong circular component. The expensive neurophysiological techniques are developed to complement imperfect clinical methods and to increase the diagnostic precision; but in a meta-analysis, these novel techniques are evaluated on the basis of the same (presumably imprecise) diagnostic criteria that these methods should improve! The lack of the golden diagnostic standard makes another strategy more preferable, i.e., a search for the measurements most reliably related to prognosis. The above-cited findings, that prognostic studies in DoC appear to have a higher quality than diagnostic studies, are in line with this view.

The aim of the present study was a systematic analysis of all publications relating any functional brain data recorded in UWS and MCS patients to their outcome several weeks or months after the measurement. Data using only anatomical brain measurements were not included in the present analysis. Each of the analyzed publications will hereafter be designated as “record.” The term “dataset” will, in contrast, refer to any individual comparison between a neurophysiological variable (e.g., fMRI activation in a specific task) and an outcome variable (e.g., Glasgow Outcome Scale—Extended, or GOSE (12)). One record can, therefore, contain many datasets.

## METHODS

### Literature Search and ES Calculation

A search in MEDLINE and SCOPUS was conducted on the 23 November 2017 by using search terms ((prognos\* OR predict\* OR outcome) AND (vegetative state OR minimally conscious state OR unresponsive wakefulness syndrome)) AND (eeg OR fmri OR event related potentials OR erp OR positron emission). No time limits were set for the search. In addition, the systematic reviews cited above in the Introduction as well as recent

informal reviews on neurophysiology of DoC, were consulted. Eight hundred ninety-seven peer-reviewed records published in English, German, or Russian, were identified. After reading abstracts and removing duplicates, 822 of them were rejected as irrelevant. Full text was sought for the other 76 records. Seven of them were rejected because they did not contain any outcome data on DoC patients, or contained outcome data already published elsewhere. Further exclusion criteria were (a) case studies or series of cases; (b) using patients' survival, and not the clinical improvement, as the only prognostic criterion; (c) presentation of the results in such a general form that the size of the observed effects cannot be calculated; and (d) reporting the data of UWS and MCS patients together with other diagnoses such as coma, exit-MCS, or locked-in syndrome: on the basis of these criteria 22 records were rejected. Regarding (d), we accepted studies in which UWS and MCS data were reported together, but not those in which the sample included more than these two diagnoses and the reported data did not give the reader a possibility to distinguish between the different diagnostic groups. The process of the selection of relevant records is shown in **Figure 1**.

The search resulted in 47 records containing a total of 381 datasets. These records are summarized in **Table 1**. Effect size was calculated for each dataset (i.e., for each predictor–outcome pair) on the basis of primary data on each individual patient presented in the tables of most studies, or chi-squared based on the same patient data, or the *t*-statistics. Only in one record, ES was calculated from a coefficient of correlation. All these parameters were converted into Cohen's *d* following the methods summarized by Lenhard and Lenhard (13). If a resulting  $2 \times 2$  table contained a zero cell (e.g., all patients having a positive neurophysiological sign recovered), the blind

application of the corresponding formulas results in  $d = \text{infinite}$ ; to avoid this, we added 0.5 to all cells, as recommended by Nakagawa and Cuthill (14). When *d*-values were included in further operations (added, averaged, etc.), they were weighted by inverse standard error (SE).

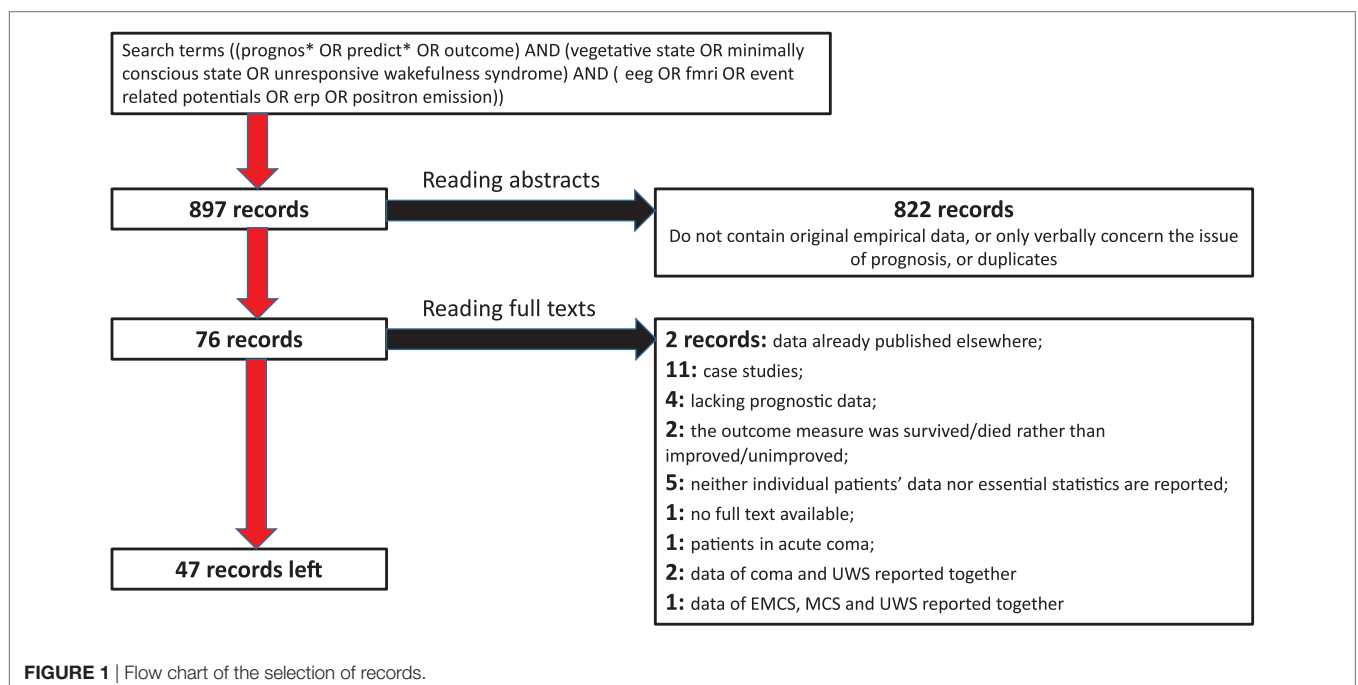
A big and still underestimated problem of all quantitative reviews is the plenty of non-reported data. Several authors (63–65) indicated that measured but unreported variables constitute one of the main sources of false positive findings ubiquitous in biology and psychology and thus an important cause of the contemporary “replication crisis” (66). When, and only when, it was evident for both present authors from the text of a paper that a neurophysiological variable was measured but not reported in relation to the outcome (or, rarely, reported as “non-significant”), the ES of this variable was assumed to be 0, and the SE of ES was assumed to be equal to the median SE calculated for the reported variables in the same record.

When the results presented several strongly correlated predictor variables (e.g., the same EEG variable in several adjacent regions), they were regarded as representing the same “construct” (1), and the mean and standard deviation (SD) for the construct were calculated according to the formulas

$$\text{Mean} = (M_1 + M_2) / N;$$

$$\text{SD} = \sqrt{\frac{(N-1)(\text{SD}_1^2 + \text{SD}_2^2) + 0.5N(M_1 + M_2 - 2M_1M_2)}{2N-1}}$$

where  $M_1$  and  $M_2$ ,  $\text{SD}_1$  and  $\text{SD}_2$  are mean and SD values for two to-be-combined variables, respectively. (Note that the formulas are so simple because both variables have the same *N*.)



**TABLE 1** | A summary of the 47 records included in the systematic review.

Reference	N (UWS/MCS)	Follow up, months	Methods	Relevant measures	Improvement criteria <sup>a</sup>
(15)	64/0	2	EEG, 24-h polysomnography	General sleep patterns	Diagnosis MCS, or GOS > 2
(16)	14/4	6–38	24-h polysomnography	Dominant EEG rhythm: beta, theta or delta	CRS-R
(17)	10/0	36	~14-h polysomnography	Sleep complexity, presence of different sleep stages	GOS
(18)	42/0	3	EEG	Sleep complexity, number of sleep spindles, presence of different sleep stages	GOS
(19)	59/47	3	EEG	Spectral power of resting state EEG in delta, theta, alpha1, alpha2, beta1 and beta2 frequency bands	LCF > 5
(20)	28/0	6	EEG	EEG amplitude normality (>20 $\mu$ V), dominant frequency, reactivity to forced eyes opening EEG combined AFR index The same as in Ref. (19)	CRS-R; change from UWS to MCS or from MCS to EMCS CRS-R; change from UWS to MCS or from MCS to EMCS
(21)	12/1	3	EEG	EEG normality according to Synek scale	LCF
(22)	4/5	6	Auditory ERP	MMN, N2 and/or P300 in control and after listening to music condition	CRS-R $\geq$ MCS
(23)	34/0	24	Short-latency EP, somatosensory EP, EEG	BAEPs grade, EEG reactivity to passive eyes opening, pain and acoustic stimuli, EEG Synek index, N20 SEP grade, P300 to a patient's own name	DRS < 22
(24)	17	12	PET	FDG-PET in the resting state	GOSE > 2
(25)	7/0	2–9	fMRI	BOLD response to speech and noise stimulation	CRS-R $\geq$ MCS
(26)	22/16	6	fMRI	fMRI BOLD response to speech and sound stimulation	CRS-R
(27)	7/4	3	fMRI	fMRI BOLD response to subject's own name	CRS = MCS
(28)	3/7	6	EEG, fMRI	EEG, BOLD response to language, music, active motor imagery instruction	GOSE > 2
(29)	43/0	24	EEG, somatosensory EP	EEG classified according to Synek scale N20 SEP grade	CRS-R $\geq$ MCS
(30)	14/0	3	EEG	Resting state EEG Index of Structural Synchrony (amplitude, length, instability, number of functional connections in Alpha, Beta1, Beta2 bands)	LCF = MCS
(31)	8/0	24	Auditory ERP	N2, P300	Recovery of awareness but no standardized assessment
(32)	20/0	NA	Auditory and visual ERP, SPECT	Auditory MMN, N100, N200, P300; visual EP present/absent; resting state brain metabolism assessed by SPECT	GOS > 2
(33)	75/38	4	Somatosensory EP	N20	CRS scores of $\geq$ 23
(34)	56/0	12	EEG, somatosensory EP, 24-h polysomnography	EEG reactivity to noxious stimulation, N20, sleep spindles in 24-h EEG All predictors scored as absent or present	GOS > 2 or transition UWS to MCS
(35)	10/0	3	Somatosensory EP	N20 grade and latency	Recovery of awareness but no standardized assessment
(36)	1/4	3	fMRI	fMRI default mode network normality	Level of consciousness according to the Multi-Society Task Force on PVS
(37, 38)	24/19	6	Auditory ERP, EEG	MMN, N400, EEG dominant background activity	DRS $\geq$ MCS
(39)	6/5	12	EEG, fMRI	EEG reactivity to warm water stimulation, fMRI activation to thermal stimulation	GOS > 2 or transition from UWS to MCS
(40)	12/10	1, 2, 3, 6, 9, 12	Auditory ERP	P300	CRS-R $\geq$ MCS
(41)	50/0	5	EEG	EEG normality according to Synek scale, EEG reactivity to pain stimulation	Regaining consciousness according to GOS, LCF
(42)	23/0	6	fMRI	fMRI BOLD response to speech (adapted affective speech)	GOS > 2 or transition from UWS to MCS
(43)	11/0	6	Polysomnography	REM sleep characteristics	Recovery of awareness but no standardized assessment
(44)	6/2	3	Auditory ERP	MMN to subject's own name stimuli, N100	CRS-R
(45)	6/5	3	PET	PET global GABA A receptor binding	CRS-R
(46)	52/0	3	fMRI	fMRI resting state connectivity	GOS > 2
(47)	5/0	0.5–2	EEG-TMS	TMS-evoked cortical responses	CRS-R

(Continued)

TABLE 1 | Continued

Reference	N (UWS/ MCS)	Follow up, months	Methods	Relevant measures	Improvement criteria <sup>a</sup>
(48)	38/0	6	EEG	Resting state EEG Approximate Entropy, EEG reactivity (stimulation protocol is not described)	GOSE > 2
(49)	56/0	12	EEG	Spectral power in Delta, Alpha, Theta, Beta, Gamma frequency bands	CRS-R = MCS
(50)	71/0	1.5	EEG, auditory ERP	92 measures including: CNV, MMN, P1, P3a, P3b; normalized and absolute spectral power of delta, theta, alpha, beta, gamma rhythms; permutation entropy, Komolgorov–Chaitin Complexity; phase lag index (PLI), spectral entropy, imaginary coherence and weighted symbolic mutual information (wSMI) in different frequency bands	CRS-R
(51)	18/51	12	PET, fMRI	Resting state FDG-PET, BOLD response to active motor and visuospatial imagery tasks	GOSE > 2
(52)	53/39	24	Auditory ERP	N400, P300	CRS-R = EMCS
(53)	9/0	2–54	PET	Resting state FDG-PET	Recovery of awareness but no standardized assessment
(54)	10/12	1–6	fMRI	BOLD response to active motor and visuospatial imagery tasks	CRS-R; change from UWS to MCS, or MCS to EMCS
(55)	39/25	12	fMRI	fMRI BOLD response to subject's own name	CRS-R
(56)	6/5	6	Auditory ERP	MMN, P300 to subject's own name	CRS-R
(57)	10/0	24	Auditory ERP	MMN	LoC > 6
(58)	10/0	24	Auditory ERP	N200, N350, P300 in active and passive paradigms	LoC > 6
(59)	11/0	26–36	Visual ERP	N2, N3, P2 amplitude and latency, P2–P3 peak to peak magnitudes of VEP	LoC > 6
(60)	10/8	1–150	EEG, 24-h polysomnography	Permutation entropy, alpha-to-theta ratio, density of slow waves, high-to-low frequencies ratio, density of sleep spindles	GOSE > 2 or CRS-R
(61)	21/0	6	Short-latency EP, EEG, somatosensory EP	BAEP, N20 SEP grade, EEG normality, approximate entropy (ApEn), cross-approximate entropy, Lempel–Ziv complexity to pain, auditory and music stimulation in comparison with eyes-closed condition	GOS > 2
(62)	36/0	12 (after injury)	Somatosensory ERP	N20, P25, N20–N25 SEP grade and amplitude	GCS ≥ MCS

N (UWS/MCS) means the number of UWS and MCS patients whose outcome and neurophysiological data were available. In the case of different number of patients available for different neurophysiological measurements, only the largest number is reported; it may be less than the total number of patients in the study.

<sup>a</sup>If GOS(E), CRS-R, LCF mentioned with no additional description, it was possible to calculate improvement criteria either way.

NA, not available, AFR index, Amplitude/Frequency/Reactivity index; UWS, unresponsive wakefulness syndrome; MCS, minimally conscious state; EMCS, Exit from MCS; GOS(E), Glasgow Outcome Scale (Extended), GCS, Glasgow Coma Scale; DRS, Disability Rating Scale; LCF, levels of cognitive functioning scale; LoC, Level of Consciousness Scale; SEP, somatosensory evoked potentials; BAEP, brain stem auditory evoked potentials; dwPLI, debiased weighted phase lag index; SPECT, single-photon emission computed tomography; CRS-R, Coma Recovery Scale-Revised.

## Outcome Criteria

The category “bad outcome” for UWS and MCS patients presumed remaining in the same condition. Deaths were included in this category only if it was clear that a patient died as a direct consequence of the brain lesion, otherwise excluded from the analysis. The category “good outcome” has, on the other hand, two different definitions: minimal clinical improvement or regaining full consciousness.<sup>1</sup> For MCS, both criteria are the same, because their minimal improvement implies the transition to Exit-MCS. But this is not true for UWS, because their minimal improvement means only the transition to MCS. As shown in Section “Results,” the two different improvement criteria of UWS yield different results.

Avantaggiato et al. (17) analyzed a group of DoC patients containing children and adolescents; because the authors presented

individual data of each patient, we selected the results for patients >13 years only. The category “good prognosis” for MCS implied the recovery of consciousness. For UWS, however, it might include either the recovery of consciousness or the transition into MCS. All 381 datasets were included in the systematic review.

## Quality Assessment

Quality of the records was estimated on the basis of the QUADAS criteria (67) that have been tailored, as recommended in the original publication, for the specific research field. Because Kondziella et al. (7) expressed concerns about possible bias in patient selection, we recorded whether a publication included a patient flow chart, and whether it described explicit exclusion criteria for UWS and MCS patients or simply mentioned that all patients admitted in the clinics for a particular time period were investigated. We also marked the records in which obviously more neurophysiological data were collected than reported in the analysis of outcome prediction. Another quality index was the use of the Coma Recovery Scale-Revised (CRS-R (68)) for DoC diagnostics, because this scale, though not being golden

<sup>1</sup> Practically, “full consciousness” is defined as reliable communication or functional use of objects. In the following, when we speak about “regaining of consciousness” we shall mean these two abilities (at least one of them) and not just minimal signs of consciousness presented also in the MCS.



standard, possesses substantially better psychometric qualities than all other instruments for the assessment of DoC (69). In addition, the impact factor (IF) of the publishing journal was included as an indirect quality criterion, because the data indicate high correlation between the IF and the informal reputation of the corresponding journal among neurologists (70).

## Meta-Analysis

Two additional inclusion criteria for meta-analyses were (1) at least three independent records reporting the same predictor variable or variables related to the same construct and (2) each of these records includes at least 10 patients. The criteria can be regarded as very liberal because, first, only three records and only 10 patients (who further should be subdivided into at least two groups) are rather low numbers, and second, the notion of construct is rather vague and permits to include into one group, for example, studies of P300 to simple tones and to patients' own names, thus increasing heterogeneity. On the basis of these criteria, 319 datasets were excluded (of course, this number would be larger if the criteria were more conservative). The remaining 62 datasets finally entered the meta-analysis.

We used a random-effects meta-analysis with restricted maximum-likelihood (REML) estimator for pooling ESs. We assessed the level of heterogeneity between studies with a standard *Q*-test statistic as well as by *I*<sup>2</sup> calculation (71). Heterogeneity was regarded as significant when  $p < 0.05$  or  $I^2 > 50\%$ . Potential publication bias for individual predictors was assessed with the Egger test for Funnel plot asymmetry and represented graphically with Begg's funnel plots of the ES versus its SE. Additionally, Rosenthal fail-safe test was also applied. All meta-analyses were performed using R package "metafor" (72) using inverted standard errors as weighting parameter.

## RESULTS

### Quality of Reporting

None of the 47 records presented a flow chart depicting patient selection. The authors of 20 records (42.6%) explicitly state that they included all patients within some exactly described time period. Nine reports (19.1%) depicted at least some inclusion and/or exclusion criteria. In the remaining 18 records, patient selection was not described.

Most selected records present their data either for each individual patient or as mean  $\pm$  SD (or SE) for each relevant group (e.g., recovered versus non-recovered). Three records present data only in a general form (e.g., as correlations). Five records (10.6%) mention the size of some effects.

CRS-R was used for the diagnosis of UWS and MCS in 29 records (61.7%); other studies employed Disability Rating Scale, Glasgow Coma Scale, or other less powerful instruments.

Quite surprisingly, only two records explicitly state that the neurologists who assessed the outcome were blinded to the neurophysiological data collected before. In six records, blindness of the outcome might be assumed because neurophysiological examination and outcome diagnostics were performed in different institutions. These eight records (17%) were combined

into one "blind" group. In the majority of the records (83%), the outcome was diagnosed with knowledge of the neurophysiological findings.

The median time between the measurement and the outcome assessment was 6 months, mean minimal time per record was 9 months (range 1–36 months), and the mean maximal time per record 16 months (range 1.5–150 months). In 42 records (89%), this interval was same for all the examined patients. Seven records used broad variable intervals for different patients (1–6, 1–30, 2–9, 6–38, 10–150, 26–36, and 24–144 months). One publication does not report the measurement–outcome interval.

The mean total sample was  $31.11 \pm 3.66$  patients, with a median of 21 patients and a range of 5–123 patients. Eight records included <10 patients, 14 records had between 10 and 19 patients. Adding the case studies filtered out at the previous stage, we come to the result that about a half of all prognostic studies included <20 patients. The records that did not describe patient selection included significantly less patients (means 14.1 versus 43.0,  $t = 5.11$ ,  $p < 0.001$ ) than records describing their selection process.

The median IF of the publishing journals was 3.87, range from 0 to 44. IF did not differ between the records with correctly versus incorrectly described patient selection. We hypothesized that studies with more patients (thus having higher power) are published in more prestigious journals, but the corresponding correlation was not significant (Spearman's  $\rho = 0.26$ ,  $p = 0.078$ ). However, studies employing CRS-R were published in journals with higher IF than studies that did not use this scale:  $p < 0.001$ , Mann–Whitney test. A few studies with blind outcome assessment included larger sample sizes than studies without outcome blindness ( $t = 2.35$ ,  $p = 0.023$ ) and were also published in more prestigious journals ( $p = 0.046$ , Mann–Whitney test).

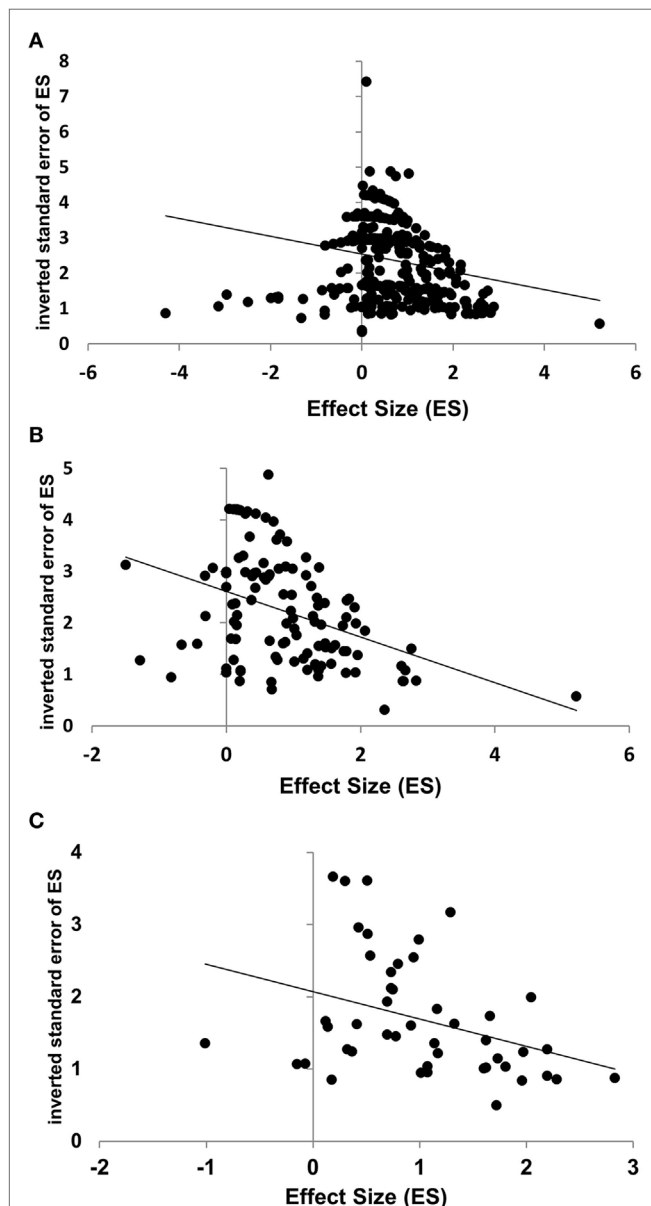
Notably, we did not find a significant relationship between any of the variables and the time elapsed from the neurophysiological measurement till the assessment of the outcome. Non-weighted ES correlated with the mean time between neurophysiological measurement and outcome assessment with Spearman's  $\rho = -0.09$ , with minimal time per study  $\rho = -0.18$ , with maximal time per study  $\rho = -0.07$  (all nonsignificant). For weighted ES, the corresponding correlations were 0.03,  $-0.06$ , and  $-0.11$ , respectively (all nonsignificant). Likewise, correlations of the time interval with the SD of ES (as a measure of its reliability) were all between 0.00 and 0.03, and correlations of the time interval with sample size were between 0.00 and 0.06, all non-significant.

Also, the year of publication did not correlate with any other measures. The bibliographic literature gives a reason to expect that later publications might have large samples or smaller ESs than earlier (73). Although the corresponding correlations were in the expected direction, they did not reach significance (year/N: Spearman's  $\rho = 0.12$ ; year/ES:  $\rho = -0.08$ ). Also, the correlation between publication year and IF was close to 0 ( $\rho = 0.03$ ).

### Publication Bias

The inverted SE (1/SE) was taken as a measure of the reliability of an ES. Across all datasets, the rank-order correlation

between ES and its  $1/SE$  was weak but significant ( $\rho = -0.22$ ,  $k = 381$ ,  $p < 0.001$ ). The result might be biased because different records contribute disproportionally to the whole mass of data. However, the positive correlation between the ES and its SE became even stronger when calculated for the selected subset of datasets included in the meta-analysis ( $\rho = -0.47$ ,  $k = 62$ ,  $p < 0.001$ ), as well as for the ESs averaged for each record ( $\rho = -0.41$ ,  $k = 47$ ,  $p = 0.004$ ). The results are shown in Figure 2.



**FIGURE 2** | Negative correlations between effect size (ES) and its reliability, estimated by the inverted standard error ( $1/SE$ ), for all individual datasets [(A): Spearman's  $\rho = -0.22$ ,  $p < 0.001$ ], datasets included in the meta-analysis [(B):  $\rho = -0.47$ ,  $p < 0.001$ ], and for mean ESs per record [(C):  $\rho = -0.41$ ,  $p = 0.004$ ]. The regression lines are presented for illustration only, not for quantitative analysis.

Note that the first analysis (across all datasets) overestimates the contribution of the records reporting many datasets. The last analysis (across averaged ES), to the contrary, may overestimate the contribution of the records presenting few or only one dataset. Despite this contrary bias, very similar results were obtained. To sum up, these data show a trend to selective publication of strong but unreliable effects. How serious the bias is in respect of each particular predictor variable will be discussed below.

## UWS and MCS

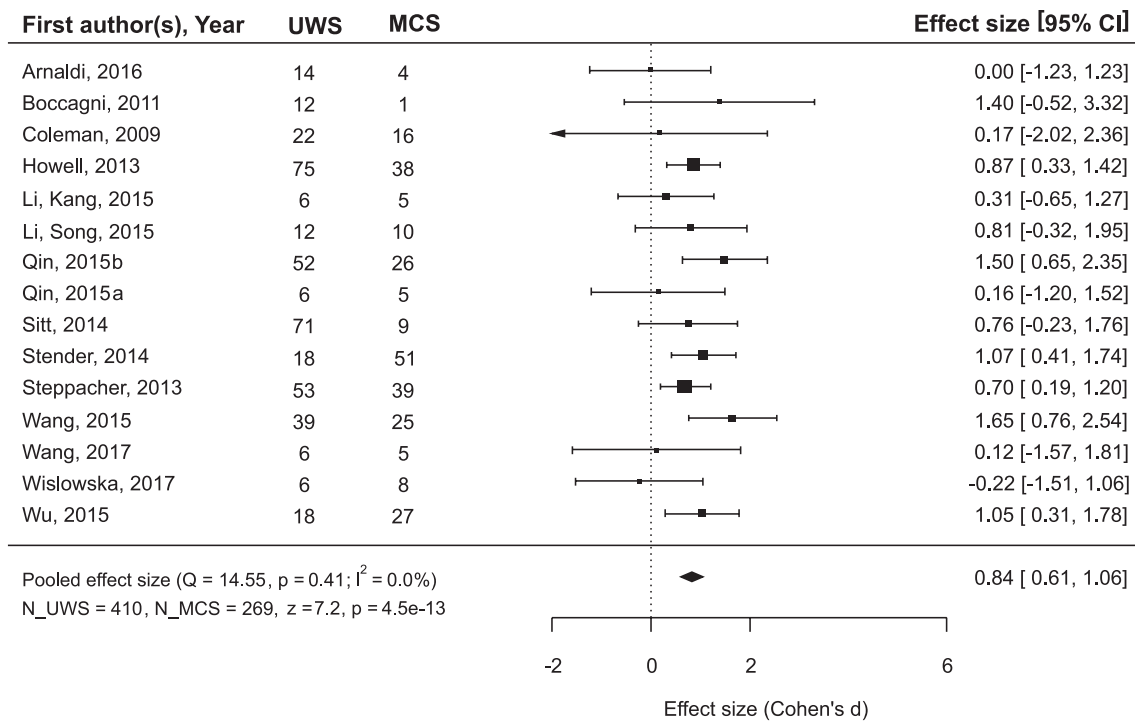
Thirteen of the 381 datasets included only MCS samples, 248 datasets included only UWS patients, and the remaining datasets included both diagnostic groups of DoC patients.

While the main issue of the present study was outcome prediction on the basis of neurophysiological data, we also asked the question whether the outcome can be predicted simply from the diagnosis. Many authors of the reviewed articles also asked this question and answered it negatively. However, a meta-analysis of the combined data from the records where both diagnosis and prognosis could be followed revealed that MCS patients recovered consciousness significantly more frequently than UWS patients (Figure 3): mean ES = 0.84, 95% CI from 0.61 to 1.06. On the other hand, if the positive outcome of UWS patients is defined as any minimal improvement, i.e., the transition to the MCS, the diagnosis loses its predictive value (Figure 4).

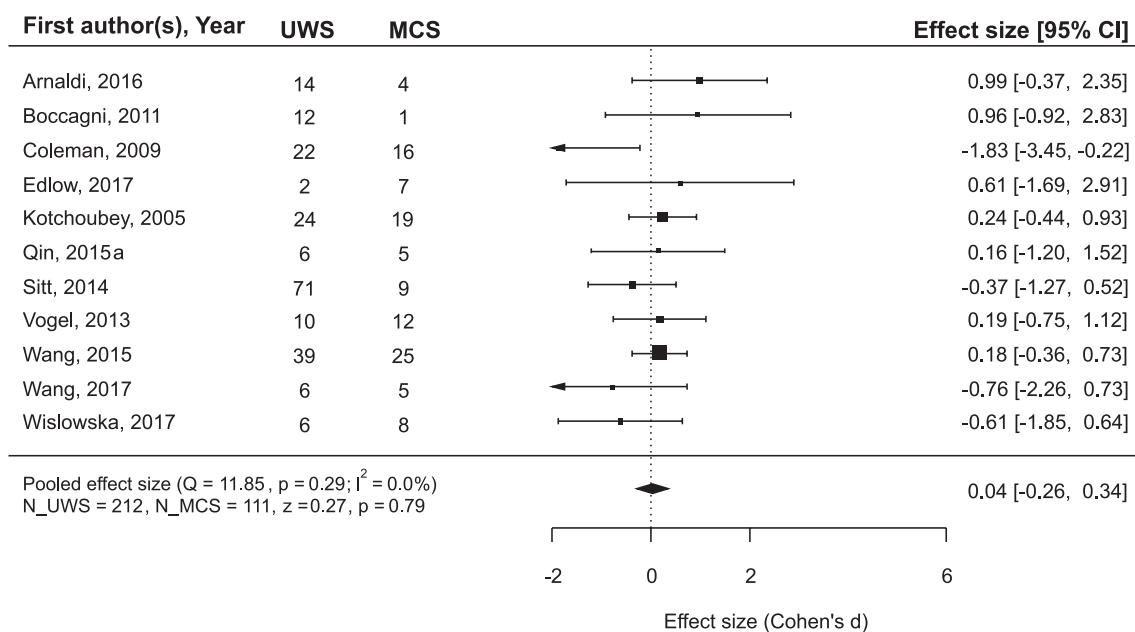
Because we found that the improvement criterion for UWS (transition to the MCS versus recovery of full consciousness, that is, exit-MCS) can play a role in the calculation of prediction effects, we compared weighted mean ES for the neurophysiological variables in three conditions: (i) prediction of the recovery of consciousness for MCS patients; (ii) prediction of the recovery of consciousness for UWS patients; and (iii) prediction of the transition to MCS for UWS patients. A one-way ANOVA across these three groups resulted in a highly significant effect:  $F(2,294) = 23.11$ ,  $p < 0.001$ . The result does not change when we limit the analysis by only those datasets that will later enter the meta-analysis [ $F(2,60) = 19.88$ ,  $p < 0.001$ ], or when we exclude all mixed datasets [ $F(2,86) = 12.08$ ,  $p < 0.001$ ]. Independently of the method of calculation, the mean weighted ES for the groups (i) and (ii) (i.e., different diagnoses, the same improvement criterion) were very similar and varied—dependent on the selected data—between 0.41 and 0.48. The mean weighted ES for the group (iii) was about three times larger (between 1.40 and 1.68) and differed significantly from both of them, although the groups (iii) and (ii) included patients with the same diagnosis and some datasets involved in these two groups might even include some of the same patients. To sum up, neurophysiological methods are significantly more successful in prediction of the transition from UWS to MCS than in prediction of the recovery of full consciousness.

## Meta-Analysis of Predictory Constructs

According to the above results, we performed the meta-analysis separately for (a) prediction of any clinical improvement (for which UWS patients means at least transition to the MCS), and



**FIGURE 3** | The results of the meta-analysis for prediction of the outcome from the diagnosis. The criterion of improvement for all patients was recovery of full consciousness.  $Q$ , the corresponding  $p$ -value and  $I^2$  are estimates of between-study heterogeneity; symbols ■ stay for the estimates of effect size (ES) in each single study, with the size of the symbol being proportional to the precision of the estimate. Error bars indicate the 95% confidence intervals of ES. The diamond ♦ is the estimate of the overall effect, the edges of the diamond represent the 95% confidence interval limits; CI, confidence interval; UWS and MCS, sample size of UWS and MCS patients in individual studies; N\_UWS and N\_MCS, overall sample size of the two patient groups. The resulting ES was tested for significance using  $z$ -criterion; the values of  $z$  and the corresponding  $p$  are given at the end of the lower left line.



**FIGURE 4** | The results of the meta-analysis for prediction of the outcome from the diagnosis. The criterion of improvement was “minimal improvement,” that is for UWS patients, it was the transition to MCS, and for MCS patients, at least the transition to Exit-MCS. As can be seen, with this improvement criterion the diagnosis does not predict outcome. The rest is the same as in **Figure 3**.

(b) prediction of the recovery of full consciousness. Sixty-two datasets comprising a total of 1,919 patients were analyzed. They involved the following potential predictors:

1. EEG reactivity to “passive” stimulation (i.e., without an active instruction). Hypothesis: stronger EEG oscillatory responses = > better prognosis.
2. EEG entropy indices. Hypothesis: higher EEG entropy = > better prognosis.
3. EEG dominant oscillatory activity. Hypothesis: background activity closer to the alpha frequency = > better prognosis.
4. EEG Synek score (74) is frequently used in the intensive care medicine for the prognosis of the outcome of acute coma. Hypothesis: higher score = > better prognosis.
5. fMRI BOLD response to passive (auditory or nociceptive) stimulation. Hypothesis: stronger response = > better prognosis.
6. Resting state PET or SPECT metabolism. Hypothesis: closer to normal brain metabolism = > better prognosis.
7. N20 component of somatosensory evoked potentials (SSEP). Hypothesis: normal N20 = > better prognosis.
8. Auditory Mismatch Negativity (MMN) to a change in ongoing acoustic stimulation. Hypothesis: larger MMN = > better prognosis.
9. Auditory P300 as an index of complex processing in cortico-subcortical networks. Hypothesis: larger amplitude or shorter latency = > better prognosis.
10. Spindle activity as an index of information processing in sleep (75). Hypothesis: presence of sleep spindles = > better prognosis.

The findings are summarized in **Figures 5** and **6** and presented in more detail in Figures S1 and S2 and Tables S2 and S3 in Supplementary Material.

Only oscillatory EEG responses to passive stimulation appear to be reliably related to both prognostic criteria (i.e., minimal clinical improvement and the recovery of full consciousness). The included datasets are highly homogenous and yield a highly significant mean ES of 1.45 on a sample of 99 patients. Another prediction variable that significantly predicted the recovery of consciousness was brain metabolism assessed by PET/SPECT. It attained a mean ES of 1.40 on a sample of 106 patients. The prognostic value of the MMN, P300, EEG entropy variables, and fMRI responses to passive stimulation was not significant and characterized by strong heterogeneity of the primary datasets.<sup>2</sup>

More promising results have been obtained in relation to the minimal improvement criterion. In addition to the EEG reactivity, significant effects are found for the MMN and sleep spindles. Formally positive results are obtained for the SSEP component N20 and the background EEG frequency, but the data are too heterogeneous to make a conclusion.

<sup>2</sup>The ES in Wijnen et al. (57) strongly differs from all other effects in the MMN group. After removing this result, the MMN data become completely homogenous ( $I^2 = 0$ ).

## DISCUSSION

Although the Section “Limitation” is frequently placed at the end of Discussion, we believe that particularly the discussion of meta-analytic data is useful to begin with limitations. One important limitation is that of the present work as such. As the manuscript was prepared for a special issue, we did not systematically address the authors of the original publications but relied solely on the published data including supplementary information. Although we believe that personal contact with the authors may have enhanced our knowledge, at the first step we did not use this strategy because it might have caused considerable delays.

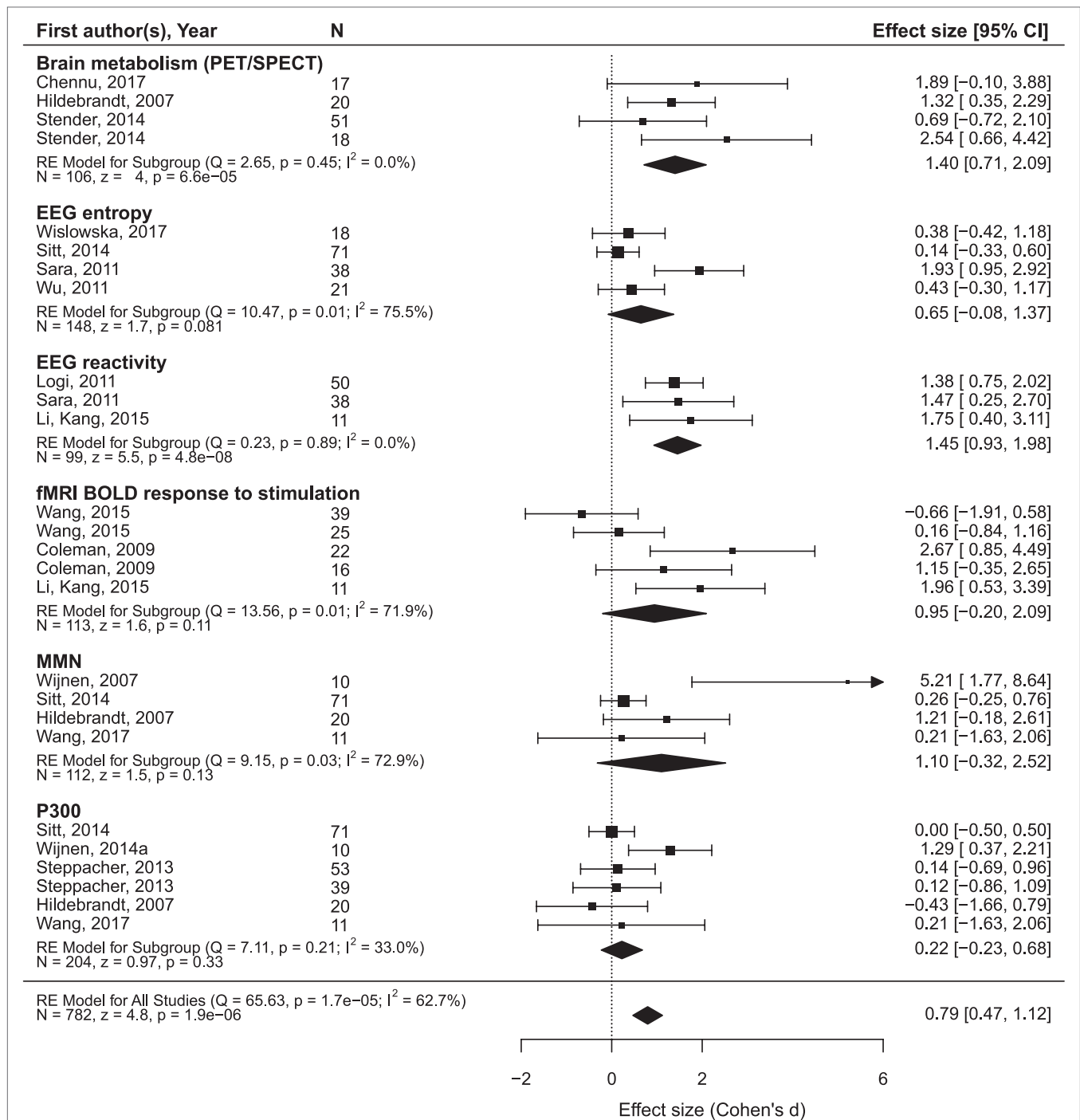
Other limitations of the meta-analysis are rather related to the limitations of the primary literature. A quantitative review can overcome some limitations of the reviewed studies, e.g., their small size (thus, it can reveal a consistent and significant effect on the basis of several inconsistent and non-significant ones), but it cannot remove the biases implied in its empirical basis.

To begin with the least, the quality of data reporting is far from the present-day standard. While Fritz et al. (76) bristled that only 42% of empirical psychological studies report the size of their effects, in the present sample ES was mentioned only in five records (10.6%). Presenting a patient flow chart is already a standard in many fields of clinical research but fully unknown in the domain of DoC. About a half of the reviewed records neither describe inclusion and exclusion criteria nor even make a simple statement that all patients admitted to the hospital during some period were included. Thus, the concern of Kondziella et al. (7) about possible bias in patient selection seems to be justified.

The majority of the reviewed studies employed a univariate approach, i.e., each predictor was separately compared with the target variable. Of course, this is a serious limitation because we know that the values of a regression strongly depend on the other predictor variables included or excluded in/from the equation. Thus, a neurophysiological variable (e.g., P300), which appears useless as a single predictor, might reveal its effect in a particular combination with other predictors. A few groups have recently attempted to overcome this limitation and employed a multivariate approach to outcome prediction in DoC (24, 50). This seems to be a perspective line of research, but now the number of such records is still too low to undertake a separate meta-analysis of these data.

The negative correlation between the description of patient selection and the number of patients suggests that selection bias might be particularly strong in small-size studies. Although the sample size in prognostic studies is on average larger than in studies comparing UWS and MCS, we found, together with single case studies, 33 records with less than 20 patients, which implies that even in the case of the equal distribution at least one of the outcome groups (recovered or non-recovered) includes <10 patients. Particularly, the studies with the total  $N < 10$  result in huge confidence intervals making any reliable conclusion impossible. Of course, small or even single case studies may have sense at the very beginning of the research process, when nothing is known about an investigated phenomenon whatsoever. However, in such a case, one can expect an increase



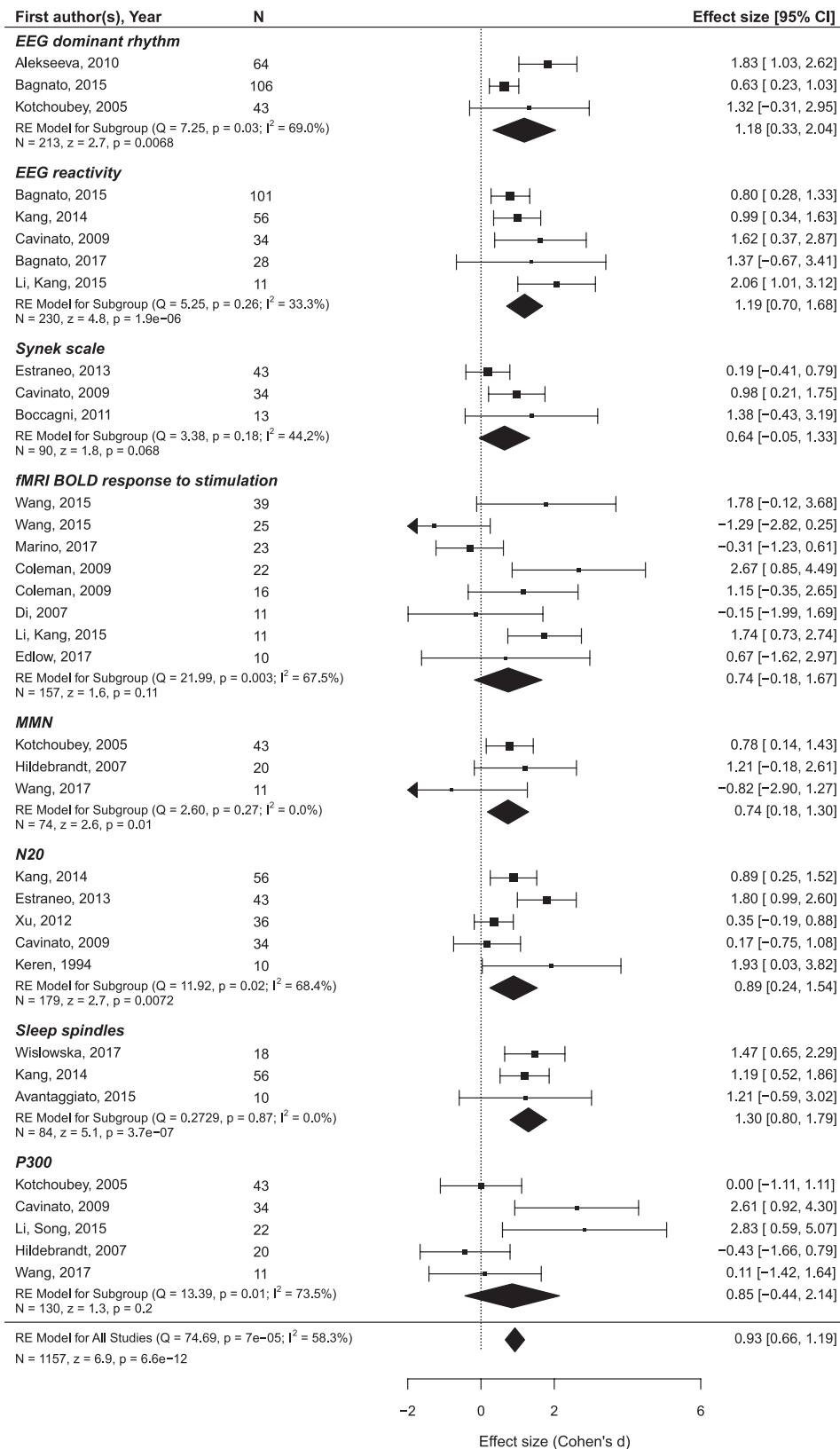


**FIGURE 5 |** The results of the meta-analysis for prediction of the outcome from neurophysiological variables. The criterion of improvement for all patients was the recovery of consciousness. RE, random effects. The rest is the same as in **Figure 3**.

of sample sizes with the year of publication, but this correlation was not significant.

Strong negative effects of underpowered studies on the quality of the reported data have thoroughly been discussed in the literature in general (63, 77, 78) and specifically in neuroscience (79, 80). Positive findings of tiny studies can only result from

chance or selective data report. Our data show a consistent and significant correlation between the size of a prognostic effect and its standard error, indicating that stronger effects are less reliable. The correlation even withstood the removal of all datasets with <10 patients. As these small samples yield particularly large SE, the variability of SE was severely restricted, which might be



**FIGURE 6** | The results of the meta-analysis for prediction of the outcome from neurophysiological variables. The criterion of improvement for UWS patients was the transition to MCS, and for MCS patients, the recovery of consciousness. The rest is the same as in **Figure 3**.

expected to reduce the correlation coefficient. This was, however, not the case (**Figure 2**).

Another important limitation of nearly all studies was the lack of outcome blindness. Only two groups of authors clearly indicated that the diagnosis of the outcome was performed by neurologists without the knowledge of predictor values. One might argue that the diagnosis of recovery of consciousness (based on the criteria of consistent communication and functional use of objects) is quite easy and can hardly be biased by neurophysiological data. Even if this argument is true for exit-MCS, it is obviously false for the other broadly used improvement criterion of UWS patients, namely the transition to MCS. As the differential diagnostics between UWS and MCS is notoriously difficult (81), any information about positive or negative neurophysiological findings could influence the diagnostic decision. If this influence really takes place, we can expect much stronger correlation of neurophysiological indices with the transition to MCS than with the transition to exit-MCS, because the latter diagnosis is easier and thus less affected by additional information.

Exactly this was true. When the improvement criterion for both diagnostic groups (UWS and MCS) was the transition to exit-MCS, the weighted average ES (in terms of Cohen's *d*) was rather moderate, in any case slightly smaller than 0.5. But the transition of UWS patients to MCS (which is quite difficult from the diagnostic point of view) was strongly related to the neurophysiological findings, with the weighted average ES being  $>1.4$ .

A potentially strong but still underestimated bias is related to unreported predictor variables. In most of the reviewed records, outcome prediction was not the main aim of the study, but rather a by-product of other analyses. Particularly, in such studies (though not only in these), many variables could be measured but not really reported. Sometimes, many variables are used in a UWS/MCS comparison but not even mentioned in relation to prognosis, although one may suppose that they were also compared with the follow-up data. Less frequently prognostic effects are referred to as "lacking" or "non-significant" without further quantification. Simmons et al. (65) suggest a very simple solution of the problem: whenever authors list their variables, they should add a short word "only." We tried to counteract this false positive effect by assigning the value of 0 to the effects of obviously omitted variables (with its SE being assumed as the median SE of the reported variables). However, this method is not only imprecise but can also be biased, first, because the real number of such omitted variables may be much larger than a reader can guess, and second, because negative effects (i.e., those which run against the starting hypothesis, such as better neurophysiological responses in non-recovered patients) can be omitted more frequently than positive effects.

With this in mind, we understand that the data of meta-analyses should be taken with great caution. Nevertheless, we believe that a glance on the meta-analytic results can be of interest. First, the analysis was strongly complicated by the high variability of the primary records. Very small number of studies using exactly the same predictor and the same improvement criterion enforced us to combine similar methods, which resulted in high heterogeneity indices such as  $I^2$ . Poor prognostic features of the characteristics of fMRI reactivity might partially

be attributed to this group of studies including fMRI responses to very different stimulations from pain to music. For the same reason, we excluded some possible predictors (e.g., responses to active behavioral instructions; ERP N400 component) that were employed in two records only.

Second, the empirical contribution of predictors does not necessarily follow their general theoretical value defined by basic neuroscience. This is quite demonstrative in the case of P300, one of the most useful and most widely employed indices in neuroscience whose effect in the prediction of the outcome turned out to be virtually 0. One might speculate that P300 is not immediately related to consciousness (37), but, rather, to a more specific function such as working memory. Another possible reason may be the extreme difficulty of the separation between different P300 subcomponents (P3a and P3b) in the target population (38). The subcomponents are usually distinguished by topography and responses to active instruction, but most DoC patients have changed ERP topography and do not respond to instruction. If the results of this preliminary analysis should be used to determine which lines of research should not be recommended for future studies, P300 is the first candidate for such a negative recommendation. Also, the importance of the (highly expensive) fMRI predictors might similarly be overestimated on the basis of their theoretical importance.

Oscillatory EEG responses to stimulation showed, to the contrary, most promising effects, which agree well with the results of Bender et al. (10) obtained on the basis of different data.

Although EEG reactivity was measured to very different stimuli [e.g., to passive (23) or forced eyes opening (19, 20), to pain (34, 41), to warm water (39), and no description was given by Sarà et al. (48)] and the definition of reactivity substantially varied, the results are very homogenous across the reports. Moreover, this was the only group of predictor variables whose predictive value was significant for both improvement criteria (transition from UWS to MCS and the recovery of consciousness). Publication bias was also presented in these data, but it was less strong than for many other predictors (see Tables S2 and S3 in Supplementary Material).

Other perspective variables are brain metabolism (estimated by means of PET or SPECT) and the presence of sleep spindles in the EEG. Recent sleep data indicate a vital importance of spindles in information processing during sleep, which affects numerous cognitive processes in the subsequent wakefulness (75, 82, 83). DoC belongs to rare medical conditions characterized by severe deficits, or even complete absence, of sleep spindles, also in patients with relatively preserved sleep structure (84, 85). We believe that the role of sleep spindles in the outcome prediction in DoC should be explored in future work.

Both MMN and SSEP are proven outcome predictors for acute coma (86, 87). However, their value for the chronic DoC remains unclear. The present findings indicate their prognostic effects for the transition from UWS to MCS but not for recovery of consciousness.

The data further show that the predictive value of the auxiliary (e.g., neurophysiological) variables should be compared with the values of clinical variables. In the currently reviewed data, MCS patients had about 4.5 times better chances (if we take the

lower limit of the 95% CI, three times better chances) to regain consciousness than UWS patients. It is true that we analyzed only records implementing the neurophysiological approach and missed similar data in the other publications not using neurophysiological variables. Nevertheless, the effect is very strong and, as far as we can judge, not strongly biased (as it was not a desired effect). This indicates the necessity to integrate neurophysiological and clinical predictors within a multivariate approach in further studies. This integration could be more productive in both diagnostic and prognostic respects than the attempts to oppose different classes of variables to each other.

These considerations can only be conceived of as preliminary. It should be stressed that all biasing factors discussed above act in the same direction, potentially increasing the number of *false positive* results. The general critique of Brok et al. (64) remains valid also for the current study: as long as the original studies do not present all information, meta-analyses can only try to diminish, but not abolish the positive bias. If we want to eliminate the bias, (i) small-size studies should be avoided (for prediction studies, groups of recovered/non-recovered should include at least 20 patients each); (ii) a flow chart should make evident the procedure of patient selection; (iii) neurologists assessing the target variable (i.e., change of the diagnosis) should be completely blinded regardless the values of neurophysiological predictors; (iv) the full list of measured variables including all potential predictors should be presented from the beginning of a report (in a Methods section); (v) the intervals (a) between the accident and the neurophysiological measurement, and (b) between this measurement and the follow-up assessment should be specified;

finally, (vi) all positive *and negative* (e.g., non-significant relationships) results should be described in the same quantitative manner, either including the size of all effects, or permitting to calculate this size (e.g., mean and SD for the recovered and non-recovered groups).

Therefore, the numbers presented in **Figures 5 and 6** and in the Supplementary Materials can now be regarded, not as estimates of real effects, but rather, as upper limits of these effects. The current state of affairs is yet far away from the level at which any practical recommendation can be given except the recommendation to be highly careful with interpretations.

## AUTHOR CONTRIBUTIONS

Both authors performed data search and analyses. The manuscript was initiated by the second author and finalized by the first author.

## FUNDING

The study was supported by the German Research Society (Deutsche Forschungsgemeinschaft, DFG), Grant KO-1753/13.

## SUPPLEMENTARY MATERIAL

The Supplementary Material for this article can be found online at <https://www.frontiersin.org/articles/10.3389/fneur.2018.00315/full#supplementary-material>.

## REFERENCES

- Lipsey MW, Wilson DB. *Practical Meta-Analysis (Applied Social Research Methods Ser., V. 49)*. Thousand Oaks, CA: SAGE (2001).
- Gurevitch J, Koricheva J, Nakagawa S, Stewart G. Meta-analysis and the science of research synthesis. *Nature* (2018) 555:175–82. doi:10.1038/nature25753
- Giacino JT, Ashwal S, Childs N, Cranford R, Jennett B, Katz DI, et al. The minimally conscious state definition and diagnostic criteria. *Neurology* (2002) 58(3):349–53. doi:10.1212/WNL.58.3.349
- Laureys S, Celesia GG, Cohadon F, Lavrijsen J, León-Carrión J, Sannita WG, et al. Unresponsive wakefulness syndrome: a new name for the vegetative state or apallic syndrome. *BMC Med* (2010) 8(1):68. doi:10.1186/1741-7015-8-68
- Liberati G, Hünfeldt T, Belardinelli MO. Questioning the dichotomy between vegetative state and minimally conscious state: a review of the statistical evidence. *Front Hum Neurosci* (2014) 8:865. doi:10.3389/fnhum.2014.00865
- Hannawi Y, Lindquist MA, Caffo BS, Sair HI, Stevens RD. Resting brain activity in disorders of consciousness. *Neurology* (2015) 84:1272–80. doi:10.1212/WNL.0000000000001404
- Kondziella D, Friberg CK, Frokjaer VG, Fabricius M, Moeller K. Preserved consciousness in vegetative and minimal conscious states: systematic review and meta-analysis. *J Neurol Neurosurg Psychiatry* (2016) 87:485–92. doi:10.1136/jnnp-2015-310958
- Rosenthal R. The “file drawer problem” and tolerance for null results. *Psychol Bull* (1979) 86:638–41. doi:10.1037/0033-2909.86.3.638
- Rothstein H, Sutton AJ, Borenstein M. *Publication Bias in Meta-Analysis: Prevention, Assessment and Adjustments*. Hoboken, NJ: Wiley (2005).
- Bender A, Jox RE, Grill E, Straube A, Lulé D. Persistent Vegetative State and Minimally Conscious State: a systematic review and meta-analysis of diagnostic procedures. *Deutsches Ärzteblatt International* (2015) 112(14):235–42. doi:10.3238/arztebl.2015.0235
- Kotchoubey B. Evoked and event-related potentials in disorders of consciousness: a quantitative review. *Conscious Cogn* (2017) 54:155–67. doi:10.1016/j.concog.2017.05.002
- Wilson JTL, Pettigrew LEL, Teasdale GM. Structured interview for the Glasgow Outcome Scale and the Extended Glasgow Outcome Scale: guidelines for their use. *J Neurotrauma* (1998) 15:573–85. doi:10.1089/neu.1998.15.573
- Lenhard W, Lenhard A. *Calculation of Effect Sizes*. Dettelbach, Germany: Psychometrica (2016). Available from: [https://www.psychometrica.de/effect\\_size.html](https://www.psychometrica.de/effect_size.html) (Accessed: February 28, 2018).
- Nakagawa S, Cuthill IC. Effect size, confidence interval and statistical significance: a practical guide for biologists. *Biol Rev Camb Philos Soc* (2007) 82:591–605. doi:10.1111/j.1469-185X.2007.00027.x
- Alekseeva EV, Alashev AM, Belkin AA, Kudrinskikh NV, Nikov PN. Prognostic evaluation of sleep in patients in a vegetative state. *Anesteziol Reanimatol* (2010) 55(4):38–42.
- Arnaldi D, Terzaghi M, Cremascoli R, De Carli F, Maggioni G, Pistarini C, et al. The prognostic value of sleep patterns in disorders of consciousness in the sub-acute phase. *Clin Neurophysiol* (2016) 127(2):1445–51. doi:10.1016/j.clinph.2015.10.042
- Avantaggiato P, Molteni E, Formica F, Gigli GL, Valente M, Lorenzini S, et al. Polysomnographic sleep patterns in children and adolescents in Unresponsive Wakefulness Syndrome. *J Head Trauma Rehabil* (2015) 30(5):334–46. doi:10.1097/HTR.0000000000000122
- Babiloni C, Sarà M, Vecchio F, Pistoia F, Sebastiano F, Onorati P, et al. Cortical sources of resting-state alpha rhythms are abnormal in persistent vegetative state patients. *Neurophysiol Clin* (2009) 120(4):719–29. doi:10.1016/j.clinph.2009.02.157
- Bagnato S, Boccagni C, Sant'Angelo A, Prestandrea C, Mazzilli R, Galardi G. EEG predictors of outcome in patients with disorders of consciousness



- admitted for intensive rehabilitation. *Neurophysiol Clin* (2015) 126(5):959–66. doi:10.1016/j.clinph.2014.08.005
20. Bagnato S, Boccagni C, Prestandrea C, Fingelkurts AA, Fingelkurts AA, Galardi G. Changes in standard electroencephalograms parallel consciousness improvements in patients with Unresponsive Wakefulness Syndrome. *Arch Phys Med Rehabil* (2017) 98(4):665–72. doi:10.1016/j.apmr.2016.09.132
  21. Boccagni C, Bagnato S, Sant'Angelo A, Prestandrea C, Galardi G. Usefulness of standard EEG in predicting the outcome of patients with disorders of consciousness after anoxic coma. *J Clin Neurophysiol* (2011) 28(5):489–92. doi:10.1097/WNP.0b013e318231c8c8
  22. Castro M, Tillmann B, Luauté J, Corneillie A, Dailier F, André-Obadia N, et al. Boosting cognition with music in patients with disorders of consciousness. *Neurorehabil Neural Repair* (2015) 29(8):734–42. doi:10.1177/1545968314565464
  23. Cavinato M, Freo U, Ori C, Zorzi M, Tonin P, Piccione F, et al. Post-acute P300 predicts recovery of consciousness from traumatic vegetative state. *Brain Inj* (2009) 23(12):973–80. doi:10.3109/02699050903373493
  24. Chennu S, Anen J, Wannez S, Thibaut A, Chatelle C, Cassol H, et al. Brain networks predict metabolism, diagnosis and prognosis at the bedside in disorders of consciousness. *Brain* (2017) 140(8):2120–2132. doi:10.1093/brain/awx163
  25. Coleman MR, Rodd JM, Davis MH, Johnsrude IS, Menon DK, Pickard JD, et al. Do vegetative patients retain aspects of language comprehension? Evidence from fMRI. *Brain* (2007) 130(10):2494–507. doi:10.1093/brain/awm170
  26. Coleman MR, Davis MH, Rodd JM, Robson T, Ali A, Owen AM, et al. Towards the routine use of brain imaging to aid the clinical diagnosis of disorders of consciousness. *Brain* (2009) 132(9):2541–52. doi:10.1093/brain/awp183
  27. Di HB, Yu SM, Weng XC, Laureys S, Yu D, Li JQ, et al. Cerebral response to patient's own name in the vegetative and minimally conscious states. *Neurology* (2007) 68(12):895–9. doi:10.1212/01.wnl.0000258544.79024.d0
  28. Edlow BL, Chatelle C, Spencer CA, Chu CJ, Bodien YG, O'Connor KL, et al. Early detection of consciousness in patients with acute severe traumatic brain injury. *Brain* (2017) 140(9):2399–414. doi:10.1093/brain/awx176
  29. Estraneo A, Moretta P, Loreto V, Lanzillo B, Cozzolino A, Saltalamacchia A, et al. Predictors of recovery of responsiveness in prolonged anoxic vegetative state. *Neurology* (2013) 80(5):464–70. doi:10.1212/WNL.0b013e31827f0f31
  30. Fingelkurts AA, Fingelkurts AA, Bagnato S, Boccagni C, Galardi G. Prognostic value of resting-state electroencephalography structure in disentangling vegetative and minimally conscious states: a preliminary study. *Neurorehabil Neural Repair* (2013) 27(4):345–54. doi:10.1177/1545968312469836
  31. Glass I, Sazbon L, Groswasser Z. Mapping “cognitive” event-related potentials in prolonged postcoma unawareness state. *Clin Electroencephal* (1998) 29(1):19–30. doi:10.1177/155005949802900109
  32. Hildebrandt H, Happe S, Deutschmann A, Basar-Eroglu C, Eling P, Brunhöber J. Brain perfusion and VEP reactivity in occipital and parietal areas are associated to recovery from hypoxic vegetative state. *J Neurol Sci* (2007) 260(1):150–8. doi:10.1016/j.jns.2007.04.035
  33. Howell K, Grill E, Klein A-M, Straube A, Bender A. Rehabilitation outcome of anoxic-ischaemic encephalopathy survivors with prolonged disorders of consciousness. *Resuscitation* (2013) 84(10):1409–15. doi:10.1016/j.resuscitation.2013.05.015
  34. Kang XG, Li L, Wei D, Xu XX, Zhao R, Jing YY, et al. Development of a simple score to predict outcome for unresponsive wakefulness syndrome. *Crit Care* (2014) 18:R37. doi:10.1186/cc13745
  35. Keren O, Sazbon L, Groswasser Z, Shmuel M. Follow-up studies of somatosensory evoked potentials and auditory brainstem evoked potentials in patients with post-coma unawareness (PCU) of traumatic brain injury. *Brain Inj* (1994) 8(3):239–47. doi:10.3109/02699059409150976
  36. Kondziella D, Fisher PM, Larsen VA, Hauerberg J, Fabricius M, Möller K, et al. Functional MRI for assessment of the default mode network in acute brain injury. *Neurocrit Care* (2017) 27(3):401–6. doi:10.1007/s12028-017-0407-6
  37. Kotchoubey B. Event-related potential measures of consciousness: two equations with three unknowns. *Prog Brain Res* (2005) 150:427–44. doi:10.1016/S0079-6123(05)50030-X
  38. Kotchoubey B. Apallic syndrome is not apallic – is vegetative state vegetative? *Neuropsychol Rehabil* (2005) 15:333–56. doi:10.1080/09602010443000416
  39. Li L, Kang XG, Qi S, Xu XX, Xiong LZ, Zhao G, et al. Brain response to thermal stimulation predicts outcome of patients with chronic disorders of consciousness. *Neurophysiol Clin* (2015) 126(8):1539–47. doi:10.1016/j.clinph.2014.10.148
  40. Li R, Song W, Du J, Huo S, Shan G. Connecting the P300 to the diagnosis and prognosis of unconscious patients. *Neural Regen Res* (2015) 10(3):473–80. doi:10.4103/1673-5374.153699
  41. Logi F, Pasqualetti P, Tomaiuolo F. Predict recovery of consciousness in post-acute severe brain injury: the role of EEG reactivity. *Brain Inj* (2011) 25(10):972–9. doi:10.3109/02699052.2011.589795
  42. Marino S, Bonanno L, Ciurleo R, Baglieri A, Morabito R, Guerrera S, et al. Functional evaluation of awareness in vegetative and minimally conscious state. *Open Neuroimag J* (2017) 11:17–25. doi:10.2174/1874440001711010017
  43. Oksenberg A, Gordon C, Arons E, Sazbon L. Phasic activities of rapid eye movement sleep in vegetative state patients. *Sleep* (2001) 24(6):703. doi:10.1093/sleep/24.6.703
  44. Qin P, Di H, Yan X, Yu S, Laureys S, Weng X. Mismatch negativity to the patient's own name in chronic disorders of consciousness. *Neurosci Lett* (2008) 448(1):24–8. doi:10.1016/j.neulet.2008.10.029
  45. Qin P, Wu X, Duncan NW, Bao W, Tang W, Zhang Z, et al. GABAA receptor deficits predict recovery in patients with disorders of consciousness: a preliminary multimodal [11C]Flumazenil PET and fMRI study. *Hum Brain Mapp* (2015) 36(10):3867–77. doi:10.1002/hbm.22883
  46. Qin P, Wu X, Huang Z, Duncan NW, Tang W, Wolff A, et al. How are different neural networks related to consciousness? *Ann Neurol* (2015) 78(4):594–605. doi:10.1002/ana.24479
  47. Rosanova M, Gosseries O, Casarotto S, Boly M, Casali AG, Bruno MA, et al. Recovery of cortical effective connectivity and recovery of consciousness in vegetative patients. *Brain* (2012) 135(4):1308–20. doi:10.1093/brain/awr340
  48. Sarà M, Pistoia F, Pasqualetti P, Sebastiano F, Onorati P, Rossini PM. Functional isolation within the cerebral cortex in the vegetative state: a nonlinear method to predict clinical outcomes. *Neurorehabil Neural Repair* (2011) 25(1):35–42. doi:10.1177/1545968310378508
  49. Schorr B, Schlee W, Arndt M, Bender A. Coherence in resting-state EEG as a predictor for the recovery from unresponsive wakefulness syndrome. *J Neurol* (2016) 263(5):937–53. doi:10.1007/s00415-016-8084-5
  50. Sitt JD, King JR, El Karoui I, Rohaut B, Faugeras F, Gramfort A, et al. Large scale screening of neural signatures of consciousness in patients in a vegetative or minimally conscious state. *Brain* (2014) 137(8):2258–70. doi:10.1093/brain/awu141
  51. Stender J, Gosseries O, Bruno MA, Charland-Verville V, Vanhaudenhuyse A, Demertzi A, et al. Diagnostic precision of PET imaging and functional MRI in disorders of consciousness: a clinical validation study. *Lancet* (2014) 384(9942):514–22. doi:10.1016/S0140-6736(14)60042-8
  52. Steppacher I, Eickhoff S, Jordanov T, Kaps M, Witzke W, Kissler J. N400 predicts recovery from disorders of consciousness. *Ann Neurol* (2013) 73(5):594–602. doi:10.1002/ana.23835
  53. Tommasino C, Grana C, Lucignani G, Torri G, Fazio F. Regional cerebral metabolism of glucose in comatose and vegetative state patients. *J Neurosurg Anesthesiol* (1995) 7:109. doi:10.1097/00008506-199504000-00006
  54. Vogel D, Markl A, Yu T, Kotchoubey B, Lang S, Müller F. Can mental imagery functional magnetic resonance imaging predict recovery in patients with disorders of consciousness? *Arch Phys Med Rehabil* (2013) 94(10):1891–8. doi:10.1016/j.apmr.2012.11.053
  55. Wang F, Di H, Hu X, Jing S, Thibaut A, Di Perri C, et al. Cerebral response to subject's own name showed high prognostic value in traumatic vegetative state. *BMC Med* (2015) 13:83. doi:10.1186/s12916-015-0330-7
  56. Wang XY, Wu HY, Lu HT, Huang TT, Zhang H, Zhang T. Assessment of mismatch negativity and P300 response in patients with disorders of consciousness. *Eur Rev Med Pharmacol Sci* (2017) 21(21):4896–906.
  57. Wijnen VJM, van Boxtel GJM, Eilander HJ, de Gelder B. Mismatch negativity predicts recovery from the vegetative state. *Clin Neurophysiol* (2007) 118(3):597–605. doi:10.1016/j.clinph.2006.11.020
  58. Wijnen VJM, Eilander HJ, de Gelder B, van Boxtel GJM. Repeated measurements of the auditory oddball paradigm is related to recovery from the vegetative state. *J Clin Neurophysiol* (2014) 31(1):65–80. doi:10.1097/01.wnp.0000436894.17749.0c
  59. Wijnen VJM, Eilander HJ, de Gelder B, van Boxtel GJM. Visual processing during recovery from vegetative state to consciousness: comparing behavioral indices to brain responses. *Neurophysiol Clin* (2014) 44(5):457–69. doi:10.1016/j.neucli.2014.08.008

60. Wisłowska M, Del Giudice R, Lechinger J, Wielek T, Heib DPJ, Pitiot A, et al. Night and day variations of sleep in patients with disorders of consciousness. *Sci Rep* (2017) 7:266. doi:10.1038/s41598-017-00323-4
61. Wu DY, Cai G, Yuan Y, Liu L, Li GQ, Song WQ, et al. Application of nonlinear dynamics analysis in assessing unconsciousness: a preliminary study. *Clin Neurophysiol* (2011) 122(3):490–8. doi:10.1016/j.clinph.2010.05.036
62. Xu W, Jiang G, Chen Y, Wang X, Jiang X. Prediction of minimally conscious state with somatosensory evoked potentials in long-term unconscious patients after traumatic brain injury. *J Trauma Acute Care Surg* (2012) 72(4):1024–30. doi:10.1097/TA.0b013e31824475cc
63. Ioannidis JPA. Why most published research findings are false. *PLoS Med* (2005) 2(8):e124. doi:10.1371/journal.pmed.0020124
64. Brok J, Thorlund K, Gluud C, Wetterslev J. Trial sequential analysis reveals insufficient information size and potentially false positive results in many meta-analyses. *J Clin Epidemiol* (2008) 61(8):763–9. doi:10.1016/j.jclinepi.2007.10.007
65. Simmons JP, Nelson LD, Simonsohn U. False-positive psychology: undisclosed flexibility in data collection and analysis allows presenting anything as significant. *Psychol Sci* (2011) 22(11):1359–66. doi:10.1177/0956797611417623
66. Begley CG, Ioannidis JP. Reproducibility in science: improving the standard for basic and preclinical research. *Circ Res* (2015) 116:116–26. doi:10.1161/CIRCRESAHA.114.303819
67. Whiting PF, Rutjes AW, Westwood ME, Mallett S, Deeks JJ, Reitsma JB, et al. QUADAS-2: a revised tool for the quality assessment of diagnostic accuracy studies. *Ann Intern Med* (2011) 155:529–36. doi:10.7326/0003-4819-155-8-201110180-00009
68. Giacino JT, Kalmar K, White J. The JFK Coma Recovery Scale-Revised: measurement characteristics and diagnostic utility. *Arch Phys Med Rehabil* (2004) 85:2020–9. doi:10.1016/j.apmr.2004.02.033
69. American Congress of Rehabilitation Medicine, Brain Injury-Interdisciplinary Special Interest Group, Disorders of Consciousness Task Force, Seel RT, Sherer M, Whyte J, Katz DI, Giacino JT, et al. Assessment scales for disorders of consciousness: evidence-based recommendations for clinical practice and research. *Arch Phys Med Rehabil* (2010) 91:1795–813. doi:10.1016/j.apmr.2010.07.218
70. Yue W, Wilson CS, Boller E. Peer assessment of journal quality in clinical neurology. *J Med Libr Assoc* (2007) 95:70–6.
71. Higgins JPT, Thompson SG. Quantifying heterogeneity in a meta-analysis. *Stat Med* (2002) 21(11):1539–58. doi:10.1002/sim.1186
72. Viechtbauer W. Conducting meta-analyses in R with the metafor package. *J Stat Softw* (2010) 36(3):1–48. doi:10.18637/jss.v036.i03
73. Brems B, Button K, Munafo M. Deep impact: unintended consequences of journal rank. *Front Hum Neurosci* (2013) 7:291. doi:10.3389/fnhum.2013.00291
74. Synek VM. Value of a revised EEG Coma Scale for prognosis after cerebral anoxia and diffuse head injury. *Clin EEG Neurosci* (1990) 21(1):25–30.
75. Rasch B, Born J. About sleep's role in memory. *Physiol Rev* (2013) 93:681–766. doi:10.1152/physrev.00032.2012
76. Fritz CO, Morris PE, Richler JJ. Effect size estimates: current use, calculations, and interpretation. *J Exp Psychol* (2012) 141(1):2–18. doi:10.1037/a0024338
77. Sedlmeier P, Gigerenzer G. Do studies of statistical power have an effect on the power of studies? *Psychol Bull* (1989) 105(2):309–16. doi:10.1037/0033-2909.105.2.309
78. Ingre M. Why small low-powered studies are worse than large high-powered studies and how to protect against “trivial” findings in research: comment on Friston (2012). *Neuroimage* (2013) 81:496–8. doi:10.1016/j.neuroimage.2013.03.030
79. Vul E, Harris C, Winkelman P, Paschler H. Puzzlingly high correlations in fMRI studies of emotion, personality, and social cognition. *Perspect Psychol Sci* (2009) 4:274–90. doi:10.1111/j.1745-6924.2009.01132.x
80. Button KS, Ioannidis JP, Mokrysz C, Nosek BA, Flint J, Robinson ES, et al. Power failure: why small sample size undermines the reliability of neuroscience. *Nat Rev Neurosci* (2013) 14:365–76. doi:10.1038/nrn3475
81. Schnakers C, Vanhaudenhuyse A, Giacino J, Ventura M, Boly M, Majerus S, et al. Diagnostic accuracy of the vegetative and minimally conscious state: clinical consensus versus standardized neurobehavioral assessment. *BMC Neurol* (2009) 9:Article35. doi:10.1186/1471-2377-9-35
82. Gais S, Molle M, Helms K, Born J. Learning-dependent increases in sleep spindle density. *J Neurosci* (2002) 22:6830–4. doi:10.1523/JNEUROSCI.22-15-06830.2002
83. Tamminen J, Ralph MAL, Lewis PA. The role of sleep spindles and slow-wave activity in integrating new information in semantic memory. *J Neurosci* (2013) 33:15376–81. doi:10.1523/JNEUROSCI.5093-12.2013
84. Pavlov YG, Gais S, Müller F, Schönauer M, Schäpers B, Born J, et al. Night sleep in patients with vegetative state. *J Sleep Res* (2017) 26:629–40. doi:10.1111/jsr.12524
85. Sebastiano RD, Visani E, Panzica F, Sattin D, Bersano A, Nigri A, et al. Sleep patterns associated with the severity of impairment in a large cohort of patients with chronic disorders of consciousness. *Clin Neurophysiol* (2018) 129(3):687–93. doi:10.1016/j.clinph.2017.12.012
86. Daltrozzo J, Wioland N, Mutschler V, Kotchoubey B. Predicting outcome of coma using event-related brain potentials: a meta-analytic approach. *Neurophysiol Clin* (2007) 118:606–14. doi:10.1016/j.clinph.2006.11.019
87. Zandbergen EGJ, Koelman JHTM, de Haan RJ, Hijdra A. SSEPs and prognosis in postanoxic coma: only short or also long latency responses? *Neurology* (2006) 67:583–6. doi:10.1212/01.wnl.0000230162.35249.7f

**Conflict of Interest Statement:** The authors declare that the research was conducted in the absence of any commercial or financial relationships that could be construed as a potential conflict of interest.

The reviewer AP and handling Editor declared their shared affiliation.

Copyright © 2018 Kotchoubey and Pavlov. This is an open-access article distributed under the terms of the Creative Commons Attribution License (CC BY). The use, distribution or reproduction in other forums is permitted, provided the original author(s) and the copyright owner are credited and that the original publication in this journal is cited, in accordance with accepted academic practice. No use, distribution or reproduction is permitted which does not comply with these terms.



# Daytime Central Thalamic Deep Brain Stimulation Modulates Sleep Dynamics in the Severely Injured Brain: Mechanistic Insights and a Novel Framework for Alpha-Delta Sleep Generation

Jackie L. Gottshall<sup>1\*</sup>, Zoe M. Adams<sup>2</sup>, Peter B. Forgacs<sup>1,2,3</sup> and Nicholas D. Schiff<sup>1,2,3</sup>

<sup>1</sup> Feil Family Brain and Mind Research Institute, Weill Cornell Medicine, New York, NY, United States, <sup>2</sup> Department of Neurology, Weill Cornell Medicine, New York, NY, United States, <sup>3</sup> Rockefeller University Hospital, New York, NY, United States

## OPEN ACCESS

### Edited by:

Roland Beisteiner,  
Medical University of Vienna, Austria

### Reviewed by:

Bornali Kundu,  
University of Utah, United States  
Srivas Chennu,  
University of Kent, United Kingdom

### \*Correspondence:

Jackie L. Gottshall  
jag2037@med.cornell.edu

### Specialty section:

This article was submitted to  
Applied Neuroimaging,  
a section of the journal  
Frontiers in Neurology

**Received:** 08 November 2018

**Accepted:** 08 January 2019

**Published:** 04 February 2019

### Citation:

Gottshall JL, Adams ZM, Forgacs PB  
and Schiff ND (2019) Daytime Central  
Thalamic Deep Brain Stimulation  
Modulates Sleep Dynamics in the  
Severely Injured Brain: Mechanistic  
Insights and a Novel Framework for  
Alpha-Delta Sleep Generation.  
Front. Neurol. 10:20.  
doi: 10.3389/fneur.2019.00020

Loss of organized sleep electrophysiology is a characteristic finding following severe brain injury. The return of structured elements of sleep architecture has been associated with positive prognosis across injury etiologies, suggesting a role for sleep dynamics as biomarkers of wakeful neuronal circuit function. In a continuing study of one minimally conscious state patient studied over the course of  $\sim 8\frac{1}{2}$  years, we sought to investigate whether changes in daytime brain activation induced by central thalamic deep brain stimulation (CT-DBS) influenced sleep electrophysiology. In this patient subject, we previously reported significant improvements in sleep electrophysiology during 5½ years of CT-DBS treatment, including increased sleep spindle frequency and SWS delta power. We now present novel findings that many of these improvements in sleep electrophysiology regress following CT-DBS discontinuation; these regressions in sleep features correlate with a significant decrease in behavioral responsiveness. We also observe the re-emergence of alpha-delta sleep, which had been previously suppressed by daytime CT-DBS in this patient subject. Importantly, CT-DBS was only active during the daytime and has been proposed to mediate recovery of consciousness by driving synaptic activity across frontostriatal systems through the enhancement of thalamocortical output. Accordingly, the improvement of sleep dynamics during daytime CT-DBS and their subsequent regression following CT-DBS discontinuation implicates wakeful synaptic activity as a robust modulator of sleep electrophysiology. We interpret these findings in the context of the “synaptic homeostasis hypothesis,” whereby we propose that daytime upregulation of thalamocortical output in the severely injured brain may facilitate organized frontocortical circuit activation and yield net synaptic potentiation during wakefulness, providing a homeostatic drive that reconstitutes sleep dynamics over time. Furthermore, we consider common large-scale network dynamics across several neuropsychiatric disorders in which alpha-delta sleep has been documented, allowing us to formulate a novel mechanistic framework for alpha-delta sleep generation. We conclude that the bi-directional modulation of sleep electrophysiology by daytime

thalamocortical activity in the severely injured brain: (1) emphasizes the cyclical carry-over effects of state-dependent circuit activation on large-scale brain dynamics, and (2) further implicates sleep electrophysiology as a sensitive indicator of wakeful brain activation and covert functional recovery in the severely injured brain.

**Keywords:** traumatic brain injury, minimally conscious state, deep brain stimulation, synaptic homeostasis hypothesis, alpha-delta sleep, sleep spindles, slow wave sleep

## INTRODUCTION

Increasing evidence suggests that many patients with disorders of consciousness experience neuronal re-organization and recovery of large-scale brain function over prolonged time periods (1–5). The presence of sleep architecture, particularly sleep spindles and slow wave sleep (SWS), has been found to correlate with prognosis following injury and therefore may be an important dimension for understanding and tracking functional improvements (6–14). In the present study we tracked long-term sleep changes in a single patient remaining in minimally conscious state over ~8.5 years. Adams et al. (15) first reported on the EEG sleep characteristics of this patient before and during ~5 years of daytime central thalamic deep brain stimulation (CT-DBS), which was initiated for the promotion of arousal regulation. Initial findings by Adams et al. showed an increase in sleep spindle frequency and SWS duration following the onset of CT-DBS treatment (15). An irregular intrusion of alpha activity during SWS was also reported prior to CT-DBS, which seemed to attenuate during CT-DBS treatment. Importantly, these results implicated daytime brain activation as modulator of sleep architecture in the severely injured brain.

Here we report on distinct changes observed ~1 year after the discontinuation of CT-DBS treatment. We find ongoing plasticity in multiple physiological aspects of sleep, providing important insight into the network-level dynamics that can be induced by daytime arousal regulation in the severely injured brain. Most notably, in the present study we identify a regression of the previously noted improvements in sleep dynamics seen over course of CT-DBS treatment. A return of the atypical SWS alpha intrusion initially reported by Adams et al. as “mixed state” is evaluated here in the context of the previously documented phenomenon “alpha-delta sleep” (16). We discuss our findings in the context of neuronal circuit mechanisms that may organize the improvement of sleep dynamics during daytime CT-DBS in the severely injured brain, as well as those that may underlie functional regression with the withdrawal of CT-DBS treatment. Finally, we explore the role of alpha-delta sleep across pathophysiologicals of neuropsychiatric disorders and propose a mechanistic explanation for alpha-delta sleep generation.

## METHODS

### Patient History

Patient subject is a 48-year-old man who suffered a severe brain injury as the result of a motor vehicle accident at the age of 17. The injury pattern is characterized by a small left thalamic

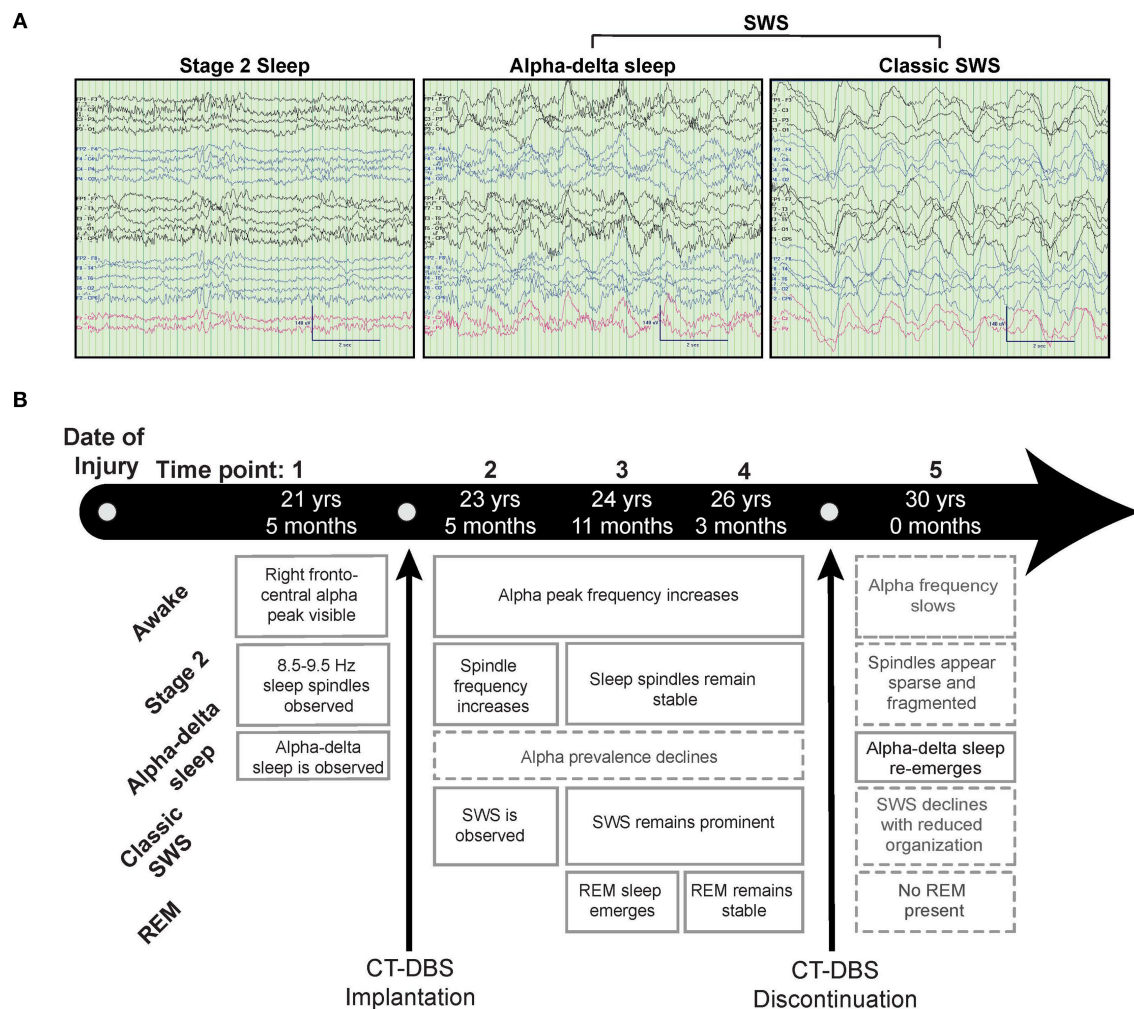
hemorrhage, as well as diffuse axonal injury with extensive atrophy of the left hemisphere (**Supplementary Figure 1**). Behavioral presentation has remained consistent with a diagnosis of minimally conscious state since the time of injury.

### Data Collection and Timeline

The patient subject was studied longitudinally at five time points (TP1-TP5) over the course of 8.5 years (**Figure 1**). Each study consisted of a 24–72 h inpatient admission (TP1 at New York Presbyterian Hospital, New York, USA; TP2-TP5 at Rockefeller University Hospital, New York, USA) under IRB approvals from Weill Cornell Medicine and Rockefeller University. Written informed consent was obtained from the patient’s surrogate for study participation, data collection and publication. During each inpatient study, behavioral responsiveness was quantified according to the Coma Recovery Scale-Revised (CRS-R) (17) at least once per day. Overnight video-EEG was collected with collodion-pasted electrodes (30 electrodes at TP1; 37 electrodes at TP2-TP5) placed according to the international 10–20 system. Signals were recorded using the Natus XLTEK system (San Carlos, CA) at impedances  $\leq 5$  k $\Omega$ . Time point one occurred at 21 years 5 months post injury. The patient subject subsequently underwent surgery for the implantation of bilateral central thalamic deep brain stimulation electrodes [clinical trial methods are described briefly below, as well as in detail in Schiff et al. (18)]. Study time points two through four were concurrent with daytime central thalamic deep brain stimulation (CT-DBS) (TP2: 23 years 5 months, TP3: 24 years 11 months, and TP4: 26 years 3 months post injury, respectively). Time point five occurred ~1 year following CT-DBS discontinuation secondary to battery depletion (TP5: 30 years 0 months post injury).

Implantation of deep brain stimulation electrode leads was aided by microelectrode recordings from the sensory relay nucleus of the thalamus on both the right and left hemispheres. Using electrophysiological localization of the sensory nucleus as known, the lateral wing of the central lateral nucleus was targeted using the Morel atlas (19) by dead reckoning. Following implantation, CT-DBS was administered on a blocked 12 h ON/OFF cycle (ON: 6AM–6PM/OFF: 6PM–6AM) over the course of ~7 ½ years. During this time, a wide range of electrode contact geometries, stimulation intensities, and frequencies of stimulation were employed. Briefly, following extensive titration testing of stimulation frequency and intensity, an optimal geometry was identified for each electrode contact based on apparent arousal effects and limitations of visible side effects. The





**FIGURE 1 |** Representative EEG and summary timeline. **(A)** Representative segments of patient subject EEG tracings during non-REM sleep show the presence of stage two (left) and SWS (middle, right) epochs. A mixed frequency signature consistent with alpha-delta sleep was also observed (middle), classified here as a subset of SWS for consistency with combined “SWS-like” states reported in Adams et al. (15). **(B)** The patient subject was studied at five time points over the course of 8.5 years, consisting of one time point before, three during, and one after CT-DBS treatment. Qualitative summaries of individual EEG states are shown for each time point.

left electrode was stimulated in bipolar mode with the lowest contact chosen as cathode and highest contact chosen as anode; the right electrode was stimulated in monopolar mode with two cathodes, placed at the lowest two contacts. During a 6 month crossover phase, stimulation at these contacts occurred for 12 h each day using a 90 ms pulse width, 130 Hz stimulation frequency, and 4 V intensity for each electrode. Following the crossover phase, a range of varying frequencies and intensities were used including a 1 year period of stimulation at each of 175 Hz and 100 Hz. For the majority of the 7½ years of CT-DBS exposure stimulation occurred at 100 Hz with other parameters held constant.

## Data Analysis

### EEG Processing

For estimates of wakeful brain dynamics, periods of resting eyes open awake states were identified by video record and

corresponding EEG was manually cleaned for the removal of eye blink and movement artifacts.

Sleep analyses included nighttime sleep EEG collected between the hours of 8 p.m. and 6 a.m., manually cleaned for movement artifacts and verified eyes-closed according to synchronous video record. Standard sleep scoring criteria were used to classify segments as stage two or SWS (20). Briefly, the patient subject was considered to be in stage two sleep if the EEG record displayed k-complexes and/or 9–16 Hz spindle-like formations across frontocentral channels. Slow wave sleep was classified by large polymorphic delta (<4 Hz) waves present over at least 20% of a 30 s epoch. The observation of an additional and constant 8–14 Hz oscillation overriding classic SWS characteristics was considered alpha-delta sleep. To maintain consistency with the previous report by Adams et al. (15), alpha-delta sleep was scored under the categorization of SWS.

## Power Spectral Estimation

Raw EEG was segmented into 30–35 representative epochs for awake, stage two sleep, and SWS states, respectively. Multitaper power spectral estimates were calculated separately for each state (21) with implementation of Hjorth Laplacian montaging from the MATLAB chronux toolbox (22). After spectral calculation, six frontocentral channels (F3, F4, FC5, FC6, C3, C4) were used for longitudinal comparison to maintain consistency with Adams et al. (15).

For longitudinal comparisons of spectral peak sizes during stage two and SWS stages, calculated spectra were normalized according to methods outlined in Gottselig et al. (23). Briefly, a power law function was fit to each spectrum in the 5–6 Hz and 17–18 Hz frequency ranges for stage two sleep, or 4–6 Hz and 23–24 Hz frequency ranges for SWS. Frequency ranges for normalization were chosen based on optimal fitting of the power law function to the underlying shape of the power spectrum across channels, excluding frequency bins of interest to avoid flattening of relevant spectral features. Absolute power of the fitted spectrum was subtracted from the calculated spectrum and resulting values were integrated across frequency bins of interest. By subtracting the best-fit underlying spectral shape, arbitrary differences in background power bias between visits were removed, allowing for estimation of magnitude change in relevant spectral features.

Dominant spindle frequency was determined from normalized stage two power spectra using a handcrafted manual click program to determine the center frequency of the largest spectral peak in the 9–16 Hz spindle range. Briefly, the spindle peak for each channel was visually identified from the normalized power spectrum and a quadratic polynomial was fit to the identified peak to determine the local power maxima and corresponding dominant spindle frequency. If no spindle peak was present no value was recorded.

## Statistics

Analyzed variables were CRS-R total score, stage two sleep spindle power (9–16 Hz) and peak spindle frequency, SWS delta power (0.5–4 Hz), and SWS alpha power (8–14 Hz). Time periods for comparison were grouped into three conditions reflecting initial pre-stimulation baseline, the active period of CT-DBS, and the post-withdrawal of stimulation phase (Pre:TP1/Active:TP2-TP4/Post:TP5). An analysis of variance (ANOVA) was performed for each variable to identify changes across CT-DBS conditions. For stage two and SWS variables, ANOVA factors included CT-DBS condition and hemisphere. To identify any changes within the active CT-DBS condition, a separate ANOVA was conducted for TP2-TP4 within each variable. *Post-hoc* comparisons were conducted using Tukey's HSD at a significance level of  $p < 0.05$ .

## RESULTS

### Visual EEG Features

**Figure 1** provides a qualitative summary of changes in EEG architecture over the course of study. Most notable was the observation at TP1 of an additional sleep signature consisting of high voltage, low frequency (<2 Hz) activity exhibiting an

overriding mid-frequency (8–14 Hz) component (**Figure 1A**, middle panel). This signature closely resembles alpha-delta sleep, characterized by Hauri and Hawkins (16) as “a mixture of 5–20% delta waves (>75  $\mu$ V, 0.5–2 c/sec) combined with relatively large amplitude, alpha-like rhythms (7–10 c/s).” Alpha-delta sleep was prominent before CT-DBS treatment (TP1), waned during active CT-DBS (TP2-TP4), and re-emerged following discontinuation of CT-DBS (TP5). Inversely, changes in healthy sleep architecture during CT-DBS treatment included the normalization of stage two sleep spindles, SWS, and awake alpha rhythms, as well as the emergence of REM sleep. Each of these healthy features demonstrated qualitative decline following CT-DBS discontinuation (**Figure 1B**).

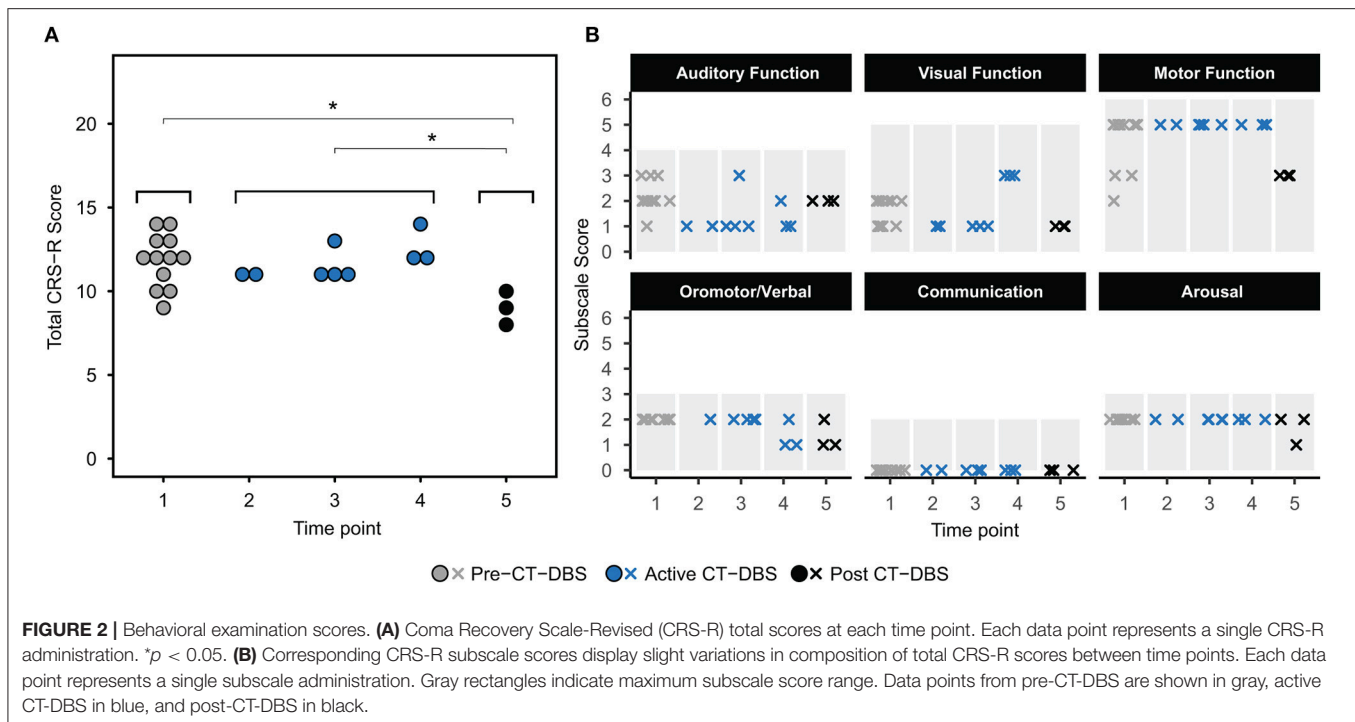
### Behavioral Examination

The CRS-R was administered at least once daily during each time point. A one-way ANOVA showed a significant effect of CT-DBS condition (pre, active, post) [ $F_{(2,21)} = 5.55$ ,  $p = 0.0116$ ], such that total CRS-R scores were significantly lower after CT-DBS cessation ( $M = 9.0$ ,  $SD = 1.0$ ) than either before CT-DBS ( $M = 11.8$ ,  $SD = 1.6$ ,  $p = 0.011$ ) or during active CT-DBS ( $M = 11.8$ ,  $SD = 1.1$ ,  $p = 0.016$ ) (**Figure 2A**). Although this reduction in CRS-R score was statistically significant, the patient subject remained within the diagnostic classification of minimally conscious state throughout the course of study. There was no change in CRS-R scores between active CT-DBS time points.

CRS-R subscale scores were also compared for a detailed view of composite CRS-R score changes. Analysis of variance was not performed due to the categorical nature of subscale classifications. Subscale scores varied slightly across time points, with the exception of the communication subscale, for which the patient subject received a score of 0 at each examination (**Figure 2B**). Altogether, although CT-DBS did not produce an increase in CRS-R scores, the withdrawal of CT-DBS correlated with a significant reduction in responsiveness at TP5.

### Power Spectra During Wake, Stage 2, and SWS

Power spectra from TP1, TP4, and TP5 were overlaid for a qualitative analysis of spectral shape before, during, and after CT-DBS, respectively. Awake power spectra showed small local changes but few global changes over time (**Figure 3A**). In the alpha range, FC6 initially demonstrated a spectral peak at ~8–9 Hz which reduced in power but increased in frequency to ~9–10 Hz by TP4 (**Figure 3A**, FC6 inset arrow). Following discontinuation of CT-DBS at TP5, the FC6 power spectrum largely flattened and showed no clear peak within the alpha range (**Figure 3A**, FC6 inset). A similar awake alpha modulation was present in C4 with a less prominent increase in alpha frequency from ~8 Hz at TP1 to ~9 Hz at TP4 (**Figure 3A**, C4 inset arrow) and a complete flattening at TP5 (**Figure 3A**, C4 inset). Additional examination of parietal and occipital channels during wakeful periods also revealed increases in alpha frequency at TP4 with slight reductions at TP5 (data not shown). Channel C3 uniquely showed prominent electrophysiological change after CT-DBS was discontinued with the emergence of a



clear spectral peak in the beta frequency range at  $\sim 12$  Hz during TP5 (Figure 3A, C3, asterisk).

In contrast to the variable results observed in the patient subject's awake EEG, spectral analysis of stage two sleep showed robust global changes over time. Power spectra were characterized by an increased peak frequency in the sleep spindle range from TP1 to TP4 across all channels (Figure 3B). Following CT-DBS discontinuation at TP5, power in the spindle range disappeared entirely in all channels except C3. At TP5, C3 showed a continued increase in peak spindle frequency, albeit displaying a smaller and less defined spectral peak (Figure 3B, C3 inset arrow). These findings are consistent with the observation of sleep spindle fragmentation across the majority of EEG channels following CT-DBS discontinuation.

SWS power spectra also demonstrated global changes over time, most notably characterized by an intrusion of 8–14 Hz power across channels prior to CT-DBS treatment at TP1, corresponding to the presence of alpha-delta sleep (Figure 3C). The 8–14 Hz alpha-delta sleep frequency signature was absent in all channels during active CT-DBS treatment at TP4, only to re-emerge following CT-DBS discontinuation at TP5. Re-emergence of alpha-delta sleep at TP5 showed increased peak frequency in the alpha range across all except for the two frontal channels (F3 and F4).

## Relationship Between Sleep Dynamics and CT-DBS

For statistical comparison, data were collapsed into three groups: “Pre CT-DBS” (TP1), “Active CT-DBS” (TP2–TP4), and “Post CT-DBS” (TP5). Global feature measurements were compared across and within CT-DBS conditions for a quantitative analysis

of the effects of CT-DBS treatment and subsequent cessation on EEG sleep dynamics.

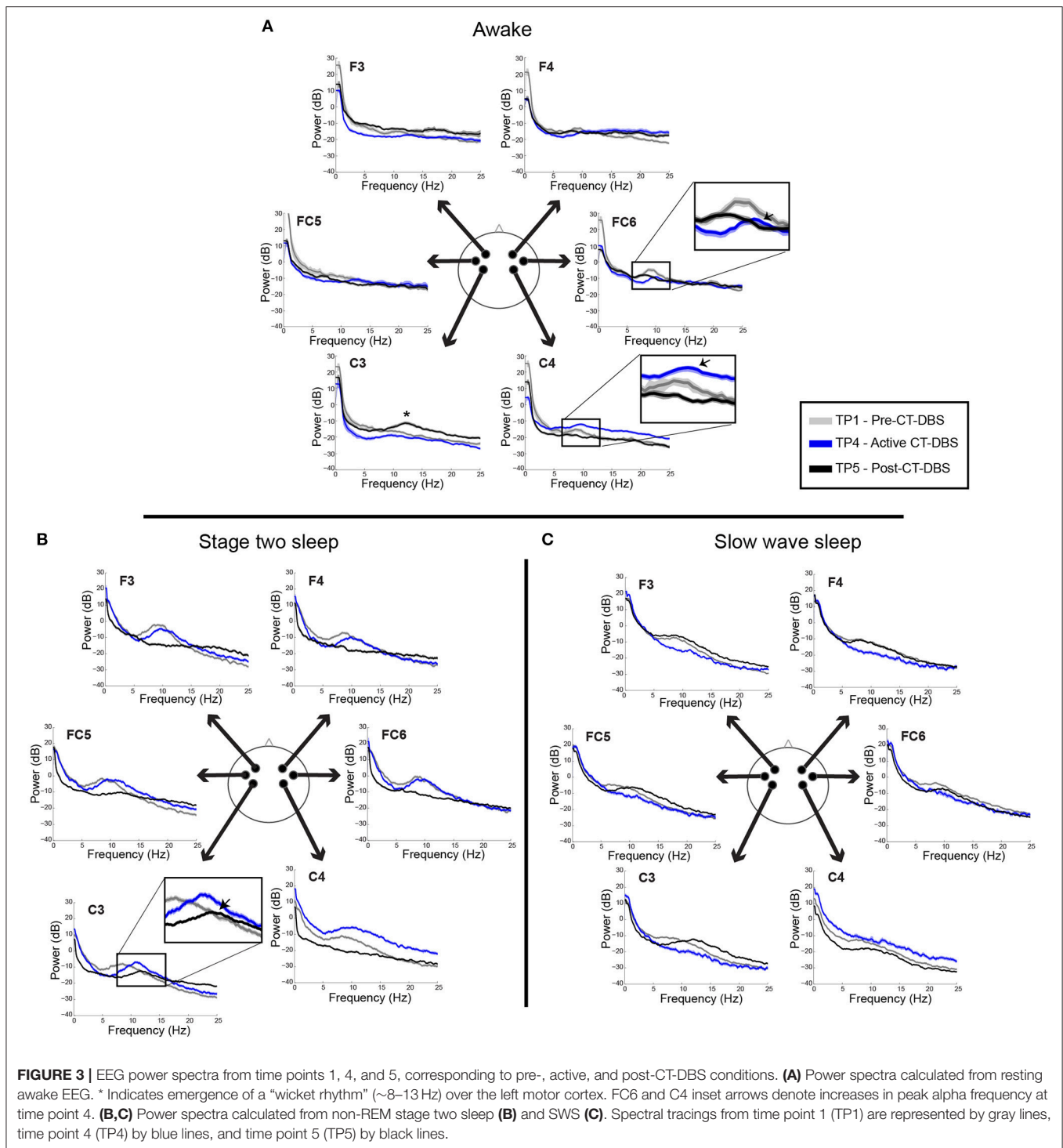
### Stage Two Sleep Spindles

Normalized stage two power spectral calculations were used to quantify changes in spindle (9–16 Hz) power over time. A two-way ANOVA with factors CT-DBS (pre, active, post) and hemisphere (left, right) showed greater spindle power in the left hemisphere [ $F_{(1)} = 6.483$ ,  $p = 0.0177$ ], as well as a highly significant main effect of CT-DBS condition [ $F_{(2)} = 20.411$ ,  $p < 0.0001$ ] (Figure 4A, Table 1). *Post-hoc* tests identified a reduction in spindle power post CT-DBS compared to both pre and active CT-DBS conditions,  $p < 0.001$  and  $p < 0.0001$ , respectively. Spindle power remained consistent across the active CT-DBS condition, with the exception of a slight increase in the left hemisphere at TP4 compared to TP2,  $p = 0.0438$ .

To quantify changes in spindle frequency, we first removed the post CT-DBS condition (TP5) from analyses due to lack of spectral peak in the spindle range in five of the six channels (see Figure 3B). A two-way ANOVA with factors CT-DBS (pre, active) and hemisphere (left, right) demonstrated significantly faster spindle frequency in both hemispheres during active CT-DBS than before CT-DBS treatment [ $F_{(1)} = 26.920$ ,  $p < 0.0001$ ] (Figure 4B, Table 1). Spindle frequency varied within active CT-DBS time points [ $F_{(2)} = 4.158$ ,  $p = 0.0425$ ], such that there was a significant slowing from TP3 to TP4,  $p = 0.0347$ , with frequency at TP4 consistent with peak spindle frequency at TP2.

### SWS Delta Power

Delta (0.5–4 Hz) power was quantified from normalized SWS power spectra as an indicator of healthy SWS electrophysiology.



A two-way ANOVA with factors CT-DBS (pre, active, post) and hemisphere (left, right) showed a global effect of CT-DBS [ $F_{(2)} = 3.932$ ,  $p = 0.033$ ] but not hemisphere, such that SWS delta power significantly increased from pre to active CT-DBS conditions,  $p = 0.0472$  (**Figure 5A**, **Table 1**). During active CT-DBS, delta power was significantly greater at TP4 than TP2 and TP3,  $p < 0.001$  and  $p = 0.001$ , respectively. Despite an empirical reduction in delta

power from TP4 to TP5, statistical analyses yielded no difference between active and post CT-DBS conditions,  $p = 0.186$ .

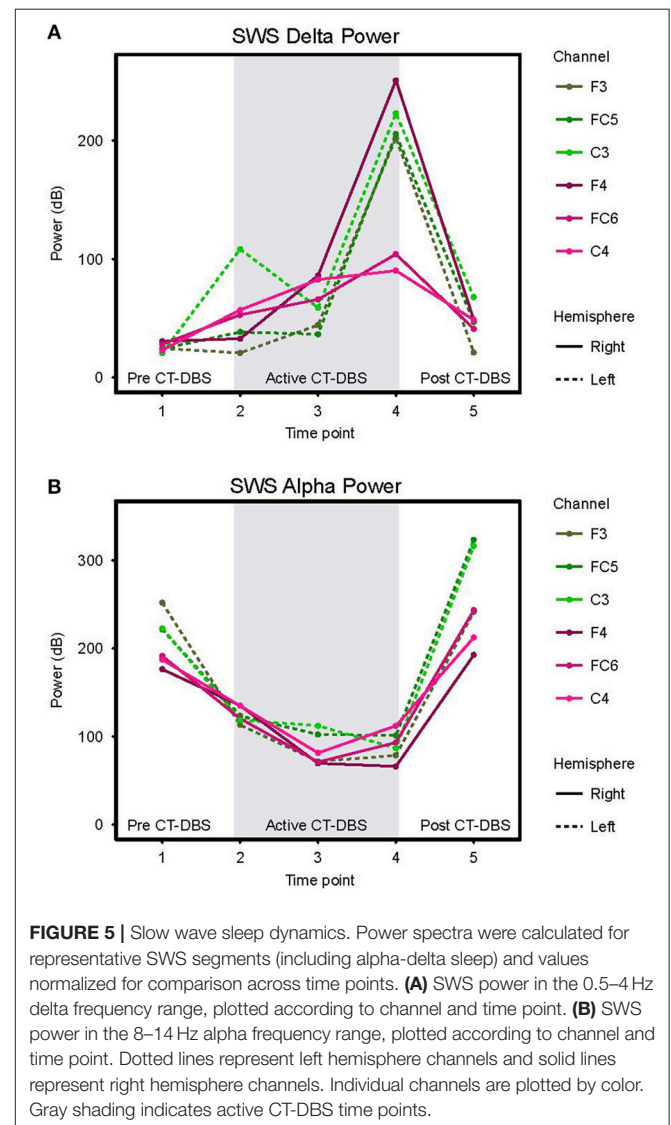
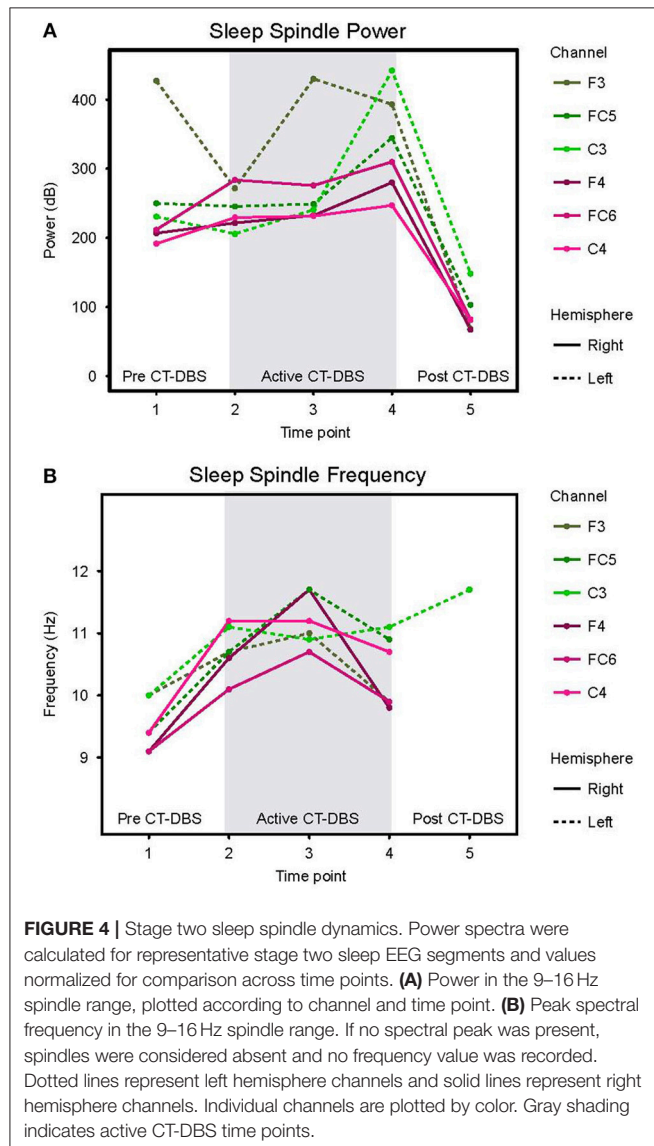
### SWS Alpha Power

Alpha (8–14 Hz) power during SWS was quantified as a marker of alpha-delta sleep expression. A two-way ANOVA with factors CT-DBS (pre, active, post) and hemisphere (left, right) yielded



a highly significant CT-DBS by hemisphere interaction [ $F_{(2)} = 5.657, p = 0.00971$ ] (**Figure 5B, Table 1**). *Post hoc* testing showed

that global alpha power was reduced from pre to active CT-DBS conditions,  $p < 0.001$ , followed by a significant rebound from active to post CT-DBS conditions,  $p < 0.001$ . This rebound



**TABLE 1 |** Average sleep variables calculated from EEG power spectral estimates.

	CT-DBS condition	Stage two spindle power (dB)	Stage two spindle frequency (Hz)	SWS delta power (dB)	SWS alpha power (dB)
Left Hemisphere	Pre	302.62 ± 108.32	9.80 ± 0.35	23.26 ± 2.08	232.04 ± 17.08
	Active	313.61 ± 90.04	10.89 ± 0.48	104.22 ± 83.29	100.82 ± 18.17
	Post	106.76 ± 39.86	11.70*	45.30 ± 23.35	293.66 ± 45.37
Right Hemisphere	Pre	203.35 ± 10.64	9.20 ± 0.17	27.30 ± 3.75	184.90 ± 7.74
	Active	256.80 ± 31.20	10.66 ± 0.64	91.39 ± 63.70	98.10 ± 28.03
	Post	76.91 ± 8.20	NA	46.10 ± 23.35	216.06 ± 25.62

\*Channel C3 only.

was larger in the left than the right hemisphere, such that SWS alpha power did not differ between hemispheres during pre or active CT-DBS conditions, but was greater in the left hemisphere following CT-DBS withdrawal,  $p = 0.010$ . SWS alpha power also differed within active CT-DBS time points [ $F_{(2)} = 13.329$ ,  $p < 0.001$ ], such that it was significantly reduced from TP2 to TP3,  $p = 0.001$ , and remained suppressed at TP4 compared to TP2,  $p = 0.003$ .

## DISCUSSION

In this longitudinal study of a single patient subject in chronic minimally conscious state, we report marked regression of sleep dynamics following the discontinuation of CT-DBS. In this patient subject, Adams et al. (15) previously demonstrated that daytime CT-DBS (6 a.m.–6 p.m.) over a 5 year period was associated with the normalization of sleep architecture and dynamics; specific changes included increased spindle frequency during stage two sleep, increased sustained SWS, and the re-emergence of REM sleep. Presently, we show regression of each of these improvements observed at 1 year after CT-DBS discontinuation (see **Figure 1** for a schematic summary) and in temporal correlation with a significant reduction in behavioral responsiveness (**Figure 2**). During stage two sleep we identify a loss of sleep spindles alongside a reduction in spectral power in the spindle range (**Figures 3B, 4**). We also find a reversion of SWS delta power to pre-CT-DBS levels (**Figures 3C, 5A**), and no instances of REM sleep. Importantly, we observe the re-emergence of a SWS-like frequency signature that had previously been suppressed by daytime CT-DBS (**Figure 5B**). This frequency signature closely resembles the “alpha-delta sleep” pattern that has been identified across several neuropsychiatric conditions (16, 24–29), leading us to re-characterize this phenomenon as alpha-delta sleep arising within the severely injured brain.

In summary, reduced behavioral responsiveness after CT-DBS discontinuation was associated with the abolishment of stage two sleep spindles, marked downregulation of SWS delta power, and the return of alpha-delta sleep. In the following sections we discuss: (1) the proposed mechanism of sleep modulation by daytime CT-DBS in the severely injured brain and implications for sleep dynamics as an indicator of wakeful engagement, (2) altered network dynamics that may underlie alpha-delta sleep expression in the severely injured brain, and (3) a novel mechanistic framework for alpha-delta sleep generation across pathophysiologies.

### Restoration of Frontostriatal Activation by CT-DBS May Drive Sleep Changes in the Severely Injured Brain

The rationale for using CT-DBS in minimally conscious state patients is two-fold: (1) the central thalamus has widespread innervation of frontal cortical and basal ganglia regions and plays a crucial role in maintaining arousal regulation during wakeful states, (2) multi-focal deafferentation is a characteristic injury pattern in severe brain injuries and is known to functionally and structurally disfacilitate central thalamic neuronal populations

(30–32). The upregulation of central thalamic neurons via CT-DBS is therefore expected to re-establish frontostriatal neuronal firing rates, thereby restoring the frontocortical regulation of sustained waking arousal needed to support organized behavior (33). Studies of CT-DBS in another post-traumatic minimally conscious state patient provided proof-of-concept that restoration of sustained frontocortical activity correlates with improvements in organized behavior. In these studies, increased neuronal activity in the frontal cortices produced by CT-DBS was associated with heightened arousal, recovery of speech, restored executive motor control over one limb, and improved feeding behaviors (18, 34). While CT-DBS in our patient subject failed to produce clinically measurable behavioral improvement, it did produce robust improvements in sleep electrophysiology. Adams et al. (15) proposed that these sustained changes in network dynamics visible during sleep were the result of daytime activation of frontostriatal systems by CT-DBS, which allowed for organized neuronal activity in intact but functionally downregulated frontostriatal networks (30, 33, 35–37).

Here we show that CT-DBS cessation temporally correlated with significant regressions in sleep electrophysiology and behavioral responsiveness, providing strong support for the hypothesis that CT-DBS modulates sleep electrophysiology via upregulation of daytime frontostriatal activation and system-level engagement. Modulation of sleep dynamics in response to diurnal neuronal activity has been well described in both animal and human studies. Across species, progressive wakefulness is associated with increased cortical excitability (38–42), increased neuronal firing rates (43, 44), and increased extrasynaptic glutamate levels (45). Subsequent non-REM sleep episodes are characterized by an initial maintenance of high neuronal firing rates, increased cortical synchrony, and upregulated slow wave activity in regions corresponding to increased neuronal activation during wakefulness (46–48). Successive non-REM sleep episodes show a progressive decline in each of these features (43). Accounting for these sleep-wake dynamics, growing evidence indicates that wakefulness creates a net increase in synaptic strengths that requires sleep processes for renormalization; a concept known as the “synaptic homeostasis hypothesis” (SHY) (49–51). Importantly, sustained high firing rates alone, such as those produced by CT-DBS, are insufficient to produce the changes in SWS observed here. Rather, SWS changes are more likely to result from system-level wakeful engagement with the environment that results in synaptic potentiation (38, 47, 52). The SHY therefore predicts that the marked improvements in sleep electrophysiology seen in our patient subject during CT-DBS reflect fundamental changes in synaptic potentiation occurring during wakefulness.

Further supporting this inference, daytime CT-DBS is known to upregulate the long-term potentiation (LTP)-related immediate early gene *zif268* within neocortex (53). Similar gene expression patterns are expressed during periods of REM sleep following wakeful LTP (54); rodent studies have implicated these REM periods as instrumental in the consolidation of CT-DBS-induced learning (53). Accordingly, the selective appearance of REM sleep with CT-DBS in our patient subject likely reflects changes in LTP-related gene expression induced by the daily

12 h CT-DBS periods. Taken together, our findings suggest that the restoration of both non-REM sleep architecture and REM sleep episodes during CT-DBS may provide an indirect marker of meaningful daytime engagement across a range of sensory and associative processing systems within the forebrain.

Our finding that improvements in sleep electrophysiology are lost following withdrawal of CT-DBS suggests further that this process can be reversed. Specifically, sub-threshold wakeful activation may insufficiently engage organized neuronal dynamics needed for synaptic potentiation. Under-activated networks would therefore fail to produce the homeostatic sleep pressure necessary for large-scale neuronal synchronization and synaptic scaling during sleep. This general mechanism has precedence in the healthy brain. Following periods of arm immobilization, healthy individuals demonstrate localized wakeful synaptic depression and reductions in sleep slow wave activity over contralateral sensorimotor cortex (55). In the deafferented brain, the reduction of thalamocortical outflow associated with CT-DBS discontinuation would be expected to result in decreased cortical activation and synaptic depression, culminating in a progressive loss of wakeful frontocortical excitability and diminished homeostatic sleep-wake processes over time. The reduced behavioral responsiveness and degradation of organized sleep architecture after CT-DBS withdrawal at TP5 supports this inference. Collectively, these observations raise the possibility that restoration of synaptic homeostasis during sleep may be a process that is re-engaged in the severely injured brain only after sufficient increases in large-scale organized neuronal firing patterns emerge across the cerebral cortex to produce a net increase in synaptic strength during wakefulness. Such reinstatement of large-scale network engagement, including both glutamatergic synaptic potentiation and GABAergic firing rates (56), provides a testable mechanism for the observed changes in sleep architecture with CT-DBS.

As an exception to the observed global regressions following CT-DBS discontinuation, channel C3 displayed retained sleep spindles and improvements in SWS delta power at TP5 (Figures 3B,C), as well as the emergence of high frequency beta and healthy “Mu” or “wicket” rhythms (~8–13 Hz) during wake (57, 58) (Figure 3A). Of note, although this patient subject was unable to communicate, he retained a high-level of emotional responsiveness consistent with his sense of humor prior to the injury. These unique dynamics underscore the structural preservation of the patient subject’s left temporal cortex (Supplementary Figure 1) as well as verify the functional preservation of his left temporal language processing capabilities. Mechanistically, continued improvements in cortical regions underlying C3 may have resulted from local restructuring as the result of restored neuronal activation across relatively preserved cortical substrate during CT-DBS. Such changes would not be unprecedented; Thengone et al. (1) recently demonstrated prominent changes in structural connectivity emanating from Broca’s area following implementation of assistive communication technology in a minimally conscious state patient. This independent EEG pattern exhibited by a localized brain region in our patient subject underscores the impact that upregulated neuronal activation can have on the

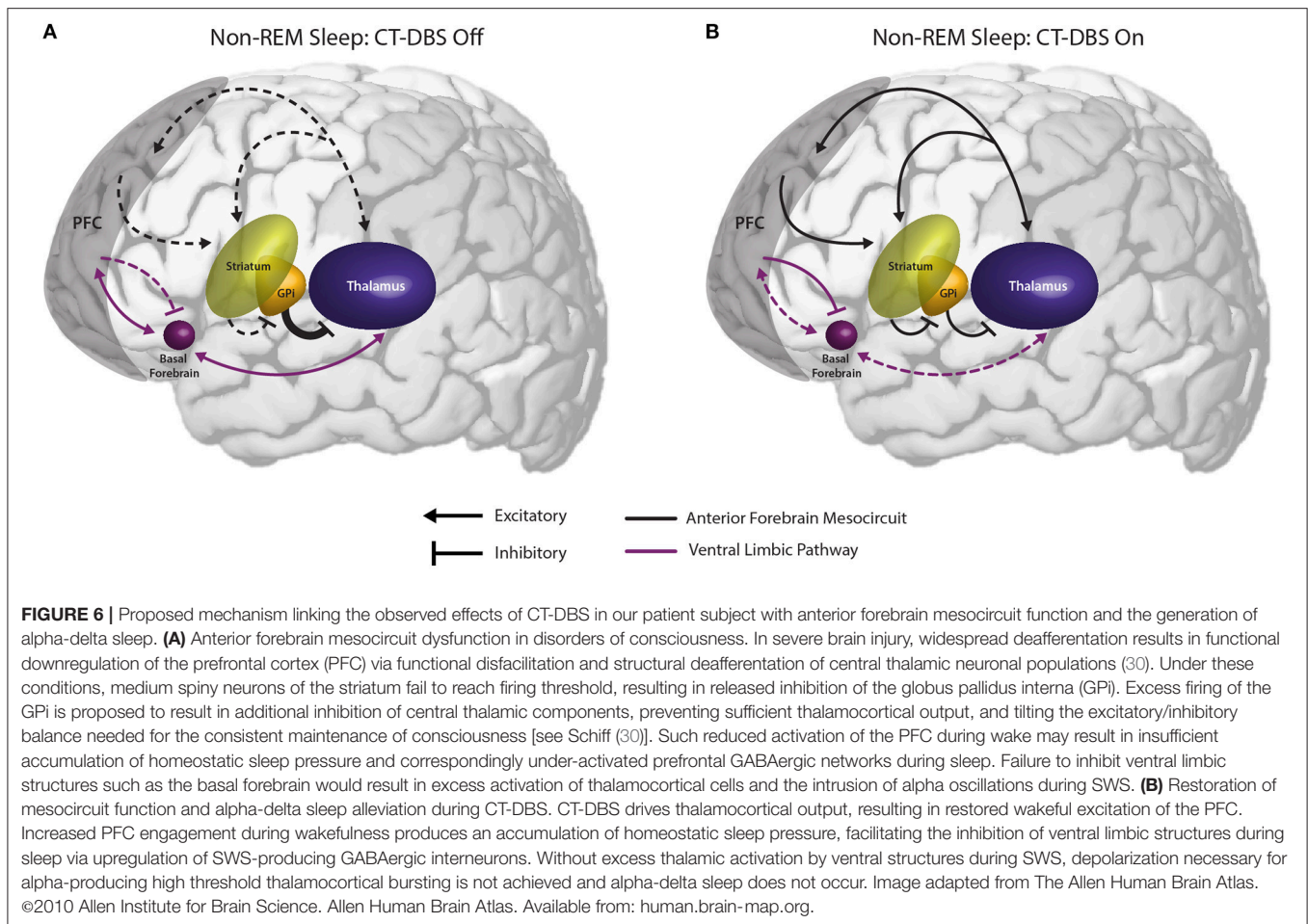
recovery of functional circuitry in structurally intact brain regions.

## An Underactive Prefrontal Cortex may Permit Ventral Limbic Over-activation, Resulting in Alpha-Delta Sleep

Perhaps the most novel and interesting finding observed here is the mixing of alpha and delta rhythms during sleep, originally reported by Adams et al. (15) and identified here as alpha-delta sleep (16). Although the functional role and underlying circuit mechanisms of alpha-delta sleep have remained elusive (59, 60), the phenomenon has been reported in a variety of conditions including fibromyalgia/chronic fatigue (25, 26), rheumatoid arthritis (24), schizophrenia (16), major depressive disorder (29) with implications for suicidality (61), anxiety (28), and in healthy individuals with induced pain and/or arousal during sleep (62). To our knowledge, this is the first report of alpha-delta sleep in the severely injured brain. The persistence of the alpha-delta sleep phenotype across a range of neurological conditions, and now severe brain injury, invites us to consider a common underlying mechanism.

We observe that the conditions in which alpha-delta sleep is reported fall into two mechanistic categories: (1) those characterized by a primary pathology of cerebral hypofrontality or (2) those characterized by a primary upregulation of ventral limbic activation. Both mechanisms result in an increase in limbic system activity during sleep, either via under-activation of the descending corticothalamic pathway needed to drive homeostatic sleep pressure or an overactivation of the ascending pathways that maintain wakefulness. Accordingly, we hypothesize that the appearance of alpha-delta sleep is indicative of a failure of the prefrontal cortex to sufficiently inhibit excitatory output from ventral structures to the thalamus during the shift into synchronized cortical activity for SWS (Figure 6). Specifically, we identify the basal forebrain as a likely generator of thalamic depolarization in alpha-delta sleep due to its cholinergic projections to the thalamus (63–65). Support for this mechanism is provided by simulation and *in vitro* studies of both alpha oscillations (66–69) and alpha-delta sleep expression (70). Regarding alpha production by basal forebrain cholinergic projections, the activation of muscarinic acetylcholine receptors on reticular nuclei, thalamocortical, and high-threshold thalamocortical cells, as well as on somatosensory and visual thalamic nuclei, has been evidenced to produce alpha oscillations in thalamic models (69) and cat *in vitro* slice recordings (67), respectively. Conversely, follow-up *in vitro* studies show that direct thalamic application of a muscarinic acetylcholine receptor antagonist reduces high-threshold thalamocortical cell bursting, and in turn thalamic and cortical alpha power (68). Additional simulation studies demonstrate that alpha-delta sleep generation may originate in aberrant thalamic depolarization during SWS, specifically of “high-threshold” thalamocortical cells that serve as the putative generators of awake alpha (70).

Critically, the novel finding that alpha-delta sleep is modulated by CT-DBS lends strong support to the validity



of this prefrontal-ventral dysfunction model of alpha-delta sleep generation. In our patient subject, CT-DBS restored bulk activation of the frontal cortices during the day, likely facilitating the reinstatement of top-down limbic inhibition (56) and driving activity-dependent increases in homeostatic sleep pressure. This increase in frontocortical GABAergic tone would be expected to carry over into sleep via sustained alterations of GABAergic firing rates (43) and the mutual reinstatement of synchronous cortical slow wave activity needed for synaptic scaling [see Allada et al. (71) for a detailed review]. With proper inhibition of ventral limbic structures by the frontal cortex during SWS, there would be minimal excess corticothalamic excitation and therefore attenuation of the alpha-delta sleep phenotype (69). In our patient subject, when CT-DBS was eventually discontinued, daytime frontocortical network activation was reduced, likely resulting in a gradual lifting of frontal inhibition over limbic structures during SWS and the observed re-emergence of alpha-delta sleep.

### Restoring Frontocortical GABAergic Tone Reduces Alpha-Delta Sleep

The prefrontal-ventral dysfunction model of alpha-delta sleep provides a consistent mechanism across several conditions in

which alpha-delta sleep has been documented. Patients with fibromyalgia demonstrate reduced gray matter volume of the frontal cortex alongside increased structural connectivity of the amygdala (72, 73). Schizophrenia is associated with prefrontal GABAergic deficits and thalamocortical hypoconnectivity (74–76). Major depression is characterized by prefrontal gray matter reductions (77) and GABAergic interneuron deficits (78, 79), as well as ventral hypermetabolism that persists from wakefulness into non-REM sleep (80). Individuals with anxiety and PTSD demonstrate reduced prefrontal regulation of the amygdala (81–83), which is present in both fear conditions and resting states (84, 85); The high prevalence of sleep disturbances in PTSD suggests that prefrontal-amygdala dysfunction persists into sleep states as well. Together, these commonalities suggest that alpha-delta sleep dynamics may be indicative of the presence and/or severity of prefrontal-ventral dysregulation across behavioral diagnoses.

In support of the generalizability of this model, the alleviation of frontal GABAergic deficits by gamma hydroxybutyrate (GHB/sodium oxybate) has been found to suppress alpha-delta sleep in several conditions (86–90). GHB is an activity-dependent neurotransmitter synthesized within GABAergic interneurons



[reviewed in detail by Maitre et al. (91)]. Importantly, these GHB-containing interneurons play a critical role in the endogenous regulation of sleep-wake cycles by inhibiting cholinergic structures such as the basal forebrain (92). At increased doses used for exogenous administration, GHB exerts inhibitory effects by directly binding GABA-B receptors (93, 94); a necessary step for the homeostatic modulation of firing rates (95). Accordingly, the demonstrated suppression of alpha-delta sleep and dose-dependent upregulation of SWS by GHB likely occurs through a GABA-B receptor-mediated process analogous to both the endogenous production of homeostatic sleep pressure through normal wakeful activity and the exogenous driving of organized frontocortical networks with CT-DBS. Kothare et al. (96) reported a case of sodium oxybate use in an 8-year-old boy with a prior disorder of consciousness produced by encephalitis at age four, providing strong support for this mechanism. The boy presented with disseminated encephalomyelitis with thalamic lesions, poor sleep efficacy, and alpha-delta sleep alongside severe cognitive and attentional regulation problems indicating prefrontal downregulation characteristic of anterior forebrain mesocircuit dysfunction (30). Following 6 months of sodium oxybate treatment beginning 4 years after the initial event, he showed improvements in all measures of sleep including increased SWS and the disappearance of alpha-delta sleep, as well as improvements in measures of attention, executive function, and impulse control. We suggest that these findings, in concert with those of our patient subject, complementarily underscore the bi-directional carry-over effects of GABAergic upregulation between sleep and wakeful states. In our patient subject, upregulation of frontocortical GABAergic circuits during wakefulness resulted in the recovery of sleep architecture; In Kothare et al.'s patient subject, upregulation of GABAergic circuits during sleep resulted in the recovery of wakeful frontocortical function. Accordingly, we emphasize the notion that state-dependent activation of GABAergic circuits exerts a 24 h cyclical influence over organized neuronal function.

## Limitations and Future Directions

The present study has important limitations to consider. Due to the single-patient, observational nature of this study, interpretations of causality must be made with caution. Nevertheless, our primary findings of regression in both behavioral responsiveness and sleep features are temporally correlated with the discontinuation of CT-DBS ~12 months prior. As there had been no changes in medication or rehabilitation that could account for the sudden shift in these features, we feel it is reasonable to attribute these changes to a shift in neuronal dynamics resulting from the withdrawal of CT-DBS.

Furthermore, it is possible that our findings and proposed model will not generalize to the larger population of individuals with disorders of consciousness. However, evidence indicates that the prevailing network dynamics observed in this patient subject are not unique, but instead mechanistically characteristic

of the severely deafferented brain (97). Larger studies of sleep dynamics in patients with disorders of consciousness are needed to further clarify the potential value of sleep electrophysiology as a meaningful indicator of wakeful brain function. Additionally, although this is the first case in which alpha-delta sleep has been characterized in a patient with severe traumatic brain injury, we have previously described this phenomenon in a small number of minimally conscious state patients (98). Accordingly, we suggest that alpha-delta sleep and the implicated network dynamics may be present across many more patient subjects. Future studies should seek to identify the prevalence of alpha-delta sleep in individuals with disorders of consciousness, as well as to experimentally investigate the described prefrontal-ventral dysfunction model as a mechanism of alpha-delta sleep generation across populations. We suggest that our proposed model provides several possible experimental evaluations to determine its predictive validity in populations with alpha-delta sleep.

## AUTHOR CONTRIBUTIONS

JG: Study concept and design, data acquisition, data analysis and interpretation, manuscript preparation and revision; ZA: Data acquisition, data analysis, manuscript revision; PF: Clinical assessment, manuscript revision; NS: Study concept and design, data acquisition, clinical assessment, data interpretation, manuscript preparation and revision.

## FUNDING

This work was supported by NIH grants #HD51912 & #HL135465, the James S. McDonnell Foundation, and the Jerold B. Katz Foundation. PF is supported by NIH NINDS K23 NS096222, Leon Levy Neuroscience Fellowship Award, NIH UL1 TR000043 NCATS Rockefeller CTSA Program, and The Stavros Niarchos Foundation.

## ACKNOWLEDGMENTS

The authors thank Dr. Jonathan Victor for guidance regarding data analysis, as well as Dr. Mary Conte for the critical reading of this manuscript. We would like to acknowledge the clinical staff at New York Presbyterian Hospital as well as Rockefeller University Hospital for providing care to the patient during inpatient visits. We are grateful to the patient and his family for their continued participation in and support of this research.

## SUPPLEMENTARY MATERIAL

The Supplementary Material for this article can be found online at: <https://www.frontiersin.org/articles/10.3389/fneur.2019.00020/full#supplementary-material>

## REFERENCES

- Thengone DJ, Voss HU, Fridman EA, Schiff ND. Local changes in network structure contribute to late communication recovery after severe brain injury. *Sci Transl Med*. (2016) 8:368re5. doi: 10.1126/scitranslmed.aaf6113
- Voss HU, Ulug AM, Dyke JB, Watts R, Kobylarz EJ, Mccandliss BD, et al. Possible axonal regrowth in late recovery from the minimally conscious state. *J Clin Invest*. (2006) 116: 2005–11. doi: 10.1172/JCI27021
- Nakase-Richardson R, Whyte J, Giacino JT, Pavawalla S, Barnett SD, Yablon SA, et al. Longitudinal outcome of patients with disordered consciousness in the NIDRR TBI model systems programs. *J Neurotrauma* (2012) 29:59–65. doi: 10.1089/neu.2011.1829
- De Tanti A, Saviola D, Basagni B, Cavatorta S, Chiari M, Casalino S, et al. Recovery of consciousness after 7 years in vegetative state of non-traumatic origin: a single case study. *Brain Inj*. (2016) 30:1029–34. doi: 10.3109/02699052.2016.1147078
- Estraneo A, Moretta P, Loreto V, Lanzillo B, Santoro L, Trojano L. Late recovery after traumatic, anoxic, or hemorrhagic long-lasting vegetative state. *Neurology* (2010) 75:239–45. doi: 10.1212/WNL.0b013e3181e8e8cc
- Rossi Sebastiano D, Visani E, Panzica F, Sattin D, Bersano A, Nigri A, et al. Sleep patterns associated with the severity of impairment in a large cohort of patients with chronic disorders of consciousness. *Clin Neurophysiol*. (2018) 129:687–93. doi: 10.1016/j.clinph.2017.12.012
- Sandsmark DK, Kumar MA, Woodward CS, Schmitt SE, Park S, Lim MM. Sleep features on continuous electroencephalography predict rehabilitation outcomes after severe traumatic brain injury. *J Head Trauma Rehabil*. (2016) 31:101–7. doi: 10.1097/HTR.0000000000000217
- Forgacs PB, Conte MM, Fridman EA, Voss HU, Victor JD, Schiff ND. Preservation of electroencephalographic organization in patients with impaired consciousness and imaging-based evidence of command-following. *Ann Neurol*. (2014) 76:869–79. doi: 10.1002/ana.24283
- Ducharme-Crevier L, Press CA, Kurz JE, Mills MG, Goldstein JL, Wainwright MS. Early presence of sleep spindles on electroencephalography is associated with good outcome after pediatric cardiac arrest. *Pediatr Crit Care Med*. (2017) 18:452–60. doi: 10.1097/PCC.0000000000001137
- Urakami Y. Relationship between sleep spindles and clinical recovery in patients with traumatic brain injury: a simultaneous EEG and MEG study. *Clin EEG Neurosci*. (2012) 43:39–47. doi: 10.1177/1550059411428718
- Valente M, Placidi F, Oliveira AJ, Bigagli A, Morghen I, Proietti R, et al. Sleep organization pattern as a prognostic marker at the subacute stage of post-traumatic coma. *Clin Neurophysiol*. (2002) 113:1798–805. doi: 10.1016/S1388-2457(02)00218-3
- Mouthon A-L, van Hedel HJA, Meyer-Heim A, Kurth S, Ringli M, Pugin F, et al. High-density electroencephalographic recordings during sleep in children with disorders of consciousness. *NeuroImage Clin*. (2016) 11:468–75. doi: 10.1016/j.nicl.2016.03.012
- Arnaldi D, Terzaghi M, Cremascoli R, De Carli F, Maggioni G, Pistarini C, et al. The prognostic value of sleep patterns in disorders of consciousness in the sub-acute phase. *Clin Neurophysiol*. (2016) 127:1445–51. doi: 10.1016/j.clinph.2015.10.042
- Avantaggiato P, Molteni E, Formica F, Gigli GL, Valente M, Lorenzini S, et al. Polysomnographic sleep patterns in children and adolescents in unresponsive wakefulness syndrome. *J Head Trauma Rehabil*. (2015) 30:334–46. doi: 10.1097/HTR.0000000000000122
- Adams ZM, Forgacs PB, Conte MM, Schiff ND. Late and progressive alterations of sleep dynamics following central thalamic deep brain stimulation (CT-DBS) in chronic minimally conscious state. *Clin Neurophysiol*. (2016) 127:3086–92. doi: 10.1016/j.clinph.2016.06.028
- Hauri P, Hawkins DR. Alpha-delta sleep. *Electroencephalogr Clin Neurophysiol*. (1973) 34:233–7. doi: 10.1016/0013-4694(73)90250-2
- Giacino JT, Kalmar K, Whyte J. The JFK coma recovery scale-revised: measurement characteristics and diagnostic utility. *Arch Phys Med Rehabil*. (2004) 85:2020–9. doi: 10.1016/j.apmr.2004.02.033
- Schiff ND, Giacino JT, Kalmar K, Victor JD, Baker K, Gerber M, et al. Behavioural improvements with thalamic stimulation after severe traumatic brain injury. *Nature* (2007) 448:600–3. doi: 10.1038/nature06041
- Morel A, Magnin M, Jeanmonod D. Multiarchitectonic and stereotactic atlas of the human thalamus. *J Comp Neurol*. (1997) 387:588–630.
- Tatum WO, Selioutski O, Ochoa JG, Clary HM, Cheek J, Drislane FW, et al. American clinical neurophysiology society guideline 7: guidelines for EEG reporting. *Neurodiagn J*. (2016) 56:285–93. doi: 10.1080/21646821.2016.1245576
- Thomson DJ. Spectrum estimation and harmonic analysis. *Proc IEEE* (1982) 70:1055–96.
- Bokil H, Andrews P, Kulkarni JE, Mehta S, Mitra PP. Chronux: a platform for analyzing neural signals. *J Neurosci Methods* (2010) 192:146–51. doi: 10.1016/j.jneumeth.2010.06.020
- Gottselig JM, Bassetti CL, Achermann P. Power and coherence of sleep spindle frequency activity following hemispheric stroke. *Brain* (2002) 125:373–83. doi: 10.1093/brain/awf021
- Drewes AM, Svendsen L, Taagholt SJ, Bjerregård K, Nielsen KD, Hansen B. Sleep in rheumatoid arthritis: a comparison with healthy subjects and studies of sleep/wake interactions. *Br J Rheumatol*. (1998) 37:71–81.
- Manu P, Lane TJ, Matthews DA, Castriotta RJ, Watson RK, Abeles M. Alpha-delta sleep in patients with a chief complaint of chronic fatigue. *South Med J*. (1994) 87:465–70.
- Roizenblatt S, Moldofsky H, Benedito-Silva AA, Tufik S. Alpha sleep characteristics in fibromyalgia. *Arthritis Rheum*. (2001) 44:222–30. doi: 10.1002/1529-0131(200101)44:1<222::AID-ANR29>3.0.CO;2-K
- Roehrs JD. Alpha delta sleep in younger veterans and active duty military personnel: an unrecognized epidemic? *J Clin Sleep Med*. (2015) 11:277. doi: 10.5664/jcsm.4546
- Sloan EP, Maunder RG, Hunter JJ, Moldofsky H. Insecure attachment is associated with the  $\alpha$ -EEG anomaly during sleep. *Biopsychosoc Med*. (2007) 1:20. doi: 10.1186/1751-0759-1-20
- Jaimcharyatam N, Rodriguez CL, Budur K. Prevalence and correlates of alpha-delta sleep in major depressive disorders. *Innov Clin Neurosci*. (2011) 8:35–49.
- Schiff ND. Recovery of consciousness after brain injury: a mesocircuit hypothesis. *Trends Neurosci*. (2010) 33:1–9. doi: 10.1016/j.tins.2009.11.002
- Maxwell WL, MacKinnon MA, Smith DH, McIntosh TK, Graham DI. Thalamic nuclei after human blunt head injury. *J Neuropathol Exp Neurol*. (2006) 65:478–88. doi: 10.1097/01.jnen.0000229241.28619.75
- Kawai N, Maeda Y, Kudomi N, Yamamoto Y, Nishiyama Y, Tamiya T. Focal neuronal damage in patients with neuropsychological impairment after diffuse traumatic brain injury: evaluation using 11 C-flumazenil positron emission tomography with statistical image analysis. *J Neurotrauma* (2010) 27:2131–8. doi: 10.1089/neu.2010.1464
- Schiff ND. Central thalamic contributions to arousal regulation and neurological disorders of consciousness. *Ann N Y Acad Sci*. (2008) 1129:105–18. doi: 10.1196/annals.1417.029
- Giacino J, Fins JJ, Machado A, Schiff ND. Central thalamic deep brain stimulation to promote recovery from chronic posttraumatic minimally conscious state: challenges and opportunities. *Neuromodulation* (2012) 15:339–49. doi: 10.1111/j.1525-1403.2012.00458.x
- Fridman EA, Beattie BJ, Broft A, Laureys S, Schiff ND. Regional cerebral metabolic patterns demonstrate the role of anterior forebrain mesocircuit dysfunction in the severely injured brain. *Proc Natl Acad Sci USA*. (2014) 111:6473–8. doi: 10.1073/pnas.1320969111
- Chatelle C, Thibaut A, Gosseries O, Bruno M-A, Demertzi A, Bernard C, et al. Changes in cerebral metabolism in patients with a minimally conscious state responding to zolpidem. *Front Hum Neurosci*. (2014) 8:917. doi: 10.3389/fnhum.2014.00917
- Williams ST, Conte MM, Goldfine AM, Noirhomme Q, Gosseries O, Thonnard M, et al. Common resting brain dynamics indicate a possible mechanism underlying zolpidem response in severe brain injury. *Elife* (2013) 2:e01157. doi: 10.7554/eLife.01157
- Vyazovskiy VV, Cirelli C, Pfister-Genskow M, Faraguna U, Tononi G. Molecular and electrophysiological evidence for net synaptic potentiation in wake and depression in sleep. *Nat Neurosci*. (2008) 11:200–8. doi: 10.1038/nn2035
- Huber R, Mäki H, Rosanova M, Casarotto S, Canali P, Casali AG, et al. Human cortical excitability increases with time awake. *Cereb Cortex* (2013) 23:332–8. doi: 10.1093/cercor/bhs014

40. Kuhn M, Wolf E, Maier JG, Mainberger F, Feige B, Schmid H, et al. Sleep recalibrates homeostatic and associative synaptic plasticity in the human cortex. *Nat Commun.* (2016) 7:12455. doi: 10.1038/ncomms12455
41. Ly JQM, Gaggioni G, Chellappa SL, Papachilleos S, Brzozowski A, Borsu C, et al. Circadian regulation of human cortical excitability. *Nat Commun.* (2016) 7:11828. doi: 10.1038/ncomms11828
42. Meisel C, Schulze-Bonhage A, Freestone D, Cook MJ, Achermann P, Plenz D. Intrinsic excitability measures track antiepileptic drug action and uncover increasing/decreasing excitability over the wake/sleep cycle. *Proc Natl Acad Sci USA.* (2015) 112:14694–9. doi: 10.1073/pnas.1513716112
43. Vyazovskiy VV, Olcese U, Lazimy YM, Faraguna U, Esser SK, Williams JC, et al. Cortical firing and sleep homeostasis. *Neuron* (2009) 63:865–78. doi: 10.1016/j.neuron.2009.08.024
44. Miyawaki H, Diba K. Regulation of hippocampal firing by network oscillations during sleep. *Curr Biol.* (2016) 26:893–902. doi: 10.1016/j.cub.2016.02.024
45. Dash MB, Douglas CL, Vyazovskiy VV, Cirelli C, Tononi G. Long-term homeostasis of extracellular glutamate in the rat cerebral cortex across sleep and waking states. *J Neurosci.* (2009) 29:620–9. doi: 10.1523/JNEUROSCI.5486-08.2009
46. Hanlon EC, Faraguna U, Vyazovskiy VV, Tononi G, Cirelli C. Effects of skilled training on sleep slow wave activity and cortical gene expression in the rat. *Sleep* (2009) 32:719–29. doi: 10.1093/sleep/32.6.719
47. Rodriguez AV, Funk CM, Vyazovskiy VV, Nir Y, Tononi G, Cirelli C. Why does sleep slow-wave activity increase after extended wake? assessing the effects of increased cortical firing during wake and sleep. *J Neurosci.* (2016) 36:12436–47. doi: 10.1523/JNEUROSCI.1614-16.2016
48. Huber R, Esser SK, Ferrarelli F, Massimini M, Peterson MJ, Tononi G. TMS-induced cortical potentiation during wakefulness locally increases slow wave activity during sleep. *PLoS ONE* (2007) 2:e276. doi: 10.1371/journal.pone.0000276
49. Tononi G, Cirelli C. Sleep function and synaptic homeostasis. *Sleep Med Rev.* (2006) 10:49–62. doi: 10.1016/j.smrv.2005.05.002
50. Tononi G, Cirelli C. Sleep and synaptic homeostasis: a hypothesis. *Brain Res Bull.* (2003) 62:143–50. doi: 10.1016/j.brainresbull.2003.09.004
51. Tononi G, Cirelli C. Sleep and the price of plasticity: from synaptic and cellular homeostasis to memory consolidation and integration. *Neuron* (2014) 81:12–34. doi: 10.1016/j.neuron.2013.12.025
52. Cirelli C. Sleep, synaptic homeostasis and neuronal firing rates. *Curr Opin Neurobiol.* (2017) 44:72–9. doi: 10.1016/j.conb.2017.03.016
53. Shirvalkar P, Seth M, Schiff ND, Herrera DG. Cognitive enhancement with central thalamic electrical stimulation. *Proc Natl Acad Sci USA.* (2006) 103:17007–12. doi: 10.1073/pnas.0604811103
54. Ribeiro S, Mello CV, Velho T, Gardner TJ, Jarvis ED, Pavlides C. Induction of hippocampal long-term potentiation during waking leads to increased extrahippocampal zif-268 expression during ensuing rapid-eye-movement sleep. *J Neurosci.* (2002) 22:10914–23. doi: 10.1523/JNEUROSCI.22-24-10914.2002
55. Huber R, Ghilardi MF, Massimini M, Ferrarelli F, Riedner BA, Peterson MJ, et al. Arm immobilization causes cortical plastic changes and locally decreases sleep slow wave activity. *Nat Neurosci.* (2006) 9:1169–76. doi: 10.1038/nn1758
56. Rudolph M, Pelletier JG, Paré D, Destexhe A. Characterization of synaptic conductances and integrative properties during electrically induced EEG-activated states in neocortical neurons *in vivo*. *J Neurophysiol.* (2005) 94:2805–21. doi: 10.1152/jn.01313.2004
57. Reiber J, Lebel M. Wicket spikes: clinical correlates of a previously undescribed EEG pattern. *Can J Neurol Sci.* (1977) 4:39–47. doi: 10.1017/S0317167100120396
58. Kuhlman WN. Functional topography of the human mu rhythm. *Electroencephalogr Clin Neurophysiol.* (1978) 44:83–93. doi: 10.1016/0013-4694(78)90107-4
59. Rains JC, Penzien DB. Sleep and chronic pain: challenges to the alpha-EEG sleep pattern as a pain specific sleep anomaly. *J Psychosom Res.* (2003) 54:77–83. doi: 10.1016/S0022-3999(02)00545-7
60. Mahowald M, Mahowald M. Nighttime sleep and daytime functioning (sleepiness and fatigue) in less well-defined chronic rheumatic diseases with particular reference to the “alpha-delta NREM sleep anomaly.” *Sleep Med.* (2000) 1:195–207. doi: 10.1016/S1389-9457(00)00029-0
61. Dolsen MR, Cheng P, Arnedt JT, Swanson L, Casement MD, Kim HS, et al. Neurophysiological correlates of suicidal ideation in major depressive disorder: hyperarousal during sleep. *J Affect Disord.* (2017) 212:160–6. doi: 10.1016/j.jad.2017.01.025
62. Drewes AM, Nielsen KD, Arendt-Nielsen L, Birket-Smith L, Hansen LM. The effect of cutaneous and deep pain on the electroencephalogram during sleep an experimental study. *Sleep* (1997) 20:632–40. doi: 10.1093/sleep/20.8.632
63. Steriade M, Parent A, Paré D, Smith Y. Cholinergic and non-cholinergic neurons of cat basal forebrain project to reticular and mediodorsal thalamic nuclei. *Brain Res.* (1987) 408:372–6. doi: 10.1016/0006-8993(87)90408-2
64. Markello RD, Spreng RN, Luh WM, Anderson AK, De Rosa E. Segregation of the human basal forebrain using resting state functional MRI. *Neuroimage* (2018) 173:287–97. doi: 10.1016/j.neuroimage.2018.02.042
65. Parent A, Paré D, Smith Y, Steriade M. Basal forebrain cholinergic and noncholinergic projections to the thalamus and brainstem in cats and monkeys. *J Comp Neurol.* (1988) 277:281–301. doi: 10.1002/cne.902770209
66. Blumenfeld H, McCormick DA. Corticothalamic inputs control the pattern of activity generated in thalamocortical networks. *J Neurosci.* (2000) 20:5153–62. doi: 10.1523/JNEUROSCI.20-13-05153.2000
67. Lorincz ML, Crunelli V, Hughes SW. Cellular dynamics of cholinergically induced alpha (8 - 13 Hz) rhythms in sensory thalamic nuclei *in vitro*. *J Neurosci.* (2008) 28:660–71. doi: 10.1523/JNEUROSCI.4468-07.2008
68. Lorincz ML, Kékesi KA, Juhász KA, Crunelli V, Hughes SW. Temporal framing of thalamic relay-mode firing by phasic inhibition during the alpha rhythm. *Neuron* (2009) 63:683–96. doi: 10.1016/j.neuron.2009.08.012
69. Vijayan S, Kopell NJ. Thalamic model of awake alpha oscillations and implications for stimulus processing. *Proc Natl Acad Sci USA.* (2012) 109:18553–8. doi: 10.1073/pnas.1215385109
70. Vijayan S, Klerman EB, Adler GK, Kopell NJ. Thalamic mechanisms underlying alpha-delta sleep with implications for fibromyalgia. *J Neurophysiol.* (2015) 114:1923–30. doi: 10.1152/jn.00280.2015
71. Allada R, Cirelli C, Sehgal A. Molecular mechanisms of sleep homeostasis in flies and mammals. *Cold Spring Harb Perspect Biol.* (2017) 9:a027730. doi: 10.1101/cshperspect.a027730
72. Ceko M, Bushnell MC, Gracely RH. Neurobiology underlying fibromyalgia symptoms. *Pain Res Treat* (2012) 2012:585419. doi: 10.1155/2012/585419
73. Lutz J, Jäger L, De Quervain D, Krauseneck T, Padberg F, Wichnalek M, et al. White and gray matter abnormalities in the brain of patients with fibromyalgia: a diffusion-tensor and volumetric imaging study. *Arthritis Rheum.* (2008) 58:3960–9. doi: 10.1002/art.24070
74. Ferrarelli F, Tononi G. Reduced sleep spindle activity point to a TRN-MD thalamus-PFC circuit dysfunction in schizophrenia. *Schizophr Res.* (2016) 180:36–43. doi: 10.1016/j.schres.2016.05.023
75. Kantrowitz J, Citrome L, Javitt D. GABAB Receptors, schizophrenia and sleep dysfunction. *CNS Drugs* (2009) 23:681–91. doi: 10.2165/00023210-200923080-00005
76. Giraldo-Chica M, Woodward ND. Review of thalamocortical resting-state fMRI studies in schizophrenia. *Schizophr Res.* (2017) 180:58–63. doi: 10.1016/j.schres.2016.08.005
77. Bora E, Fornito A, Pantelis C, Yücel M. Gray matter abnormalities in major depressive disorder: a meta-analysis of voxel based morphometry studies. *J Affect Disord.* (2012) 138:9–18. doi: 10.1016/j.jad.2011.03.049
78. Rajkowska G, O'Dwyer G, Teleki Z, Stockmeier CA, Miguel-Hidalgo JJ. GABAergic neurons immunoreactive for calcium binding proteins are reduced in the prefrontal cortex in major depression. *Neuropsychopharmacology* (2007) 32:471–82. doi: 10.1038/sj.npp.1301234
79. Hasler G, van der Veen J, Tümonis T, Meyers N, Shen J, Drevets WC. Reduced prefrontal glutamate/glutamine and  $\gamma$ -aminobutyric acid levels in major depression determined using proton magnetic resonance spectroscopy. *Arch Gen Psychiatry* (2007) 64:193–200. doi: 10.1001/archpsyc.64.2.193.PDF
80. Nofzinger EA, Buysse DJ, Germain A, Price JC, Meltzer CC, Miewald JM, et al. Alterations in regional cerebral glucose metabolism across waking and non-rapid eye movement sleep in depression. *Arch Gen Psychiatry* (2005) 62:387–96. doi: 10.1001/archpsyc.62.4.387
81. Stevens JS, Jovanovic T, Fani N, Ely TD, Glover EM, Bradley B, et al. Disrupted amygdala-prefrontal functional connectivity in civilian women

- with posttraumatic stress disorder. *J Psychiatr Res.* (2013) 47:1469–78. doi: 10.1016/j.jpsychires.2013.05.031
82. Brown VM, Labar KS, Haswell CC, Gold AL, Beall SK, Van Voorhees E, et al. Altered resting-state functional connectivity of basolateral and centromedial amygdala complexes in posttraumatic stress disorder. *Neuropsychopharmacology* (2014) 39:351–9. doi: 10.1038/npp.2013.197
  83. Liao W, Qiu C, Gentili C, Walter M, Pan Z, Ding J, et al. Altered effective connectivity network of the amygdala in social anxiety disorder: a resting-state fMRI study. *PLoS ONE* (2010) 5:e15238. doi: 10.1371/journal.pone.0015238
  84. Kim MJ, Gee DG, Loucks RA, Davis FC, Whalen PJ. Anxiety dissociates dorsal and ventral medial prefrontal cortex functional connectivity with the amygdala at rest. *Cereb Cortex* (2011) 21:1667–73. doi: 10.1093/cercor/bhq237
  85. Prater KE, Hosanagar A, Klumpp H, Angstadt M, Phan KL. Aberrant amygdala-frontal cortex connectivity during perception of fearful faces and at rest in generalized social anxiety disorder. *Depress Anxiety* (2013) 30:234–41. doi: 10.1002/da.22014
  86. Moldofsky H, Inhaber NH, Guinta DR, Alvarez-Horine SB. Effects of sodium oxybate on sleep physiology and sleep/wake-related symptoms in patients with fibromyalgia syndrome: a double-blind, randomized, placebo-controlled study. *J Rheumatol.* (2010) 37:2156–66. doi: 10.3899/jrheum.091041
  87. Scharf M, Baumann M, Berkowitz D. The effects of sodium oxybate on clinical symptoms and sleep patterns in patients with fibromyalgia. *J Rheumatol.* (2003) 30:1070–4.
  88. Tanaka Z, Mukai A, Takayanagi Y, Muto A, Mikami Y, Miyakoshi T, et al. Clinical application of 4-hydroxybutyrate sodium and 4-butyrolactone in neuropsychiatric patients. *Psychiatry Clin Neurosci.* (1966) 20:9–17. doi: 10.1111/j.1440-1819.1966.tb00055.x
  89. Maremmani AGI, Bacciardi S, Rovai L, Rugani F, Dell'Osso L, Maremmani I. Sodium oxybate as off-label treatment for anxiety disorder: successful outcome in a low-energy anxious resistant patient. *Addict Disord their Treat.* (2015) 14:198–202. doi: 10.1097/ADT.0000000000000055
  90. Schwartz TL. Gamma hydroxy butyric acid and sodium oxybate used to treat posttraumatic stress disorder. *CNS Spectr.* (2007) 12:884–6. doi: 10.1017/S1092852900015649
  91. Maitre M, Klein C, Mensah-Nyagan AG. Mechanisms for the specific properties of  $\gamma$ -hydroxybutyrate in brain. *Med Res Rev.* (2016) 36:363–88. doi: 10.1002/med.21382
  92. Anacleit C, Pedersen NP, Ferrari LL, Venner A, Bass CE, Arrigoni E, et al. Basal forebrain control of wakefulness and cortical rhythms. *Nat Commun.* (2015) 6:8744. doi: 10.1038/ncomms9744
  93. Nava F, Carta G, Bortolato M, Gessa GL.  $\gamma$ -Hydroxybutyric acid and baclofen decrease extracellular acetylcholine levels in the hippocampus via GABAB receptors. *Eur J Pharmacol.* (2001) 430:261–3. doi: 10.1016/S0014-2999(01)01163-3
  94. Kaupmann K, Cryan JF, Wellendorph P, Mombereau C, Sansig G, Klebs K, et al. Specific gamma-hydroxybutyrate-binding sites but loss of pharmacological effects of gamma-hydroxybutyrate in GABAB(1)-deficient mice. *Eur J Neurosci.* (2003) 18:2722–30. doi: 10.1111/j.1460-9568.2003.03013.x
  95. Vertkin I, Styr B, Slomowitz E, Ofir N, Shapira I, Berner D, et al. GABA B receptor deficiency causes failure of neuronal homeostasis in hippocampal networks. *Proc Natl Acad Sci USA.* (2015) 112:E3291–9. doi: 10.1073/pnas.1424810112
  96. Kothare SV, Adams R, Valencia I, Faerber EC, Grant ML. Improved sleep and neurocognitive functions in a child with thalamic lesions on sodium oxybate. *Neurology* (2007) 68:1157–8. doi: 10.1212/01.wnl.0000258658.00692.36
  97. Schiff ND. Mesocircuit mechanisms underlying recovery of consciousness following severe brain injuries: model and predictions. In: Monti M, Sannita W, editors. *Brain Function and Responsiveness in Disorders of Consciousness*. Cham: Springer International Publishing. (2016) p. 195–204.
  98. Gottshall JL, Adams ZM, Forgacs PB, Nauvel TJ, Schiff ND. Novel characterization of an architecturally distinct sleep stage and its implications for recovery from the minimally conscious state. In: *Cognitive Neuroscience Society 24th Annual Meeting*. San Francisco, CA (2017).

**Conflict of Interest Statement:** The authors declare that the research was conducted in the absence of any commercial or financial relationships that could be construed as a potential conflict of interest.

Copyright © 2019 Gottshall, Adams, Forgacs and Schiff. This is an open-access article distributed under the terms of the Creative Commons Attribution License (CC BY). The use, distribution or reproduction in other forums is permitted, provided the original author(s) and the copyright owner(s) are credited and that the original publication in this journal is cited, in accordance with accepted academic practice. No use, distribution or reproduction is permitted which does not comply with these terms.





# Do Sensory Stimulation Programs Have an Impact on Consciousness Recovery?

Lijuan Cheng<sup>1†</sup>, Daniela Cortese<sup>2†</sup>, Martin M. Monti<sup>3,4</sup>, Fuyan Wang<sup>1</sup>,  
Francesco Riganello<sup>2</sup>, Francesco Arcuri<sup>2</sup>, Haibo Di<sup>1\*</sup> and Caroline Schnakers<sup>5\*</sup>

<sup>1</sup> International Vegetative State and Consciousness Science Institute, Hangzhou Normal University, Hangzhou, China,

<sup>2</sup> Research in Advanced Neurorehabilitation, S. Anna Institute, Crotone, Italy, <sup>3</sup> Department of Psychology, University of California, Los Angeles, Los Angeles, CA, United States, <sup>4</sup> Department of Neurosurgery, David Geffen School of Medicine at UCLA, Los Angeles, CA, United States, <sup>5</sup> Research Institute, Casa Colina Hospital and Centers for Healthcare, Pomona, CA, United States

## OPEN ACCESS

### Edited by:

Roland Beisteiner,  
Medizinische Universität Wien, Austria

### Reviewed by:

Martin Kronbichler,  
University of Salzburg, Austria  
Friedemann Mueller,  
Schön Klinik, Germany  
Ingrid Brands,  
Libra Rehabilitation & Audiology,  
Netherlands

### \*Correspondence:

Caroline Schnakers  
cschnakers@casacolina.org  
Haibo Di  
dihai19@aliyun.com

<sup>†</sup>These authors have contributed  
equally to this work

### Specialty section:

This article was submitted to  
Applied Neuroimaging,  
a section of the journal  
Frontiers in Neurology

**Received:** 29 March 2018

**Accepted:** 13 September 2018

**Published:** 02 October 2018

### Citation:

Cheng L, Cortese D, Monti MM,  
Wang F, Riganello F, Arcuri F, Di H and  
Schnakers C (2018) Do Sensory  
Stimulation Programs Have an Impact  
on Consciousness Recovery?  
Front. Neurol. 9:826.  
doi: 10.3389/fneur.2018.00826

**Objectives:** Considering sensory stimulation programs (SSP) as a treatment for disorders of consciousness is still debated today. Previous studies investigating its efficacy were affected by various biases among which small sample size and spontaneous recovery. In this study, treatment-related changes were assessed using time-series design in patients with disorders of consciousness (i.e., vegetative state—VS and minimally conscious state—MCS).

**Methods:** A withdrawal design (ABAB) was used. During B phases, patients underwent a SSP (3 days a week, including auditory, visual, tactile, olfactory, and gustatory stimulation). The program was not applied during A phases. To assess behavioral changes, the Coma Recovery Scale-Revised (CRS-R) was administered by an independent rater on a weekly basis, across all phases. Each phase lasted 4 weeks. In a subset of patients, resting state functional magnetic resonance imaging (fMRI) data were collected at the end of each phase.

**Results:** Twenty nine patients ( $48 \pm 19$  years old; 15 traumatic; 21 > a year post-injury; 11 VS and 18 MCS) were included in our study. Higher CRS-R total scores (medium effect size) as well as higher arousal and oromotor subscores were observed in the B phases (treatment) as compared to A phases (no treatment), in the MCS group but not in the VS group. In the three patients who underwent fMRI analyses, a modulation of metabolic activity related to treatment was observed in middle frontal gyrus, superior temporal gyrus as well as ventro-anterior thalamic nucleus.

**Conclusion:** Our results suggest that SSP may not be sufficient to restore consciousness. SSP might nevertheless lead to improved behavioral responsiveness in MCS patients. Our results show higher CRS-R total scores when treatment is applied, and more exactly, increased arousal and oromotor functions.

**Keywords:** brain injuries, consciousness, persistent vegetative state, minimally conscious state, sensory stimulation

## INTRODUCTION

Amantadine is till now the only treatment that has shown its efficacy in patients with severe brain injury (1). Finding new ways to treat patients recovering from disorders of consciousness is therefore one of the biggest challenge facing clinicians (2). Patients can stay during months to years in disorders of consciousness such as vegetative state (which is characterized by the presence of arousal but the absence of awareness) or minimally conscious state (which is characterized by the presence of fluctuating but reproducible signs of consciousness but an absence of reliable communication), leading to a financial and ethical conundrum for the families (3, 4). Sensory stimulation programs (SSP) have been the most studied treatment in the neurorehabilitation field (5). These programs are based on the idea that an enriched environment benefits brain plasticity and improves the recovery of injured brains (6).

Rosenzweig and coworkers who were the first to introduce “environmental enrichment” in the field of animal research four decades ago showed that the morphology and physiology of the brain can be altered by modifying the quality and intensity of environmental stimulation (7, 8). Enriched environment has been associated with changes in cortical thickness (9, 10), changes in neurons size, number and connections (11–16). Exposure to such environment has shown to be beneficial following experimental brain lesions (17–19), particularly, in terms of recovery of cognitive (e.g., learning and memory) and motor functions (20–22). Enriched environment following brain injury has also shown additional beneficial effects such as decreasing lesion size or enhancing dendritic branching (6, 23–25).

Based on animal research, the Institutes for the Achievement of Human Potential (IAHP) have introduced SSP in the field of neurorehabilitation. Despite the lack of scientific evidence in human subjects, these programs were supported on the principle that they could enhance the rehabilitative process by avoiding environmental deprivation and promoting synaptic reinnervation, thus accelerating the recovery from disorders of consciousness in severely brain injured patients (26). Numerous studies have investigated SSP in patients with disorders of consciousness [for a review see: (5, 27, 28)]. While Padilla (5) concluded that the current literature provided strong evidence that multimodal sensory stimulation improves arousal and enhances clinical outcomes for patients in a coma or persistent vegetative state, both Meyer (28) and Cossu (27) reported that there was conflicting evidence regarding the clinical relevance and the benefit of sensory stimulation in patients recovering from coma. Most studies are, indeed, affected by various methodological biases such as, among others, poor description of the disorders of consciousness, poor validity, and/or sensitivity of the outcome measure, small sample size as well as spontaneous recovery. Indeed, these studies were mostly performed in the acute stage, a period during which spontaneous recovery has the highest probability to occur. Interestingly, several recent studies investigated whether the improvements observed after SSP exceeded spontaneous recovery using a time-series design. However, they all included a small number of patients ( $n < 15$ ) (29–31). Finally, neuroimaging data was collected in a subset

of patients. Only one study recently investigated the changes in brain activity related to treatment. Pape and coworkers examined the effects of a unimodal stimulation program in 15 patients using familiar auditory stimulation and found higher activation in the language network in the treated group as compared to the control group, suggesting that coupling behavioral measures with neuroimaging may help to understand what impact sensory stimulation has on the recovering brain (32).

Therefore, the aim of this study was to assess the impact of SSP on the recovery of consciousness (as measured by the Coma Recovery Scale-Revised) and to determine treatment-related changes using a time-series design in a group of patients with disorders of consciousness (i.e., VS and MCS).

## METHODS

### Inclusion/Exclusion Criteria

Severely brain injured patients diagnosed as being in a vegetative state (VS) (3) or in a minimally conscious state (MCS) (4) were recruited from the Rehabilitation Center for Brain Damage of Wujing Hospital (Hangzhou, China) and the Research in Advanced Neurorehabilitation of S. Anna Institute (Crotone, Italy). Patients were only followed during their stay in the inpatient rehabilitation unit. Patients were included in the study if they (a) were at least 18 years old, (b) were at least a month post-injury, and (c) presented periods of spontaneous eye opening. Traumatic and non-traumatic etiologies were included in this study. Patients were excluded if they had (a) a documented history of prior brain injury, (b) premorbid history of uncorrected visual or hearing impairments, (c) premorbid history of developmental, psychiatric, or neurologic illness resulting in documented functional disability up to the time of the injury, (d) acute illness, (e) emerged from MCS during the first A phase as assessed by the Coma Recovery Scale—Revised (33), and (f) medical complications during the study. Information regarding patients’ comorbidities and education were not collected. This study was carried out in accordance with the recommendations of the ethics committee of the Hangzhou Normal University (Hangzhou, China) and the S. Anna Institute (Crotone, Italy). The study was approved by the ethics committee of each participating center. Written informed consent was obtained from the patients’ legal surrogate in accordance with the Declaration of Helsinki.

### Behavioral Data Acquisition and Analyses Procedure

Time series design was chosen to address previous criticisms on spontaneous recovery (34). Indeed, one advantage of this design is to compare baselines to treatment and, therefore, to measure how the presence/absence of the target treatment modulates the outcome measure within each participant. An ABAB withdrawal design (where A = baseline and B = treatment) was preferred to an AB or ABA design since it provided an opportunity to repeatedly collect data on the relationship between the treatment and the outcomes of interest. Each phase of this ABAB design lasted 4 weeks, as previously used (27, 29). During A phases, no SSP was administered, the patients only received until 3 h a

day for 5 days a week of comprehensive rehabilitation including nursing care as well as physical therapy, respiratory therapy and speech therapy. During B phases, a SSP (described below) was also administered 3 times a week (i.e., Monday, Wednesday, and Friday; twice a day), as agreed with the medical staff.

The Coma Recovery Scale—Revised (CRS-R) (33) was chosen as our outcome measure and was administered once weekly (i.e., Saturday) for the full length of the study (i.e., across all phases) to assess changes in behavioral responsiveness. The Chinese and Italian translations of the scale were used in this study (35, 36). The CRS-R was designed to differentiate VS from MCS patients and is recommended by the American Congress of Rehabilitation Medicine to assess patients with disorders of consciousness (37). It consists of 23 hierarchically-arranged items divided into six subscales assessing auditory, visual, motor, oromotor, communication, and arousal functions. The rater performing the CRS-R assessments was not involved in the administration of the SSP and was not aware of the study design (i.e., ABAB). In each center, the same rater assessed the patients every week.

## SSP

The administration of SSP corresponds to the B phases of our procedure. Based on the literature, we opted for a multi-sensory stimulation program including auditory, visual, tactile, olfactory, and gustatory stimuli (5, 28). Familiar stimulations were used since it has been shown that there is a higher probability to observe an improved behavioral response when emotional stimuli are presented (5, 38). Each stimulation was administered three times, on the patient's right and left side alternatively (inter-stimulus interval of 20 s). The order in which sensory stimulations were applied was randomized for each session. The program lasted around 20 min per session.

The program included the following stimulation: (a) Visual stimulation. A picture of the family member with whom the patient had the closest relationship before the injury was presented to the patient. If not possible to obtain, a picture with a high positive valence (valence of 8 according to the International Affective Picture System) was used (39). The picture was slowly moved 45 degrees to the right and left of the vertical midline and 45 degrees above and below the horizontal midline. (b) Auditory stimulation. The patient's favorite music before the injury was chosen. If not possible to obtain, classical music was used. (c) Tactile stimulation. Fingertips were used to apply firm pressure down the patient's arm, from the shoulder to the wrist. Areas with fractures as well as skin or muscular lesions were not stimulated. (d) Olfactory stimulation. The smell the patient preferred before the injury (or, by default, vanilla concentrate) was presented underneath the patient's nose. In case of tracheotomy, the entrance of the cannula was covered. (e) Gustatory stimulation. The flavor the patient preferred before the injury (or, by default, vanilla concentrate) was chosen. A stick soaked of this flavor was introduced into the patient's mouth.

Several recommendations had to be followed such as: applying the treatment while the patients were in a wakeful state with eyes open in a setting with minimal ambient noise and respecting a 30 min rest before each session (i.e., absence of nursing care).

## Statistical Analyses

A mixed-design ANCOVA was performed on the CRS-R total scores with phase (ABAB) and week (1-2-3-4) as within-subject factors, diagnosis (VS vs. MCS) and etiology (traumatic vs. non-traumatic) as between-subjects factors, and time since injury as a covariate. The effect size was estimated, for each significant result, using a partial- $\eta^2$  statistic (small:  $\eta_p^2 \geq 0.01$ ; medium:  $\eta_p^2 \geq 0.06$ ; large:  $\eta_p^2 \geq 0.14$ ) (40). Planned comparisons were intended to be used to compare CRS-R total scores during B phases (treatment) vs. A phases (no treatment) for both VS and MCS groups but also within each group, separately. Wilcoxon tests were performed to compare CRS-R mean subscores during A phases and B phases for both VS and MCS groups but also within each group, separately.

## fMRI Data Acquisition and Analyses

Neuroimaging data were acquired at one of the two centers which had Magnetic Resonance Imaging (MRI), the Rehabilitation Center for Brain Damage of Wujing Hospital (Hangzhou, China). Using a 1.5 Tesla Siemens Magnetom Essenza MRI system (Siemens AG, Munich, Germany). Resting state functional MRI (fMRI) data were collected in a subset of patients at the end of each phase (on the fourth week) to assess the effects of the treatment on brain activity. Inclusion criteria were: stability of vital parameters and absence of contra-indications for entering the MRI environment. The preprocessed data was used to calculate, on a single-subject basis, the Amplitude of Low Frequency Fluctuations (ALFF) across the whole brain (band frequency of interest: 0.01–0.1 Hz). Results were Z-scored across the full brain. Group data was analyzed using a repeated measures ABAB design, to assess the effect of phase on the ALFF maps. For more information regarding the fMRI acquisition and analyses, see **Supplementary Material**.

## RESULTS

### Participants

Twenty nine patients ( $48 \pm 19$  years old; 19 men; age range: 20–79 years) were included in this study. The etiology of brain injury was traumatic ( $n = 15$ ), anoxic ( $n = 5$ ), ischemic stroke ( $n = 5$ ), hemorrhagic ( $n = 3$ ), or metabolic ( $n = 1$ ). The time since injury was more than a year for 21 patients (1.04–10.7 years) and less than a year for eight patients (41–348 days). According to CRS-R scores (**Table 1**), 11 patients presented a stable diagnosis of VS and 18 patients presented a stable diagnosis of MCS during the first A phase. Eighteen patients were recruited at the Rehabilitation Center for Brain Damage of Wujing Hospital (Hangzhou, China) and 11 at Research in Advanced Neurorehabilitation, S. Anna Institute (Crotone, Italy). To test differences in patients' population among both centers, *T*-tests and Chi-squares were used to compare variables that are known to impact patients' outcome (2): time since injury, etiology (i.e., traumatic vs. non-traumatic) and diagnosis (i.e., VS vs. MCS). We did not find any difference between centers ( $t_{(27)} = 1.53$ ,  $p = 0.14$ ;  $\chi^2_{(1)} = 0.96$ ,  $p = 0.33$ ; and,  $\chi^2_{(1)} = 1.65$ ,  $p = 0.2$ , respectively). The medications most frequently administered included; antispastics, anticonvulsants, anti-acid,

**TABLE 1** | Demographic data for minimally conscious (MCS) and vegetative (VS) patients.

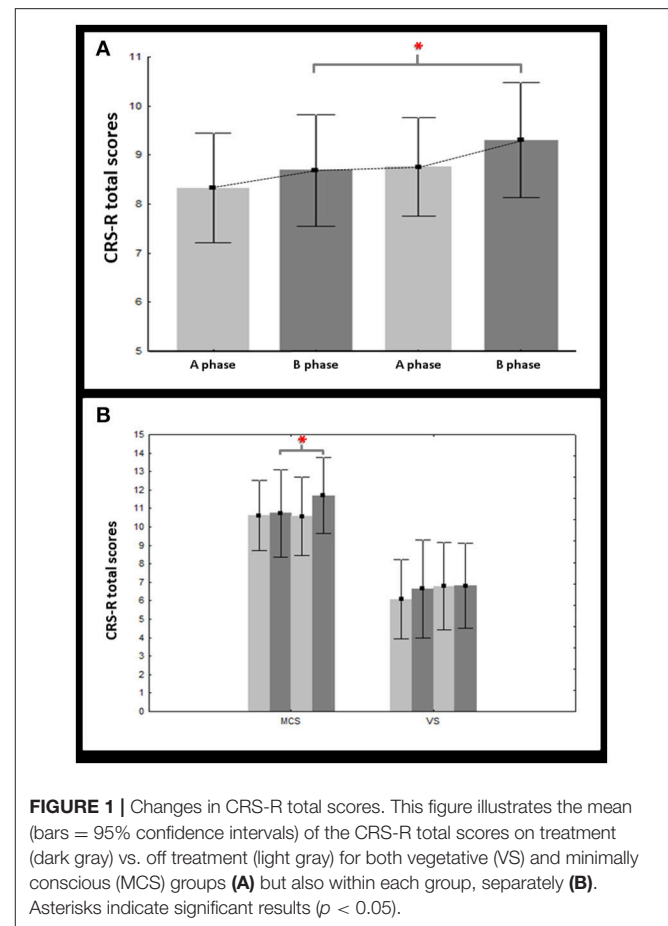
Patient	Etiology	TSI	CRS-R	AF	VF	MF	OF	C	Ar
MCS 1	Traumatic	4.8y	13	2	3	5	1	0	2
MCS 2	Traumatic	3.2y	10	2	3	2	1	0	2
MCS 3	Traumatic	4.48y	10	0	3	5	0	0	2
MCS 4	Stroke	2.87y	13	2	3	4	2	0	2
MCS 5	Stroke	2.93y	10	2	3	2	1	0	2
MCS 6	Traumatic	2.93y	9	2	3	2	1	0	1
MCS 7	Stroke	2.91y	15	4	5	2	1	1	2
MCS 8	Anoxic	1.04y	19	4	5	5	2	1	2
MCS 9	Traumatic	2.4y	10	2	3	2	1	0	2
MCS 10	Traumatic	5.52y	13	2	3	5	1	0	2
MCS 11	Hemorrhage	10.07m	9	1	3	2	1	0	2
MCS 12	Stroke	3.53m	13	3	1	5	2	0	2
MCS 13	Traumatic	1.27y	9	2	1	2	2	0	2
MCS 14	Traumatic	5.47m	8	2	2	2	0	0	2
MCS 15	Traumatic	11.6m	14	3	4	4	1	0	2
MCS 16	Traumatic	6.9m	5	0	0	4	1	0	0
MCS 17	Traumatic	2.19y	11	2	3	2	2	0	2
MCS 18	Anoxic	2.42y	12	1	3	5	1	0	2
VS 1	Traumatic	3.95y	8	1	1	2	2	0	2
VS 2	Traumatic	1.45y	7	1	1	2	1	0	2
VS 3	Hemorrhage	1.09y	6	2	0	2	1	0	1
VS 4	Hemorrhage	1.81y	7	2	0	2	1	0	2
VS 5	Traumatic	7.23m	6	0	0	2	2	0	2
VS 6	Metabolic	5.36y	7	2	0	2	1	0	2
VS 7	Anoxic	3.77m	7	1	1	2	2	0	1
VS 8	Stroke	1.28y	7	1	0	2	2	0	2
VS 9	Traumatic	1.33y	7	1	1	2	1	0	2
VS 10	Anoxic	1.37m	8	2	1	2	1	0	2
VS 11	Anoxic	10.7y	7	1	0	2	2	0	2

TSI, Time Since Injury (y = years/m = months); CRS-R, total scores for the Coma Recovery Scale-Revised (AF, Auditory Function; VF, Visual Function; MF, Motor Function; OF, Oromotor Function; C, communication; Ar, Arousal). The highest CRS-R total scores (and its subscores) on the first A phase (baseline) are mentioned.

laxatives, analgesics, mucolytics, vitamins, and supplements. None of our patients received Amantadine (or Zolpidem), which could have an impact on the patient's consciousness recovery (1, 2).

## Behavioral Results

Using a mixed-design ANCOVA, a main effect of phase (ABAB) [ $F_{(3)} = 3.17$ ,  $p = 0.03$ ] was found. The effect size was found to be medium ( $\eta_p^2 = 0.12$ ). We did not find any interaction with the time since injury [ $F_{(3)} = 0.65$ ,  $p = 0.58$ ], the etiology (i.e., traumatic vs. non traumatic) [ $F_{(3)} = 0.36$ ,  $p = 0.78$ ], or the diagnosis [ $F_{(3)} = 1.35$ ,  $p = 0.26$ ]. We have to note that we also found a main effect of the diagnosis [ $F_{(1)} = 39.78$ ,  $p < 0.001$ ], which is not surprising since this variable (particularly, being conscious/MCS) is known to impact patients' general outcome (41) (**Supplementary Material** and **Figure 1**). Using planned comparisons, we found a significant difference [ $F_{(1)} =$



6.98,  $p = 0.01$ ] between B phases (treatment) and A phases (no treatment); CRS-R total scores being higher during treatment. However, when considering the diagnosis, CRS-R total scores were found to be higher during treatment in MCS patients [ $F_{(1)} = 7.18$ ,  $p = 0.01$ ] but not in VS patients [ $F_{(1)} = 1.28$ ,  $p = 0.27$ ] (**Figure 1**).

Regarding subscores, higher scores during treatment (B phases vs. A phases) were only found for the oromotor subscale ( $T = 2.73$ ,  $p = 0.006$ ) and the arousal subscale ( $T = 2.8$ ,  $p = 0.005$ ). Such difference was confirmed in MCS patients ( $T = 2.07$ ,  $p = 0.04$  and  $T = 2.22$ ,  $p = 0.03$ , respectively) but not in VS patients (**Table 2**).

## fMRI Results

fMRI scans were performed across each phase on seven patients. Patients who exhibited motion greater than one voxel (i.e., 3 mm) were excluded from the analysis. Therefore, data of only three patients (i.e., MCS 7, MCS 8, and VS 11) were considered for analyses. Because of the small number of patients, group analyses were performed using a fixed-effects model (42), and significance was assessed using a non-parametric permutation test (available in FSL) at a significance level of  $p < 0.005$  uncorrected. Regions exhibiting significant activations were identified using the MNI structural atlas, and further specified with the Harvard-Oxford



**TABLE 2 |** Results for the Wilcoxon tests performed to compare CRS-R subscores (average  $\pm$  standard deviation) during A phases and B phases for both VS and MCS groups but also within each group, separately.

MCS/VS	A phases	B phases	<i>p</i>
Auditory	1.33 $\pm$ 0.71	1.35 $\pm$ 0.80	0.95
Visual	1.82 $\pm$ 1.39	1.84 $\pm$ 1.35	0.64
Motor	2.51 $\pm$ 1.11	2.56 $\pm$ 1.19	0.57
Oromotor	1.20 $\pm$ 0.38	1.34 $\pm$ 0.41	0.006*
Communication	0.04 $\pm$ 0.16	0.08 $\pm$ 0.32	0.18
Arousal	1.74 $\pm$ 0.26	1.83 $\pm$ 0.19	0.005*
<b>MCS</b>			
Auditory	1.49 $\pm$ 0.83	1.60 $\pm$ 0.88	0.30
Visual	2.63 $\pm$ 1.12	2.60 $\pm$ 1.08	0.97
Motor	2.94 $\pm$ 1.23	3.03 $\pm$ 1.28	0.36
Oromotor	1.18 $\pm$ 0.45	1.33 $\pm$ 0.47	0.04*
Communication	0.07 $\pm$ 0.20	0.13 $\pm$ 0.40	0.18
Arousal	1.82 $\pm$ 0.26	1.91 $\pm$ 0.17	0.03*
<b>VS</b>			
Auditory	1.07 $\pm$ 0.36	0.95 $\pm$ 0.43	0.08
Visual	0.49 $\pm$ 0.37	0.60 $\pm$ 0.62	0.39
Motor	1.82 $\pm$ 0.17	1.78 $\pm$ 0.35	0.68
Oromotor	1.21 $\pm$ 0.24	1.36 $\pm$ 0.33	0.07
Communication	0 $\pm$ 0	0 $\pm$ 0	1
Arousal	1.62 $\pm$ 0.21	1.7 $\pm$ 0.14	0.08

Significant results are indicated by an asterisk ( $p < 0.05$ ).

atlas and the ICBM Deep Nuclei Probabilistic atlas (43, 44). The group ALFF analyses revealed higher activation during treatment in the right middle frontal gyrus ( $t = 1.71$ ,  $p = 0.001$ ; peak voxel:  $x = 21$ ,  $y = 70$ ,  $z = 54$ ) and right superior temporal gyrus ( $t = 1.88$ ,  $p = 0.001$ ; peak voxel:  $x = 20$ ,  $y = 62$ ,  $z = 31$ ) as well as the bilateral ventro-anterior thalamic nucleus ( $t = 1.26/1.23$ ,  $p = 0.002/0.003$ ; peak voxels:  $x = 49/40$ ,  $y = 59/59$ ,  $z = 38/35$ , for the left and right hemispheres, respectively) (Figure 2).

## DISCUSSION

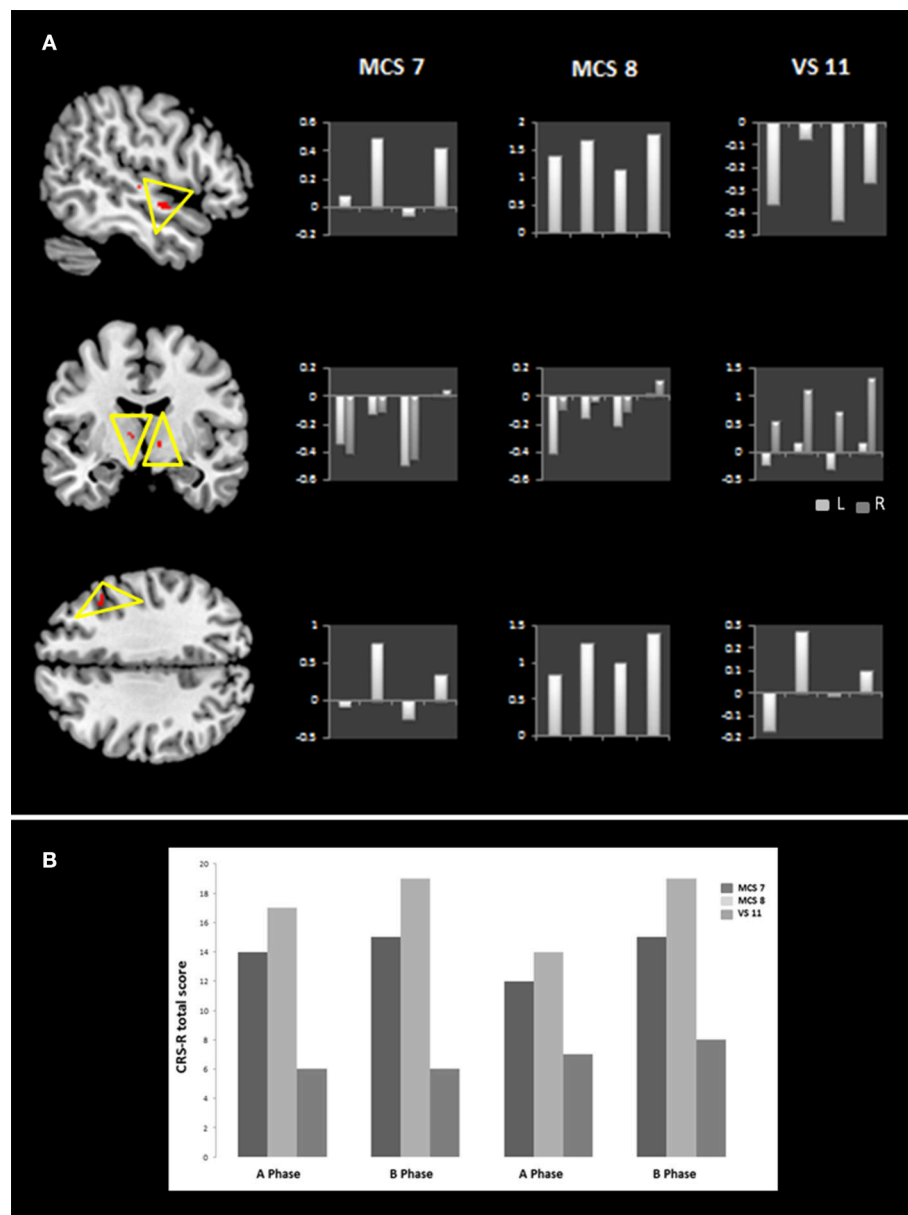
The aim of this study was to assess the impact of SSP on the recovery of consciousness and to determine treatment-related changes using a time-series design in patients with disorders of consciousness (i.e., VS and MCS). Our results suggest that SSP may not be sufficient to restore consciousness. However, SSP might lead to improved behavioral responsiveness in MCS patients. Our results show higher CRS-R total scores when treatment is applied with increased arousal and oromotor function but no changes for the other subscales (i.e., visual, motor, or communication).

Our results showed higher CRS-R total scores when treatment was applied (B phases) as compared to when treatment was not applied (A phases) (with a medium effect size). The time since injury or the etiology did not seem to have an impact on our dataset. However, patients who were diagnosed as being in a MCS obtained higher CRS-R total

scores during treatment than off treatment while patients who were diagnosed as being in a VS did not show such changes. We should however, nuance our findings since we did not find an interaction between CRS-R changes through each phases and diagnosis (VS/MCS) which indicates that the significant changes that we found for our planned comparison (when compiling both A phases versus both B phases) are in fact smaller when each phase is considered separately. Higher CRS-R subscores were also found during treatment for the oromotor and arousal subscales but not for the other subscales (i.e., visual, motor, or communication). These findings were mainly present in MCS patients (i.e., higher oromotor and arousal subscores during treatment) but not in VS patients. We have to mention that even though we found significant results in two subscales of the CRS-R, we could not show, because of statistical limitation, that these changes were significantly higher as compared to the other subscales. Therefore, specific treatment related improvements in arousal and verbal functions should be further investigated and confirmed in the future.

Previous studies using time series and performed in smaller samples ( $n < 15$ ) have reported a modulation of behavioral responses related to treatment based on standardized scales assessing the level of consciousness (29, 30). Using emotionally relevant multi-modal stimulation, Di Stefano and coworkers have found an increased responsiveness in terms of the number of behaviors but also in terms of complexity, based on the Wessex Head Injury Matrix (45). Additionally, even though it did not reach significance, MCS tend to show more behavioral responsiveness than VS patients similarly to our findings. The authors also suggested that the use of emotional stimuli (as used in this study) might have optimized arousal and facilitates behavioral responsiveness (30). Improved arousal has also been shown in studies using a controlled design based on the Glasgow Coma Scale (28, 46, 47). Finally, recent studies have shown that SSP using emotional stimuli have a higher likelihood to lead to increased responsiveness while studies using neuroimaging showed higher metabolic brain activity in response to self-relevant stimuli (5, 38, 48).

The behavioral changes observed (increased arousal and oromotor function) also seem to be in line with our neuroimaging data. Indeed, treatment-related metabolic changes were observed in the superior temporal gyrus, the middle frontal gyrus, and the ventral anterior thalamic nucleus. The superior temporal and middle prefrontal gyri are typically recruited by a number of cognitive processes including language (49) while the ventral anterior thalamic nucleus is known to be a major source of projection to the premotor sections of the frontal cortex, and is involved in motor planning and speech (50). The thalamus also plays a key role in arousal and consciousness. According to the mesocircuit theory, projections from thalamus to associative cortical areas (including temporal and frontal) are crucial for sustaining organized behaviors and integrating information across different regions of cortex (51). Moreover, the ventral anterior nucleus receives neuronal inputs from the basal ganglia which seems to serve a critical role in the



**FIGURE 2 |** Brain areas with treatment-related metabolic changes. The left side of (A) illustrates, at the group level, areas with treatment-related metabolic changes which include the right middle frontal gyrus, the right superior temporal gyrus as well as the bilateral ventro-anterior thalamic nucleus (L = left, R = right) ( $p < 0.005$  voxel-wise uncorrected). On the right side of (A), z-scores for each activated area are also reported at each phase (ABAB) for patients MCS 7, MCS 8, and VS 11. (B) Shows the CRS-R total scores on the last week of each phase (ABAB) for patients MCS 7, MCS 8, and VS 11.

maintenance of behavioral and electrocortical arousal, as well as wakefulness (52–54). Finally, Pape and coworkers found higher activation in the superior temporal and prefrontal gyri in the treated group as compared to the control group, following an unimodal (familiar auditory) stimulation. Anecdotally, the authors also observed higher arousal and more vocalizations in the treated group (32). Besides the neuroimaging modulation observed, the behavioral results obtained in the patients who underwent fMRI, particularly, MCS7 and MCS8 (who were

chronic non-traumatic patients; respectively, 2.91 and 1.04 y post injury), also seem to show fluctuations according to the presence/absence of treatment. VS 11 (who was chronic non-traumatic patient; 10.7 y post injury) did not show such fluctuations (but a constant increase which is difficult to interpret as related to our treatment). This observation is parallel to what we found at the group level since changes in CRS-R scores were mainly observed in the MCS group. Nevertheless, we have to nuance this interpretation since VS 11 had a significantly

longer time post injury (10 y), which might also explain why we don't see changes related to treatment. We also have to stress that our neuroimaging findings were based on an extremely small subsample ( $n = 3$ ), which makes it difficult to formulate firm conclusions. Nonetheless, except Pape et al. (32), no studies have reported neuroimaging findings. Such findings are important since they allow us to start better understanding the mechanisms of action of a particular treatment, here, the SSP. We nevertheless do realize that the generalization of these results is quite limited and that these data are very preliminary.

Our study aimed to address various methodological biases existing in previous studies such as poor description of disorders of consciousness, poor validity, and/or sensitivity of the outcome measure, small sample size as well as spontaneous recovery. Patients recruited in this study were assessed and diagnosed either in a VS or in a MCS based on the CRS-R. The CRS-R is currently the most validated and sensitive scale available to perform behavioral assessment in patients with severe brain injury and to stratify with high accuracy the level of consciousness (37). On the other hand, time series withdrawal design was also chosen not only to address the sample size but also the spontaneous recovery issue. Indeed, withdrawal designs (here, ABAB) provided a high degree of experimental control while being relatively straightforward to plan and implement. Such design allows to repeatedly compare baseline to treatment in order to measure the outcome with and without the intervention, and therefore offers a better control for the impact of natural recovery. Another advantage is that, as compared to controlled designs, within-subject measures requests no matching processes and a smaller sample size (since the sample is not divided between an intervention and a control group). Our study is the first one to include a large sample ( $n = 29$ ) using time-series design, confirming previous preliminary findings (29–31). Only one recent study using a controlled design included 30 patients per group. Indeed, Salmani et al. (48) evaluated the effects of SSP including emotional stimulation on the level of consciousness and showed higher GCS and CRS-R total scores in the end of the intervention in patients receiving emotional SSP as compared to neutral SSP, suggesting that family-centered affective stimulation is more effective in improving the level of consciousness.

This study has several limitations. First, even though the time since injury did not seem to influence the behavioral changes observed during treatment, the majority of our patients were chronic (21 of 29 patients were more than a year post injury), decreasing our chances to see spontaneous recovery but most likely also reducing our chances to see consciousness improvement. Also, the size of VS ( $n = 11$ ) and MCS ( $n = 18$ ) groups did not allow us to explore further the difference of outcome observed. Our neuroimaging data was collected in a very small sample limiting the interpretation of our findings. A double-blinded design was not used in this study. The CRS-R

rater was blinded regarding the ABAB design but knew that the study was about applying treatment to patients with disorders of consciousness. The therapist applying the SSP and the patients' family were not blinded. The aim of the study was not to determine the time, the frequency, the duration and type of program (multi-modal, unimodal, or sensory regulation) (47) requested to optimize the recovery of patients with severe brain injury. One could argue that the effects observed might be due to changes in therapy independent from our treatment. Nevertheless, changes might likely have happened at random in our sample ( $n = 29$ ); i.e., it is most likely that not all our patients stopped or started a therapy at the same time but rather stopped or started a therapy at different time through the study. The withdrawal design we used allowed us to look at behavioral changes that are time locked to treatment as opposed to random changes in treatment. Besides, the statistics we used (mixed design ANCOVA) also controls for such bias and ensures that the effects observed represent a global tendency of the group (that is time locked to treatment). Our data cannot speak on whether the presently applied SSP also leads to lasting changes in level of consciousness and therefore really leads to lasting rehabilitation benefits (in contrast to short-lived changes in responsiveness that might vanish as soon as the SSP is discontinued). Future studies will have to include long term follow-up in order to answer this important issue. Finally, since a controlled design was not used, one cannot clearly determine, in this study, whether improvements are due to specific aspects of our SSP (such as emotional stimulation) or non-specific aspects (such as more time devoted to patients, or non-specific arousal effect).

In conclusion, our study showed a modulation of behavioral responses in a larger sample using time series design. Our results suggest that, even if it may not be sufficient to restore consciousness, SSP might lead to improved behavioral responsiveness in MCS patients. Combined with other validated therapeutics (such as Amantadine) (1), SSP might optimize patients' recovery. Further investigation is nevertheless warranted to test this hypothesis.

## AUTHOR CONTRIBUTIONS

CS and HD: conception, design, and supervision of the work; LC, FW, DC, FR, and FA: acquisition and analysis of behavioral data; FW and MM: acquisition and analysis of fMRI data; CS and HD: interpretation of data for the work; LC, DC, and CS: drafting the work; MM, FW, FR, FA, and HD revising critically for important intellectual content.

## SUPPLEMENTARY MATERIAL

The Supplementary Material for this article can be found online at: <https://www.frontiersin.org/articles/10.3389/fneur.2018.00826/full#supplementary-material>

## REFERENCES

- Giacino JT, Whyte J, Bagiella E, Kalmar K, Childs N, Khademi A, et al. Placebo-controlled trial of amantadine for severe traumatic brain injury. *N Engl J Med.* (2012) 366:819–26. doi: 10.1056/NEJMoa1102609
- Whyte J. Disorders of consciousness: the changing landscape of treatment. *Neurology* (2014) 82:1106–7. doi: 10.1212/WNL.0000000000000276
- The Multi-Society Task Force on PVS. Medical aspects of the persistent vegetative state. *N Engl J Med.* (1994) 330:1499–508.
- Giacino JT, Ashwal S, Childs N, Cranford R, Jennett B, Katz DI, et al. The minimally conscious state: definition and diagnostic criteria. *Neurology* (2002) 58:349–53. doi: 10.1212/WNL.58.3.349
- Padilla R, Domina A. Effectiveness of sensory stimulation to improve arousal and alertness of people in a coma or persistent vegetative state after traumatic brain injury: a systematic review. *Am J Occup Ther.* (2016) 70:7003180030p1–8. doi: 10.5014/ajot.2016.021022
- Schnakers C, Magee WL, Harris B. Sensory stimulation and music therapy programs for treating disorders of consciousness. *Front Psychol.* (2016) 7:297. doi: 10.3389/fpsyg.2016.00297
- Rosenzweig MR. Environmental complexity, cerebral change, and behavior. *Am Psychol.* (1966) 21:321–32. doi: 10.1037/h0023555
- Rosenzweig MR, Bennett EL, Hebert M, Morimoto H. Social grouping cannot account for cerebral effects of enriched environments. *Brain Res.* (1978) 153:563–76. doi: 10.1016/0006-8993(78)90340-2
- Rosenzweig MR, Bennett EL, Krech D. Cerebral effects of environmental complexity and training among adult rats. *J Comp Physiol Psychol.* (1964) 57:438–9. doi: 10.1037/h0046387
- Beaulieu C, Colonnier M. Effect of the richness of the environment on the cat visual cortex. *J Comp Neurol.* (1987) 266:478–94. doi: 10.1002/cne.902660404
- Diamond MC, Krech D, Rosenzweig MR. The effects of an enriched environment on the histology of the rat cerebral cortex. *J Comp Neurol.* (1964) 123:111–20. doi: 10.1002/cne.901230110
- Holloway RL. Dendritic branching: some preliminary results of training and complexity in rat visual cortex. *Brain Res.* (1966) 2:393–6. doi: 10.1016/0006-8993(66)90009-6
- Mollgaard K, Diamond MC, Bennett EL, Rosenzweig MR, Lindner B. Quantitative synaptic changes with differential experience in rat brain. *Int J Neurosci.* (1971) 2:113–27. doi: 10.3109/00207457109148764
- Greenough WT, Volkmar FR, Juraska JM. Effects of rearing complexity on dendritic branching in frontal and temporal cortex of the rat. *Exp Neurol.* (1973) 41:371–8. doi: 10.1016/0014-4886(73)90278-1
- Turner AM, Greenough WT. Differential rearing effects on rat visual cortex synapses. Synaptic and neuronal density and synapses per neuron. *Brain Res.* (1985) 329:195–203.
- Kozorovitskiy Y, Gross CG, Kopil C, Battaglia L, McBrean M, Stranahan AM et al. Experience induces structural and biochemical changes in the adult primate brain. *Proc Natl Acad Sci USA.* (2005) 102:17478–82. doi: 10.1073/pnas.0508817102
- Johansson B. B. (1996). Functional outcome in rats transferred to an enriched environment 15 days after focal brain ischemia. *Stroke.* 27:324–6.
- Koopmans GC, Brans M, Gómez-Pinilla F, Duis S, Gispen WH, Torres-Aleman, et al. Circulating insulinlike growth factor and functional recovery from spinal cord injury under enriched housing conditions. *Eur J Neurosci.* (2006) 23:1035–46. doi: 10.1111/j.1460-9568.2006.04627.x
- Sale A, Berardi N, Maffei L. Enrich the environment to empower the brain. *Trends Neurosci.* (2009) 32:233–9. doi: 10.1016/j.tins.2008.12.004
- Farrell R, Evans S, Corbett D. Environmental enrichment enhances recovery of function but exacerbates ischemic cell death. *Neuroscience* (2001) 107:585–92. doi: 10.1016/S0306-4522(01)00386-4
- Hicks RR, Zhang L, Atkinson A, Stevenson M, Veneracion M, Seroogy KB. Environmental enrichment attenuates cognitive deficits, but does not alter neurotrophin gene expression in the hippocampus following lateral fluid percussion brain injury. *Neuroscience* (2002) 112:631–7. doi: 10.1016/S0306-4522(02)00104-5
- Ronnback A, Dahlqvist P, Svensson PA, Jernas M, Carlsson B, Carlsson LM, et al. Gene expression profiling of the rat hippocampus one month after focal cerebral ischemia followed by enriched environment. *Neurosci Lett.* (2005) 385:173–8. doi: 10.1016/j.neulet.2005.05.016
- Kolb B, Gibb R. Environmental enrichment and cortical injury: behavioral and anatomical consequences of frontal cortex lesions. *Cereb Cortex.* (1991) 1:189–98. doi: 10.1093/cercor/1.2.189
- Passineau MJ, Green EJ, Dietrich WD. Therapeutic effects of environmental enrichment on cognitive function and tissue integrity following severe traumatic brain injury in rats. *Exp Neurol.* (2001) 168:373–84. doi: 10.1006/exnr.2000.7623
- Nithianantharajah J, Hannan AJ. Enriched environments, experienced dependent plasticity and disorders of the nervous system. *Nat Rev Neurosci.* (2006) 7:697–709. doi: 10.1038/nrn1970
- LeWinn EB, Dimancescu MD. Environmental deprivation and enrichment in coma. *Lancet* (1978) 2:156–7.
- Cossu G. Therapeutic options to enhance coma arousal after traumatic brain injury: state of the art of current treatments to improve coma recovery. *Br J Neurosurg.* (2014) 28:187–98. doi: 10.3109/02688697.2013.841845
- Meyer MJ, Megyesi J, Meythaler J, Murie-Fernandez M, Aubut JA, Foley N, et al. Acute management of acquired brain injury Part III: an evidence-based review of interventions used to promote arousal from coma. *Brain Inj.* (2010) 24:722–9. doi: 10.3109/02699051003692134
- Oh H, Seo W. Sensory stimulation programme to improve recovery in comatose patients. *Clin Nurs.* (2003) 12:394–404. doi: 10.1046/j.1365-2702.2003.00750.x
- Di Stefano C, Cortesi A, Masotti S, Simoncini L, Piperno R. Increased behavioural responsiveness with complex stimulation in VS and MCS: preliminary results. *Brain Inj.* (2012) 26:1250–6. doi: 10.3109/02699052.2012.667588
- Lotze M, Schertel K, Birbaumer N, Kotchoubey B. A long-term intensive behavioral treatment study in patients with persistent vegetative state or minimally conscious state. *J Rehabil Med.* (2011) 43:230–6. doi: 10.2340/16501977-0653
- Pape TL, Rosenow JM, Steiner M, Parrish T, Guernon A, Harton B, et al. Placebo-controlled trial of familiar auditory sensory training for acute severe traumatic brain injury: a preliminary report. *Neurorehabil Neural Repair* (2015) 29:537–47. doi: 10.1177/1545968314554626
- Giacino JT, Kalmar K, Whyte J. The JFK coma recovery scale-revised: measurement characteristics and diagnostic utility. *Arch Phys Med Rehabil.* (2004) 85:2020–9. doi: 10.1016/j.apmr.2004.02.033
- Byiers BJ, Reichle J, Symons FJ. Single-subject experimental design for evidence-based practice. *Am J Speech Lang Pathol.* (2012) 21:397–414. doi: 10.1044/1058-0360(2012/11-0036)
- Di H, He M, Zhang Y, Cheng L, Wang F, Nie Y, et al. Chinese translation of the Coma Recovery Scale-Revised. *Brain Inj.* (2017) 31:363–5. doi: 10.1080/02699052.2016.1255780
- Sacco S, Altobelli E, Pistorini C, Cerone D, Cazzulani B, Carolei A, et al. Validation of the Italian version of the Coma Recovery Scale-Revised (CRS-R). *Brain Inj.* (2011) 25:488–95. doi: 10.3109/02699052.2011.558043
- Seel RT, Sherer M, Whyte J, Katz DI, Giacino JT, Rosenbaum AM, et al. Assessment scales for disorders of consciousness: Evidence-based recommendations for clinical practice and research. *Arch Phys Med Rehabil.* (2010) 91:1795–813. doi: 10.1016/j.apmr.2010.07.218
- Perrin F, Castro M, Tillmann B, Luauté J. Promoting the use of personally relevant stimuli for investigating patients with disorders of consciousness. *Front Psychol.* (2015) 6:1102. doi: 10.3389/fpsyg.2015.01102
- Lang PJ, Bradley MM, Cuthbert BN. *International Affective Picture System (IAPS): Gainesville: NIMH: The Center for Research in Psychophysiology.* University of Florida (1997).
- Cohen J. *Statistical Power Analysis for the Behavioural Sciences.* New York, NY: Academic Press (1969).
- Estraneo A, Trojano L. Prognosis in disorders of consciousness. In: Schnakers C, Laureys S, editors. *Coma and Disorders of Consciousness.* London: Springer-Verlag (2018). p. 17–36.
- Monti MM. Statistical analysis of fMRI time-series: a critical review of the GLM Approach. *Front Hum Neurosci.* (2011) 5:28. doi: 10.3389/fnhum.2011.00028



43. Desikan RS, Segonne F, Fischl B, Quinn BT, Dickerson BC, Blacker D, et al. An automated labeling system for subdividing the human cerebral cortex on MRI scans into gyral based regions of interest. *Neuroimage* (2006) 31:968–80. doi: 10.1016/j.neuroimage.2006.01.021
44. Mazziotta J, Toga A, Evans A, Fox P, Lancaster J, Zilles K, et al. A probabilistic atlas and reference system for the human brain: International Consortium for Brain Mapping (ICBM). *Philos Trans R Soc Lond B Biol Sci.* (2001) 356:1293–322. doi: 10.1098/rstb.2001.0915
45. Shiel A, Horn SA, Wilson BA, Watson MJ, Campbell MJ, McLellan DL, et al. The Wessex Head Injury Matrix (WHIM) main scale: a preliminary report on a scale to assess and monitor patient recovery after severe head injury. *Clin Rehabil.* (2000) 14:408–16. doi: 10.1191/0269215500cr326oa
46. Hall ME, MacDonald S, Young GC. The effectiveness of directed multisensory stimulation versus non-directed stimulation in comatose CHI patients: pilot study of a single subject design. *Brain Injury* (1992) 6:435–45. doi: 10.3109/02699059209008139
47. Wood RL, Winkowski TB, Miller JL, Tierney L, Goldman L. Evaluating sensory regulation as a method to improve awareness in patients with altered states of consciousness: a pilot study. *Brain Injury* (1992) 6:411–8. doi: 10.3109/02699059209008137
48. Salmani F, Mohammadi E, Rezvani M, Kazemnezhad A. The effects of family-centered affective stimulation on brain-injured comatose patients' level of consciousness: a randomized controlled trial. *Int J Nurs Stud.* (2017) 74:44–52. doi: 10.1016/j.ijnurstu.2017.05.014
49. Dronkers NF, Wilkins DP, Van Valin RD, Redfern BB, Jaeger JJ. Lesion analysis of the brain areas involved in language comprehension. *Cognition* (2004) 92:145–77. doi: 10.1016/j.cognition.2003.11.002
50. Nieuwenhuys R, Voogd J, van Huijzen C. *The Human Central Nervous System*. 4th ed. New York, NY: Springer (2008).
51. Schiff ND. Recovery of consciousness after brain injury: a mesocircuit hypothesis. *Trends Neurosci.* (2010) 33:1–9. doi: 10.1016/j.tins.2009.11.002
52. Vetrivelan R, Qiu MH, Chang C, Lu J. Role of basal ganglia in sleep-wake regulation: neural circuitry and clinical significance. *Front Neuroanat.* (2010) 4:145. doi: 10.3389/fnana.2010.00145
53. Lazarus M, Chen JF, Urade Y, Huang ZL. Role of the basal ganglia in the control of sleep and wakefulness. *Curr Opin Neurobiol.* (2013) 23:780–5. doi: 10.1016/j.conb.2013.02.001
54. Lutkenhoff ES, Chiang J, Tshibanda L, Kamau E, Kirsch M, Pickard JD, et al. Thalamic and extrathalamic mechanisms of consciousness after severe brain injury. *Ann Neurol.* (2015) 78:68–76. doi: 10.1002/ana.24423
55. Power JD, Mitra A, Laumann TO, Snyder AZ, Schlaggar BL, Petersen SE. Methods to detect, characterize, and remove motion artifact in resting state fMRI. *Neuroimage* (2014) 84:320–41. doi: 10.1016/j.neuroimage.2013.08.048

**Conflict of Interest Statement:** The authors declare that the research was conducted in the absence of any commercial or financial relationships that could be construed as a potential conflict of interest.

Copyright © 2018 Cheng, Cortese, Monti, Wang, Riganello, Arcuri, Di and Schnakers. This is an open-access article distributed under the terms of the Creative Commons Attribution License (CC BY). The use, distribution or reproduction in other forums is permitted, provided the original author(s) and the copyright owner(s) are credited and that the original publication in this journal is cited, in accordance with accepted academic practice. No use, distribution or reproduction is permitted which does not comply with these terms.

# Advantages of publishing in Frontiers



## OPEN ACCESS

Articles are free to read  
for greatest visibility  
and readership



## FAST PUBLICATION

Around 90 days  
from submission  
to decision



## HIGH QUALITY PEER-REVIEW

Rigorous, collaborative,  
and constructive  
peer-review



## TRANSPARENT PEER-REVIEW

Editors and reviewers  
acknowledged by name  
on published articles

## Frontiers

Avenue du Tribunal-Fédéral 34  
1005 Lausanne | Switzerland

**Visit us:** [www.frontiersin.org](http://www.frontiersin.org)

**Contact us:** [info@frontiersin.org](mailto:info@frontiersin.org) | +41 21 510 17 00



## REPRODUCIBILITY OF RESEARCH

Support open data  
and methods to enhance  
research reproducibility



## DIGITAL PUBLISHING

Articles designed  
for optimal readership  
across devices



## FOLLOW US

[@frontiersin](https://twitter.com/frontiersin)



## IMPACT METRICS

Advanced article metrics  
track visibility across  
digital media



## EXTENSIVE PROMOTION

Marketing  
and promotion  
of impactful research



## LOOP RESEARCH NETWORK

Our network  
increases your  
article's readership